

THE SEDIMENTOLOGY AND RESERVOIR CHARACTERISTICS
OF THE LOWER ACACUS FORMATION, NC2 CONCESSION,
HAMADA BASIN, NW LIBYA
(PART I)

CENTRE FOR NEWFOUNDLAND STUDIES

**TOTAL OF 10 PAGES ONLY
MAY BE XEROXED**

(Without Author's Permission)

OMAR BOUZID ELFIGIH





National Library
of Canada

Acquisitions and
Bibliographic Services Branch

395 Wellington Street
Ottawa, Ontario
K1A 0N4

Bibliothèque nationale
du Canada

Direction des acquisitions et
des services bibliographiques

395, rue Wellington
Ottawa (Ontario)
K1A 0N4

Your file / Votre référence

Our file / Notre référence

NOTICE

The quality of this microform is heavily dependent upon the quality of the original thesis submitted for microfilming. Every effort has been made to ensure the highest quality of reproduction possible.

If pages are missing, contact the university which granted the degree.

Some pages may have indistinct print especially if the original pages were typed with a poor typewriter ribbon or if the university sent us an inferior photocopy.

Reproduction in full or in part of this microform is governed by the Canadian Copyright Act, R.S.C. 1970, c. C-30, and subsequent amendments.

AVIS

La qualité de cette microforme dépend grandement de la qualité de la thèse soumise au microfilmage. Nous avons tout fait pour assurer une qualité supérieure de reproduction.

S'il manque des pages, veuillez communiquer avec l'université qui a conféré le grade.

La qualité d'impression de certaines pages peut laisser à désirer, surtout si les pages originales ont été dactylographiées à l'aide d'un ruban usé ou si l'université nous a fait parvenir une photocopie de qualité inférieure.

La reproduction, même partielle, de cette microforme est soumise à la Loi canadienne sur le droit d'auteur, SRC 1970, c. C-30, et ses amendements subséquents.

Canada

**THE SEDIMENTOLOGY AND RESERVOIR CHARACTERISTICS
OF THE LOWER ACACUS FORMATION, NC2 CONCESSION,
HAMADA BASIN, NW LIBYA.**

(PART I)

BY

C OMAR BOUZID ELFIGIH

**A thesis submitted to the School of Graduate
Studies in partial fulfilment of the
requirements for the degree of
Master of Sciences.**

**Department of Earth Sciences,
Memorial University of Newfoundland.**

November 1991

St. John's

Newfoundland



National Library
of Canada

Acquisitions and
Bibliographic Services Branch

395 Wellington Street
Ottawa, Ontario
K1A 0N4

Bibliothèque nationale
du Canada

Direction des acquisitions et
des services bibliographiques

395, rue Wellington
Ottawa (Ontario)
K1A 0N4

Your file / Votre référence

Our file / Notre référence

The author has granted an irrevocable non-exclusive licence allowing the National Library of Canada to reproduce, loan, distribute or sell copies of his/her thesis by any means and in any form or format, making this thesis available to interested persons.

L'auteur a accordé une licence irrévocable et non exclusive permettant à la Bibliothèque nationale du Canada de reproduire, prêter, distribuer ou vendre des copies de sa thèse de quelque manière et sous quelque forme que ce soit pour mettre des exemplaires de cette thèse à la disposition des personnes intéressées.

The author retains ownership of the copyright in his/her thesis. Neither the thesis nor substantial extracts from it may be printed or otherwise reproduced without his/her permission.

L'auteur conserve la propriété du droit d'auteur qui protège sa thèse. Ni la thèse ni des extraits substantiels de celle-ci ne doivent être imprimés ou autrement reproduits sans son autorisation.

ISBN 0-315-82657-6

Canada

National Library
of Canada

Canadian Theses Service

Bibliothèque nationale
du Canada

Service des thèses canadiennes

NOTICE

THE QUALITY OF THIS MICROFICHE
IS HEAVILY DEPENDENT UPON THE
QUALITY OF THE THESIS SUBMITTED
FOR MICROFILMING.

UNFORTUNATELY THE COLOURED
ILLUSTRATIONS OF THIS THESIS
CAN ONLY YIELD DIFFERENT TONES
OF GREY.

AVIS

LA QUALITE DE CETTE MICROFICHE
DEPEND GRANDEMENT DE LA QUALITE DE LA
THESE SOUMISE AU MICROFILMAGE.

MALHEUREUSEMENT, LES DIFFERENTES
ILLUSTRATIONS EN COULEURS DE CETTE
THESE NE PEUVENT DONNER QUE DES
TEINTES DE GRIS.

ABSTRACT

Analyses of core and wireline logs from twenty one (21) wells distributed inside and outside the study area demonstrate that the Lower Acacus Formation consists regionally (across the Hamada Basin) of at least fourteen progradational sandstone units (A1-A14) from south to north. Locally, in the study area, at least nine progradational sandstone units (A6-A14) exist. On the basis of a best-facies-fit approach the stratigraphic framework indicates deltaic packages change laterally northward, in a progradational fashion, from fluvial-channel sands to coastal-deltaic sands and silts and eventually to offshore-marine reworked sands and shales. The depositional patterns of some sandstone units in the Lower Acacus Formation are lobate. Sand axes in each unit are offset from those in the older units due to sediment loading and differential compaction within the delta complex. From core data and log responses the Lower Acacus sandstones are interpreted to have been deposited as deltaic lobes during shoreline progradation, where each lobe consists of two lithofacies; (1) a horizontal cross-laminated, clean sandstone or proximal delta front lithofacies which has the best reservoir quality, low clay content, and (2) a bioturbated silty-sandstone or distal delta front

lithofacies (marginal), with poor reservoir quality and high clay content.

Secondary porosity, found to be the dominant porosity type in the Lower Acacus Sandstones, was derived mainly from partial dissolution of carbonate cements, some detrital grains, and rock fragments. This porosity is characterized by oversized, elongate, corroded and irregular pore spaces. Primary pores are minor, but where present are small, concavo-convex and triangular in thin-section cross-sectional shape and are usually associated with quartz-supported clean sandstones.

Core plug porosity quantifies total porosity but does not distinguish micro-porosity from macroporosity (effective porosity), and shows an insignificant relationship with corresponding permeability values due to microporosity associated with clay-rich sandstones. Thin-section porosity on the other hand most significantly reflects corresponding permeability values and identifies meaningful correlation after the elimination of clay-rich sandstones.

Oil-bearing sands with high reservoir quality are found to be closely related to sedimentary environmental facies. The best reservoir quality sandstone units are found in the proximal delta front facies at the top of

deltaic lobes in wells which occur in the central and southern part of the study area. They are characterized by an average porosity of 20.3%, an average permeability 921 md., an average hydrocarbon saturation of 62% and a cutoff point of 48% for formation water saturation. The cumulative estimation (total hydrocarbon estimation) of hydrocarbons from multiple pay zones in the Lower Acacus Sandstones on a per well basis is 803 BOPD with 0.931 MMCFGPD, while the estimated oil-in-place for all structures producing from the Lower Acacus Sandstones in the study area is calculated to be about 190.12 MMSTBOIP and 117.19 MMSCFGIP.

Information from wells in the study area, with specific reference to GR log shapes, and integrated with sand isopach maps has resulted in paleogeographic maps which illustrate the depositional history of the Lower Acacus Formation and provides the basis for future exploration prospects.

ACKNOWLEDGMENTS

I am indebted to Dr.J.D. Harper, Earth Sciences Department, Memorial University of Newfoundland, for initial persuasion to undertake this project and who supervised all stages of its preparation. His continuing encouragement and helpful criticism is gratefully acknowledged.

I greatly appreciate the hard work of Mr. Wilfred Marsh, Memorial University of Newfoundland, who photographed (PMT) the illustrations and whose suggestions resulted in material improvement of the presentation of this work.

I thank the Arabian Gulf Oil Company (AGOCO) Benghazi-Libya, for providing the financial support for this research, as well as the cores, rock thin-sections, well logs and field information upon which this study is based.

DEDICATION

This thesis is dedicated to my wife, and my son (WAIL) whose unsurpassable encouragement, patience and moral support made all this possible.

Also, this work is to be as a remembrance to the memory of my son

**** (S E R A J) ****

(January.8.1991 - March.5.1991).

CONTENTS

PART I	Page
ABSTRACT.....	ii
ACKNOWLEDGEMENTS.....	v
DEDICATION.....	vi
LIST OF TABLES.....	xi
LIST OF FIGURES.....	xiii
LIST OF ABBREVIATIONS USED.....	xxviii
INTRODUCTION.....	1
GENERAL GEOLOGY OF THE HAMADA BASIN AND STUDY AREA.....	12
- Tectonic Framework.....	12
- Stratigraphy.....	26
Stratigraphic Remarks.....	26
Memouniat Formation (Cambro-Ordovician).....	30
Tanezzuft Formation (Lower Silurian).....	35
Acacus Formation (Upper Silurian).....	43
Lower Acacus.....	45
Middle Acacus.....	46
Upper Acacus.....	46
DATA BASE AND METHODOLOGY.....	54
- Data Base.....	54
- Methodology.....	55
1- Subsurface Studies.....	55
2- Core Study.....	61
3- Thin-Section Study.....	61

4- Petrophysical Study.....	62
WIRELINE-LOG CHARACTERISTICS.....	65
SANDSTONE TRENDS AND MORPHOLOGY.....	86
- Cross Sections.....	86
- Isopach Maps.....	90
- Log Facies Maps.....	114
- Sandstone Percentage Map.....	129
- Sand-Shale Ratio Map.....	129
DEPOSITIONAL ENVIRONMENTS AND LITHOFACIES.....	135
- Depositional Environments and Processes.....	135
- Lithofacies.....	141
- Depositional Model-Lower Acacus Sandstone.....	154
PETROGRAPHY.....	159
- Detrital Grains.....	159
- Authigenic Minerals.....	169
- Compaction.....	172
PETROPHYSICS AND RESERVOIR QUALITY-SUMMARY.....	173
- Petrophysics.....	173
Porosity and Permeability Study.....	173
Petrophysical Log Interpretation.....	192
1- Log Interpretation of A14 Sand/Silt Unit, Well E1-NC2, Lower Acacus Formation.....	192
2- Log Interpretation of A12 Sand/Silt Unit, Well F1-NC2, Lower Acacus Formation.....	215
3- Log Interpretation of A8 Sand/Silt Unit, Well C1-NC2, Lower Acacus Formation.....	238

4- Log Interpretation of A8 Sand/Silt Unit, Well A1-NC2, Lower Acacus Formation.....	259
- Reservoir Quality-Summary.....	276
STRATIGRAPHIC APPLICATION.....	283
- Acacus South formation.....	283
- Paleogeographic Map.....	286
FUTURE EXPLORATION STRATEGY AND RECOMMENDATION.....	289
CONCLUSIONS.....	294
REFERENCES.....	302

PART II

APPENDICES.....	316
-----------------	-----

Appendix I: Core Description and Core Photographs of the Lower Acacus Formation, NC2

Concession, Hamada Basin, NW Libya.....	317
Well E1-NC2.....	317
Well C1-NC2.....	330
Well T1-23.....	344
Well A1-NC2.....	354
Well Q1-23.....	361
Well B1-61.....	379
Well B3-61.....	391
Well C1-61.....	417
Well D1-61.....	440

Appendix II: Cores Illustrating Sedimentary Structures of the Lower Acacus

Formation, NC2 Concession, Hamada Basin, NW Libya.....	475
Appendix III: Thin-Section-Lithofacies of the Lower Acacus Formation, NC2 Concession, Hamada Basin, NW Libya.....	493
Appendix IV: Thin-Section-Petrographic Information of the Lower Acacus Formation, NC2 Concession, Hamada Basin, NW Libya.....	507
Appendix V: Thin-Section-Porosity Type of the Lower Acacus Formation, NC2 Concession, Hamada Basin, NW Libya.....	543
Appendix VI: Staining Method.....	568

ENCLOSURES

TABLES

	Page
Table 1. Petrographic data of Lower Acacus Sandstones NC2 concession, Hamada Basin, NW Libya.....	160
Table 2. Porosity-Permeability data of routine core analyses for all sandstone samples from Lower Acacus Formation, NC2 concession, Hamada Basin, NW Libya.....	174
Table 3. Porosity-Permeability data of sandstone samples containing $\leq 3\%$ matrix from Lower Acacus Formation, NC2 concession, Hamada Basin, NW Libya.....	178
Table 4. Log evaluation for A14 sand/silt unit, well E1-NC2, Lower Acacus Formation, NC2 concession, Hamada Basin, NW Libya.....	199
Table 5. Log evaluation for A12 sand/silt unit, well F1-NC2, Lower Acacus Formation, NC2 concession, Hamada Basin, NW Libya.....	221
Table 6. Log evaluation for A8 sand/silt unit, well C1-NC2, Lower Acacus Formation, NC2 concession, Hamada Basin, NW Libya.....	245
Table 7. Log evaluation for A8 sand/silt unit, well A1-NC2, Lower Acacus Formation, NC2 concession, Hamada Basin, NW Libya.....	264

Table 8. Reservoir characteristics of oil and gas producing wells in the study area, NC2 concession, Hamada Basin, NW Libya, for which core-thin-section data, log data and DST data were available for sandstone unit intervals in the Lower Acacus Formation.....	281
Table 9. Total estimate reserves of oil and gas in the Lower Acacus Sandstones, NC2 concession, Hamada Basin, NW Libya.....	282

FIGURES

Figure	Page
Figure 1. Location map of Libya and the Hamada Basin (Ghadames Basin).....	3
Figure 2. North-south cross section showing the setting of the Paleozoic-Mesozoic Hamada Basin (after Conant and Goudarzi, 1967).....	5
Figure 3. Location map of the study area (from TDL, AGOCO, 1988).....	7
Figure 4. Location map of the study area defined by latitude and longitude (from TDL, AGOCO, 1988).....	9
Figure 5. Tectonic map of Libya showing the basins and the structural elements of Hamada Basin.....	14
Figure 6. Regional structural cross section illustrating the concept of stratigraphic and structural relations in the Hamada Basin, NW Libya (after N.O.C., Exploration Department, 1981).....	16
Figure 7. Type of structures in the Hamada Basin NW Libya (modified map, after BEICIP, 1975, Western Libya Exploration study, National Oil Corporation).....	18
Figure 8. Structural relief during Early Paleozoic and Devonian times (after Klitzsch, 1971).....	21

Figure 9. Area of the exposed Precambrian rocks (adapted from Karasek R.M., 1981).....	23
Figure 10. General Paleozoic stratigraphic framework for the Hamada Basin, NW Libya.....	29
Figure 11. Geological map showing type areas of Cambro-Ordovician Memouniat Sandstone at Jabal Gargaf (modified, after Collomb, 1962; Vos, 1981b).....	32
Figure 12. Distribution of Cambro-Ordovician strata (after Klitzsch, 1970).....	34
Figure 13. Map showing the type locality of the Silurian-Devonian section (after Klitzsch 1969).....	38
Figure 14. Distribution of Silurian (Tanezzuft-Acacus) strata (after Klitzsch, 1970).....	40
Figure 15. Isopach map of Tanezzuft Formation, NC2 concession, Hamada Basin, NW Libya.....	43
Figure 16. Isopach map of the Lower Acacus Formation, NC2 concession, Hamada Basin, NW Libya.....	49
Figure 17. Isopach map of the Middle Acacus Formation, NC2 concession, Hamada Basin, NW Libya.....	51
Figure 18. Isopach map of the Upper Acacus Formation, NC2 concession, Hamada Basin, NW Libya.....	53
Figure 19. Gamma-Ray (GR) log patterns of the deltaic sand/silt of the Lower Acacus Formation, NC2 concession, Hamada Basin, NW Libya.....	68

Figure 20-A. Gamma-Ray (GR) log characteristics for the fluvial sands of the Lower Acacus Formation (in well C1-61), NC2 concession, and of the Acacus South formation (in wells II1-NC7 and C1-NC7A, south of NC2 concession), Hamada Basin, NW Libya..... 72

Figure 20-B. Spontaneous-Potential (SP) and Gamma-Ray (GR) Logs for the fluvial sands of the Lower Acacus Formation (in well B3-61, NC2 concession), and of the Acacus South formation (in well III1-NC7, south of NC2 concession), Hamada Basin, NW Libya..... 74

Figure 20-C. Spontaneous-Potential (SP) and Gamma-Ray (GR) logs for the fluvial sands of the Lower Acacus Formation (in well B3-61, NC2 concession), and of the Acacus South formation (in well C1-NC7A, south of NC2 concession), Hamada Basin, NW Libya..... 76

Figure 21. Gamma-Ray (GR) log patterns of the marine sands in the Lower Acacus Formation, NC2 concession, Hamada Basin, NW Libya..... 79

Figure 22. Spontaneous-Potential (SP) and Gamma-Ray (GR) log patterns for some sand sequences in well B2-NC2 and well D1-NC2, Lower Acacus Formation, NC2 concession, Hamada Basin, NW Libya..... 83

Figure 23. Spontaneous-Potential (SP) and Gamma-Ray (GR) log patterns for the same sand unit in well C1-61, Lower Acacus Formation, NC2 concession, Hamada Basin, NW Libya..... 85

Figure 24. Net sandstone isopach map of the Lower Acacus Formation, NC2 concession, Hamada Basin, NW Libya..... 92

Figure 25. Isopach map of the A8 sandstone unit, Lower Acacus Formation, NC2 concession, Hamada Basin, NW Libya..... 97

Figure 26. Isopach map of the A9 sandstone unit, Lower Acacus Formation, NC2 concession, Hamada Basin, NW Libya..... 99

Figure 27. Isopach map of the A10 sandstone unit, Lower Acacus Formation, NC2 concession, Hamada Basin, NW Libya..... 101

Figure 28. Isopach map of the A12 sandstone unit, Lower Acacus Formation, NC2 concession, Hamada Basin, NW Libya..... 103

Figure 29. Isopach map of the A14 sandstone unit, Lower Acacus Formation, NC2 concession, Hamada Basin, NW Libya..... 105

Figure 30-A. Depositional patterns and axes of successive sandstone units (A8-A14), of the Lower Acacus Formation, NC2 concession, Hamada Basin, NW Libya..... 108

Figure 30-B. Depositional patterns and axes of successive sandstone units (A8-A14), in the southern delta system, Lower Acacus Formation, NC2 concession, Hamada Basin, NW Libya..... 110

Figure 30-C. Depositional patterns and axes of successive sandstone units (A8-A14), in the possible eastern delta system, Lower Acacus Formation, NC2 concession Hamada Basin, NW Libya..... 112

Figure 31. Log facies map for A8 sand/silt unit, Lower Acacus Formation, NC2 concession, Hamada Basin , NW Libya..... 116

Figure 32. Log facies map for A9 sand/silt unit, Lower Acacus Formation, NC2 concession, Hamada Basin, NW Libya..... 118

Figure 33. Log facies map for A10 sand/silt unit, Lower Acacus Formation, NC2 concession, Hamada Basin, NW Libya..... 120

Figure 34. Log facies map for A12 sand/silt unit, Lower Acacus Formation, NC2 concession, Hamada Basin, NW Libya..... 122

Figure 35. Log facies map for A14 sand/silt unit, Lower Acacus Formation, NC2 concession, Hamada Basin, NW Libya..... 124

Figure 36. Gravity anomaly map of the Hamada Basin, NW Libya, (Adapted from Bouger gravity map of Libya; Essed, A.S., 1978).....	128
Figure 37. Sandstone percentage map of the Lower Acacus Formation, NC2 concession, Hamada Basin, NW Libya.....	132
Figure 38. Sand-Shale ratio map of the Lower Acacus Formation, NC2 concession, Hamada Basin, NW Libya.....	134
Figure 39. Type log of the well E1-NC2, NC2 concession, Hamada Basin, NW Libya.....	137
Figure 40. Gamma-Ray (GR) log pattern of the deltaic facies in the Lower Acacus Formation, NC2 concession, Hamada Basin, NW Libya.....	145
Figure 41. Well-log motif (SP & GR) showing characteristics of the fluvial channel facies and their sequences in the Lower Acacus Formation, NC2 concession, Hamada Basin, NW Libya.....	147
Figure 42. Schematic depositional model for the Lower Acacus Formation, NC2 concession, Hamada Basin, NW Libya.....	158
Figure 43. Detrital plot for Lower Acacus Sandstones, NC2 concession, Hamada Basin, NW Libya.....	163

- Figure 44. Texture, composition and log character of the Lower Acacus Sandstone, NC2 concession, Hamada Basin, NW Libya..... 165
- Figure 45. Core plug porosity (ϕ_c) versus air permeability (K_{air}) for all sandstone samples from the Lower Acacus Formation, NC2 concession, Hamada Basin, NW Libya..... 185
- Figure 46. Thin-section porosity (ϕ_u) versus air permeability (K_{air}) for sandstone samples containing $\leq 3\%$ matrix from the Lower Acacus Formation, NC2 concession, Hamada Basin, NW Libya..... 187
- Figure 47. Porosity measured in core plugs (ϕ_c) versus porosity measured in thin section (ϕ_u) for sandstone samples containing $> 3\%$ matrix, from the Lower Acacus Formation, NC2 concession, Hamada Basin, NW Libya..... 189
- Figure 48. Porosity measured in core plugs (ϕ_c) versus porosity measured in thin section (ϕ_u) for sandstone samples containing $\leq 3\%$ matrix from the Lower Acacus Formation, NC2 concession, Hamada Basin, NW Libya..... 191
- Figure 49. Resistivity logs (MSFL, ILD, SFL), sonic log (DT) with bit size (BS), caliper log (CALI), gamma-ray log (GR),

and spontaneous-potential log (SP),
 for A14 sand/silt unit, well E1-NC2,
 NC2 concession, Hamada Basin, NW Libya..... 194

Figure 50. Combination neutron-density logs
 (NPHI-RHOB), photo-electric index log
 (PEF), with gamma-ray log (GR), bit size
 (BS), and caliper log (CALI), for A14
 sand/silt unit, well E1-NC2, Lower Acacus
 Formation, NC2 concession, Hamada Basin,
 NW Libya..... 196

Figure 51. Grain size determination by water
 saturation (S_w) versus corrected
 log average porosity ($\phi_{w.c}$) crossplot
 for A14 sand/silt unit, well E1-NC2,
 Lower Acacus Formation, NC2 concession,
 Hamada Basin, NW Libya..... 203

Figure 52. Water saturation (S_w) versus irreducible
 water saturation (S_{wir}) crossplot for
 determining relative permeability to
 gas (K_{rg}) for A14 sand/silt unit, well
 E1-NC2, Lower Acacus Formation,
 NC2 concession, Hamada Basin, NW Libya..... 205

Figure 53. Water saturation (S_w) versus irreducible
 water saturation (S_{wir}) crossplot for
 determining relative permeability to

water (K_{rw}) for A14 sand/silt unit, well
E1-NC2, Lower Acacus Formation,
NC2 concession, Hamada Basin, NW Libya..... 208

Figure 54. Water saturation (S_w) versus irreducible
water saturation (S_{wir}) crossplot for
determining relative permeability to
oil (K_{ro}) for A14 sand/silt unit, well
E1-NC2, Lower Acacus Formation,

NC2 concession, Hamada Basin, NW Libya..... 210

Figure 55. Water saturation (S_w) versus irreducible
water saturation (S_{wir}) crossplot for
determining percent water-cut (35°API gravity
oil) for A14 sand/silt unit, well E1-NC2,
Lower Acacus Formation, NC2 concession,
Hamada Basin, NW Libya..... 213

Figure 56. Resistivity logs (MSFL, ILD, SFL), sonic
log (DT) with bit size (BS), caliper log
(CALI), gamma-ray log (GR), and spontaneous-
potential log (SP), for A12 sand/silt unit,
well F1-NC2, Lower Acacus Formation,
NC2 concession, Hamada Basin, NW Libya..... 217

Figure 57. Combination neutron-density logs
(NPHI-RHOB), photo-electric indexlog (PEF),
with bit size (BS), gamma-ray logs
(SGR, CGR), and caliper log (CALI), for

A12 sand/silt unit, well F1-NC2,
Lower Acacus Formation, NC2 concession,
Hamada Basin, NW Libya..... 220

Figure 58. Grain size determination by water saturation

(S_w) versus corrected average log porosity
($\phi_{v,c}$) crossplot, for A12 sand/silt unit,
well F1-NC2, Lower Acacus Formation,
NC2 concession, Hamada Basin, NW Libya..... 223

Figure 59. Corrected average log porosity ($\phi_{v,c}$)

versus irreducible water saturation (S_{wir})
crossplot for determining total permeability
for A12 sand/silt unit, well F1-NC2,
Lower Acacus Formation, NC2 concession,
Hamada Basin, NW Libya..... 226

Figure 60. Water saturation (S_w) versus irreducible

water saturation (S_{wir}) crossplot for
determining relative permeability to gas
(K_g) for A12 sand/silt unit, well F1-NC2,
Lower Acacus Formation, NC2 concession,
Hamada Basin, NW Libya..... 228

Figure 61. Water saturation (S_w) versus irreducible

water saturation (S_{wir}) crossplot for
determining relative permeability to water
(K_w) for A12 sand/silt unit, well F1-NC2,
Lower Acacus Formation, NC2 concession,

	Hamada Basin, Nw Libya.....	231
Figure 62.	Water saturation (S_w) versus irreducible water saturation (S_{win}) crossplot for determining percent water-cut (35°API gravity oil) for A12 sand/silt unit, well F1-NC2, Lower Acacus Formation, NC2 Concession, Hamada Basin, NW Libya.....	233
Figure 63.	Water saturation (S_w) versus irreducible water saturation (S_{win}) for determining relative permeability to oil (K_{ro}) for A12 sand/silt unit, well F1-NC2, Lower Acacus Formation, NC2 concession, Hamada Basin, NW Libya.....	237
Figure 64.	Resistivity logs (MSFL, ILD, SFL), sonic log (DT) with bit size (BS), caliper log (CALI), gamma-ray log (GR), and spontaneous- potential log (SP), for A8 sand/silt unit, well C1-NC2, Lower Acacus Formation, NC2 concession, Hamada Basin, NW Libya.....	242
Figure 65.	Combination neutron-density logs (NPHI-RHOB), photo-electric index log (PEF), with gamma ray log (GR), bit size (BS), and caliper log (CALI), for A8 sand/silt unit, well C1-NC2, Lower Acacus Formation, NC2 concession, Hamada Basin, NW Libya.....	244

- Figure 66. Grain size determination by water saturation (S_w) versus corrected average log porosity ($\phi_{v,c}$) crossplot for A8 sand/silt unit, well C1-NC2, Lower Acacus Formation, NC2 concession, Hamada Basin, NW Libya..... 247
- Figure 67. Water saturation (S_w) versus Irreducible water saturation (S_{wir}) crossplot for determining relative permeability to gas (K_{rg}) for A8 sand/silt unit, well C1-NC2, Lower Acacus Formation, NC2 concession, Hamada Basin, NW Libya..... 250
- Figure 68. Water saturation (S_w) versus irreducible water saturation (S_{wir}) crossplot for determining relative permeability to water (K_{rw}) for A8 sand/silt unit, well C1-NC2, Lower Acacus Formation, NC2 concession, Hamada Basin, NW Libya..... 252
- Figure 69. Water saturation (S_w) versus irreducible water saturation (S_{wir}) crossplot for determining relative permeability to oil (K_{ro}) for A8 sand/silt unit, well C1-NC2, Lower Acacus Formation, NC2 concession, Hamada Basin, NW Libya..... 256
- Figure 70. Water saturation (S_w) versus irreducible water saturation (S_{wir}) crossplot for

determining percent water-cut (35°API gravity oil) for A8 sand/silt unit, well C1-NC2, Lower Acacus Formation, NC2 concession, Hamada Basin, NW Libya..... 258

Figure 71. Resistivity logs (MSFL, ILD, SFL), sonic log (DT) with bit size (BS), caliper log (CALI), gamma-ray log (GR), and spontaneous-potential log (SP), for A8 sand/silt unit, well A1-NC2, Lower Acacus Formation, NC2 concession, Hamada Basin, NW Libya..... 261

Figure 72. Combination neutron-density logs (NPFI-RHOB) with gamma-ray log (GR), bit size (BS), and caliper log (CALI), for A8 sand/silt unit, well A1-NC2, Lower Acacus Formation, NC2 concession, Hamada Basin, NW Libya..... 263

Figure 73. Grain size determination by water saturation (S_w) versus corrected average log porosity ($\phi_{av,c}$) crossplot for A8 sand/silt unit, well A1-NC2, Lower Acacus Formation, NC2 concession, Hamada Basin, NW Libya..... 267

Figure 74. Water saturation (S_w) versus irreducible water saturation (S_{wirr}) crossplot for determining relative permeability to water (K_{rw}) for A8 sand/silt unit, well A1-NC2,

- Lower Acacus Formation, NC2 concession,
Hamada Basin, NW Libya..... 269
- Figure 75. Water saturation (S_w) versus irreducible
water saturation (S_{wirr}) crossplot for
determining relative permeability to gas (K_{rg})
for A8 sand/silt unit, well A1-NC2, Lower
Acacus Formation, NC2 concession, Hamada
Basin, NW Libya..... 271
- Figure 76. Water saturation (S_w) versus irreducible
water saturation (S_{wirr}) crossplot for
determining relative permeability to oil
(K_{ro}) for A8 sand/silt unit, well A1-NC2,
Lower Acacus Formation, NC2 concession,
Hamada Basin, NW Libya..... 273
- Figure 77. Corrected average log porosity ($\phi_{av,c}$)
versus irreducible water saturation (S_{wirr})
crossplot for determining total permeability
for A8 sand/silt unit, well A1-NC2, Lower
Acacus Formation, NC2 concession, Hamada
Basin, NW Libya..... 275
- Figure 78. Type logs for the Acacus South formation,
in well C1-NC7A and Well III-NC7, Hamada
Basin, NW Libya..... 285
- Figure 79. Paleogeographic map depicting depositional
facies of the Lower Acacus Formation,

Hamada Basin, NW Libya..... 288

LIST OF ABBREVIATIONS USED

American Petroleum Institute.....	API
Air Permeability.....	K_{air}
Alternations.....	alter
Appendix.....	App.
Arabian Gulf Oil Company.....	AGOCO
As above.....	a/a
At.....	@
Barrels of oil per day.....	BOPD
Billion standard cubic feet of gas in place.....	MMSCFIP
Bioturbated.....	Biot
Bit size.....	BS
Black.....	blk
Bottom.....	bott
Brown.....	brn
Burrowed.....	Burr
Burrowed structures.....	Burr.stru
Calcareous.....	calc
Calcite cement.....	C
Caliper log.....	CALI
Carbonaceous.....	Car
Cased Hole Drill Stem Test.....	CH.DST

Chamosite.....	Cham
Chert.....	Chr
Chlorite.....	Chl
Clay.....	Cly
Clay clasts.....	Cly clas
Coarse grained.....	CG, c grd
Clay volume.....	V_{cly}
Compensated Gamma-Ray log.....	CGR
Complex sandstone.....	cplx. ss
Contact.....	Co
Contorted laminations.....	Cont.lam
Contorted structures.....	Cont.stru
Core Number.....	C#
Core plug porosity.....	ϕ_c
Corrected average log porosity.....	ϕ_{avc}
Corrected density porosity.....	ϕ_D
Corrected neutron porosity.....	ϕ_N
Corrected sonic porosity.....	ϕ_s
Cream.....	crm
Cross-laminations.....	x.lam
Crossed nicols.....	X.N
Cubic feet per barrel.....	cc.ft/bbl
Deep Induction Laterolog.....	ILD
Degree (American Petroleum Institute).....	°API
Degree Fahrenheit.....	°F

Density.....	ρ_b
Density log.....	RHOB
Density porosity.....	ϕ_D
Dolomite.....	Dolo
Drill Stem Test.....	DST
Drill Stem Test Interval.....	DST Intv.
Enclosure.....	Encl.
Enclosures.....	Encls.
Fair.....	fr
Feet.....	ft
Feldspar.....	Feld
Ferruginous.....	Ferr
Figure.....	Fig
Figures.....	Figs
Fine.....	F, fn
Fissile.....	fiss
Flaky.....	flky
Fluid contact.....	F/C
Fine to medium grained.....	F-MG, fn-mgrd
Friable Sandstone.....	Frb.ss
Gamma-Ray log.....	GR
Gas Oil Ratio.....	GOR
Gas Volume Factor.....	Bg
Glaucanite.....	G
Good.....	gd

Gram per cubic centimeter.....	gm/cc
Gray.....	gy
Grayish.....	gyish
Green.....	grn
Hydrocarbon.....	H
Hydrocarbon saturation.....	S_h
Inch.....	IN
Indistinctive.....	Indist
Irreducible water saturation.....	S_{wir}
Kaolinite.....	K
Kelly Bushing.....	K.B
Lamination.....	lam
Lenticular.....	lent
Lenticular sand.....	lent.sd
Lenses.....	L
Load features.....	Lf
Lower Acacus Sandstone unit number 1 to Lower Acacus Sandstone unit number 14.....	A1-A14
Marine Sandstone.....	M.ss
Matrix.....	MX
Maximum.....	max
Meter.....	m
Mica.....	mic.
Mica muscovite.....	Ms
Microspherically focused log.....	MSFL

Millidarcy.....	md
Milliseconds per foot.....	μ sec/ft
Million cubic feet of gas per day.....	MMCFGPD
Million stock tank barrels of oil in place.....	MMSTBOIP
Millivolt.....	MV
Minimum.....	min
Moderately sorted.....	m.sort
Moderate to well sorted.....	m-w.sort
Monocrystalline Quartz.....	MQ, Qm
Neutron porosity.....	ϕ_N
Neutron porosity log.....	NPFI
Northwest.....	NW
Occasionally.....	occ
Ohm.....	Ω
Ohm-meter.....	OHMM
Oil Volume Factor.....	O.v.F
Open Hole Drill Stem Test.....	OH.DST
Other minerals.....	Oth
Page.....	p.
Parallel.....	Par
Parallel laminations.....	Par.lam
Parts.....	pts
Partial crossed nicols.....	P.X.N
Photo-Electric Index log.....	PEF
Polycrystalline Quartz.....	PQ, Qp
Poor.....	pr

Poorly sorted.....	pr.sort
Pore spaces.....	P
Porosity.....	\emptyset
Pounds per square inch.....	PSI
Quartz overgrowth.....	O
Relative permeability to gas.....	K_{rg}
Relative permeability to oil.....	K_{ro}
Relative permeability to water.....	K_{rw}
Resistivity.....	Res.
Resistivity of flushed zone.....	R_{fo}
Resistivity of invaded zone.....	R_i
Resistivity of uninvaded zone.....	R_u
Rippled.....	rippl
Rock fragment.....	RF
Rounded.....	rd
Sand.....	sd
Sandstone.....	ss
Shale.....	sh, SH
Shale laminations.....	sh.lam
Shallow focused log.....	SFL
Siderite.....	Sid
Silicate cement.....	Silc
Silt.....	slt
Silty sand lenses.....	slty.sd.L
Silty sandstone.....	slty.ss
Spectral Gamma-Ray log.....	SGR

Spontaneous-Potential Log.....	SP
Sonic log (Transit time).....	DT, ΔT
Sonic porosity.....	ϕ_s
South.....	S
Standard cubic feet.....	SCF
Subangular.....	subang
Subfissile.....	subfiss
Subparallel.....	subpar
Subrounded.....	subrd
Technical Data Library.....	TDL
Thin-section.....	T.S.
Thin-section porosity.....	ϕ_u
Vertical burrows.....	Vr. Burr
Very bioturbated.....	V. Biot
Very laminated.....	V. lam
Very fine grained.....	VFG, vf.grd
Very fine to fine grained.....	vf-f.grd
Water cut.....	WC
Water saturation.....	S_w
Wavy laminated.....	w. lam
Whitish.....	wtish
Well sorted.....	w.sort
With minor.....	w/minor

INTRODUCTION

The Hamada Basin, also called the Ghadames Basin in some of the literature, is situated in north-western Libya and extends into Tunisia and Algeria (Fig. 1).

Hamada Basin, on the whole, can be classified as an interior sag basin of Paleozoic-Mesozoic age according to the classification of Kingston et al. (1983), in which a thick sequence, mainly of clastic rocks, has been deposited during Paleozoic time (Fig. 2).

The study area is located on the northern flank of the Hamada Basin (Fig. 3), and has a nearly rectangular shape (Fig. 4) defined by the coordinates:

NW	31° 50' N	/	10° 45' E
NE	31° 50' N	/	11° 50' E
SE	31° 30' N	/	11° 50' E
SE	31° 30' N	/	11° 40' E
SE	31° 25' N	/	11° 40' E
SW	31° 25' N	/	10° 45' E

The Compagnie des Petroles Total (Libya) (CPT (L)) started exploring this area in the 1960's and most of its production was from the Lower Acacus Sandstones. In 1971-1975 BEICIP, a consulting organization, made an exploration study and evaluation of the Hamada Basin. Their report covered, in general, the stratigraphy of the

**Figure 1. Location map of Libya and the Hamada
Basin (Ghadames Basin).**



OBB-91

Figure 2. North-south cross section showing the setting of the Paleozoic-Mesozoic Hamada Basin (after Conant and Goudarzi, 1967).

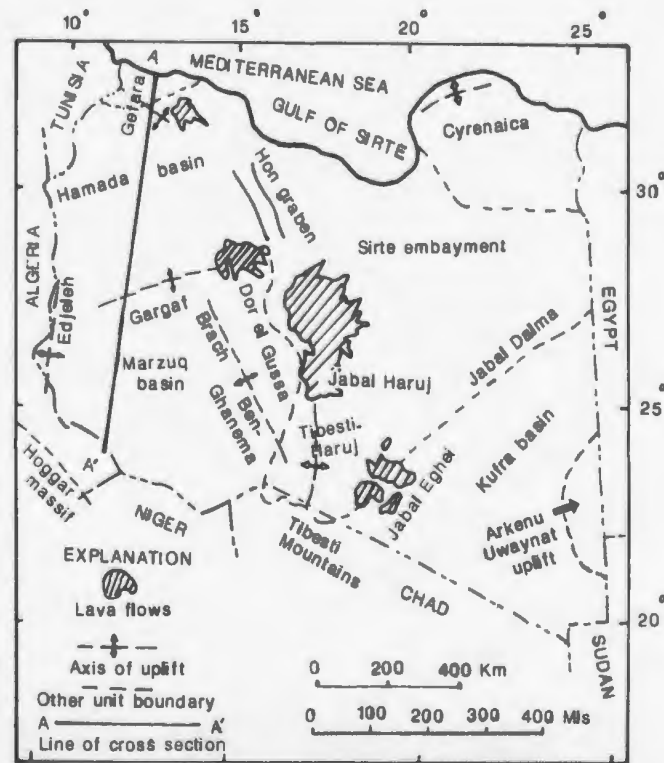
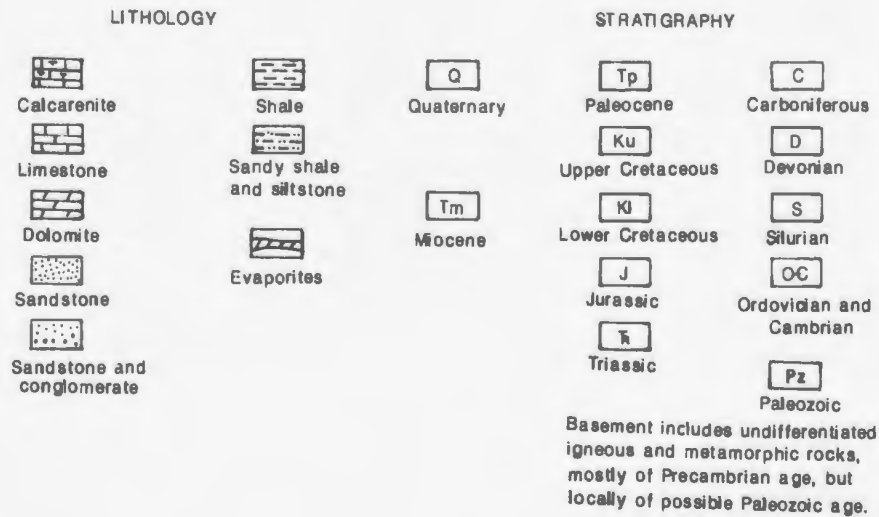
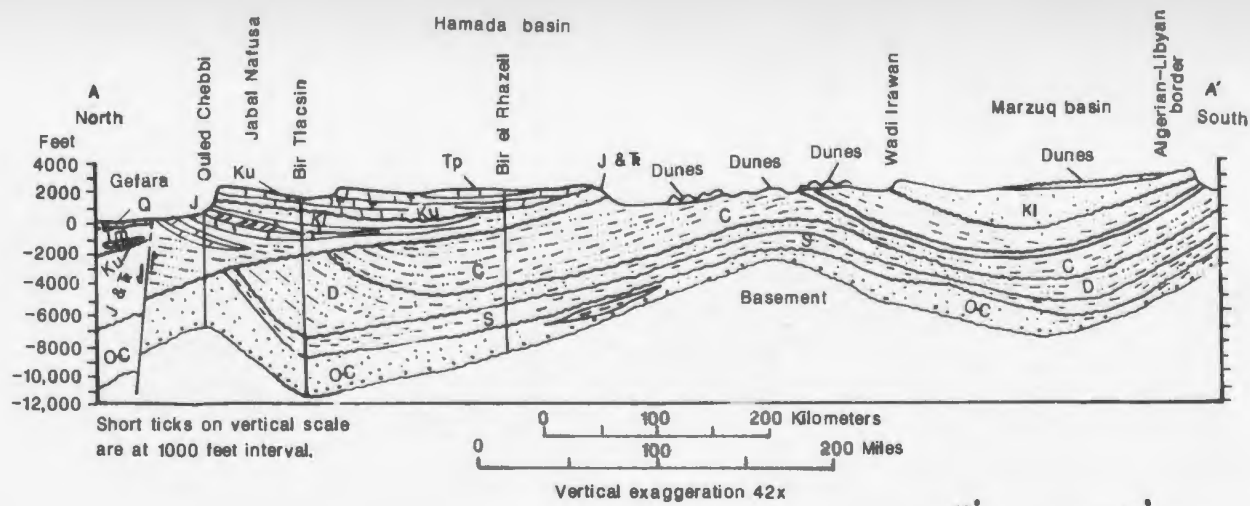


Figure 3. Location map of the study area (from
TDL, AGOCO, 1988).

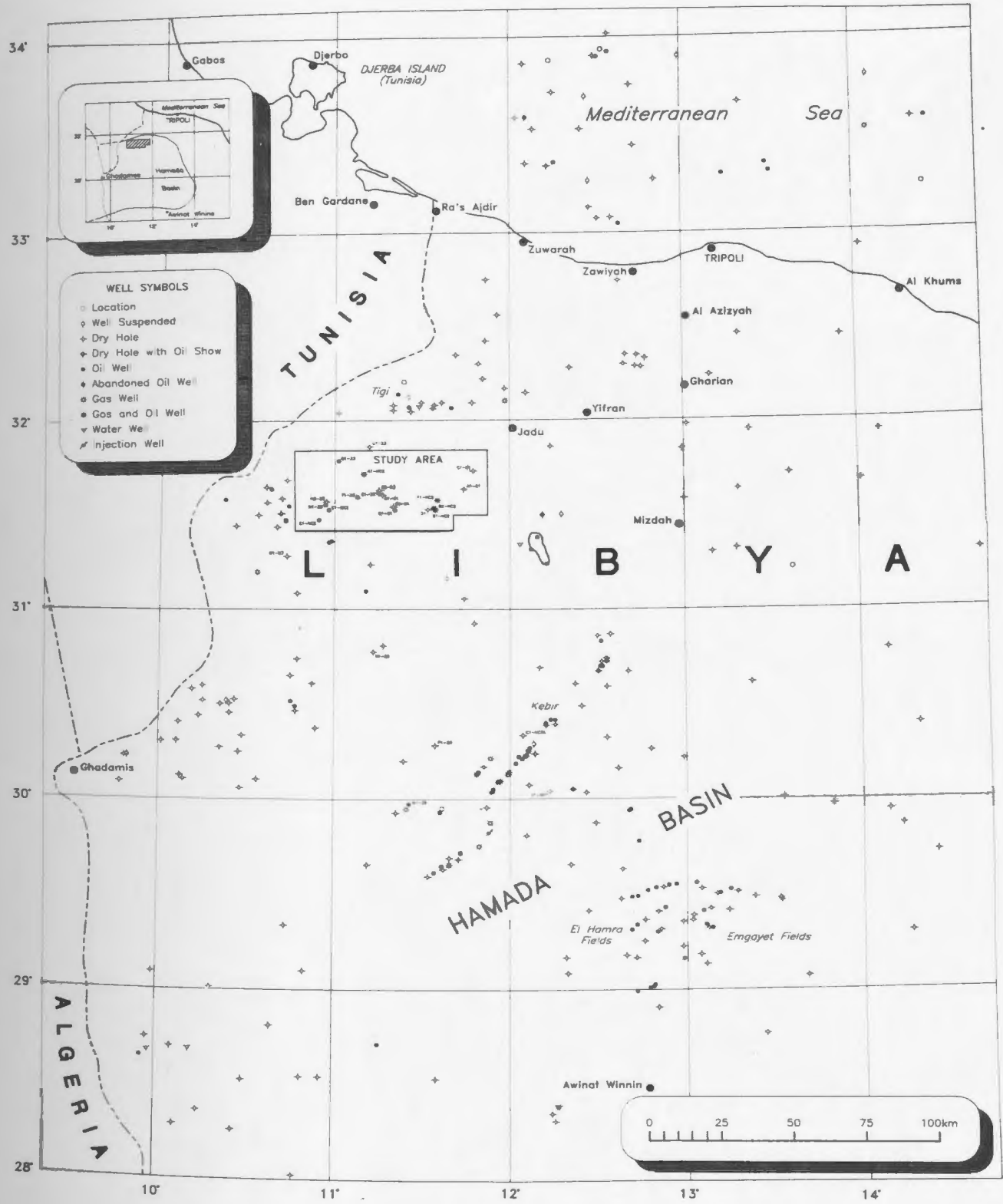
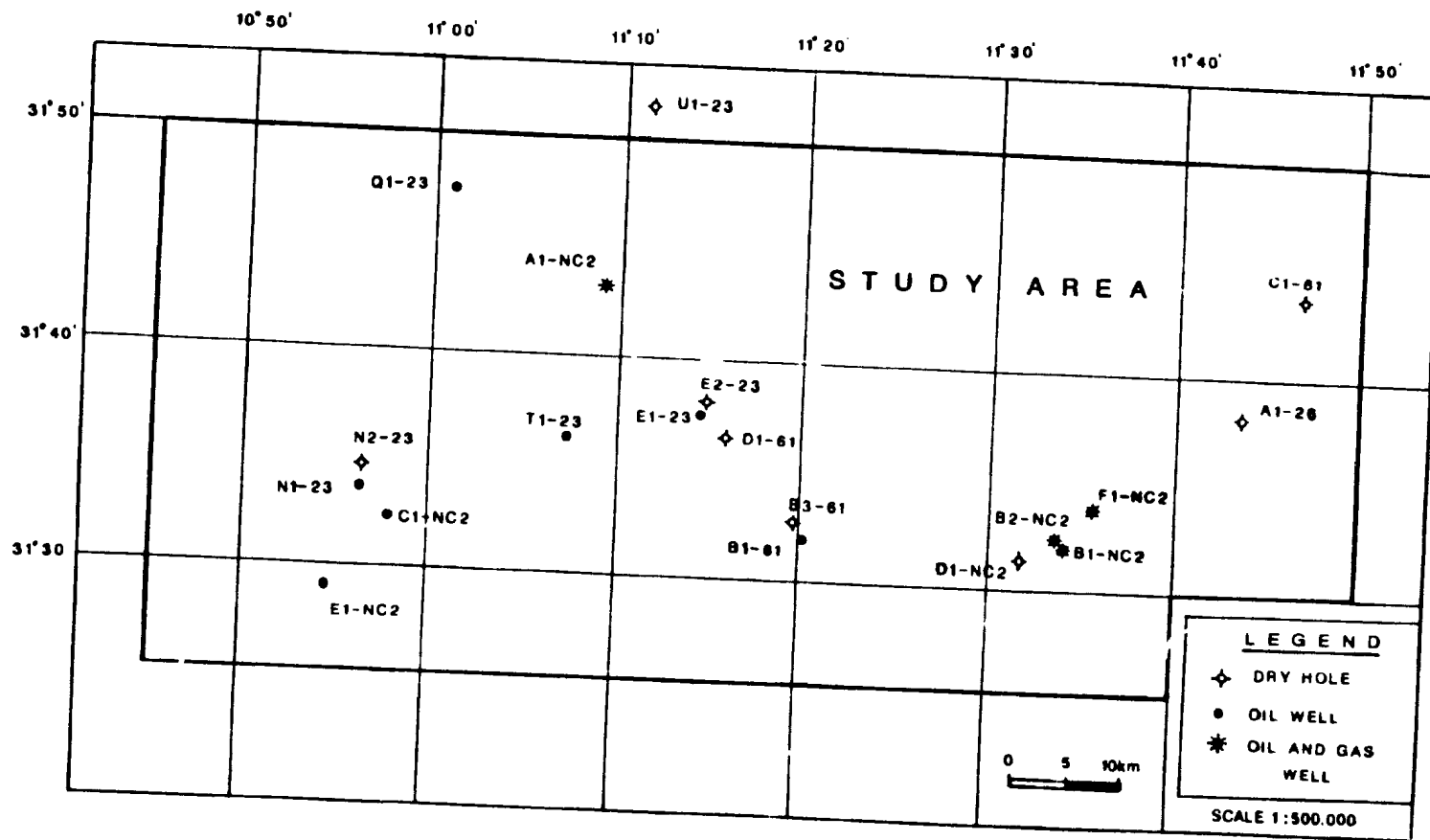


Figure 4. Location map of the study area defined by latitude and longitude (from the TDL, AGOCO, 1988).



geological formation, the history and entrapment of oil. Subsequently, the Arabian Gulf Oil Company has started exploration of the northern flank of the Hamada Basin (this present study area) and has already drilled seven wells. Hydrocarbons from various lenses in the Lower Acacus Sandstones have been encountered.

The Lower Acacus Formation (considered to be the main productive reservoir in the study area) is present at depths of 8500-9000 feet and has a thickness of about 1000-1510 feet.

Multiple sand lenses forming multiple pay-zones have been encountered in most of the drilled wells in this area.

Detailed sedimentological analysis of complex sandstones, such as those found in the Lower Acacus Formation, can contribute to the future exploration success of any reservoir sandstones in this formation. Also, variations in reservoir quality within the sandstones, due to either depositional or diagenetic processes, can be documented.

Since no study had been carried out for reservoir quality in this area, this present study was proposed to carry out the above tasks. The main goals of this study are to characterize these potential sandstones in terms of their depositional origin, and their important reservoir

quality variations from one area to another, and to predict the location and reservoir quality of all sandstones that may be penetrated on the basis of the geological conclusions for this study.

GENERAL GEOLOGY OF THE HAMADA BASIN
AND THE STUDY AREA

TECTONIC FRAMEWORK

Hamada Basin (Ghadames Basin) is situated in north-western Libya between:

Latitudes. 28° 37' N & 32° 18' N

Longitudes. 9° 00' E & 13° 30' E

It is bounded from the north by Gefara Arch, from the south by Gargaf Arch, from the east by Tripoli-Soda Arch, and from the west by Thampoka Arch (Fig. 5). The present shape of the Hamada Basin, as depicted in Figure 6 (N.O.C., Exploration Department, 1981), shows that it has a poly-genetic developmental history. The basin was formed as an interior sag basin, in the classification of Kingston et al. (1983), before the Hercynian epeirogeny. Subsequently, it took the form of a marginal sag basin and then, after the Cretaceous, it became an interior sag basin.

Therefore, the basin has characteristic depositional environments which resulted in the formation of source rock (the Silurian shale); also shallow marine and nonmarine conditions produced the presently observed widespread extent of sandstones and shales, forming reservoirs and seals (unpublished AGOCO Report, 1988). The basin contains a series of highs, some of them with NE-SW trend as in the eastern and the southeast part of the basin. Some highs

Figure 5. Tectonic map of Libya showing the basins and the structural elements of Hamada Basin (modified after Said F.M., 1974; Bellini E. and Massa D., 1978).

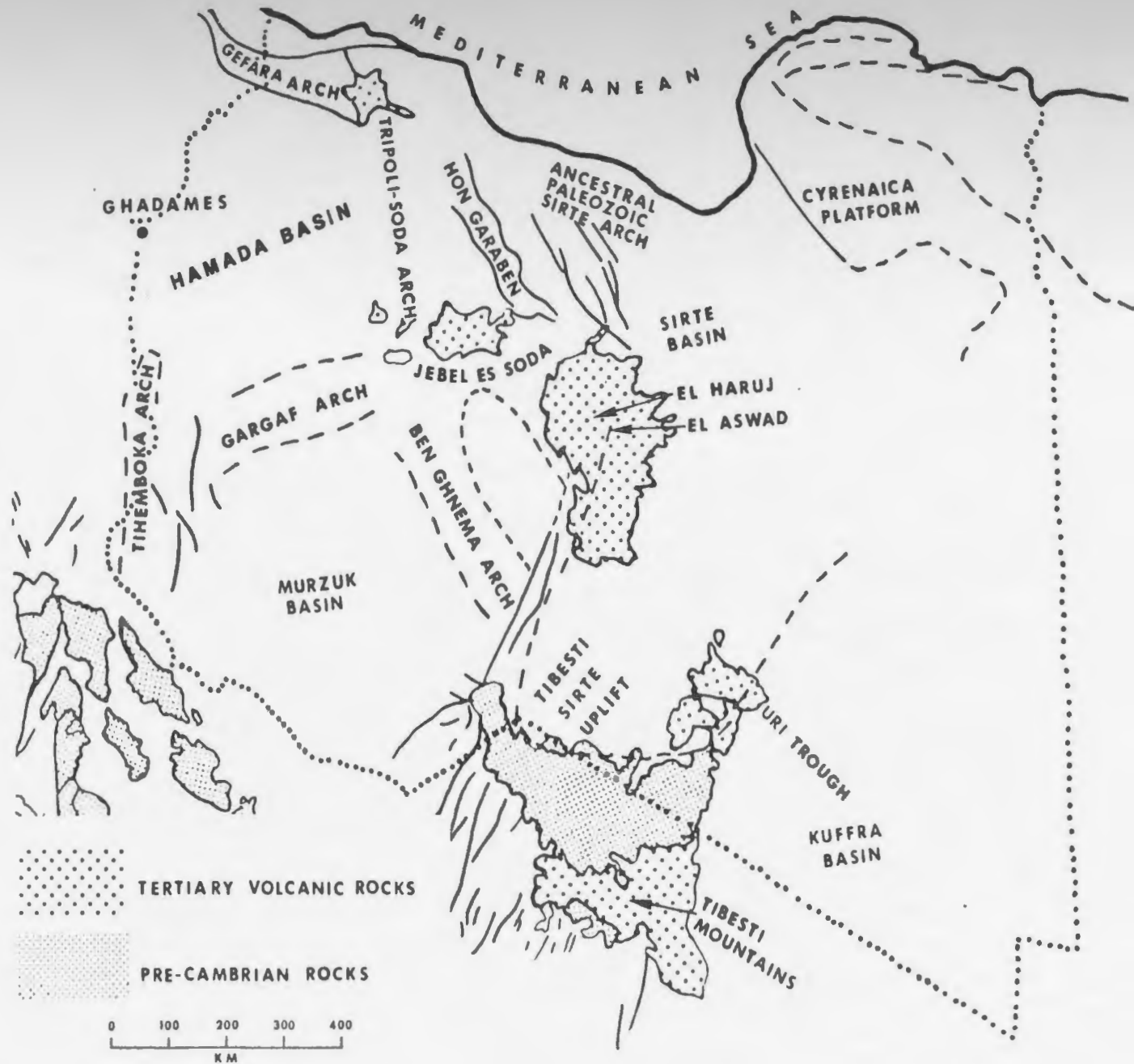


Figure 6. Regional structural cross section illustrating concept of stratigraphic and structural relations in the Hamada Basin, north-western Libya (after N.O.C. Exploration Department, 1981).
Cal. Unc.= Caledonian unconformity.
Her. Unc.= Hercynian unconformity.

NORTH
TRIPOLITANIA
RIDGE

HAMADA BASIN

GARGAF
UPLIFT

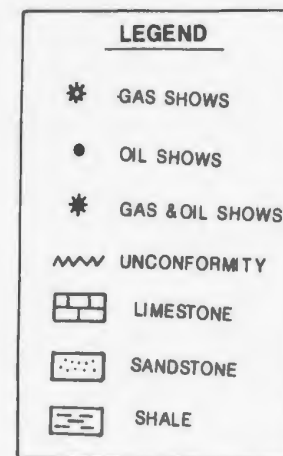
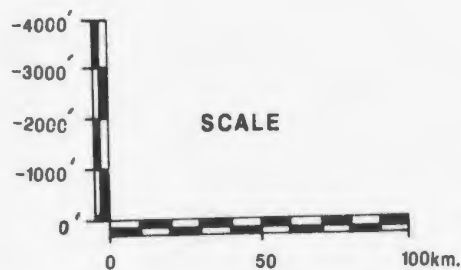
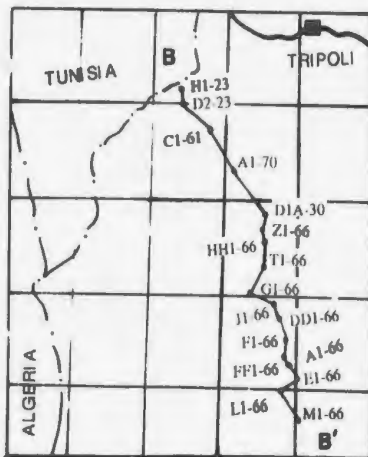
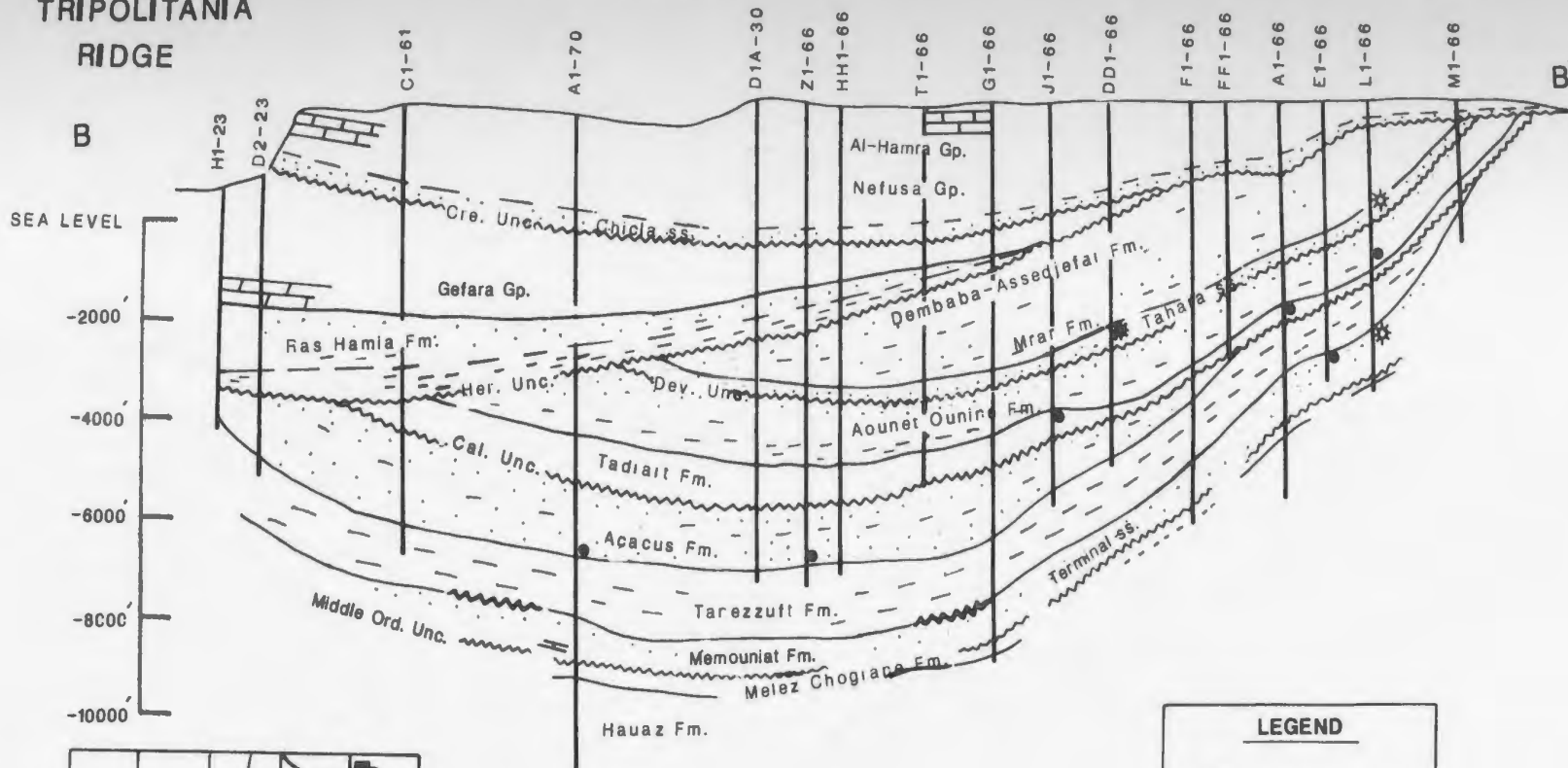
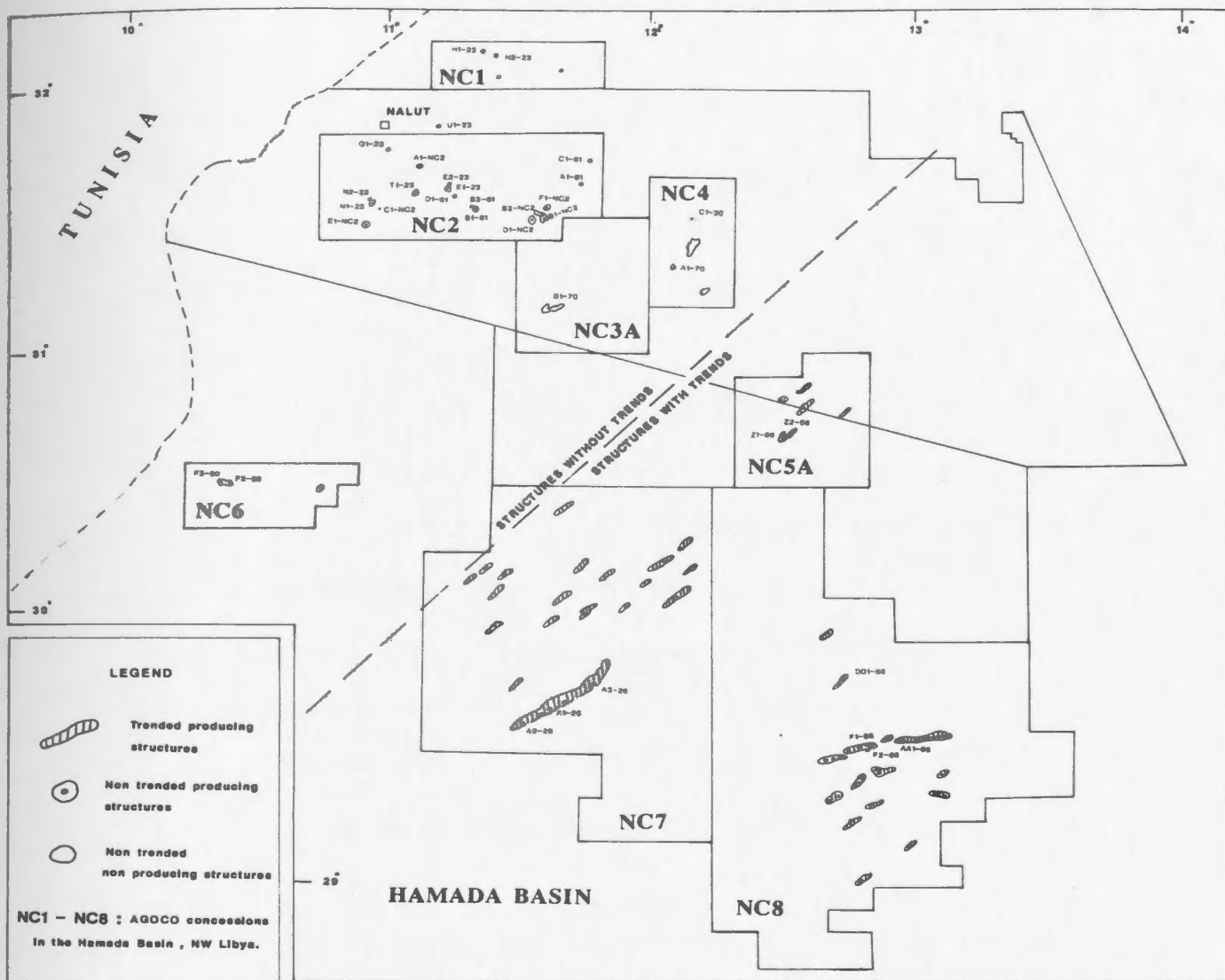


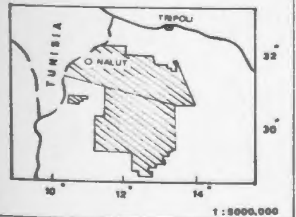
Figure 7. Type of structures in the Hamada Basin
north-western Libya (modified map, after
BEICIP, 1975, Western Libya Exploration
Study, National Oil Corporation).



LEGEND

- Trended producing structures
- Non trended producing structures
- Non trended non producing structures

NC1 - NC8 : AGOCO concessions
In the Hamada Basin, NW Libya.



Scale 1 : 1000,000

BEICIP - 1975
N.O.C. - LIBYA

are almost without a trend as in the northern flank of the basin (Fig. 7). These high areas "... may reflect the pre-Cambrian basement ridges and folds in the sedimentary cover.." (BEICIP, 1975 ; unpublished AGOCO Report, 1988).

The study area, being part of the larger Hamada Basin, reflects the clear influence of the basinal tectonic setting on the Paleozoic sequence.

During the Precambrian, the area experienced several strong orogenic movements, but the present configuration of the Paleozoic sediments "...is due to epeirogenic movements resulting in drape and differential compaction of this cover on the topography of the basement.." (unpublished AGOCO Report, 1988).

According to Klitzsch (1971), the structural elements during Early Paleozoic-Devonian time (Fig. 8) in Libya were generated as follows:

- 1- Precambrian rocks were exposed in Jabal Aouinet, Jabal Tibisti and Jabal Eghei and, in the subsurface, in Sirte Basin and Hamada Basin (Fig. 9). During Precambrian time, orogenic movements of Archean age (Goudarzi, 1970) caused fold-type structures, and sediments of unknown thickness were metamorphosed. The last Precambrian orogeny was followed by a long period of erosion.

- 2- Cambrian sediments overlie folded Precambrian rocks with unconformity. Sediments of Cambrian age

Figure 8. Structural relief during Early
Paleozoic and Devonian times
(after Klitzsch, 1971).

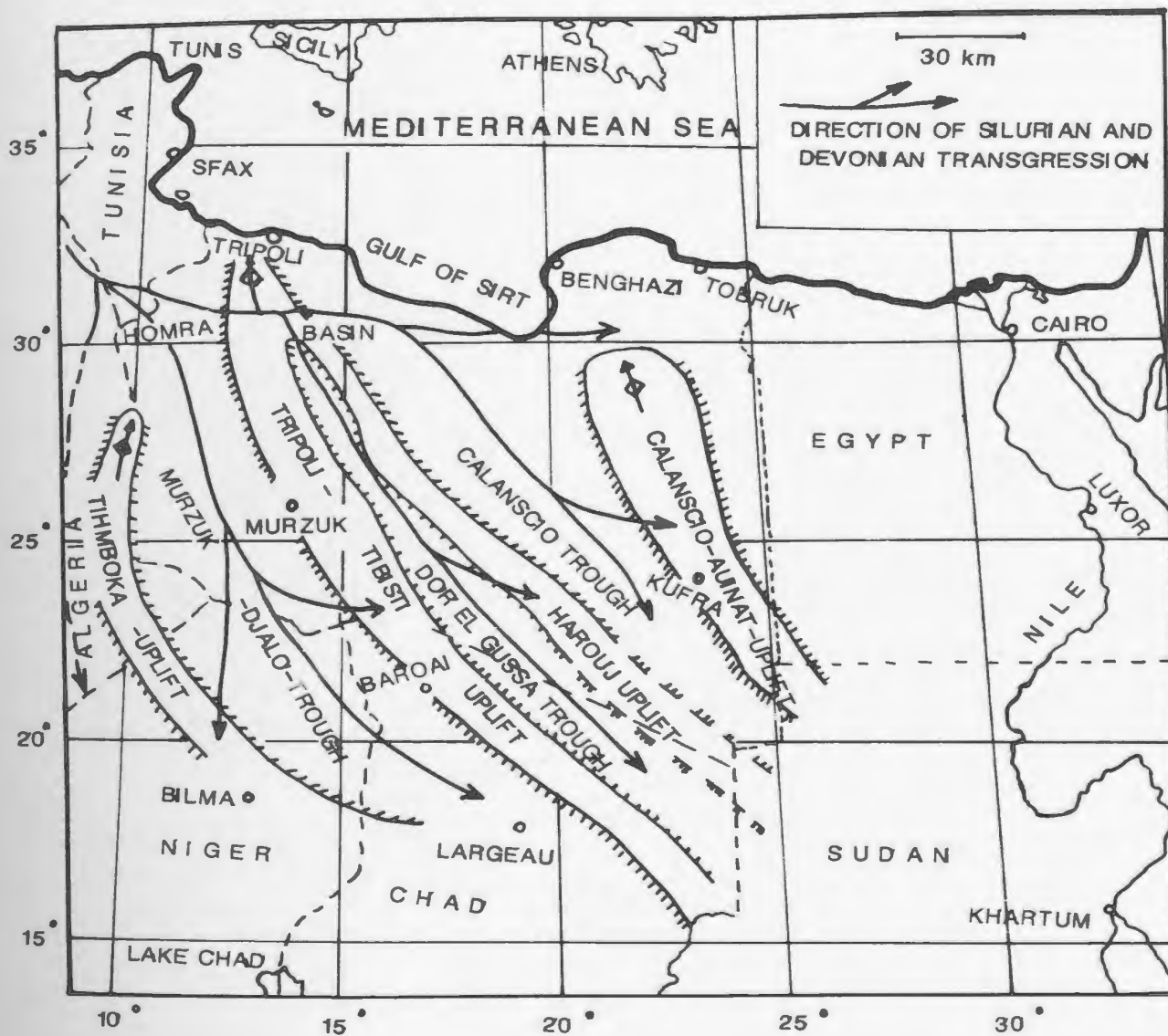
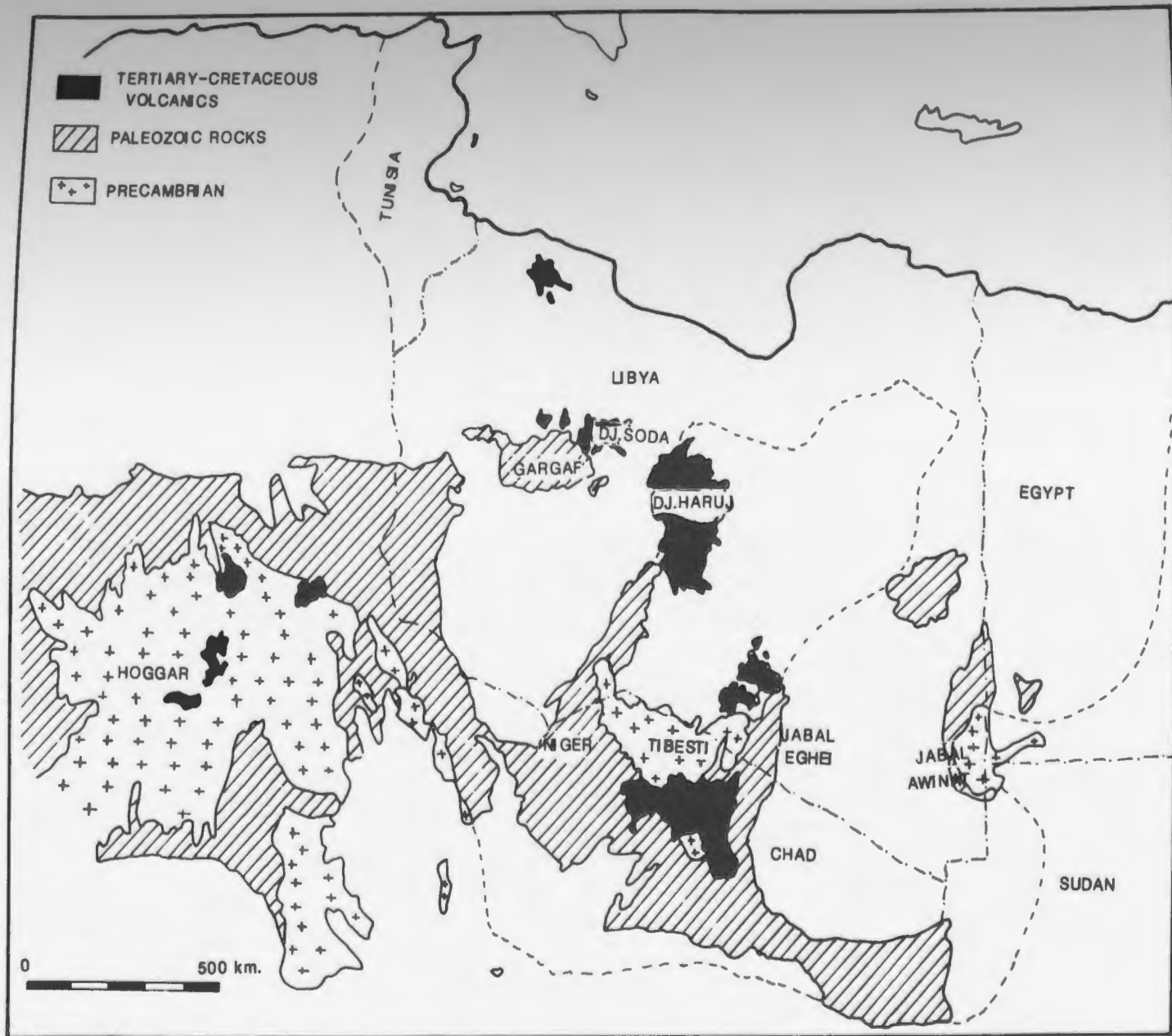


Figure 9. Area of the exposed Precambrian rocks
(adapted from Karasek R.M., 1981).



comprise the Hassauna Formation and are exclusively clastic; they consist of fine to coarse-grained and partly conglomeritic sandstones (Klitzsch, 1981), and have been interpreted to be of continental origin.

3- Structural relief during Early Paleozoic time trended NW-SE (Klitzsch, E., 1971). A series of troughs and uplifts were developed. The troughs are characterized by very thick intervals of Paleozoic sediments (Murzuk-Gialo Trough, Dor-Elgossa Trough and Calinscio Trough), whereas the uplifts are characterized by reduced deposition and increased erosion (Triboli-Tibisti Uplift, Haroudj Uplift and Calinscio-Aouinet Uplift) (Fig. 8). These uplifts are of great importance because their axial strike is the same as the axes of the Paleozoic transgressions (Klitzsch, 1981) which inundated large parts of the African craton and deposited Paleozoic sediments in the troughs.

4- Ordovician seas transgressed most of Libya after the early Caledonian movements, depositing fine grained sandstones (Haouaz Formation) and locally silty shale (Melez-Chograne Formation) (Klitzsch, 1981). During the Late Ordovician a partial retreat of Ordovician seas resulted in deposition of the Memouniat Formation. This Formation consists of "... fine grained, thick-bedded, partly ferruginous sandstones in the east of the Hamada

Basin.." (Collomb, 1962), homogeneous, cross-bedded, unfossiliferous sandstones in the middle part of the basin, and fine grained silty sandstones with shale beds of shallow marine origin in the western part of the Basin.

5- During Silurian times, the first major penetration of the sea in western Libya reached into Chad and Niger to the south (Louis C. Conant and Gus H. Goudarzi, 1967).

During the Early Silurian, subsidence of those NW-SE striking troughs lying between uplifts continued (Klitzsch, E., 1981). Within the troughs, thick graptolitic marine sediments of the Tanezzuft Formation were deposited, while on the uplifts only a thin sequence of sediments was deposited. During the Late Silurian, epeirogenic movements and reactivation of source areas afforded the influx of the Upper Silurian detrital sediments; thereby forming the Acacus Formation. Active detrital input, "... balanced by continued rises in sea level, allowed the persistent basinward progradation of the depositional system in the Hamada Basin (NW) and in the Murzuk Basin (SW).." (Karasek, 1981).

STRATIGRAPHY

Stratigraphic Remarks

Stratigraphic terminology used in this thesis corresponds to that used in Libya because at this stage of geologic investigation in the Hamada Basin it is important that local workers understand and appreciate the information and interpretations presented. This terminology, in the context of the international stratigraphic code, is a mix of formal and informal terms in both formal and informal mode. However it is the terminology understood by the workers in this frontier geologic region. This present study lays the basis for future regional formalization of both surface and subsurface terms, and for correspondence to the stratigraphic code.

Generally, the Paleozoic sedimentary record from Cambrian to Carboniferous of the Hamada Basin (Fig. 10) is characterized by four major regional unconformities that may be related to the rapid fluctuation of part of the craton with respect to sea level (Sloss, L.L., 1974). The timing of the unconformities represented are:

Middle Ordovician, Late Silurian-Early Devonian,
Late Devonian-Early Carboniferous, and Late
Carboniferous-Early Permian.

This present study deals with the stratigraphy of the Lower Paleozoic Silurian section. This sedimentary interval is bounded by regional unconformities of Middle Ordovician below and Late Silurian-Early Devonian age above. The sedimentary sequence in the Silurian interval is defined as a major sedimentary cycle deposited during one tectonic phase (Fig. 6, p. 10), and having three stages representing the three elements of one major transgressive-regressive cycle (White, David A., 1980). The first stage corresponds to nonmarine to shallow marine deposits forming the basal transgressive sandstones of Memouniat Formation. The second stage is the marine transgression and the formation of Tanezzuft shale, and the third stage is the regressive part of the cycle represented by the Acacus Sandstones. This thesis concentrates on the lower part of the third stage of the cycle (Lower Acacus Formation) (Fig. 10).

Stratigraphic data in this study have been obtained as a result of the petroleum exploration which has occurred in the study area (NC2 Concession; northern flank of the Hamada Basin).

Exploration in this area has been confined to date to that interval of section between the Upper Memouniat Formation of Cambro-Ordovician age and the Upper Acacus Formation of Late Silurian age.

Figure 10. General Paleozoic stratigraphic framework
for the Hamada Basin, NW Libya.

Memouniat Formation (Cambro-Ordovician)

The term Memouniat was introduced by Massa and Collomb (1960) after Jabal Memouniat (27° 45' N: 13° 00' E) (Fig. 11) in the western part of Jabal Gargaf (Banerjee, 1980).

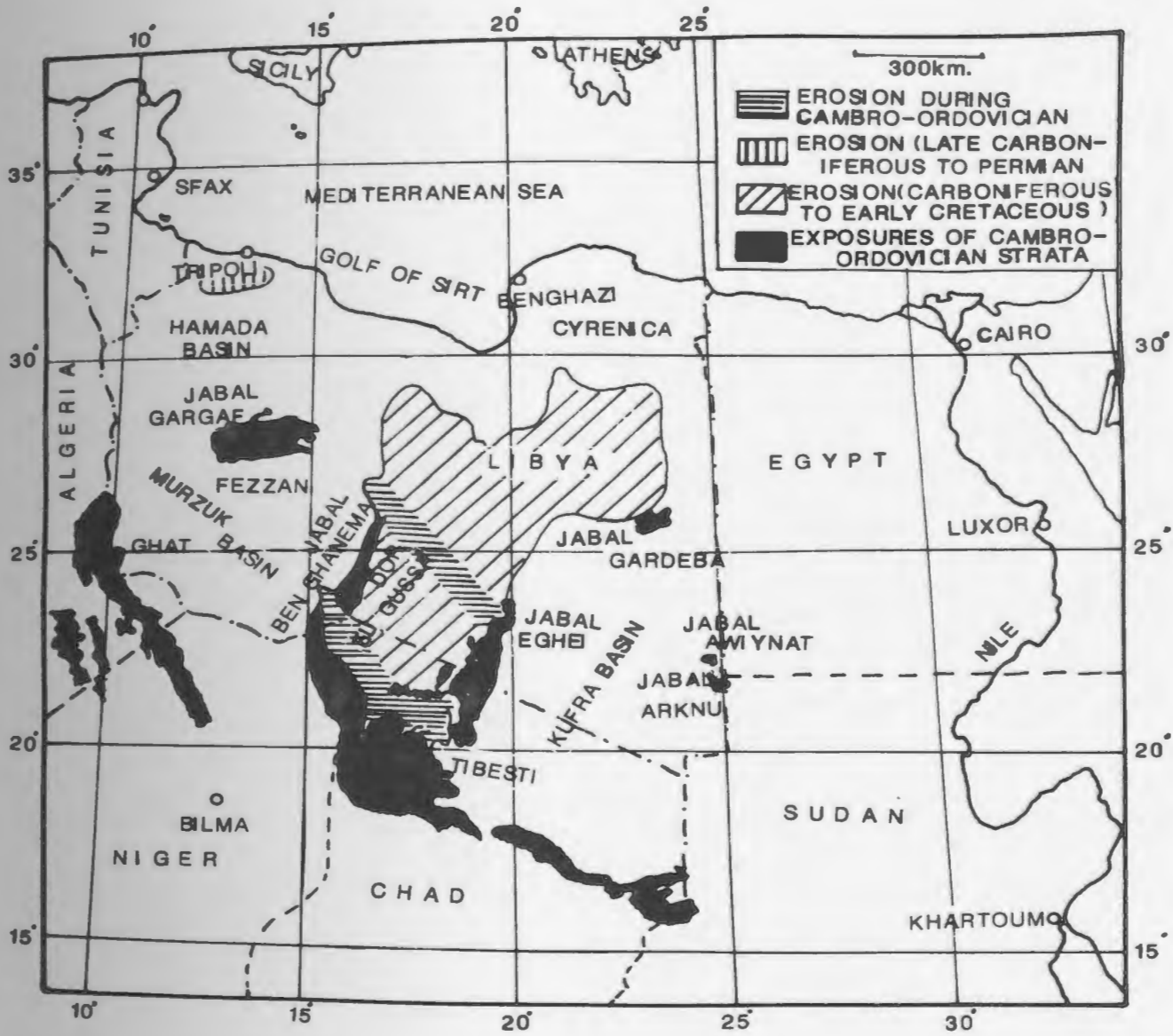
Regionally, the formation is exposed at the southern edge of the Hamada Basin at Jabal Gargaf (Klitzsch, E., 1981,), in Ghat area to the southwest, in Jabal Ben Ghanema (Dor-ElGussa area) in Fazzan, Jabal Eghei to the south, and Jabal al Awynat and Jabal Arknu area in southern Cyrenica (Fig. 12). Thickness of the Memouniat Formation is generally 328 feet (100 m) to 549 feet (140 m) in the type locality (Jabal Memouniat area), "... thinning in the SSE to about 98 feet (30 m) in the Dor-ElGussa area.." (Banerjee, 1980). Its thickness, as recorded in the E1-23 well is 610 feet (186 m).

Within the western part of Libya and especially in the Jabal Gargaf area, the Memouniat Formation consists of "...fine grained to silty sandstone with clayey and ferruginous matrix and with shale beds.." (AGOCO, unpublished report). In these beds, "... well-preserved brachiopods and pelecypods were found.." (Collomb, 1962; Banerjee, 1980).

The lower boundary of the Memouniat Formation is unconformable with the older Formations and the upper

Figure 11. Geological map showing type areas of
Cambro-Ordovician Memouniat Sandstone at
Jabal Gargaf (modified, after Collomb,
1962; Vos, 1981b).

Figure 12. Distribution of Cambro-Ordovician
strata (after Klitzsch, 1970).



boundary is unconformable with the Silurian Tanezzuft Formation (Klitzsch, 1966; Banerjee, 1980).

In the study area, subsurface information indicates that a sandstone band ranging in thickness from 20 to 45 feet (6 to 13.7 m) is found in the top part of this Formation. This band is known as the Terminal sandstone and is found throughout the NC2 Concession, Hamada Basin (AGOCO, unpublished report).

According to unpublished AGOCO reports, the Memouniat Formation consists of light brown, fine to very fine grained sandstone, subrounded, occasionally pyritic. The lower part of the Memouniat Formation below the Terminal Sandstone consists of alternations of sandstones, siltstone and shale.

Tanezzuft Formation (Lower Silurian)

The term Tanezzuft was formally introduced by Desio (1936) after Wadi Tanezzuft, about 65 km northeast of Ghat from where the type section (25° 00' N: 10° 10' E) was described (Banerjee, 1980).

According to Klitzsch (1969) (Fig. 13), the type locality is at the southern part of Wadi Tanezzuft in southwestern Fazzan (Klitzsch, 1981). The Formation is also exposed at the southern edge of the Hamada Basin

(Fig. 14) "...in the area of Jabal Gargaf, along the western and eastern flanks of the Murzuk Basin extending into Algeria, Niger and Chad, and in some areas surrounding the Kufra Basin.." (Klitzsch, 1981; Klitzsch, 1970), "... and in northern Dor-ElGussa in central Libya.." (Klitzsch, 1970; Collomb, 1962; Banerjee, 1980).

The subsurface distribution of the Tanezzuft Formation (Fig. 14) "... is limited to the Hamada Basin in the northwestern Libya, the major part of the Murzuk Basin in southwestern Libya, the Kufra Basin in southeastern Libya and Western Desert Basin in northeastern Libya.." Klitzsch, 1981). The thickness of the Formation, "... reached a maximum of 1558 feet (475 m) south of Ghat, 1319 feet (402 m) in Klitzsch's type section, about 1115 feet (340 m) on the western flank of Murzuk Basin, and 525 feet (160 m) thick in Dor-ElGussa area, finally wedging out southward.." (Banerjee, 1980; Klitzsch, 1966).

Klitzsch (1969-1970) described the Tanezzuft Formation as graptolitic grey marine shale. The Formation is silty with sandstone lenses and some thin sandstone beds in the lower part, and unconformably overlies the Cambro-Ordovician units. The upper boundary is gradational and conformable with the Acacus Sandstone (Banerjee, 1980).

In the study area (NC2 Concession), and from deep drilled wells, the Tanezzuft Formation consists of thick

Figure 13. Map showing the type locality of the
Silurian-Devonian sections:

- (1) Tanezzuft Shale
- (2) Lower Acacus Sandstone
- (3) Upper Acacus Sandstone
- (4) Top Acacus Sandstone and Tadrart
Sandstone

(after Klitzsch, 1969)

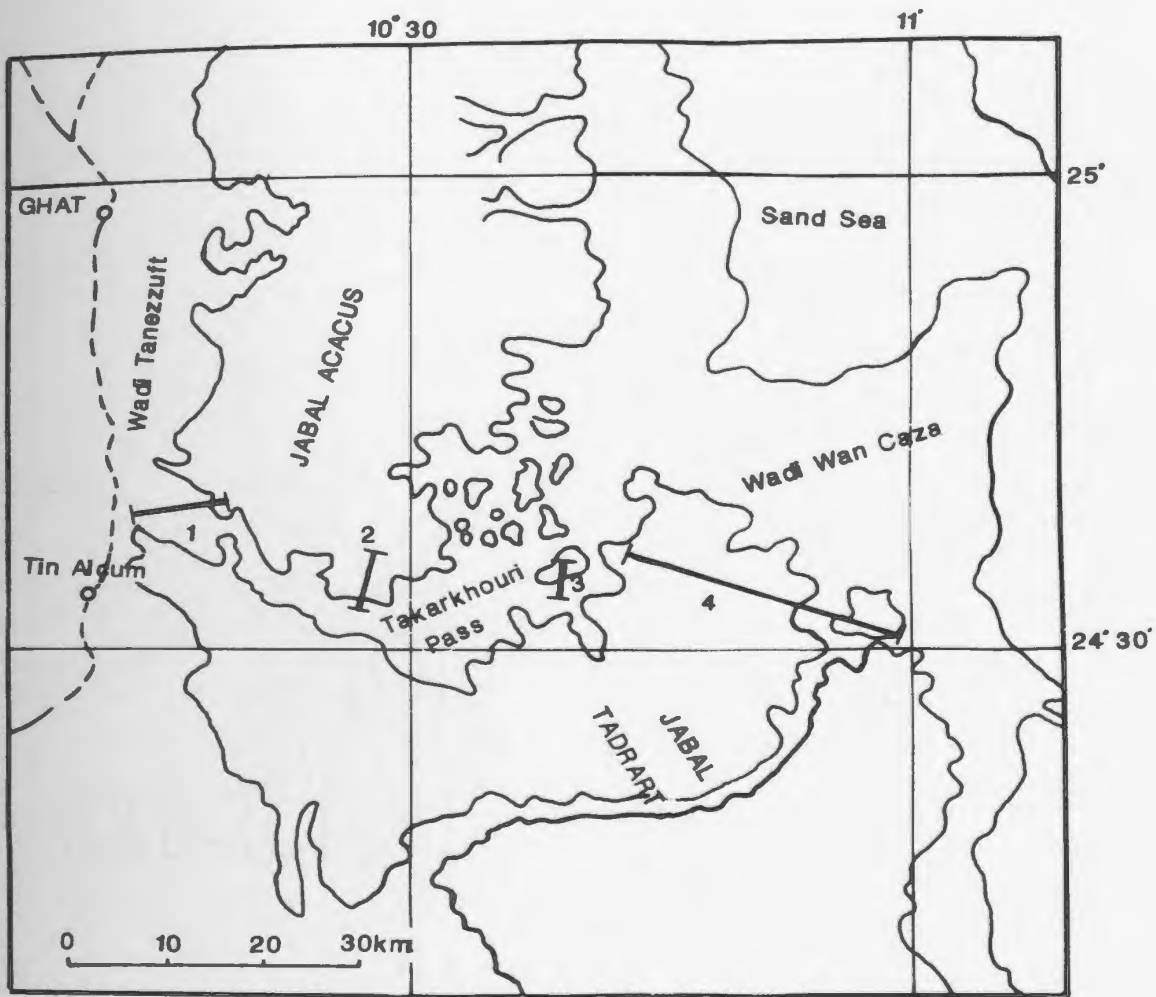
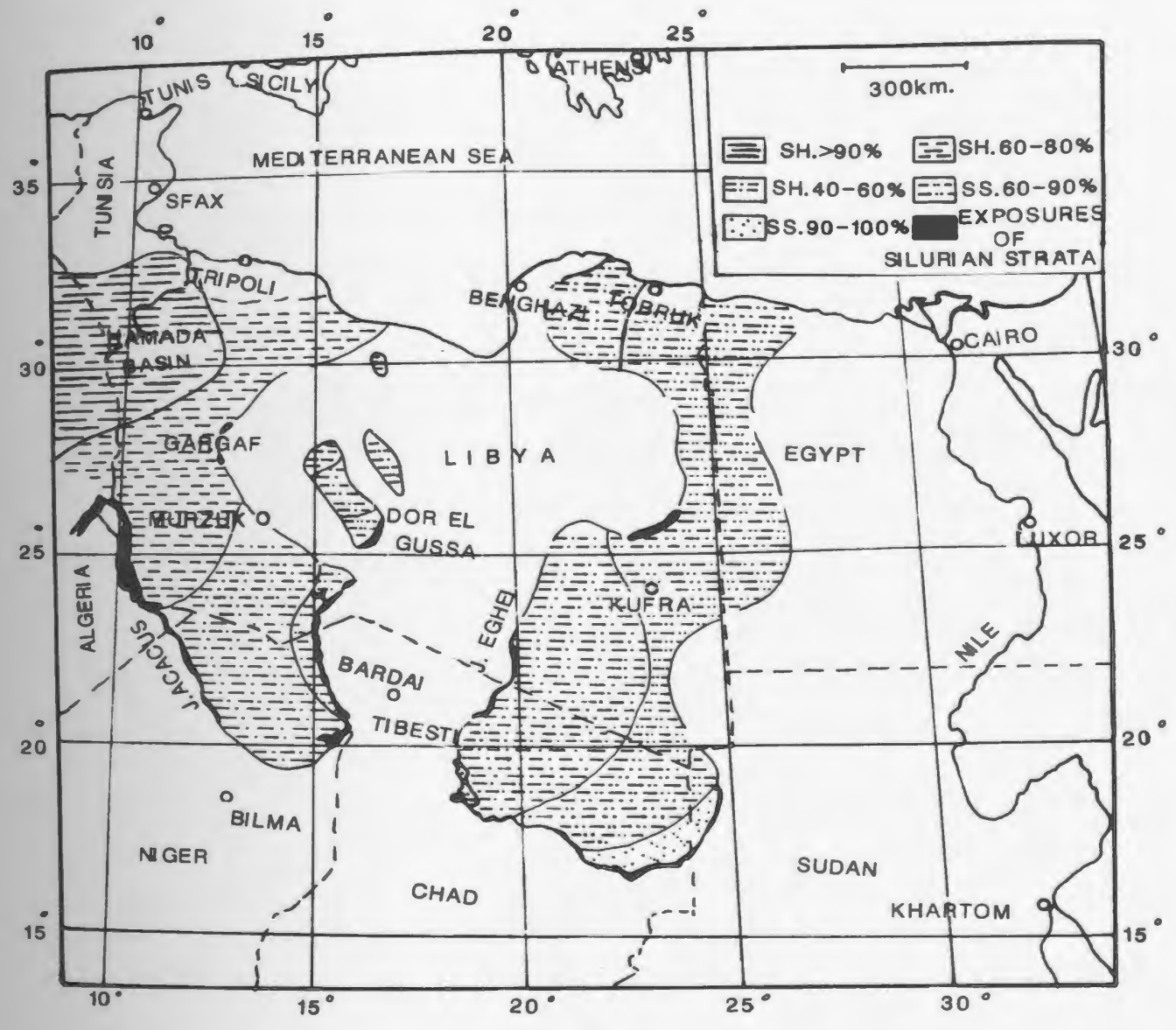


Figure 14. Distribution of Silurian (Tanezzuft-
Acacus) strata (after Klitzsch, 1970).



graptolitic shales attaining a thickness of about 1280 feet (390 m) (Fig. 15), and reflects basin deepening to the northwest in the vicinity of Well Q1-23, which is "... the direction of major Silurian transgression..." (Bishop, 1975). The shales are dark grey, micaceous, fissile, and in places are interbedded with siltstone and thin beds of sandstone (unpublished AGOCO Reports).

The Tanezzuft shale extends over the whole area of the Hamada Basin and constitutes a good seal for the Terminal sandstone reservoirs of the Memouniat Formation. These shales are believed to be the "... major source rock of Saharan oil..." (Bishop, 1975), are also the main source rock of the Hamada Basin (BEICIP, 1971; unpublished AGOCO reports).

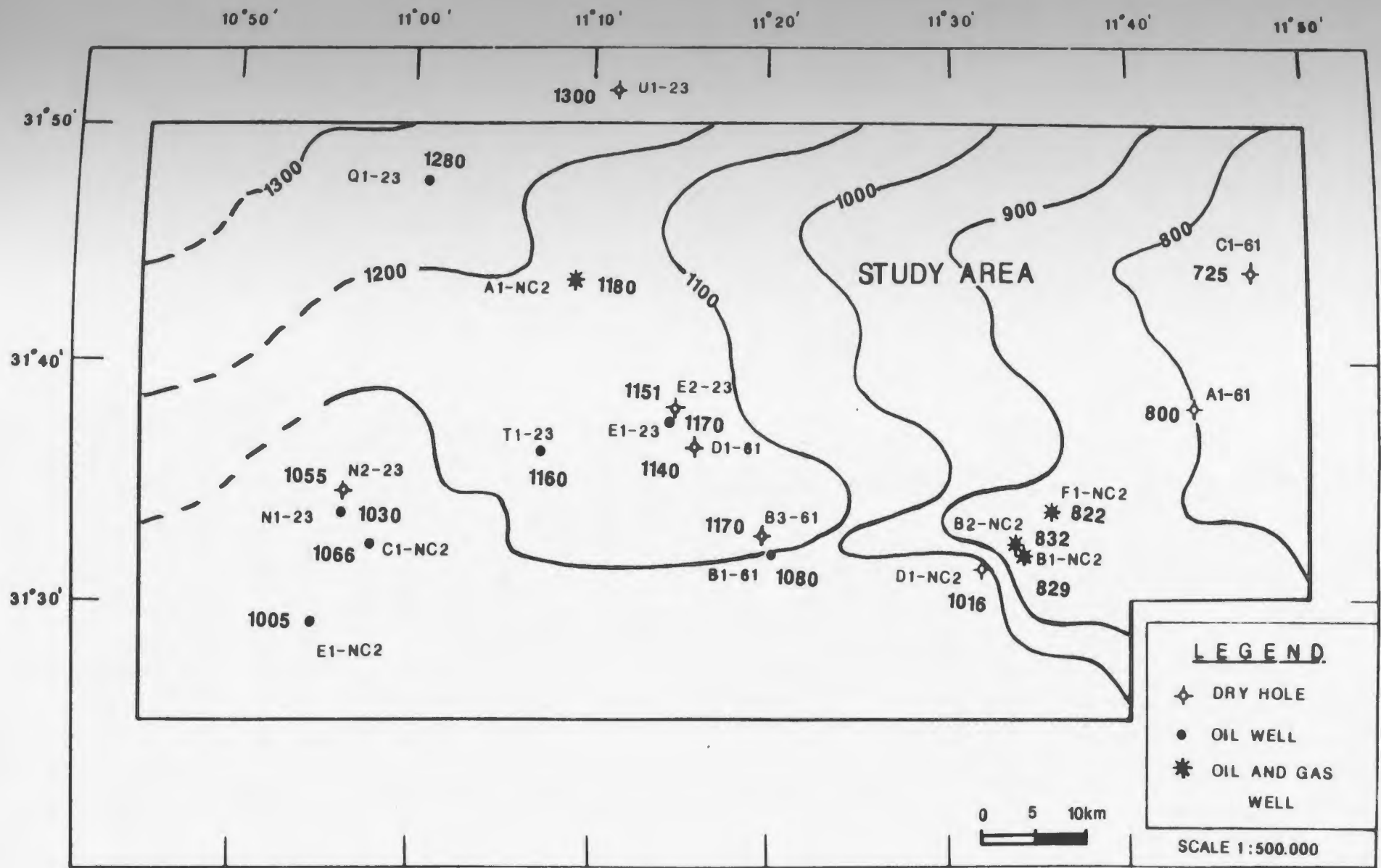
Acacus Formation (Upper Silurian)

The term was introduced by Desio (1936a) after Jabal Acacus in the Ghat (24° 54' N: 10° 12' E) area, southwest Libya (Banerjee, 1980).

Its first description by Desio (1936a) referred to outcrops in the area of Wadi Tanezzuft (24° 38' N: 10° 27' E) wherefrom Klitzsch (1965-1969) described his type section (Fig. 13).

According to Klitzsch (1969), the approximate exposed section of Acacus Formation is about 1132 feet (345 m.) white, grey and brown, mainly fine grained sandstone, thin

Figure 15. Isopach map of Tanezzuft Formation,
NC2 concession, Hamada Basin, NW Libya
(C.I. = 100 feet).



OBE-91

Isopach map of the Tanezzuft Formation, NC2 concession, Hamada Basin, NW Libya. (C.I 100 feet).

to thick-bedded, with clean sandstone near the top and shale beds in the lower part. Frequent trace fossils, which occur on thin-bedded sandstone bedding planes, indicate shallow water deposition (Banerjee, 1980). The Acacus Formation west of the Jabal Al Haruj al Aswad consists chiefly of sandstone with minor siltstone interbeds (Goudarzi, 1970).

The maximum thickness of the Acacus Formation is about 1525 feet (465 m) in the north Dor-ElGussa. Its outcrop (Fig. 14) in the Ghat area extends along Jabal Acacus to about 25° 38' N (Klitzsch, 1981), at the eastern edge of Murzuk Basin. It is also exposed at the southern edge of the Hamada Basin in the northern flank of Jabal Gargaf, while it is missing at the southern flank of Jabal Gargaf (Klitzsch, 1963; Banerjee, 1980), and in the environment of the Kufra Basin (Klitzsch, 1981).

The lower boundary with the Tanezzuft Formation is not clearcut, always being gradational (Bellini and Massa, 1978). The upper boundary with the overlying Tadrart Sandstone is "... erosive and discordant.." (Banerjee, 1980).

Subsurface distribution (Fig. 14) of the Acacus Formation is limited to the Hamada Basin in northwestern Libya, to the Murzuk Basin southwestern Libya, to the Kufra Basin in southeastern Libya and to the Western Desert Basin in northeastern Libya (Klitzsch, 1970; Klitzsch, 1981).

In the study area, from subsurface information, the Acacus Formation is predominantly sandy/silty formation (unpublished AGOCO Report). According to BEICIP (1973), the Acacus Formation can be divided into three main parts: Acacus A, Acacus B and Acacus C, or Lower Acacus, Middle Acacus and Upper Acacus, respectively.

This division has been based on the lithologic differences between the parts. The Lower and Upper Acacus are predominantly sandstones. The Middle Acacus is dominantly shales. The Lower and Upper Acacus are generally separated by a thick interval of about 300 to 400 feet (91 to 122 m) of mainly silty shale beds, namely the Middle Acacus Formation, which are easily picked up on well logs.

Lower Acacus:

The Lower Acacus is composed predominantly of sandstones, which are fine to medium grained, poor to moderately sorted with kaolinitic cement, with occasional feldspar grains, and with some shale alternations (unpublished AGOCO Report), and is characterized by coarsening-upward sandstone sequences on gamma ray logs.

The Lower Acacus is the main hydrocarbon productive unit in the study area, in which most the

sandstone units are potentially productive. The total thickness of this unit ranges from 700 to 1655 feet (213 to 505 m) in the study area (Fig. 16).

Middle Acacus:

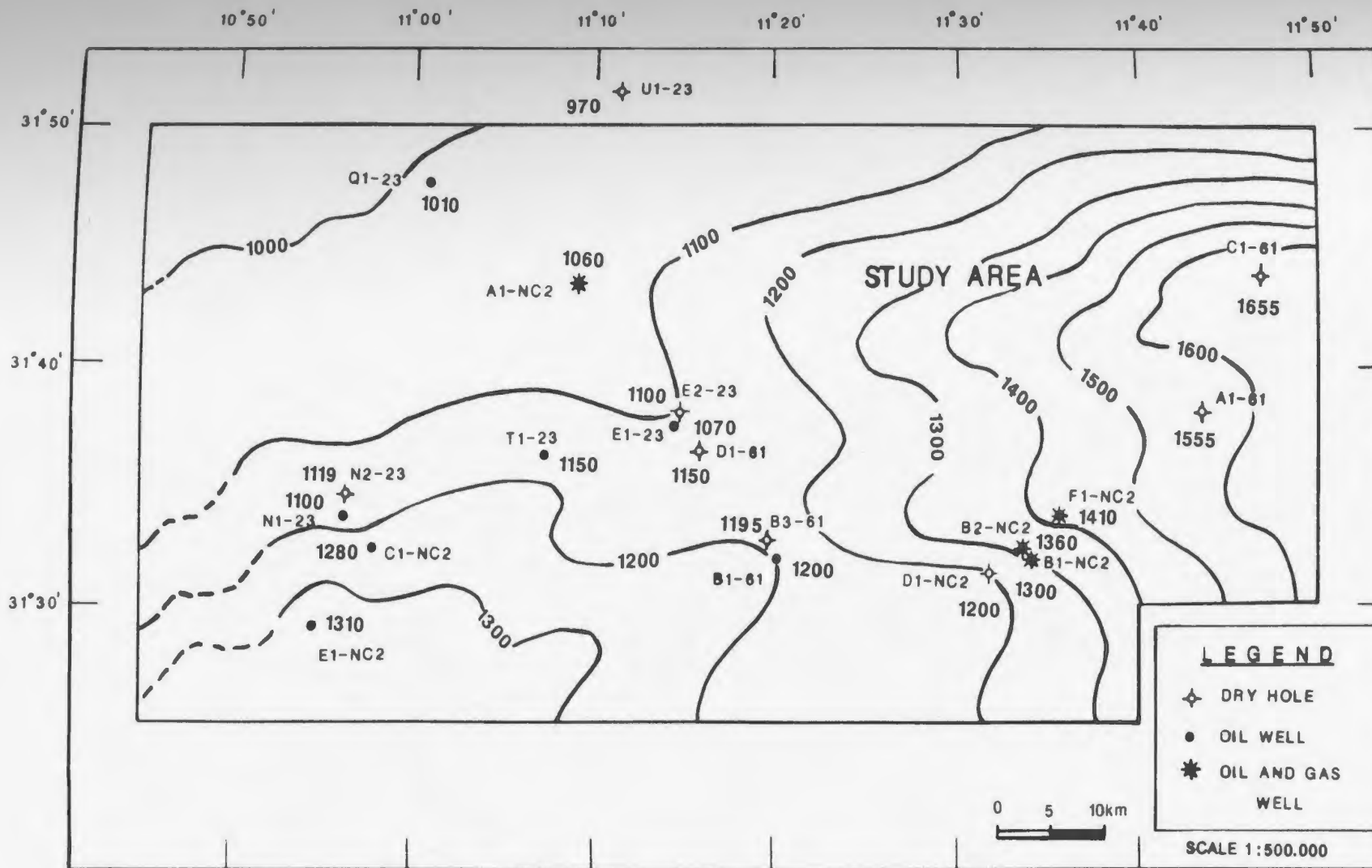
The Middle Acacus interval is predominantly a silty shale unit in which the shale is grey, green, firm to brittle, subfissile, occasionally micaceous, noncalcareous, pyritic interbedded with some sandstone lenses (daily AGOCO Wellsite reports). Its thickness ranges from 300 to 400 feet (91 to 122 m) in the study area (Fig. 17).

Upper Acacus:

The Upper Acacus consists mainly of white, light grey, occasionally brown sandstone, fine to very fine grained, moderately sorted sandstone with kaolinitic cement, characterized by the frequent occurrence of ferruginous sandstone at top. These sandstones are interbedded with grey to dark grey, firm, subfissile, silty, noncalcareous shale (daily AGOCO Wellsite reports). These fluvial channel sandstones are recorded as fining-upward sequences and blocky log response on gamma ray logs. The thickness of this unit is about 375 to 980 feet (114 to 299 m) in the

study area (Fig. 18), with a trend of thickening to the north-northwest.

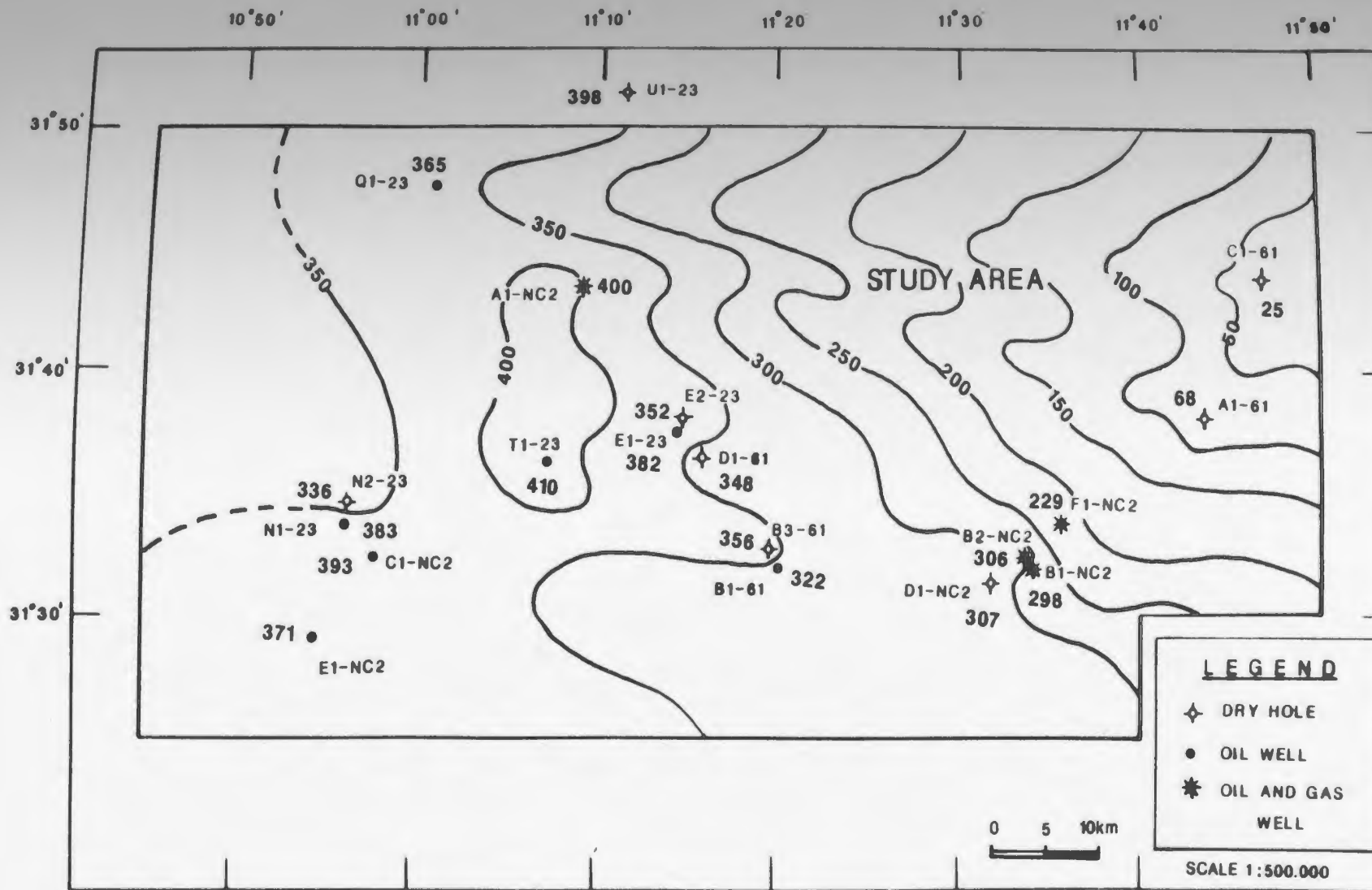
Figure 16. Isopach map of the Lower Acacus
Formation, NC2 concession, Hamada Basin,
NW Libya (C.I. = 100 feet).



OBE-91

Isopach map of the Lower Acacus Formation, NC2 concession, Hamada Basin, NW Libya. (C.I 100 feet).

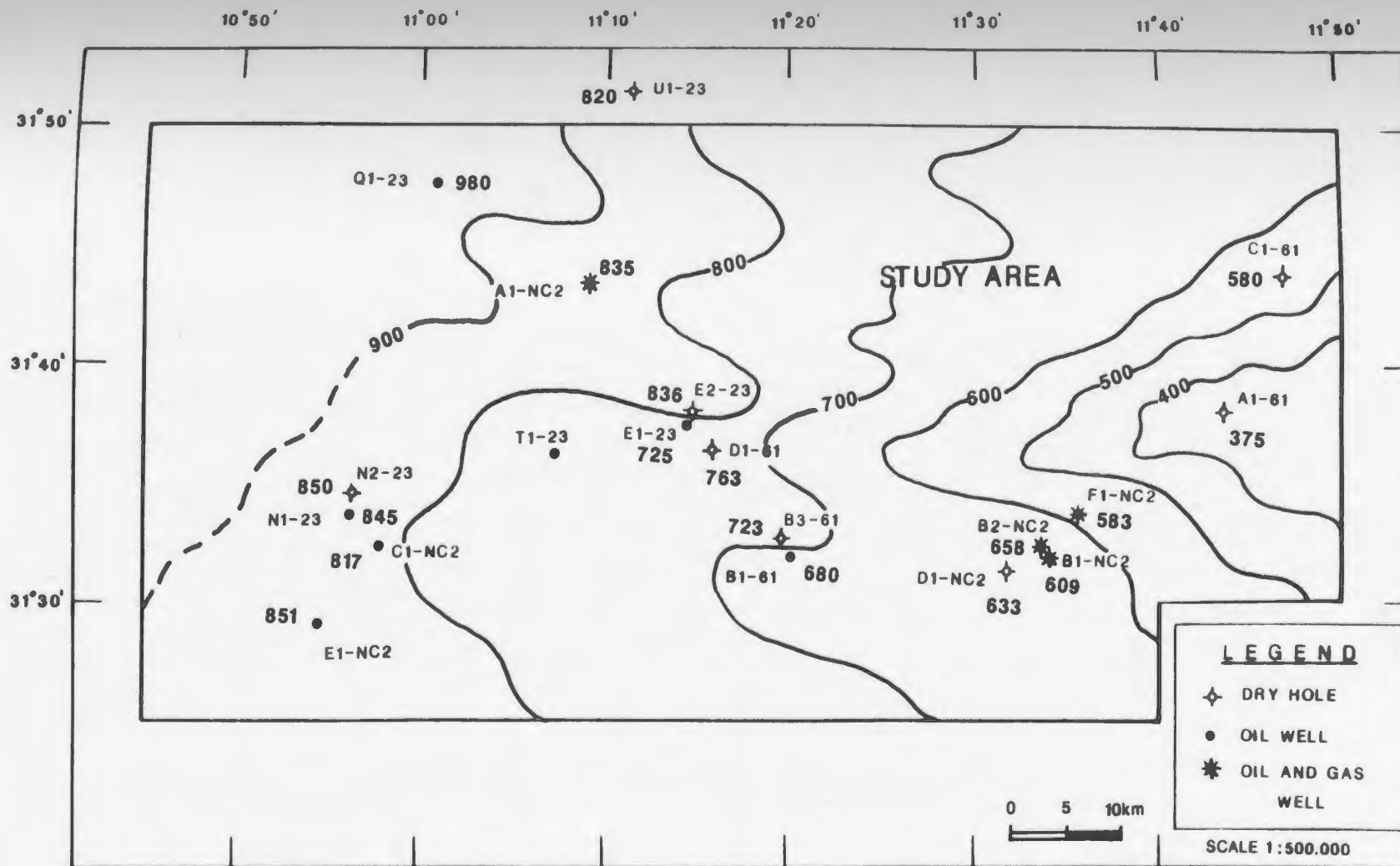
Figure 17. Isopach map of the Middle Acacus
Formation, NC2 concession, Hamada Basin,
NW Libya (C.I. = 50 feet).



OBE-91

Isopach map of the Middle Acacus Formation, NC2 concession, Hamada Basin, NW Libya. (C.I 50 feet).

Figure 18. Isopach map of the Upper Acacus
Formation, NC2 concession, Hamada Basin,
NW Libya (C.I. = 100 feet).



OBE-91

Isopach map of the Upper Acacus Formation, NC2 concession, Hamada Basin, NW Libya. (C.I 100 feet).

DATA BASE AND METHODOLOGY

Data Base

The available subsurface geological data are basic spontaneous potential logs, gamma ray logs, and sonic logs (TDL, AGOCO) recorded for most the 18 wells drilled in the study area (NC2 concession, northern flank of the Hamada Basin), and for a few other wells from outside the study area. In addition, neutron-density logs where available, have been included (see Appendix for list of wells and data types). Some 1230 feet (375 m) of core were cut in 10 wells at different stratigraphic levels in the Lower Acacus Sandstones. Some 170 petrographic thin sections, from different intervals in Lower Acacus Sandstones were prepared for this study by AGOCO Lab Technicians (December 1990). A number of 45 sample plugs were cut in some sandstone intervals in the 10 cored wells, prepared and analysed by Core-Lab AGOCO-Benghazi for porosity-permeability. Logs of the hydrocarbon shows, in addition to well-test results (TDL, AGOCO-Benghazi), are available for some wells in the study area. Less often available are the core petrophysical analyses and completion reports. In a few wells the only data at hand were the daily wellsite geological sheets, and internal unpublished oil company reports.

Methodology

Four principal methods of study have been used:

1. Subsurface studies.
 - (a) Subsurface well log correlation.
 - (b) Map construction.
2. Core study.
3. Thin-section study.
4. Petrophysical study.

1. Subsurface studies:

- (a) Subsurface well log correlation

Well log data were obtained by courtesy of the Arabian Gulf Oil Company (AGOCO)-Benghazi, Libya. The relevant wells are marked on the location map (Fig. 4) and are widely distributed throughout the study area.

Environmental interpretation of sedimentary facies using well log data has a major role in the search for hydrocarbons, through to enabling the prediction of location, geometry and trend of porous reservoir units. Three cross-sections have been constructed in stratigraphic format to show the stratigraphic and environmental relationships of the sandstone reservoirs in the Lower Acacus Formation (Encls.1,2 & 3). Two north-south cross-sections show the regional

picture since they cross approximately the whole basin parallel to the interpreted depositional dip. The third cross-section, trending NE-NNW, is at an angle to the proposed NE depositional dip and joins the NNW cross-sections. This third cross-section is restricted to the study area (see Encls.1,2 & 3).

Two types of wireline logs were used for this study:

- (a-1) Spontaneous-Potential (SP) log.
- (a-2) Gamma-Ray (GR) log.

(a-1) Spontaneous-Potential (SP) Log

The Spontaneous-Potential log is the record and continuous measurement of the electrical properties of the Formation. Since rock matrix materials are non-conductive, the electrical properties recorded are "... a function of the contained fluids and differences in salinities between mud filtrate and formation water within permeable beds.." (Asquith and Gibson, 1982). SP logs measure "...the cumulative effect of electrofiltration and electrochemical potential within the formation (potential differences); those properties essentially being proportional to permeability.." (Schlumberger, 1972).

Some difficulties arise in correlation, especially at well C1-61 where the SP log shows a reversed response to gamma ray. The reasons for this reversal will be discussed later (Pages 80,81).

(a-2) Gamma-Ray (GR) Log

Gamma-ray logs are essentially responsive to the natural radioactivity of the formation. They can be used to identify lithologies and for correlation (Asquith and Gibson, 1982). Shale-free sandstones have low concentrations of radioactive material and give low gamma ray readings. In the absence of carbonates which also tend to have a low gamma response, we can generally assume that for low gamma ray sandstones the lithology is reworked, high energy sands having high textural maturity (Serra, 1984) as a result of removal of clay-sized particles during deposition leaving medium to coarse grain size, and very well sorted sands.

In some situations, caving of boreholes and varying hole size can affect the gamma ray response (Schlumberger, 1972), while the presence of some potassium feldspars and mica in sandstones can give a relatively high gamma ray reading (Asquith and Gibson, 1982). It is evident that, although both types of well logs (SP and GR) measure different properties,

they are both indirectly measuring grain size profiles. As well, both logs provide information about the lithologic boundary conditions. In passing abruptly from a sand to a shale, a sharp contact will be recorded, while conversely, in a shale/sand transitional zone gradual changes will be traced. The use of log interpretation as a measure of grain size profile has developed because many depositional environments tend to generate characteristic grain size profiles as those environments migrate laterally and are preserved in vertical sequences (Serra, 1989).

Examples of grain size profile from this study include the upward coarsening of sandstone sequences in wells (T1-23, C1-NC2 and E1-NC2) at the central and southern part of the study area as well as the fining upward trends or profiles of sandstone sequences inside the study area, as in B3-61 well and C1-61 well to the east, and outside the study area in the south as in III1-NC7 and C1-NC7A wells (see Encls. 1,2 and 3). In general, both spontaneous-potential and gamma-ray logs were used in this study to identify and define sandstone sequences, although only gamma-ray logs were available for most of the wells indicated in Encl.1 to Encl.3.

(b) Map Construction

(b-1) Isopach Maps

The isopach map of the Tanezzuft shale (Fig. 15) was constructed to shed light on the paleostructure and areas of maximum shale development at the time of deposition. Since some wells in the study area have not been drilled deep enough to penetrate the Tanezzuft Shale, thickness estimation relative to the nearby wells has been utilized.

Isopach maps of each of the three parts of the Acacus Formation (Lower Acacus Formation, Middle Acacus Formation and Upper Acacus Formation; Fig. 16 to Fig. 18), have been constructed to show the general formation thickness distribution, and to reflect the paleotectonic setting in the study area. With regards to the Lower Acacus Formation, mapping of the total isopach (Fig. 16) has been important in order to assess basic ideas of the depositional history in the study area. The depositional patterns of the sandstones and their thickness distributions are best observed in the net sandstone thickness map (Fig. 24) which measures the net thickness of sandstone intervals which record readings of 75 API units or less on gamma-ray logs.

Also, construction of isopach maps for important specific sandstone horizons (clean sandstone) in each sequence (Fig. 25 to Fig. 29) was provided to illustrate sandstone morphology which may reflect the patterns of the depositional environment.

(b-2) Sandstone Percentage Map

After determination of the sand line on GR log, sandstone thickness of 75 API units or less were recorded and the percentage of these sandstone units were computed by dividing the net sand thickness by total thickness (genetic units thickness) for each well. The resulting map (Fig.37) shows the relative amount of sand in the stratigraphic sequence.

(b-3) Sand-Shale Ratio Map

This type of map illustrates the areal relationship of the ratio between the net sand thickness of one depositional sequence to the shale thickness in the same depositional sequence. This provides an effective means for displaying the interrelations between these two lithologic components with a single set of contours (Krumbein and Sloss, 1963).

In general the interplay between sand and shale, expressed as a ratio, provides insight to the

quality of the reservoir sandstones in a particular area. By this means the sandstone percentage contrasted to the interbedded marine shale in a particular area (Fig.38) may be predicted.

All above maps will be discussed under the topic of Sandstone Trends and Morphology (p.86).

2. Core Study

Interpretation of subsurface well log data in the study area (NC2 concession, northern flank of the Hamada Basin, NW Libya), has been integrated with the real rock section by means of core. Wireline logs must be calibrated with real rock information which provides data concerning associated lithologies, texture, sedimentary structures, etc.

A total of 1230 feet (375 m) of core intervals cut at different levels in the sandstones of Lower Acacus Formation have been studied for description of basic lithology and sedimentary structures (see Appendix I & II).

3. Thin-Section Study

Thin-section petrographic information for this study was obtained from point counts (300 points per slide) of 70 thin sections. Samples were taken from

10 cored wells for thin-sectioning. Samples selected for petrographic analysis are typically silty, very fine to medium grained. Some samples included very silty shales. Thin-section examination has been used to aid in the construction of the environmental model.

4. Petrophysical Study

In this study the porosity-permeability variation (conducted by AGOCO Lab, Benghazi, Libya), oil and water saturation (from well log analysis) and formation pressure values (from formation testing reports, AGOCO, Benghazi, Libya) were determined for some sandstone intervals in the 10 cored wells.

For the porosity-permeability study, sample plugs were cut from sandstone cores in 10 cored wells during the core study stage, through the assistance of the Arabian Gulf Oil Company technical staff. The sample plugs were analysed using techniques and methodology recommended by the American Petroleum Institute (1956 and 1960) and Curtis, (1971). Porosity data were obtained using a volumetric porosimeter and by applying Boyle's Law (American Petroleum Institute, 1960). Grain volume of a sample is measured using

a Boyle's Law helium porosimeter.

Laboratory procedures for determining porosity and permeability:

The dry weight of sample is determined, and bulk volume measured by mercury displacement. Grain density and porosity are calculated. Permeability is determined by gas methods. Nitrogen pressure (N 15 PSI) is applied to one face of the sample (in Hassler Cell, under 250 PSI); this is called upstream pressure. Flow of gas through the sample is measured from the opposite face (downstream pressure).

Permeability of a sample is obtained by entering its dimensions, applied pressure (upstream), the flow rate, viscosity of nitrogen, as well as downstream pressure into Darcy's equation (American Petroleum Institute, 1956, 1960; Curtis, 1971). Standards with known values are used in the calculation.

In this study porosity-permeability data have been compared to the geologic data from the core , and from the electrical log data for each sedimentary facies with the purpose of identifying possible trends of increase or decrease of porosity and permeability. The core-plug porosity values have been compared with thin-section porosity values for some producing

sandstone units taking into consideration the corresponding permeability values.

Petrophysical results calculated from the electrical logs and Schlumberger charts are: average corrected log porosity ($\phi_{av.c}$), true formation resistivity (R_t), clay volume (V_{cl}), hydrocarbon saturation (S_h), water saturation (S_w) and irreducible water saturation (S_{wirr}). These values define reservoir sandstone quality at different locations in the study area.

Other reservoir parameters such as formation pressure, oil gravity, gas-oil ratio (GOR), and flow rates for some tested sandstone intervals, have been obtained from company formation testing reports.

WIRELIN-LOG CHARACTERISTICS

Cores are not available for some wells (E1-23, D1-NC2 and A1-61). Cores are available in some wells for specific sandstone unit intervals, but other sandstone units have no cores. This fact necessitates that other types of data must be used to identify environmental facies and evaluate reservoir characteristics. Wireline-logs, which are run routinely on most wildcat wells, were investigated as facies indicators or as sedimentological tools (Serra, 1989) for identifying the different sand-body types. Each log pattern is characteristic of a particular part or subenvironment (Visher, Satta and Phares, 1971) in the subsurface; thereby permitting interpretation of the history of a specific unit in the Lower Acacus Formation.

Some basic observations made on Gamma-Ray curves (GR) and Spontaneous-Potential curves (SP) (if available) were:

1. Nature of basal contact of the sandstone unit; is it sharp or gradational?
2. Trend of the electric curve; is it inclined upsection to the left (coarsening-upward sand unit with clay content decreasing upward), or inclined upsection to the right (fining-upward sand unit with clay content increasing upward), or blocky (clay content relatively uniform)?

3. Nature of the curve; is it smooth or serrated because of thin shale interbeds? (Gilreath and Stephens, 1975; Nelson and Glaister, 1978).

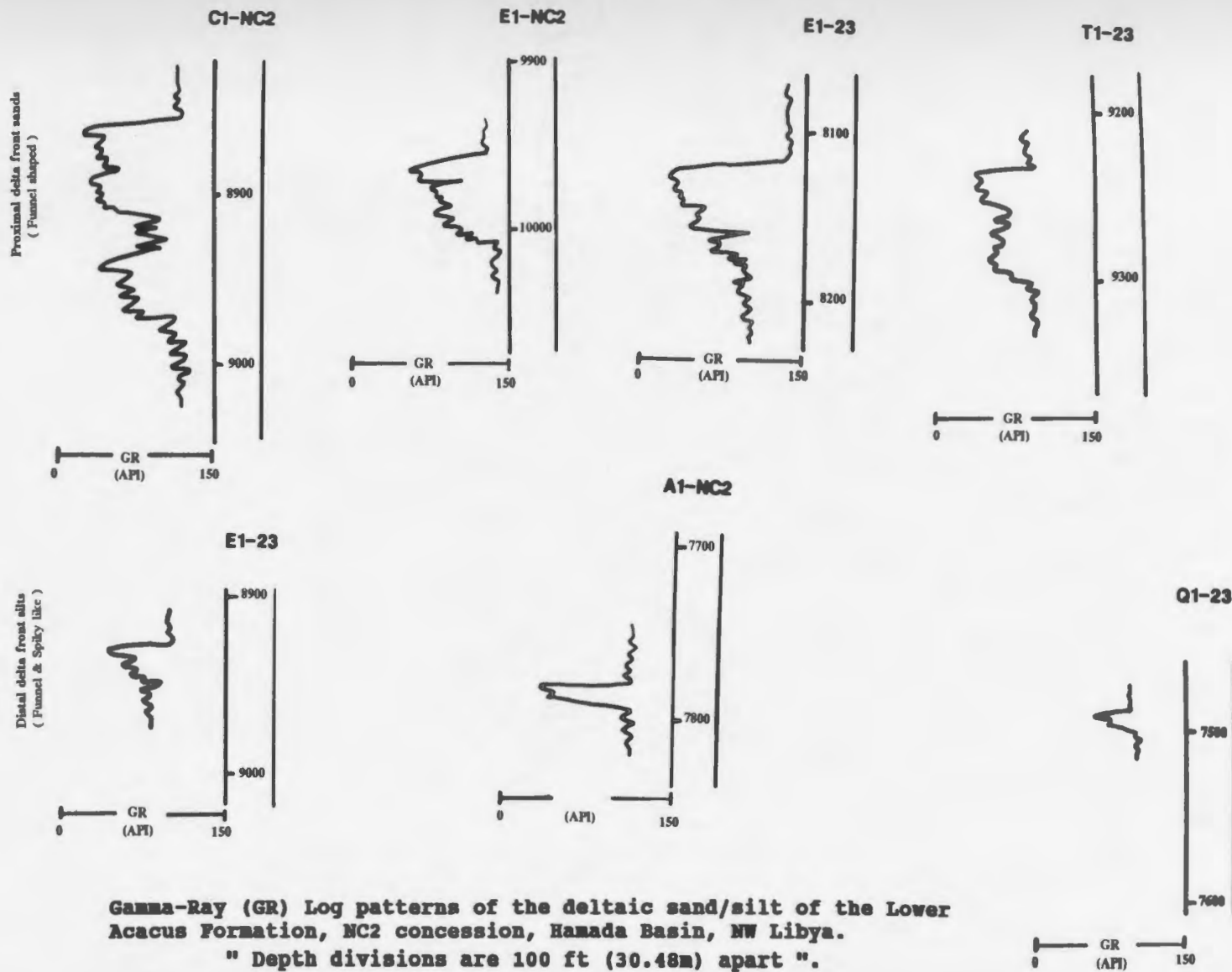
The following discussion of well log character and depositional environment interpretation is based both on literature analogies as referenced, and in the knowledge of the details of drill core described later in the thesis (refer to p.135 and 141). Thus the core serve to verify the generalizations drawn from the logs and literature analogies regarding depositional environment.

The main Gamma-Ray (GR) characteristics and Spontaneous-Potential (SP) characteristics (in most cases) of various facies observed in the cored sand intervals in the Lower Acacus Formation for wells in the study area, and for some wells outside the study area, are grouped in Figures 19-21, and are discussed below:

1. A funnel shaped gamma-ray curve (deltaic sands), is characterized by a gradational basal contact with an upsection slope to the left (Fig. 19). This slope reflects a notable upsection increase in grain size (coarsening-upward) and decrease in clay content. The nature of the lower part of the GR curve in most sand units of this type is serrated because of the presence of silty/shale interbeds. This category is found to correspond with sand/silt sequences "...of prograded

Figure 19. Gamma-Ray log patterns of the
deltaic sand/silt of the Lower Acacus
Formation, NC2 concession, Hamada Basin,
NW Libya.

DELTAIC SANDS
 COARSENING UPWARD
 FUNNEL SHAPED/SPIKY LIKE
 GRADATIONAL BASE
 (DELTA FRONT SANDS/SILT)



Gamma-Ray (GR) Log patterns of the deltaic sand/silt of the Lower Acacus Formation, NC2 concession, Hamada Basin, NW Libya.

" Depth divisions are 100 ft (30.48m) apart "

delta front.." (Serra, 1989). Good porosity and permeability and highest oil saturation can be expected toward the top of the sand unit. Moreover, in the delta front facies packages, the minor spike-shaped log response of silty-shaly sandstone units is readily recognized at the seaward margin of the funnel-shaped sand facies. This spiky log character represents the distal delta front silt facies of the prograded deltaic body.

2. Among fluvial channel sand responses, three types of curves are observed and are represented in Figures 20 A, B and C.

2-A. Fining upwards, bell shaped, sharp base (channel sands): The gamma-ray (GR) sloping up-section to the right corresponds with channel sand sequences. The sands are characterized by a sharp basal contact and a generally fining-upward sequence: reflected by an abrupt left deviation at the base and by a slope to the right respectively. The GR curve in most units of this type is serrated (Fig. 20-A).

2-B. Fining upward, partially blocky, sharp base (channel sands):

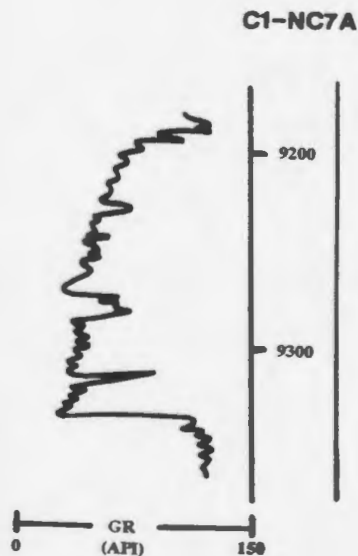
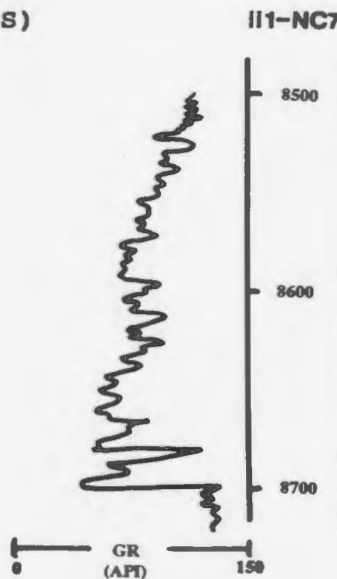
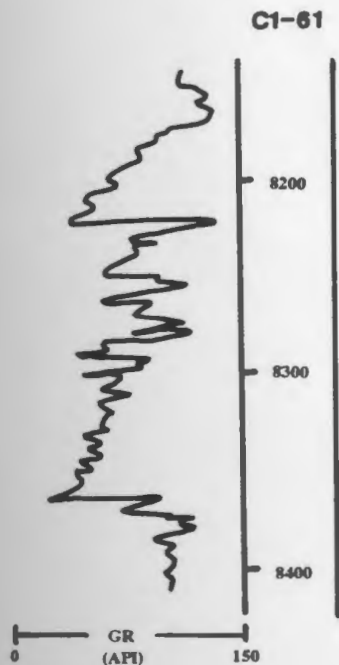
The SP and GR curves are generally smooth in the lower part and becomes more serrated toward the top (Fig. 20-B), with an overall fining-upward trend as evidenced by SP and GR curves sloping to the right.

2-C. Blocky, uniform-serrated, sharp base (stacked channel sands):

The SP and GR curves are nearly vertical and are characterized by uniform to serrated blocky form (Fig. 20-C), which indicates variation in clay content. This type of curve can be identified with sand sequences composed of stacked channels (Nelson and Glaister, 1978; Serra, 1984). Such log characters were detected in the southern part of the study area in well B1-61 and outside the study farther to the south in well C1-NC7A.

Figure 20-A. Gamma-Ray log characteristics for the fluvial sands of the Lower Acacus Formation (in well C1-61, NC2 concession), and of the Acacus South formation (in wells II1-NC7 and C1-NC7A, south of NC2 concession), Hamada Basin, NW Libya. Refer to page 283 for discussion of definition of Acacus South formation.

FLUVIAL SANDS
FINING UPWARD
BELL SHAPED
SHARP BASE
(CHANNEL SANDS)



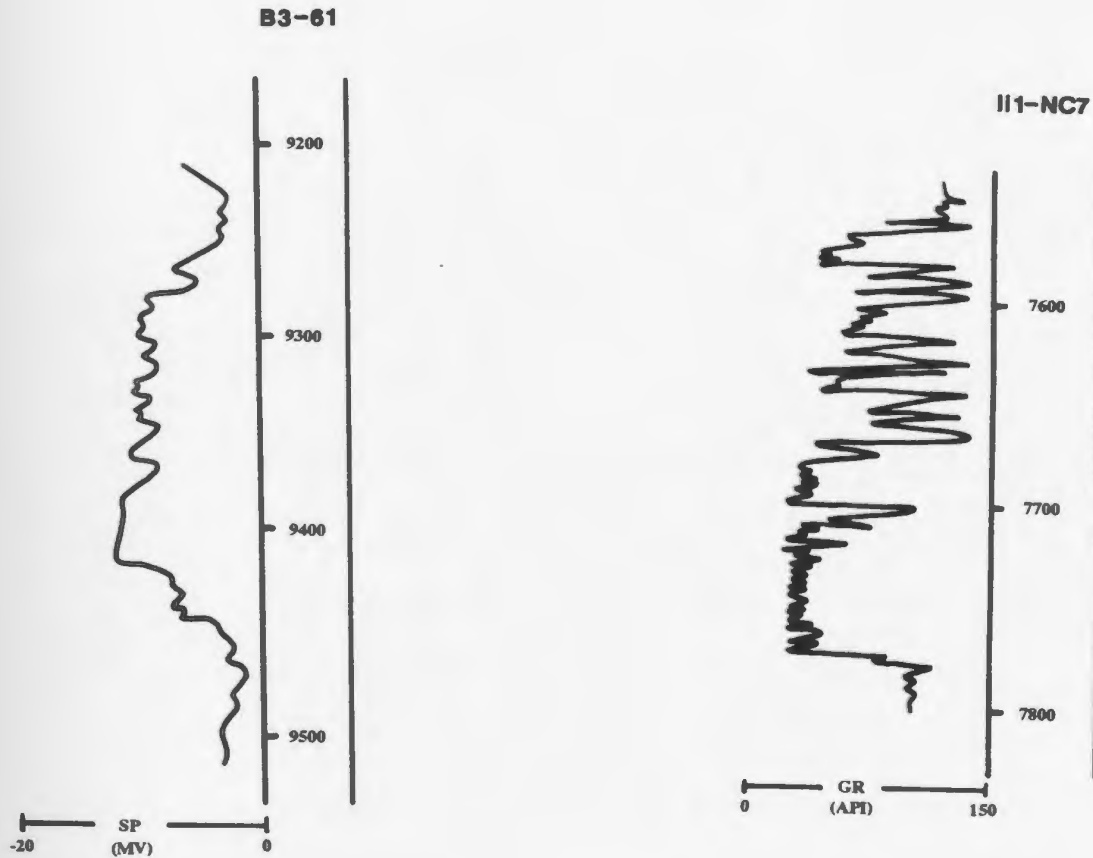
A- Gamma-Ray (GR) Log characteristics for the fluvial sands of the Lower Acacus Formation (in well C1-61, NC2 concession), and of the Acacus South Formation (in well III-NC7 and well C1-NC7A, South of NC2 concession), Hamada Basin, NW Libya.

" Depth divisions are 100 ft (30,48m) apart "

Figure 20-B. Spontaneous-Potential (SP) and Gamma-Ray (GR) logs for the fluvial sands of the Lower Acacus Formation (in well B3-61, NC2 concession), and of the Acacus South formation (in well I11-NC7, south of NC2 concession), Hamada Basin, NW Libya. Refer to page 283 for discussion of definition of Acacus South formation.

FLUVIAL SANDS
FINING UPWARD-PARTIALLY BLOCKY
BELL SHAPED
SHARP BASE
(CHANNEL SANDS)

74



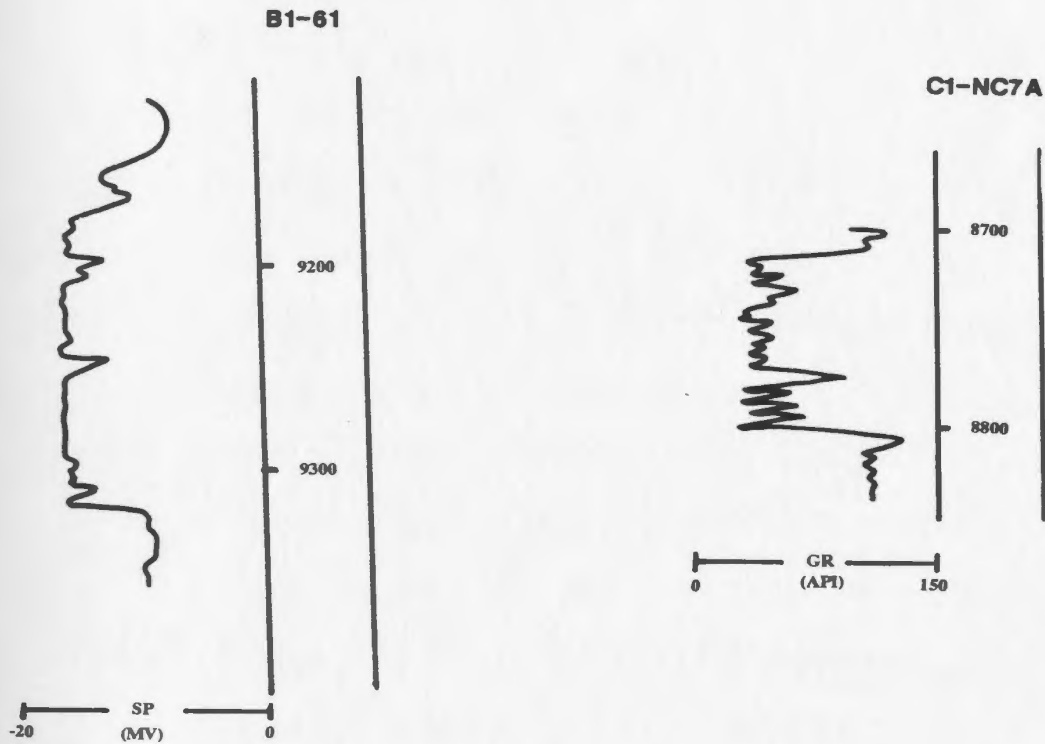
B- Spontaneous-Potential (SP) and Gamma-Ray (GR) Logs for the Fluvial sands of the Lower Acacus Formation (in well B3-61, NC2 concession), and of the Acacus South Formation (in well II1-NC7 and well C1-NC7A, South of NC2 concession), Hamada Basin, NW Libya.

" Depth divisions are 100 ft (30.48m) apart ".

OBE-91

Figure 20-C. Spontaneous-Potential (SP) and Gamma-Ray (GR) logs for the fluvial sands of the Lower Acacus Formation (in well P3-61, NC2 concession), and of the Acacus South formation (in well C1-NC7A, south of NC2 concession), Hamada Basin, NW Libya. Refer to page 283 for discussion of definition of Acacus South formation.

FLUVIAL SANDS
BLOCKY, UNIFORM-SERRATED
SHARP BASE
(STACKED CHANNEL SANDS)



C- Spontaneous-Potential (SP) and Gamma-Ray (GR) Logs for the fluvial sands of the Lower Acacus Formation (in well B1-61, NC2 concession), and of the Acacus South Formation (in well C1-NC7A, South of NC2 concession), Hamada Basin, NW Libya.

" Depth divisions are 100 ft (30.48m) apart "

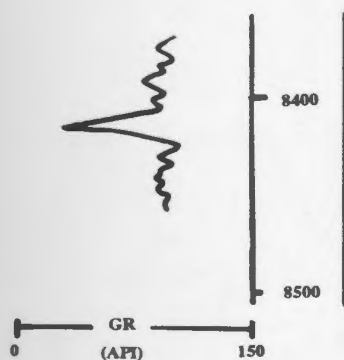
3. Spiky, dominantly sharp base, reworked marine sand:
A spiky or tapered spiky nature of GR curve (Fig. 21), is found to correspond with thin, less extensive sand stringers classified in this study as reworked marine sands. These occur very commonly between shales along the northern edge of the low-sand areas in wells A1-NC2, Q1-23 and U1-23. This character probably represents relief-fill deposits (Coleman and Prior, 1980). It is also found in the central and southern parts of the study area associated with sequences of transgressive marine shales. These deposits are characterized by abrupt contacts with the overlying and underlying shales. Rarely does this log character occur in sections with notable upward coarsening from underlying shales where contacts are gradational, or in fining-upward sections where the GR has a sharp basal contact. Spiky marine sands may have good reservoir quality where associated with the cleaning-up of sands by marine processes (as in well Q1-23 at 8461 feet).

This discussion of the different log response characteristics indicates that vertical patterns interpreted from electric logs can be related to sequences

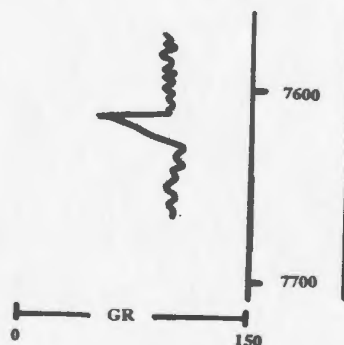
Figure 21. Gamma-Ray (GR) log patterns of the marine sands in the Lower Acacus Formation, NC2 concession, Hamada Basin, NW Libya.

**MARINE SANDS
SPIKY
DOMINANTLY SHARP BASE
OCCASIONALLY GRADATIONAL BASE
(REWORKED MARINE SANDS)**

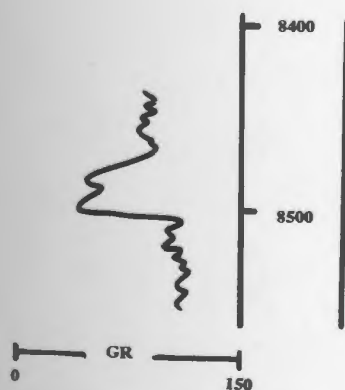
E1-23



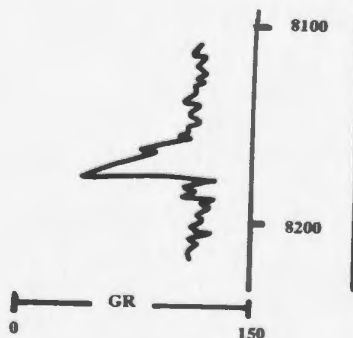
Q1-23



Q1-23



A1-NC2



Gamma-Ray Log (GR) patterns of the marine sands in the Lower Acacus Formation, NC2 concession, Hamada Basin, NW Libya.

" Depth divisions are 100 ft (30.48m) apart "

of texture and lithologies described from the cored sand intervals (Appendix I). As a result in this study where core control is available, it is possible to extrapolate environmental facies into non-cored wells on the basis of GR log characteristics alone.

SP log characteristics were investigated for comparison with GR curves in those wells where the two log types were available (B1-61, B3-61 and C1-61). The comparison indicates that the SP curve is usually less definitive and of lower resolution than the coincident GR log (Fig. 22). In some cases (eg. well C1-61), the trends are even reversed (Fig. 23).

An SP curve is less reliable than the GR for interpreting the various depositional facies of Lower Acacus Formation because it is severely affected by a number of factors such as:

- (i) salinity variations in the formation fluids or in drilling mud; SP curve is a function of salinity contrast between mud filtrate and formation (Schlumberger, 1972 ; Asquith et al, 1982). Hence, if the resistivity of mud filtrate and formation water are about equal, the SP deflection will be small and the curve will be rather featureless (Fig. 22).
- (ii) The SP curve is affected by depth of invasion and decreases as invasion deepens (Serra, 1984) opposite

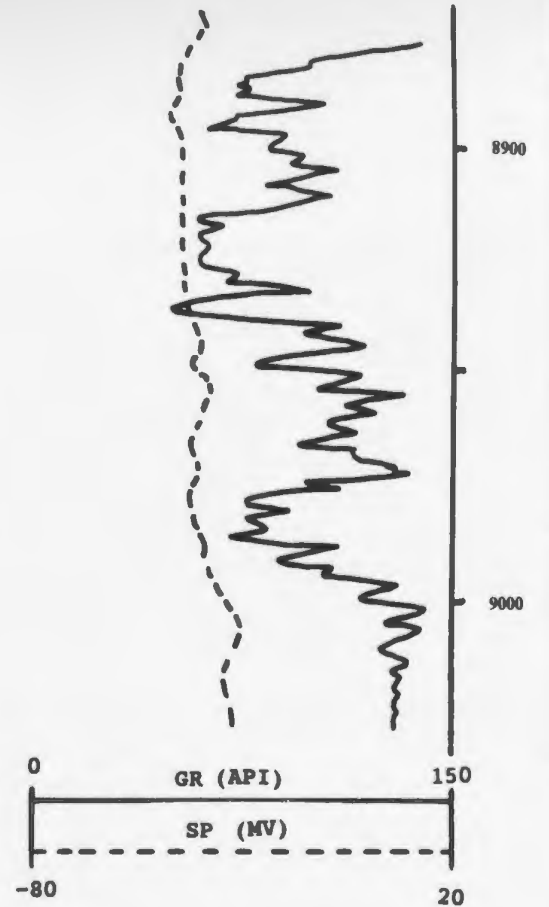
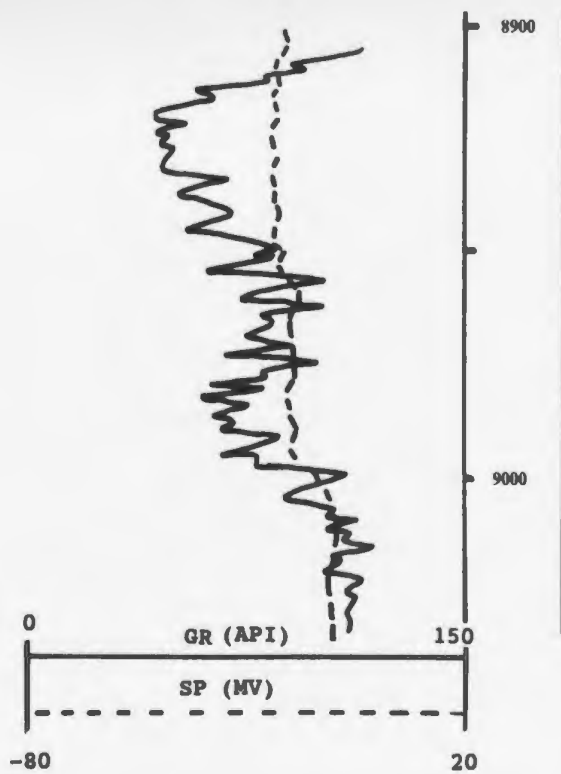
to porous sandstone unit. Figure 23 illustrates an SP curve and a GR curve for the same sand interval in well C1-61. A highly serrated SP curve is observed with sharp basal contact. The trend of the SP curve from 7780 ft to 7818 ft (2372- 2384 m.) is inclined to right (shale content increasing upward), reflecting a fining-upward sequence typical of channel sands of fluvial environment. The GR curve indicates a gradational basal contact with a notable overall increase in grain size, and a decrease in shale content upward. The GR curve inclined to the left, therefore suggests a coarsening-upward sequence which would be typical of a regressive sand unit. The core section that was cut at the top of this unit in well C1-61 (Core #4, Fig.App.22) indicates that the unit is composed of silty to very fine sandstone of occasional shale laminae at the base and fine to medium grained clean sandstone at top. Hence, the core emphasizes that the GR curve response is reliable.

- (iii) Technical reasons should not be ignored which may be responsible in part for the lesser reliability of SP curve, "...including SP anomalies due to noise.."
(Shlumberger, 1972 ; Dewan, 1983).

Figure 22. Spontaneous-Potential (SP) and Gamma-Ray (GR) log patterns for some sand sequence in well B2-NC2 and well D1-NC2, Lower Acacus Formation, NC2 concession, Hamada Basin, NW Libya.

B2-NC2
Hamada Basin
NW Libya

D1-NC2
Hamada Basin
NW Libya

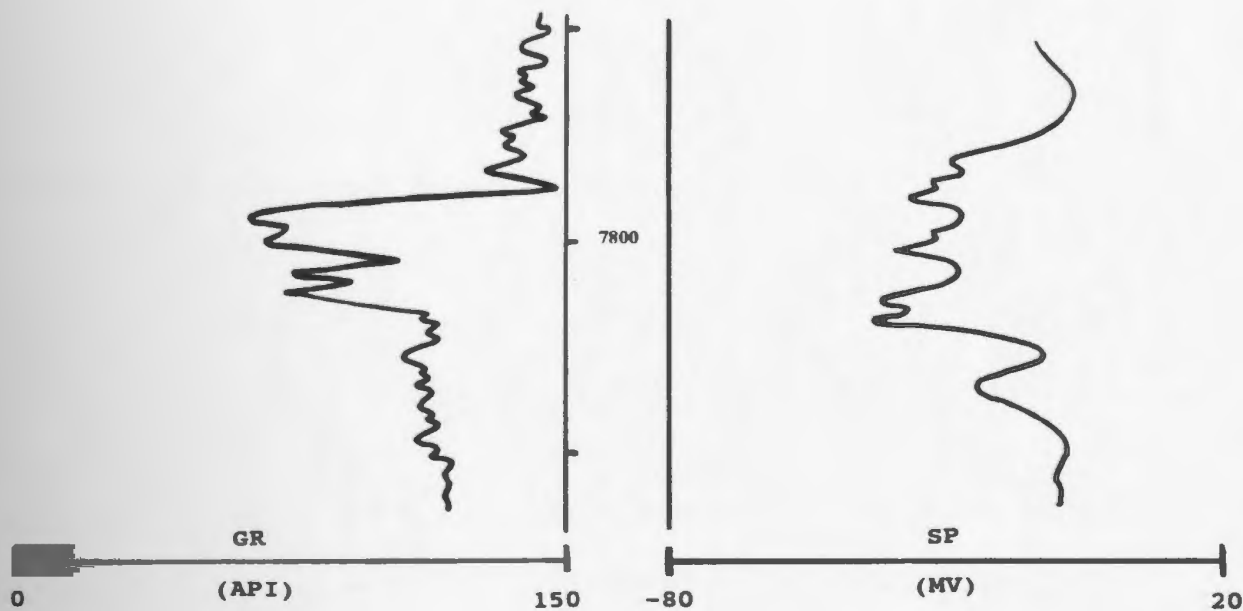


Spontaneous-Potential (SP) and Gamma-Ray Log patterns for some sand sequences in well B2-NC2 and well D1-NC2, Lower Acacus Formation, NC2 concession, Hamada Basin, NW Libya.
Note: the SP curve is usually less definitive and featureless.

" Depth divisions are 50 ft (15.24m) apart "

Figure 23. Spontaneous-Potential (SP) and Gamma-Ray (GR) log patterns for the same sand unit in well C1-61, Lower Acacus Formation, NC2 concession, Hamada Basin, NW Libya.

C1-61
Hamada Basin
NW Libya



Spontaneous-Potential (SP) and Gamma-Ray (GR) Log patterns for the same sand unit in well C1-61, Lower Acacus Formation, NC2 concession, Hamada Basin, NW Libya.
Note: the trend of the SP curve is reversed and the logs suggest two different types of sand sequences.

" Depth divisions are 50 ft (15.24m) apart ".

OBE-91

SANDSTONE TRENDS AND MORPHOLOGY

Cross-Sections

Three stratigraphic cross-sections were constructed to determine the depositional characteristics of the individual sandstones in the Lower Acacus Formation. Two regional cross-sections trending from south to north were constructed in which wells from outside the study area were used to delineate the extent of different types of sandstone units and to complete the depositional picture. The third cross section from northeast to northwest-north, was constructed using 8 wells to reveal depositional patterns in the eastern side of the study area. The three stratigraphic cross-sections, with their environmental interpretations are shown in Enclosure 1 to Enclosure. 3. Using a combination of gamma-ray log characteristics and some core section data, the Lower Acacus Sandstones in the study area can be defined in terms of cyclic intervals of regressive sand pulses. By this means the Lower Acacus Formation is divided into 14 coarsening-upward units (A1-A14), interbedded with transgressive marine shale packages, with elusive stratigraphic relationships in which stratigraphic markers between two or three adjacent wells are not regionally continuous. New stratigraphic markers have to be selected to provide a stratigraphically

meaningful relationship in which the litho-facies packages can be correlatable in terms of lateral and vertical changes. The overlying Middle Acacus shale represents one of the utilized markers between some of the wells and its significance can be appraised by referring to the regional cross sections (Encl. 1 and Encl. 2); between wells E1-23, A1-NC2, Q1-23 and U1-23, and cross section (Encl. 3); between wells B2-NC2, D1-NC2, A1-NC2, Q1-23 and U1-23. This correlation indicates that the contact between the Tanezzuft marine shale and the overlying Lower Acacus Formation is transitional and diachronous, climbing upsection all the way from south to north, which is also the direction of increasing marine shales from 850 feet (259 m.) in well II1-NC7 south, to 1280 feet (390 m.) in well Q1-23 offshore. In all deep drilled wells, a highly radioactive marker of organic shale occurs at the base of the Tanezzuft marine shale and is considered to be a good stratigraphic marker.

In the two S-N regional cross sections (Encl. 1 and Encl. 2), the land-to-seaward sequence for a given sandstone unit is from multistory fluvial sands to the south, in the vicinity of II1-NC7 and C1-NC7A wells, to coastal-deltaic sands and silts in wells concentrated in the southern and central parts of the study area, and to

marine shales and reworked marine sands of the offshore environment to the north in wells A1-NC2, Q1-23 and U1-23.

In the third cross-section (Encl. 3), the lateral relations of depositional environments from northeast to northwest-north is similar to that in the previous south-north trending cross-sections. An exception is the possibility that an area of fluvial channel systems may be concentrated farther to the east outside the study area. One channel system was observed in the A8 sand/silt unit level, through which sediments of A8 sand/silt unit have been distributed in the west and southeast directions. Coastal-deltaic sands and silts are very well illustrated in this cross section (Encl. 3) as being prograded deltaic lobes from the east through wells C1-61, A1-61 and F1-NC2 which gradually change to marine shale and reworked marine sands in the vicinity of B1-NC2, B2-NC2 and D1-NC2 to the southeast, and toward A1-NC2, Q1-23 and U1-23 wells to the north.

The vertical sequence of a single deltaic lobe may be different from one area to another and depends on where the lobe is being penetrated by the wells (i.e., vertical sequences from proximal parts of a lobe are different from those cut through marginal parts). The ideal vertical sequences from the proximal part of the lobe down to the

distal (marginal) part to the prodelta marine shale can be seen especially in those wells located in the central and southern part of the study area (T1-23, E1-NC2, C1-NC2). Based on the Gamma-Ray log signature, the vertical sequence in cross-sections is characterized by a number of log facies which are:

Spiky-shale log facies representing the reworked marine sands and the prodelta marine shales, which gradually change upward into the coarsening-upward coastal-deltaic log facies represented by two components; very silty sandstone at base and clean sandstone at top.

The stratigraphic framework of Lower Acacus Formation sandstones as revealed in the three cross-sections can be summarized as follows:

- * Individual sandstone units begin with marine shales representing a transgressive phase and terminate with a regressive deltaic sand/silt phase (progradational units). This latter phase is overlain by less persistent, thin, reworked marine sands representing the destructional phase. Thus, each of the sandstone units make up major progradational sequences bounded by local or regional time-stratigraphic markers.
- * Major river systems occur to the south of the study area. These systems flowed northward.

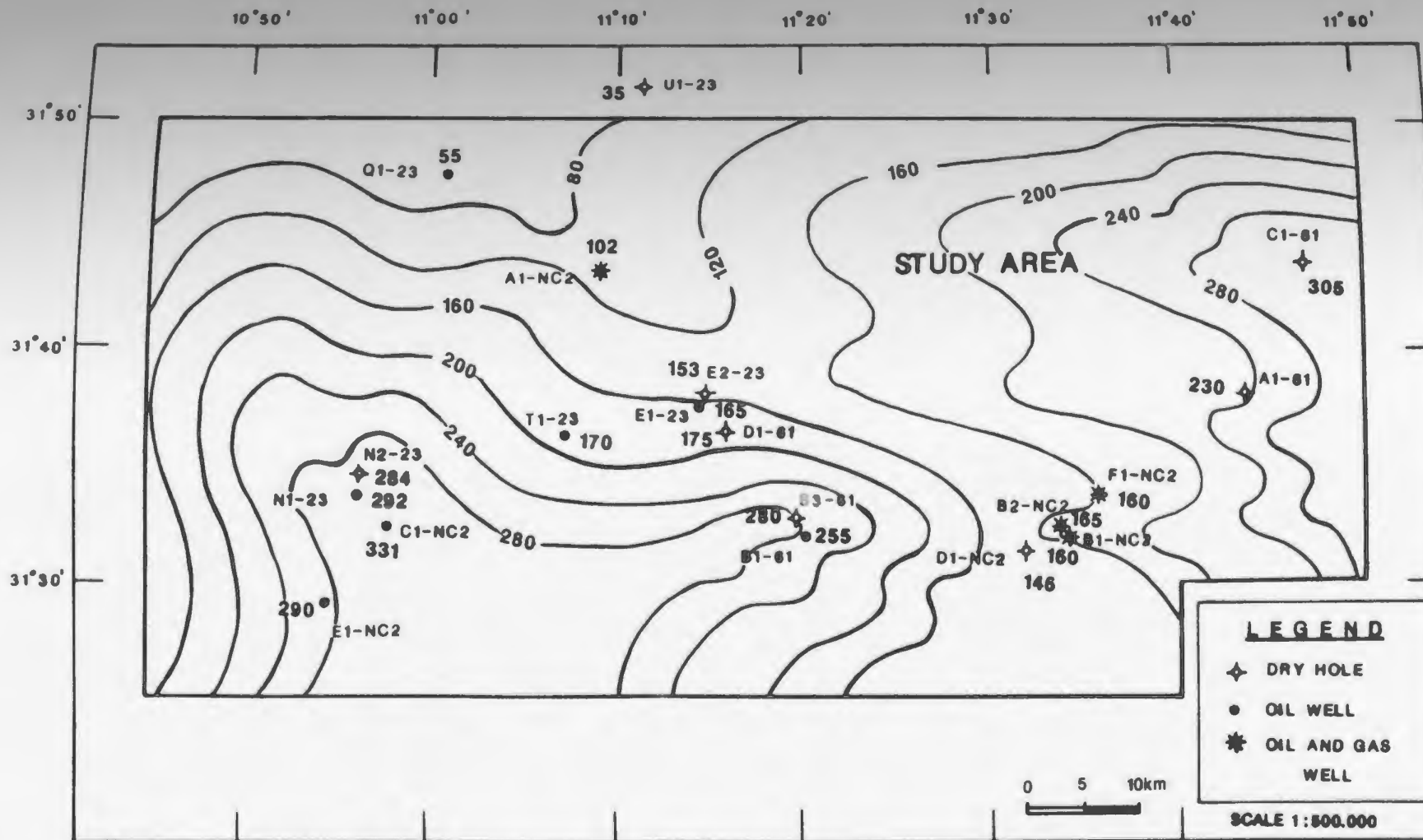
- * The largest delta lobes prograded 28-31 miles (45-50 km.) northward in the study area. The resulting vertical accumulation of sands averaged 45 feet (14 m.). The cross-section further illustrates the diachronous stratigraphic relationship between the Lower Acacus deltaic sandstones and the Tanezuft marine shales. Refer to the "transitional boundary" indicated on enclosures 1-3.

Isopach Maps

Well control in this study is not sufficient to map the details of facies distribution, because in some areas no wells exist (especially in the northern part of the study area). Also, the wells are quite widely spaced, especially between well A1-61 and well A1-NC2; well A1-61 and well Q1-23; well A1-NC2 and well C1-61. Therefore, depositional patterns and areas of major sediment input are better observed where subsurface control is more abundant as is the case in the southern part of the study area.

Net sandstone isopach maps were constructed by measuring the thickness of sandstone that recorded a reading of 75 API or less on the gamma-ray log. Trends and morphology of the Lower Acacus sandstones are illustrated by the net sandstone isopach map (Fig.24) of all sandstone units sequences (A8-A14). The map outlines a large lobate delta complex, 75 km. wide (strike direction) and

Figure 24. Net sandstone isopach map of the
Lower Acacus Formation, NC2 concession,
Hamada Basin, NW Libya.



OBE-91

Net Sandstone isopach map of the Lower Acacus Formation, NC2 concession, Hamada Basin, NW Libya. "C.I 40 feet"

(Sandstones of Gamma-ray Log readings 75 API or less).

approximately 32.5 Km. long (dip direction), in the southern part of the study area.

Sandstone units (A8-A14) in well C1-NC2, well E1-NC2, well N1-23, well N2-23, well B1-61 and well B3-61, are interpreted in this study to be delta front sands (proximal delta front facies), while the silty sandstone bodies in the vicinity of E1-23 and A1-NC2 represent the distal portions of the lobate delta in the northward direction.

A second deltaic system on the east side of the study area (around well C1-61 and well A1-61 area) shows thick lobes outlined by 280, 240, 200 and 160 feet isopach contours. This system progrades from east to west towards well A1-NC2 and to the southeast towards wells B2-NC2 and D1-NC2. Due to the lack of well control between wells C1-61 and A1-NC2 the lobe configurations are not as clear as those in the southern portion of the study area. Five net isopach maps were mapped for the lower sandstone units (A8, A9 & A10), the middle sandstone unit (12) and upper sandstone unit (14) (Fig.25 to Fig.29). In each the sandstone thickness is different from well to well. The well-logs confirm that each of these sandstone intervals were developed as cyclic units, having distinct sequences that begin with a prominent marine shaly unit at the base, and grade upward into bioturbated, interbedded silty sandstones to clean sandstones at top. Each of these

sequences are variable in thickness from 150 to 350 feet (46 to 106 m.). It can be determined from well log correlation (Encl. 1 and Encl. 2) that these sandstone units represent northward-prograding sand bodies, each reflecting a separate deltaic lobe. The sandstone thickness variations in the lower sandstone units (A8, A9 and A10) are as follows:

Unit A8 has a minimum thickness of about 33 feet (10 m.) in well E1-23 and is a maximum of 120 feet (36 m.) thick in well B1-61. The unit is about 35 feet (10.5 m.) to 65 feet (20 m.) in wells C1-61 and F1-NC2 respectively. The thickest A8 sandstone interval in wells B1-61 to the south and C1-61 to the east, display linear, channel-like contour configuration on map view (Fig. 25). The log response in these wells record overall fining upward sequences to blocky log signatures (Fig. 31). These signatures may represent the accumulation of fluvial channel deposits responsible for the distribution of deltaic sands and silts from south to north as sourced from B1-61 and B3-61 areas and from east to westward and southeast direction as sourced from C1-61 area.

Unit A9 has a minimum thickness of 12 feet (3.6 m.) in well E1-23 (which is believed to be in the distal part of the lobe) and a maximum of 30 feet (9 m.) in well B1-61 (Fig.26). From south to north, this unit (A9) prograded

only a short distance so that a full lobate patterns is not observed beyond well B3-61 in the north.

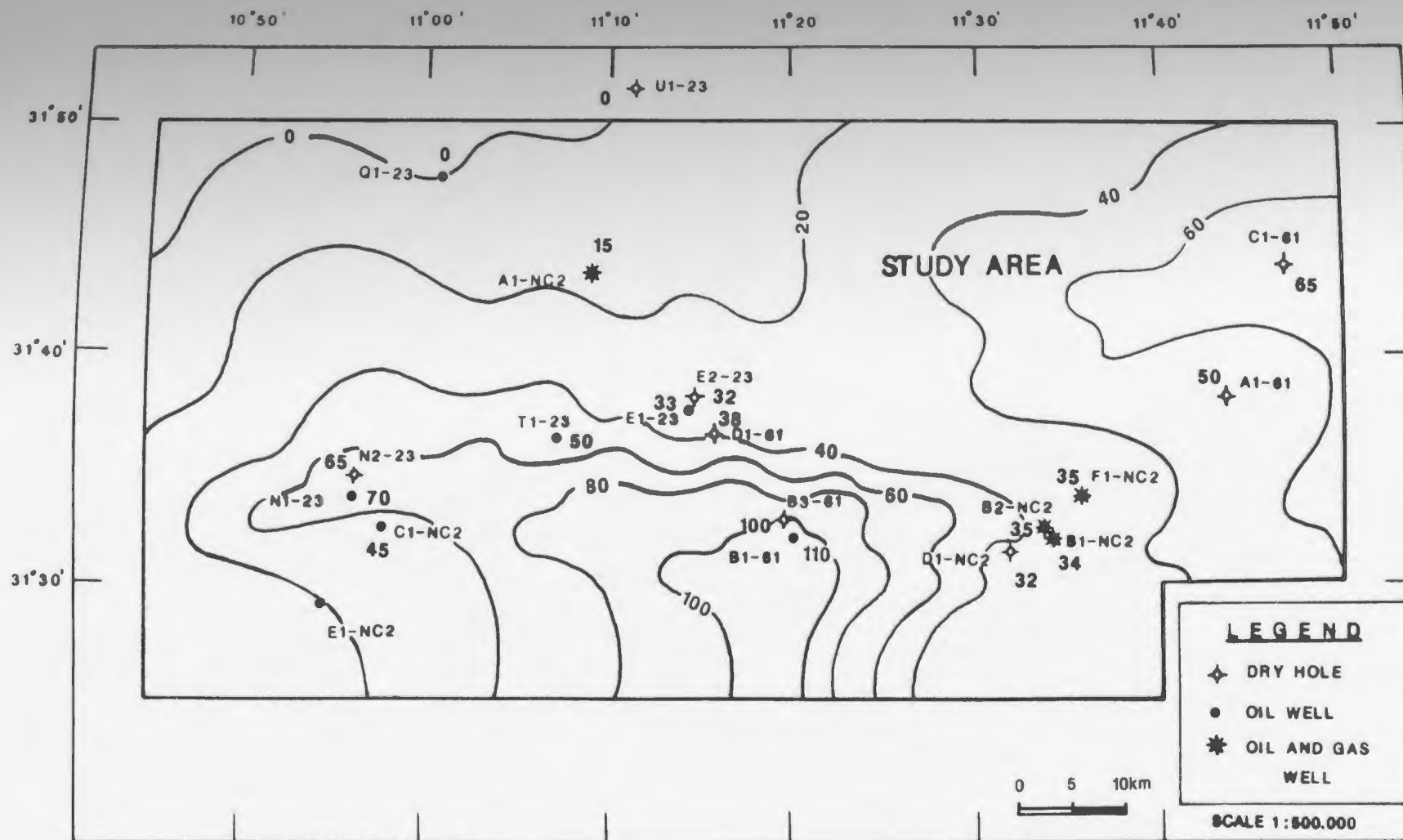
Unit A10 represents a more progradational sand body than unit A9, with more pronounced lobate contour patterns covering 35 km. (dip direction) over a width of 70 km. (strike direction). A minimum thickness of 23 feet (7 m.) in well A1-NC2 occurs at the distal part of this deltaic lobe (marginal) (Encl. 1). A maximum thickness of 58 feet (18 m.) occurs in well B1-61 (Fig.27).

In the eastern side of the study area, a second A10 lobate pattern may be seen, having a minimum thickness of 20 feet (6 m.) in well B1-NC2, and a maximum thickness of 42 feet (13 m.) in well A1-61.

In the middle unit A12, similar lobate patterns may be seen to indicate south-north progradation with a slight shift of the axis towards well B1-61. A minimum thickness of about 20 feet (6 m.) occurs in well E1-23 and a maximum thickness of about 55 feet (17 m.) occurs in well B1-61. Progradation of the eastern lobe to the west is still present with changes in thickness from maximum of 75 feet (23 m.) in well C1-61 to a minimum thickness of 13 feet (4 m.) towards well D1-NC2 (Fig. 28).

For the uppermost unit A14, a lobate pattern still exists in the south with a significant shift of depo-centre (Fig.29) from well B1-61 to well C1-61 for maximum 75 feet

Figure 25. Isopach map of the A8 sandstone unit,
Lower Acacus Formation, NC2 concession,
Hamada Basin, NW Libya.

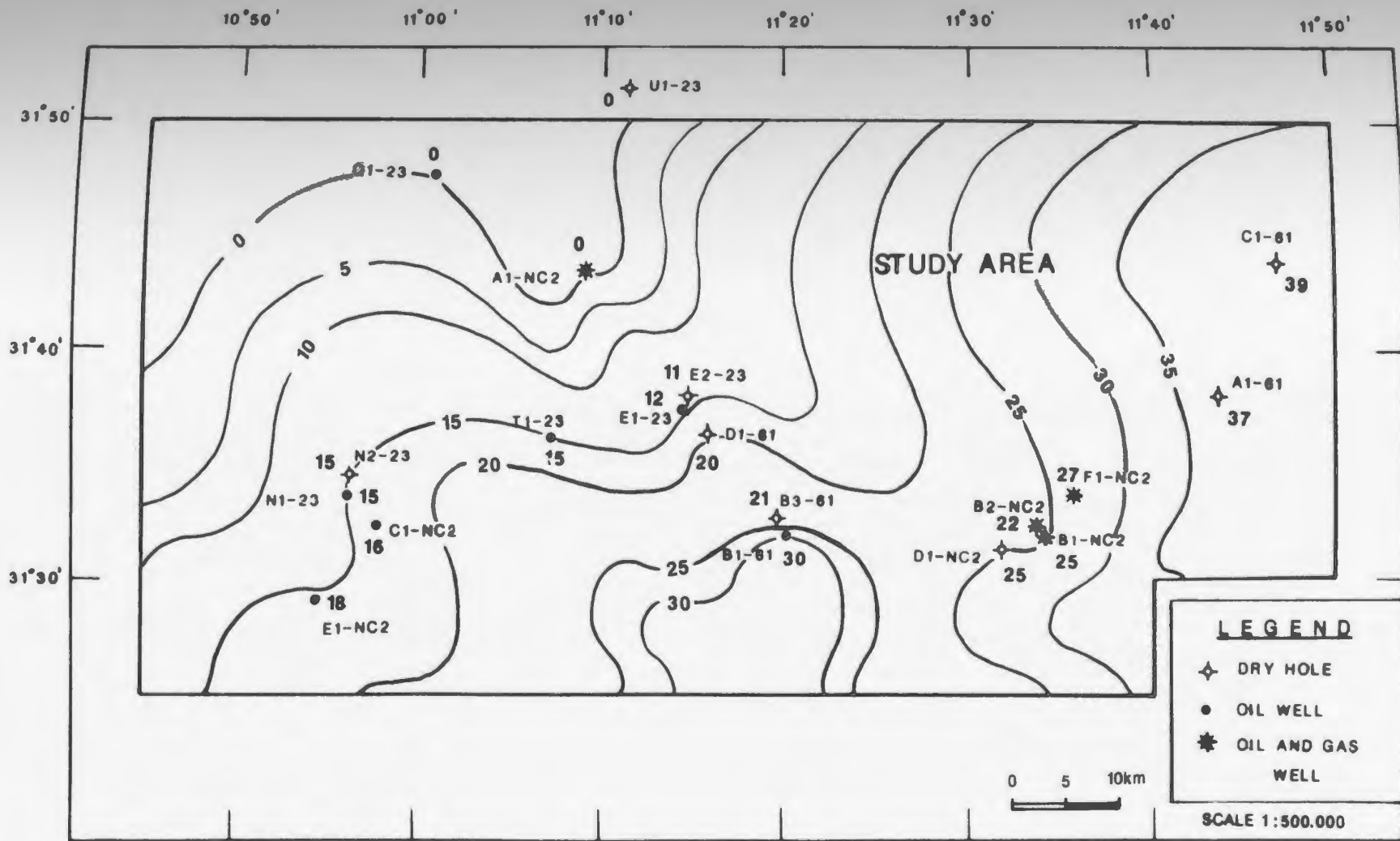


OBE-91

Isopach map of the A8 Sandstone unit, Lower Acacus Formation, NC2 concession, Hamada Basin, NW Libya. "C.I 20 feet"

(Sandstones of Gamma-ray Log readings 75 API or less).

Figure 26. Isopach map of the A9 sandstone unit,
Lower Acacus Formation, NC2 concession,
Hamada Basin, NW Libya.

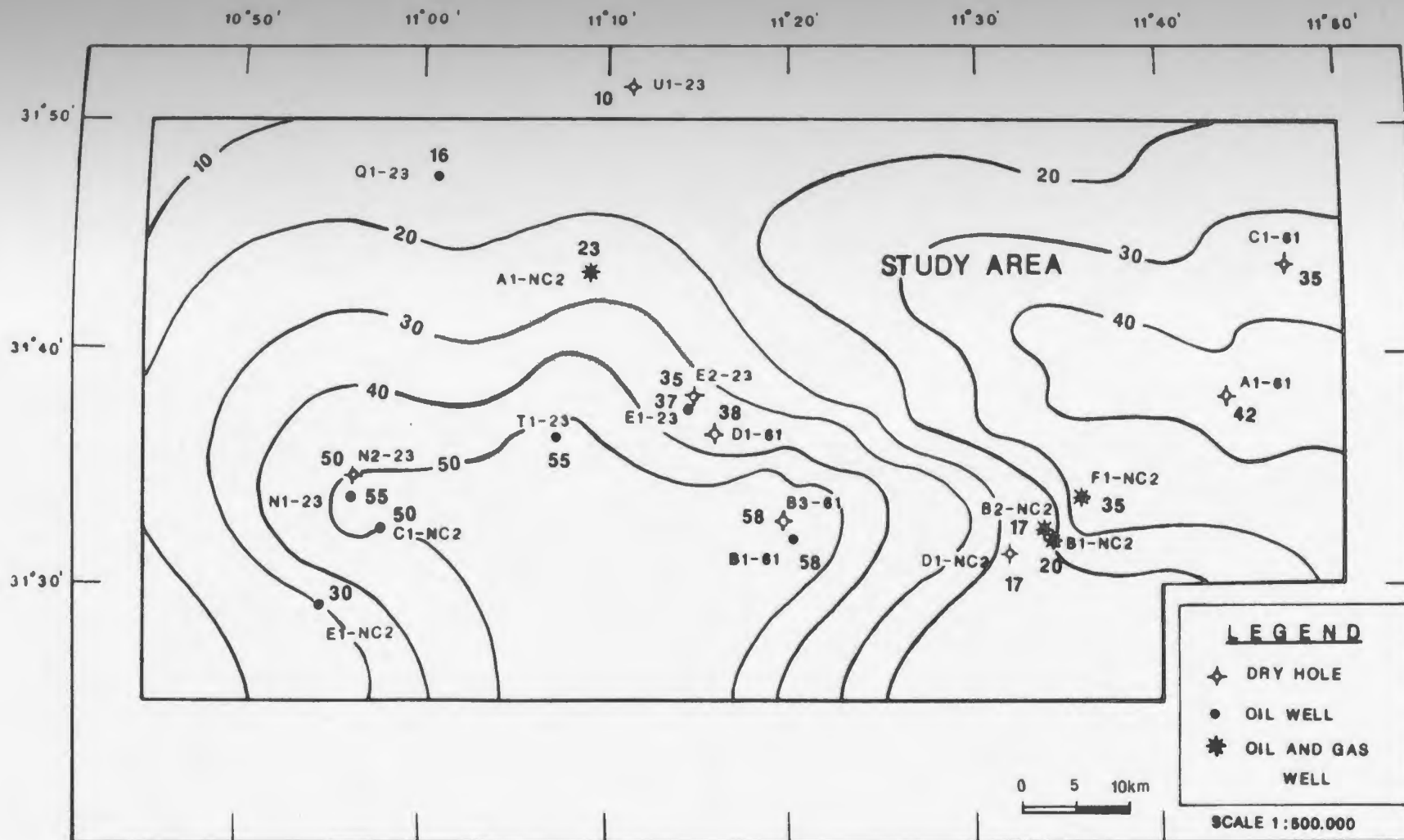


OBE-91

Isopach map of the A9 Sandstone unit, Lower Acacus Formation, NC2 concession, Hamada Basin, NW Libya. "C.I 5 feet"

(Sandstones of Gamma-ray Log readings 75 API or less).

Figure 27. Isopach map of the A10 sandstone unit,
Lower Acacus Formation, NC2 concession,
Hamada Basin, NW Libya.

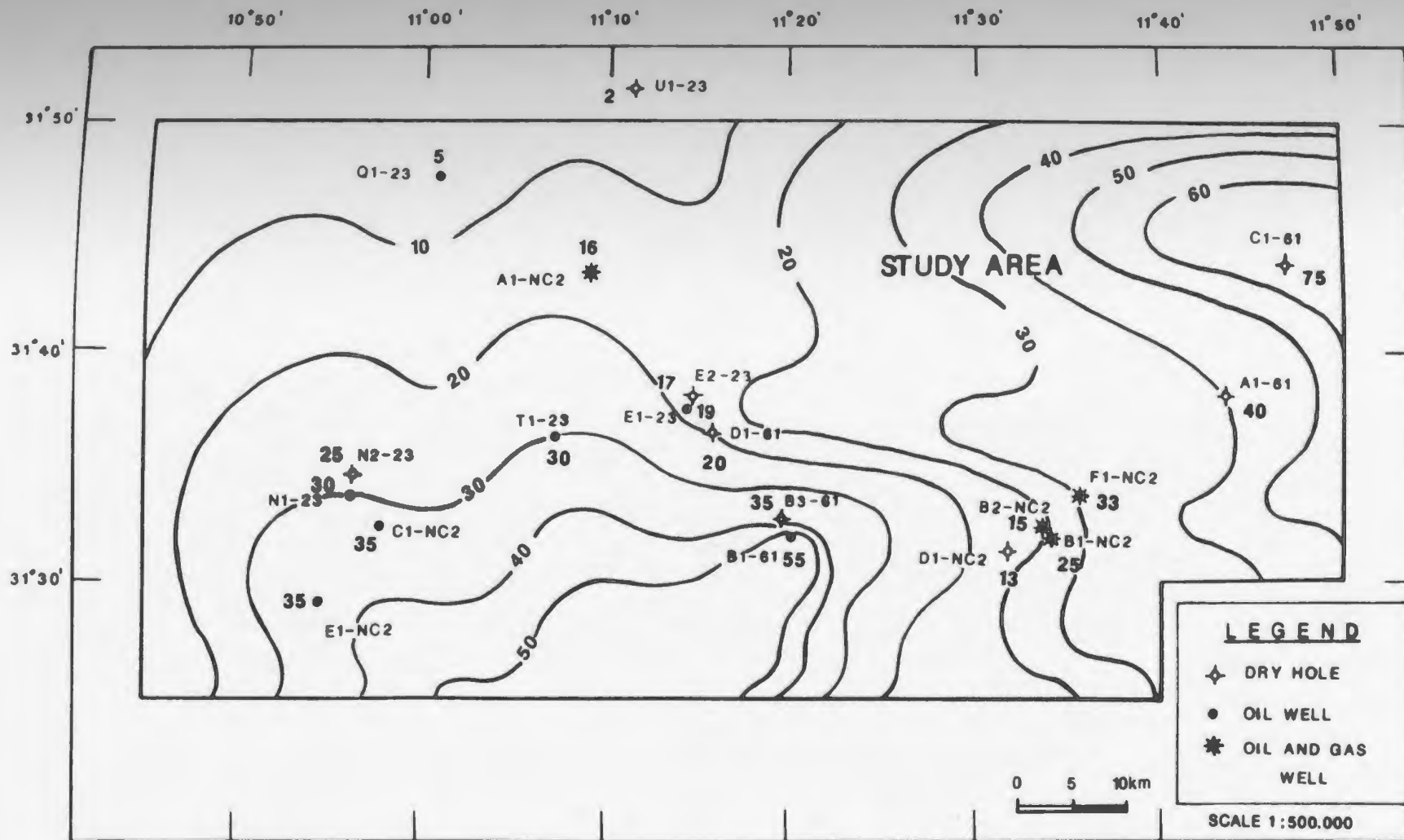


OBE-91

Isopach map of the A10 Sandstone unit, Lower Acacus Formation, NC2 concession, Hamada Basin, NW Libya. "C.I 10 feet"

(Sandstones of Gamma-ray Log readings 75 API or less).

Figure 28. Isopach map of the A12 sandstone unit,
Lower Acacus Formation, NC2 concession,
Hamada Basin, NW Libya.

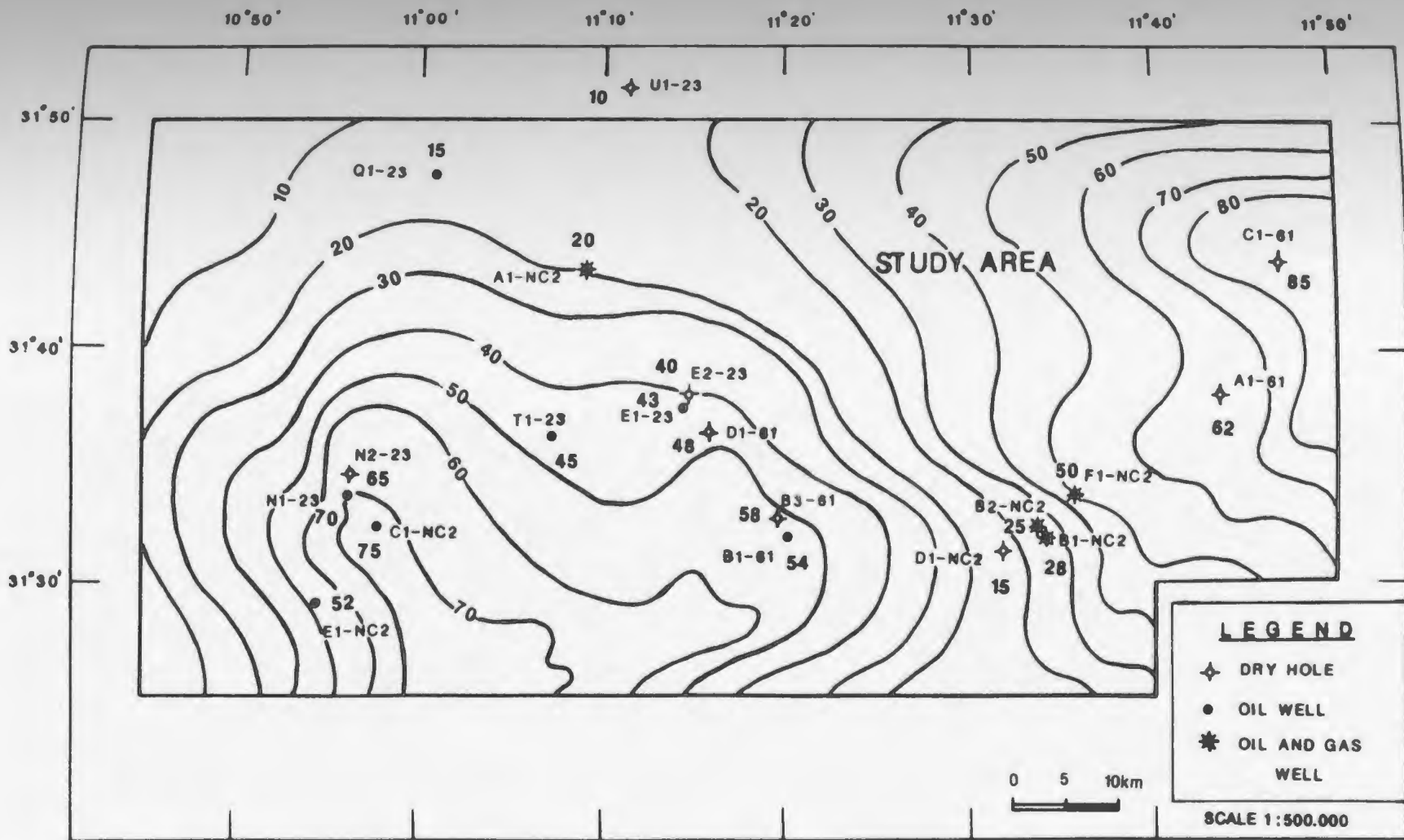


OBE-91

Isopach map of the A12 Sandstone unit, Lower Acacus Formation, NC2 concession, Hamada Basin, NW Libya. "C.I 10 feet"

(Sandstones of Gamma-ray Log readings 75 API or less).

Figure 29. Isopach map of the A14 sandstone unit,
Lower Acacus Formation, NC2 concession,
Hamada Basin, NW Libya.



OBE-91

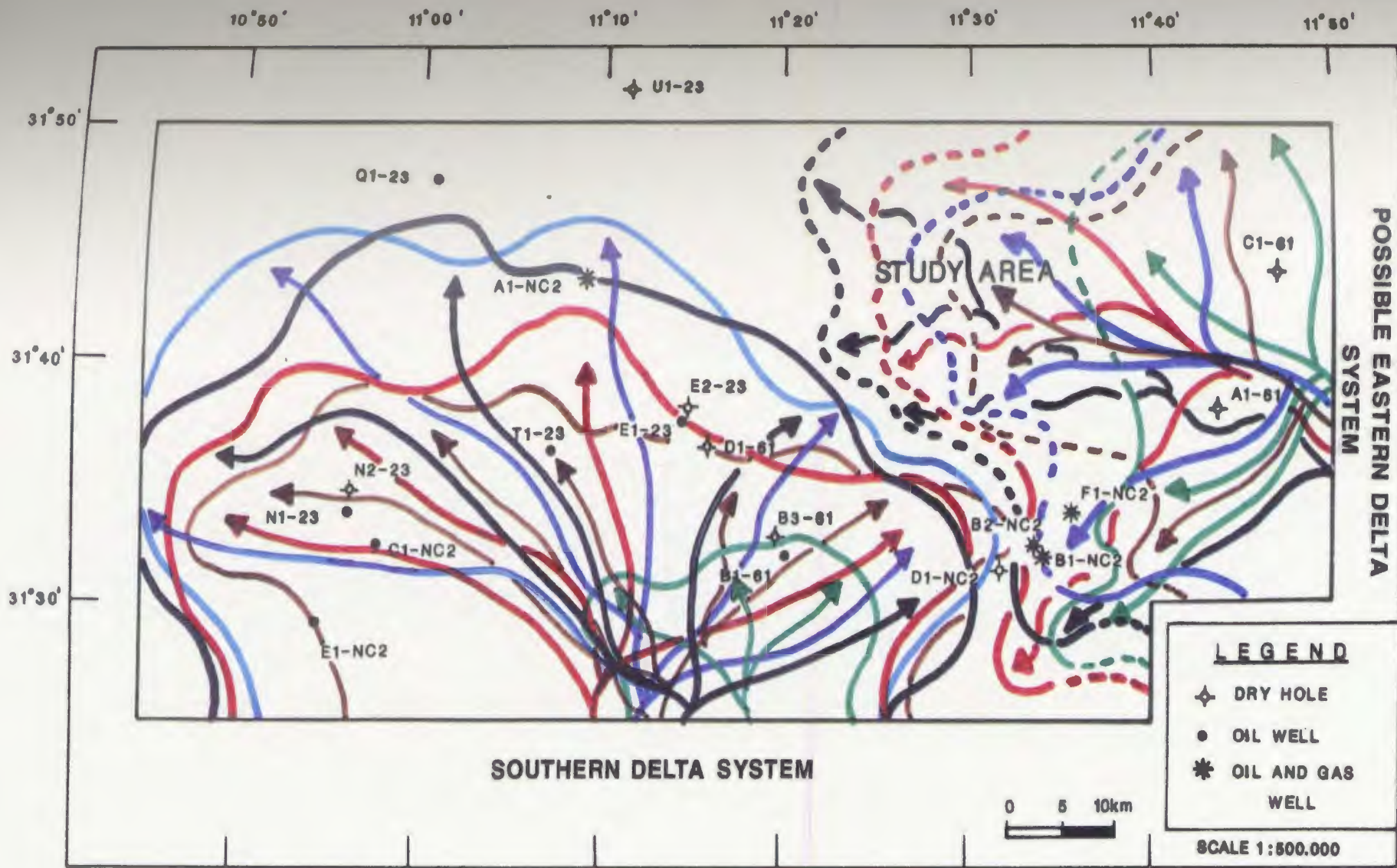
Isopach map of the A14 Sandstone unit, Lower Acacus Formation, NC2 concession, Hamada Basin, NW Libya. "C.I 10 feet"

(Sandstones of Gamma-ray Log readings 75 API or less).

(23 m.) sandstone thickness. A minimum thickness of about 20 feet (6 m.) is encountered at well A1-NC2 which represents the marginal well on this lobe. In the eastern side of the study area, sand thickness declines from 85 feet (26 m.) in well C1-61 to 25 feet (8 m.) in well B2-NC2. To the eastern side of the study area, the influence of another deltaic depo-centre may be seen, but the concentration of sandstones have a more lobate pattern at least at the southern part of the study area.

The data illustrate that each sandstone body originated in different lobes in different times. Shifting of depositional axes occurred, as can be seen when the isopach maps (Fig. 25 to Fig. 29) of the five sandstone units (A8 to A14) are superimposed on each other (Figs. 30A-30C). Different distances of progradation and shifts of depositional axes can be seen which may reflect either the intensity or the duration of sediment supply in each deltaic system. Unit A9 has the least progradational extent. Units A8 and A12 have approximately the same progradational extents covering 30 km. in dip direction (south-north) and 70km. in strike direction (east-west). Units A10 and A14 had the greatest progradational distances covering 40 km. in dip direction and 75 km. in strike direction. Each sandstone lobe shows some shift from the earlier deposited lobe, a phenomenon which may be related

Figure 30-A. Depositional patterns and axes of successive sandstone units (A8-A14), of the Lower Acacus Formation, NC2 concession, Hamada Basin, NW Libya.



— A9 Sandstone Unit

— A12 Sandstone Unit

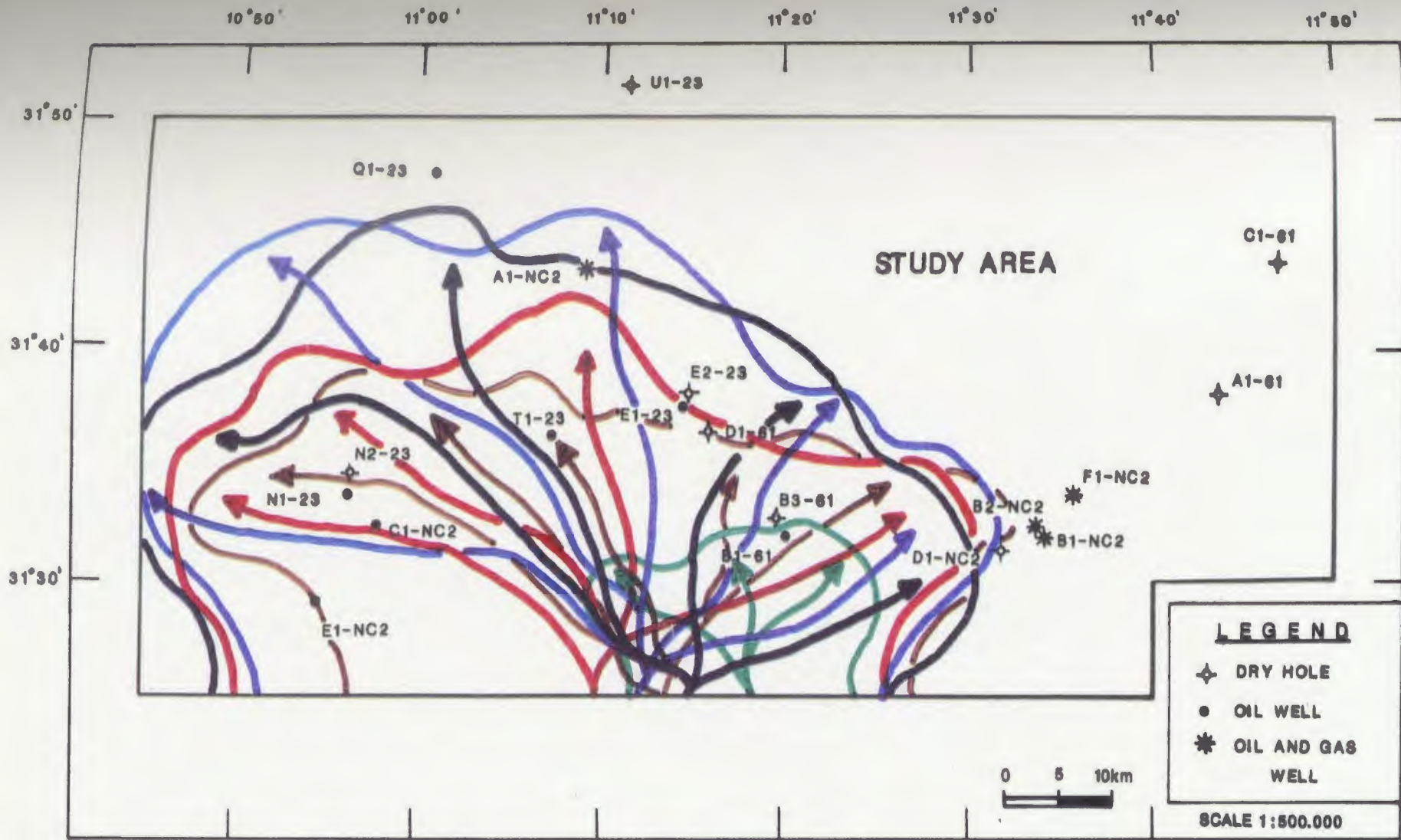
— A14 Sandstone Unit

— A8 Sandstone Unit

— A10 Sandstone Unit

OBE-91

Figure 30-B. Depositional patterns and axes of successive sandstone units (A8-A14), in the southern delta system, Lower Acacus Formation, NC2 concession, Hamada Basin, NW Libya.

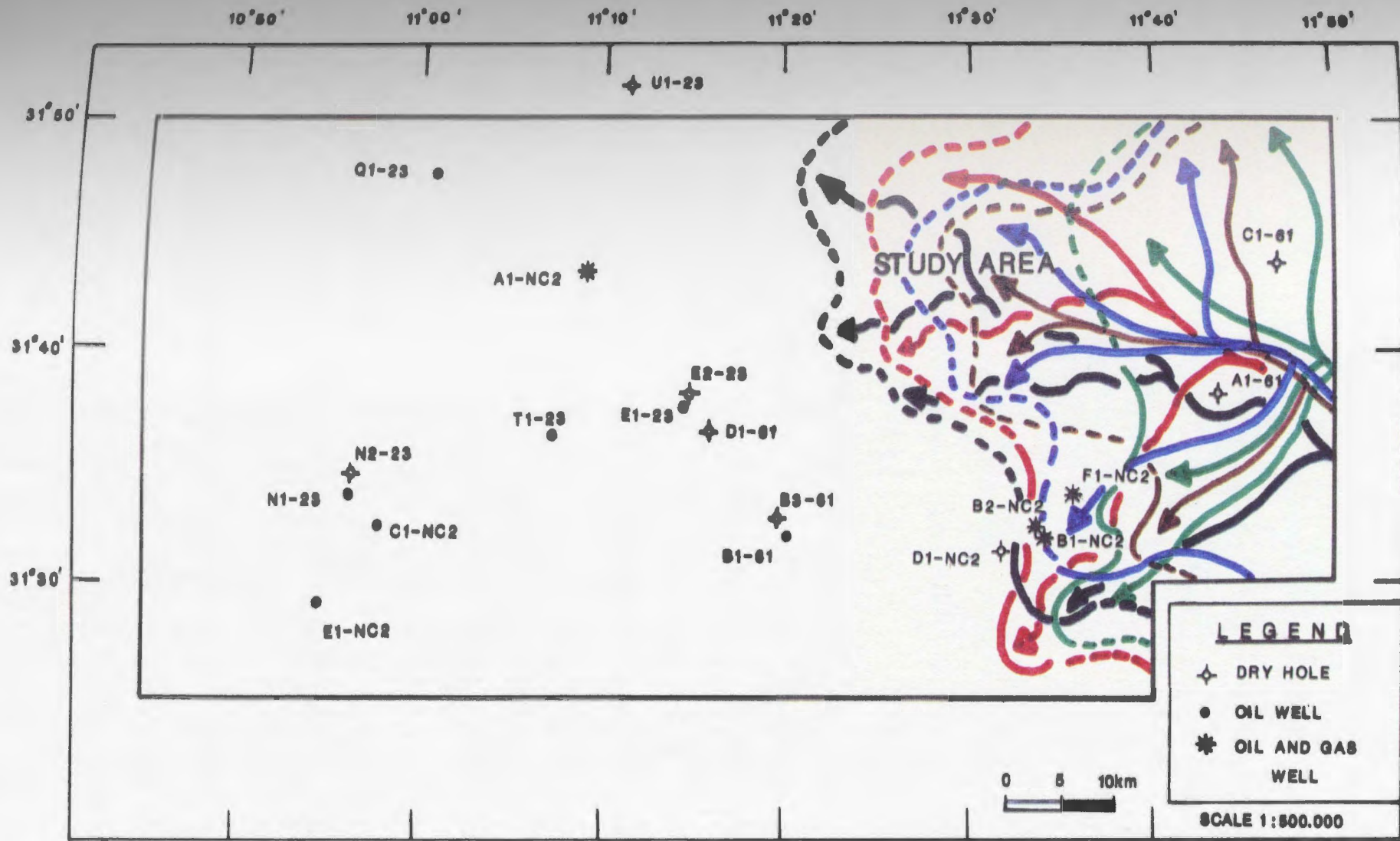


— A9 Sandstone Unit
— A8 Sandstone Unit

— A12 Sandstone Unit
— A10 Sandstone Unit

— A14 Sandstone Unit

Figure 30-C. Depositional patterns and axes of successive sandstone units (A8-A19), in the possible eastern delta system, Lower Acacus Formation, NC2 concession, Hamada Basin, NW Libya.



OBE-91

- A9 Sandstone Unit
- A12 Sandstone Unit
- A14 Sandstone Unit
- A8 Sandstone Unit
- A10 Sandstone Unit

to "...sediment loading and differential compaction over the lower sand/shale units..", (Brown Jr., 1975 ; Blatt, Middleton and Murray, 1980 ; Coleman, 1981).

From the sandstone thickness maps the patterns of sandstone distribution and size of delta system in each lobe are well illustrated (Fig. 25 to Fig. 29). The thickness and areal extent of the deltaic sandstones vary greatly depending upon the rate of sediment supply, tectonic setting of the basin, and the wave and current energy conditions on the coast (Saxena, 1976b). "...Rapidly subsiding areas like those in the Gulf Coast, produce a significant thickness of deltaic sands.." (Coleman and Prior, 1980; Coleman, 1981), but have a relatively short areal extent. In the modern Mississippi delta "...the distributary mouth bars are made up of sands 200 to 300 feet (61 - 91 m.) thick and 3.2 km. (2 miles) to 9.6 km. (6 miles) wide (along depositional strike) and 3.2 km. (2 miles) to 6.4 km. (4 miles) long (along depositional dip).." (Saxena, 1976b). In the NC2 concession, Hamada Basin, northwest Libya where the Silurian deltas of the Lower Acacus Formation developed in a stable basin, the sandstone lobes in each deltaic system exhibit thicknesses of 20 feet (6 m.) to 85 feet (26 m.). These sandstone lobes extend over long distances from 25 km. (16 miles) to 80 km.

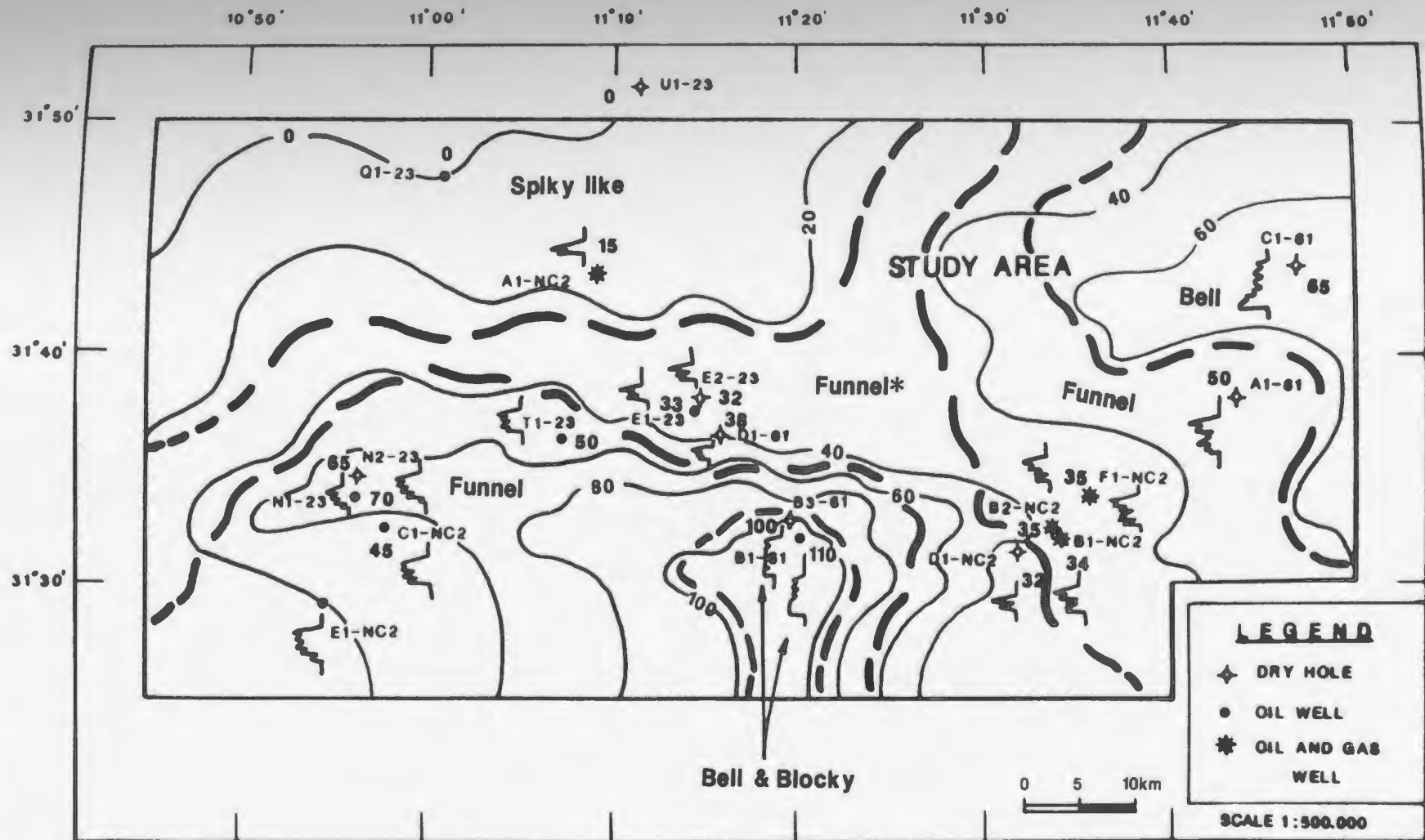
(50 miles) wide along depositional strike and 15 km. (9.3 miles) to 40 km. (25 miles) along depositional dip. This suggests that the greater the distance of progradation the greater the lateral accretion and the thinner the vertical accumulation in this relatively stable basin.

Log Facies Maps

Log facies can be defined as "...the set of log responses which characterize a bed or unit and permits it to be distinguished from the others.." (Serra, 1985; Serra, 1989). With sufficient well control, as is the case in the southern part of the study area, and by using log shapes, log facies maps can be established for the previously discussed five sandstone units (A8-A14) in the Lower Acacus Formation. Figures 31 to 35 are log facies maps which show the different facies and their log characterization in each deltaic lobe for each drilled well (see wireline-log characteristics, P.64). Integration of the log shapes with isopach maps showing the geometry of each sandstone unit, makes it possible to interpret depositional environments (Bulling and Breyer, 1989) in each deltaic lobe.

As indicated earlier (p.69) bell-shaped and blocky serrated log facies is interpreted to represent fining upward sequences of fluvial sandstones which range in

Figure 31. Log facies map for A8 sand/silt unit,
Lower Acacus Formation, NC2 concession,
Hamada Basin, NW Libya.



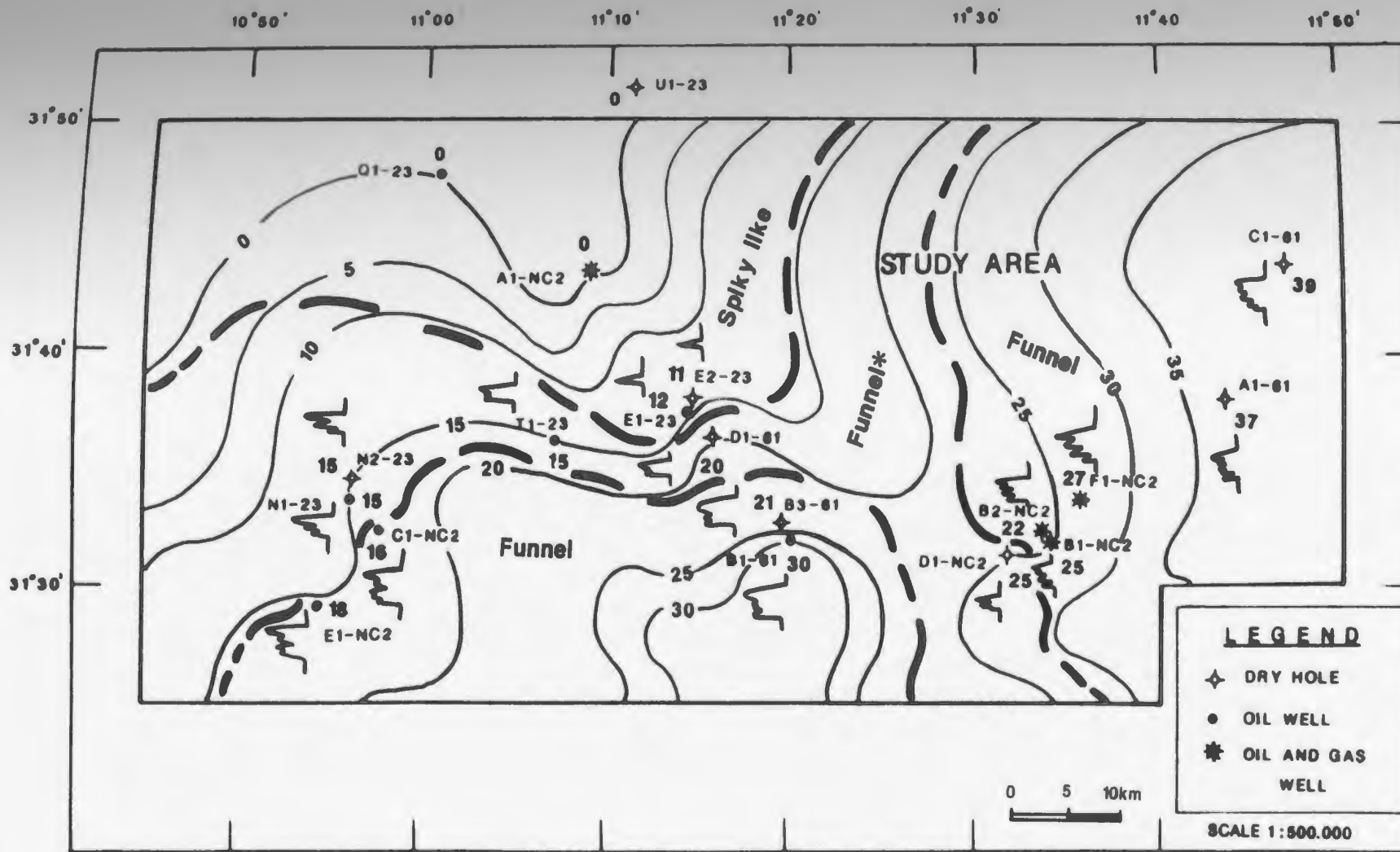
Key:

Bell & Blocky serrated shaped = Channel sand facies.
 Funnel shaped = Proximal delta front sand facies.
 Funnel* & Spiky like shaped = Distal delta front (marginal) silt facies.

OBE-91

Log facies map for A8 sand/silt unit, Lower Acacus Formation, NC2 concession, Hamada Basin, NW Libya.

Figure 32. Log facies map for A9 sand/silt unit,
Lower Acacus Formation, NC2 concession,
Hamada Basin, NW Libya.

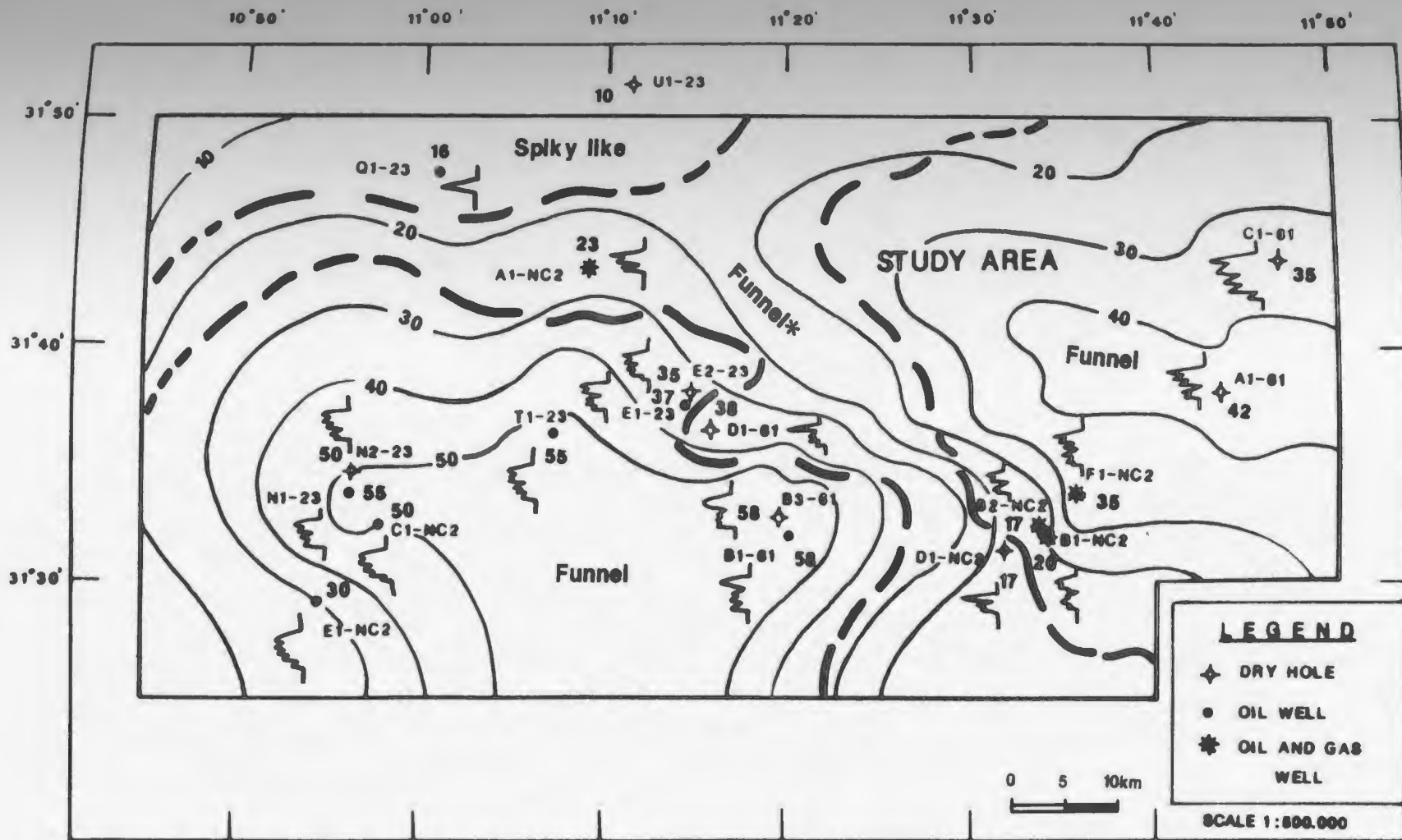


Key:

Funnel shaped = Proximal delta front sand facies.
 Funnel* & Spiky like = Distal delta front (marginal) silt facies.

Log facies map for A9 sand/silt unit, Lower Acacus Formation, NC2 concession,
 Hamada Basin, NW Libya.

Figure 33. Log facies map for A10 sand/silt unit,
Lower Acacus Formation, NC2 concession,
Hamada Basin, NW Libya.



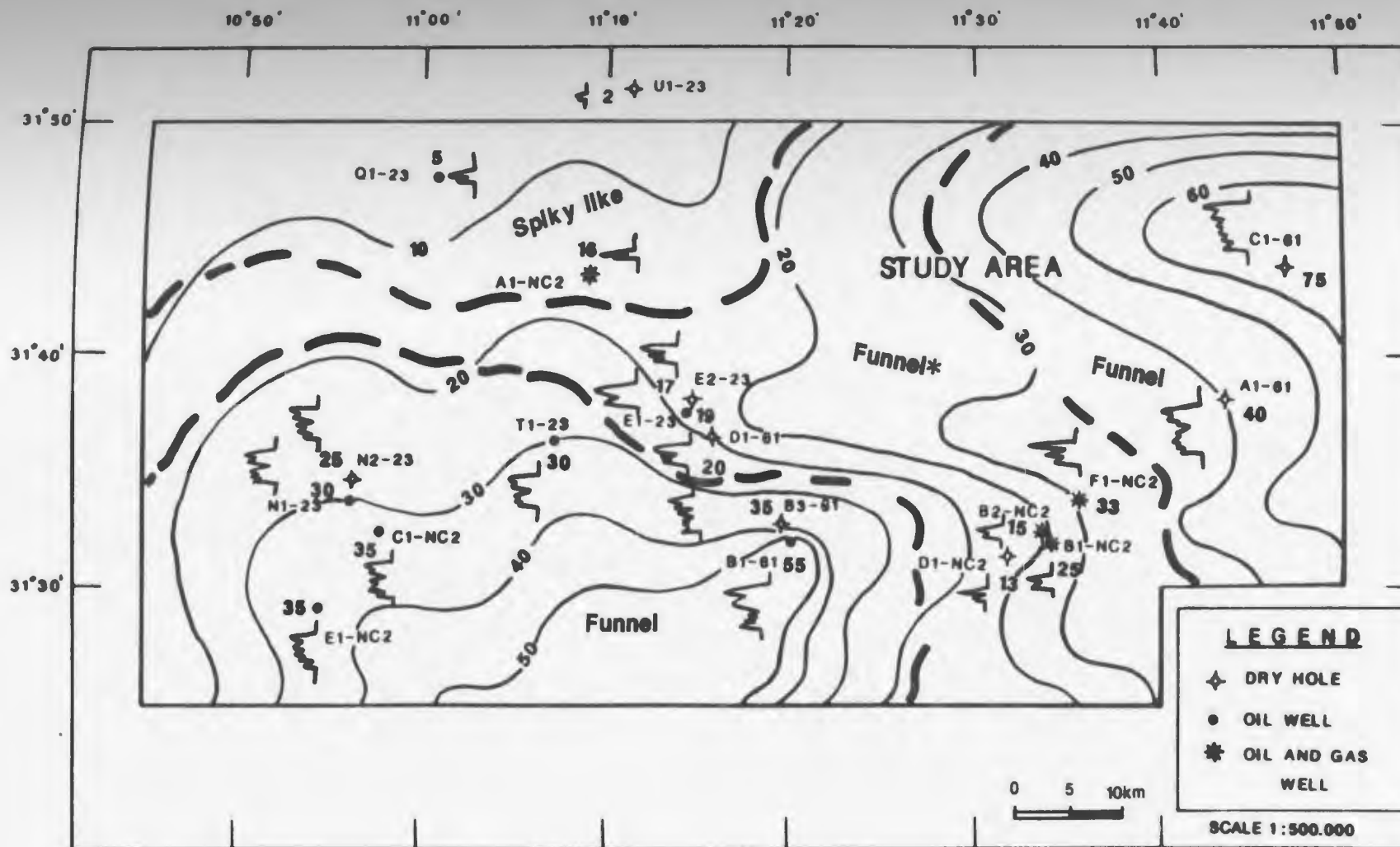
Key:

Funnel shaped = Proximal delta front sand facies.
 Funnel* & Spiky like shaped = Distal delta front (marginal) silt facies.

Log facies map for A10 sand/silt unit, Lower Acacus Formation, NC2 concession,
 Hamada Basin, NW Libya.

OBE-91

Figure 34. Log facies map for A12 sand/silt unit,
Lower Acacus Formation, NC2 concession,
Hamada Basin, NW Libya.



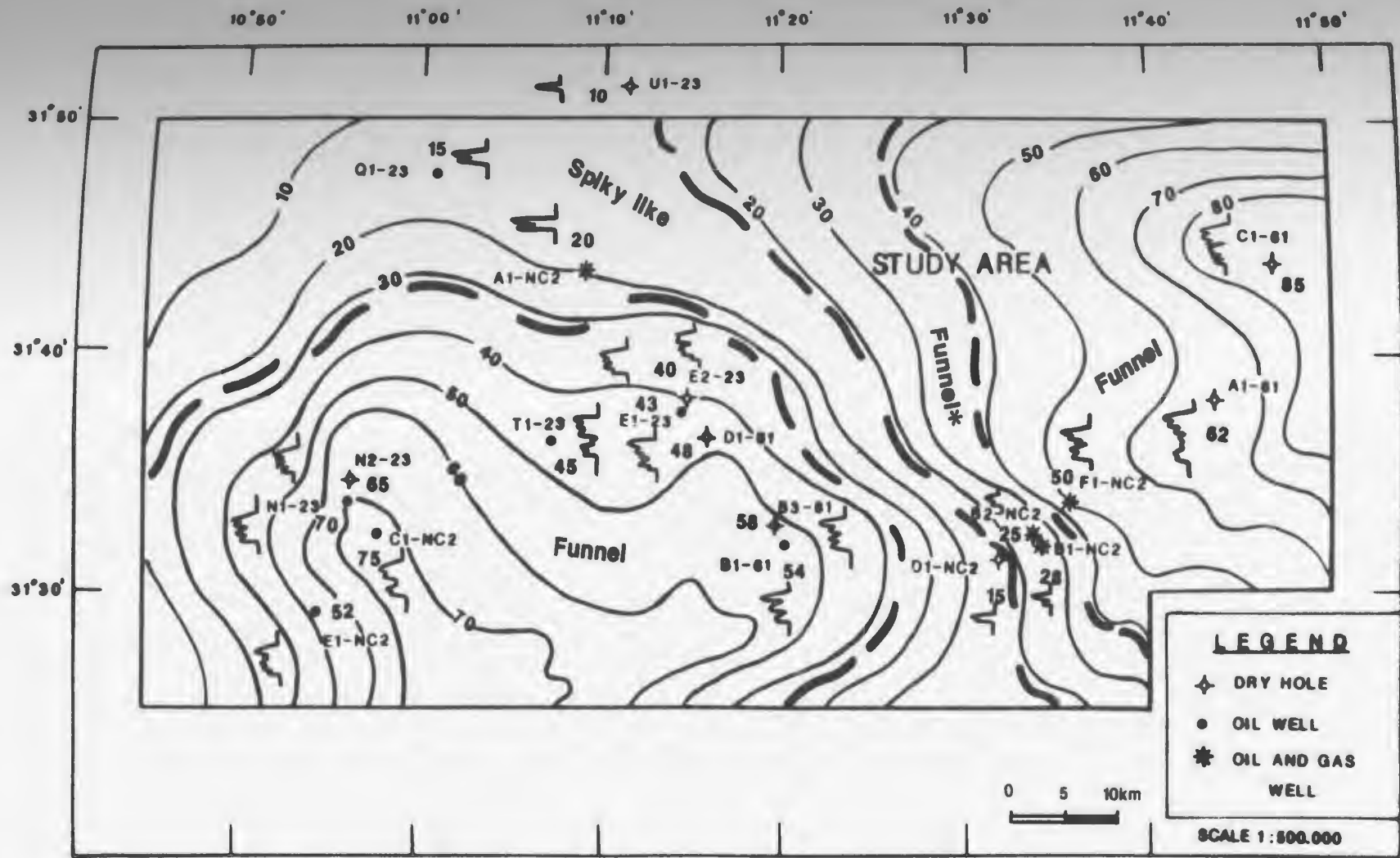
Key:

Funnel shaped = Proximal delta front sand facies.
 Funnel* & Spiky like shaped = Distal delta front (marginal) silt facies.

Log facies map for A12 sand/silt unit, Lower Acacus Formation, NC2 concession, Hamada Basin, NW Libya.

OBE-91

Figure 35. Log facies map for A14 sand/silt unit,
Lower Acacus Formation, NC2 concession,
Hamada Basin, NW Libya.



Key:

Funnel shaped = Proximal delta front sand facies.
 Funnel* & Spiky like = Distal delta front (marginal) silt facies.

Log facies map for A14 sand/silt unit, Lower Acacus Formation, NC2 concession, Hamada Basin, NW Libya.

thickness from 65 to 110 feet (20 to 34 m.) in well B1-61 and C1-61 respectively. Fluvial sandstone occur as linear sand bodies deposited in channels. These channels trend northward (in case of wells B1-61 and B3-61) and westward (in case of well C1-61), and are the means by which the sands and silts of A8 unit were transported to the deltaic shoreline in the study area.

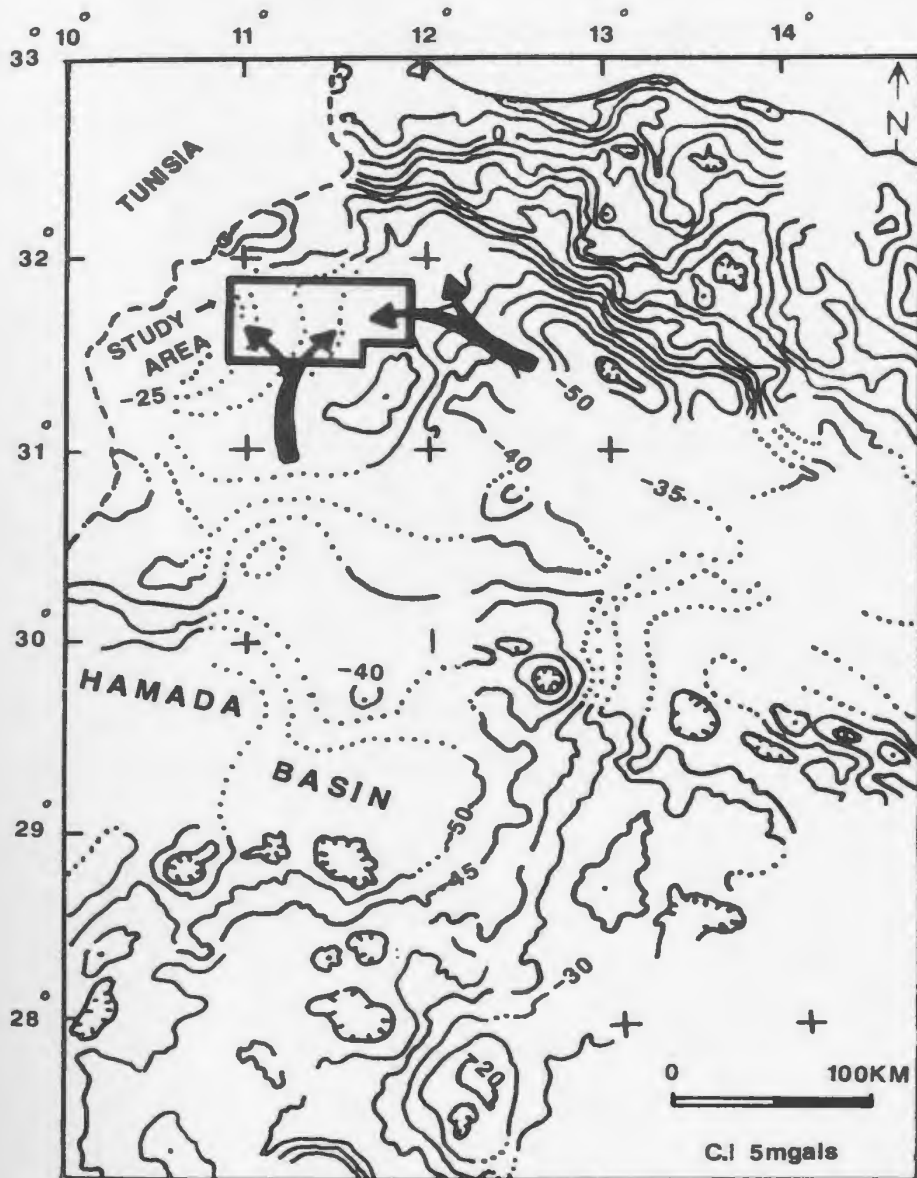
Funnel-shaped log facies (p.66) represent coarsening-upward sequences and are commonly associated with deltaic deposits. These shapes represent proximal delta front sands of 35 to 75 feet (11 to 23 m.) thick which overlie with gradational base the underlying silty shales. These funnel shapes are occasionally associated with sandstones of bell and blocky serrated log signature. Such an example can be seen in A8 unit (Encls. 2 and 3).

The seaward extent of this funnel facies is the small scale, 16 to 35 feet (5 to 11 m.) thick funnel-star (Funnel *) shaped silty sandstone unit of the distal delta front. These are the transitional units between funnel sands and spiky-like silty sandstone units of the most marginal deltaic facies. As thin deltaic lobes extend seaward from the main thick sand bodies, a thin (usually cuts low isopachs of ≤ 16 feet), spiky-like silt unit enclosed between shales is observed which represents the distal end of the deltaic lobe. A good example can be seen

in Figs.34 & 35, between wells A1-NC2, Q1-23, & U1-23, where the sand facies change transitionally to the north from the funnel-shaped of the proximal delta front facies, to the funnel-star shape of the distal delta front, to the spiky-like shape of the silt and shale facies of distal delta front margin.

Additional support for the existence of two deltaic systems, one sourced from south and the other from east, is revealed by the gravity map (Fig. 36, Essed, 1978) on the top of basement. Gravity highs to the south and east-southeast of the study area suggest basement highs between which northward and westward transported sediments reached the coastline and contributed to the existence of deltaic systems in the study area.

Figure 36. Gravity anomaly of the Hamada Basin,
NW Libya. (Adapted from Bouger gravity
map of Libya; Essed, A.S., 1978).



Key:



Possible fluvial transport directions relative to basement gravity anomalies.

Gravity map of the Hamada Basin, NW Libya.

Sandstone Percentage Map

Figure 37 depicts the relative amount of sandstone to the total thickness of the Lower Acacus Formation. The general decreasing trends of sandstone percentage are to the north in the vicinity of well A1-NC2 (10%) and well Q1-23 (8%), and to the southeast in the vicinity of wells F1-NC2 (13%), B1-NC2 (12%), B2-NC2 (12%) and D1-NC2 (12%). Sand percentages tend to be low because there is a high percentage of shale in these sequences. In this study the sand-shale ratio map best communicates the nature of the interrelation between these two lithologies.

Sand-Shale Ratio Map

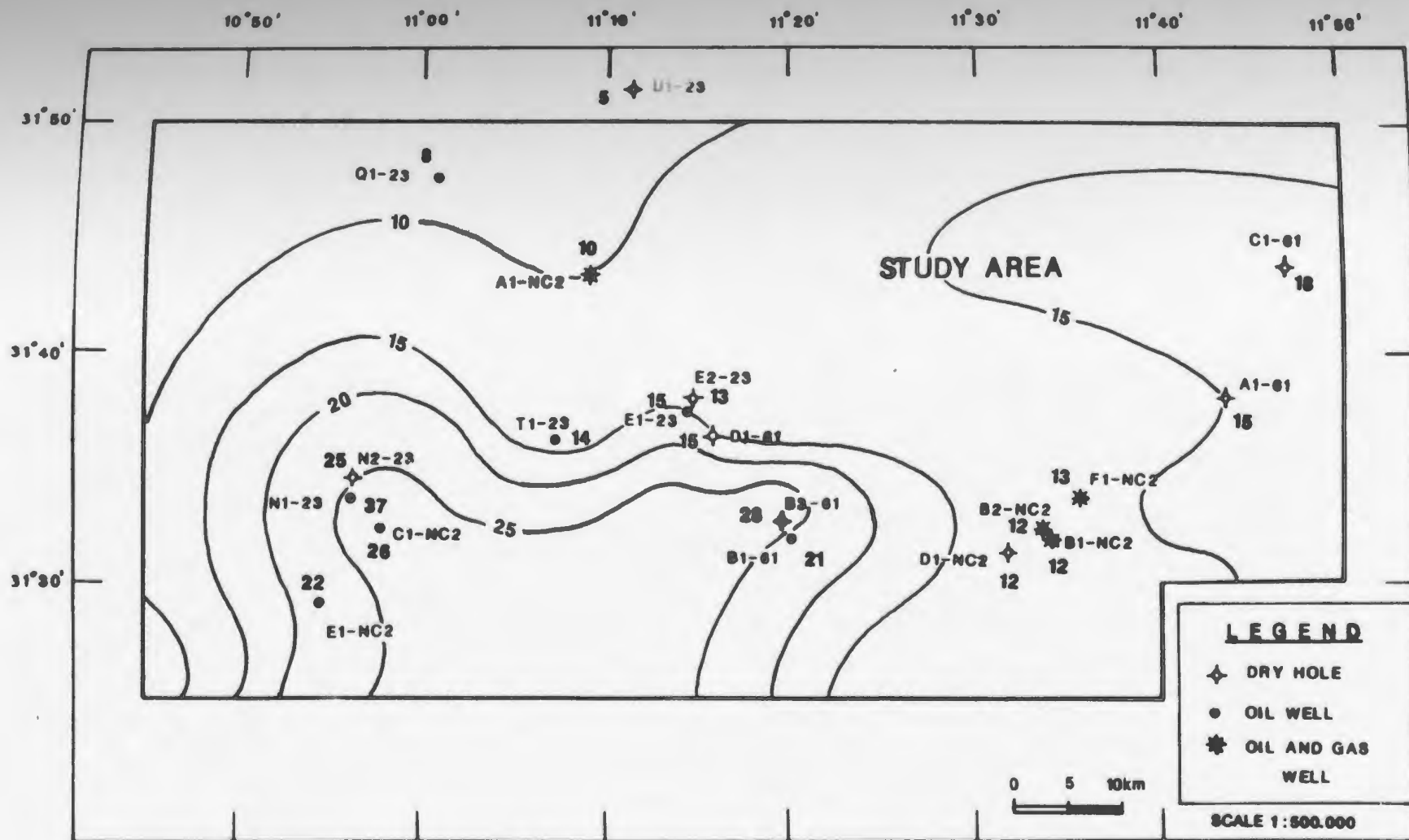
The thickness ratio of sand relative to shale (Fig. 38) reveals the interrelation between these two lithologic components (Krumbein and Sloss, 1963).

The inter-play between sand and shale can be expressed by ratio contours $1/4$, $1/6$, $1/8$ and $1/10$, where the $1/4$ contour represents one fourth of a foot of sandstone per one foot of shale; similarly for the other ratio contours. In Figure 38 the ratio contours divide the study area into an area of relatively high sandstone ratio concentrated to the south in wells E1-NC2, C1-NC2, N1-23, T1-23 and B1-61

and to the east in wells A1-61 and C1-61, and an area where the mainly shaly units are concentrated to the north in wells A1-NC2, Q1-23 and U1-23 and to the southeast of the study area in wells B1-NC2, B2-NC2, D1-NC2 and F1-NC2.

Comparison of the percentage map (Fig. 37) with the ratio map (Fig. 38) indicates equivalent contour configurations where ratio contours $1/4$, $1/6$, $1/8$ and $1/10$ correspond to the sandstone percentages of 25%, 17%, 13% and 10% respectively. Since we are dealing with only two end members-sand & shale the maps are the same; the contours differ in value only.

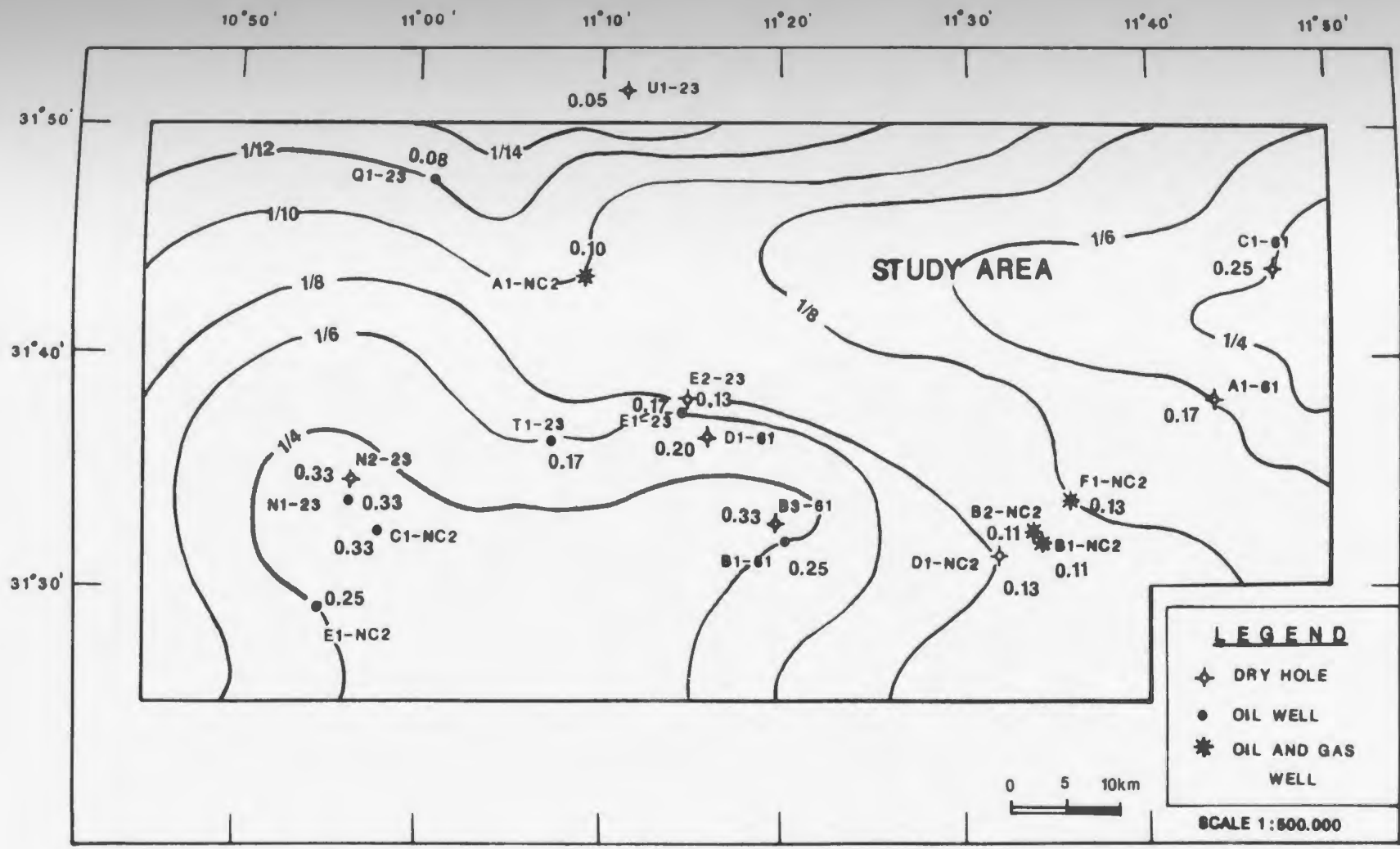
Figure 37. Sandstone percentage map of the Lower
Acacus Formation, NC2 concession,
Hamada Basin, NW Libya.



OBE-91

Sandstone percentage map of the Lower Acacus Formation, Hamada Basin,
NW Libya. " C.I 5 percent "

Figure 38. Sand-Shale ratio map of the Lower Acacus
Formation, NC2 concession, Hamada Basin,
NW Libya.



OBE-91

Sand-Shale ratio map of the Lower Acacus Formation, NC2 concession, Hamada Basin, NW Libya.

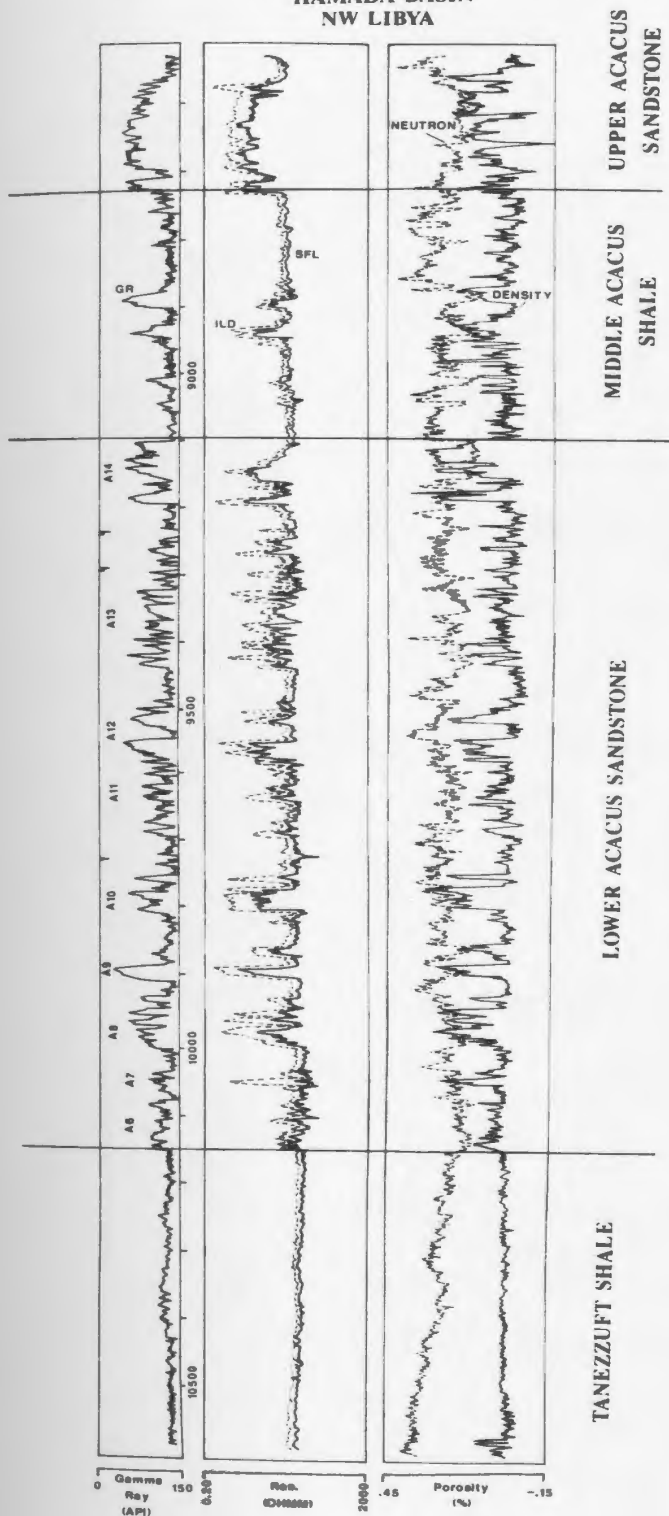
DEPOSITIONAL ENVIRONMENTS AND LITHOFACIES

Depositional Environments and Processes

The Acacus Formation in the Northern flank of the Hamada Basin is divided into the Lower and Upper Acacus sandstone units separated by interbedded shales and siltstones of the Middle Acacus unit. This present study is restricted to the Lower Acacus sandstone, in which a number of coarsening-upward sandstone units have been encountered (Fig. 39). Stratigraphic correlation of well logs of the Lower Acacus Sandstone (Encls. 1, 2 & 3) and detailed study of cores (App.I) substantiate the interpretation that this unit originated as a deltaic complex deposited during "...shoreline progradation under a high rate of sedimentation.." (Weimer, 1978). Three important processes; progradation, channel shifts and abandonment of deltaic bodies, have dominated the sedimentation throughout the northern flank of the Hamada Basin. An ideal delta cycle is characterized by the deposition of sedimentary packages 200-300 feet (61-91 m.) thick of sediments by active northward progradation of distributaries in the Hamada Basin area. This progradation (constructional phase) is due to the northward sediment influx with a relative low rate of subsidence, and to some

Figure 39. Type log of the well E1-NC2, NC2
concession, Hamada Basin, NW Libya.

E1-NC2
 NC2 CONCESSION
 HAMADA BASIN
 NW LIBYA



Type Log of Well E1-NC2, NC2 Concession, Hamada Basin ,
 NW Libya, Showing The GR, Resistivity and Porosity Logs of
 The Lower Acacus Sandstone Units.
 Note: The Coarsening-upward Nature of Each Sandstone Unit .
 Depth Divisions on Logs Are 100 Ft (30.48 M) Apart.

extent with associated compaction (Galloway, 1975; McBride, Weidler and Wolleben, 1975), by which larger thicknesses of sands and silts are accommodated, and thick delta lobes responsible for the deposition of delta front deposits are developed, which are characterized by a specific electric log pattern reflecting a coarsening-upward nature.

Channels shift because of high rates of sedimentation in shallow water in the absence of any significant subsidence (relatively stable basin). More sediment comes into the basin than can be accumulated in a given location. Deposition of this sediments acts as an obstacle which causes major channel shifting from the original site to nearby lower areas for gradient advantage (Saxenna, 1976a ; Blatt, Middleton and Murray, 1980). When a delta undergoes a channel shift, the delta is abandoned and subsequently is then subjected to marine encroachment (destructional phase) involving reworking of the constructive delta surface (Fisher and McGowen, 1969; Coleman, 1981). Wave reworking and modification of the abandoned delta front produces the marine sands of spiky log nature which overlie the earlier delta front deposits, Eventually, deposition of marine shales occurs as a result of net transgressive conditions. This orderly repetition of depositional events and shifting sites of sedimentation results in "...numerous overlapping

of vertical regressive deltaic sequences separated by shallow marine deposits.." (Coleman, 1981). The overall sequence of the Lower Acacus Formation consists of an alternating sequence of sandstones and shales with an overall thickness of about 1180 feet (360 m.). In the study area, nine persistent sandstone units have been observed in the Lower Acacus Formation and termed in ascending order; the A6, A7, A8, A9, A10, A11, A12, A13 and A14 units (Fig. 39 and Encls. 1 to 3).

The sandstone units have gradational lower contacts, coarsen upward in response to an upward increase in flow regime and sand content and are abruptly overlain by dark gray, greenish black marine shale (Fig. 39 and Fig. 40).

According to (Berg, 1986), the upward transition from marine shale to siltstone to sandstone is typical of deposition within a prograding sand body of deltaic origin. Within the study area the Lower Acacus Sandstone units studied in core sections exhibit sequences of sedimentary structure and texture (see Appendix I & 2) indicative of coastal-deltaic to shallow marine origin. These units are interpreted to have formed as distributary mouth bars (proximal delta front) characterized by fine to medium grained sandstone, with horizontal lamination to low angle laminations and some carbonaceous debris, overlying the bioturbated calcareous silty sandstone unit of the delta

fringe (distal delta front) where the diversity of bioturbation" suggest deposition in shallow-neritic environment of low energy conditions." (Keltch et al., 1990) (see Appendix I for core description).

The regressive episodes that deposited the Lower Acacus Sandstone units were punctuated by a period of rapid transgression with deposition of dark gray, greenish black, silty marine shale. Minor bodies of sandstones enclosed within the marine shale are believed to be the result of the delta-front edge being reworked by longshore currents (Berg, 1986). Such processes may have been the mechanism that produced the linear morphology observed, and which is characterized by relatively very fine to fine grained rarely medium grained, glauconitic calcareous sandstones. Such sand bodies are very common at the northern edge of each delta lobe along the sequence in the study area (Encls. 1 to 3).

Sandstone of fluvial origin is encountered only in well B1-61 at 9140-9310 feet, in well B3-61 at 9275-9437 feet, and in well C1-61 at 8135-8365 feet as judged from the response of the borehole logs (Encl. 3). The logs record responses which are blocky serrated and bell shaped, suggesting the upward-fining sandstone sequence of mainly fluvial origin (fluvial channels). These fluvial channels

cut through the surrounding deltaic sands (lobes) depositing, thick, and less continuous sandstone bodies, through which northward and westward transported sands are responsible for the formation of some delta lobes in the study area. (Example; In the case of wells B1-61 and B3-61, fluvial channels of blocky-serrated SP log response have been observed at 9140-9310 ft. and at 9275-9437 ft. respectively. These are interpreted to be the feeder channels for the deltaic lobes of A7 and A8 units deposited to the north in wells D1-61 and E1-23 (see Encl.2). In the case of well C1-61, a fluvial channel of bell shaped GR response has been observed at 8135-8365 ft. This channel may be responsible for the formation of the deltaic lobes of A7 and A8 units deposited westward in well A1-61 (see Encl.3))

Lithofacies

Lithofacies are the key to determining depositional environments of the Lower Acacus Sandstones, NC2 concession, Hamada Basin, northwest Libya. Furthermore, reservoir quality of these sandstones is directly related to lithofacies variability.

Thirty-four (34) core sections have been cut through different intervals in the Lower Acacus Sandstones with a total of 1230 feet (375 m.). The recovered cores account

for 89% of the total cored section. Friable sand accounts an additional 4% of the total section. Approximately 7% of the total section is missing due to reboxing, sampling, well trade, or parts of the cores are mislocated or misoriented. Wireline-logs were used to minimize these problems.

14 cores demonstrate the validity of environmental interpretations of well log responses against the different types of sandstones through the sequence. These cores are cut in the following wells:

E1-NC2; C #1, #2 (9105-9126 ft, 9126-9146 ft)
(Figs. App.I-1, App.I-3).

C1-NC2; C #1, #2 (9621-9642 ft., 9642-9672 ft.)
(Figs. App.I-4, App.I-5).

T1-23; C #2 (8458-8502 ft.) (Figs. App.I-6, App.I-7).

Q1-23; C #1, #2 (7440-7470 ft., 7470-7485 ft.)
(Figs. App.I-10, App.I-13).

C #3 (8170-8200 ft.) (Figs. App.I-11,
App.I-13).

C #4 (8461-8497 ft.) (Figs. App.I-12,
App.I-13).

B1-61; C #4 (8459-8518 ft.) (Figs. App.I-14,
App.I-15).

B3-61; C #5 (9310-9365 ft.) (Figs. App.I-18,
App.I-19).

C1-61; C #3 (7507-7555 ft.) (Figs. App.I-21,
App.I-24).

C #4 (7770-7828 ft.) (Figs. App.I-22,
App.I-24).

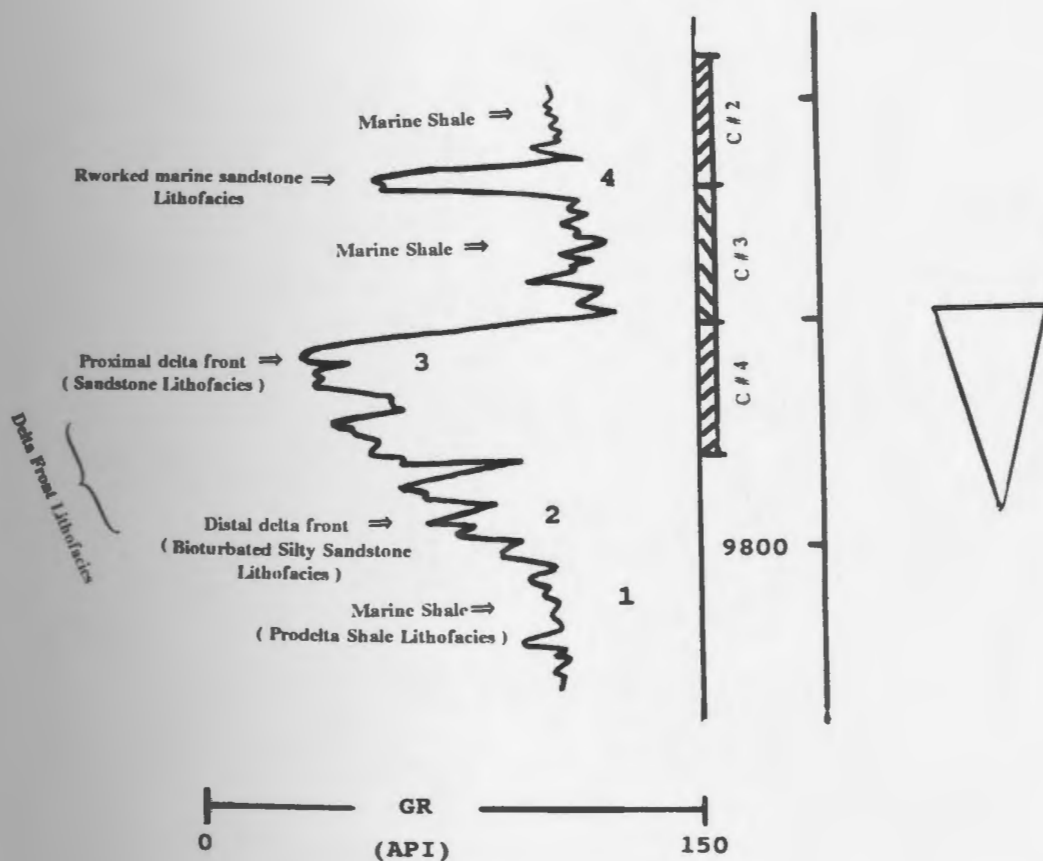
and
D1-61; C #10 (8845-8885 ft.) (Figs. App.I-27,
App.I-28).

Five lithofacies types (types 1 - 5) (see Figures 40 and 41) are recognized within the Lower Acacus Sandstone. These lithofacies are based on particular associations of rock types, sedimentary structures, and electric log patterns. They are presented below in depositional sequence from base to top:

1. Dark gray, greenish black, finely laminated occasionally bioturbated shale (marine).
2. Bioturbated silty sandstone (distal delta front, marginal).
3. Horizontal to low angle cross-laminated to indistinct laminated, fine to medium grained sandstone. This equates to the proximal delta front of Weimer, 1978 & represents the principle hydrocarbon producing lithofacies in the study area.
4. Glauconitic, calcareous, wavy laminated, very fine to fine grained sandstone (reworked marine sandstone) (Fig. 40)
5. Low angle, cross-laminated to parallel laminated, medium to fine grained sandstone which is occasionally silty and clayey with some bioturbation. This corresponds to the sandstones of fluvial origin.

Figure 40. Gamma-Ray (GR) log pattern of the deltaic facies in the Lower Acacus Formation, NC2 concession, Hamada Basin, NW Libya.

**C1-NC2
Hamada Basin
NW Libya**



Gamma-ray log (GR) patterns of the deltaic facies in the Lower Acacus Formation, NC2 Concession, Hamada Basin, NW Libya.

Lithofacies Descriptions:

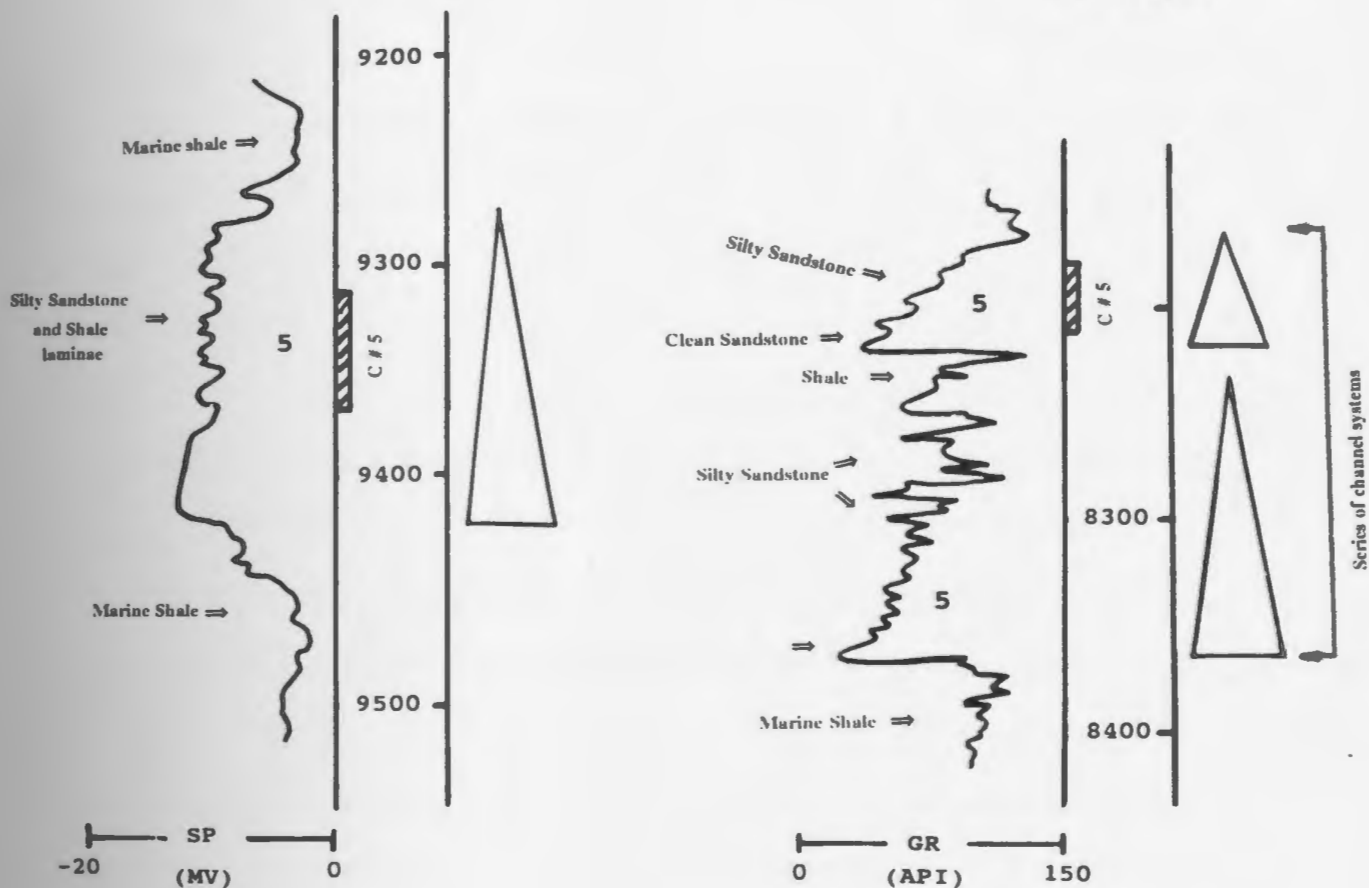
- 1-Dark gray, black, laminated occasionally bioturbated marine shale.
- 2-Bioturbated silty sandstone.
- 3-Horizontal, cross laminated, carbonaceous fine to medium grained sandstone.
- 4-Glauconitic, wavy laminated, rippled, reworked marine sandstone.

" Depth divisions are 50 ft (15.24m) apart "

Figure 41. Well-log motif (SP & GR) showing characteristics of the fluvial channel facies and their sequences in the Lower Acacus Formation, NC2 concession, Hamada Basin, NW Libya.

**B3-61
Hamada Basin
NW Libya**

**C1-61
Hamada Basin
NW Libya**



Well-log motif (SP & GR) showing characteristics of the fluvial channel lithofacies and their sequences in the Lower Acacus Formation, NC2 concession, Hamada Basin, NW Libya.

Left electric log (SP) from well B3-61 indicating fining-upward to blocky log nature, the curve is generally smooth at the base opposite to the clean sandstone and becomes serrated as the silty sandstone and shale laminae (channel fill deposits) increase toward the top. Lithofacies 5- Low angle cross laminated to horizontal laminated, occasionally bioturbated complex sandstone.

Right gamma-ray log (GR) from well C1-61 indicating series of channel systems of typical fining-upward log nature. Lithofacies 5- Clean sandstone to silty-clayey sandstone.

" Depth divisions are 100 ft (30.48m) apart "

1. Finely laminated - Bioturbated shale

This facies consists mainly of thick sequences of dark gray, greenish black shale occasionally micaceous with rippled lenticular silty sand lenses (0.05-1 feet thick) (App.II - A) occasionally are finely laminated when burrowing has not obscured the laminae (App.II - B). Some soft sediment deformation features are locally preserved (App.II - C,D) and tend to be silty at the top of the section. The facies becomes more highly bioturbated and burrowed in places at the base (App.II - E). The pervasive burrowing activity in the silty shale beds indicates "...relatively slow depositional rates in the absence of substantial wave and current agitation.." (Chan and Dott, 1986). Generally this facies is characterized by a predominance of black shale, lack of abundant sedimentary structures (App.II - F) and a relative increase in the bioturbation down section.

2. Bioturbated silty sandstone

Occurring gradationally at the top of the marine shale with a thickness of 2 to 7 feet (0.6 to 2.1 m.) thick, this facies consists of very silty sandstone which is occasionally very fine grained, dark gray, grayish cream in colour. Some ripple lamination

occurs, but the facies is usually bioturbated and burrowed with very distorted structure as in well C1-NC2 at 9648 ft, and well E1-NC2 at 9515 ft and well A1-NC2 at 7826.5 ft (App.II - G,H & I). The sediment tends to be calcareous and to show a high percentage of clay matrix (10%-15%). There are occasional minor contorted laminations, especially in well C1-NC2 at 9633 feet and 9651 feet. In well T1-23 at 8468 ft. these contortions may be due to differential loading (Coleman and Gagliano, 1965; Erxleben, 1975). The facies has a generally gradational contact with the upper fine to medium relatively cleaned sandstone (App.II - J).

(See App.III-D,E for thin-section-lithofacies type).

3. Horizontal-low angle cross laminated, carbonaceous sandstone.

Overlying the bioturbated silty sandstone are sandstones which are calcareous in part and which occasionally contain carbonaceous debris and clay clasts (App.II - K). This sandstone consists of moderately to well sorted, subangular to rounded grains. The sandstones of this lithofacies are texturally mature and show an upward decrease in matrix percent ($\leq 3\%$) (Fig. 45).

Sedimentary structures include horizontal parallel to indistinctive lamination (App.II - L) or low angle cross-laminations at top of the unit (App.II - M) suggesting a relatively high energy lithofacies. Most core sections of sandstone units of this facies are slabbed and occasionally have vertical burrows (App.II - N) of "...skolithos trace fossils..." (Chamberlain, 1978) which indicates high energy environments.

The vertical sequence of the above lithofacies (1-3) shows a difference in texture and an increase of sedimentary structures upward; from laminated to bioturbated shale (lithofacies No.1), to bioturbated silty sandstone (lithofacies No.2), to fine to medium grained sandstone with horizontal to cross laminations (lithofacies No.3). This suggests a transitional relationship from prodelta-marine shale (No. 1) to delta-front & coastal silts and sands (No. 2, No. 3). (See App.III-A,B and C for thin section lithofacies type).

In addition to the sandstones of the constructional delta front facies, some local sandstone lenses (lithofacies No.4) occur along the fringes of the delta (Brown, 1975), enclosed within the marine shale (App.II - O).

4. Glauconitic, calcareous, wavy laminated sandstone.

These sandstones are less extensive than lithofacies 2 and 3, with thicknesses ranging from 2 to 20 feet (0.61 to 6.1 m.). They occasionally show either a general fining-upward or coarsening-upward log signature. They usually occur as sand lenses (or stringers) of spiky log nature (Fig. 40) as can be seen clearly in well Q1-23 from 8180 to 8193 ft., and from 7459 to 7470 ft. (Encl. 1).

These sand lenses are composed of very fine to fine-grained sandstone or occasionally of medium grained sandstone, silty at the base, glauconitic (App.III- F, App.IV- O,P) (similar sandstones have been described by Hubert et al, 1972). The tops of analogous stringers were either "...shallow or deep and reworked by waves and current action..." (Turner and Conger, 1981). Such processes were responsible for the relatively quartz-rich sand. Both wave and current action could have produced the common thin wavy lamination to low angle cross laminations (App.II- P). Rarely, there is bioturbation.

In general, these marine sand bodies are most prominent in the northern part of the study area, especially in well A1-NC2, well Q1-23 and well U1-23 (Encls. 1 to 3). The less extensive nature of these

sand lenses and their locations in front of each deltaic sand package attests to a destructional phase origin for these sands. They may have been formed by intermittent wave or current activity.

(See App.III-F,G for thin section-lithofacies type)

5. Low angle cross laminated to parallel laminated medium to fine grained complex sandstone.

The presence of channel system deposits are emphasized by isolated, thick, less continuous sandstone bodies of fining-upward or blocky serrated log nature (Fig. 41). They are observed to occur especially in well B1-61 from 9140 to 9310 feet, in well B3-61 from 9275 to 9437 feet and in well C1-61 from 8135 to 8365 feet (Encl. 2 & 3). The exact extension and configuration of these channels is difficult to interpret from the existing well control. It is possible that these channels can be correlated with channels to the south in wells III-NC7 and C1-NC7A. That possibility is presented in this study (see regional stratigraphic cross section Encl. 2).

The lowest sequence of these sandstone units was not cored, only the uppermost fluvial channel was recovered in well B3-61 (Fig. App.I-18) and in well C1-61 (Fig. App.I-23). Based on log interpretation,

the fluvial channels in the study area (Encls. 2 & 3) rest abruptly on the marine shale and cut through the deltaic sand units (A7 and A8).

The sediment of this lithofacies is generally massive, unbedded with some low angle cross-lamination and horizontal lamination. It represents a relatively clean sublithofacies at base and fines upward from light-gray whitish gray fine to medium grained sandstone to dark gray, silty sandstone with matrix percent increasing to >15% (see p.168). This interval represents the low energy sublithofacies of channel-filling deposits which occur during late stage of deposition as the channels are filled and abandoned (Tillman and Jordan, 1987).

Small fining-upward and coarsening-upward cycles are repeated along the cored interval at different levels in the channel sandstones. These cycles are interbedded with dark gray shale (Fig. App.I-18) and thin-section samples show that the channels are filled with complex, poorly sorted, fine silty sands and clayey sands (with grain size ranging from 0.05-0.12 mm.) with increase in clay matrix upward (App.III-L,M). This lithofacies represent fluvial channel deposits which prograded northward and cut through the delta facies, leaving a strong imprint of

superimposed fluvial character on the sandstone facies complex.

Channel lithofacies of similar ancient environments have been described by Cherven (1978); Hyne, Cooper and Dickey (1979); Berg (1979) and Rice (1980). (See App.III-H to M for thin-section-lithofacies type).

Depositional Model-Lower Acacus Sandstone:

The Lower Acacus Sandstone core intervals (App.I) display clear vertical transition from marine to nearshore-coastal deltaic rock types, where the entire core sections represent different lithofacies of deltaic complex environments. From well-log characteristics and correlation in Enclosures 1 to 3, the Lower Acacus Formation displays an ordering of the depositional sequence that makes it possible to construct a generalized depositional model for the Lower Acacus sandstones (Fig. 42). 14 sand-silt units (A1-A14) have been recognized and their lateral relationship from continental to marine environments can be seen.

The sandstone units may be visualized as individual lobate bodies (as supported by the isopach patterns; Fig.

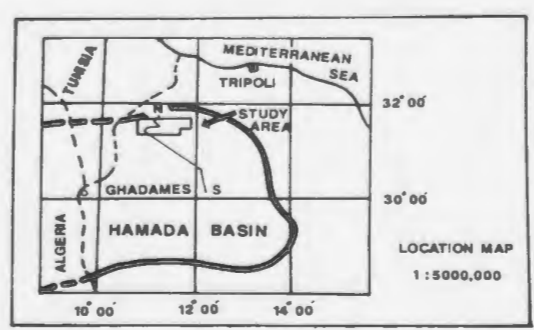
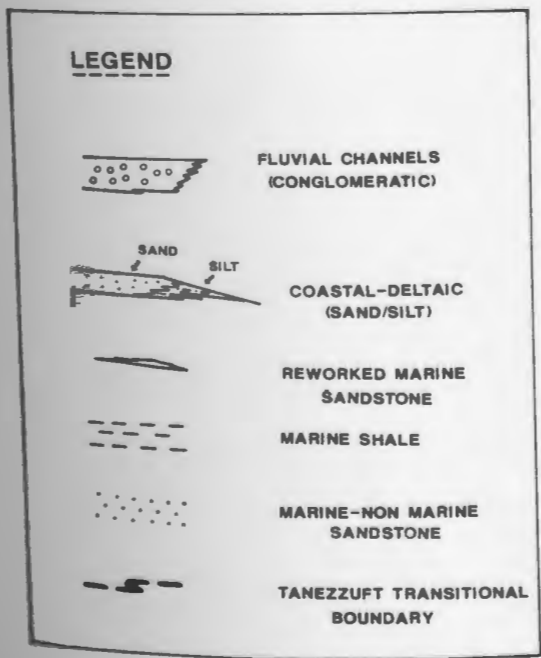
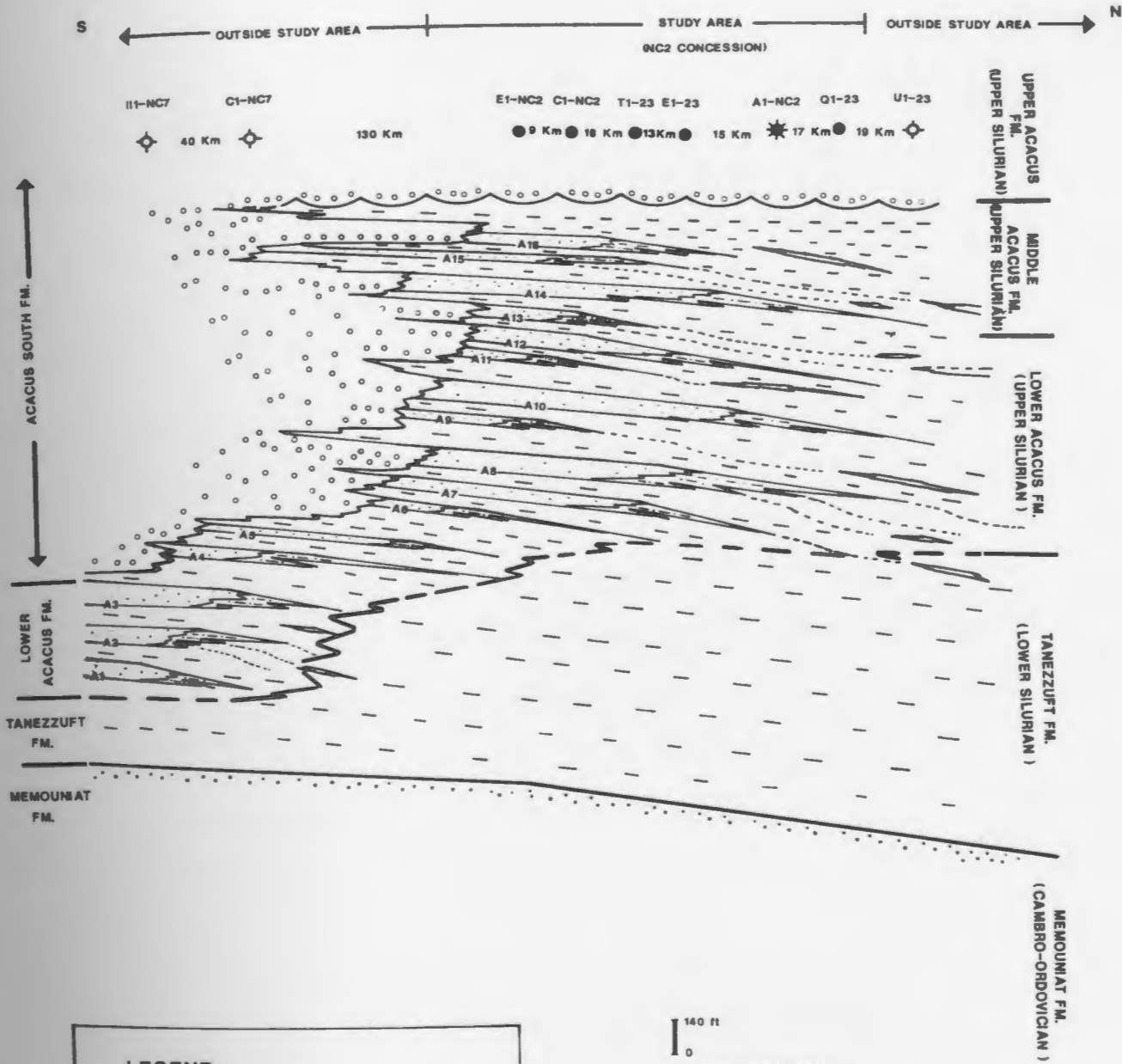
25 to Fig. 29), composed of silty sandstone (distal part of the lobe) succeeded by clean, fine to medium grained, occasionally carbonaceous, sandstones (proximal part of the lobe). Each individual lobe was sourced from the south and was confined to a local area during a regression phase (or progradation of shoreline) until the distributary system shifted. A new delta lobe formed at an adjacent site once the shift occurred. Eventually, the deltaic lobe was abandoned and inundated during a period of marine transgression and buried by thick deposits of marine shale.

Individual vertical sequences in any well can penetrate different lobes at different positions (proximal part of the lobe or marginal part of the lobe). As a result one can conclude that the northern side of the study area in the vicinity of well A1-NC2, well Q1-23 and well U1-23, will be characterized by the more silty-shaly sandstones of the marginal part of the northward prograded sand bodies. Wells in the southern and central part of the study area in the vicinity of wells E1-NC2, C1-NC2 and T1-23 have the greatest chance to recover clean sandstones of the proximal delta front facies of the various deltaic lobes.

Similar sequences have been identified for the Mississippi delta (Coleman and Gagliano, 1964). This

schematic depositional model depicts that the transition from Tanezzuft shale (Lower Silurian) to regressive coastal-deltaic Lower Acacus sandstone lobes (Upper Silurian) is diachronous.

Figure 42. Schematic depositional model for the Lower
Acacus Formation, Hamada Basin, NW Libya.



OBE-91

PETROGRAPHY

Petrographic information for this study was obtained from pointcounts (300 point per slide) of 70 thin-sections. Samples for thin-sectioning were taken from 25 cores in the Lower Acacus sandstones, and were prepared through the assistance of the Arabian Gulf Oil Company technical staff, Benghazi, Libya. Both line and line-traversed ribbon methods (Galehouse, 1971) of pointcounting have been used, following the description scheme recommended by Harwood (1988). All thin-sections were stained for carbonate (Dickson, 1965, 1966; Miller, 1988). For procedures and staining techniques for carbonate in thin-section, see Appendix VI.

The petrographic analyses reveal the primary and authigenic mineral composition and texture for all examined sandstone units.

Detrital grains

The Lower Acacus sandstone is very fine to medium grained. Mean grain size of individual sandstone intervals ranges from 0.15 mm. - 0.34 mm. (Table 1). Average grain size for the total sand volume is 0.24 mm. Monocrystalline quartz grains are very common and subangular to well rounded. The degree of roundness increases with increasing

TABLE 1: Petrographic Data of Lower Acacus Sandstones, NC2 Concession, Hamada Basin, NW Libya.

Sand Unit	Well Name	Depth Interval (ft)	No of Samples	Grain Size (mm) ^b			Detrital Composition (%) ^c						Cement (%) ^d			Perm (md)	Poro (%)
				min	max	mean	Q	Qp	Feld	RI	Oth	Mx	Sil	Carb	Cly		
Am sd	A1-NC2	7814-7817	2	0.10	0.23	0.16	81	-	3	7	1	7	-	11	7	1085	19.0
Am sd	C1-NC2	9622-9630	2	0.20	0.30	0.25	84	8	-	7	tr	2	6	8	3	30	18.1
A9 sd/silt		9645-9649	1	0.20	0.70	0.45	80	-	-	20	tr	-	9	2	-	-	19.0
A8 sd/silt		9703-9725	2	0.27	0.40	0.34	97	-	tr	3	tr	-	18	4	-	856	20.0
A14 sd/silt	E1-NC2	9105-9145	10	0.10	0.24	0.17	77	1	tr	15	2	5	8	5	8	96	16.0
A12 sd/silt		9512-9514	1	0.15	0.40	0.28	70	13	-	14	-	3	9	20	3	11	14.6
A8 sd/silt		9960-9975	2	0.16	0.40	0.28	97	-	1	2	-	-	18	5	-	955	20.0
A14 sd/silt	T1-23	8454-8473	2	0.17	0.38	0.28	82	-	3	4	7	4	8	5	3	14704	18.0
Am sd		8489-8490	1	0.20	0.40	0.30	85	-	2	8	5	-	3	12	2	368	17.4
Am sd	Q1-23	7461-8481	7	0.14	0.32	0.23	84	tr	3	4	6	3	4	10	6	753	8.3
A14 sd/silt	B1-61	8420-8490	7	0.16	0.37	0.26	87	tr	2	6	2	3	5	9	6	1734	18.0
Am sd	B1-61	8750-8764	3	0.15	0.35	0.25	91	tr	2	4	1	1	6	8	5	381	13.0
A12 sd/silt		8893-8960	5	0.11	0.22	0.16	89	tr	2	5	3	1	7	13	2	130	11.0
A11 sd/silt		8969-8979	3	0.15	0.29	0.22	82	1	2	6	3	5	2	13	3	98	15.0
At sd		9311-9360	5	0.12	0.24	0.18	80	tr	3	7	4	5	2	6	6	48	16.8
A12 sd/silt	C1-61	7510-7529	4	0.18	0.38	0.28	91	-	2	4	2	1	6	9	3	6121	18.2
A10 sd/silt		7775-7795	2	0.15	0.38	0.26	87	-	1	6	3	3	-	4	5	279.2	17.8
At sd		8199-8208	2	0.16	0.31	0.23	81	-	1	9	3	5	2	8	7	-	14.4
A12 sd/silt	D1-61	8236-8319	4	0.16	0.35	0.25	90	-	2	4	1	3	3	13	4	436	17.0
A13 sd/silt		8420-8454	2	0.06	0.23	0.14	76	1	2	9	3	8	2	16	10	161	11.5
A10 sd/silt		8845-8872	3	0.17	0.32	0.24	85	-	3	8	3	1	4	10	1	-	-
Means of All Samples				0.15	0.34	0.24	85	1.2	1.5	7	2.3	3	6.5	9.1	4	1313	15.4

OBB-91

- ^a A8-A14 sd/silt - Acacus Deltaic Sand-Silt units; Am sd = Acacus Marine Sands; At sd = Acacus Fluvial Sands
- ^b Long Axis Measurements.
- ^c Qm = Monocrystalline Quartz; Qp = Polycrystalline Quartz; Feld = Feldspars; RI = Rock Fragments; Oth = Other Minerals; Mx = Matrix; tr = Traces.
- ^d Sil = Silica; Carb = Carbonates (Calcite, Dolomite or Siderite); Cly = Clay Cement.
- ^e Perm = Permeability, Data from Lab Core Analysis.
- ^f Poro = Average Porosity, Data from Lab Core Analysis

grain size and sorting. The mean grain size ranges from 0.16 mm. to 0.45 mm. Each sandstone unit in the Lower Acacus Formation intervals displays a distinct coarsening-upward trend (Fig. 39).

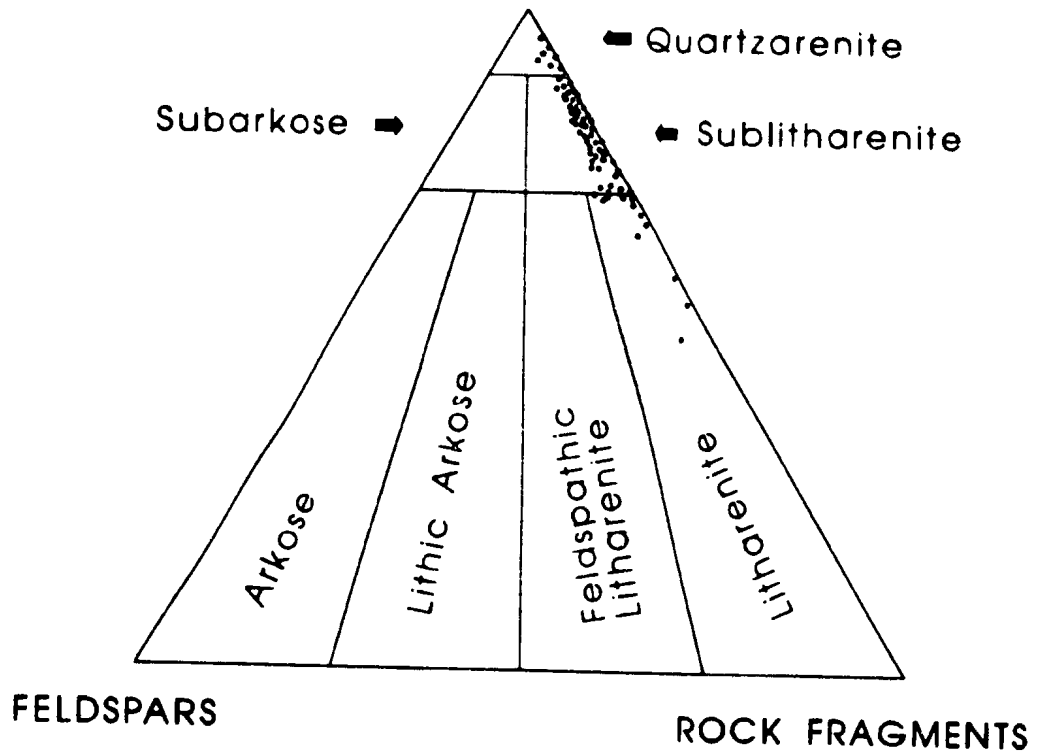
Based on Folk's (1980) compositional classification scheme of sandstone, the average detrital composition of the Lower Acacus sandstones is that of sublitharenite, with some samples of quartzarenite and others of lithic-arenite (Fig. 43). Framework grains average 85% monocrystalline quartz, 1.25% polycrystalline quartz, 1.5% feldspar, 7.00% rock fragments, 2.3% other minerals and. The feldspar content is considered to be very low or absent, while monocrystalline quartz and rock fragments are considered to be the most dominant detrital constituents in the Lower Acacus sandstones and vary widely. The quartz content increases up-section (App.III - A), with quartz grain ranging from a low of 55% in the silty-very fine grained sandstone to a high of 97% in the fine to medium grained sandstone (Fig.44).

The increase in percentage of quartz is interpreted to be due to "...winnowing of detrital matrix as a result of increasing current velocities.." (Franklin and Tieh, 1989). Quartz grains show straight (non-undulose) to undulose extinction, suggesting a contribution of granitic source terrane (Padki and Fox, 1989). Polycrystalline quartz

Figure 43. Detrital plot for Lower Acacus Sandstones,
NC2 concession, Hamada Basin, NW Libya.

QUARTZ

163

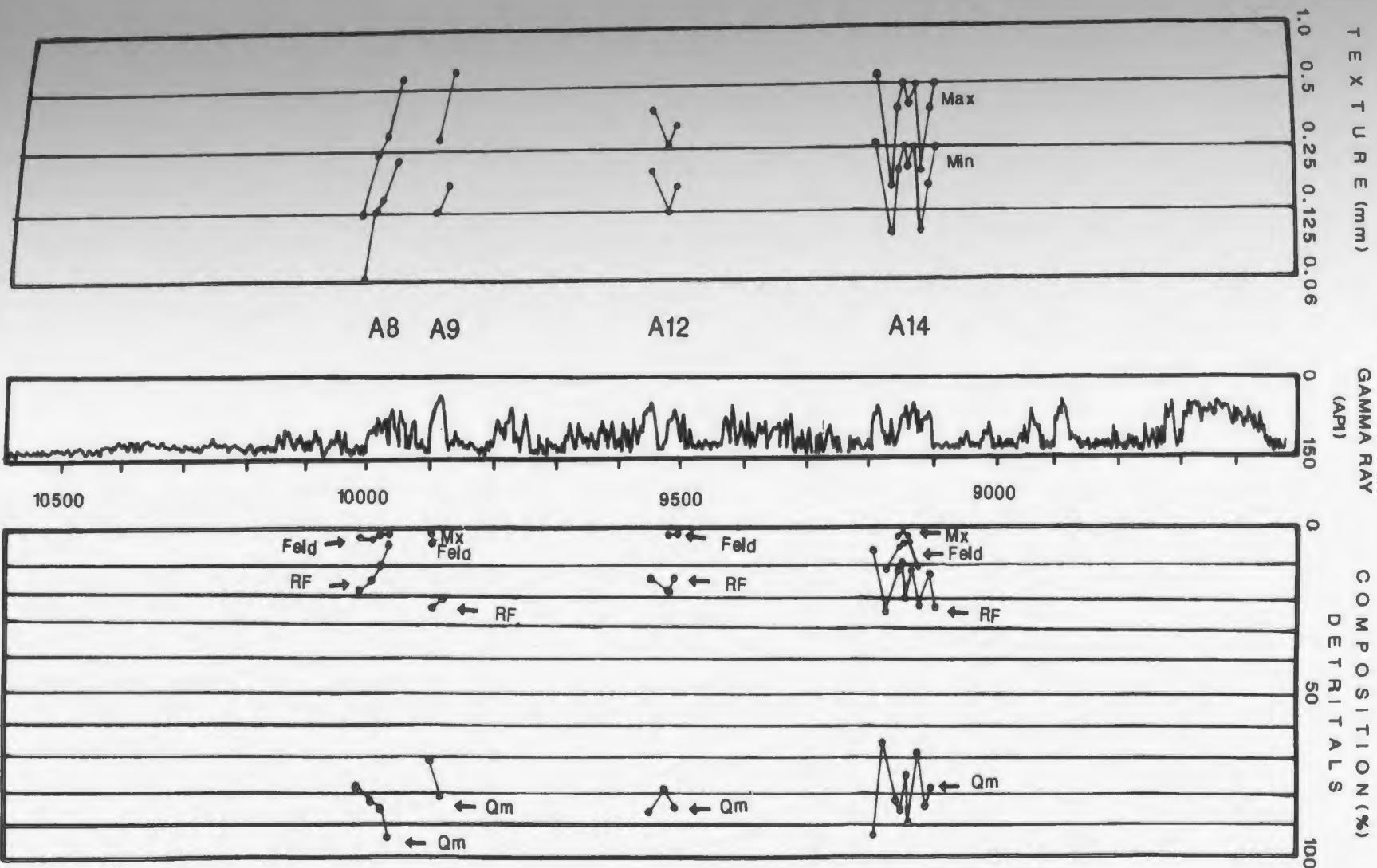


**Detrital Plot For The Lower Acacus Sandstones
NC2 Concession, Hamada Basin, NW Libya.**

" QPR classification of sandstones "
after Folk, 1980.

08E-91

Figure 44. Texture, composition and log character of
the Lower Acacus Sandstones, NC2
concession, Hamada Basin, NW Libya.



OBF-91

Texture, composition and log character of the Lower Acacus Sandstone, NC2 concession, Hamada Basin, NW Libya. Detrital composition is divided into monocrystalline quartz (Qm), Feldspar (Feld), rock fragment (RF) and clay matrix (Mx). Depth divisions are 100 ft (30.48m) apart.

grains are much less abundant, representing an average of 1.2% of the total detrital composition when present. The grains have the form of stretched and/or foliated polycrystalline quartz (App.IV - A), implying that metamorphic rocks were minor (possible) contributors to the sediment. Feldspar grain content is consistently low, ranging from 0 to 3% and comprising only an average of 1.5% of the detrital composition. Most feldspar grains (App.IV - E,G), exhibit albite twinning (polysynthetic twinning) and gridiron structure (Kerr, 1977). Feldspar may be altered to clay minerals which precipitated in adjacent pores, especially in the silty-very fine sandstone (App.III - L, App.IV - ZZ). Feldspar percentage in the clean sands decreases slightly upward toward the A14 unit from approximately 2-3% in the clean A8 sand unit to about 0-1% in the clean A14 sand unit (Fig. 44).

Rock fragments represent the other dominant detrital constituent after monocrystalline quartz, averaging 7% of the total detrital grain population. Rock fragments are of igneous, metamorphic and sedimentary origin. The igneous and metamorphic rock fragments are volumetrically minor constituents representing only 2% or less of the total detrital composition. Igneous rock fragments, comprising only a trace of the total rock fragments are identified by

a glassy to chert-like appearance combined with a presence of microgranules and laths of unknown crystals (App.IV- H). Metamorphic rock fragments make up an average of 2% or less of the total rock fragment population, and consist of large grains of numerous, elongate, stretched polycrystalline quartz with vein-like foliated structures (App.IV - C), and occasionally with unidentified crystals (possible feldspar laths) set in a very finely crystalline matrix (App.IV- D). Sedimentary rock fragments average 5% to 6% of the detrital composition. Clay clasts and chert fragments are the most prevalent with some traces of detrital carbonate particles; especially detrital dolomite and very minor skeletal fragments.

Clay clasts are brown to dark brown (2-3 mm.) (App.IV -F), composed mainly of finely crystalline clay minerals, are occasionally deformed by the surrounding rigid quartz grains. In a few cases it appeared that compaction may have crushed or ruptured the occasional clay clast to the point that the "clast" could not be distinguished from matrix. In such cases the material was counted as matrix. Chert fragments are present ubiquitously in all samples and are identified by low relief. Very uniform microcrystalline quartz occasionally varies to dense isotropic aggregates (Scholle, 1979), with no visible speckled texture (App.IV - E,H). Detrital dolomite

fragments in trace amount were identified by their rhombic shape of crystal, their cloudy color, and lack of response to stain (App.IV - J). The remainder of the detrital composition is composed of other accessory minerals and organic matter comprising an average of 2.3% of the total detrital composition, and clay matrix which comprise only 3% of the rock constituents.

The accessory minerals identified include zircon, prismatic tourmaline grains, muscovite, chlorite, chamosite and glauconite pellets (App.IV - K to P). Organic matter as carbonaceous debris occurs as very well rounded grains and elongate fragments that are usually found in the fine to medium grained sandstones at the top of the coarsening upward sequence (App.IV - Q,R). The clay matrix consists of clay material of less than 0.0039 mm. size which may be of different modes of occurrences; dispersed clay matrix between rigid quartz grains or silty shale laminae (App.III - D,E). These modes of occurrence may be modified by bioturbation where clays may line burrows (App.IV - S) or may be irregularly dispersed (Wilson and Pittman, 1977).

Clay-matrix contents range from 0 to 3% in the fine to medium grained sandstones at the top of each coarsening-upward sequence, while the bioturbated silty-sandstones down-section range from 5% to 15% clay matrix (Fig. 44).

The bioturbated silty-sandstone units have relatively high percentages of clay content, that is directly related to the churning, reworking and redistribution of the original shale laminae into dispersed clay-matrix.

Source terrane for the Lower Acacus sandstones in the study area was mixed igneous, metamorphic and sedimentary as inferred from the composition of the constituent grains.

Authigenic Minerals

Quartz overgrowth, carbonate and clay minerals comprise the authigenic constituents which average about 20% of the bulk rock composition. Silica cement is present in the form of overgrowths and direct contact between quartz grains. Tangential, straight and concavo-convex grain contacts are present in Lower Acacus sandstones. It is obvious, all samples having quartz overgrowth are characterized by straight contact which may result from "...contact of overgrowths on adjacent grains rather than pressure solution.." (Lumsden, Pittman and Buchanan, 1971). Quartz overgrowths (App. IV - T,U) form euhedral crystal terminations and are much most abundant in the well sorted, clean, cross laminated and fine to medium grained sandstones with high quartz content. Quartz overgrowths formed initially on the rounded to well rounded quartz grain surfaces where their sharp crystal faces point out

and project into adjacent quartz grain or probably into pore spaces and fill it partially. The general amount of silica cement varies inversely with clay-matrix content. The high clay content in the bioturbated silty-sandstone may inhibit the precipitation of silica cement (App.III - D,E). Carbonate cement, dominantly calcite and dolomite, occurs pervasively or partially in samples ranging from 4% to 20%, averaging of 9.1 of the bulk rock composition (Table 1). After staining all carbonate cemented samples by Alizarin red, the calcite has taken the red stain whereas dolomite remains unaffected. The abundance of calcite cement varies between samples. Cement increases in the interpreted marine sandstones lithofacies in well T1-23 at 8489 feet and in well Q1-23 at 8180 feet (App.III - G), and down-section (in the coarsening-upward sandstone sequences) towards the bioturbated silty sandstone lithofacies. Cement also occurs as patchy calcite and dolomite at top of the coarsening-upward sandstone units near the shale-sandstone contacts (App.IV - V). It may be inferred that, at the shale-sandstone boundaries, shale dewatering was responsible for the calcite cementation as well as the local concentrations of carbonate materials in the shale (Franklin and Tieh, 1989).

Dolomite cement occurs in patchy fashion in the top portions of the fine to medium grained sandstones as well

as in some silty-sandstone units down-section. Euhedral dolomite occurs as pore filling crystals, with moderate relief, creamy-brownish to gray color, and of rhombic outline (App.IV - V,W). In many instances calcite and dolomite cements have been dissolved, leaving behind large pores which subsequently, in some sandstones, were filled with oil (App.III - G).

Siderite occurs locally in some silty-sandstone samples down-section, characterized by brown stain and by dark brown single rhombic crystals (App.IV - X,Y).

Clay cements, comprising an average 4% of the bulk composition of these sandstones; consist mostly of kaolinite and other clay minerals such as chlorite in minor amount. Clay cements which are abundant in the bioturbated silty-sandstones (distal delta front lithofacies), and in some of the interpreted marine sandstones (reworked marine sandstone lithofacies) probably precipitated as a result of dissolution of feldspar and rock fragments (Tillman and Jordan, 1987). Kaolinite is (App.IV - Z) is the most abundant clay cement in the argillaceous samples of the Lower Acacus Formation. It occurs as patches of fine crystal aggregates filling pores and may have the highest potential for reducing reservoir quality in these samples.

Minor amounts of authigenic chlorite plates of dark brown, to greenish, to occasionally anomalous colors

(App.IV - L) which may have been formed by the alteration of unstable detrital grains and other clay minerals. These plates are usually associated with micas and are randomly oriented with respect to each other. They show some evidence of compaction but no evidence of abrasion from transport. This can be interpreted to indicate that the chlorite is authigenic (Lumsden, Pittman and Buchanan, 1971), and in part responsible for the formation of the clay matrix hashes between quartz grains. It may also be the case that a degree of compaction was involved.

Compaction

Since compaction caused by sediment loading can be expected in deltaic environments, it is important to note that the Lower Acacus Sandstone shows relatively deformed labile grains in some samples including micas and chlorite plate fragments (App.IV - ZZZZZ).

PETROPHYSICS AND RESERVOIR QUALITY-SUMMARY

Petrophysics:

Forty-five (45) core plug samples were taken from the Lower Acacus sandstones from the following wells: A1-NC2, C1-NC2, E1-NC2, Q1-23, T1-23, B1-61, B3-61, C1-61 and D1-61. Routine core analysis of these plugs included air permeability (K_{air}), core plug helium porosity (ϕ_c) and grain density (Table 2) were conducted by the AGOCO core lab, Benghazi-Libya. Porosities are found to range from 6.4% to 28.3%, and permeabilities range from 4 millidarcies to greater than 30,000 millidarcies. The reservoir properties and the quality of the Lower Acacus sandstones are governing by a complex relationship between the mineralogical composition and the environment and site of deposition.

Porosity and Permeability Study

Core plug helium porosity (ϕ_c) represents the total sandstone porosity (Ehrenberg, 1990), and combines the low quality microporosity found to be associated with clay-matrix rich sandstones with the macroporosity (thin-section measurable porosity) found to be associated with clean, clay-free sandstones. The combination of these two types

TABLE 2:

Porosity Permeability Data of Routine Core Analyses for All Sandstone Samples from Lower Acacus Formation, NC₂ Concession, Hamada Basin, NW Libya.

Well Name	Sample Number	Depth (ft.)	Permeability ^a K _{air} (md)	Porosity (%) ^b		Grain Density (gm/cc)
				Ø _c	Ø _{ts}	
A ₁ -NC ₂	1	7817	1085	19.7	14.0	2.65
C ₁ -NC ₂	2	9630	25	16.1	13.0	2.63
	3*	9645	-	26.3	25.0	2.66
E ₁ -NC ₂	4	9703	250	19.6	17.0	2.56
	5	9725	3133	27.9	24.0	2.68
	6	9111	418	14.8	10.5	2.66
	7	9115	31	11.7	6.5	2.62
	8	9131	24	20.7	17.5	2.62
	9	9141	4	16.1	12.5	2.69
	10	9143	4	13.3	6.0	2.69
	11	9512	11	14.6	12.0	2.68
Q ₁ -23	12	7461	252	19.6	17.0	2.65
	13	8485	47	6.4	2.4	2.64
T ₁ -23	14	8454	30879	20.2	17.5	2.66
	15	8472	1254	16.2	7.0	2.65
	16	8489	368	17.4	9.0	2.66
B ₁ -61	17	8462	262	12.0	4.0	2.66
	18	8479	2331	23.3	19.5	2.67
B ₃ -61	19	8484	2609	28.2	26.5	2.67
	20	8756	703	28.3	24.5	2.67
	21	8764	58	15.4	13.0	2.68
	22	8893	113	21.2	18.5	2.65
	23*	8908	-	15.2	7.0	2.66
	24	8929	278	15.4	5.5	2.67
	25	8974	11	14.0	5.0	2.62
	26	9311	90	24.4	5.0	2.65
	27	9328	94	20.8	17.5	2.69
	28	9345	7	22.5	14.5	2.64
C ₁ -61	29*	9360	-	18.3	11.0	2.63
	30	7510	5719	21.4	18.0	2.65
	31	7522	13	16.8	14.0	2.65
	32	7525	18384	21.8	18.5	2.65
	33	7529	20	11.5	7.5	2.62
	34	7775	12	12.2	9.0	2.67
	35	7795	532	26.1	18.3	2.67
	36	8199	1856	14.4	5.6	2.68
	37*	8208	-	-	12.3	2.68

cont'd

TABLE 2:

Porosity-Permeability Data of Routine Core Analyses for All Sandstone Samples from Lower Acacus Formation, NC2 Concession, Hamada Basin, NW Libya.

Well Name	Sample Number	Depth (ft.)	Permeability ^a K _{air} (md)	Porosity (%) ^b		Grain Density (gm/cc)
				Ø _c	Ø _{ts}	
D1-61	38	8236	247	17.4	16.3	2.65
	39	8240	368	17.3	15.5	2.69
	40	8319	234	18.1	11.0	2.64
	41	8420	363	12.2	8.5	2.66
	42*	8454	-	-	9.0	2.65
	43*	8845	-	-	13.0	2.66
	44*	8866	320	-	15.0	2.67
	45*	8872	-	-	8.0	2.65

OBE-91

^a K_{air} = Permeability (Millidarcy), from Lab Core Analysis.

^b Ø_c = Core Plug Helium Porosity, from Lab Core Analysis
Ø_{ts} = Thin-Section Porosity, from point counting thin-section

* = Samples unsuitable for Lab analysis.

Note: Permeability, Porosity (Ø_c) and Grain Density tests were conducted by Core Lab, AGOCO, Benghazi, Libya in February, 1990.

of porosities (microporosity and macroporosity) makes the porosity-permeability relationship more complex and hard to understand. For example, the core plug helium porosity (ϕ_c) of A14 sand/silt unit in well T1-23 at 8454 ft. is 20.2% and permeability 30879 md. The core plug helium porosity of the same A14 sand/silt unit in well B1-61 at 8484 ft. is 28.2% with a lower permeability of 2604 md. Significant porosity/permeability variations occur throughout the Lower Acacus Sandstones. These variations are considered to be due to decreased pore space interconnection as clay matrix percent increases. Clay-rich samples commonly have a relatively low permeability with a significant microporosity, regardless of whether the clays are detrital or authigenic in origin (Franklin and Tieh, 1989). Some of the argillaceous sandstones are highly microporous, due mainly to the abundance of clay-matrix. These microporosities can be identified by the tiny accumulations of oil droplets in the clay matrix (App. IV - ZZ, ZZZ).

Microporosity is difficult to identify and quantify petrographically, simply because of its small size and the nature of its association with the clay-matrix and its occurrence in very fine grained sandstone samples. Generally, "...microporosity does not contribute much to permeability, but is responsible for the irreducible water saturation (S_{wir}) in sandstones..." (Pittman, 1979). The

combination of microporosity with macroporosity in clay-rich sandstones can affect measurably those permeability values measured from core plugs.

Macroporosity (thin-section measurable porosity) (ϕ_u) has been interpreted to be a "...measure of the effective porosity that contributes most significantly to permeability and from which hydrocarbons can potentially be displaced by production operations.." (Ehrenberg, 1990). This type of porosity can be identified in thin-sections of fine to medium grained, clean sandstones. Under the microscope it includes both small primary intergranular porosity and secondary porosity formed by dissolution processes, excluding the microporosity associated with very fine grained and silty sandstones.

Thin-section analyses for porosity begin with point counting macroporosity (300 points per thin-section) in sandstone samples containing $\leq 3\%$ matrix (Table 3). Such analysis involves clay-free pores having approximate diameters greater than 0.05 mm. (50 μm .). Intergranular macroporosities are identified in thin-section by their position and shape among detrital grains. Identification of dissolution macroporosities in thin-section is by means of their size, location and shape (outline) with respect to the surrounding grains. In some instances identification is

TABLE 3:

Porosity-Permeability Data of Sandstone Samples Containing $\leq 3\%$ Martix from Lower Acacus Formation, NC2 Concession, Hamada Basin, NW Libya.

Well Name	Sample Number	Depth (ft.)	Permeability ^a K _{air} (md)	Porosity(%) ^b	
				ϕ_c	ϕ_{ts}
C1-NC2	2	9630	25	16.1	13.0
	3*	9645	-	26.3	25.0
	4	9703	250	19.6	17.0
	5	9725	3133	27.9	24.0
E1-NC2	6	9111	418	14.8	10.5
	8	9131	24	20.7	17.5
	9	9141	4	16.1	12.5
	11	9512	11	14.6	12.0
Q1-23	12	7461	252	19.6	17.0
T1-23	14	8454	30879	20.2	17.5
B1-61	18	8479	2331	23.3	19.5
	19	8484	2609	28.2	26.5
B3-61	20	8756	703	28.3	24.5
	22	8893	113	21.2	18.5
	27	9328	94	20.8	17.5
	28	9345	7	22.5	14.5
C1-61	31	7522	13	16.8	14.0
	32	7525	18384	21.8	18.5
	34	7775	12	14.0	11.0
	35	7795	532	26.1	18.3
D1-61	37*	8208	-	-	13.3
	38	8236	247	17.4	16.3
	39	8240	368	17.3	15.5
	44*	8866	320	-	15.0

OBE-91

^a K_{air} = Permeability (Millidarcy), from Lab Core Analysis.

^b ϕ_c = Core Plug Helium Porosity, from Lab Core Analysis
 ϕ_{ts} = Thin-Section Porosity, from point counting thin-sections.

* = Samples unsuitable for Lab analysis.

affected by the presence of grain remnants or partial residual cement.

The majority of pore spaces studied in the Lower Acacus Sandstones are secondary in origin; primary porosity contributes only about 8% to the total number (45) of examined thin sections. Primary pores are concavo-convex, of triangular shape (App.V - A,B) and have sharp straight uncorroded boundaries with the surrounding grains. These pores vary in size due to grain compaction and precipitation of some authigenic clay materials. Primary pores are usually associated with quartz-rich samples of primarily silicate cement at the top of the coarsening-upward sand/silt unit (in wells E1-NC2 at 9131 ft., 9141 ft.; T1-23 at 8454 ft. and B1-61 at 8484 ft.). Some small pores may show some evidences of being secondary; formed as a result of calcite cement dissolution, it can be defined as being a replica of residual primary porosity (App.V - C,D).

Four types of secondary porosities occur in the Lower Acacus Sandstones according to the classification of Schmidt and McDonald, 1979:

1. Partial dissolution: The most common secondary pores occur as a result of partial leaching of the soluble cement material, being either calcite (App.V - E,F) or dolomite (App.V - G,H), as evidenced by remnant

patches of calcite or dolomite cements and the corroded grain boundaries adjacent to pore. Such porosity can also be recognized as a result of partial dissolution of unstable grains like feldspar grains (App.V _ I to L) where part of the grain which has not dissolved and corroded is adjacent to a pore which can be identified as an incomplete mold (Schmidt, 1977). This type of pore characterizes the Lower Acacus marine sands (Am) in well Q1-23 and occurs in some Lower Acacus sand/silt units of fine to medium grains near the top of the unit (A9, A14) in well C1-NC2 and well D1-61.

2. Oversized pores: These pores developed as a result of total dissolution of soluble grains or total dissolution of cement and have a significant larger diameter than that of the adjacent grains (greater than 0.2 mm.). These are the second most abundant pore type in the Lower Acacus Sandstones. Oversized pores are characterized by some irregular grain edges, floating grains (App.V - O,P) or inhomogeneity of packing (App.V - Q,R). In some reservoir sandstones oversized pores (> 0.3mm) can be identified by the large accumulation of hydrocarbon as in well C1-NC2 at 9703 ft. (App.IV - ZZZZ).

3. Recognizable molds: The third type of pore in the Lower Acacus Sandstones exhibits the shape of crystals or grains in which crystal outlines may be seen with some irregularity in the pore edges (App.V - S to V). These type of pores are very common in A8 sand/silt unit of well C1-NC2 at 9703 ft., and A12 sand/silt unit of well B3-61 at 8893 ft.
4. Elongate pores: These are present along the edges of packed quartz grains and show evidence of cement dissolution with more than 0.5 mm. long. They are typically best developed where the lithology changes from fine to medium grained sandstone to very fine grained silty sandstone at the bottom of the coarsening-upward sand/silt units in well C1-NC2 at 9725 ft. (App.V - W,X) and in well B1-61 at 8420 ft. (App.V - Y,Z).

Graphic representation is provided for comparison of core plug porosity (ϕ_c), thin-section porosity (ϕ_u), and those permeability values (K_{air}) indicated in Table 2 and Table 3. These graphs illustrate the most effective and reliable measured porosity whose values are best correlatable and are related to the measured permeability (Figs. 45 to 48). Data points of core plug porosity (ϕ_c) versus air permeability (K_{air}) values

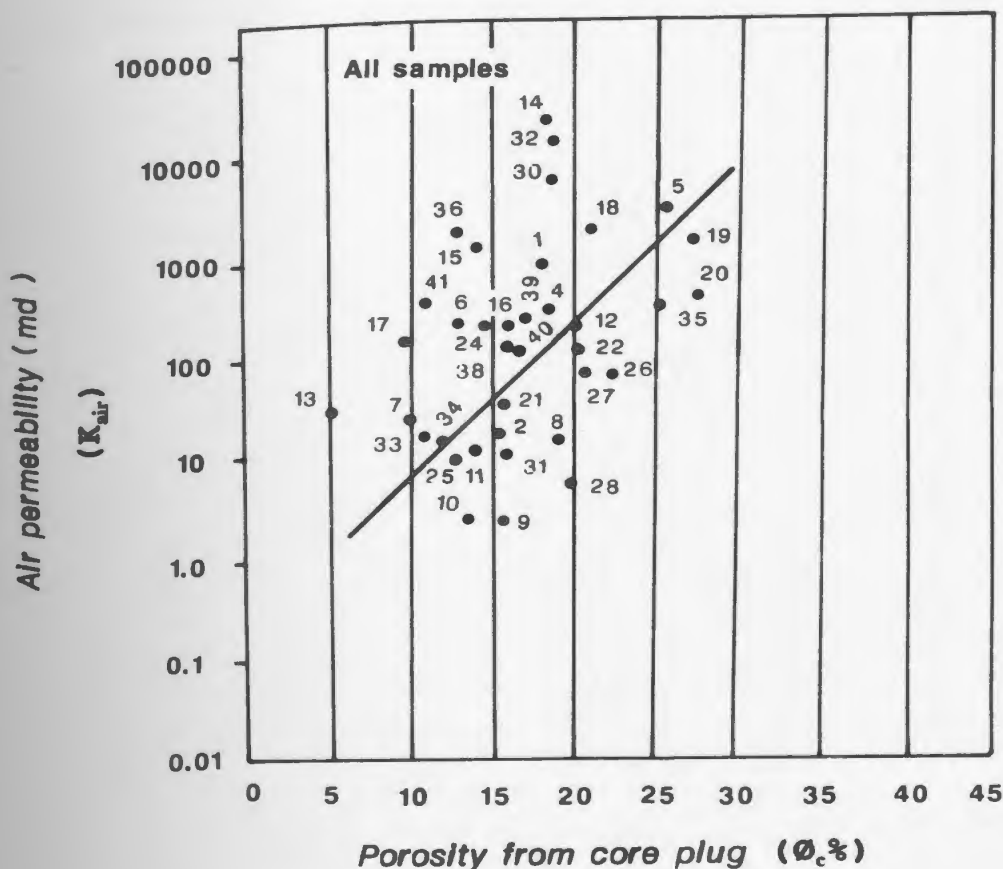
(Fig. 45) (values of ϕ_c and K_{air} obtained from Table 2) are randomly distributed and give no apparent correlation between points. This occurs because of the core plug porosities combine microporosities associated with low quality silty and very-fine grained sandstone samples with macroporosity (thin-section porosity) associated with high quality, clean fine to medium grained sandstone samples having little or very low amounts of clay-matrix ($\leq 3\%$). Figure 46 (values of ϕ_u and K_{air} obtained from Table 3) illustrates thin-section porosity (ϕ_u) versus air permeability (K_{air}) and shows a better fit correlation line. The data show a trend that may suggest that the measured thin-section porosity (macroporosity) in clean (clay free-matrix samples) reflects closely the true porosity, with values (Table 3) being more closely related to the measured rock permeability.

In order to prove this relationships, graphic representation of core plug porosity (ϕ_c) to thin-section porosity (ϕ_u) for samples having greater than 3% clay-matrix and for those having less than 3% clay-matrix (Figs. 47 and 48) was proposed. Clay-matrix percentage was obtained from pointcounting for clay-matrix versus grains in thin-sections.

Figure 47 shows plug porosity (ϕ_c) versus thin-section

porosity (ϕ_u) for those samples which contain more than 3% clay-matrix (the very silty sandstones). Less oriented porosity points can be seen which may be attributed to the high clay-matrix percentage included in the core plug porosity (ϕ_c). In Figure 48, a significant and obvious change in this relationship may be seen. Data points obtained from sandstones containing less than 3% clay-matrix improved the correlation between core plug porosity (ϕ_c) and thin-section porosity (ϕ_u). The data suggest that, in the first case (Fig. 47), a very weak correlation relationship between the two porosities (ϕ_c and ϕ_u) is due mainly to high clay-matrix percentages found in the very silty sandstone samples. In the second case (Fig. 48), by excluding all samples containing greater amount of clay-matrix (>3%), the core plug porosity (ϕ_c) is found to be more representative of the thin-section porosity (ϕ_u) (the effective macroporosity).

Figure 45. Core plug porosity ($\phi_c\%$) versus air permeability (K_{air}) for all sandstone samples from the Lower Acacus Formation, NC2 concession, Hamada Basin, NW Libya.



Core plug porosity ($\phi_c\%$) versus air permeability (K_{air}) for all sandstone samples from the Lower Acacus Formation, NC2 concession, Hamada Basin, NW Libya.

Note that samples unsuitable for permeability or porosity Lab analysis (Table 2) are not included on the plot.

Key is as follows : A1-NC2 well; 1 = Sublitharenite @ 7817 ft (2382m).

C1-NC2 well; 2 = Sublitharenite @ 9630 ft (2936m), 4 = Quartzarenite @ 9703 ft (2958m), 5 = Quartzarenite @ 9725 ft (2965m).

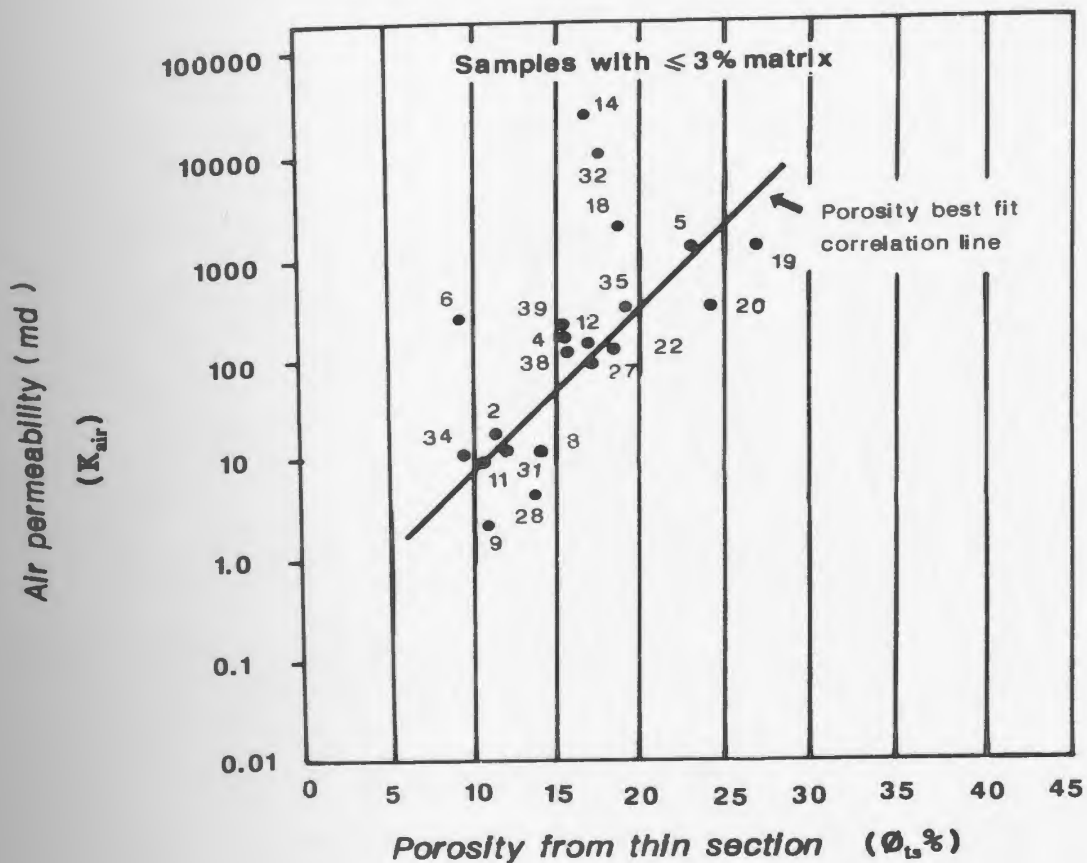
E1-NC2 well 6 = Sublitharenite @ 9111 ft (2778m), 7 = Sublitharenite @ 9115 ft (2779m), 8 = Quartzarenite @ 9131 ft (2784m), 11 = Sublitharenite @ 9512 ft (2900m). Q1-23; 12 = Quartzarenite @ 7461 ft (2275m), 13 = Litharenite @ 8485 ft (2587). T1-23 well; 14 = Sublitharenite @ 8454 ft (2577m),

15 = Litharenite @ 8472 ft (2583m), 16 = Sublitharenite @ 8489 ft (2588m). B1-61 well; 17 = Sublitharenite @ 8462 ft (2580m), 18 = Sublitharenite @ 8479 ft (2585m), 19 = Quartzarenite @ 8756 ft (2670m). B3-61 well; 20 = Quartzarenite @ 8756 ft (2670m), 21 = Sublitharenite @ 8764 ft (2672m),

22 = Sublitharenite @ 8893 ft (2711m), 24 = Sublitharenite @ 8929 ft (2722m), 25 = Sublitharenite @ 8974 ft (2736m), 26 = Litharenite @ 9411 ft (2839m), 27 = Sublitharenite @ 9328 ft (2844m), 28 = Sublitharenite @ 9345 ft (2849m). C1-61 well; 30 = Quartzarenite @ 7510 ft (2290m),

31 = Quartzarenite @ 7522 ft (2293m), 32 = Quartzarenite @ 7525 ft (2294m), 33 = Sublitharenite @ 7529 ft (2295m), 34 = Sublitharenite @ 7775 ft (2370m), 35 = Sublitharenite @ 7795 ft (2377m), 36 = Litharenite @ 8199 ft (2500m). D1-61; 38 = Quartzarenite @ 8236 ft (2511m), 39 = Sublitharenite @ 8240 ft (2512m), 40 = Sublitharenite @ 8319 ft (2536m), 41 = sublitharenite @ 8420 ft (2567m).

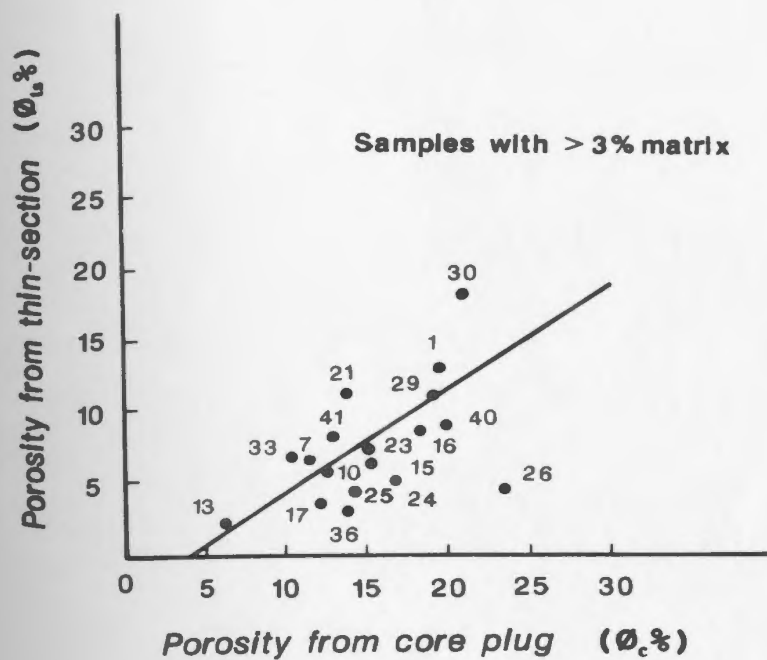
Figure 46. Thin-section porosity ($\phi_u\%$) versus
air permeability (K_{air}) for sandstone
samples containing $\leq 3\%$ matrix from
the Lower Acacus Formation, NC2
concession, Hamada Basin, NW Libya.



Thin-section porosity ($\phi_L\%$) versus air permeability (K_{air}) -
for sandstone samples containing $\leq 3\%$ matrix from the Lower Acacus
Formation, NC2 concession, Hamada Basin, NW Libya.
Note that samples unsuitable for permeability or porosity Lab
analysis (Table 3) are not included on plot.

Key is as follows : C1-NC2 well; 2= Sublitharenite @ 9639 ft (2936m), 4= Quartzarenite @ 9703 ft (2958m),
5= Quartzarenite 9725 ft (2965m). E1-NC2 well; 6= Sublitharenite @ 9111 ft (2778m), 8= Quartzarenite @ 9131 ft (2784m), 9= Sublitharenite
@ 9141 ft (2787m), 11= Sublitharenite @ 9512 ft (2900m). Q1-23 well; 12= Quartzarenite @ 7461 ft (2275m).
T1-23 well; 14= Sublitharenite @ 8454 ft (2577m). B1-61 well; 18= Sublitharenite @ 8479 ft (2585m), 19= Sublitharenite @ 8484 ft (2670m).
B3-61 well; 20= Quartzarenite @ 8756 ft (2670m), 22= Sublitharenite @ 8893 ft (2711m), 27= Sublitharenite @ 9328 ft (2844m).
28= Sublitharenite @ 9345 ft (2849m). C1-61 well; 31= Quartzarenite @ 7522 ft (2293m), 32= Quartzarenite @ 7525 ft (2294m),
34= Sublitharenite @ 7775 ft (2370m), 35= Sublitharenite @ 7795 ft (2377m). D1-61 well; 38= Quartzarenite @ 8236 ft (2511m),
39= Sublitharenite @ 8240 ft (2512m).

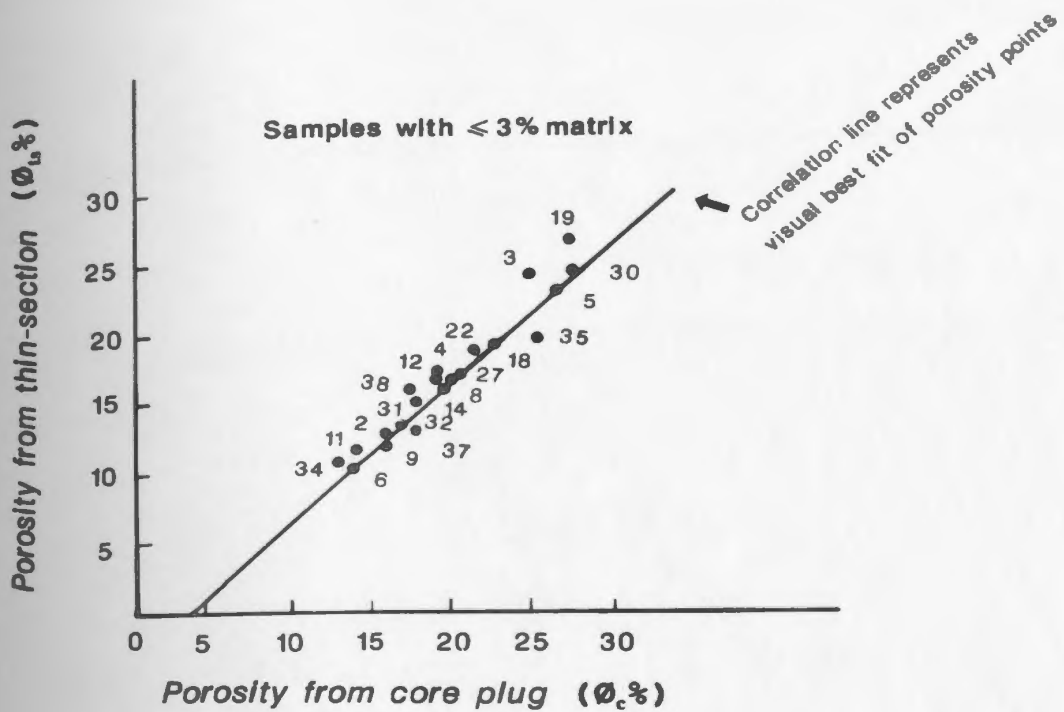
Figure 47. Porosity measured in core plugs (ϕ_c) versus porosity measured in thin-section (ϕ_t) for sandstone samples containing > 3% matrix, from the Lower Acacus Formation, NC2 concession, Hamada Basin, NW Libya.



Porosity measured in core plugs ($\phi_c\%$) versus porosity measured in thin-sections ($\phi_{ts}\%$) for sandstone samples containing > 3% matrix, from the Lower Acacus Formation, NC2 concession, Hamada Basin, NW Libya.

OBE-91

Figure 48. Porosity measured in core plugs (ϕ_c) versus porosity measured in thin-sections (ϕ_s) for sandstone samples containing $\leq 3\%$ matrix from the Lower Acacus Formation, NC2 concession, Hamada Basin, NW Libya.



Porosity measured in core plugs ($\phi_c\%$) versus porosity measured in thin-sections ($\phi_{ts}\%$) for sandstone samples containing $\leq 3\%$ matrix from the Lower Acacus Formation, NC2 concession, Hamada Basin, NW Libya.

Petrophysical Log Interpretation

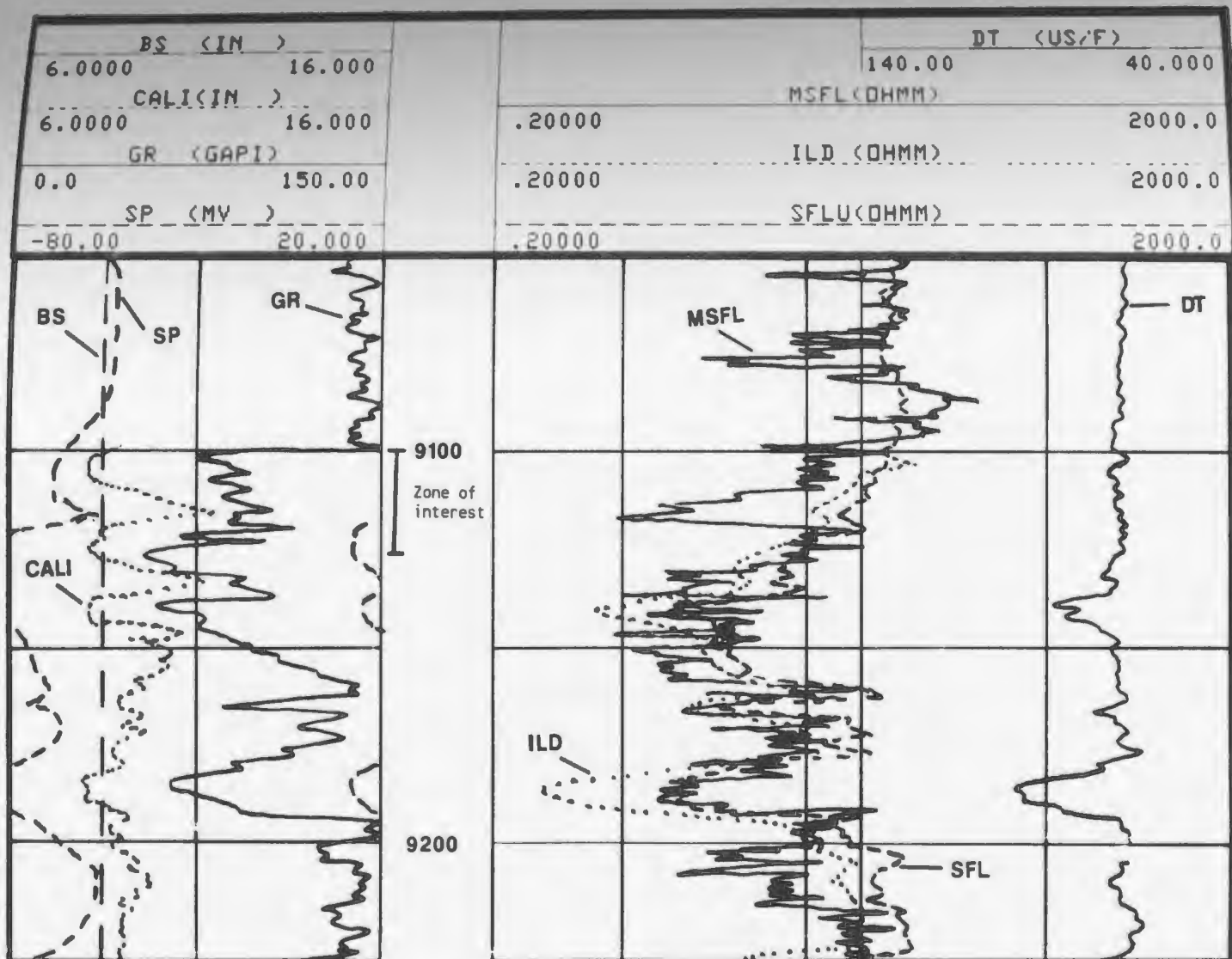
Log interpretation is an effective exploration tool. A successful exploration program takes petrophysical log interpretations into consideration at an early step in order to define the reservoir characteristics and to reduce risk of problems when drilling new wells. For that reason the following log interpretations will demonstrate application of the findings of this study to selected productive zones in the formation.

1. Log interpretation of A14 sand/silt unit (9100-9125 ft.) (proximal delta front lithofacies, #3), well E1-NC2, Lower Acacus Formation:

Careful examination of the log response recorded through the A14 sand/silt unit at the top of the Lower Acacus Formation provides the following information. The log suite includes resistivity measurements (MSFL, SFL and ILD), Sonic log (DT), SP log, Gamma-ray log and Caliper log (Fig. 49), and a combination Neutron-Density log with Gamma-ray log and Caliper (Fig. 50).

The microspherically focussed log (MSFL) measures the resistivities of the flushed zone (R_{fo}), while the Shallow Focused Log (SFL) measures the resistivities of the Invaded Zone (R_i) and the Induction Laterolog Deep (ILP) measures the true resistivity of the uninvaded zone (R_t)

Figure 49. Resistivity logs (MSFL, ILD, SFL),
sonic log (DT) with bit size (BS),
caliper log (CALI), gamma-ray log (GR),
and spontaneous-potential log (SP), for
A14 sand/silt unit, well E1-NC2, NC2
concession, Hamada Basin, NW Libya.

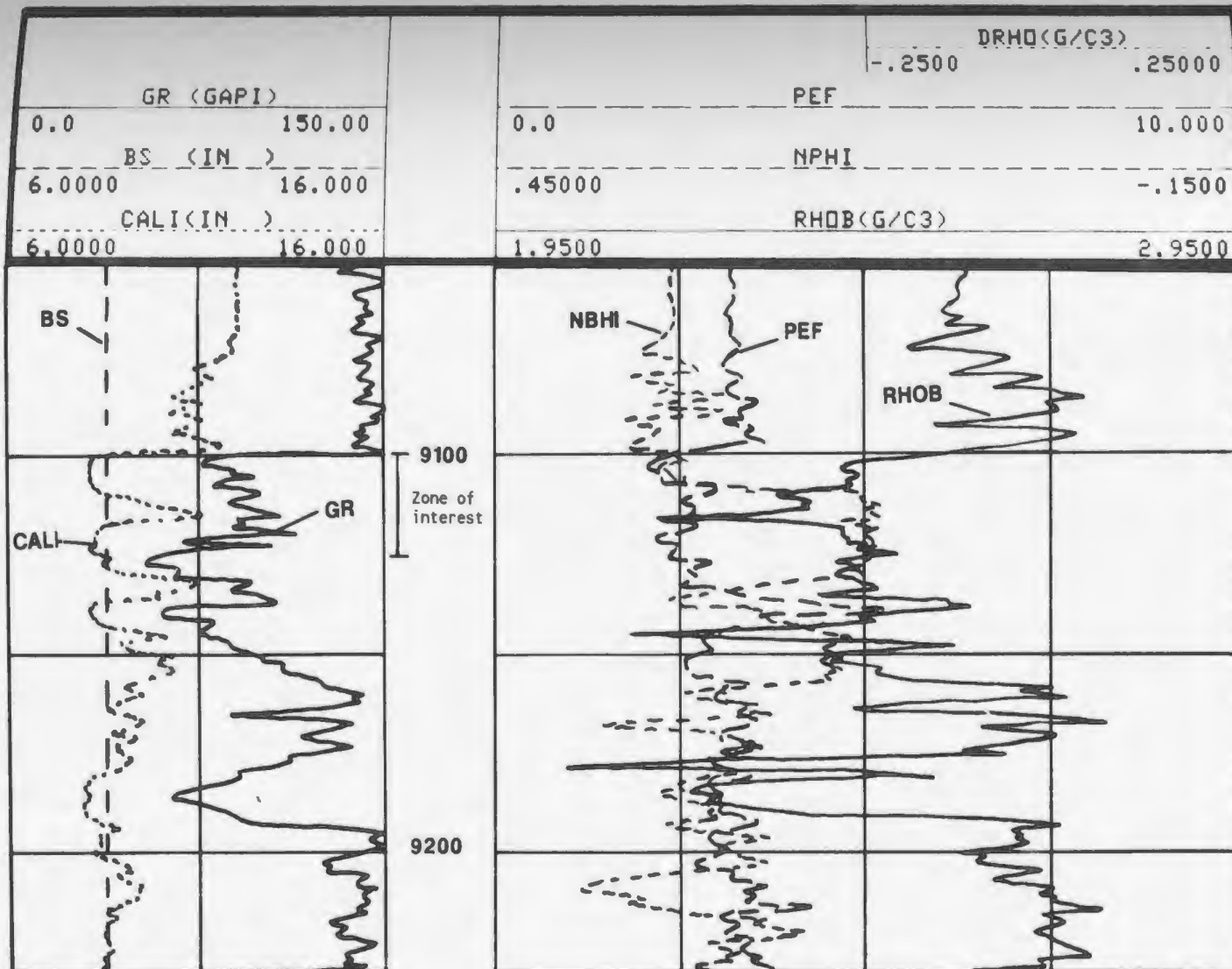


Schlumberger, 1987

Resistivity logs (MSFL,ILD,SFL), sonic log (DT) with bit size (BS), caliper log (CALI), gamma ray log (GR), and spontaneous potential log (SP), for A14 sand/silt unit, well E1-NC2, NC2 concession, Hamada Basin, NW Libya.

" Depth divisions are 50 ft (15.24m) apart "

Figure 50. Combination neutron-density logs (NPHI-RHOB), photo-electric index log (PEF), with gamma-ray log (GR), bit size (BS), and a caliper log (CALI), for A14 sand/silt unit, well E1-NC2, Lower Acacus Formation, NC2 concession, Hamada Basin, NW Libya.



Schlumberger, 1987

Combination Neutron-Density logs (NPHI-RHOB), photo-electric index log (PEF), with gamma ray log (GR), bit size (BS), and caliper log (CALI), for A14 sand/silt unit, well E1-NC2, Lower Acacus Formation, NC2 concession, Hamada Basin, NW Libya.

" Depth divisions are 50 ft (15.24m) apart "

(Schlumberger, 1972; Serra, 1984; Asquith and Gibson, 1982). The resistivity parameter of greatest interest is R_v because it is related to "...the hydrocarbon saturation (S_h)..." (Schlumberger, 1972). Therefore correct determination of R_v is most important.

Cores of unit A14 in well E1-NC2 (C #1 and C #2; Fig. App.I-1) found that this unit is fine to medium grained carbonaceous sandstone with some shale interbedding, and were from overall coarsening-upward sequence. A porous and permeable sand, is indicated on the SP log (Fig. 49) from 9100 to 9130 by a leftward deflection of the curve from the shale line, and is characterized by offscale behavior. High values on the gamma-ray log (90-105 API) suggest the presence of some shale (slightly shaly unit). A decrease in hole diameter occurs at 9100-9110 ft. and at 9120-9130 ft. on the caliper log (Fig. 49). The decrease in hole diameter indicates the presence of mud cake (Schlumberger, 1974), which means invasion has taken place.

Scrutinizing the resistivity logs to identify invasion zones is very important. Between depth 9100 and 9117 feet the resistivity logs (MSFL, SFL and ILD) read different values of resistivities and the curves separate. This separation suggests that invasion has taken place (Schlumberger, 1972; Asquith and Gibson, 1982) and

hydrocarbons are present since R_t falls in the range of 23-32 Ohmm (Table 4). The lessening of separation between MSFL and ILD logs (Fig. 49) and the decrease of R_t to 0.7 Ohmm at 9130 ft. in the lower sand zone indicates higher water saturation (S_w) ranging from 57% to 100% (shale bearing) between 9128 and 9130 ft.. That means lower hydrocarbon saturation (S_h) to 43% at 9128 ft. and to 0% at 9130 ft.

This variation in S_w and S_h helps to locate the oil water contact for this unit which coincides with the depth 9128 ft. as S_w increases to 57%. It is very important to recognize that, within this sand unit sequence, shale interbeds which isolate the various oil bearing sands delineating the oil/shale type of contacts are very common. Porous and permeable zones which occur intermittently through the interval from 9100 ft. to 9130 ft., are identified by reading the sonic log (Fig. 49) and the combination neutron-density log (Fig. 50). Zones of different porosity and permeability in the A14 sand/silt unit have been encountered and calculated from core section using core lab analysis indicating good average porosity of 15.7% and average permeability 158 md. in this unit (Table 4). Zones of porosity and permeability are not clearly seen on sonic log. This may be due to the shale interbeds, but one can recognize an increase and relative

TABLE 4
Log Evaluation for A14 Sand/Silt Unit, E1-NC2 Well, Lower Acacus Formation, NC2 Concession, Hamada Basin, NW Libya.

Depth (ft)	GR (API)	V _{clay} (%)	R _t (Ω)	Δt (μs/ft)	Ø _S (%)	Ø _{Sc} (%)	ρ _b (gm/cc)	Ø _D (%)	Ø _{Dc} (%)	Ø _N (%)	Ø _{Nc} (%)	Ø _{av c} (%)	S _w (%)	S _h (%)	S _{wirr} (%)
9100	75	28	23	69	11	6	2.55	9	2	23	15	8	33	67	25
9102	90	42	32	70	12	4	2.45	17	4	19	6	5	45	55	40
9104	98	50	23	70	12	2	2.43	16	2	19	4	2	100	-	100
9106	92	45	20	70	12	3	2.43	16	3	20	7	3	81	19	60
9108	87	40	19	70	12	4	2.40	17	5	21	9	6	48	52	33
9110	98	50	17	70	12	2	2.34	23	6	20	5	4	77	23	50
9112	100	52	15	72	14	3	2.37	21	4	19	3	3	80	20	70
9114	111	63	11	70	12	2	2.36	22	3	19	2	3	100	-	68
9116	95	48	12	70	12	3	2.25	32	15	19	5	9	52	48	22
9118	97	50	14	70	11	2	2.43	17	2	19	4	3	80	20	61
9120	87	40	13	69	12	3	2.42	17	5	19	7	5	71	29	40
9122	105	57	8	70	11	2	2.45	16	2	18	2	2	100	0	100
9124	60	14	6	69	12	9	2.42	15	12	18	15	12	43	57	16
9126	98	5	5	70	14	11	2.46	15	14	19	18	14	41	59	14
9128	48	21	4	72	15	9	2.42	16	10	21	14	11	57	43	20
9130	57	11	7	84	21	18	2.43	16	14	15	12	15	100	-	13

OBE-91

Remarks:

GR_{max} = 150 API, GR_{min} = 45 API, R_w = 0.02 Ω
 Clay volume (V_{cl}) = [(GR - GR_{min}) / (GR_{max} - GR_{min})]
 Corrected sonic porosity (Ø_{sc}) = Ø_S - (V_{cl} × Ø_{S,cl})
 Corrected density porosity (Ø_{dc}) = Ø_D - (V_{cl} × Ø_{D,cl})
 Corrected neutron porosity (Ø_{nc}) = Ø_N - (V_{cl} × Ø_{N,cl})
 Water Saturation (S_w) = $\sqrt{\frac{F - R_w}{R_0}}$ (Archie Equation)
 Hydrocarbon Saturation (S_h) = 1 - S_w

decrease in the interval transit time(DT) between 69 and 75 μ sec./ ft. that may be because of the alternating sand and shale laminae. On the combination neutron-density log (Fig. 50), the intermittently porous and permeable zones are seen by an increase in both neutron and density porosities opposite to the different sand zones. At depth 9110 ft. to 9118 ft., the neutron log records low porosity and is deflected to the right, while the density log records high porosity and is deflected to the left and showing decrease in density readings (from 2.35 to 2.10 gm./cc.) leaving a good "...separation between the two curves which indicates the effect of gas.." (Denno, 1978) in this sand zone. In some places a higher neutron porosity is recorded than density porosity especially at 9104-9106 ft. and at 9118-9122 ft. This is probably due to the alternating shales which "...have a high hydrogen ion concentration.." (Schlumberger, 1972; Asquith and Gibson, 1982).

Calculation of water saturation (Table 4) by applying the Archie equation (Schlumberger, 1972; Fertl, 1978), gives values of 33% to 57%, obtained by using the Schlumberger (1972, 1974) shaly sand equations to correct for the effect of shale. Generally, clay-rich sandstones (high clay volume, V_{cl}) have high S_w values, while the fine to medium

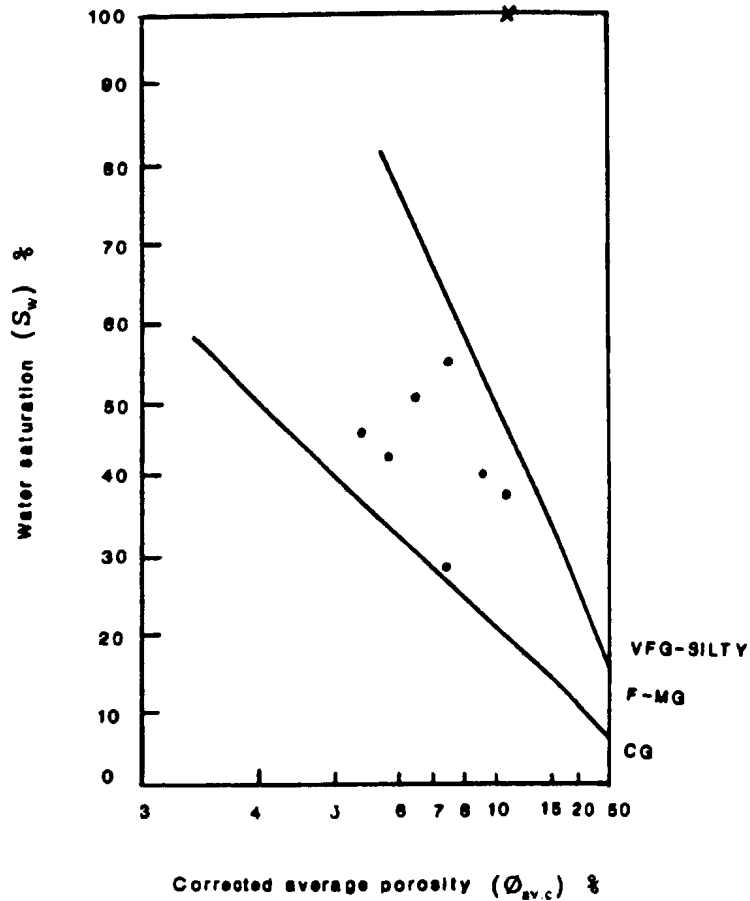
grained sandstones (Sublitharenite to Quartzarenite) have relatively low S_w .

Water-free oil and gas production has been recovered from the upper 25 feet (9100-9125 ft.) (AGOCO, DST reports) and has been characterized by average water saturation from 33% to 52%, even though there is a relative high water saturation at 9116 ft. of 52%, because "...reservoir sandstone at irreducible water saturation (S_{wir})..." (Asquith and Gibson, 1982).

If Archie water saturation (S_w) and average corrected log porosity ($\phi_{v,c}$) are crossplotted (Fig. 51), a grain size ranging from fine to medium grain is shown on the plot. This confirms the core sample examination which indicates a fine to medium grained sandstone. The data point at 9130 ft. shows very fine grained sandstone, which on the log appears to be a shale bearing point of high concentration of water saturation.

Reservoir grain size, along with shale contents that vary from one place to another, are the reasons for the variation in relative permeability to gas (K_{rg}) (Fig. 52). Points having high shale content showing low relative gas permeability ranging from 0.04 to 0.10 md., at high S_{wir} of 40% to 70%. Points having low shale contents and characterized by fine to medium grained sandstones show high relative-gas permeability ranging from 0.2 to 1.0 line

Figure 51. Grain size determination by water saturation (S_w) versus corrected average log porosity ($\phi_{w.c}$) crossplot for A14 sand/silt unit, well E1-NC2, Lower Acacus Formation, NC2 concession, Hamada Basin, NW Libya.



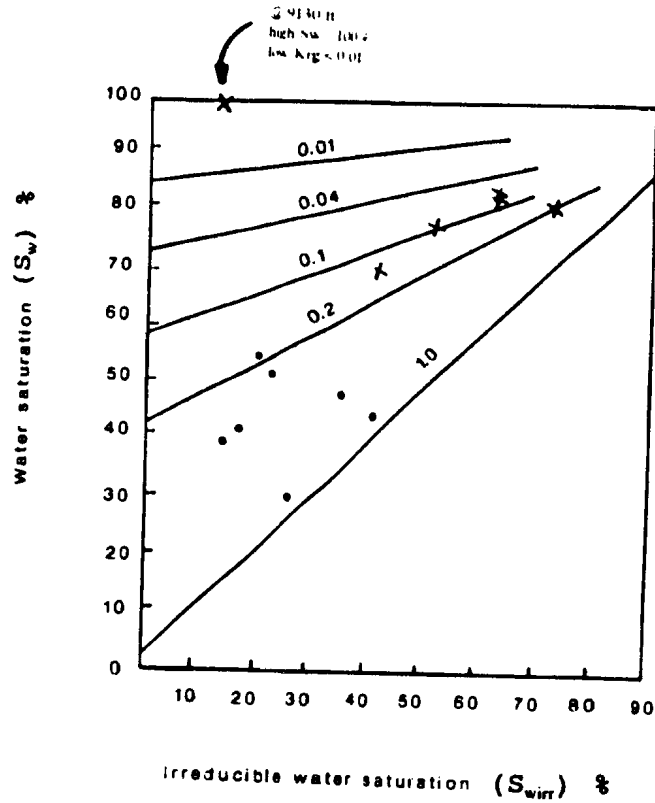
KEY:
 VFG-SILTY = very fine grained to silty sandstone points.
 F-MG = fine to medium grained sandstone points.
 CG = coarse grained sandstone points.
 x = very fine grained to silty sandstone points.
 ● = fine to medium grained sandstone points.

Grain size determination by water saturation (S_w) versus corrected average log porosity ($\phi_{av,c}$) crossplot for A14 sand/silt unit, well E1-NC2, Lower Acacus Formation, NC2 concession, Hamada Basin, NW Libya.

Note, Shale points of GR reading > 75 API are not included.

(Chart after Schlumberger, 1972 ; Asquith et al, 1982).

Figure 52. Water saturation (S_w) versus irreducible water saturation (S_{wir}) crossplot for determining relative permeability to gas (K_{rg}) for A14 sand/silt unit, well E1-NC2, Lower Acacus Formation, NC2 concession, Hamada Basin, NW Libya.



KEY:

- x Shale points.
- Fine to medium grained sandstone points.

Water saturation (S_w) versus irreducible water saturation (S_{wirr}) crossplot for determining relative permeability to gas (K_{rg}) for A14 sand/silt unit, well E1-NC2, Lower Acacus Formation, NC2 concession, Hamada Basin, NW Libya.

(Chart after Schlumberger, 1972 ; Asquith et al, 1982).

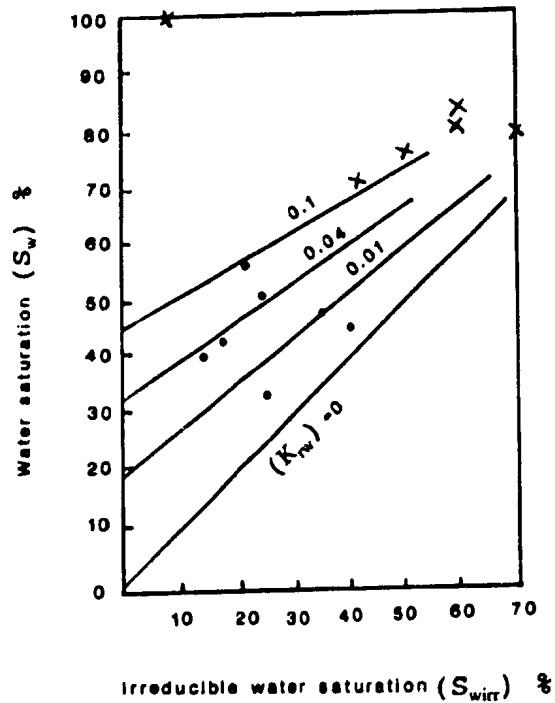
(20 to 100 md.) at S_{wirr} between 15% to 40%.

As relative gas permeability (K_{rg}) in the very fine and silty sandstone (at 9130 ft.) is decreased (Fig. 52) the corresponding relative permeability to water (K_{rw}), is increased (>0.1 md.) (Fig. 53). With the addition of high water saturation (S_w) associated with the silty and very fine grained sandstone, the reservoir at some point will produce some salt water.

The relative permeability to water (K_{rw}) plots (Fig. 53) illustrate that some of the tested zones in this unit have low K_{rw} ranging from 0 to 0.1 with the possibility of producing some water, but during testing no water recovered. In this case the reservoir is believed to be at irreducible water saturation (minimum water saturation) (Schlumberger, 1972) despite the high water saturation values. The average water saturation (S_w) calculated for the tested interval (9090-9125 ft.) was about 44% (see Table 8).

Relative permeability to oil (K_{ro}) of the different zones of different grain sizes are shown on a crossplot of S_{wirr} versus S_w (Fig. 54). Data showing the shale points fall in the area of $K_{ro} = 0$ meaning 0% oil, while data points of fine to medium grained sandstones fall between $K_{ro} = 0.3$ and $K_{ro} = 1.0$ (30%-100%) representing zones which may produce 30% to 100% oil as they are characterized by

Figure 53. Water saturation (S_w) versus irreducible water saturation (S_{wir}) crossplot for determining relative permeability to water (K_{rw}) for A14 sand/silt unit, well E1-NC2, Lower Acacus Formation, NC2 concession, Hamada Basin, NW Libya.



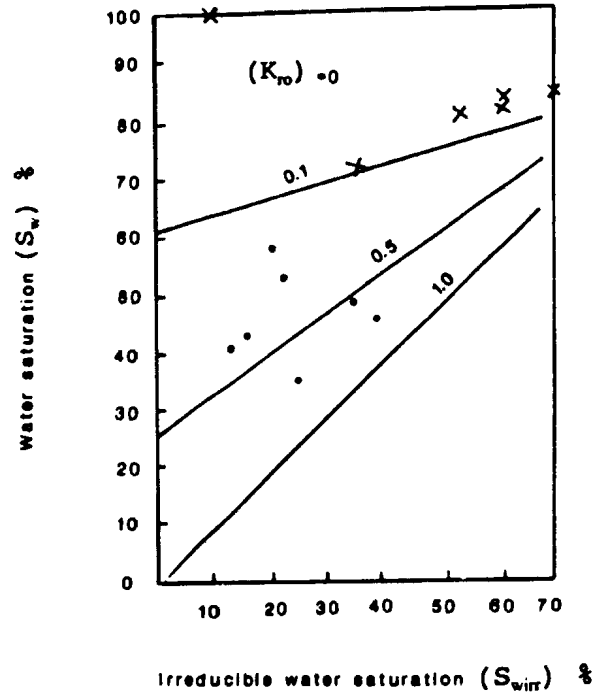
KEY:

- x Shale points.
- Fine to medium grained sandstone points.

Water saturation (S_w) versus irreducible water saturation (S_{wirr}) crossplot for determining relative permeability to water (K_{rw}) for A14 sand/silt unit, well E1-NC2, Lower Acacus Formation, NC2 concession, Hamada Basin, NW Libya.

(Chart after Schlumberger, 1972 ; Asquith et al, 1982).

Figure 54. Water saturation (S_w) versus irreducible water saturation (S_{wir}) crossplot for determining relative permeability to oil (K_{ro}) for A14 sand/silt unit, well E1-NC2, Lower Acacus Formation, NC2 concession, Hamada Basin, NW Libya.



KEY:

- x Shale points.
- o Fine to medium grained sandstone points.

Water saturation (S_w) versus irreducible water saturation (S_{wirr}) crossplot for determining relative permeability to oil (K_{ro}) for A14 sand/silt unit, well E1-NC2, Lower Acacus Formation, NC2 concession, Hamada Basin, NW Libya.

(Chart after Schlumberger, 1972 ; Asquith et al, 1982).

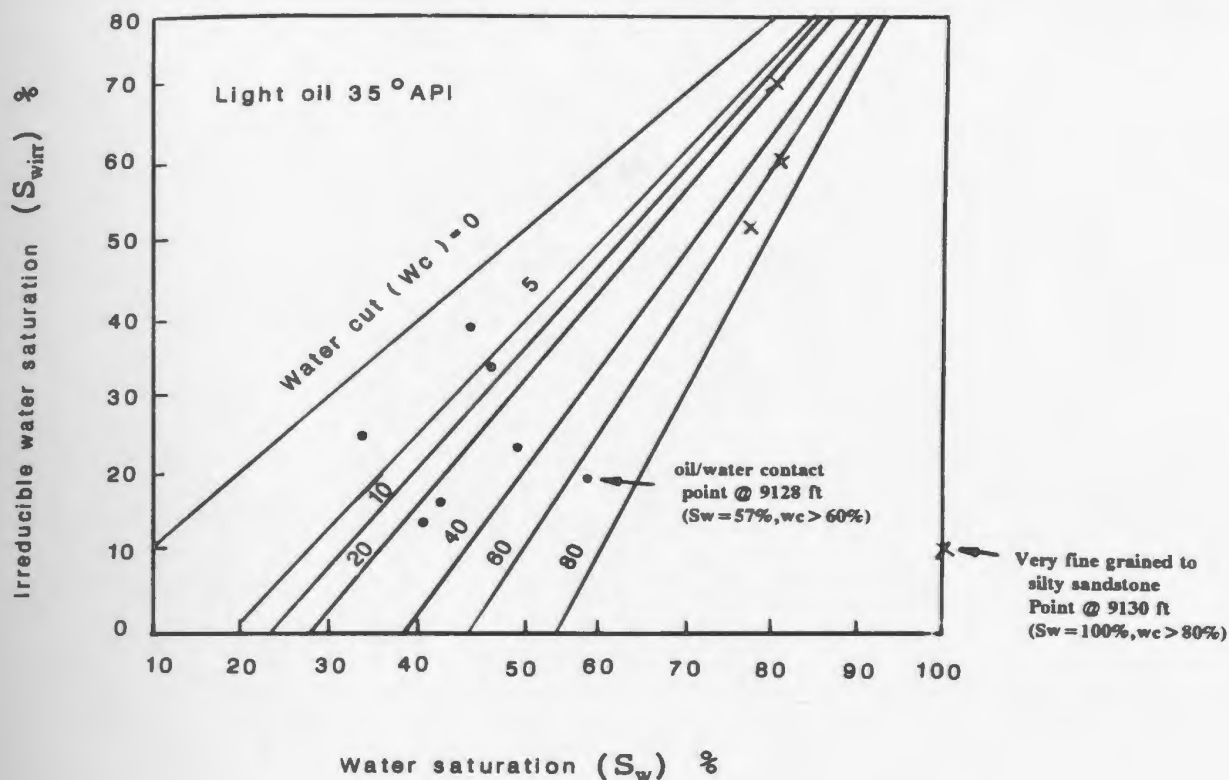
the variation in water saturation relatively. However, as points occur with increasing distance from the 100% ($K_{ro} = 1.0$) line, there is a high chance to produce some water.

The data point of silty and very fine grained sandstone at 9130 ft., falls in the area of $K_{ro} = 0$ which means that at this point one can expect the well to produce only water.

Since light oil of 32.7° API has been recovered from the tested interval (9090-9125 ft.) (AGOCO DST reports), a percent water cut plot (Fig. 55) has 8 points, 7 points characterized by fine to medium grained sandstones and show a water cut variation from 0% to a high of 70% and only one point is showing water cut (Wc) greater than 80%. It is of interest to note that the oil bearing zone (9090-9125 ft.) is characterized by points with water cut ranging from 0% to 40% (Fig. 55). These water cut (Wc) values (0-40%) are favourable for this kind of sandstones to produce only oil even if they have water saturation of 48%, (i.e, till this point the reservoir is at its minimum water saturation with cutoff point of 48% formation water saturation is considered).

Fortunately, the lower water bearing sand zones (at 9128-9130 ft.) were not tested (not perforated) so that the well produced only oil and gas (AGOCO DST reports), but during analysis a high water cut (Wc) of 70% was

Figure 55. Water saturation (S_w) versus irreducible water saturation (S_{wir}) crossplot for determining percent water-cut (35°API gravity oil) for A14 sand/silt unit, well E1-NC2, Lower Acacus Formation, NC2 concession, Hamada Basin, NW Libya.

**KEY:**

- × Shale points.
- Fine to medium grained sandstone points.

Water saturation (S_w) versus irreducible water saturation (S_{wirr}) crossplot for determining percent water-cut (35°API gravity oil) for A14 sand/silt unit, well E1-NC2, Lower Acacus Formation, NC2 concession, Hamada Basin, NW Libya.

(Chart after Schlumberger, 1972 ; Fertl et al, 1978).

encountered at the lower sand zone at 9128 ft. (and of S_w 57%) the point at which oil-water contact should be delineated while increasing water cut (W_c) to greater than 80% at 9130 ft. (of S_w 100%), the point at which production of water should be expected.

The tested interval (9090-9125 ft.) is produced oil and gas, the calculated open flow rate of gas was 0.017 MMCFGPD (17,000 cubic feet gas per day), with bottom shut-in pressure of 3343 pounds per inch (PSI), at a bottom hole temperature of 170°F, high tubing pressure 830 PSI, and a gas-oil ratio of 17 cu. ft./bbl.

The calculated oil production per day is 1020 barrels of oil per day (BOPD) (AGOCO DST reports). The estimated oil and gas in place from the A14 sand/silt unit tested interval (9090-9125) is 7.4 MMSTBOIP and 6.2 MMMCFGIP which is calculated using the following parameters:

Areal closure = 4 km²

= 988.4 Acres

Net pay = 20 ft.

Corrected average log porosity ($\phi_{n.c.}$) = 13%

Water saturation (S_w) = 48%

Hydrocarbon saturation (S_h) = 52%

Estimated oil volume factor (O.V.F.) in the Lower Acacus Formation = 1.4 cu. ft./bbl.

Estimated gas volume factor (β_g) in the Lower Acacus Formation = 160.4 SCF/cu. ft.

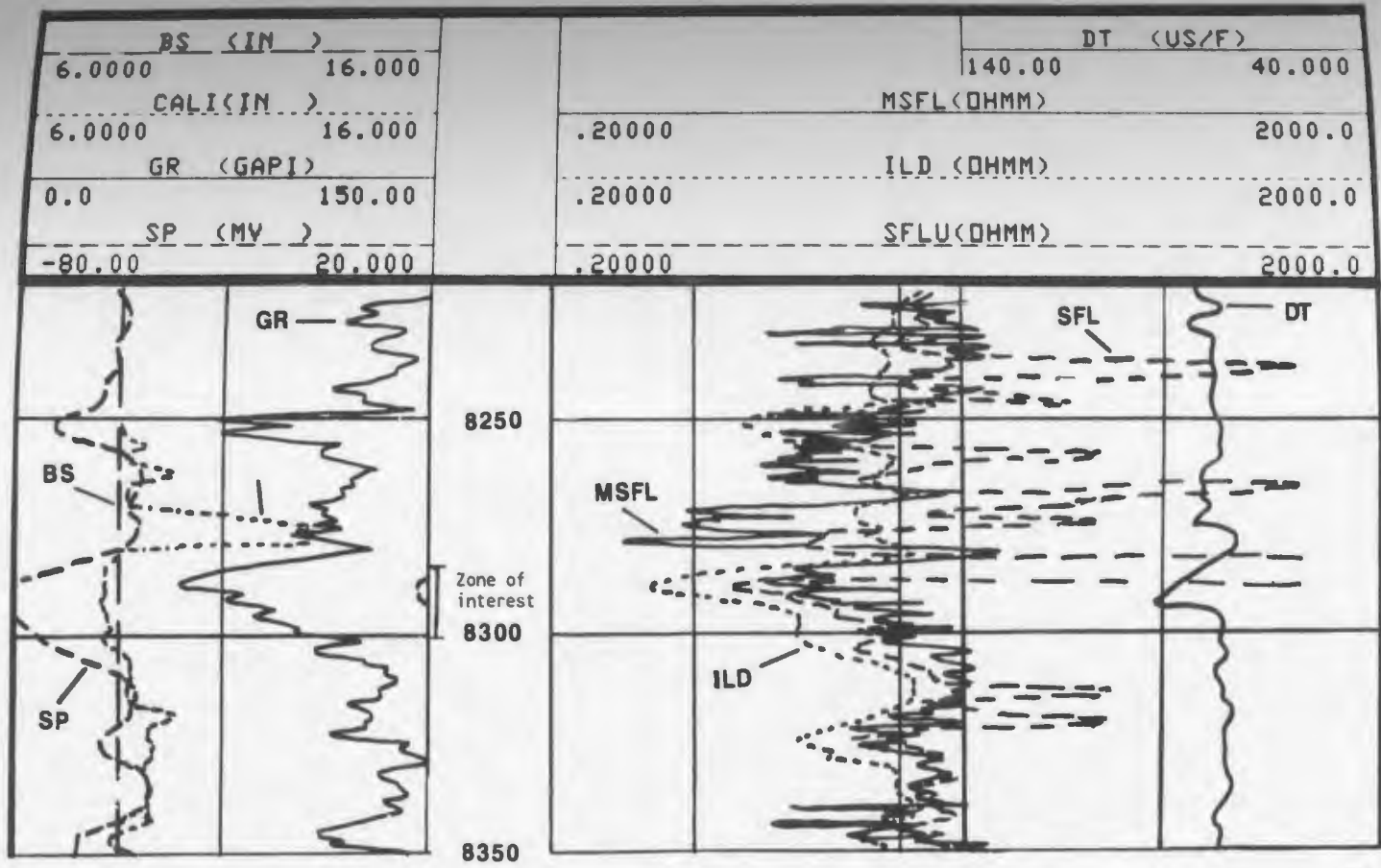
2. Log interpretation of A12 sand/silt unit (8284-8300 ft.) (distal delta front lithofacies, #2), well F1-NC2, Lower Acacus Formation:

A12 sand/silt unit in well F1-NC2 occurs from 8284 to 8300 ft. and is read on the SP curve (Fig. 56) by an over-scale left deflection from the shale line, indicating porous and permeable sand. A relatively low value of 68 to 75 API is recorded on the gamma-ray log opposite to the sand zone, while high values are opposite to shaly sand zones ranging from 80 to 98 API, especially at the bottom of the interval between 8290 and 8300 ft.

The caliper log shows a decrease in hole diameter opposite to the sand zone interval, indicating that mud cake has developed, and invasion of drilling fluid has taken place. An increase in caliper log curve (Fig. 56) above and below the tested interval opposite to shale (8260-8280 ft. and 8310-8340 ft.) indicates hole enlargement due to caving and washout shales. On the deep induction log (ILD), the readings of true formation resistivity (R) increase from 8284 to 8287 ft. (1-2 Ohmm) (Table 5).

Increase in resistivities can mean that hydrocarbons are present (Schlumberger, 1972; Asquith and Gibson, 1982). The deep induction log (ILD) reading decreases (0.6-0.7 Ohmm) opposite to the water bearing zone, which the contact of which can be expected at 8288 ft.

Figure 56. Resistivity logs (MSFL, ILD, SFL), sonic log (DT) with bit size (BS), caliper log (CALI), gamma-ray log, and spontaneous-potential log (SP), for A12 sand/silt unit, well F1-NC2, Lower Acacus Formation, NC2 concession, Hamada Basin, NW Libya.



Schlumberger, 1987

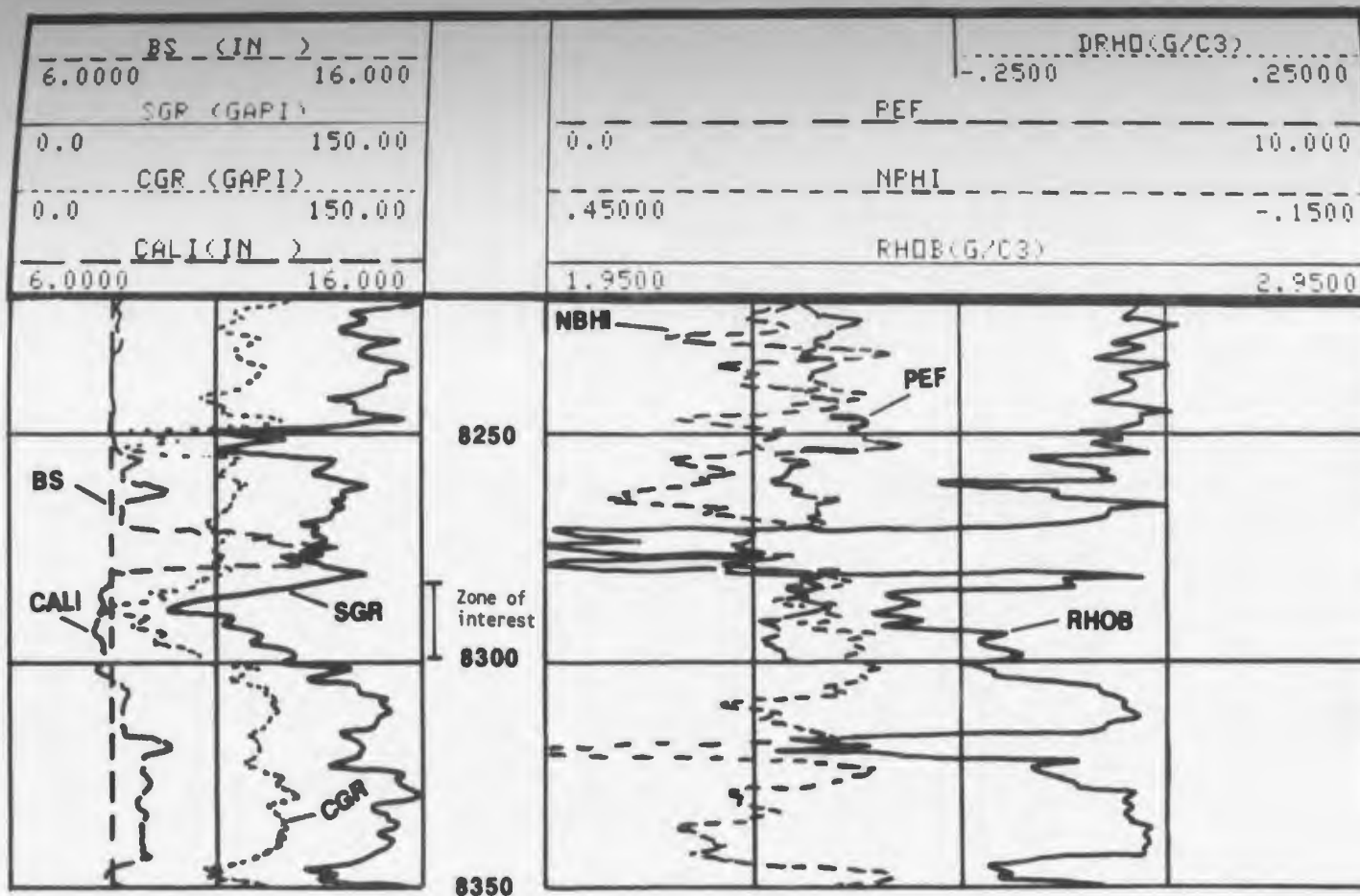
Resistivity logs (MSFL,ILD,SFL), sonic log (DT) with bit size (BS), caliper log (CALI), gamma ray log (GR), and spontaneous potential log (SP), for A12 sand/silt unit, well F1-NC2, NC2 concession, Hamada Basin, NW Libya.

" Depth divisions are 50 ft (15.24m) apart "

Porosity of this unit from 8284 to 8292 ft. is indicated by a high (80 to 90 μ sec./ft.) interval transit time (DT) as evidenced by the left deflection on the sonic log (Fig. 56) and by the combination neutron-density log (Fig. 57). Grain size determination from the cross plot of water saturation (S_w) versus porosity (\emptyset) indicates, fine to medium grained sandstones. Very fine-silty sandstone is also present, as indicated by the data points at 8288 ft., 8289 ft. and 8280 ft. (Fig. 58). However, because of the presence of very fine-silty sandstones and shaly sandstones at the bottom of the interval, the relative water saturation will be increased from 23% in the fine to medium grained sandstones to 71% in the very silty, shaly sandstones, but the well is not producing free water, and is still at its minimum water saturation (S_{wirr}).

As grain sizes decrease, the possibility of the presence of shale increases in this unit. The neutron log and the density log may reveal some of this clay effect on sand porosity. High values for neutron porosity (\emptyset_N) through the tested interval range from 23% to 28% with corresponding relative decrease in density porosity (\emptyset_D) from 15% to 20%. "... The differences between neutron porosity and density porosity can only be related to the hydrogen ions bound in the lattice of shale..." (Dewan, 1983). Unfortunately, this sand/silt unit has not been

Figure 57. Combination neutron-density logs (NPFI-RHOB), photo-electric index log (PEF) with bit size (BS), gamma-ray logs (SGR-CGR), and caliper log (CALI), for A12 sand/silt unit, well F1-NC2, Lower Acacus Formation, NC2 concession, Hamada Basin, NW Libya.



Schlumberger, 1987

Combination Neutron-Density logs (NPHI-RHOB), photo-electric index log (PEF), with bit size (BS), gamma ray logs (SGR,CGR), and caliper log (CALI), for A12 sand/silt unit, well F1-NC2, Lower Acacus Formation, NC2 concession, Hamada Basin, NW Libya.

" Depth divisions are 50 ft (15.24m) apart "

TABLE 5
Log Evaluation for A12 Sand/Silt Unit, F1-NC2 Well, Lower Acacus Formation, NC2 Concession,
Hamada Basin, NW Libya

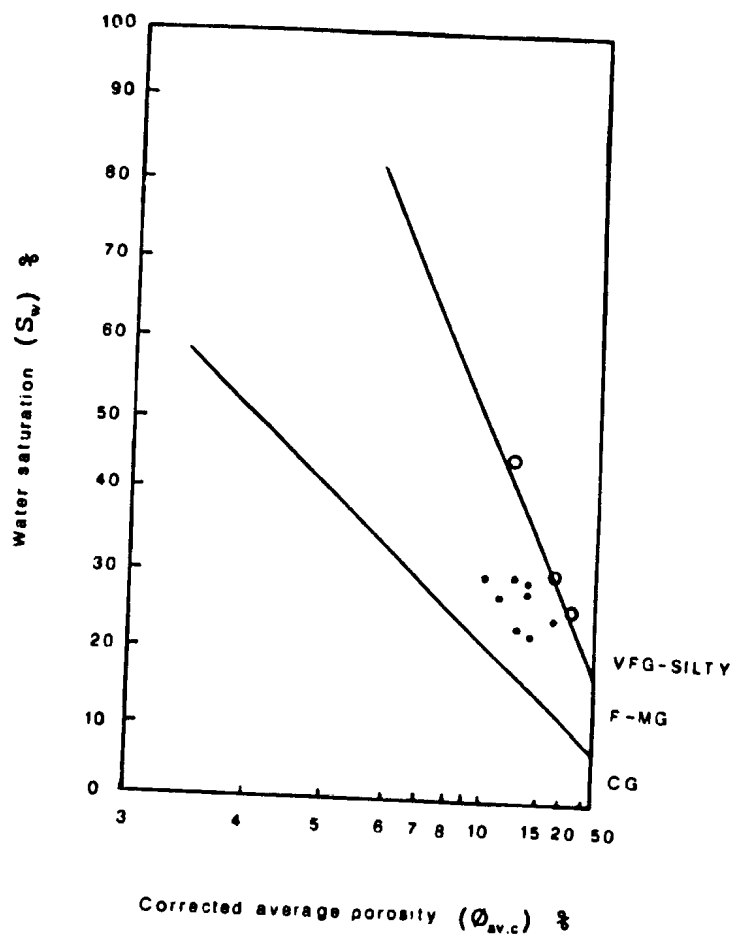
Depth (ft)	GR (API)	V _{clay} (%)	R _t (Ω)	Δt (μs/ft)	Ø _S (%)	Ø _{Sc} (%)	ρ _b (gm/cc)	Ø _D (%)	Ø _{Uc} (%)	Ø _N (%)	Ø _{Nc} (%)	Ø _{av c} (%)	S _w (%)	S _h (%)	S _{wirr} (%)
8284	80	42	2	80	20	10	2.45	15	6	26	13	14	28	72	14
8285	76	37	1.5	85	23	13	2.36	20	11	27	16	13	25	75	15
8286	75	36	1	88	26	16	2.40	18	10	27	16	14	29	71	14
8287	60	21	1	90	27	20	2.38	19	14	28	22	18	26	74	11
8288	68	19	0.6	93	25	12	2.35	21	10	22	18	11	27	73	20
8289	70	31	0.7	87	20	13	2.35	11	12	23	13	16	30	70	20
8290	75	36	0.8	82	21	12	2.40	18	10	23	12	11	15	55	18
8291	72	33	1	80	20	12	2.38	19	11	26	16	13	31	69	15
8292	70	31	1.5	80	20	12	2.36	20	12	27	17	15	23	77	13
8294	90	53	1.5	70	12	2	2.31	22	13	27	11	8	41	59	25
8296	75	36	2	71	12	5	2.35	21	12	25	14	10	30	70	20
8298	98	61	2	70	12	0	2.44	16	3	26	7	3	94	6	67
8300	98	61	2	72	13	0	2.35	21	5	26	7	4	71	29	51

Remarks:

GR_{max} = 135 API
 GR_{min} = 40 API
 R_w = 0.002 Ω

OBE-91

Figure 58. Grain size determination by water saturation (S_w) versus corrected average log porosity ($\phi_{av,c}$) crossplot, for A12 sand/silt unit, well F1-NC2, Lower Acacus Formation, NC2 concession, Hamada Basin, NW Libya.



KEY:
 VFG-SILTY - very fine grained to silty sandstone points.
 F-MG - fine to medium grained sandstone points.
 CG - coarse grained sandstone points.
 ○ - very fine grained to silty sandstone points.
 ● - fine to medium grained sandstone points.

Grain size determination by water saturation (S_w) versus corrected average log porosity ($\phi_{av,c}$) crossplot for A12 sand/silt unit, well F1-NC2, Lower Acacus Formation, NC2 concession, Hamada Basin, NW Libya.

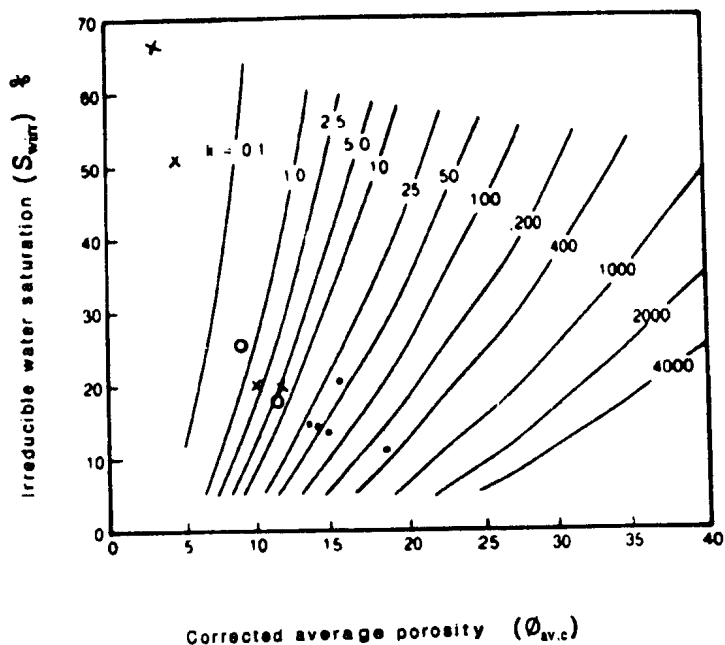
Note, Shale points of GR reading > 75 API are not included.

(Chart after Schlumberger, 1972 ; Asquith et al, 1982).

cored so that we can not obtain any value of permeability. Shale laminae can also create permeability problems.

In this case, in order to estimate the total permeability for this rock and the relative permeabilities to all fluid phases, a crossplot (Fig. 59) of corrected average porosity (ϕ_{nc}) and irreducible water saturation (S_{wir}) (Schlumberger, 1972) is presented. This crossplot indicates a permeability range of 25 md. to 400 md. for the fine to medium grained sandstones, while a low permeability of less than 5 md. characterizes the very fine and shaly sandstones in the lower part of the unit, i.e from 8288 to 8300 ft. Figure 60 illustrates data points of relative permeability to gas with values less than 0.1 md. at 8298 and 8300 ft. equivalent to the shaly points. These points can be expected to have more water in their tiny pore spaces. Points with relative permeability to gas between line 0.2 and line 0.4 (20-40 md.) occur at 8290 and 8294 it is correspond to the very fine-grained silty sandstone at the bottom of the interval (8284-8300 ft). These sands have a high chance of producing some water. Points falling between permeability lines 0.6 and 1.0 (60 md. and 100 md.) (8284-8290 ft) having a high relative permeability to gas (K_g) which should produce less water. As the gas relative permeability (K_g) values decrease (down the interval, at 8298 -8300 ft) the water relative permeability (K_w) values

Figure 59. Corrected average log porosity ($\phi_{v,c}$) versus irreducible water saturation (S_{wir}) crossplot for determining total permeability for A12 sand/silt unit, well F1-NC2, Lower Acacus Formation, NC2 concession, Hamada Basin, NW Libya.



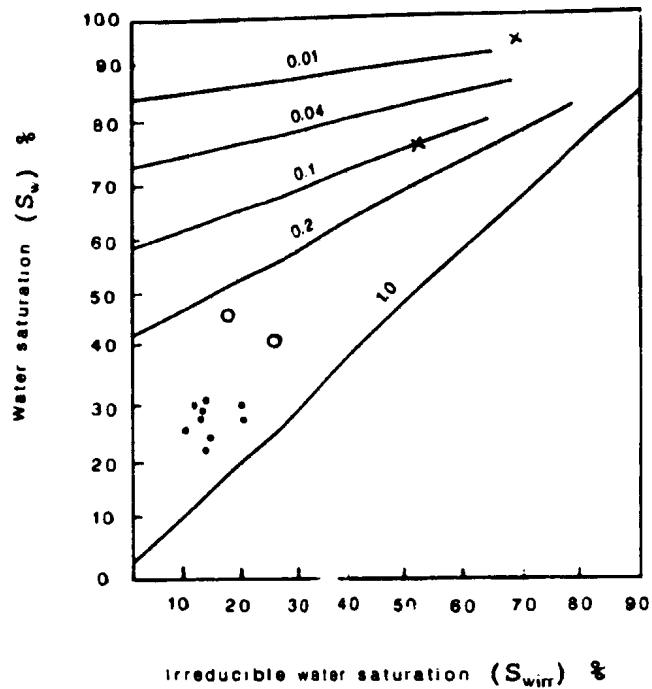
KEY:

- x Shale points.
- o Very fine grained to silty sandstone points.
- Fine to medium grained sandstone points

Corrected average porosity ($\phi_{av,c}$) versus irreducible water saturation (S_{wirr}) crossplot for determining total permeability for A12 sand/silt unit, well F1-NC2, Lower Acacus Formation, NC2 concession, Hamada Basin, NW Libya.

(Chart after Schlumberger, 1979).

Figure 60. Water saturation (S_w) versus irreducible water saturation (S_{wirr}) crossplot for determining relative permeability to gas (K_{rg}) for A12 sand/silt unit, well F1-NC2, Lower Acacus Formation, NC2 concession, Hamada Basin, NW Libya.

Relative permeability to gas (K_{rg})

KEY:

- x Shale points.
- Very fine grained to silty sandstone points.
- Fine to medium grained sandstone points

Water saturation (S_w) versus irreducible water saturation (S_{wirr}) crossplot for determining relative permeability to gas (K_{rg}) for A12 sand/silt unit, well F1-NC2, Lower Acacus Formation, NC2 concession, Hamada Basin, NW Libya.

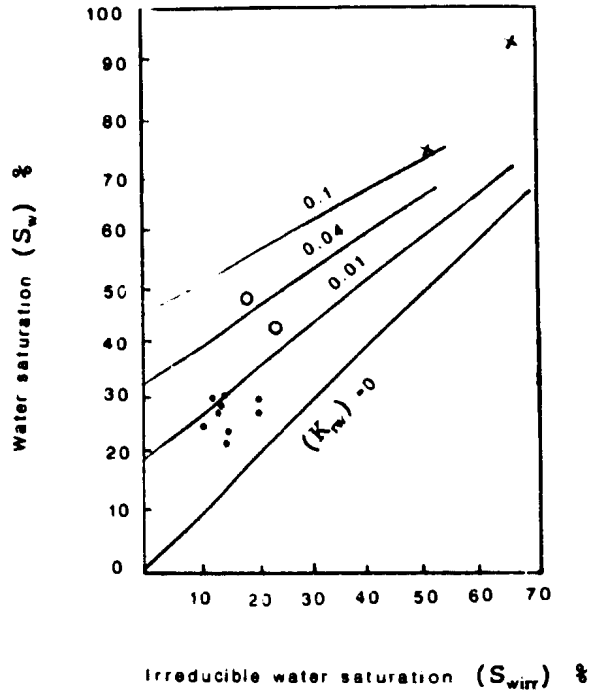
(Chart after Schlumberger, 1972 ; Asquith et al, 1982).

increase (from 1 to 100 md.) as the tested interval changes in grain size and lithology (very fine sandstone and silty sandstone). The K_w values for the fine to medium grained sandstones are less than 1 md. (less than 0.01 permeability line) (Fig. 61). During perforation test No.6 (8284-8292 ft) the well produced clean oil with gas but no water. Again, the water in this case may be held in the micropores, but is still residual, mobile and at its minimum (Schlumberger, 1972; Pittman, 1979). A percent water-cut plot (Fig. 62) shows the water-bearing points in this unit, i.e. two shaly points from depth 8298 ft. and 8300 ft. each having water-cuts greater than 60%. Two very fine-silty sandstone points from depth 8290 ft. and 8294 ft. have water-cuts between 20% and 60% lines.

Both the shaly points and the very fine-silty sandstone points are indicate a tendency to yield some water. The fine to medium grained sandstone points at the top of the tested interval (8284-8289 ft) are of low water-cut percentages between 0-20% lines, in fact they have water-cut (Wc) values less than 20% which may confirm the perforation test results which indicated water free production (AGOCO DST reports).

The relative permeabilities to oil (K_{ro}) of the data points in the studied interval are shown on crossplot of water saturation (S_w) and irreducible water saturation

Figure 61. Water saturation (S_w) versus irreducible water saturation (S_{wirr}) crossplot for determining relative permeability to water (K_{rw}) for A12 sand/silt unit, well F1-NC2, Lower Acacus Formation, NC2 concession, Hamada Basin, NW Libya.



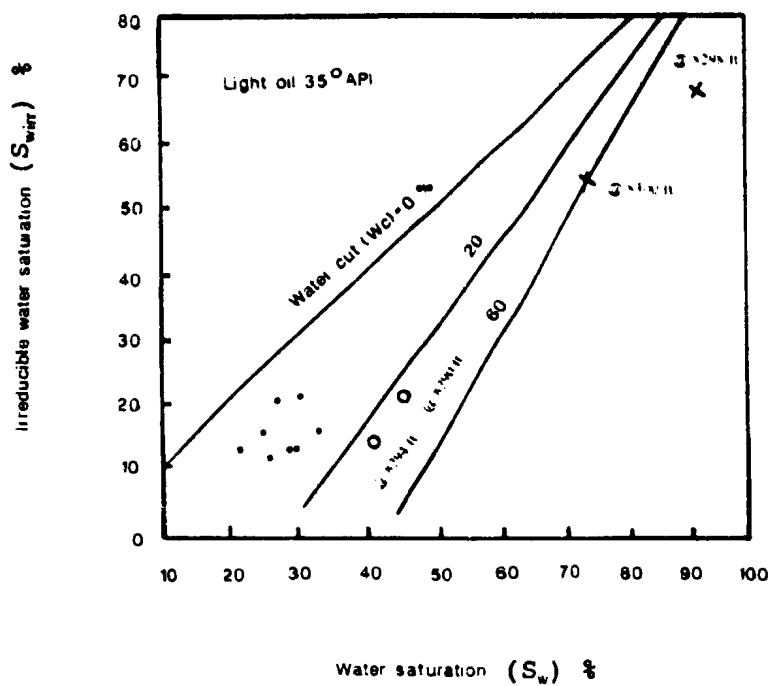
KEY:

- x Shale points.
- o Very fine grained to silty sandstone points.
- Fine to medium grained sandstone points

Water saturation (S_w) versus irreducible water saturation (S_{wirr}) crossplot for determining relative permeability to water (K_{rw}) for A12 sand/silt unit, well F1-NC2, Lower Acacus Formation, NC2 concession, Hamada Basin, NW Libya.

(Chart after Schlumberger, 1972 ; Asquith et al, 1982).

Figure 62. Water saturation (S_w) versus irreducible water saturation (S_{wir}) crossplot for determining percent water-cut (35°API gravity oil) for A12 sand/silt unit, well F1-NC2, Lower Acacus Formation, NC2 concession, Hamada Basin, NW Libya.



Key:

- x Shale points.
- o Very fine grained to silty sandstone points.
- Fine to medium grained sandstone points.

Water saturation (S_w) versus irreducible water saturation (S_{wirr}) crossplot for determining percent water-cut (35°API gravity oil) for A12 sand/silt unit, well F1-NC2, Lower Acacus Formation, NC2 concession, Hamada Basin, NW Libya.

(Chart after Schlumberger, 1972 ; Fertl et al, 1978).

(S_{win}) (Fig. 63). Data points corresponding to fine to medium grained sandstones have a high K_{ro} between 0.5 and 1.0 lines (50 md. and 100 md.), and represent zones which should produce oil.

As grain size changes (very fine silty sandstone to shaly sandstone) there occurs an increase in distance from the $K_{ro} = 1$ line (100% line) of the value of K_{ro} between 0 and less than 0.5 (0 to < 50%). This indicates the possibility of an increasing amount of water toward the bottom part of the tested interval.

Formation testing reports (AGOCO DST reports) have indicated that this interval was perforated from 8284 ft. to 8292 ft. and yielded clean oil (35° API) with some gas. The open flow rate of gas was 5.212 MMCFGPD at high tubing pressure of 1220 PSI and a bottom hole shut-in pressure of 2996 PSI at bottom hole temperature of 160° F, with gas/oil ratio (GOR) of 6021 cu. ft./bbl. The estimated oil production per day is 865.6 BOPD, oil gravity 35° API at 60° F. The estimated oil and gas reserves from the gross interval (8284 to 8300 ft.) in the A12 sand/silt unit of Lower Acacus Formation in well F1-NC2 is 1.7 million stock tank barrels of oil in place (MMSTBOIP) and 1.4 billion of cubic feet gas in place (MMCFGIP). These oil and gas reserves have been based on the following parameters:

Areal closure = 371 acres

Net pay = 10 ft.

Corrected average log porosity ($\phi_{av,c}$) = 12%

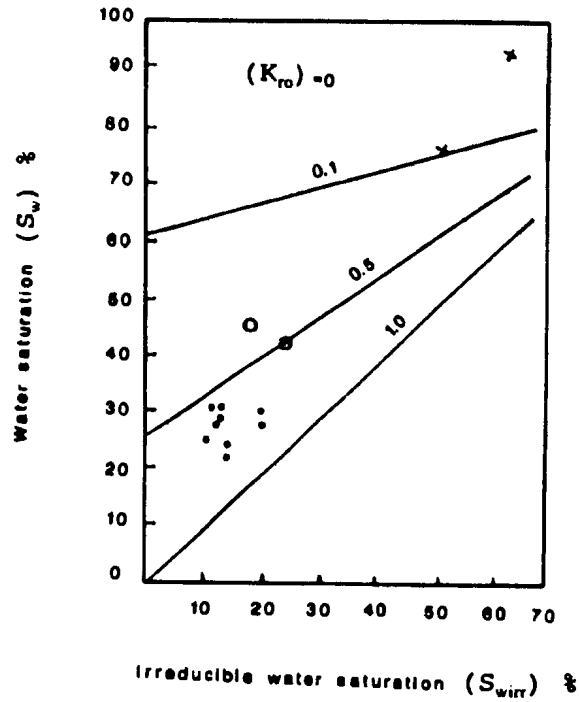
Water saturation (S_w) = 31%

Hydrocarbon saturation (S_h) = 69%

Estimated oil volume factor (O.V.F.) in the
Lower Acacus Formation = 1.4 cu. ft./bbl.

Estimated gas volume factor (B_g) in the
Lower Acacus Formation = 160.4 SCF/cu. ft.

Figure 63. Water saturation (S_w) versus irreducible water saturation (S_{wirr}) crossplot for determining relative permeability to oil (K_{ro}) for A12 sand/silt unit, well F1-NC2, Lower Acacus Formation, NC2 concession, Hamada Basin, NW Libya.



KEY:

- x Shale points.
- o Very fine grained to silty sandstone points.
- Fine to medium grained sandstone points

Water saturation (S_w) versus irreducible water saturation (S_{wirr}) crossplot for determining relative permeability to oil (K_{ro}) for A12 sand/silt unit, well F1-NC2, Lower Acacus Formation, NC2 concession, Hamada Basin, NW Libya.

(Chart after Schlumberger, 1972 ; Asquith et al, 1982).

3. Log interpretation of A8 sand/silt unit (9704-9730 ft.) (proximal delta front lithofacies, #3), well C1-NC2, Lower Acacus Formation:

Figures 64 and 65 indicate that the log suite used in the C1-NC2 well includes SP log, GR log, Caliper log, Resistivity logs (SFL, MSFL and ILD), Sonic log (DT), and a combination Neutron-density log with a Gamma-ray (GR) log and caliper log (CALI). The SP log in Figure 64 is featureless with no deflection either to the right or to the left opposite to either shale or sand intervals. This response is very common in most logs in the study area, and may be due to salinity variation between drilling mud and formation water, or may be due to mechanical problems. Regardless of the SP log response, the GR log (Fig. 64) shows low values (29-50 API) opposite sand zones, with high values (60-97 API) opposite shale or shaly sandstone zones (Table 6), due to their greater concentration of radioactivity than that found in sandstone (Helander, 1984). The GR log curve reveals the alternation of shale throughout the sandstone sequence, as indicated by the relatively high GR readings.

On the caliper log, mud cake development is important because it indicates a permeable zone (Asquith and Gibson, 1982). Mud cake forms by the accumulation of the drilling mud particles on the borehole walls when porous and permeable zone such as that at 9704-9728 ft. is invaded

with drilling fluids. This causes a decrease in hole diameter (note that the bit size (BS) is 8.5 inches and the hole has been reduced to 8 inches; hence, the 0.5 inches is the mud cake thickness).

On the resistivity logs, a separation between (ILD) deep induction log and the microspherically focused log (MSFL) indicates invasion has taken place (Schlumberger, 1974) in the interval between 9704 and 9716 ft. The deep induction log (ILD) reads relatively high resistivity values for R_t from 1 to 2 Ohmm. (Fig. 64) increased true formation resistivity (R_t) indicates the presence of hydrocarbons.

However, in the interval between 9716 to 9718 ft. all the resistivity logs (SFL, MSFL and ILD) meet at one point and show no separation, suggesting no invasion, opposite an impermeable, non-porous zone composed mainly of shale, as indicated by GR log curve (Fig. 64). The resistivity curves from 9720 to 9730 ft. tend to separate as invasion takes place coincident with a permeable, porous sand zone. The curves also show high resistivity, which indicates the presence of hydrocarbons.

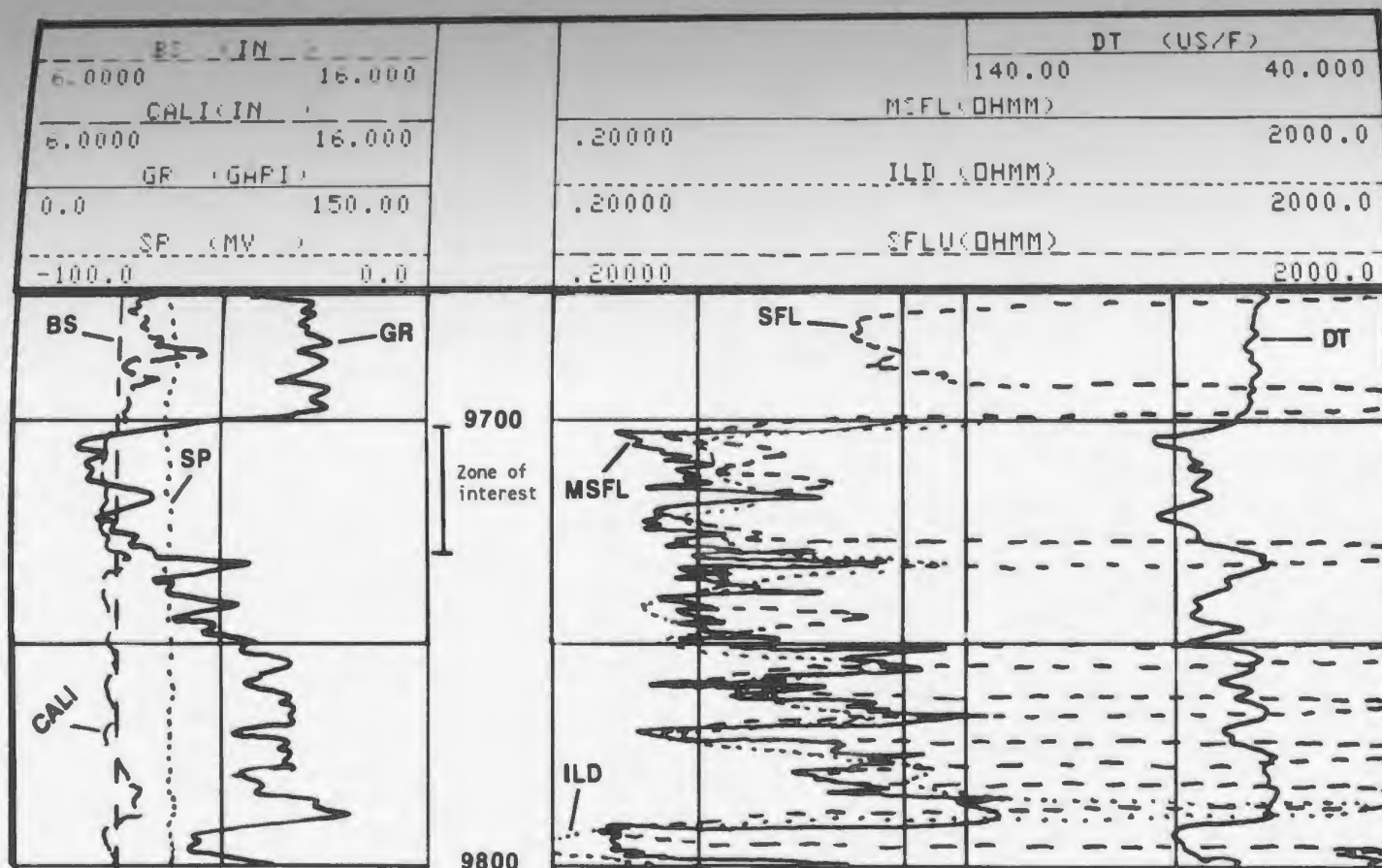
Porosity in the sand zones from 9704 to 9716 ft. and from 9720 and 9728 ft. is recognized by the high (84-93 μ sec./ft.) interval transit time (DT) on the sonic

log, while porosity in the shale bearing zones from 9716 to 9720 ft. and from 9728 to 9730 ft. is apparent by the low (67-79 μ sec./ft.) interval transit time (DT) (Fig. 64).

On the neutron-density porosity logs recorded over the A8 sand/silt unit interval from 9704 to 9730 ft., the neutron log has recorded porosity at the top of the sand unit between 9706 ft. and 9708 ft. with values 25% and 27% respectively. The density log has recorded relatively high porosities at the same mentioned depths with values of 32% and 30% respectively. The differences in porosity values indicated by neutron-density logs (Fig. 65) cause a slight separation of the two porosity curves which can be explained by the possible presence of gas at the top part of this zone (Denno, 1978). Another point of interest is that the neutron-density curves also indicate separation (low neutron porosity of 22%) and of high apparent density porosity of 24%) between 9735 ft. and 9739 ft., indicating another gas bearing sand zone of a separate pool.

The reservoir's grain size ranges from fine to medium grained sandstone as determined by petrographic and core section studies (C #4, Fig.App.I-4) in this unit. Confirmation of grain size in this unit as being fine to medium grained is made after a crossplot (Fig. 66) of water saturation (S_w); calculated by Archie equation (Table 6)

Figure 64. Resistivity logs (MSFL, ILD, SFL), sonic log (DT) with bit size (BS), caliper log (CALI), and spontaneous-potential log (SP), for A8 sand/silt unit, well C1-NC2, Lower Acacus Formation, NC2 concession, Hamada Basin, NW Libya.

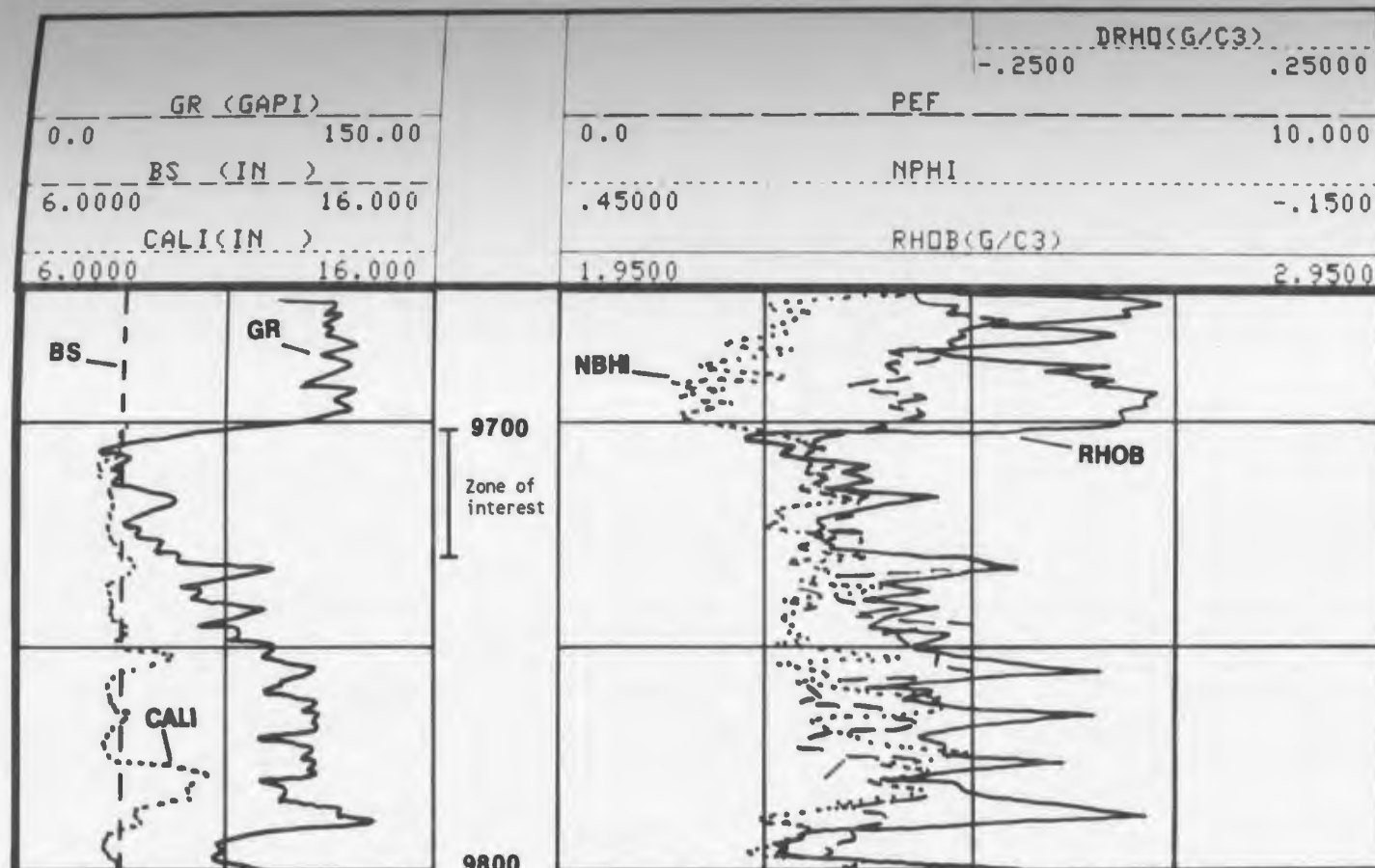


Schlumberger, 1986

Resistivity logs (MSFL,ILD,SFL), sonic log (DT) with bit size (BS), caliper log (CALI), gamma ray log (GR), and spontaneous potential log (SP), for A8 sand/silt unit, well C1-NC2, NC2 concession, Hamada Basin, NW Libya.

" Depth divisions are 50 ft (15.24m) apart "

Figure 65. Combination neutron-density logs (NPHI-RHOB), photo-electric index log (PEF), with gamma-ray log (GR), bit size (BS), and caliper log (CALI), for A8 sand/silt unit, well C1-NC2, Lower Acacus Formation, NC2 concession, Hamada Basin, NW Libya.



Schlumberger, 1986

Combination Neutron-Density logs (NPHI-RHOB), photo-electric index log (PEF), with gamma ray log (GR), bit size (BS), and caliper log (CALI), for A8 sand/silt unit, well C1-NC2, Lower Acacus Formation, NC2 concession, Hamada Basin, NW Libya.

" Depth divisions are 50 ft (15.24m) apart "

TABLE 6

Log Evaluation for A8 Sand Silt Unit, C₁-NC₂ Well, Lower Acacus Formation, NC₂ Concession, Hamada Basin NW Libya

Depth (ft)	GR (API)	V _{clay} (%)	R _t (°)	ΔI (μs/ft)	Φ _S (%)	Φ _{Sr} (%)	ρ _b (gm/cc)	Φ _D (%)	Φ _{Dc} (%)	Φ _N (%)	Φ _{Nc} (%)	Φ _{AVC} (%)	S _w (%)	S _{ir} (%)	S _{irr} *
9704	45	16	1.7	90	26	21	2.22	31	25	33	28	25	19	81	8
9706	35	6	1	93	28	26	2.23	32	26	25	23	25	23	77	8
9708	37	8	1.2	90	26	23	2.26	30	24	27	25	24	22	78	8
9710	32	3	1.2	84	24	23	2.33	28	27	28	27	26	22	78	7
9712	29	0	1.3	84	24	24	2.32	23	23	28	28	25	22	78	8
9714	32	3	1.4	86	25	24	2.28	24	23	30	29	25	21	78	8
9716	50	21	2	86	25	19	2.37	19	12	28	22	18	26	73	11
9718	60	31	2	79	18	10	2.36	20	10	31	22	14	32	68	15
9720	37	8	0.9	92	27	24	2.26	27	24	33	31	26	26	74	7
9722	40	11	1	91	27	23	2.26	27	23	31	28	25	25	75	8
9724	48	19	1.2	86	25	19	2.33	28	21	29	23	21	28	72	10
9726	50	21	1.4	84	24	18	2.33	28	21	29	23	21	26	74	10
9728	75	46	2	88	17	5	2.43	15	0	29	15	6	75	34	34
9730	97	68	5	67	8	0	2.51	9	2	27	7	3	94	6	67

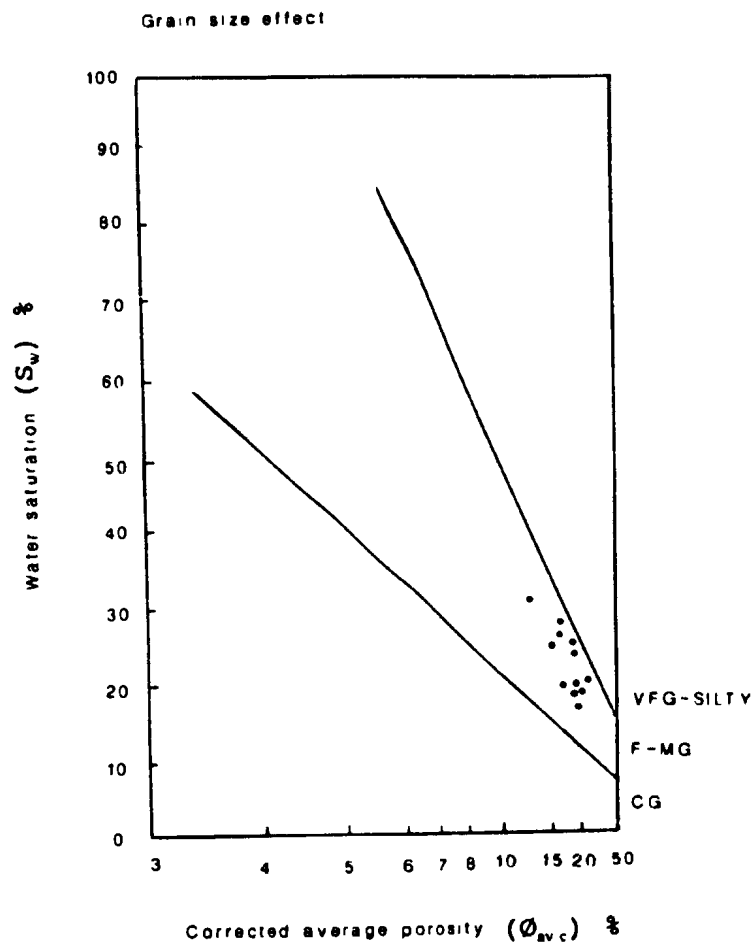
OBE-91

Remarks:

GR_{max} = 130 API, GR_{min} = 30 API, R_{av} = 0.0012

* Value for Irreducible Water Saturation, S_{irr}, used on relative permeability crossplot figures is based on S_{irr} = $\sqrt{1 - F_{0.5}^2}$ where F = 0.51 - 0.5

Figure 66. Grain size determination by
watersaturation (S_w) versus corrected
average log porosity ($\phi_{av,c}$) crossplot for
A8 sand/silt unit, well C1-NC2, Lower
Acacus Formation, NC2 concession, Hamada
Basin, NW Libya.



KEY

- VFG-SILTY - very fine grained to silty sandstone points
- F-MG - fine to medium grained sandstone points
- CG - coarse grained sandstone points
- - fine to medium grained sandstone points

Grain size determination by water saturation (S_w) versus corrected average log porosity ($\phi_{av,c}$) crossplot for A8 sand/silt unit, well C1-NC2, Lower Acacus Formation, NC2 concession, Hamada Basin, NW Libya.
Note, Shale points of GR reading > 75 API are not included.

(Chart after Schlumberger, 1972 ; Asquith et al, 1982).

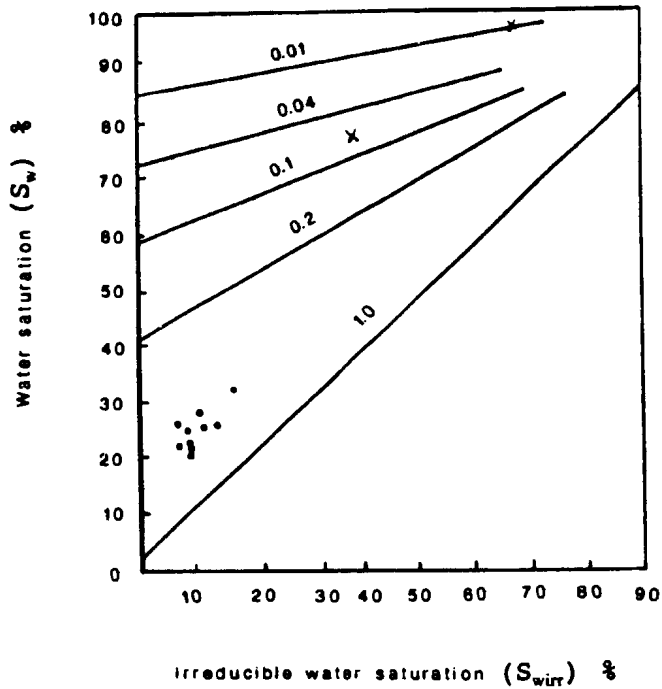
versus the corrected average log porosity ($\phi_{av,c}$), calculated from porosity logs (Table 6). Since the reservoir contains some shale, the relative permeability to gas and oil or even water if present may be lowered. A plot of the relation between water saturation (S_w) and irreducible water saturation (S_{wirr}) (Fig. 67) shows all points are clustered. High relative gas permeability (K_{rg}) ranges between the 0.2 line and the 1.0 line (20 md. and 100 md.), indicating good relative gas permeability (K_{rg}) at low irreducible water saturation (S_{wirr}) ranging from 7% to 15% for these intervals of fine to medium grained sandstones.

High water saturations of 66% to 94% are indicated for the lower shaly zone (9728-9730 ft), even after applying a shale volume correction equation for the sandstone.

At points 9728 ft. and 9730 ft., the shale content is the reason for the low relative permeability to gas (Fig. 67) which is less than the 0.1 line (<10 md.). At these two particular points the reservoir is not at irreducible water saturation ($S_{wirr} = 33\%$ and $S_{wirr} = 67\%$ respectively) (see Table 6) and may produce some water.

As K_{rg} values increase, relative permeability to water decreases (Fig. 68) to a level which is almost less than the 0.01 line (<0.01 md.) for the fine to medium grained sand. At this level the reservoir will not produce water.

Figure 67. Water saturation (S_w) versus irreducible water saturation (S_{wir}) crossplot for determining relative permeability to gas (K_{rg}) for sand/silt unit, well C1-NC2, Lower Acacus Formation, NC2 concession, Hamada Basin, NW Libya.



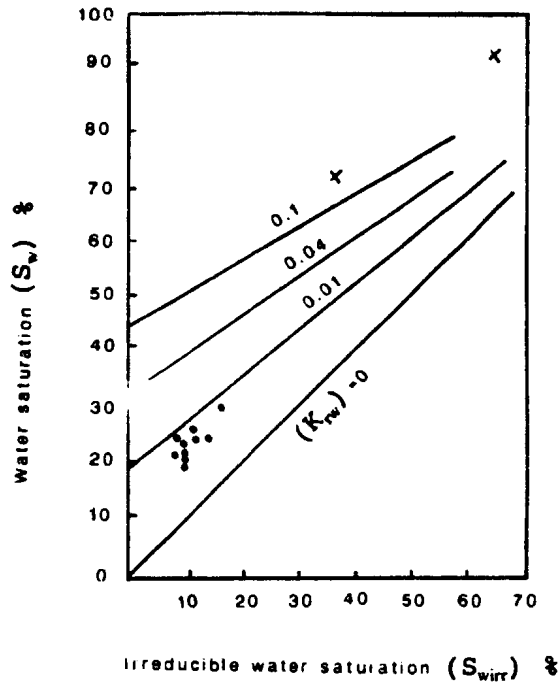
KEY:

- x Shale points.
- Fine to medium grained sandstone points.

Water saturation (S_w) versus irreducible water saturation (S_{wirr}) crossplot for determining relative permeability to gas (K_{rg}) for AS sand/silt unit, well C1-NC2, Lower Acacus Formation, NC2 concession, Hamada Basin, NW Libya.

(Chart after Schlumberger, 1972 ; Asquith et al, 1982).

Figure 68. Water saturation (S_w) versus irreducible water saturation (S_{wirr}) crossplot for determining relative permeability to water (K_{rw}) for A8 sand/silt unit, well C1-NC2, Lower Acacus Formation, NC2 concession, Hamada Basin, NW Libya.



KEY:

- x Shale points.
- Fine to medium grained sandstone points.

Water saturation (S_w) versus irreducible water saturation (S_{wirr}) crossplot for determining relative permeability to water (K_{rw}) for AS sand/silt unit, well C1-NC2, Lower Acacus Formation, NC2 concession, Hamada Basin, NW Libya.

(Chart after Schlumberger, 1972 ; Asquith et al, 1982).

The relationship of grain size and water saturation is such that very fine grained sands or shaly sands (at 9728-9730 ft.) have high irreducible water saturation and, consequently, they also have a high values of water volume held in the small pores (Asquith and Gibson, 1982; Schlumberger, 1972).

Figure 69 illustrates the relative permeability to oil (K_{ro}) of different zones of different lithology and grain size. On a crossplot of S_{wirr} versus S_w , points clustering between relative permeability lines 0.5 and 1.0 (50-100 md.) respectively show zones which should produce oil, but as the data plots fall more distance from the $K_{ro} = 1.0$ line, the chance of producing some water will be expected. When the lower part of the A8 sand/silt unit in well C1-NC2 was perforated from 9720 to 9730 ft. and tested, the unit produced clean oil with gas, with some traces of water cut (0-5%) (Fig. 70). There is an oil-shale contact at 9728 ft. in this reservoir. The well potential at this interval (9720-9730 ft.) was 730 barrels of oil per day (BOPD) of oil gravity 34.5° API and 159,000 cubic feet of gas per day (159 MCFGPD) with a gas/oil ratio of 218 cu.ft.g./bbl. (Table 8).

An estimate of oil and gas reserves by volumetric calculation of gross A8 sand/silt unit (9704-9730 ft.) in well C1-NC2 of Lower Acacus Formation is 16.8 MMSTBOIP,

1.4 MMCFGIP, using the following parameters:

Areaal closure = 5 km²

= 1235.5 Acres

Net pay = 16 ft.

Corrected average log porosity ($\phi_{av,c}$) = 22%

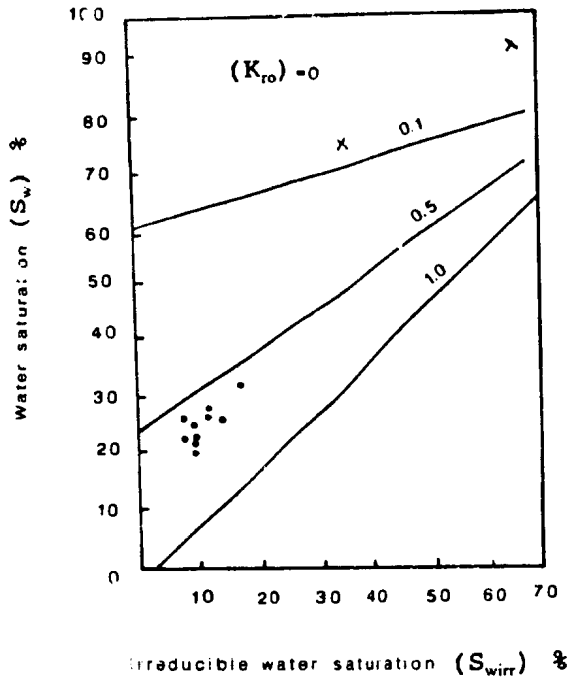
Water saturation (S_w) = 30%

Hydrocarbon saturation (S_h) = 70%

Estimated oil volume factor (O.V.F.) in the Lower
Acacus Formation = 1.4 cu. ft./bbl.

Estimated gas volume factor (Bg) in the Lower
Acacus Formation = 160.4 SCF/cu. ft.

Figure 69. Water saturation (S_w) versus irreducible water saturation (S_{wir}) crossplot for determining relative permeability to oil (K_{ro}) for A8 sand/silt unit, well C1-NC2, Lower Acacus Formation, NC2 concession, Hamada Basin, NW Libya.



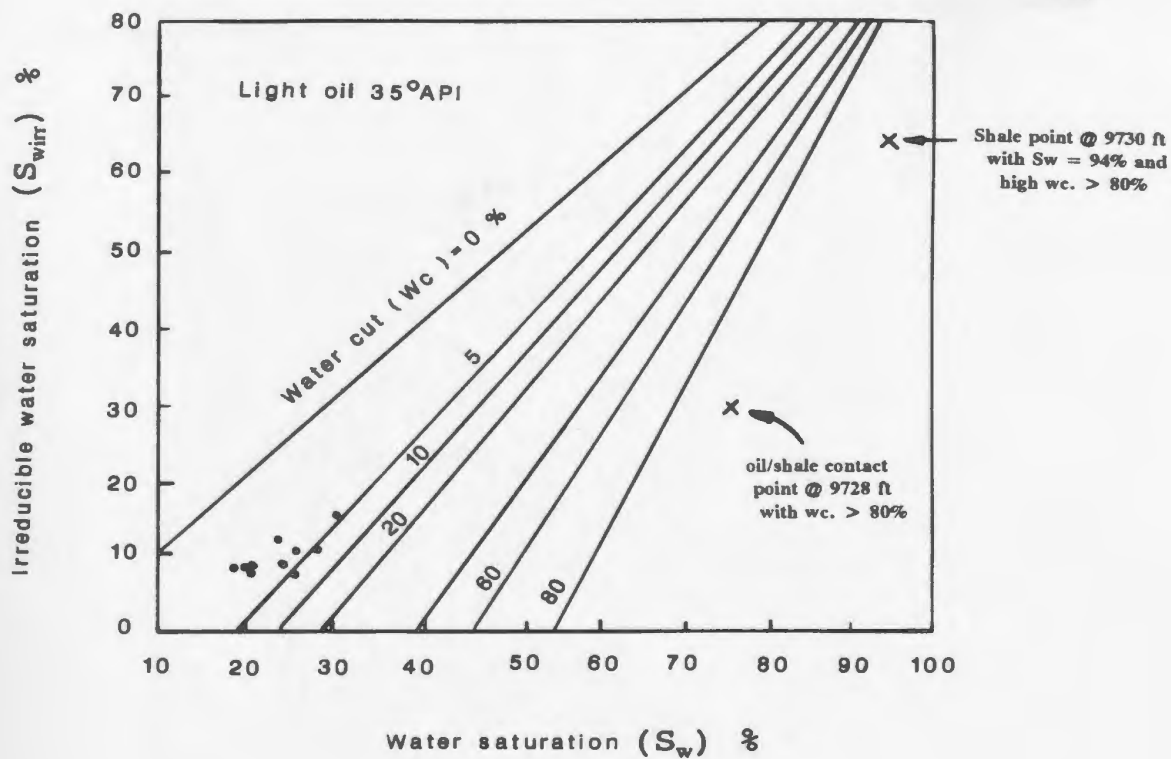
KEY:

- x Shale points.
- Fine to medium grained sandstone points.

Water saturation (S_w) versus irreducible water saturation (S_{wirr}) crossplot for determining relative permeability to oil (K_m) for A8 sand/silt unit, well C1-NC2, Lower Acacus Formation, NC2 concession, Hamada Basin, NW Libya.

(Chart after Schlumberger, 1972 ; Asquith et al, 1982).

Figure 70. Water saturation (S_w) versus
irreducible water saturation (S_{wirr})
crossplot for determining percent water-
cut (35° API gravity oil) for A8 sand/silt
unit, well C1-NC2, Lower Acacus Formation,
NC2 concession, Hamada Basin, NW Libya.



KEY:

- × Shale points.
- Fine to medium grained sandstone points.

Water saturation (S_w) versus irreducible water saturation (S_{wirr}) crossplot for determining percent water-cut (35°API gravity oil) for A8 sand/silt unit, well C1-NC2, Lower Acacus Formation, NC2 concession, Hamada Basin, NW Libya.

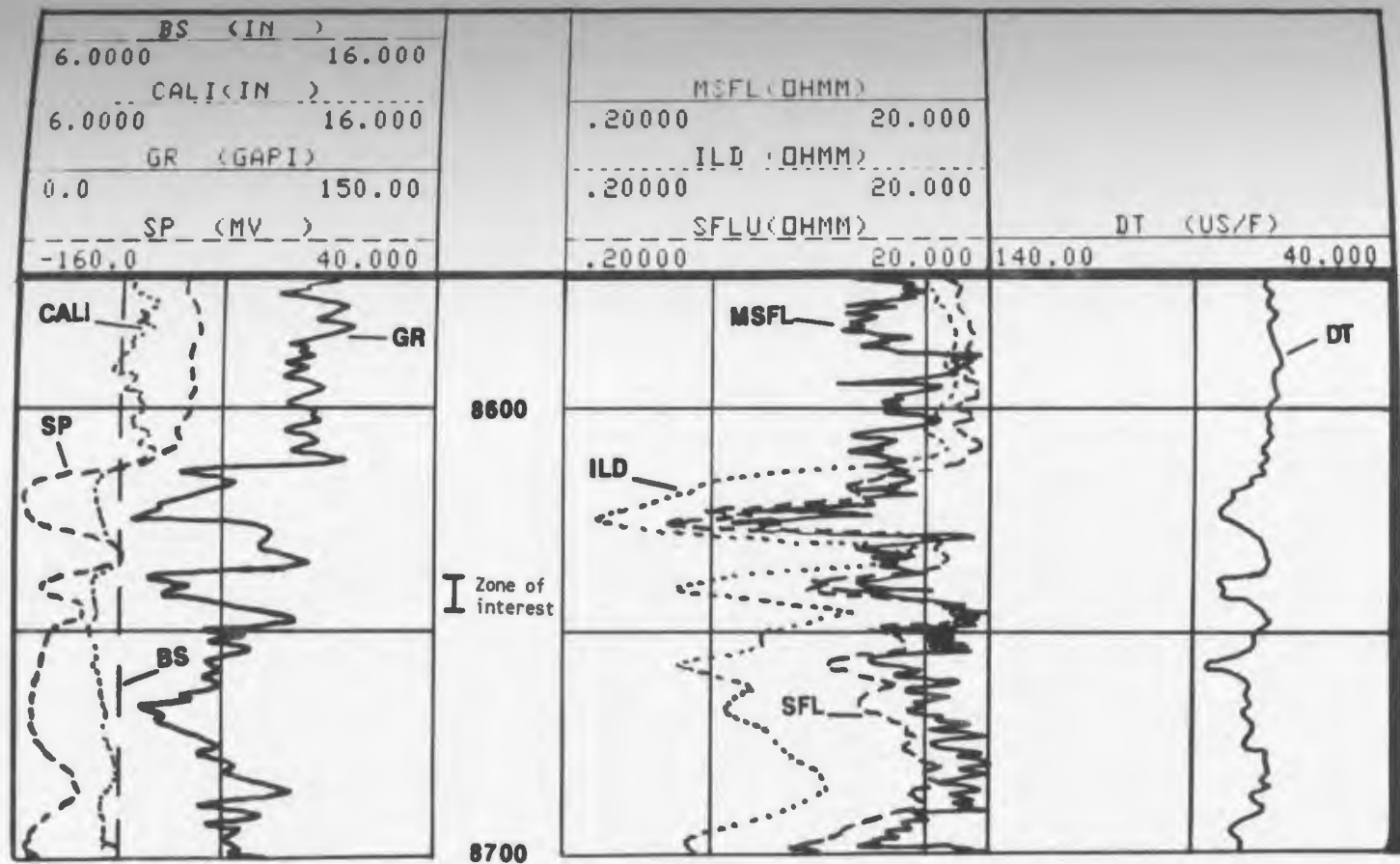
(Chart after Schlumberger, 1972 ; Fertl et al, 1978).

4. Log interpretation of A8 sand/silt unit (8638-8644 ft.) (distal delta front lithofacies, #2) well A1-NC2, Lower Acacus Formation:

The A8 sand/silt unit at depth 8638 to 8644 ft. in well A1-NC2 on the northern side of the study area represents the lateral extension of A8 sand/silt unit in C1-NC2. Environmental interpretation of this unit at well A1-NC2 places it in the distal part (marginal) of the delta lobe which prograded from south to north across the study area.

This unit is shown on SP curve (Fig. 71) by a leftward deflection from the base shale line, which indicates the presence of some porous and permeable sand in the interval in question. The separation between the deep induction curve (ILD) and the short focused curve (SFL) indicates that some invasion has taken place (Fig. 71) and that sand may have some permeability. The porosity can be determined from the Sonic log by means of the interval transit time (DT) which measures 73 to 82 μ sec./ft. (Table 7). Examination of the neutron-density log (Fig. 72) reveals neutron porosity (ϕ_N) is higher than density porosity (ϕ_D) (Table 7) and records a neutron porosity reading of 21-27%, and density porosity readings of 12-21%. The higher neutron porosity (ϕ_N) is recorded "...due to the hydrogen ions concentration..." (Denoo, 1978; Asquith and Gibson, 1982) associated with the shale laminae and the very silty grains

Figure 71. Resistivity logs (MSFL, ILD, SFL),
sonic log (DT) with bit size (BS),
caliper log (CALI), gamma-ray log (GR),
and spontaneous-potential log (SP), for
A8 sand/silt unit, well A1-NC2, Lower
Acacus Formation, NC2 concession, Hamada
Basin, NW Libya.

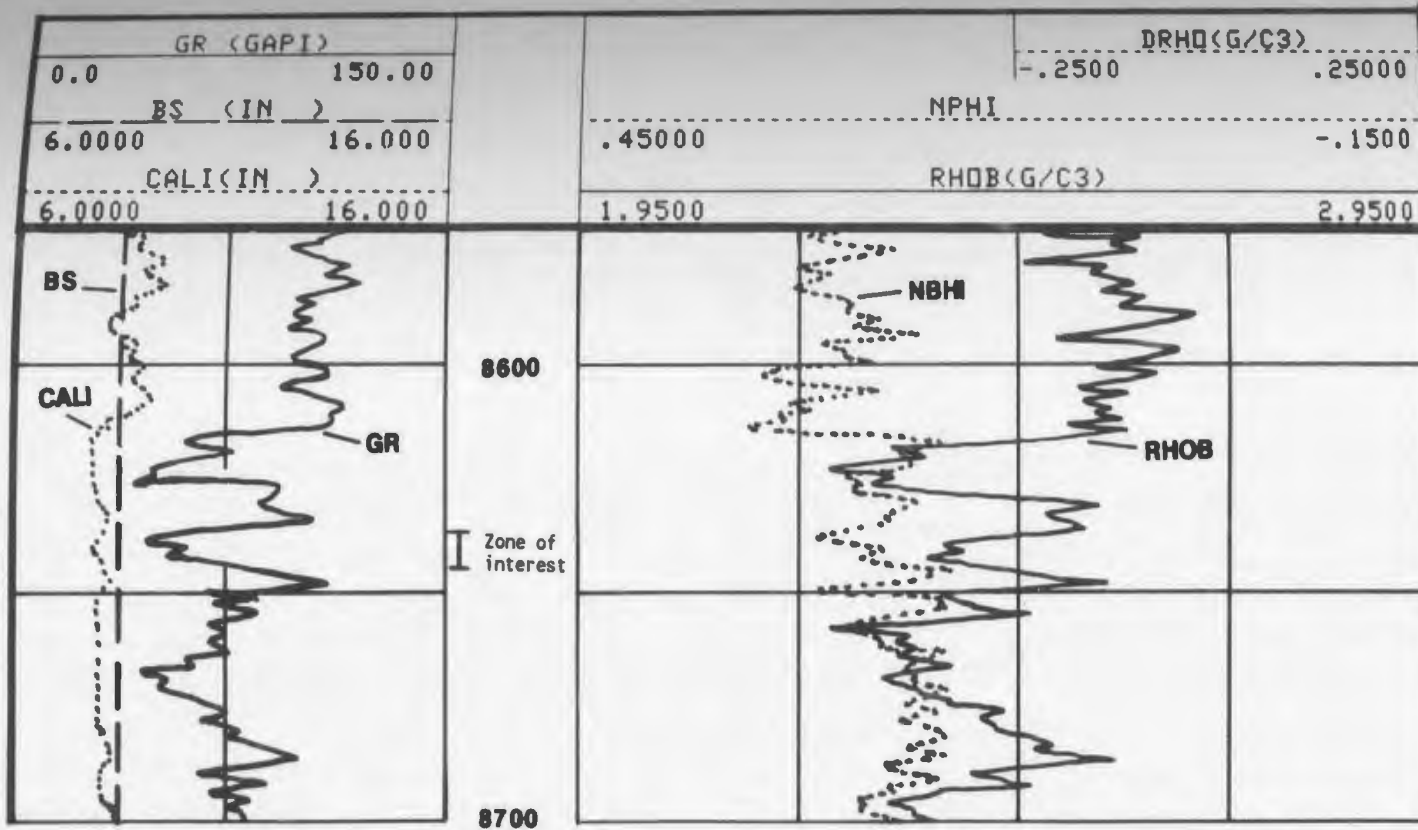


Schlumberger, 1985

Resistivity logs (MSFL,ILD,SFL), sonic log (DT) with bit size (BS), caliper log (CALI), gamma ray log (GR), and spontaneous potential log (SP), for AS sand/silt unit, well A1-NC2, NC2 concession, Hamada Basin, NW Libya.

" Depth divisions are 50 ft (15.24m) apart "

Figure 72. Combination neutron-density logs (NPHI-RHOB) with gamma ray log (GR), bit size (BS), and caliper log (CALI), for A8 sand/silt unit, well A1-NC2, Lower Acacus Formation, NC2 concession, Hamada Basin, NW Libya.



Schlumberger, 1985

Combination Neutron-Density logs (NPHI-RHOB), with gamma ray log (GR), bit size (BS), and caliper log (CALI), for A8 sand/silt unit, well A1-NC2, Lower Acacus Formation, NC2 concession, Hamada Basin, NW Libya.

" Depth divisions are 50 ft (15.24m) apart ".

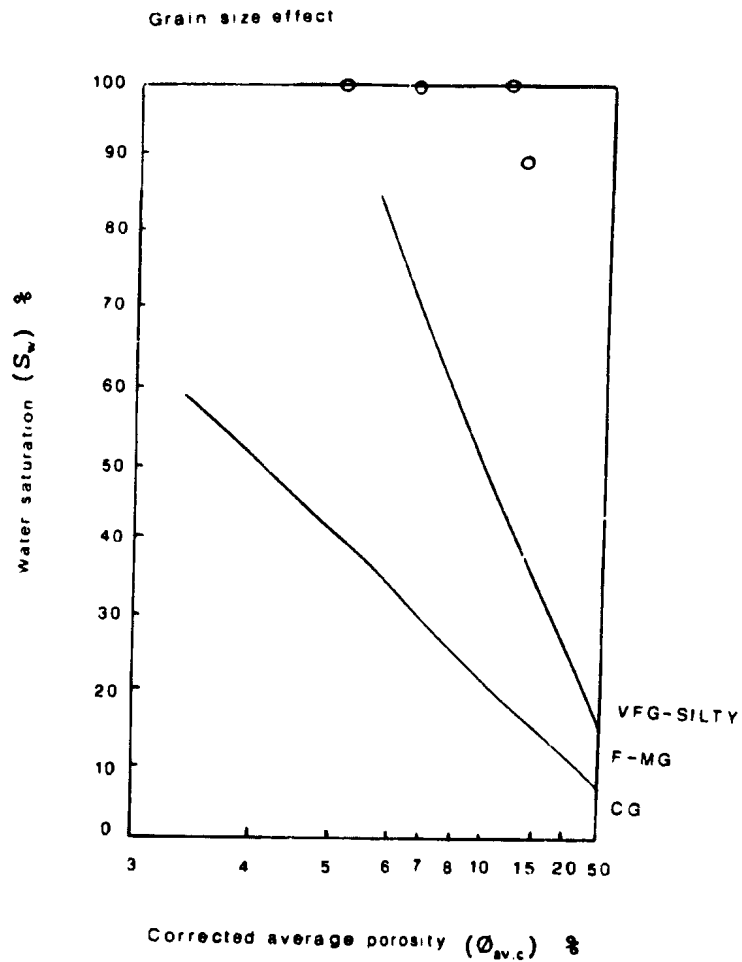
in this unit.

Because of the location and setting of this unit on the proposed deltaic lobe body, and because no core have been cut in this unit, the grain size determination from a crossplot (Fig. 73) of corrected average log porosity ($\phi_{av,c}$) and water saturation (S_w from Archie equation) is very important.

From Figure 73, the grain size of this unit in well A1-NC2 is determined to indicate very fine grained sandstones with high water saturation (S_w between 88%-100%). High water production should be expected. Data on the crossplot of water saturation (S_w) versus irreducible water saturation (S_{wir}) (Fig. 74) show a high relative permeability to water (K_{rw}) where all points are over 0.1 line (10 md.) As K_{rw} values are high, the relative permeability values to gas (K_{rg}) and to oil (K_{ro}) of Figure 75 and Figure 76 respectively will be very low ($K_{rg} < 0.01$ md. and $K_{ro} = 0$ md.); hence, this unit will produce just water.

The crossplot of corrected average log porosity ($\phi_{av,c}$) versus irreducible water saturation (S_{wir}) (Fig. 77) shows points with values less than 0.1 md. to approximately 7 md. These values are considered to be very low permeability points due mainly to the very fine-grained and the clay-rich nature of this unit.

Figure 73. Grain size determination by water saturation (S_w) versus corrected average log porosity ($\phi_{v.c}$) crossplot for A8 sand/silt unit, well A1-NC2, Lower Acacus Formation, NC2 concession, Hamada Basin, NW Libya.



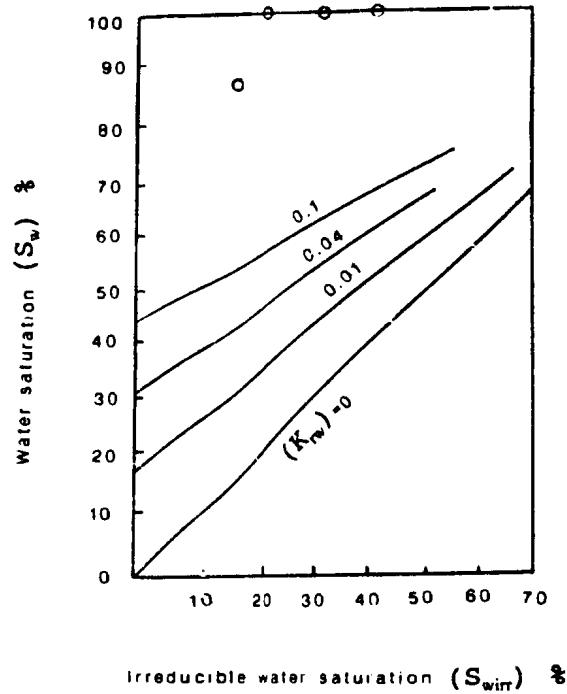
KEY:
 VFG-SILTY = very fine grained to silty sandstone points.
 F-MG = fine to medium grained sandstone points.
 CG = coarse grained sandstone points.
 O = very fine grained to silty sandstone points.

Grain size determination by water saturation (S_w) versus corrected average log porosity ($\phi_{av,c}$) crossplot for A8 sand/silt unit, well A1-NC2, Lower Acacus Formation, NC2 concession, Hamada Basin, NW Libya.

Note, Shale points of GR reading > 75 API are not included.

(Chart after Schlumberger, 1972 ; Asquith et al, 1982).

Figure 74. Water saturation (S_w) irreducible
water saturation (S_{wirr}) crossplot for
determining relative permeability to
water (K_{rw}) for A8 sand/silt unit, well
A1-NC2, Lower Acacus Formation, NC2
concession, Hamada Basin, NW Libya.



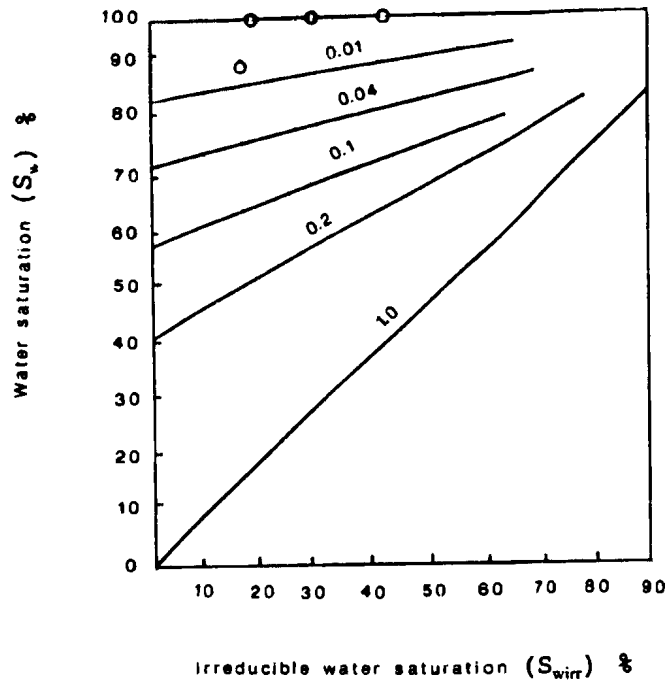
KEY:

○ Very fine grained to silty sandstone points.

Water saturation (S_w) versus irreducible water saturation (S_{wirr}) crossplot for determining relative permeability to water (K_{rw}) for A8 sand/silt unit, well A1-NC2, Lower Acacus Formation, NC2 concession, Hamada Basin, NW Libya.

(Chart after Schlumberger, 1972 ; Asquith et al, 1982).

Figure 75. Water saturation (S_w) irreducible
water saturation (S_{wir}) crossplot for
determining relative permeability to gas
(K_{rg}) for A8 sand/silt unit, well A1-NC2,
Lower Acacus Formation, NC2 concession,
Hamada Basin, NW Libya.



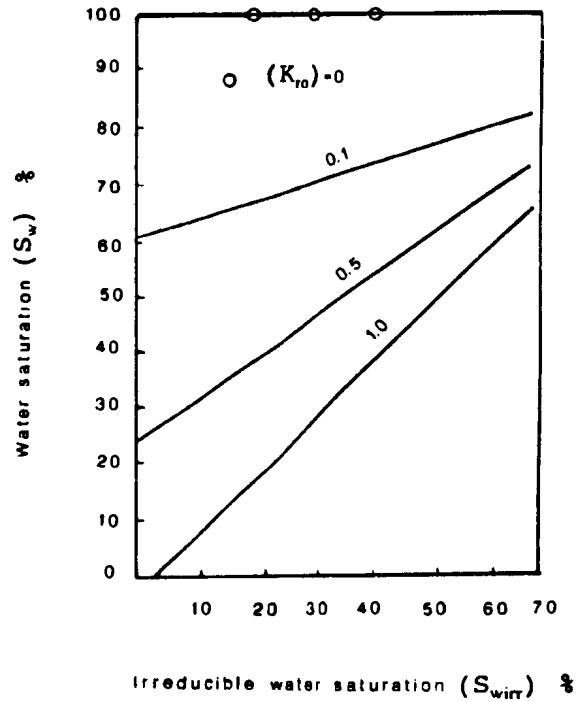
KEY:

○ Very fine grained to silty sandstone points.

Water saturation (S_w) versus irreducible water saturation (S_{wirr}) crossplot for determining relative permeability to gas (K_{rg}) for A8 sand/silt unit, well A1-NC2, Lower Acacus Formation, NC2 concession, Hamada Basin, NW Libya.

(Chart after Schlumberger, 1972 ; Asquith et al, 1982).

Figure 76. Water saturation (S_w) irreducible
water saturation (S_{wir}) crossplot for
determining relative permeability to oil
(K_{ro}) for A8 sand/silt unit, well A1-NC2,
Lower Acacus Formation, NC2 concession,
Hamada Basin, NW Libya.



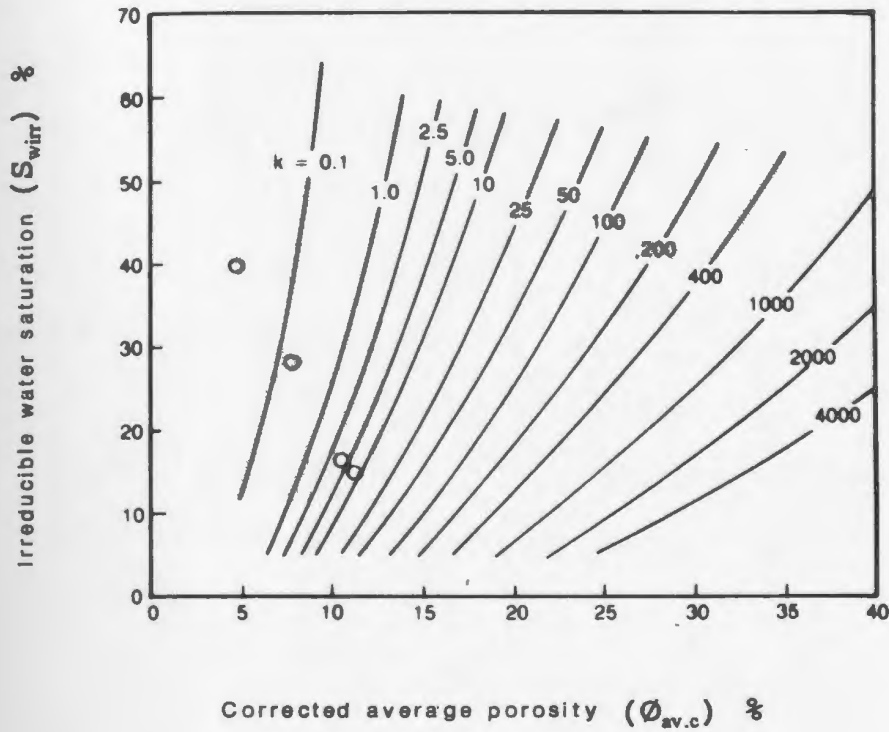
KEY:

○ Very fine grained to silty sandstone points.

Water saturation (S_w) versus irreducible water saturation (S_{wirr}) crossplot for determining relative permeability to oil (K_{ro}) for A8 sand/silt unit, well A1-NC2, Lower Acacus Formation, NC2 concession, Hamada Basin, NW Libya.

(Chart after Schlumberger, 1972 ; Asquith et al, 1982).

Figure 77. Corrected average porosity (ϕ_{av})
versus irreducible water saturation
(S_{wirr}) crossplot for determining total
permeability for A8 sand/silt unit, well
A1-NC2, Lower Acacus Formation,
NC2 concession, Hamada Basin, NW Libya.



KEY-

○ Very fine grained to silty sandstone points.

Corrected average porosity ($\phi_{av.c}$) versus irreducible water saturation (S_{wirr}) crossplot for determining total permeability for A8 sand/silt unit, well A1-NC2, Lower Acacus Formation, NC2 concession, Hamada Basin, NW Libya.

(Chart after Schlumberger, 1979).

Referring to the resistivity logs (Fig.73) the ILD curve shows a rapid decrease in resistivity which begins almost at the top of the interval (8638 ft.) and persists in the lower part of the unit (8640-8644 ft.). This indicates the interval to be water-bearing.

All data used in the evaluation of this unit and, of the position (site) of this unit relative to the main prograded sand body, support the evidence of poor reservoir quality and that low hydrocarbon potential may be expected in this unit.

Reservoir Quality-Summary:

Reservoir quality (porosity and permeability) varies vertically within each depositional sand/silt unit and laterally along the depositional dip from south to north across the study area. The best reservoir quality of sandstones occurs at the tops of the deltaic progradational sand/ silt units (A8, A9, A10, A12 and A14) in the proximal delta front sand facies in wells located in central and southern parts of the study area (E1-NC2, C1-NC2, N1-23, T1-23, E1-23, B1-61, B1-NC2, B2-NC2 and F1-NC2). Poor reservoir quality is usually characterized by clay-matrix rich, very silty sandstones of the distal delta front silt facies. This poor quality occurs in wells located at the

distal edge (marginal) of the progradational deltaic lobes especially in the northern side of the study area (wells A1-NC2, Q1-23 and U1-23).

Reservoir characteristics are plotted in Table 8 and show core and thin section data (core plug porosity and permeability and thin section porosity), log data (log porosity and fluid saturation) and drill stem tests data (formation pressure and quality of hydrocarbons) for these producing sandstone units the Lower Acacus Formation.

The average porosity measured in the core plug samples from the clean, fine to medium grained sandstone units is 20.3% (ranges from 14% to 27.9%) with average permeability 921 md. (ranges from 47 md. up to 3133 md.), while the average porosity measured in thin sections is 16% (ranges from 10% to 24%) and the corrected average porosity calculated from log responses (Neutron, Density and Sonic logs) is 15.3%.

The bioturbated silty-sandstones and clayey laminated sandstones have an average core porosity 10% (which is 50% lower than that in the clean sandstones), while the average thin section porosity is 5.8% and of average permeability 149 md. (Table 2).

Formation water saturation (S_w) were obtained by using the standard Archie equation ($S_w = \sqrt{F_x(R_w - R_i)}$), gives

values ranging from 26% to 48% in the hydrocarbon-bearing clean sandstone units. Relatively high water saturation values ranging from 49% to 100% (Table 8) characterize those water bearing reservoir sandstones which have some clay contents (V_{cl}) which ranges from 45% to 68% (Tables 4 to 7).

A cutoff point of 48% for formation water saturation is considered in this study to be the point at which the well may still be producing clean oil (with no water). Above this point some water will certainly be produced in small amount (oil-cut salt water status) as in A12 sand/silt unit of well B2-NC2 at 8582-8609 ft. of $S_w = 51$ and $S_h = 49$ (Table 8), or in great amount (salt water bearing formation status) as in A9 sand/silt unit of well E1-NC2 at 9879-9895 ft. of $S_w = 100\%$, $S_h = 0$ (Table 8).

The mean hydrocarbon saturation in the fine to medium grained, clean sandstones is 52% where the highest oil saturation value was encountered in A14 sand/silt unit of well C1-NC2 at 8842 ft. (Table 8). The mean oil saturation in the bioturbated silty-sandstones and clayey sandstones is 16.3% as encountered from well E1-NC2 at 9104-9106 ft., well F1-NC2 at 8298-8300 ft., well C1-NC2 at 9730 ft. and from well A1-NC2 at 8642 ft. (Tables 4 to 7).

Bottom hole shut-in pressure (BHSIP) is obtained from formation testing reports (AGOCO, Benghazi) of the various

drill stem tests (DST) in wells B2-NC2, C1-NC2, E1-NC2, F1-NC2, Q1-23, T1-23 and B1-61 (Table 8) in the study area. High formation pressure readings (4078 PSI) occur at 9988 ft. in A8 sand/silt unit of well E1-NC2, while the lowest pressure reading (2922 PSI) was recorded at 7928 ft. in A14 sand/silt unit of well F1-NC2. These values reflect an average formation pressure of 3500 PSI with an average normal pressure gradient (Flanigan, 1981) of 0.38 PSI/ft.

In general, the value of reservoir pressure of any producing sand unit in a single well increases with depth, but the original reservoir pressure for the same sand unit between different wells may not be the same. The original reservoir pressure in the A14 sand/silt unit measured 3343 PSI in well E1-NC2, 3470 PSI in well C1-NC2, 3273 PSI in well T1-23, and 3260 PSI in well B1-61 (Table 8). These pressure changes can be attributed to a general "...decrease in sand contents..." (Flanigan, 1981) of this interval from south to north towards well T1-23 and well B1-61 (as illustrated in net sandstone isopach map, Fig. 24, sand percentage map Fig. 37 and sand-shale ratio map Fig. 38). In fact, sand-shale percentages can change locally and create formation pressure variations. This occurred between wells C1-NC2, T1-23 and E1-NC2. Well C1-NC2 has the highest formation pressure (3470 PSI) in A14

sand/silt unit as compared to the pressures of wells T1-23 and E1-23 (3343 PSI and 3273 PSI respectively), despite the fact that well C1-NC2 is located midway between the other two.

The average API gravity is 35° API; the A14 sand/silt unit 29.5° API to 35° API, the A12 sand/silt unit 35° API to 38.5° API, the A10 sand/silt unit 35° API to 37.9° API, the A9 sand/silt unit 32.9° API, the A8 sand/silt unit 34.5 to 35.5° API and the Am (Acacus marine sand unit in well Q1-23) 41.5° API (Table 8). The average gas/oil ratio (GOR) is 3221 cubic feet per barrel (cu.ft./bbl.). The estimated average production per well in the study area is 803 barrels of oil per day (BOPD) with 0.931 million cubic feet of gas per day (MMCFGPD), while the total estimated oil and gas reserves in the multiple pay zones (A8-A14 sand units) of the Lower Acacus Formation for all potential structures in the study area (Table 9) is about 190.12 million stock tank barrels of oil in place (MMSTBOIP), and 117.19 billion standard cubic feet of gas in place (MMMSCFGIP).

TABLE 8
Reservoir characteristics of some oil and gas producing wells in the study area, NC₂ Concession, Hamada Basin, NW Libya,
for which Core Thin Section Data, Log Data and DST Data were available for some sandstone unit intervals
in the Lower Acaus Formation

Well Name	Tested Sand Unit	Tested Interval (ft)	Core and Thin Section Data				Log Data						DST Data							
			K _{int}	φ	φ _c	φ _{sp}	R	S _w	S _h	F/C	OH DST	CH DST	BHSIP	P. Grd	GOR	API	Est. BOFPD	Est. MMCFGPD	DST R	
			(md)	(%)	(%)	(%)	(%)	(%)	(%)			(psi)	(psi/ft)	(cc/stb)			(bbl)	(MMcf)		
B ₁ -NC ₂	A12	8562-8574	-	-	-	19	2	39	41	ow	8569	10	3339	0.39	7629.98	38.5	220	1.1	●	
	A12	8582-8609	-	-	-	10	1.5	51	49	ow	8592	9	3343	0.39	13124	52			●	
	A10	8687-8710	-	-	-	8	1.5	52	48	ow	8701	7	3193	0.39	13694	37.9			●	
C ₁ -NC ₂	A14	8842-8861	-	-	-	14	8	18	82	ow	8870	1	3470	0.39	530	60.6	1130	0.599	●	
	A9	9615-9641	125	21.2	19	16	2	46	54	ow	9649	2	3881	0.40	456	32.9			●	
	A8	9720-9730	3133	27.9	24	22	2	26	74	o sh	9728	4	3929	0.40	218	34.5	730	0.158	●	
E ₁ -NC ₂	A14	9090-9125	158	15.7	11.5	13	16	44	56	o sh	9120	1	3343	0.36	17	32.7	1020	0.018	●	
	A12	9543-9579	-	-	-	14	18	31	69	o sh	9573	4	3566	0.36		35	860		●	
	A10	9745-9779	-	-	-	13	0.5	90	10	ow	9753	3	3940	0.41		35	220		●	
	A9	9879-9895	-	-	-	19	1	100	-	-	-	2	4032	0.41					●	
	A8	9945-9988	-	-	-	13	9	41	59	o sh	9953	1	4078	0.41		35.5			●	
F ₁ -NC ₂	A14	7928-7933	-	-	-	15.5	4	32	68	ow	7940	9	2922	0.37	157	29.5	1005	0.158	●	
	A14	7963-7970	-	-	-	17	2.5	37	63	ow	7968	8	2960	0.37	11356	35			●	
	A12	8284-8292	-	-	-	12	1.5	37	63	o sh	8298	6	2996	0.36	6021	35	866	5.2	●	
Q ₁ -23	Am	8461-8520	47	19.6	17	20	13	38	62	o sh	8500	7	3271	0.39	155	41.5	516	0.079	●	
T ₁ -23	A14	8414-8470	47	18.2	12.2	15	24	37	63	ow	8467	1	3273	0.37			1220		●	
		8813-8855	-	-	-	23	5	48	52	ow	8849	3	3398	0.37		40	1200		●	
	A10	9045-9070	-	-	-	19	7	49	51	ow	9065	4	3454	0.38			520		●	
	A10	9093-9122	-	-	-	20	5	57	43	ow	9111	5	3463	0.38			320		●	
	A8	9223-9249	-	-	-	24	7	35	65	o sh	9249	6	3487	0.38	123	35	1130	0.139	●	
B ₁ -61	A14	8403-8458	330	14	10	12	5	38	62	o sh	8430	2	3260	0.38		34	1093		●	
	A14	8460-8517	1734	25.5	20	18	3	49	51	ow	8490	3	3260	0.38		34			●	

* K_{int} - Air permeability in Millidarcy from Lab core analysis. φ - Core plug helium porosity from Lab core analysis. φ_c - Thin-section porosity from point counting thin sections.

^b φ_{av} - Corrected Average Log Porosity (Corrected neutron porosity + Corrected density porosity + Corrected sonic porosity) / (R - True resistivity of formation). S_w - Water Saturation. S_h - Hydrocarbon Saturation. F/C - Type of fluid contact. All Log Data have been calculated by applying Archie Equation: $S_w = \frac{1}{\sqrt{K_{int} \phi^{1.4} R^{1.66}}}$

^c OH DST - Number of open hole drill stem test. CH DST - Number of closed hole drill stem test. BHSIP - Bottom hole shut-in pressure. P. Grd - True air gradient. GOR - Gas/Oil ratio. API - Oil gravity. Est. BOFPD - Estimated barrels of oil per day. Est. MMCFGPD - Estimated million cubic feet of gas per day. DST R - Drill stem test result.

- Oil
- Oil and Gas
- Oil/Gas with traces of salt water
- Oil and Salt water
- Salt water

(All DST Data from formation testing service reports: AGOC/Bengha/Libya)

TABLE 9

Total Estimated Reserves of Oil and Gas
in the Lower Acacus Sandstones, NC₂
Concession, Hamada Basin, NW Libya.

STRUCTURE	OIL RESERVES (MMSTBOIP)	GAS RESERVES (MMMSCFGIP)
B-NC ₂	9.5	60.19
C-NC ₂	74.55	22.40
E-NC ₂	7.4	6.2
F-NC ₂	28	8.65
B-61	8.37	-
E-23	32.20	10.05
N-23	5.76	4.85
Q-23	1.92	-
T-23	22.42	4.85
TOTAL RESERVES	190.12	117.19

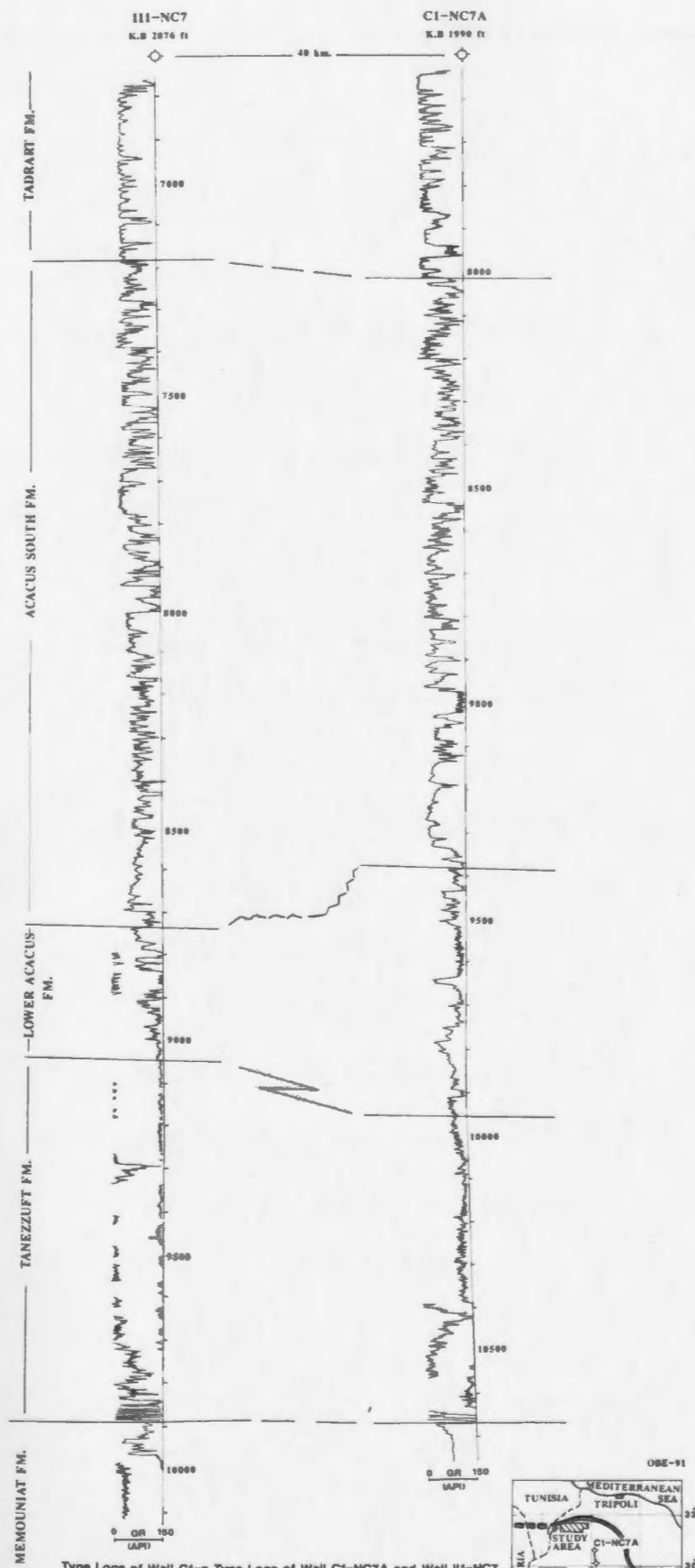
STRATIGRAPHIC APPLICATION

The study area has provided information which makes it possible to address stratigraphic ties with the Kebir area to the south. Correlation of the Kebir area stratigraphic sequence with data in the study area is on the basis of best-facies-fit correlation providing sense for the regional depositional setting with the study area. On this basis, correlation shows that the Acacus South formation interval in wells outside the study area to the south (C1-NC7A, II1-NC7) is stratigraphically partially equivalent to Lower Acacus Formation in the study area to the north. (See enclosures 1 & 2).

Acacus South formation

This formation is introduced informally for the first time in this study on the basis of the geographic location and subsurface well log data from wells C1-NC7A and II1-NC7 south of the study area. No type section has been previously described. The unit occurs from a drill depth of 7860 ft. to 9387 ft. in well C1-NC7A and from a drill depth of 7190 ft. to 8740 ft. in well II1-NC7 (Fig. 78). The average subsurface thickness is 1500 ft. According to well-log descriptions by AGOCO geologists, this unit is composed of light gray, cream, medium to coarse grained

Figure 78. Type logs for the Acacus South formation,
in well C1-NC7A and well III-NC7, Hamada
Basin, NW Libya.



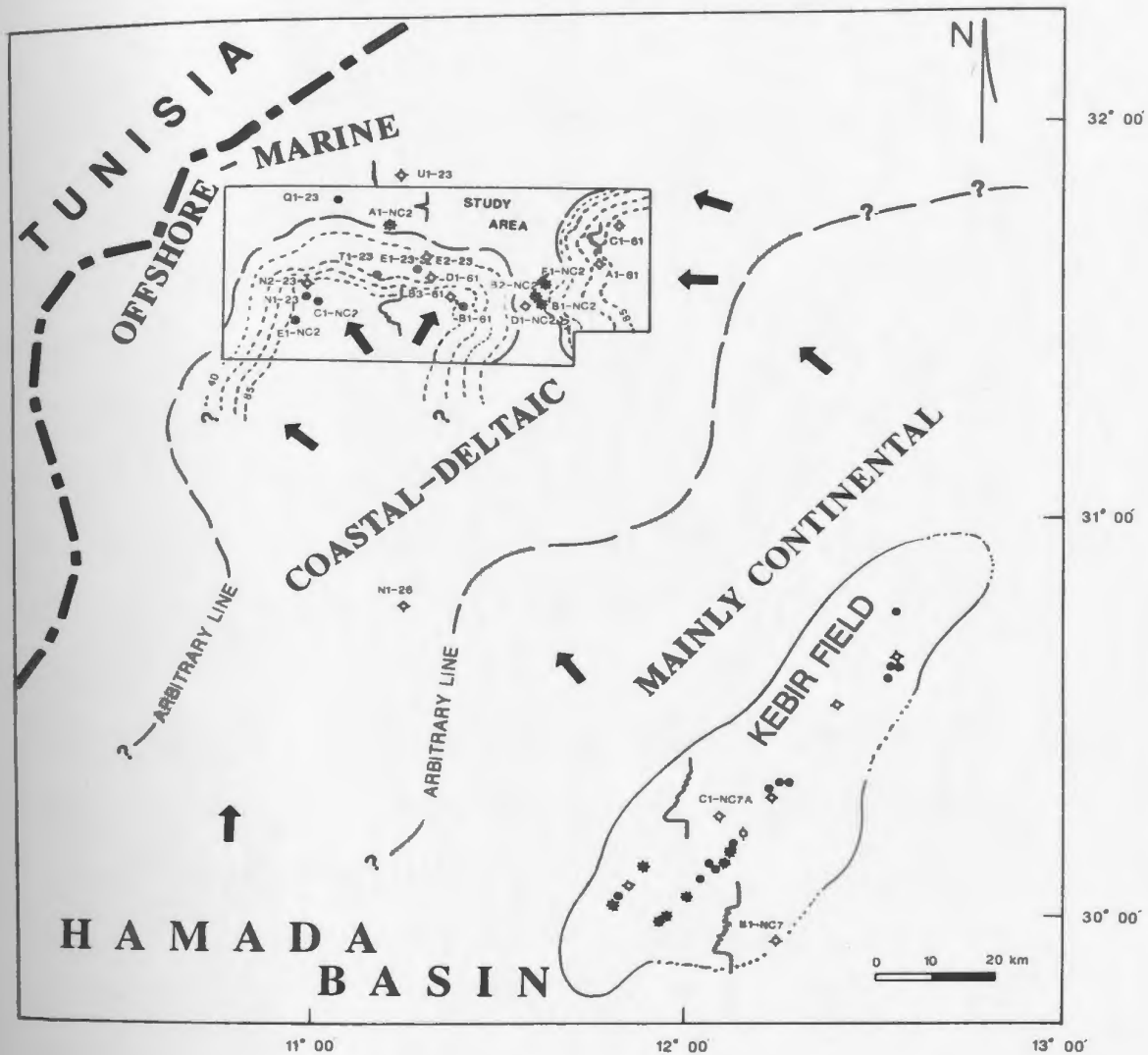
Type Logs of Well CI-n Type Logs of Well CI-NC7A and Well III-NC7, Hamada Basin, NW Libya, Showing The Gamma-Ray Log Response and The Stratigraphic Position of The Acacus South Formation. Note: The Fining-Upward Nature of Each Sandstone Sequence in The Acacus South Formation.

sandstone, conglomeratic with some shale alternations. The base of the unit is marked with a marine shale bed which is considered in this study to lie unconformably upon the Lower Acacus Sandstone. The top of the unit may be erosive with the overlying Tadrart Formation (Lower Devonian). The Acacus South formation is interpreted to be a product of continental sedimentation by fluvial channel systems which prograded northward (Encls. 1 & 2), as inferred from GR log characteristics. A regional picture of facies distribution is depicted on a paleogeographic map (Fig. 79).

Paleogeographic Map

Figure 79 illustrates the various depositional elements for the Lower Acacus Formation. From south to north, the Hamada Basin can be divided into a fluvial continental zone, a coastal-deltaic zone and an offshore-marine zone. The boundary lines separating these zones are based in part on log responses in the study area and in well control outside the study area (at wells C1-NC7A and III1-NC7). Extension of these boundaries is arbitrary.

Figure 79. Paleogeographic map depicting depositional
facies of the Lower Acacus Formation,
Hamada Basin, NW Libya.



PALEOGEOGRAPHIC MAP DEPICTING DEPOSITIONAL FACIES OF THE LOWER ACACUS FORMATION, HAMADA BASIN , NW LIBYA.

	POSSIBLE TRANSPORTATION DIRECTIONS
	ARBITRARY LINES BASED ON LOGS
	NET SANDSTONE ISOPACH CONTOUR LINES IN METERS

OBE-91

FUTURE EXPLORATION STRATEGY
AND RECOMMENDATIONS

According to the depositional framework of the Lower Acacus Sandstones and to the drilling and testing information already obtained it is possible to interpret that a significant amount of oil and gas remains to be recovered from the sandstones of the Lower Acacus Formation. The following exploration steps are suggested for future exploration and production from the Lower Acacus Sandstones:

1. Delineate the depositional dip and strike in the study area by constructing the total isopach map of the Lower Acacus Formation.
2. Construct a number of stratigraphic cross-sections through the prospect area along depositional dip and strike (if possible) using GR log response.
3. Study all cross-sections and identify the type of log responses for each sandstone unit. Relate those responses to depositional environments (coarsening-upward sand unit; coastal-deltaic, fining-upward sand unit; fluvial, spiky; marine sand, etc....).
4. Construct sandstone isopachs for those sandstone intervals (or interesting sandstone units) of 75 API

or less gamma-ray log (GR) deflections to outline net sandstone trends and to identify sedimentation patterns, and delta type (fluvial versus wave dominated).

5. Plot all drilling (lithologic description of cuttings and core sections) and testing (production DST) data on the cross-sections and relate these informations to the depositional environments through the sequence.
6. Identify productive sandstones throughout the study area. Map their thickness to identify their depositional trends as an aid for locating new prospects.

The above-mentioned steps effectively relate exploration and production of the deltaic Lower Acacus Sandstones to their depositional environments based mainly on available core data, sandstone distribution and gamma-ray log characteristics.

Recommendations

In the study area (NC2 Concession), SP-log characteristics have been investigated and compared with GR-log characteristics. The SP curve is less reliable than the GR curve for interpreting the various depositional facies because it is severely affected by many factors

such as salinity variation in the formation in the drilling fluid (Schlumberger, 1972; Asquith et al., 1982) as well as other technical reasons (Dewan, 1983).

When using well-log correlation to determine stratigraphy in the study area, it is best to select the best-facies-fit approach strategy, rather than hanging all wells on one datum because there is not a common stratigraphic marker which occurs in all correlatable wells in the study area.

When investigating porosity and permeability relationships of the Lower Acacus Sandstones, thin-section porosity (macroporosity) must be correlated with permeability values rather than core-plug porosity. Insignificant relationships between permeability and core-plug porosity occur, because of the inclusion of clay-matrix porosity (microporosity associated with clay-rich samples).

The best reservoir quality has been encountered in specific sandstone units distributed in the central and southern parts of the study area (in the vicinity of wells E1-23, T1-23 and wells E1-NC2, B1-61). This identifies first priority prospects to be drilled in this area when supported seismically. Good porosity and permeability has been encountered from some sandstone units (A12 and A14 of well C1-61) in the eastern part of the study area but, due

to the lack of well control (especially in the area between well A1-NC2 and well C1-61 and between well Q1-23 and well C1-61), the sandstone distribution patterns have not been delineated firmly. Further stratigraphic drilling in this area is recommended for second priority prospects.

Structural and stratigraphic traps occur in the study area. In the central and southern parts of the study area, small isolated structural closures (of 50-80 ft. in T1-23 area, E1-23 area, C1-NC2 area and E1-NC2 area) have been identified seismically (seismic sections-Hamada basin, TDL, AGOCO, 1988) which reflect "...pre-existing highs of the basement..." (unpublished AGOCO report). Stratigraphic cross-sections (Enclosures 1-3), identify that the down-dip changes of deltaic sand to shale northward provide some basis for structural traps in the central and southern parts of the study area. Stratigraphic traps within the deltaic sands need some investigation through synthetic seismic modelling. Stratigraphic control may also be involved in creating traps in the Lower Acacus Formation. Stratigraphic traps may also be present where the interpreted marine sandstones (in the northern side of the study area) offlap and pinch out updip to marine shale (which may be the case of (Am) unit of well Q1-23 at 8485ft.).

Production test intervals have to be selected properly. Log interpretation of some sandstone intervals, indicates that high water-cut values are from the lower porosity and shaly zones; therefore, the lower (water-bearing) zones such as those in well B2-NC2 at 8582-8609 ft. should not be perforated.

This study should be extended to cover the Hamada Basin to the south, where better resolution paleogeographic maps can be made to provide the basis for prospecting new areas.

This study has addressed the depositional petrofabric of the sandstones in the Lower Acacus Formation. The influence of diagenesis on these types of sandstones is evidenced by the presence of secondary porosity and associated clay minerals. A second phase of study is recommended to analyse and evaluate the diagenetic petrofabric of these sandstones.

CONCLUSIONS

In the study area, sandstones of the Lower Acacus Formation were deposited in an overall deltaic setting. Well correlation both inside and outside the study area, incorporating interpreted facies derived from cores and GR-log characteristics, indicates that the Lower Acacus Formation consists regionally of fourteen (A1-A14) sand/silt units in the Hamada Basin (Encls. 1 and 2). Nine (A6-A14) of these units occur locally in the study area. These units are bounded in the stratigraphic sequence by either 1) regional stratigraphic markers (equivalent to organic shales of either the Tanezzuft Formation or the Middle Acacus shale) or 2) local stratigraphic markers which have been obtained by correlation of physical stratigraphic indicators between close wells. Each of these sand/silt units originated as deltaic lobes during shoreline progradation. This interpretation is based on:

1. The overall coarsening-upward sandstone sequences in the Lower Acacus Formation.
2. The changes in lithology from bioturbated silty sandstone into horizontal-crosslaminated sandstones. These sands were deposited in high energy environments which are interpreted to record progradational events (Berg, 1986).

3. The presence of carbonaceous material in parts of the clean sandstones (in well E1-NC2 @ 9105 ft. and @ 9111 ft., and in well C1-NC2 @ 9645 ft. and @ 9703).
4. The formation of several depositional lobes as a result of channel shifts and course changes (Saxena, 1976; Blatt, Middleton and Murray, 1980).
5. Stratigraphic correlations (Encls. 1-3) have revealed at least nine regressive cycles (in the study area) during which the individual Lower Acacus Sandstone lobes were deposited; each separated by transgressive shallow marine shale (Coleman, 1981).
6. Stratigraphic log correlation which suggests that the occurrence of local sandstone lenses (marine sandstone) of destructional origin occur at the fringes of each delta lobe (Brown Jr., 1975).
7. Fluvial channel systems to the south of the study area (Kebir field, in wells I11-NC7 and C1-NC7A) in the central Hamada Basin. These fluvial systems are interpreted to have been the source of sediment for the delta lobes to the north.
8. Lobate patterns interpreted from isopach maps for some of the productive sandstone units (Figures 25 to 29).
9. Superposition of the isopach patterns of selected stratigraphic units (A8, A9, A10, A12 and A14). This identifies the fact that depositional lobes and axes

in each unit are offset from those in the older units. This may have been the result of "...sediment loading and differential compaction over the lower sediments.." (Brown, 1975; Coleman, 1980; Blatt, Middleton and Murray, 1980), thereby providing structural control for delta progradation.

Within the established stratigraphic framework the interpreted deltaic facies in the study area change laterally in a predictable manner northward. In this context horizontal-crosslaminated, medium grained sandstones in the south change to bioturbated silty sandstone with high clay content and eventually to finely laminated to bioturbated marine shales and reworked offshore marine sands in the north. Data from core revealed the vertical relationship of facies: bioturbated shales grading upsection to increasingly laminated sandstones up-section. These relationships suggest that the deltaic lobe section may be subdivided into two parts; a lower lithofacies (type 2) with its silty grain size, high clay matrix content, high bioturbation, and "...low flow-regime structures.." (Keltch, B.W. et al., 1989), and an upper lithofacies (type 3) with its coarser grain size and somewhat higher flow-regime structures. The former

lithofacies may represent the distal part of a delta; the latter may represent the proximal part of a delta front (Wiemer, 1978).

Petrographic analyses of core thin-sections of Lower Acacus Sandstones reveal, in general, texturally mature, moderately sorted sandstones of complex mineralogy. Lower Acacus Sandstones are very fine to fine grained with an average grain size of 0.24 mm. Their average detrital composition is that of sublitharenite (Folk, 1980) with framework detrital grains averaging 85% monocrystalline quartz, 1.2% polycrystalline quartz, 1.5 feldspar, 7% rock fragments and 2.3% other minerals (muscovite, zircon, tourmaline) and of average 3% clay-matrix. Authigenic minerals, represented by quartz overgrowth, form euhedral crystal terminations and are very abundant in those well sorted clean sandstones where the silica cement varies inversely with clay matrix content.

High clay minerals such as Kaolinite have filled most pore spaces between grains in the bioturbated silty sandstone lithofacies and in the marine sandstones. These clays may have been partially precipitated as a result of the dissolution of unstable feldspar grains and rock fragments (Tillman and Jordan, 1987).

Carbonate cement (calcite and dolomite) occurs pervasively or in patches in the bioturbated silty sandstones and in the marine sandstones, or in the coarse grained laminated sandstones respectively. In many instances these calcite and dolomite cements have been dissolved, leaving behind large pores which subsequently in some cases were filled with oil.

The present porosity in the Lower Acacus Sandstones appears to be dominantly secondary in origin (by the criteria of Schmidt and McDonald, 1979). Secondary porosity was primarily derived from partial dissolution of the carbonate cementing materials and of some unstable detrital feldspar grains and some rock fragments. Trace amounts of primary porosity are present and associated with the clean, fine to medium grained and quartz supported sandstones.

Graphic representation of porosity and permeability for some cored sandstone intervals shows the relationship between core plug helium porosity (ϕ_c) and air permeability (K_{air}) from laboratory analyses. The relationship between core plug porosity (ϕ_c) and air permeability values (K_{air}) permits the conclusion that the randomly distributed porosity values, which show no correlation with corresponding permeability values, are basically related to

the abundance of clay-matrix and to grain size variation in the core plug porosity (ϕ_c). Analysis of the relationship between thin-section porosity (ϕ_u) (macroporosity) and permeability (K_{av}) indicates that the true relationship between porosity and permeability in the sandstones of Lower Acacus Formation can be assessed better with thin-section porosity (ϕ_u) (macroporosity), than the use of core plug porosity (ϕ_c). The latter combines macroporosity and microporosity (associated with clay-rich samples) (Ehrenberg, 1990), thereby misleading the actual relationship between porosity and permeability.

The reservoirs having the best overall quality are fine to medium grained sandstones which occur at the top of each deltaic lobe. These sandstones represent the proximal delta front lithofacies where average effective thicknesses range from 20 to 70 feet. Poor reservoir quality characterizes those bioturbated silty-sandstones, matrix-rich distal delta front facies, which show lateral variation of reservoir quality northward (in the vicinity of well A1-NC2, well Q1-23 and well U1-23) and south-eastward (in the vicinity of well D1-NC2).

The optimum or best reservoir conditions in most cases depend not only on the net sandstone thickness but also on the environmental facies within each deltaic lobe. The

best quality sandstones occur in wells in the central and southern part of the study area, with average core plug porosity 20.3% and average air permeability 921 md. Values of formation water saturations (S_w) for some interesting zones, obtained from the standard Archie equation (Schlumberger, 1972, 1974; Fertl, 1978; Asquith et al., 1982) range from 26% to 48% in the hydrocarbon bearing sandstones. A cutoff point of 48% for formation water saturation was used in the calculation of total oil and gas reserves. The average bottom hole shut-in pressure (obtained from DST reports) is 3500 PSI. The average oil gravity (API) from the producing sandstone units (A8, A9, A10, A12 and A14) is 35° API. The estimated average oil and gas production per well from the effective sandstone units (A8, A9, A10, A12 and A14) in the study area is 803 barrels of oil per day (BOPD), of 35° API gravity oil and 0.931 million cubic feet of gas per day (MMCFGPD), while the estimated oil and gas reserves in the multiple sandstone pay zones of the Lower Acacus Formation for all potential structures in the study area is about 190.12 million stock tank barrels of oil in place (MMSTBOIP), and 117.19 billion standard cubic feet of gas in place (MMSCFIP).

The reliability of wireline logs used in illustrating the fundamental depositional facies and to assist the

understanding of the depositional model for the Lower Acacus Formation was investigated in detail. For all wells in the study area, the gamma-ray log (GR) was found to be of higher quality and more reliable for all sequences than is the spontaneous-potential log (SP). In some instances, the GR log helps in facies identification in the absence of cores and rock lithological descriptions.

Using the available well control, a regional paleogeographic map (Fig. 79) has been constructed using log facies and depositional-sand patterns (mainly in the study area). This map depicts the depositional history of the Lower Acacus Formation and provide a basis for predicting regional facies distribution across the Hamada Basin.

This study, based on a best-facies-fit correlation approach, has greatly increased understanding of environmental and reservoir facies relationships in the study area. Such an approach is essential to define the potential sandstones, their depositional origin, and their reservoir characteristics throughout the study area.

REFERENCES

- American Petroleum Institute, (1956). Recommended practice for determining permeability of porous media. Division of Production, Dallas, Texas 75201, 27 P.
- American Petroleum Institute, (1960). Recommended practice for core-analysis procedure. API Recommended practice 40 (RP 40), Production Department, First edition, Dallas, Texas 75201, 55 P.
- Arabian Gulf Oil Company, (1981). Regional structure section for Ghadames Basin. (ed. N.O.C., Exploration Department, Feb.1981), AGOCO, Benghazi, A.G./GL 3131.
- Arabian Gulf Oil Company, (1988). Geologic base map of western Libya, Technical Data Library (TDL), AGOCO, Benghazi, Scale 1 : 1000,000.
- Arabian Gulf Oil Company, (1988). Location map of the study area (NC2 Concession), Hamada Basin, NW Libya. Technical Data Library (TDL), AGOCO, Benghazi, Scale 1 : 500,000.
- Arabian Gulf Oil Company, (1988). Location Map of the study area (NC2 Concession) defined by latitude and longitude, Hamada Basin, NW Libya. Technical Data Library (TDL), AGOCO, Benghazi, Scale 1 : 500,000.
- Asquith, G. and Gibson, C., (1982). Basic well log analysis for geologists, methods in exploration series. The American Association of Petroleum Geologists, Tulsa, Oklahoma, 218 P.

- Banerjee, Syamadas, (1980). Stratigraphic lexicon of Libya.
Department of Geological Researches and Mining, Bulletin No.13,
Industrial Research Centre, Tripoli, Libya, 300 P.
- BEICIP, (1971-1975). Evaluation and geological study of the western
part of Libya (Ghadames Basin), Final Report, N.O.C., Libya,
197 P.
- BEICIP, (1975). Geological map of type of structures in the Hamada
Basin, North-western Libya, Exploration Study, N.O.C., Libya,
Scale 1 : 5000,000.
- Bellini, E. and Massa, D. (1978). A stratigraphic contribution to
the Paleozoic of the southern basins of Libya. In: Symposium on
the Geology of Libya, Second Edition, Vol. I, (eds. Salem,M.J.
and Busrewil,M.T.), Tripoli Libya , P.3-56.
- Berg, R.R., (1979). Oil and gas in delta-margin facies of Dakota
Sandstone, Lone Pine Field, New Mexico. The American
Association of Petroleum Geologists Bulletin, Vol.63, No.6,
P.886-904.
- Berg, R.R., (1986). Dakota Sandstone, Lone Pine Field, northwestern
New Mexico. In: Reservoir Sandstones, Deltaic Sandstones
(Chapter 6) Prentice-Hall, Inc., Englewood Cliffs,
New Jersey 07632,P.241-259.
- Berg, R.R., (1986). Sussex Sandstone, House Creek field,
Northeastern Wyoming. In: Reservoir Sandstones, Shelf
Sandstone (Chapter 8), Prentice-Hall, Inc., Englewood Cliffs,
New Jersey 07632, P.367-382.
- Bishop, William, F. (1975). Geology of Tunisia and adjacent parts

- of Algeria and Libya. The American Association of Petroleum Geologists Bulletin, Vol.59, No.3, P.413-450.
- Blatt, H., Middleton, G. and Murray, R., (1980). Environments and facies, ancient coastal deposits. In: Origin of Sedimentary Rocks, Second Edition, P.673-689.
- Brown Jr., L. F. (1975). Role of sediment compaction in determining geometry and distribution of fluvial and deltaic sandstones (Case Study: Pennsylvanian and Permian Rocks of North-Central Texas). In: Developments in Sedimentology, 18A, (Chapter 5), (eds. Chilingarian and Wolf), Elsevier Scientific Publishing Company, P.247-292.
- Bulling, T. P. and Breyer, J. A. (1989). Exploring for subtle traps with high-resolution paleogeographic maps: Reklaw 1 interval (Eocene), South Texas. The American Association of Petroleum Geologists Bulletin, Vol.73, No.1, P.24-39.
- Chamberlain C. K., (1978). Recognition of trace fossils in cores In: Trace Fossil concept (ed. Basan, P. B.), Society of Economic Paleontologists and Mineralogists, Short Course, No.5, Oklahoma City, P.119-166.
- Chan, M. A. and Dott Jr, R. H., (1986). Depositional facies and progradational sequences in Eocene wave-dominated deltaic complex southwestern Oregon. The American Association of Petroleum Geologists Bulletin, Vol.70, No.4, P.415-429.
- Cherven, V. B., (1978). Fluvial and deltaic facies in the Sentinel Butte Formation, Central Williston Basin. Journal of Sedimentary Petrology, Vol.48, P.159-170.

- Coleman, J. M., and Gagliano, S. M. (1964-1965). Cyclic sedimentation in the Mississippi River deltaic plain. Gulf Coast Association of Geological Societies Transactions, Vol.14, P.67-80.
- Coleman, J. M. and Gagliano, S. M. (1965). Sedimentary structures: Mississippi River deltaic plain. In: Primary Sedimentary Structures and their Hydrodynamic Interpretation (ed. Middleton, G. V.) Society of Economic Paleontologists and Mineralogists, Special Publication, No.12, Tulsa, Oklahoma, U.S.A, P.133-148.
- Coleman, J. M. (1976). Deltas: Processes of deposition and models for exploration. Continuing Education Publication Company, Inc. 102P.
- Coleman, J. M. and Prior, D. B. (1980). Deltaic sand bodies. In: Continuing Education Course Note Series # 15, The American Association of Petroleum Geologists, Department of Education, Tulsa, Oklahoma 74101, 171P.
- Coleman, J. M. (1981). Delta processes of deposition and models for exploration, Second Edition, Burgess Publication Company, CEPCO Division, 124P.
- Collomb, G. R. (1962). Etude Géologique due Jebel Fazzan et de sa Bordere Paléozoïque. Notes, Mém. Fr. Pétrole, Paris, No.1, 26p.
- Conant, L. C. and Goudarzi, G. H., (1967). Stratigraphic and tectonic framework of Libya. The American Association of petroleum Geologists, Vol.51, No.5, P.719-730.

- Curtis, D. M., (1970). Miocene deltaic sedimentation, Louisiana Gulf Coast. In: Deltaic sedimentation, modern and ancient (eds. Morgan, J. P. and Shaver, R. H.). Society of Economic Paleontologists and Mineralogists, Special Publication, No.15, P.293-308.
- Curtis, Bruce F., (1971). Measurement of porosity and permeability (Chapter 14). In: Procedures in sedimentary petrology (ed. Carver, Robert E.,1971), University of Georgia, Athens, Georgia, P.335-364.
- Denoo, Stand, (1978). Neutron-density log is a valuable open-hole porosity tool. In: Practical log analysis-9, Oil and Gas Journal, Vol.76, No.39, (September. 25. 1978), P.96-102.
- Dewan, J. T., (1983). Essentials of modern open-hole log interpretation. Pennwell Publishing Company, Tulsa, Oklahoma, 361P.
- Dickson, J. A. D., (1965). A modified staining technique for carbonates in thin section. Nature, Vol.205, P.587.
- Dickson, J. A. D., (1966). Carbonate Identification and genesis as revealed by staining. Journal of Sedimentary Petrology, Vol.36, No.2, P.491-505.
- Ehrenberg, S. N., (1990). Relationship between diagenesis and reservoir quality in the sandstones of the Garn Formation, Haltenbanken, Mid-Norwegian Continental Shelf. American Association of Petroleum Geologists Bulletin, Vol.74, No.10, P.1538-1558.

- Essed, A., (1978). Gravity map of Libya from Master research: personal copy provided to Dr.J. Harper, 1986.
- Ferm, John C., (1970). Allegheny deltaic deposits. In: Deltaic Sedimentation, Modern and Ancient (eds. Morgan, J. P. and Shaver, R. H., 1971). Society of Economic Paleontologists and Mineralogists, Special Publication, No. 15, Tulsa, Oklahoma, P.246-255.
- Fertl, W. H., (1978). Rwa method-fast formation evaluation. In: Practical Log Analysis-8, Oil and Gas Journal, (May 15,1978 - Sept.19,1979), P.73-76.
- Fertl, W. H. and Vercellino, W.C., (1978). Predict water cut from well logs. In: Practical Log Analysis-4, Oil and Gas Journal, Vol.76, No.25, (June 19,1978), P.111-116.
- Fisher, W. L. and McGowen, J. H. (1969). Depositional systems in Wilcox Group (Eocene) of Texas and their relation to occurrence of Oil and Gas. The American Association of Petroleum Geologists Bulletin, Vol.53, No.1, P.30-54.
- Flanigan, T. E., (1981). Abnormal formation pressures: recognition, distribution, and implications for geophysical prospecting, Brazoria County, Texas. Gulf Coast Association of Geological Societies Transactions, 31.st Annual Meeting (October 21-23,1981), Texas, P.97-103.
- Folk, Robert L. (1980). Petrography of sedimentary rocks. Hemphill Publishing Company, Austin, Texas, 184P.
- Franklin, Stanley P. and Tieh, Thomas T., (1989). Petrography, diagenesis, and reservoir properties of the Dakota Sandstone of

- West Lindrith Field, Rio Arriba County, New Mexico.
- In: Petrogenesis and Petrophysics of Selected Sandstone Reservoirs of the Rocky Mountain Region (eds. Coalson, E. B., Kaplan, S. S., Keighin, C. Wm., Oglesby, C. A. and Robinson, J. W.), Denver, Colorado (1989), P.117-321.
- Galehouse, Jon S., (1971). Point counting (Chapter 16).
- In: Procedures in Sedimentary Petrology (ed. Carver, Robert E., 1971), University of Georgia Athens, Georgia, P.385-406.
- Galloway, W. E., (1975). Process framework for describing the morphologic and stratigraphic evolution of deltaic depositional systems. In: Deltas, Models for Exploration (ed. Broussard, M. L.). Houston Geological Society, P87-98.
- Gilreath, J. A. and Stephans, R. W., (1975). Interpretation of log responses in a deltaic environment. In: Finding and Exploring Ancient Deltas in Subsurface, American Association of Petroleum Geologists, Marine Geology Workshop, Introductory Papers (C), Dallas, Texas, 1975, 31P.
- Goudarzi, G. H., (1970). Geology and mineral resources of Libya- a reconnaissance. U.S.Geol. Surv., Prof. Paper, 660, 104P.
- Harwood, G. (1988), Microscopic Techniques: II, Principles of Sedimentary Petrology (Chapter 5). In: Techniques in Sedimentology (ed. Tucker, M., 1988), P.108-173.
- Halender, Donald, P. (1984). Fundamentals of formation evaluation, Second Printing, OGCI Publications, Oil and Gas Consultants International, Inc., Tulsa Oklahoma, 332P.
- Hubert, J. F., Butera, J. G. and Rice, R. F., (1972). Sedimentology

of Upper Cretaceous Cody-Parkman delta, Southwestern Powder River Basin, Wyoming. In: Geological Society of America Bulletin, Vol.83, P.1649-1670.

Hyne, Norman J., Cooper, William A. and Dickey, Parke A., (1979).

Stratigraphy of intermontane, lacustrine delta, Catatumbo River, Lake Maracaibo, Venezuela. The American Association of Petroleum Geologists Bulletin, Vol.63, No.11, P.2042-2057.

Karasek, Richard Mark, (1981). Structural and stratigraphic

analysis of the Paleozoic Murzuk and Ghadames Basins, Western Libya. Unpublished Ph.D. Thesis, University of South Carolina, 146p.

Keitch, Brian W.; Wilson, Dail A. and Potter, Paul E., (1990).

Deltaic depositional controls on Clinton sandstone reservoirs, Senecaville Gas Field, Guernsey County, Ohio. In: Sandstone Petroleum Reservoirs (eds. Barwis, John H., McPherson, John, G. and Studlick, Joseph R. J., 1990). Springer-Verlag New York Inc., P.263-280.

Kerr, Paul F., (1977). Optical Mineralogy. McGraw-Hill Inc., 4th. Edition, 492P.

Kingston, D., R.; Dishroom, C., P. and Williams, P. A., (1983).

Global basin classification system. The American Association of Petroleum Geologists Bulletin, Vol.67, No. 12, P.2175-2193.

Kingston, D., R.; Dishroom, C., P. and Williams, P. A., (1983).

Hydrocarbon plays and global basin classification. The American Association of Petroleum Geologists Bulletin, Vol.67, No.2, P.2194-2198.

- Klitzsch, E., (1966). Geology of the northeast flank of the Murzuk Basin (Dejebel Ben Ghanema-Dor el Gussa Area). In: Petroleum Exploration Society of Libya, 8th. Annual Field Conf., P.19-32.
- Klitzsch, E., (1970). Die Strukturgeschichte der Zentralsahara. Neue Erkenntnisse zum Bau und zum Paläogeographic eines Tafellandes. Geol. Rundsch, 59/2, 459-527.
- Klitzsch, E., (1971). The structural development of parts of North Africa since Cambrian time. In: Symposium of Geology of Libya (ed. Gray, C.), Faculty of Sciences, University of Libya, Tripoli, P.253-262.
- Klitzsch, E., (1981). Lower Paleozoic Rocks of Libya, Egypt, and Sudan. In: Lower Paleozoic of The Middle East, Eastern and Southern Africa, and Antarctica (ed. Holland, C. H.), P.131-161.
- Krumbein, W. C. and Sloss, L. L. (1963). Stratigraphy and sedimentation. Second Edition, Freeman, W. H. and Company, San Francisco, 660P.
- Lumsden, D. N., Pittman, E. D., and Buchanan, R. S., (1971). Sedimentation and petrology of Spiro and Foster Sands (Pennsylvanian), McAlester Basin, Oklahoma. The American Association of Petroleum Geologists Bulletin, Vol.55, No.2, P.254-266.
- McBride, E. F., Weidie, A. E. and Wolleben, J. A., (1975). Deltaic and associated deposits of difunta Group (Late Cretaceous to Paleocene), Parras and Lapopa Basins, Northeastern Mexico. In: Deltas, Models for Exploration

- (ed. Broussard, M. L.). Houston Geological Society, P.485-522.
- Miller, J. (1988). Microscopical Techniques: I. Slices, slides, staining and peels, 4.5- Etching and Staining (Chapter 4). In: Techniques in Sedimentology (ed. Tucker, M., 1988), P.96-101.
- National Oil Corporation - Libya, (1981). Regional Structural Cross-section illustrating concept of stratigraphic and Structural relations in the Hamada Basin, North Western Libya. (N.O.C., Exploration Department, 1981).
- Nelson, H. W. and Glaister, R. P., (1978). Subsurface environmental facies and reservoir relationships of the McMurray Oil Sands, Northeastern Alberta. Bulletin of Canadian Petroleum Geology, Vol.26, No.2, P.177-207.
- Pakdi, Dewaduen C. and Fox, James E., (1989). Petrography and petrophysics of the Upper Cretaceous Turner Sandy Members of The Carlile Shale at Todd Field, Power River Basin, Wyoming. In: Petrogenesis and Petrophysics of Selected Sandstone Reservoirs of The Rocky Mountain Region (eds. Coalsom, E. B., Kaplan, S. S., Keighin, C. Wm., Oglesby, C. A., and Robinson, J. N.), Denver, Colorado (1989), P.235-244.
- Pittman, Edward D. (1979). Porosity, diagenesis and productive capability of sandstone reservoirs. In: Aspects of Diagenesis (eds. Scholle, P. A. and Schluger, P. R., 1979), Society of Economic Paleontologists and Mineralogists, Special Publication, No.26, P.159-173.
- Rice, Dudley D., (1980). Coastal and deltaic sedimentation of Upper

- Cretaceous Eagle Sandstone: relation to shallow gas accumulations, North-Central Montana. The American Association of Petroleum Geologists Bulletin, Vol.64, No.3, P.316-338.
- Said, F. Mohamed, (1974). Sedimentary history of the Paleozoic rocks of the Ghadames Basin in Libya Arab Republic; Unpublished M.Sc. Thesis, University of South Carolina, 39P.
- Saxena, R. S., (1976a). Modern Mississippi Delta depositional environments and processes: American Association of Petroleum Geologist-Society of Economic Paleontologists and Mineralogists, Field Trip Guidebook. New Orleans, Louisiana, May 23-26, 1976, P.9-88.
- Saxena, R. S., (1976b). Sand bodies and sedimentary environments of the Mississippi Delta- an excellent model for exploration in deltaic sandstone reservoirs. Texaco Inc., Louisiana, Presented at Cairo, Egypt, November 15-17, 1976, 53P.
- Schmidt, V., McDonald, D. A. and Platt, R. L. (1977). Pore geometry and reservoir aspects of secondary porosity in sandstones. Bulletin of Canadian Petroleum Geology, Vol.25, No.2, P.271-290.
- Schmidt, V. and McDonald, D. A., (1979). Texture and recognition of secondary porosity in sandstones. In: Aspects of Diagenesis (eds.Scholle, P. A. and Schluger, P. R., 1979), Society of Economic Paleontologists and Mineralogists, Special Publication, No.26, P.209-225.
- Schlumberger, (1972). Log interpretation manual/principles, Vol.I, Houston, Schlumberger Well Services, Inc., 113P.

- Schlumberger, (1974). Log interpretation manual/applications, Vol.II, Houston, Schlumberger Well Services, Inc., 116P.
- Schlumberger, (1979). Log Interpretation/Charts, Houston, Schlumberger Well Services, Inc., 93P.
- Scholle, Peter A., (1979). A color illustrated guide to constituents, Textures, Cements, and Porosities of Sandstones and Associated Rocks. The American Association of Petroleum Geologists, Memoir 28, Tulsa, Oklahoma (1979), 201P.
- Serra, O., (1984). Fundamentals of well-log interpretation.
1. The Acquisition of Logging Data. Developments in Petroleum Sciences, 15A, P.95-133
- Serra, O. (1985). Sedimentary environments from wireline logs (Mark of Schlumberger), 1st. Edition, 211P.
- Serra, O. (1989). Sedimentary environments from wireline logs (Mark of Schlumberger), 2nd. Edition, 243p.
- Sloss, L. L., and Speed, R. C., (1974). Relationships of cratonic and continental-margin tectonic episodes. In: Tectonics and Sedimentation, Society of Economic Paleontologists and Mineralogists, Special Publication, No.22, P.98-119.
- Tillman, R. W. and Jordan, D. W., (1987). Sedimentology and subsurface geology of deltaic facies, Admire 650' Sandstone, Eldorado Field, Kansas. The Society of Economic Paleontologists and Mineralogists, Special Publication. No.40, Tulsa, Oklahoma, P.221-291.
- Turner, J. R. and Conger, S. J., (1981). Environment of deposition and reservoir properties of the Woodbine Sandstone at Kurten

- Field, Brazos County, Texas, Gulf Coast Association of Geological Society Transactions, Vol.31, P.213-232.
- Visher, Glenn S., Sandro, S. B. and Phares, R. S., (1971). Pennsylvanian delta patterns and petroleum occurrences in eastern Oklahoma. The American Association of Petroleum Geologists Bulletin, Vol.55, No.8, P.1206-1230.
- Vos, Richard G., (1981a). Deltaic sedimentation in the Devonian of western Libya. Sedimentary Geology, Vol.29, No.1, P.67-88.
- Vos, Richard G. (1981b). Sedimentology of an Ordovician fan delta complex, Western Libya. Sedimentary Geology, Vol.29, No.2, P.153-170.
- Weimer, Robert J., (1970). Rates of deltaic sedimentation and intrabasin deformation, Upper Cretaceous of Rocky Mountain Region. In: Deltaic Sedimentation, Modern and Ancient, (eds.Morgan, J., P. and Shaver, R. H., 1971), Society of Economic Paleontologists and Mineralogists, Special Publication, No.15, Tulsa, Oklahoma, P.270-292.
- Weimer, Robert J., (1978). Shallow water marine environments (shelf-neritic). In: Deltaic and Shallow Marine Sandstones: Sedimentation, Tectonics and Petroleum Occurrences. Continuing Education Course Note Series # 2, The American Association of Petroleum Geologists, Department of Educational Activities, P.141-167.
- Weimer, Robert J., (1978). Stratigraphic principles (concepts). In: Deltaic and Shallow Marine Sandstones: Sedimentation, Tectonics and Petroleum Occurrences. Continuing Education

Course Note Series # 2, The American Association of Petroleum Geologists, Department of Educational Activities, P.9-106.

White, David A., (1980). Assessing oil and gas plays in facies-cycle wedges. The American Association of Petroleum Geologists Bulletin, Vol.64, No.8, P.1158-1178.

**THE SEDIMENTOLOGY AND RESERVOIR CHARACTERISTICS
OF THE LOWER ACACUS FORMATION, NC2 CONCESSION,
HAMADA BASIN, NW LIBYA.**

(PART II)

BY

C OMAR BOUZID ELFIGIH

**A thesis submitted to the School of Graduate
Studies in partial fulfilment of the
requirements for the degree of
Master of Sciences.**

**Department of Earth Sciences,
Memorial University of Newfoundland.**

November 1991

St. John's

Newfoundland

**THE SEDIMENTOLOGY AND RESERVOIR CHARACTERISTICS
OF THE LOWER ACACUS FORMATION, NC2 CONCESSION,
HAMADA BASIN, NW LIBYA.**

(PART II)

BY

C OMAR BOUZID ELFIGIH

**A thesis submitted to the School of Graduate
Studies in partial fulfilment of the
requirements for the degree of
Master of Sciences.**

**Department of Earth Sciences,
Memorial University of Newfoundland.**

November 1991

St. John's

Newfoundland

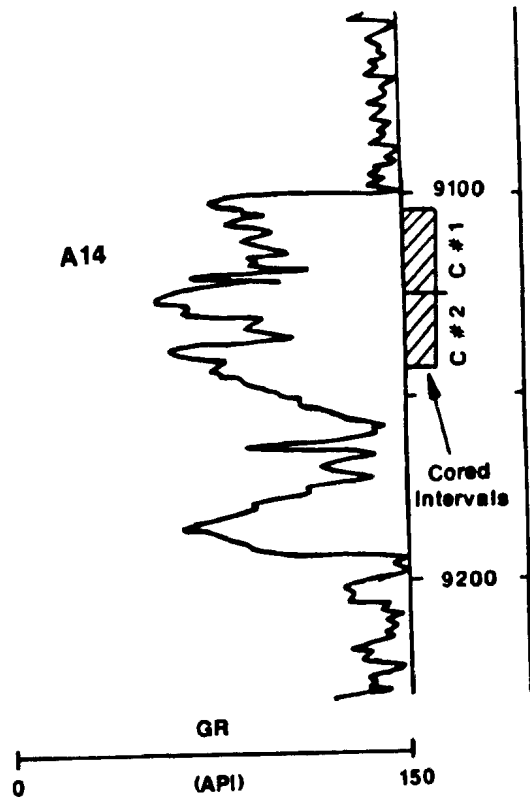
PART II
APPENDICES

APPENDIX I

**Core Descriptions and Core Photographs of
The Lower Acacus Formation, NC2 Concession,
Hamada Basin, NW Libya.**

Figure App.I.1. Cores description (C#1,C#2) of Well E1-NC2,
Lower Acacus Formation, NC2 Concession,
Hamada Basin, NW Libya.
" Location of Well Shown in Figure.4 "

E1-NC2
K.B. 1772 FT



Gamma-Ray Log (GR) Signatures and Cored Intervals (9105-9126ft; 9126-9146ft) for Well E1-NC2, Lower Acacus Formation, NC2 Concession, Hamada Basin, NW Libya.
" Depth divisions are 50 ft (15.24m) apart ".

APPENDIX I

Well E1-NC2

Formation Lower Acacus

Concession NC2
Hamada Basin, Libya

Core No. 1 & 2

Interval 9105-9126ft
9126-9148ft

Depth (ft)	T.S.	Gross Lithology	Grain Size							Sed. Structures and Accessories	Rock Description	Lithofacies	Oil Stain			Porosity			DST Intv.	DST Result	
			gy	slt	vf/s	fs	me	ss	vcs				h	m	L	gd	fr	pr			
9100																					
9110									Horizontal even parallel laminae	SS, Lt. gy., occ. tan, fn-m grd, w. sort, w/ minor slty sh lam, car, and mud clasts, calc. in parts	Even Par. Lam. SS	Oil Stain				Porosity					Oil and Gas
9120									Bioturbation	SLTY SS, gy, dk. gy, blot., w. sh lam.	Blot. Sltty SS										
9130									Lenticular sand lenses	SH, dk gy, fss., finely lam., blot., w. lent. ad. lenses.	Blot. Sltty SH										
9140									Burrow	SS, a/a @105-9111 ft lam. to indist. lam., occ. x. lam. at top, burr. at some places.	Even Par. X. Lam. SS										
9150									Low angle cross laminations	SH, dk gy, fss., finely lam., mic., non calc.	Finely Lam. SH										
										SS, gy, lt. gy, vf-f grd, slty, blot. at the base, par.-indist. lam.	Even Par. Inds. Lam. SS										
										Sh. blk, blot.	Blot. Sltty SH										

Gross Lithology

- Sandstone
- Siltstone
- Shale

Sedimentary Structures

- Horizontal even parallel laminae
- Lenticular sand lenses
- Burrow
- Bioturbation
- Low angle cross laminations

Accessories

- Carbonaceous debris
- Mud clasts

DST Result

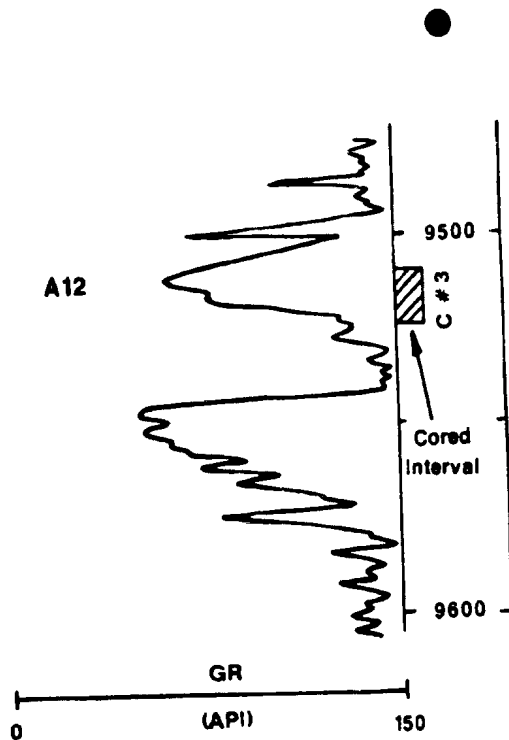
- Oil and Gas

APPENDIX I

Figure App.I.2. Core description (C#3) of Well E1-NC2,
Lower Acacus Formation, NC2 Concession,
Hamada Basin, NW Libya.

" Location of Well Shown in Figure.4 ".

E1-NC2
K.B. 1772 FT



Gamma-Ray Log (GR) Signatures and Cored Interval (9509-9524ft) for well E1-NC2, Lower Acacus Formation, NC2 Concession, Hamada Basin, NW Libya.

" Depth divisions are 50 ft (15.24m) apart "

APPENDIX I

Well E1-NC2

Formation Lower Acacus

Concession NC2

Core No. 3

Interval 9509-9524.5ft

Hamada Basin, Libya

Depth (ft)	T.S.	Gross Lithology	Grain Size							Sed. Structures and Accessories	Rock Description	Lithofacies	Oil Stain			Porosity			DST Intv.	DST Result
			dy	slt	vfs	fs	ms	cs	vcs				h	m	L	gd	fr	pr		
9500																				
9510	●								 	SS, lt. gy, wtish gy, vf-f grd, subang-subrd, m. sort, w/mud clasts, par. lam, calc	Par. lam. SS									
9520									 	SLTY SS, lt. gy, dk gy, slty, pr. sort, biot., calc.	Biot. Slt. SS									
9530									 	SH, gy, dk grn, fss-subfss, biot. at places, w/lent. slty sd lenses, mic, occ. lam. at the base	Biot. SH									

Gross Lithology

-  Sandstone
-  Siltstone
-  Shale

Sedimentary Structures

-  Horizontal even parallel laminae
-  Lenticular silty sand lenses
-  Bioturbation

Accessories

-  Mud clasts

DST Result

APPENDIX I

Figure App.I.3. Core Photos (C#1-C#3) of Well E1-NC2,
Lower Acacus Formation, NC2 Concession,
Hamada Basin, NW Libya.

" Detailed Descriptions of Lithofacies are
Included in Figures.App.I.1,App.I.2 ".

APPENDIX I



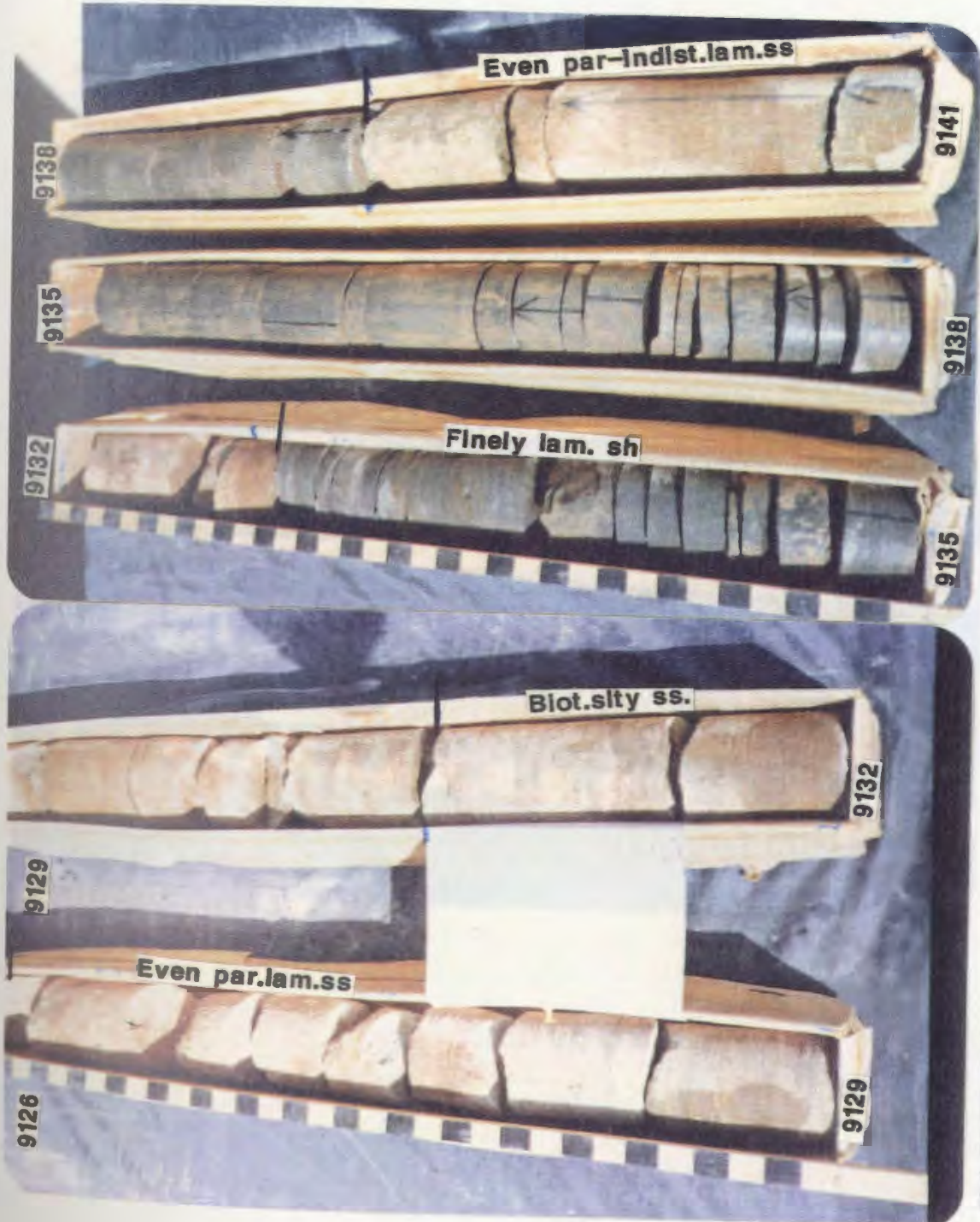
E1-NC2, C#1

APPENDIX I



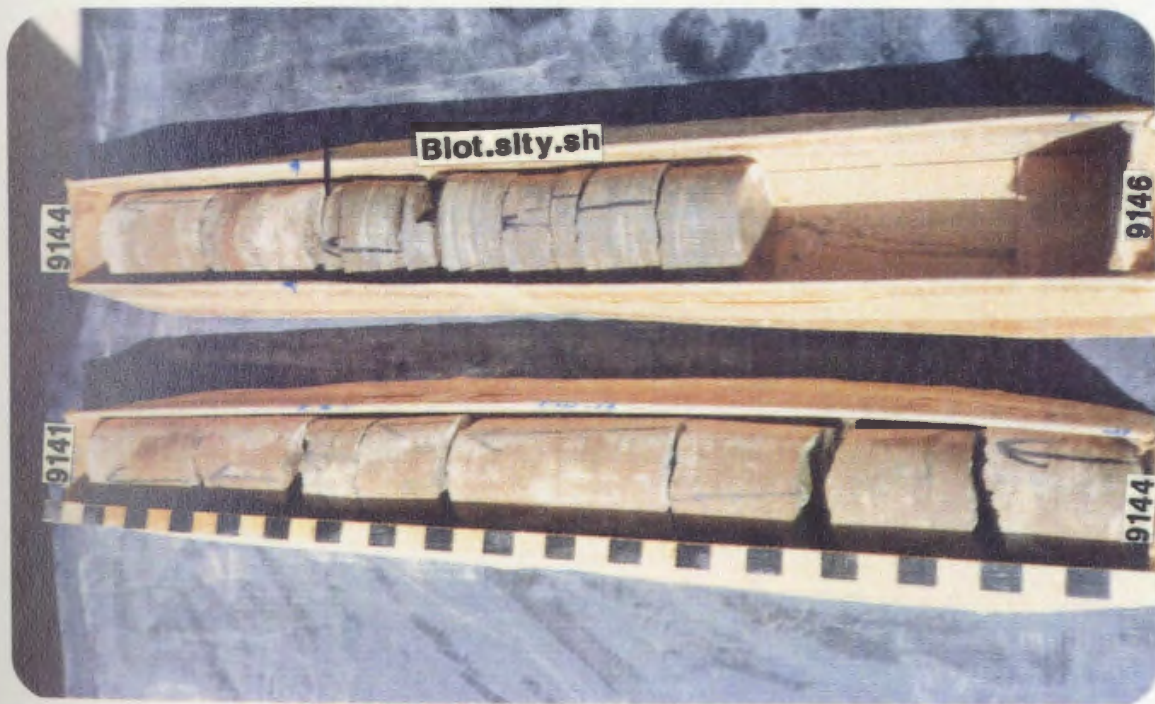
E1-NC2, C#1

APPENDIX I



E1-NC2, C#2

APPENDIX I



E1-NC2, C#2

APPENDIX I



E1-NC2,C#3

APPENDIX I

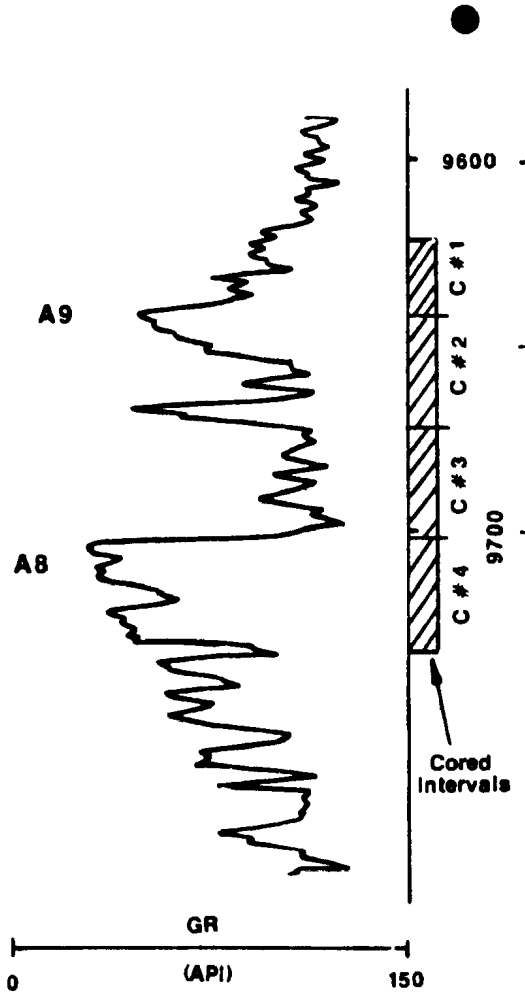


E1-NC2,C#3

APPENDIX I

Figure App.I.4. Cores Description (C#1-C#4) of Well C1-NC2,
Lower Acacus Formation, NC2 Concession,
Hamada Basin, NW Libya.
" Location of Well Shown in Figure.4 "

C1-NC2
K.B. 1855 FT



Gamma-Ray Log (GR) Signatures and Cored Intervals (9621-9642ft; 9642-9672ft; 9672-9702ft; 9702-9731ft) for Well C1-NC2, Lower Acacus Formation, NC2 Concession, Hamada Basin, NW Libya. " Depth divisions are 50 ft (15.24m) apart ".

APPENDIX I

Well C1-NC2

Formation Lower Acacus

Concession NC2

Core No. 3

Interval 9672-9702ft

Hamada Basin, Libya

Depth (ft)	T.S.	Gross Lithology	Grain Size							Sed. Structures and Accessories	Rock Description	Lithofacies	Oil Stain			Porosity			DST Intv.	DST Result
			dy	silt	vis	fs	ms	ca	vcs				h	m	L	gd	fr	pr		
9670									=	SH, dk gy, gyish grn, fess, lam. at the top, w/lent. silty sd lenses, biot. at the base	Lam. SH									
9680))			SS, lt gy, gyish wt., vf-f grd, m. sort, w/mud clasts and rip-up clasts, indist. lam, silty, occ. calc.	Indist. lam. SS							
9690									=	SH, dk gy, fess, finely lam, w/lent. silty sd lenses. No Recovery	Finely lam SH									
9700									=			SH, dk gy, grn, fess, flky, lam.	Finely lam. SH							

Gross Lithology

- Sandstone
- Siltstone
- Shale
- No Recovery

Sedimentary Structures

- Horizontal even parallel laminae
- Lenticular silty sand lenses
- Rip-up clasts
- Bioturbation

Accessories

- Mud clasts

DST Result

APPENDIX I

Well C1-NC2

Formation Lower Acacus

Concession NC2

Hamada Basin, Libya

Core No. 4

Interval 9702-9732ft

Depth (ft)	T.S.	Gross Lithology	Grain Size						Sed. Structures and Accessories	Rock Description	Lithofacies	Oil Stain			Porosity			DST Intv.	DST Result
			cl	silt	v/s	fs	ms	cs				vc	h	m	L	gd	fr		
9700																			
9710																			
9720																			
9730																			
9740																			

Gross Lithology

- Sandstone
- Siltstone
- Shale

Sedimentary Structures

- Low angle cross laminations
- Horizontal even parallel laminae
- Wavy laminations
- Bioturbation

Accessories

- Mud clasts

DST Result

- Oil & Gas

APPENDIX I

Figure App.I.5. Core Photos (C#1-C#4) of Well C1-NC2,
Lower Acacus Formation, NC2 Concession,
Hamada Basin, NW Libya.

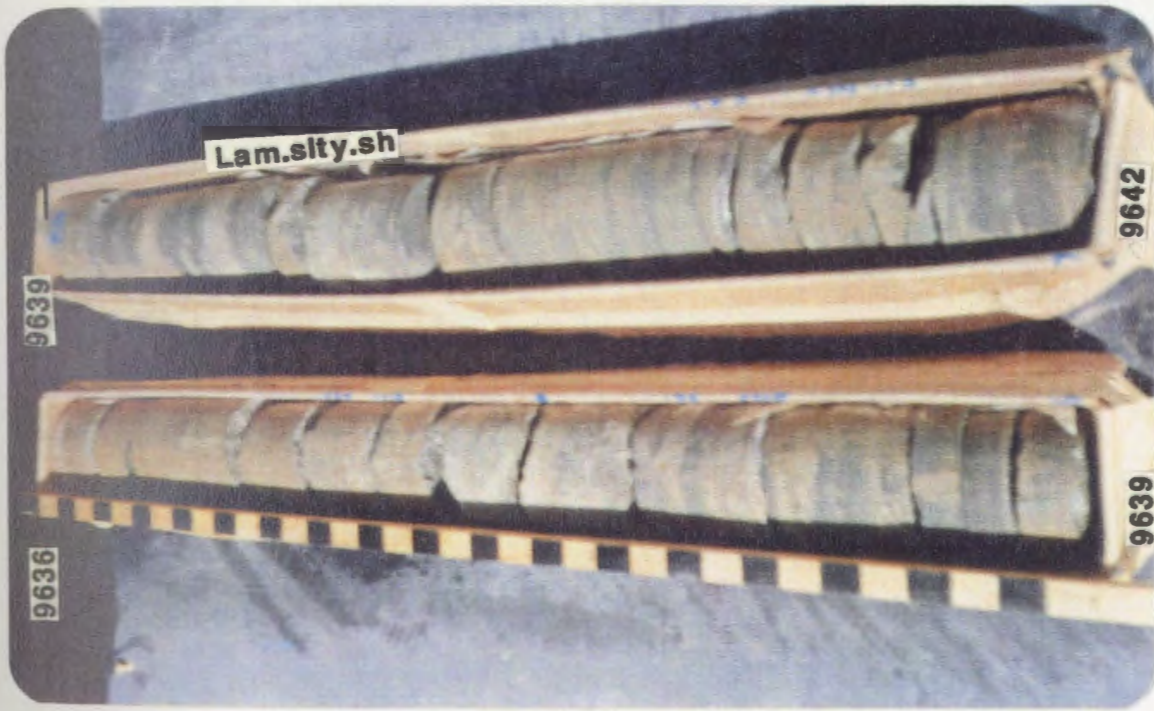
" Detailed Descriptions of Lithofacies are
Included in Figure App.I.4 ".

APPENDIX I



C1-NC2,C#1

APPENDIX I



C1-NC2, C#1

APPENDIX I



C1-NC2, C#2

APPENDIX I

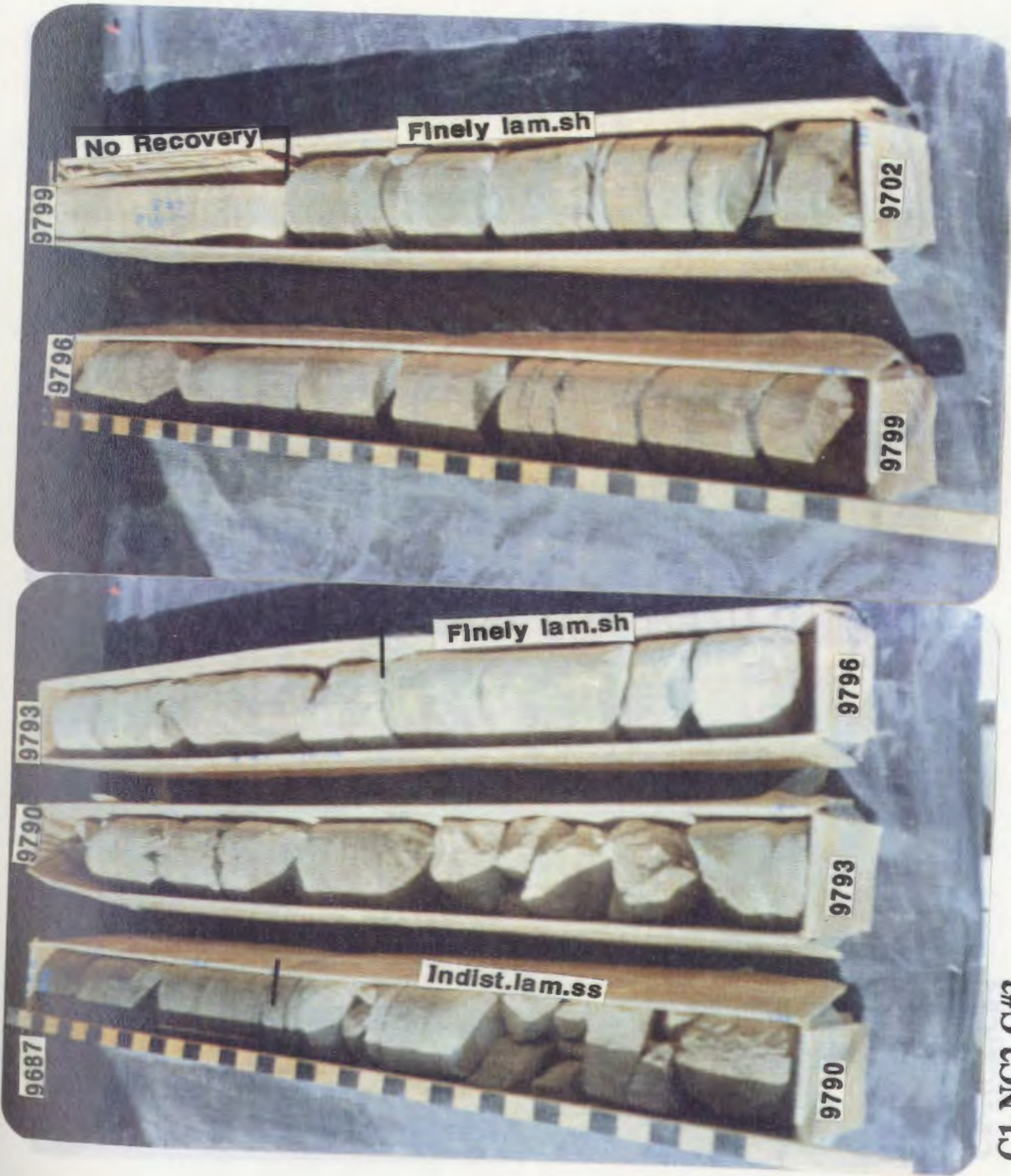


C1-NC2,C#2

APPENDIX I

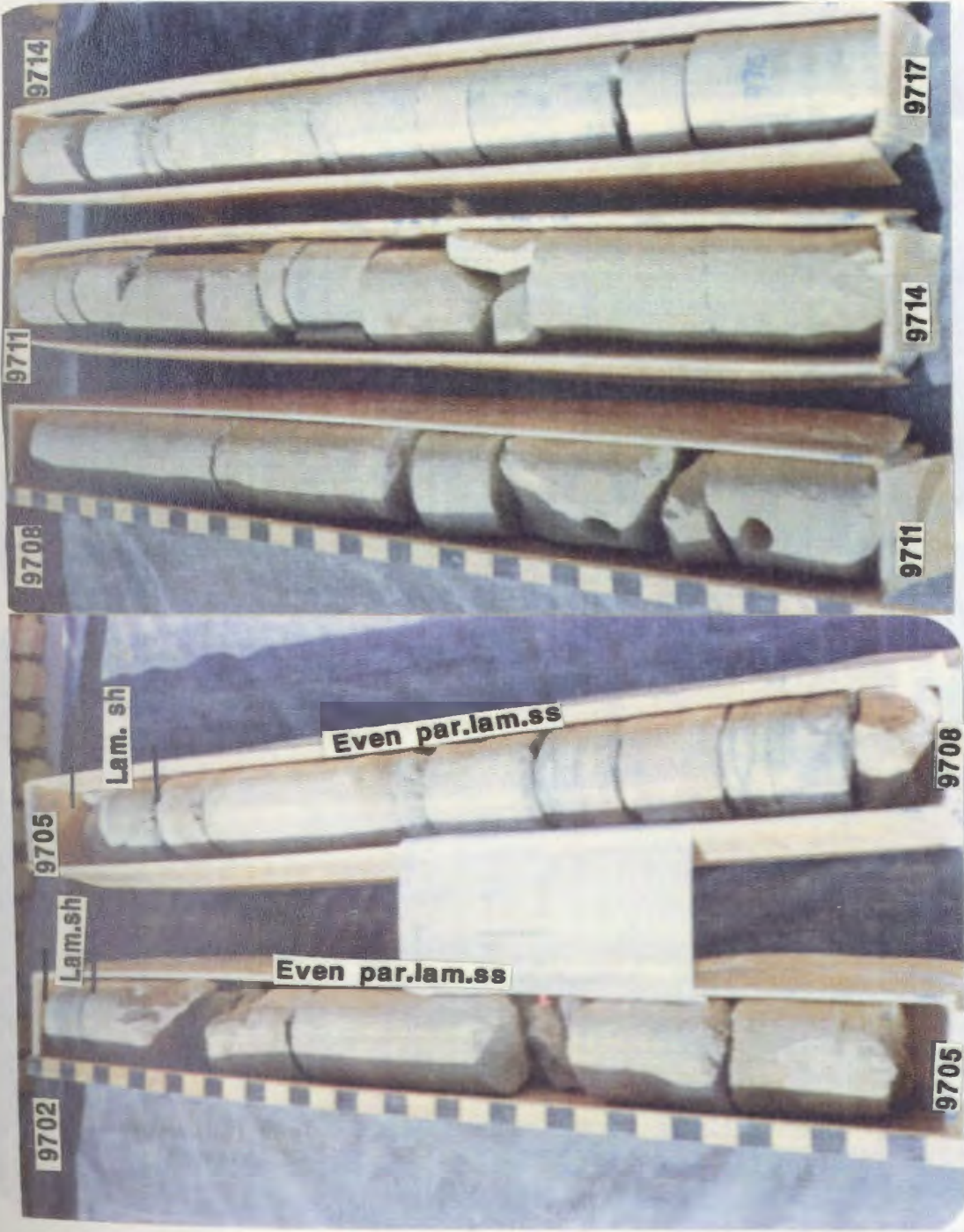


C1-NC2, C#3



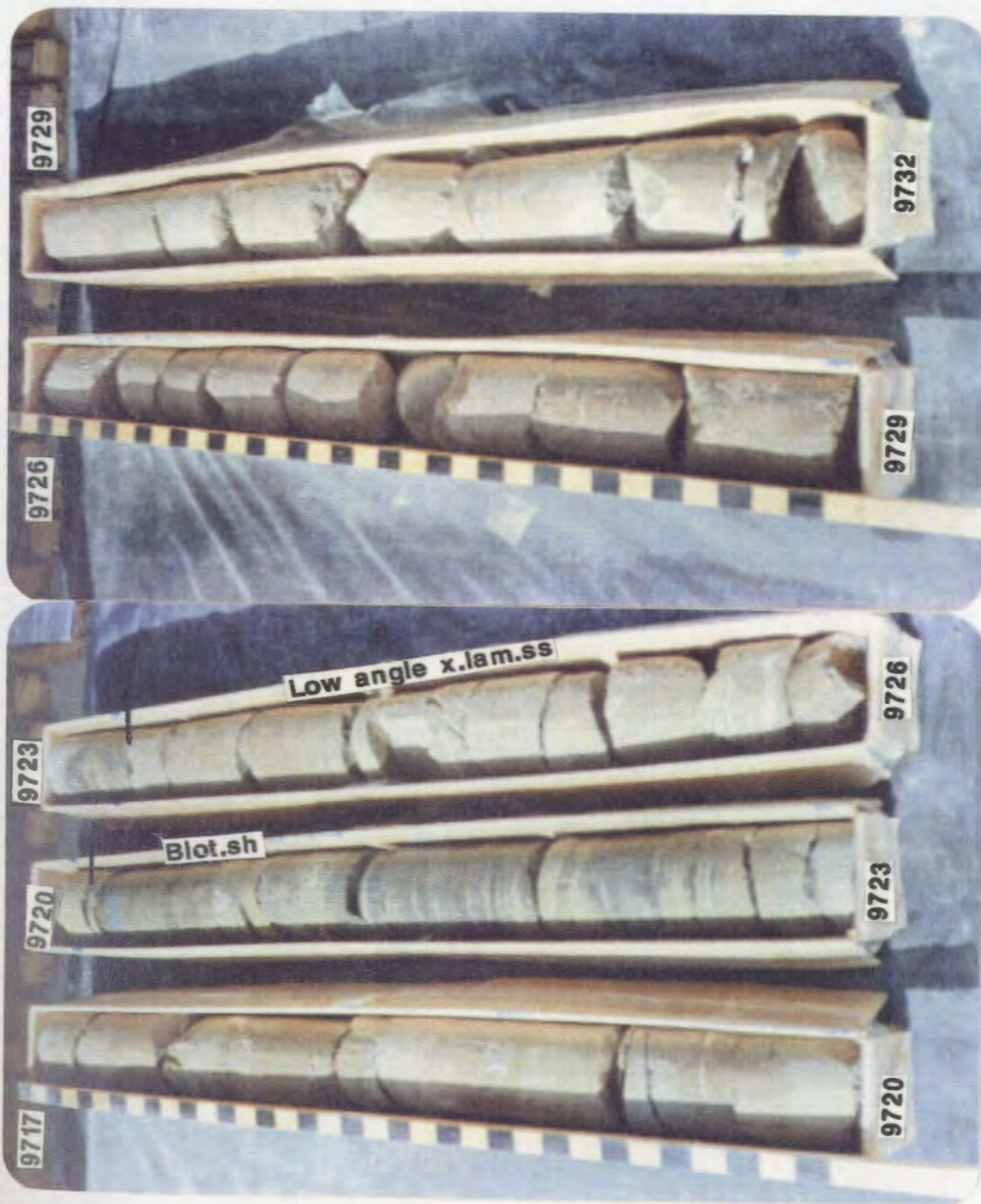
C1-NC2, C#3

APPENDIX I



C1-NC2, C#4

APPENDIX I

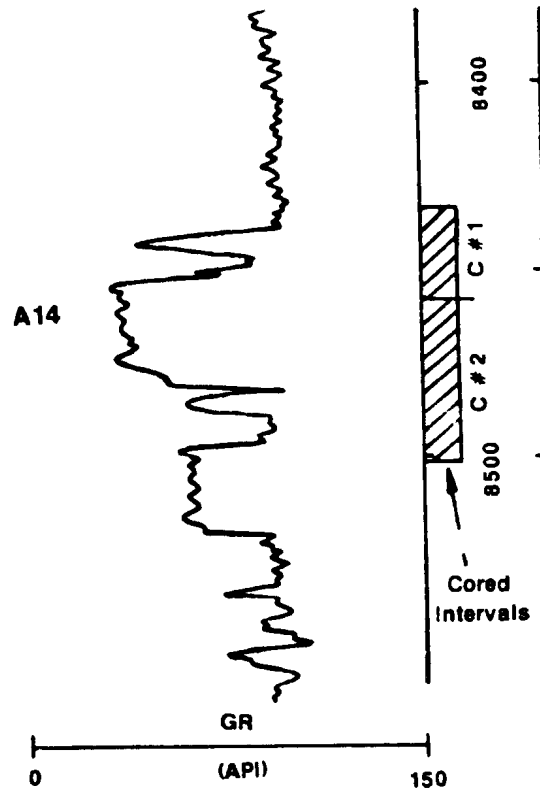


C1-NC2, C#4

APPENDIX I

Figure App.I.6. Cores Description (C#1,C#2) of Well T1-23,
Lower Acacus Formation, NC2 Concession,
Hamada Basin, NW Libya.
" Location of Well Shown in Figure.4 "

T1-23
K.B. 2056 FT



Gamma-Ray Log (GR) Signatures and Cored Intervals (8435-8458ft; 8458-8502ft) for Well T1-23, Lower Acacus Formation, NC2 Concession, Hamada Basin, NW Libya.
" Depth divisions are 50 ft (15.24m) apart "

APPENDIX I

Well T1-23

Formation Lower Acacus

Concession NC2

Core No. 1

Interval 8435-8458ft

Hamada Basin, Libya

Depth (ft)	T.S.	Gross Lithology	Grain Size							Sed. Structures and Accessories	Rock Description	Lithofacies	Oil Stain			Porosity			DST Intv.	DST Result
			dy	slt	v/s	fs	ms	cs	vcs				h	m	L	gd	tr	pr		
8430																				
8440		X							= G	SS, Lt. gy, m. grd, lam., Glauconitic pts, calc.	Glauc. par. lam. SS									
		-							//	SLTY SS, gy, dk gy, blot.	Blot. Silty SS									
8450		-							=	SH, gy, grn, firm, subfines-fine, flky, mic, lam.	Lam. SH									
		.							-	SS, Lt. gy, occ. lt brn, m. grd, subang-subrd, m. sort, mud clasts and rip up clasts, partly calc.	Indist. lam. SS									
8460		X								No Recovery										

Gross Lithology

- Sandstone
- Siltstone
- Shale
- No Recovery

Sedimentary Structures

- Horizontal even parallel laminae
- Rip-up clasts
- Bioturbation

Accessories

- Mud clasts
- Glauconite

DST Result

- Oil

APPENDIX I

Well T1-23

Formation Lower Acacus

Concession NC2

Core No. 2

Interval 8458-8502ft

Hamada Basin, Libya

Depth (ft)	T.S.	Gross Lithology	Grain Size						Sed. Structures and Accessories	Rock Description	Lithofacies	Oil Stain			Porosity			DST Intv.	DST Result
			dy	sit	v/s	fs	ms	cs				vcs	h	m	L	gd	tr		
8450																			
8460								Low angle cross lamination	SS, LT.gy, crmish wt, m.grd, subang-rd, w.sort, w/ x lam.	Low angle X-lam.SS								●	
								Horizontal even parallel laminae	SH, dk gy, blk, flss, lam.	Finely lam.SH								●	
								Wavy Laminations	SS, Lt.gy, grnsh wt, occ.tan, vf-m.grd, subang-subrd, w.sort, w/micro X-lam., rip-up clasts, partly calc.	Low angle x-lam.SS									
8470								contorted structures	SLTY SS, gy, dk gy, biot, w/cont.stru.	Biot.Slty SS									
								Lenticular silty sand lenses	SH, a/a (8460-8461ft)	Finely lam. SH									
								Rip-up clasts	SS, gy, dk gy, vf-grd, w/par. lam. at the top, slty, biot. at 8476ft.	par.lam. SS									
8480								Bioturbation	SH, dk gy, dk grn, occ.blk, flss, flky, mic, w/par-subpar. lam, w/minor slty ss lenses, non calc.	Finely lam.SH									
8490									SS, wtish gy, crm, m.grd, subang-rd, m.sort, glauc.in pts, w/wavy lam.	Glauc. wavy lam.SS									
									SH, gy, grn biot, non calc.	Biot.SH									
8500									No recovery										

Gross Lithology

- Sandstone
- Siltstone
- Shale
- No Recovery

Sedimentary Structures

- Low angle cross lamination
- Horizontal even parallel laminae
- Wavy Laminations
- contorted structures
- Lenticular silty sand lenses
- Rip-up clasts
- Bioturbation

Accessories

- Mud clasts
- Glaucanite

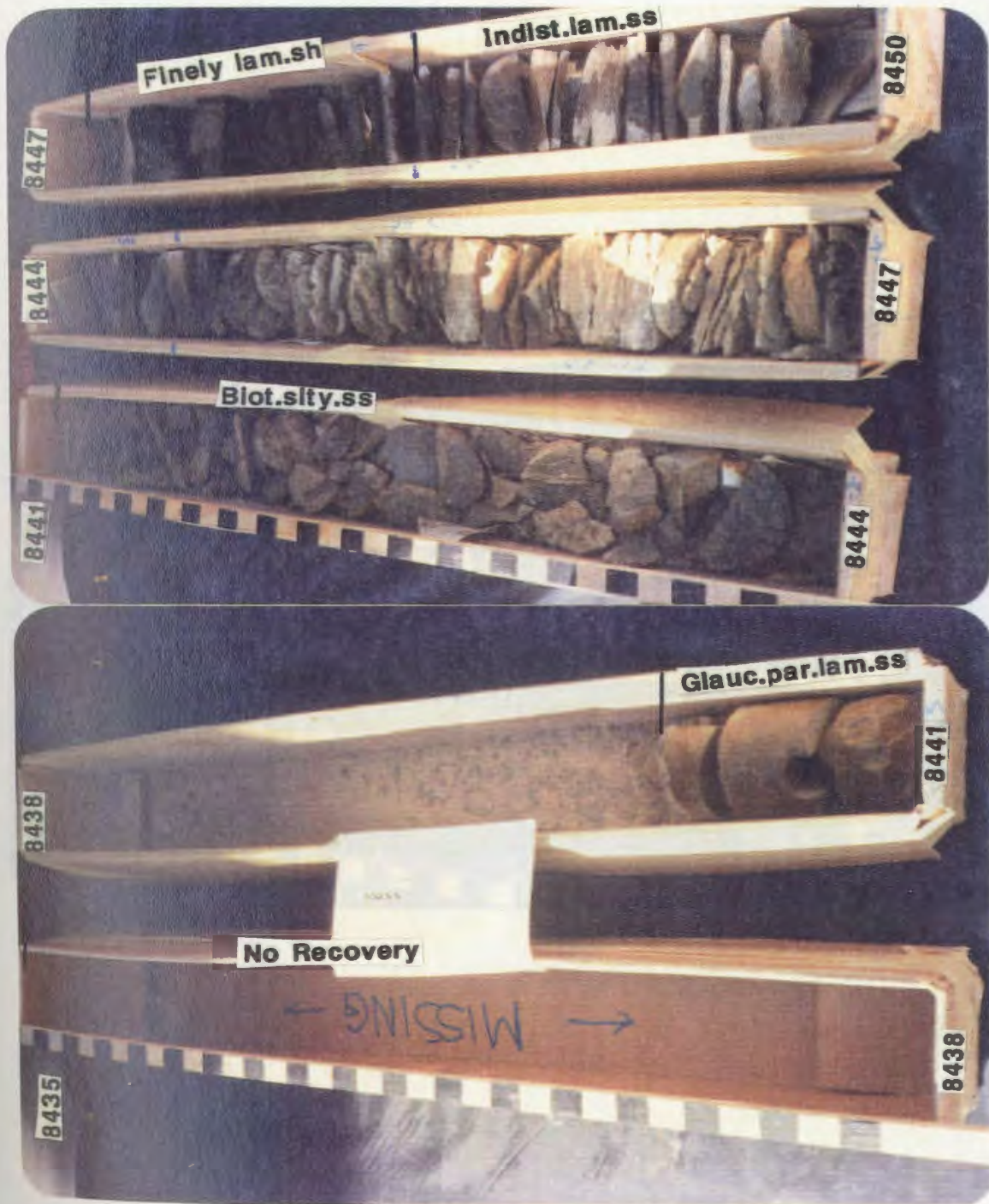
DST Result

- Oil

APPENDIX I

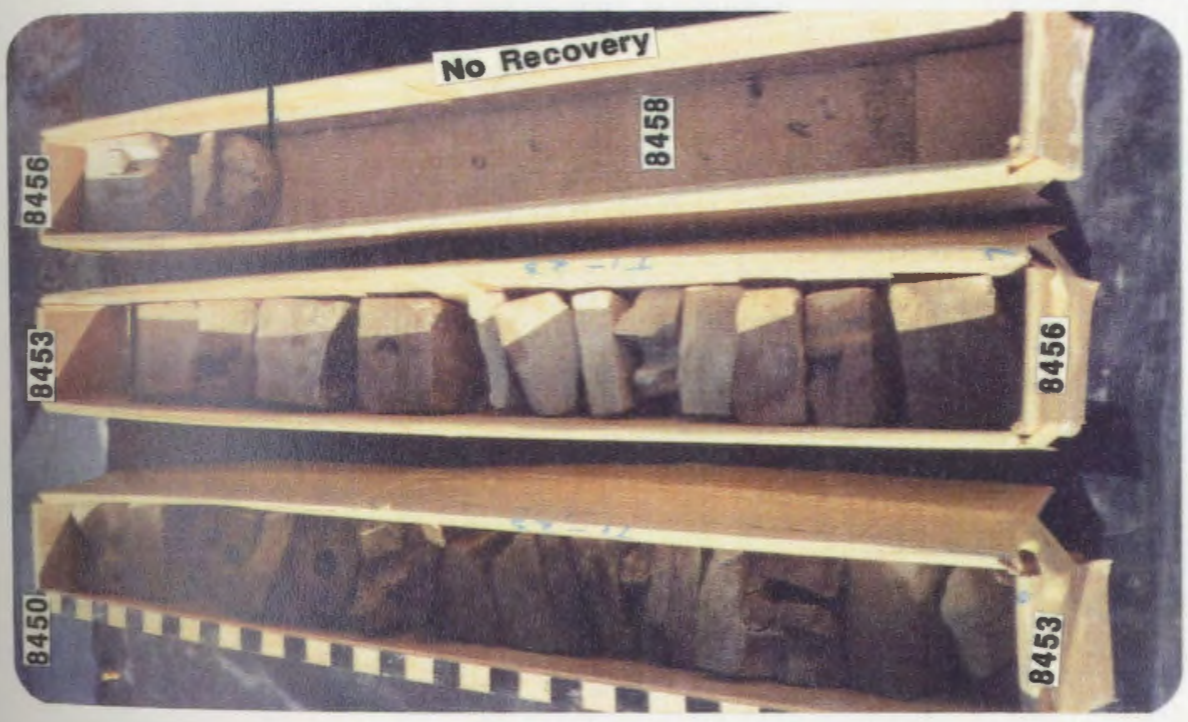
Figure App.I.7. Core Photos (C#1,C#2) of Well T1-23,
Lower Acacus Formation, NC2 Concession,
Hamada Basin, NW Libya.
" Detailed Descriptions of Lithofacies are
in Figure App.I.6 "

APPENDIX I



T1-23,C#1

APPENDIX I



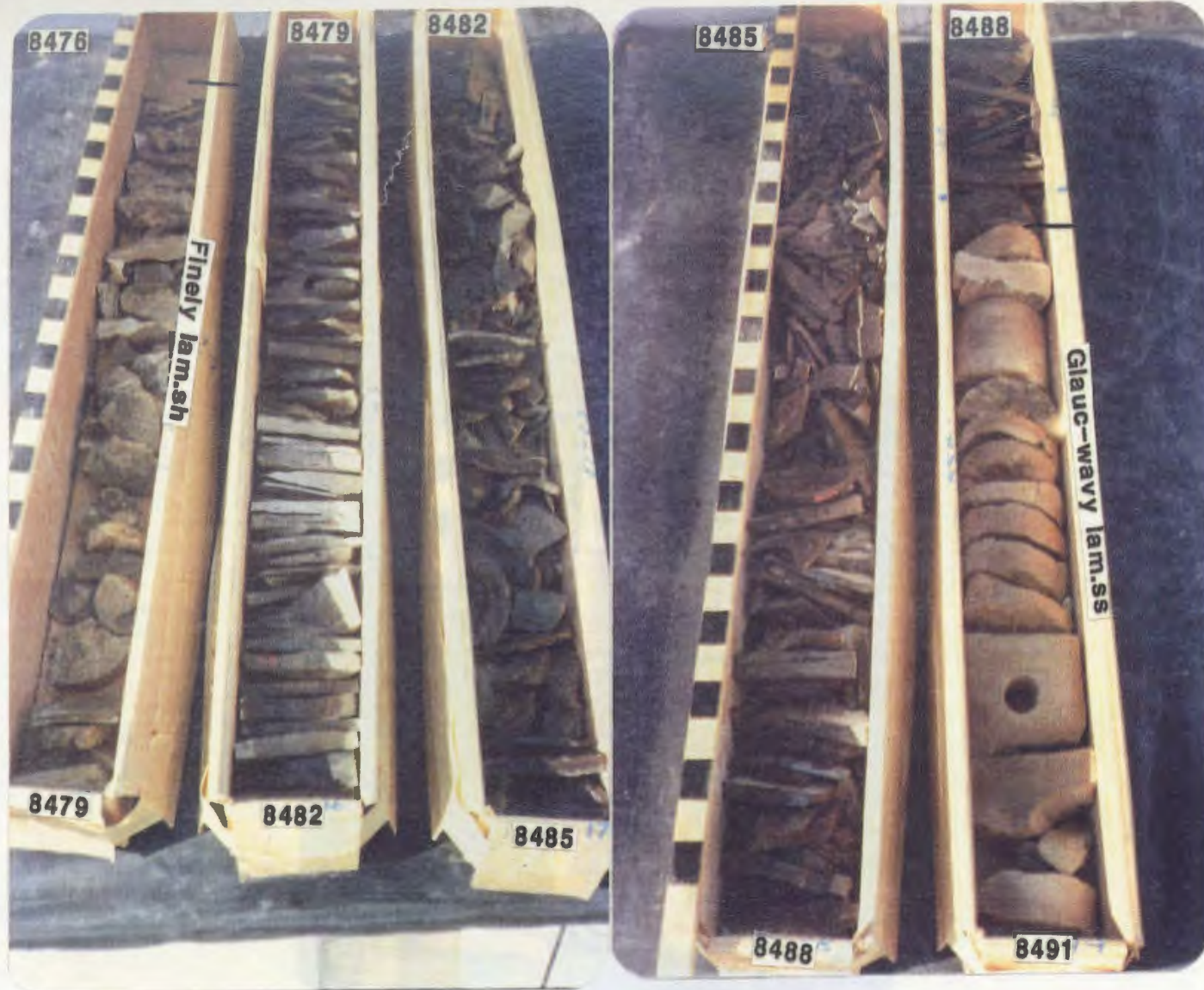
T1-23,C#1

APPENDIX I



T1-23, C#2

APPENDIX I



T1-23,C#2

APPENDIX I

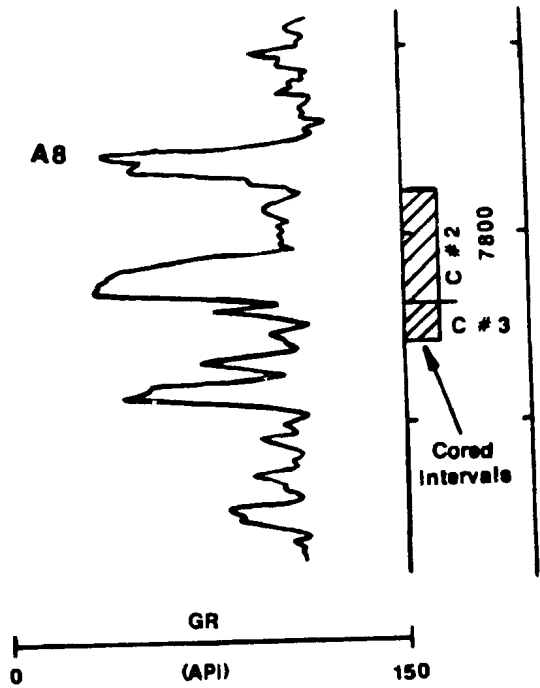


T1-23, C#2

APPENDIX I

Figure App.I.8. Cores Description (C#2,C#3) of Well A1-NC2,
Lower Acacus Formation, NC2 Concession,
Hamada Basin, NW Libya.
" Location of Well Shown in Figure.4 "

A1-NC2
K.B. 2160 FT



Gamma-Ray Log (GR) Signatures and Cored Intervals (7789-7819ft;
7819-7829ft) for Well A1-NC2, Lower Acacus Formation,
NC2 Concession, Hamada Basin, NW Libya.
" Depth divisions are 50 ft (15.24m) apart "

APPENDIX I

well A1-NC2

Formation Lower Acacus

Concession NC2

Core No. 2 & 3

Interval
7789-7819ft
7819-7829ft

Hamada Basin, Libya

Depth (ft)	T.S.	Gross Lithology	Grain Size						Sed. Structures and Accessories	Rock Description	Lithofacies	Oil Stain			Porosity			DST Inty	DST Result
			cl	silt	vs	fs	ms	cs				vcs	h	m	L	gd	fr		
7780																			
7790									   	SH, gy, grn, frm, subfiss-fiss, flky, mic, w/ thin lent. silty sd lenses biot.	Biot.SH								
7800									 										
7810									  	SS., tan, lt brn, vf-grd, subang-subrd, pr-m. sort, w/ low angle x-lam. at the top, occ. bio. at the base, w/ some alter. of Sh lam.	Low angle x-lam. SS							⊕	
7820									 	SLTY SS, dk gy, burr.	Burr. SLTY SS								
7830										SH, dk gy, blk, fiss, flky, mic, v.lam, non calc.	Finely lam. SH								

Gross Lithology

-  Sandstone
-  Siltstone
-  Shale

Sedimentary Structures

-  Low angle cross laminations
-  Horizontal even parallel laminae
-  Wavy Laminations
-  Lenticular silty sand lenses
-  Burrows
-  Bioturbation

Accessories

-  Mud clasts

DST Result

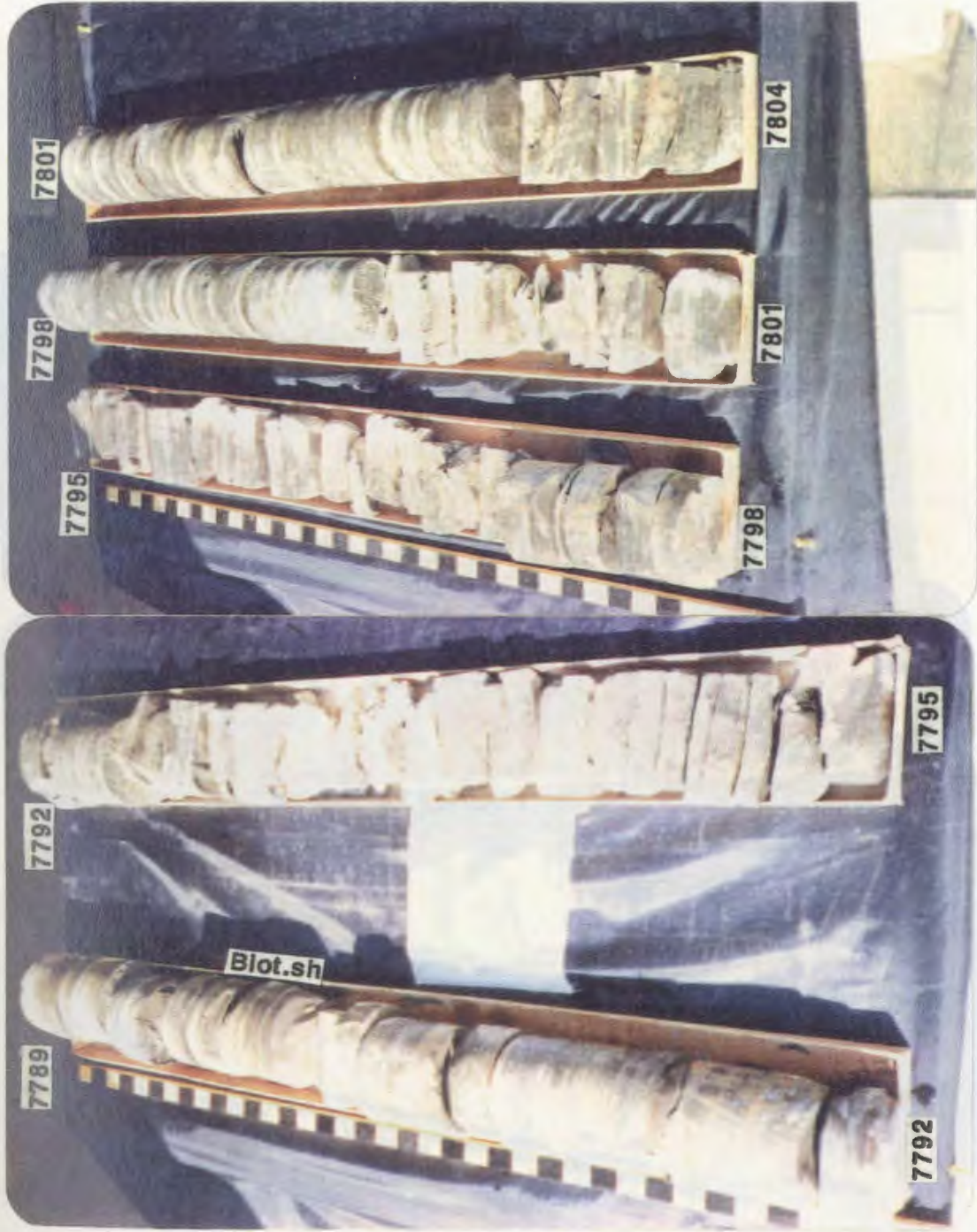
-  Water

APPENDIX I

Figure App.I.9. Core Photos (C#2,C#3) of Well A1-NC2,
Lower Acacus Formation, NC2 Concession,
Hamada Basin, NW Libya.

" Detailed Descriptions of Lithofacies are
Included in Figure App.I.8 ".

APPENDIX I



A1-NC2, C#2

APPENDIX I



A1-NC2, C#2

APPENDIX I



A1-NC2,C#3

APPENDIX I

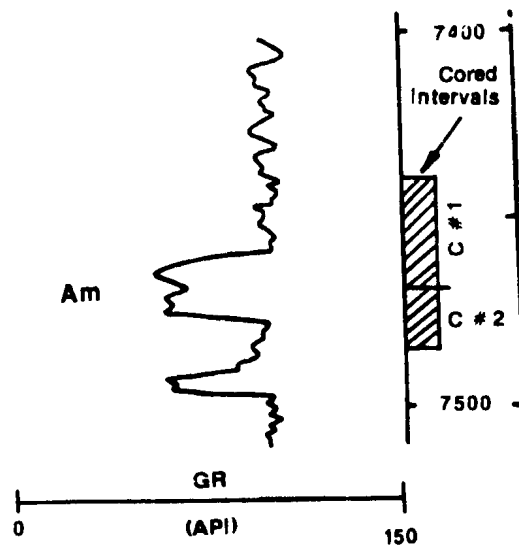
Figure App.I.10. Cores Description (C#1,C#2) of Well Q1-23,
Lower Acacus Formation, NC2 Concession,
Hamada Basin, NW Libya.

" Location of Well Shown in Figure.4 "

APPENDIX I

361

Q1-23
K.B. 2040 FT



Gamma-Ray Log (GR) Signatures and Cored Intervals (7440-7470ft;
7470-7485ft) for Well Q1-23, Lower Acacus Formation,
NC2 Concession, Hamada Basin, NW Libya.

" Depth divisions are 50 ft (15.24m) apart "

APPENDIX I

Well Q1-23

Formation Lower Acacus

Concession NC2
Hamada Basin, Libya

Core No. 1 & 2

Interval 7440-7470ft
7470-7485ft

Depth (ft)	T.S.	Gross Lithology	Grain Size						Sed. Structures and Accessories	Rock Description	Lithofacies	Oil Stain			Porosity		DST Inv.	DST Result
			cl	silt	v/s	fs	ms	cs				vcs	h	m	L	gd		
7440									 ◇ ◇ 	SH, gy, dk grn, fss, fky, lam, w/minor silty sd lenses, mic.	Finely lam. SH							
7450									 									
7460	●								 ~ G	SS, gy, whitish gy, f, grd, subang-subrd, m-w sort, mic. in pts, glauc., w/wavy ripple struc. calc.	Glauc. wavy rippled SS							
7470	●								 = G	SH, dk grn, dk gy, fss, lam. SS, a/a (7460-7467ft)	Lam. SH Glauc. wavy rippled SS							
									}} }}	No Recovery SH, dk gy, gyish grn, btrl., biot.	Biot. SH							
7480									}}									
7490																		

Gross Lithology

- Sandstone
- Siltstone
- Shale
- No Recovery

Sedimentary Structures

- Horizontal even parallel laminae
- Wavy laminations
- Lenticular silty sand lenses
- Bioturbation

Accessories

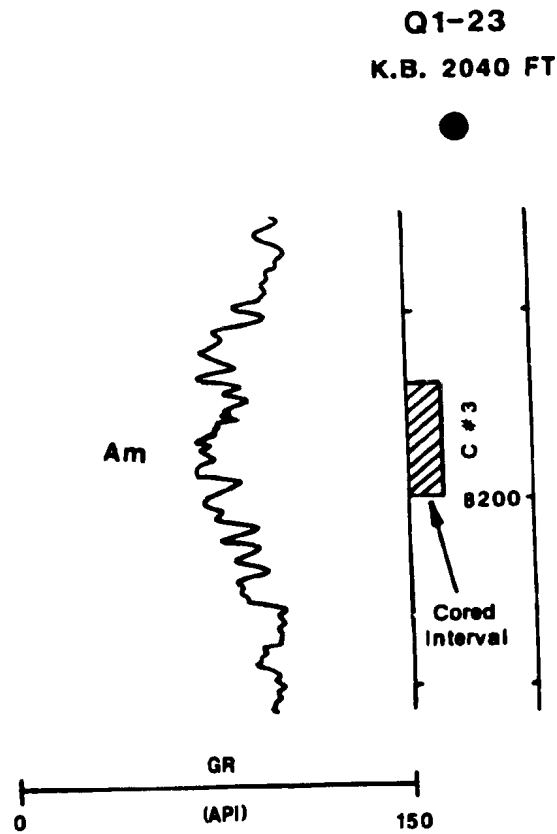
- G Glaucanite

DST Result

APPENDIX I

Figure App.I.11. Core Description (C#3) of Well Q1-23,
Lower Acacus Formation, M2 Concession,
Hamada Basin, NW Libya.

" Location of Well Shown in Figure.4 ".



Gamma-Ray Log (GR) Signatures and Cored Interval (8170-8200ft) for Well Q1-23, Lower Acacus Formation, NC2 Concession, Hamada Basin, NW Libya.

" Depth divisions are 50 ft (15.24m) apart "

APPENDIX I

Well Q1-23

365

Formation Lower Acacus

Concession NC2

Core No. 3

Interval 8170-8200ft

Hamada Basin, Libya

Depth (ft)	T.S.	Gross Lithology	Grain Size						Sed. Structures and Accessories	Rock Description	Lithofacies	Oil Stain			Porosity			DST Intv.	DST Result
			dy	sit	v/s	fs	ms	cs				ycs	h	m	L	gd	fr		
8170									SH, dk gy, brtl, biot.	Biot.SH									
								SS, wtish gy, crm, m, grd, frb, subang-rd, w. sort, w/par.lam, calc, glauc.	Glauc.par. lam.SS									●	
8180	●							SH, a/a (8170-8173ft)	Biot.SH									●	
								SS, crm, wtish gy, f-m grd, frb, indist.lam, occ.w/par.lam and wavy rippled struc. at the base, glauc.in pts, calc.	Glauc.wavy par.lam SS										
8190	●																		
								No Recovery											
								SS, a/a @187-8193ft, m, grd, w/par.lam., glauc, calc.	Glauc.par. lam SS										
8200								No Recovery											

Gross Lithology

- Sandstone
- Shale
- No Recovery

Sedimentary Structures

- Horizontal even parallel laminae
- Wavy Laminations
- Bioturbation

Accessories

- G Glaucanite

DST Result

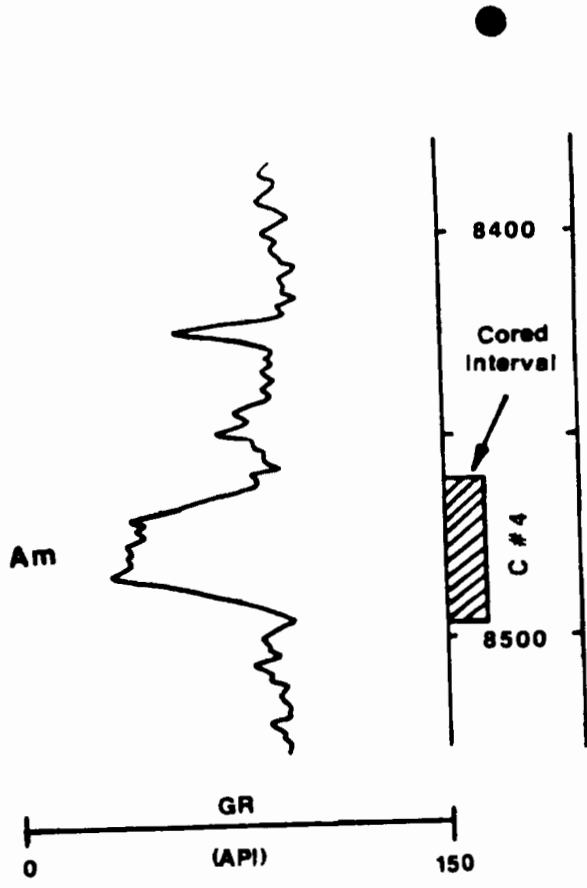
- Oil

APPENDIX I

Figure App.I.12. Core Description (C#4) of Well Q1-23,
Lower Acacus Formation, NC2 Concession,
Hamada Basin, NW Libya.

" Location of Well Shown in Figure.4 "

Q1-23
K.B. 2040 FT



Gamma-Ray Log (GR) Signatures and Cored Interval (8461-8497ft) for Well Q1-23, Lower Acacus Formation, NC2 Concession, Hamada Basin, NW Libya. " Depth divisions are 50 ft (15.24m) apart "

APPENDIX I

Well Q1-23

Formation Lower Acacus

Concession NC2

Core No. 4

Interval 8461-8497ft

Hamada Basin, Libya

Depth (ft)	T.S.	Gross Lithology	Grain Size							Sed. Structures and Accessories	Rock Description	Lithofacies	Oil Stain			Porosity			DST Intv.	DST Result
			dy	sit	v/s	f/s	m/s	cs	vcs				h	m	L	gd	fr	pr		
8460	●									G 	SS,lt gy, wtish gy,f-m grd, subang-subrd,w.sort, w/micro x-lam,w/clay clasts,glauc.in pts. SLTY SS,dk gy,biot.,w/Sh lam at places. No Recovery SLTY SS, a/a (8464-8468ft) No Recovery SLTY SS, a/a (8464-8468ft) No Recovery	Glauc. low angle x-lam.SS Biot. SLTY SS Biot. SLTY SS Biot. SLTY SS								★
8470											SS,lt gy, m.grd,subang-rd,m-w.sort,w/micro x-lam, w/some minor Sh lam., glauc,calc. SS,lt gy,vf-f grd,subang-subrd,m-w sort,burr., glauc,calc. SH, dk gy,dk grn,mic in pts, biot.,non calc.	Glauc., micro x-lam.SS Glauc., calc.SS Biot.SH.								
8480	●										SS,lt gy, m.grd,subang-rd,m-w.sort,w/micro x-lam, w/some minor Sh lam., glauc,calc.	Glauc., micro x-lam.SS							★	
8490	●									G	SS,lt gy,vf-f grd,subang-subrd,m-w sort,burr., glauc,calc.	Glauc., calc.SS								
8500											SH, dk gy,dk grn,mic in pts, biot.,non calc.	Biot.SH.								
8510																				

Gross Lithology

- Sandstone
- Siltstone
- Shale
- No Recovery

Sedimentary Structures

- Low angle cross laminations
- Wavy Laminations
- Bioturbation
- Burrows

Accessories

- Mud clasts
- G Glaucanite

DST Result

- ★ Oil & Gas

APPENDIX I

Figure App.I.13. Core Photos (C#1-C#4) of Well Q1-23,
Lower Acacus Formation, NC2 Concession,
Hamada Basin, NW Libya.

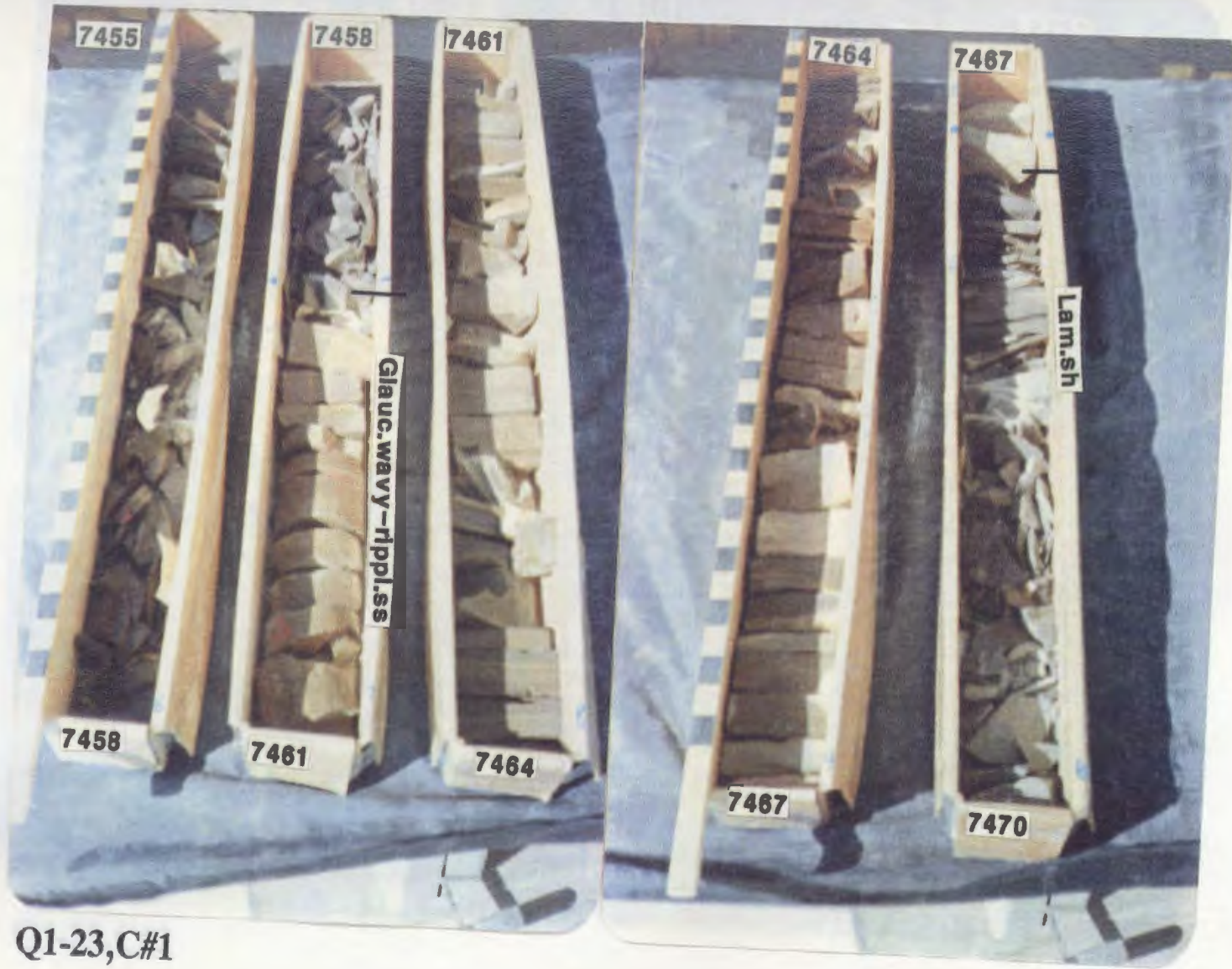
" Detailed Descriptions of Lithofacies are
Included in Figures App.I.10-AI.12 ".

APPENDIX I.



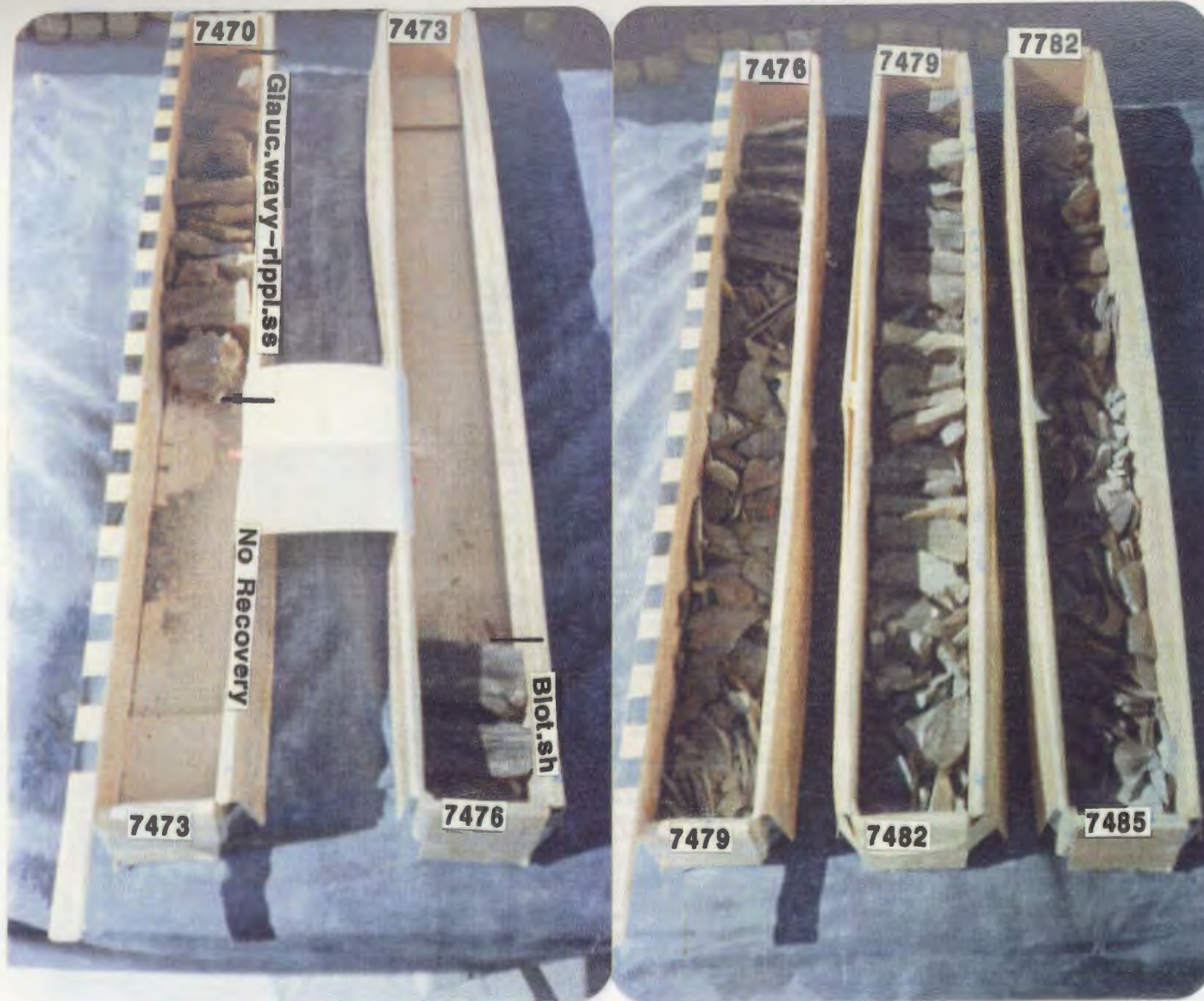
Q1-23,C#1

APPENDIX I



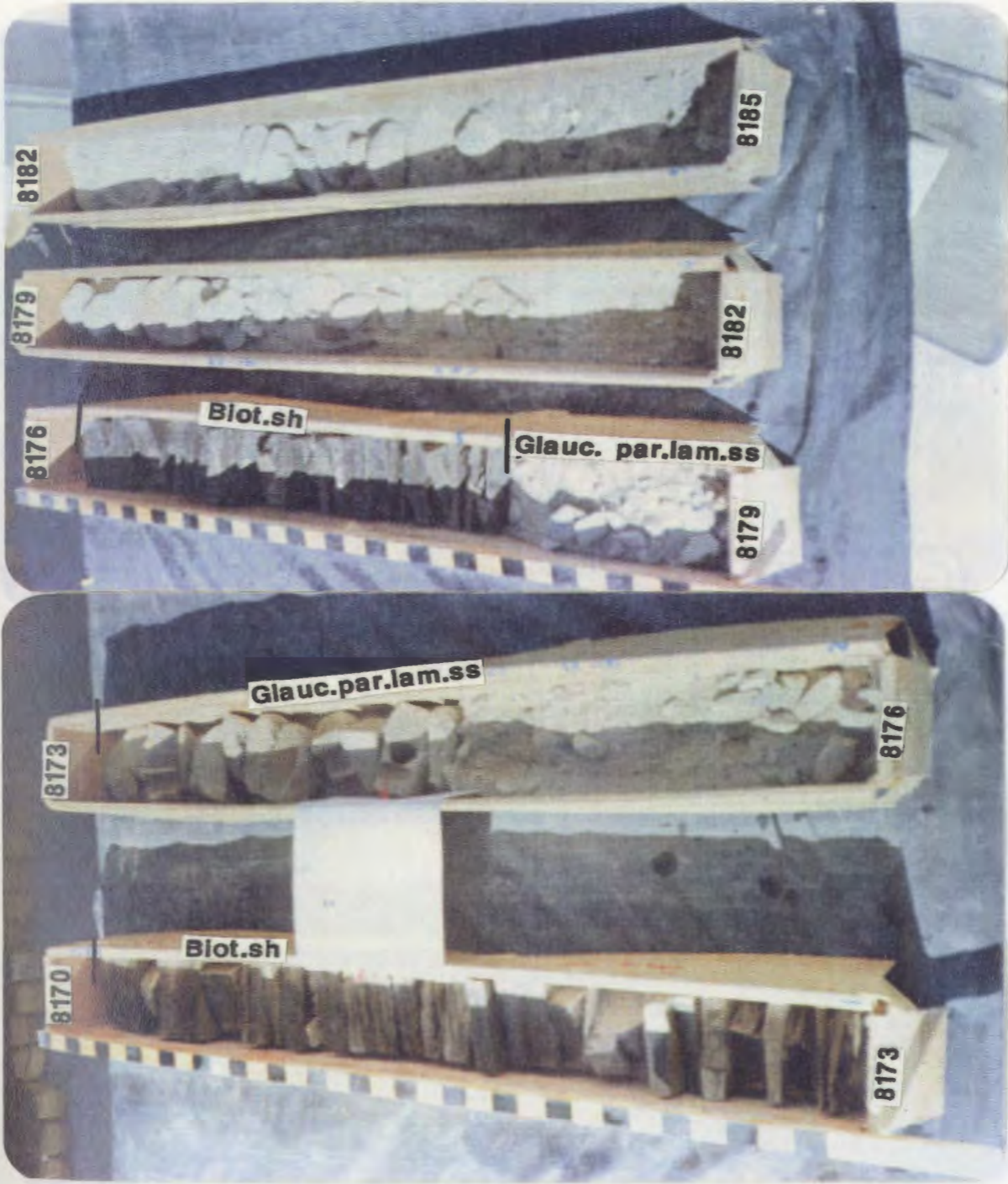
Q1-23,C#1

APPENDIX I



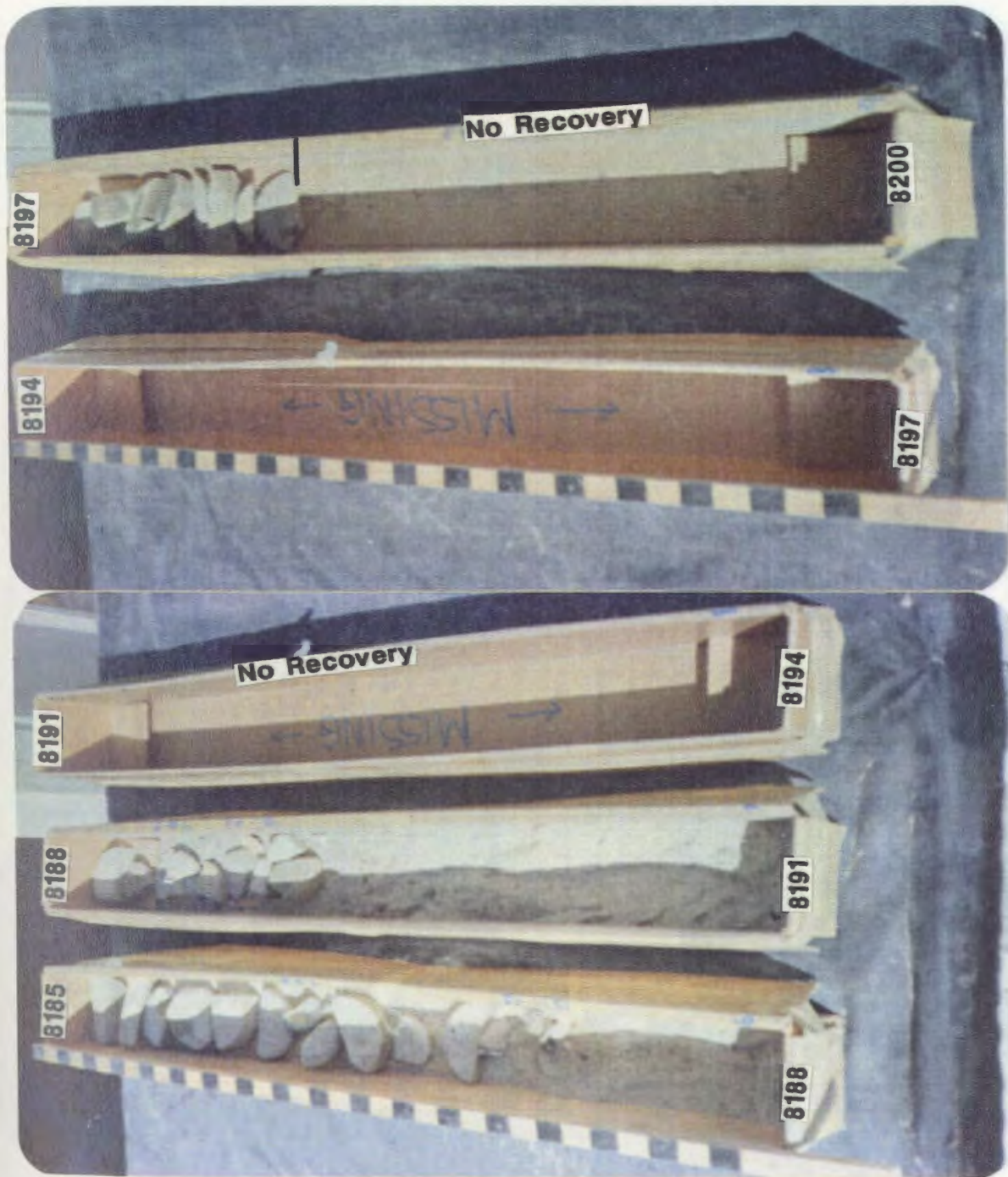
Q1-23,C#2

APPENDIX I



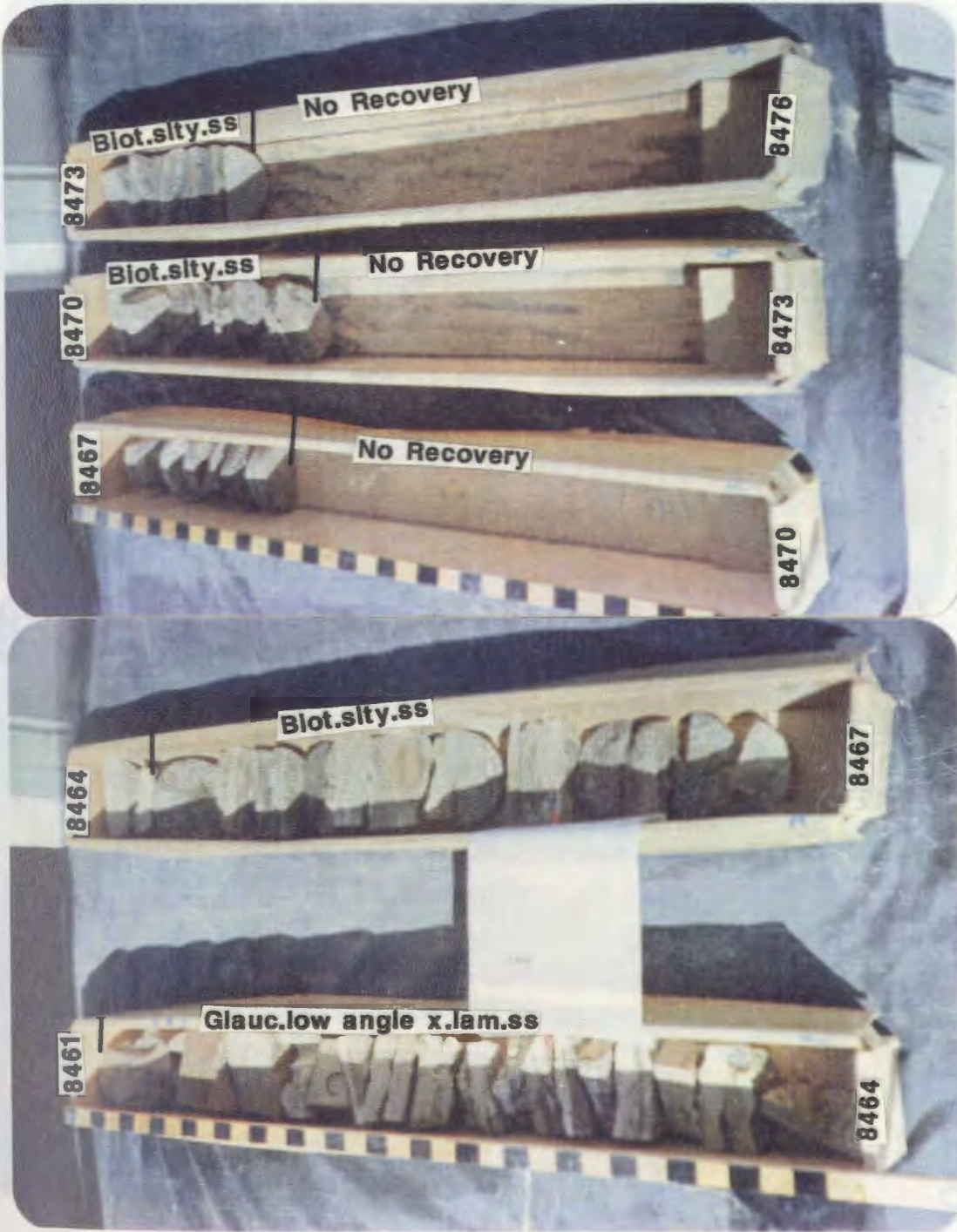
Q1-23, C#3

APPENDIX I



Q1-23, C#3

APPENDIX I



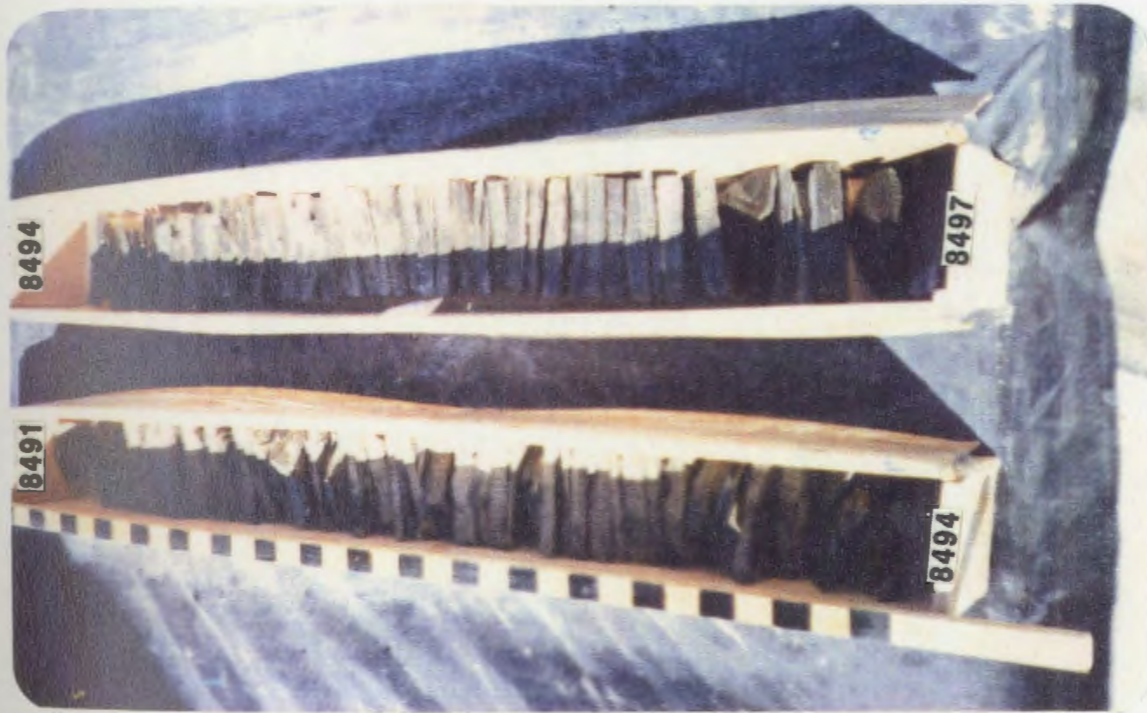
Q1-23, C#4

APPENDIX I



Q1-23,C#4

APPENDIX I



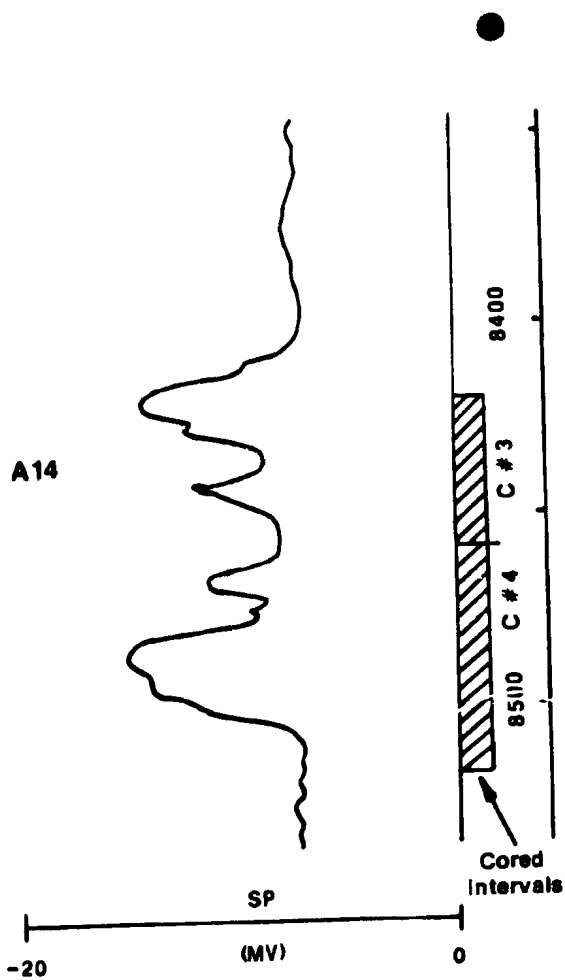
Q1-23, C#4

APPENDIX I

Figure App.I.14. Cores Description (C#3,C#4) of Well B1-61,
Lower Acacus Formation, NC2 Concession,
Hamada Basin, NW Libya.

" Location of Well Shown in Figure.4 ".

B1-61
K.B. 2037 FT



Gamma-Ray Log (GR) Signatures and Cored Intervals (8420-8459ft; 8459-8518ft) for Well D1-61, Lower Acacus Formation, NC2 Concession, Hamada Basin, NW Libya.
" Depth divisions are 50 ft (15.24m) apart "

APPENDIX I

Well B1-61

Formation Lower Acacus

Concession NC2
Hamada Basin, Libya

Core No. 3

Interval 8420-8459ft

Depth (ft)	T.S.	Gross Lithology	Grain Size							Sed. Structures and Accessories	Rock Description	Lithofacies	Oil Stain			Porosity			DST Intv.	DST Result
			cl	sl	vf	fs	ms	cs	vcs				h	m	L	gd	fr	pr		
8420	●		[Grain Size Data]								SS, gy, lt gy, wtish gy, f-m grd, subang-rd, m-w sort, indist. lam, car., mud clasts, calc. in pts	Car. indist. lam. SS								●
8430											SH, dk grn, dk gy, subfss, partly biot.	Biot. SH								
8440											SH, dk grn, dk gy, fss, flky, mic, w/lent. silty sd lenses, v.lam.	Lam. SH								
8450											SS, lt gy, crm, m. grn, w/wavy lam., calc.	wavy lam. calc. SS								
8460											SH, a/a (8430-8441ft) No Recovery									

Gross Lithology

- Sandstone
- Siltstone
- Shale
- No Recovery

Sedimentary Structures

- Horizontal even parallel laminae
- Wavy laminations
- Lenticular silty sand lenses
- Rip-up clasts
- Bioturbation

Accessories

- Carbonaceous debris
- mud clasts

DST Result

- Oil

APPENDIX I

Well B1-61

Formation Lower Acacus

Concession NC2

Core No. 4

Interval 8459-8518ft

Hamada Basin, Libya

Depth (ft)	T.S.	Gross Lithology	Grain Size						Sed. Structures and Accessories	Rock Description	Lithofacies	Oil Stain			Porosity			DST Intv.	DST Result
			dy	silt	vfs	fs	ms	cs				vcs	h	m	L	gd	fr		
8460									SH, dk gy, dk grn, flss, lam.	Lam. SH									
									SS, wtish gy, gy, vf-m grd, subang-rd, m-w sort, car w/micro x-lam, rip-up clasts, silty at 8464ft.	Car. SS									
									SH, dk gy, subfiss, biot. No Recovery	Biot. SH									
8470									SH, a/a (8465-8467ft)	Biot. SH									
									SS, lt gy, vf, grd, silty at the bott., subang-subrd, car. w/par. lam, calc. No Recovery	Even par. lam. car SS									
8480									SS, lt gy, lt grn, vf-m grn, subang-rd, w. sort, car w/mud clasts, rip-up clasts, indist. lam, silty, partly calc.	Indist. lam. car. SS									
8490									Silty SS, dk gy, v. silty, ang-subang, pr. sort, biot., calc	Biot. Silty SS									
									SH, dk gy, dk grn, occ. blk, subfiss, mic, biot., occ. w/lent. silty sd lenses.	Biot. SH									
8500									no Recovery										
8510									SH, dk gy, flss, flky, v. lam., non calc.	Finely lam. SH									

Gross Lithology

- Sandstone
- Siltstone
- Shale
- No Recovery

Sedimentary Structures

- Low angle cross laminations
- Horizontal even parallel laminae
- Lenticular silty sand lenses
- Rip-up clasts
- Burrows
- Bioturbation

Accessories

- Carbonaceous debris
- mud clasts

DST Result

- Oil

APPENDIX I

Figure App.I.15. Core Photos (C#3,C#4) of Well B1-61,
Lower Acacus Formation, NC2 Concession,
Hamada Basin, NW Libya.

" Detailed Descriptions of Lithofacies are
Included in Figure App.I.14 ".

APPENDIX I



B1-61,C#3

APPENDIX I



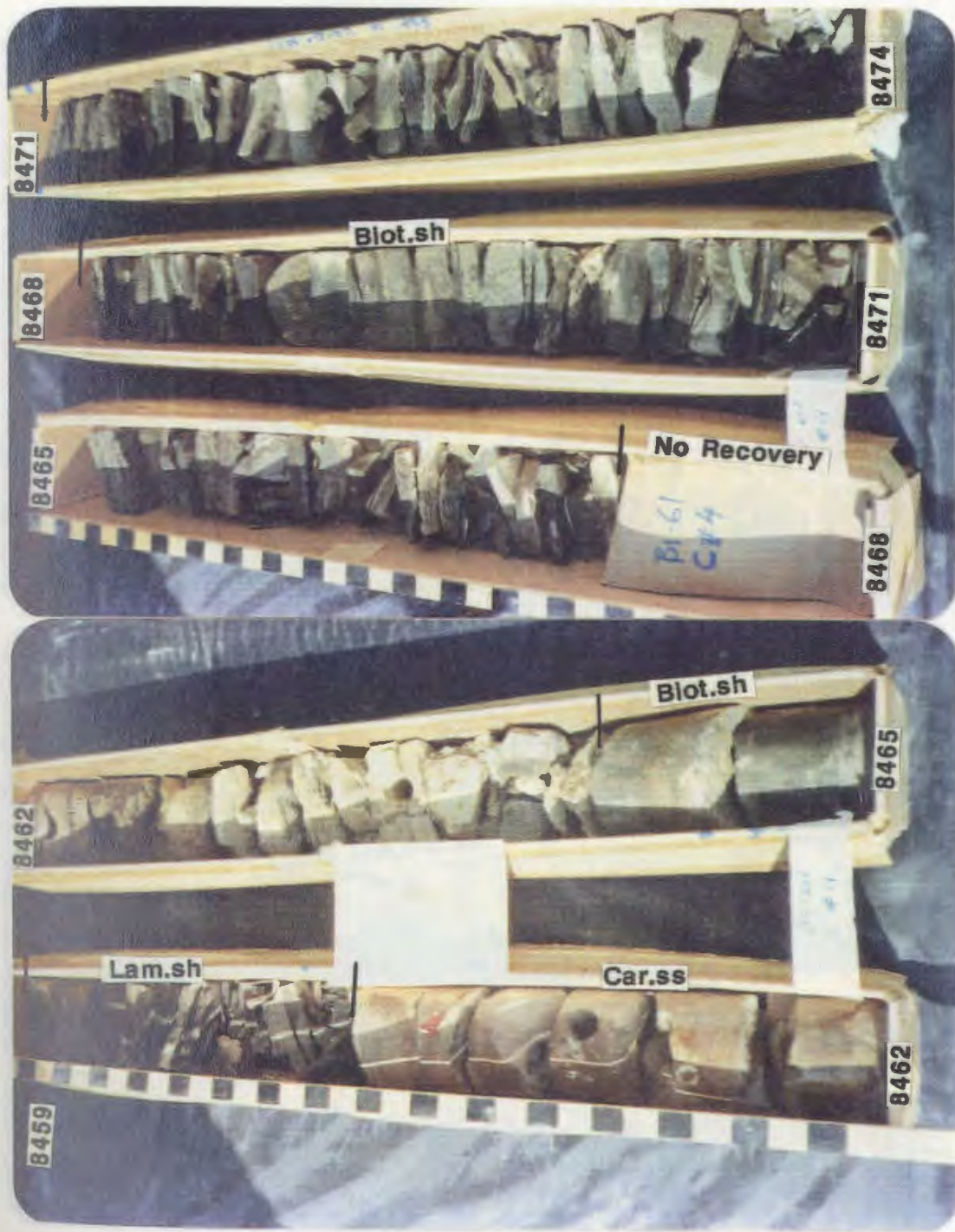
B1-61,C#3

APPENDIX I

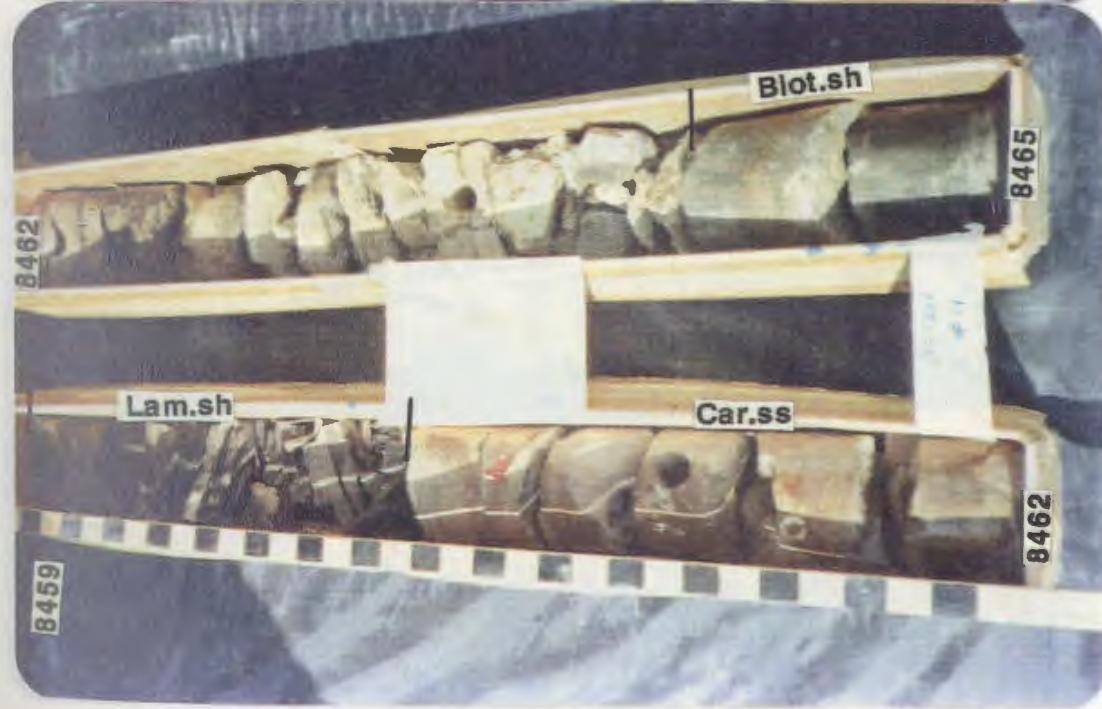


B1-61, C#3

APPENDIX I



B1-61, C#4



APPENDIX I



B1-61,C#4

APPENDIX I



B1-61,C#4

APPENDIX I



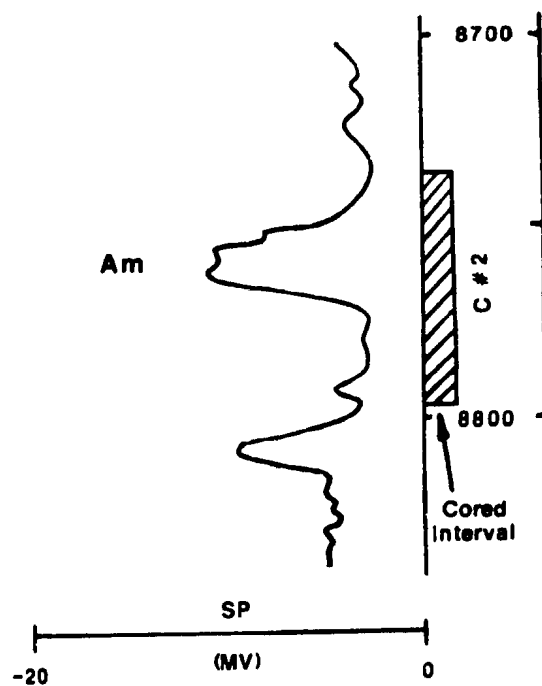
B1-61, C#4

APPENDIX I

Figure App.I.16. Core Description (C#2) of Well B3-61,
Lower Acacus Formation, NC2 Concession,
Hamada Basin, NW Libya.

" Location of Well Shown in Figure.4 "

B3-61
K.B. 2050 FT

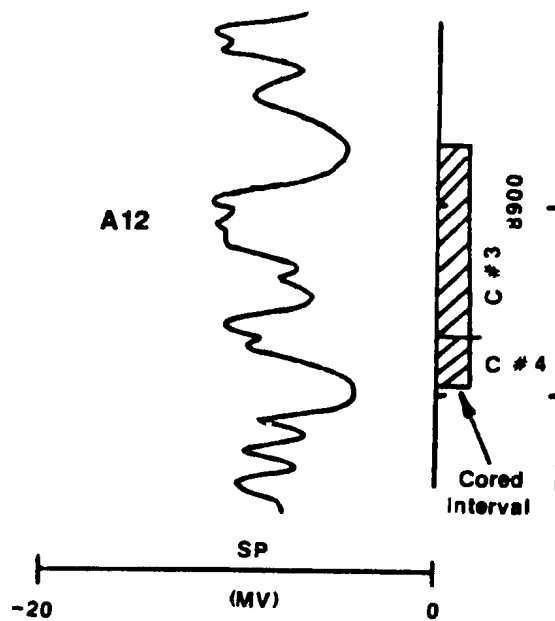


Gamma-Ray Log (GR) Signatures and Cored Interval (8736-8796ft) for Well B3-61, Lower Acacus Formation, NC2 Concession, Hamada Basin, NW Libya. " Depth divisions are 50 ft (15.24m) apart ".

APPENDIX I

Figure App.I.17. Cores Description (C#3,C#4) of Well B3-61,
Lower Acacus Formation, NC2 Concession,
Hamada Basin, NW Libya.
" Location of Well Shown in Figure.4 "

B3-61
K.B. 2050 FT



Gamma-Ray Log (GR) Signatures and Cored Intervals (8885-8945ft; 8945-8998ft) for Well B3-61, Lower Acacus Formation, NC2 Concession, Hamada Basin, NW Libya.
 " Depth divisions are 50 ft (15.24m) apart "

APPENDIX I

Well B3-61

Formation Lower Acacus

Concession NC2

Core No. 3

Interval 8885-8945ft

Hamada Basin, Libya

Depth (ft)	T.S.	Gross Lithology	Grain Size							Sed. Structures and Accessories	Rock Description	Lithofacies	Oil Stain			Porosity			DST Intv.	DST Result
			dy	slt	vfs	fs	ms	cs	vcs				h	m	L	gd	fr	pr		
8880									∞ ∞	SH, gy, dk gy, biot.	Biot. SH									
8900									◆	SS, lt gy, lt grn, f-m grd, frb. at places, subang-rd, w. sort, w/ mud clasts, car., wavy rippled lam. at the top, slty at the base.	wavy rippled lam. car. SS									
									∞	SLTY SS, dk gy, biot. SS, a/a (8892ft)	Biot. SLTY SS wavy lam. SS									
8920									==	SH, dk gy, dk grn, fiss, mic, v. lam. at top, w/ tr. of biot at the base.	Lam. SH									
										No Recovery										
									∞	SLTY SS, dk gy, biot.	Biot. SLTY SS									
8940									∞	SH, a/a (8914-8924ft)	Biot. SH									
										No Recovery										
8960																				
8980																				

Gross Lithology

- Sandstone
- Siltstone
- Shale
- No Recovery

Sedimentary Structures

- Horizontal even parallel laminae
- wavy laminations
- Bioturbation

Accessories

- Mud clasts
- Carbonaceous debris

DST Result

APPENDIX I

Well **B3-61**

Formation **Lower Acacus**

Concession **NC2 Hamada Basin, Libya**

Core No. **4**

Interval **8945-8998ft**

Depth (ft)	T.S.	Gross Lithology	Grain Size							Sed. Structures and Accessories	Rock Description	Lithofacies	Porosity			DST Intv.	DST Result
			dy	silt	v/s	fs	ms	cs	vcs				h	m	L		
8940																	
8950	●								SS	SH, dk gy, dk grn, occ. flss, w/ent. silty sd lenses at places, occ. biot. at the base	Biot. SH						
									SS, G	SS, lt gy, w/ish gy, f. grn, f. grd, w/micro x-lam, wavy rippled lam, w/tr. of glauc.	Wavy-rippled Glauc, SS						
									SS	SH, a/a (8945-8950ft) v. Biot.	Biot. SH						
8960	●								SS, =	SS, a/a (8950-8951ft) w/par. lam., calc,	Par. Jam. calc. SS						
									SS, S	SH, dk gy, biot. non calc.	Biot. SH						
8970	●								SS, S, >	SS, gy, w/ish gy, occ. tan, f-m grd, subang-subrd, w. sort, w/rip-up clasts, mud clasts, occ. biot. at the base	Indist. Jam. SS					⊕	
									U	No Recovery							
8980	●								SS	SLTY SS, dk gy, dk grn, biot.	Biot SLTY SS						
									SS, =	SH, gy, dk gy, occ. blk, flss, mic, v. lam.	Finely lam. SH						
8990									SS, =	No Recovery							

Gross Lithology

- Sandstone
- Siltstone
- Shale
- No Recovery

Sedimentary Structures

- Low angle cross laminations
- Horizontal even parallel laminae
- Wavy laminations
- Lenticular silty sand lenses
- Burrows
- Bioturbation
- Rip-up clasts

Accessories

- Mud clasts
- Glaucinite

DST Result

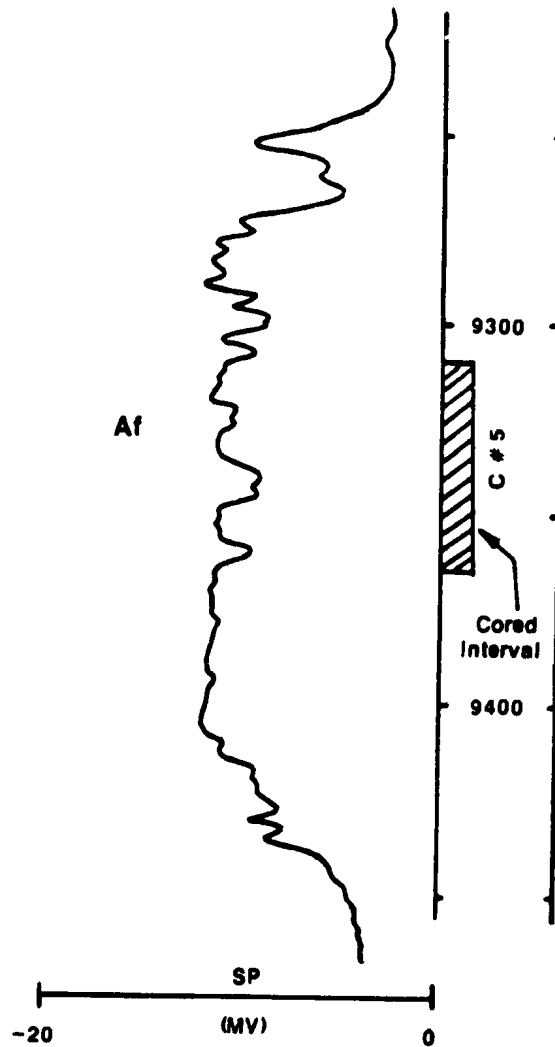
- Water

APPENDIX I

Figure App.I.18. Core Description. (C#5) of Well B3-61,
Lower Acacus Formation, NC2 Concession,
Hamada Basin, NW Libya.
" Location of Well Shown in Figure.4 ".

B3-61

K.B. 2050 FT



Gamma-Ray Log (GR) Signatures and Cored Interval (9310-9365ft) for Well B3-61, Lower Acacus Formation, NC2 Concession, Hamada Basin, NW Libya.

" Depth divisions are 50 ft (15.24m) apart "

APPENDIX I

Well B3-61

Formation Lower Acacus

Concession NC2

Core No. 5

Interval 9310-9365ft

Hamada Basin, Libya

Depth (ft)	T.S.	Gross Lithology	Grain Size						Sed. Structures and Accessories	Rock Description	Lithofacies	Oil Stain		Porosity		DST Inty.	DST Result
			cl	sl	v/s	fs	ms	cs				vc	h	m	g		
9310	•		█	█	█	█	█	█	✓ ✓	SS, lt gy, crm, m-vf grd, slty at the top, m-sort, w/minor x-lam. at the base, also w/some par.lam., occ.burr. struc. at top.	ParJam-Biot.cplx SS						
9320			█	█	█	█	█	█	ss	SH, dk gy, dk grn, v.biot.	Biot.SH						
9330	•		█	█	█	█	█	█	ss	SS, lt gy, crm, occ.lt grn, vf-f grd, m.sort, w/par lam. at the top, occ.biot at the base.	par.Jam. SS						
			█	█	█	█	█	█	ss	SH, a/a (9320-9325ft) No Recovery	Biot.SH						
9340			█	█	█	█	█	█	ss	SS, lt gy, f.grd, m.sort, par.lam. SH, dk gy, biot.	ParJam.SS Biot.SH						
	•		█	█	█	█	█	█	◆	SS, lt gy w/ sh gy, f-vf grd ang -subang, pr-m sort, occ. w/low angle x lam, and par.lam.	Low angle x-lam-par lam. cplx SS						
9350	•		█	█	█	█	█	█	ss	SLTY SS, gy, dk gy, v.slty, biot.	Biot. SLTY SS						
	•		█	█	█	█	█	█	ss	SH, dk gy, dk grn, biot. No Recovery	Biot.SH						
9360	•		█	█	█	█	█	█	◆	SS, lt gy, m.grd, subang-rd, m-w sort, w/micro lam. No Recovery	Low angle x-lam.SS						
			█	█	█	█	█	█	ss	SS, a/a (9357-9359ft) No Recovery	ParJam.SS						

Gross Lithology

- Sandstone
- Siltstone
- Shale
- No Recovery

Sedimentary Structures

- Low angle cross laminations
- Horizontal even parallel laminae
- Burrows
- Bioturbation

Accessories

- Mud clasts

DST Result

APPENDIX I

Figure App.I.19. Core Photos (C#2-C#5) of Well B3-61,
Lower Acacus Formation, NC2 Concession,
Hamada Basin, NW Libya.

" Detailed Descriptions of Lithofacies are
Included in Figures App.I.16-App.I.18 ".

APPENDIX I



B3-61,C#2

APPENDIX I



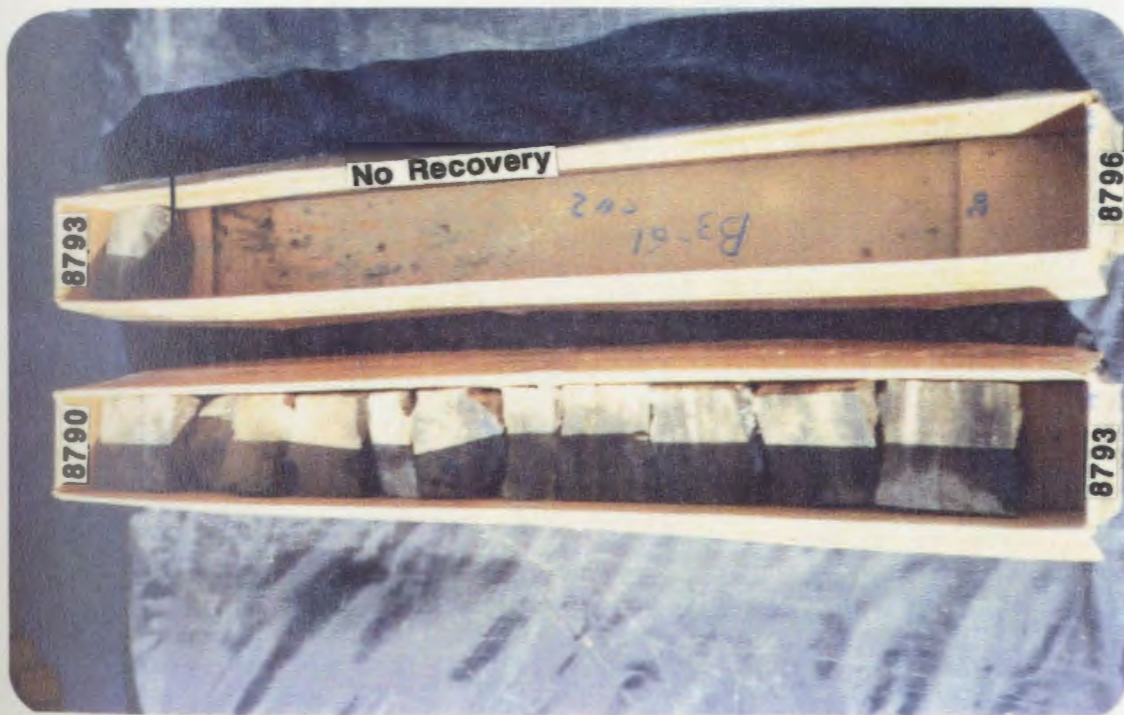
B3-61, C#2

APPENDIX I



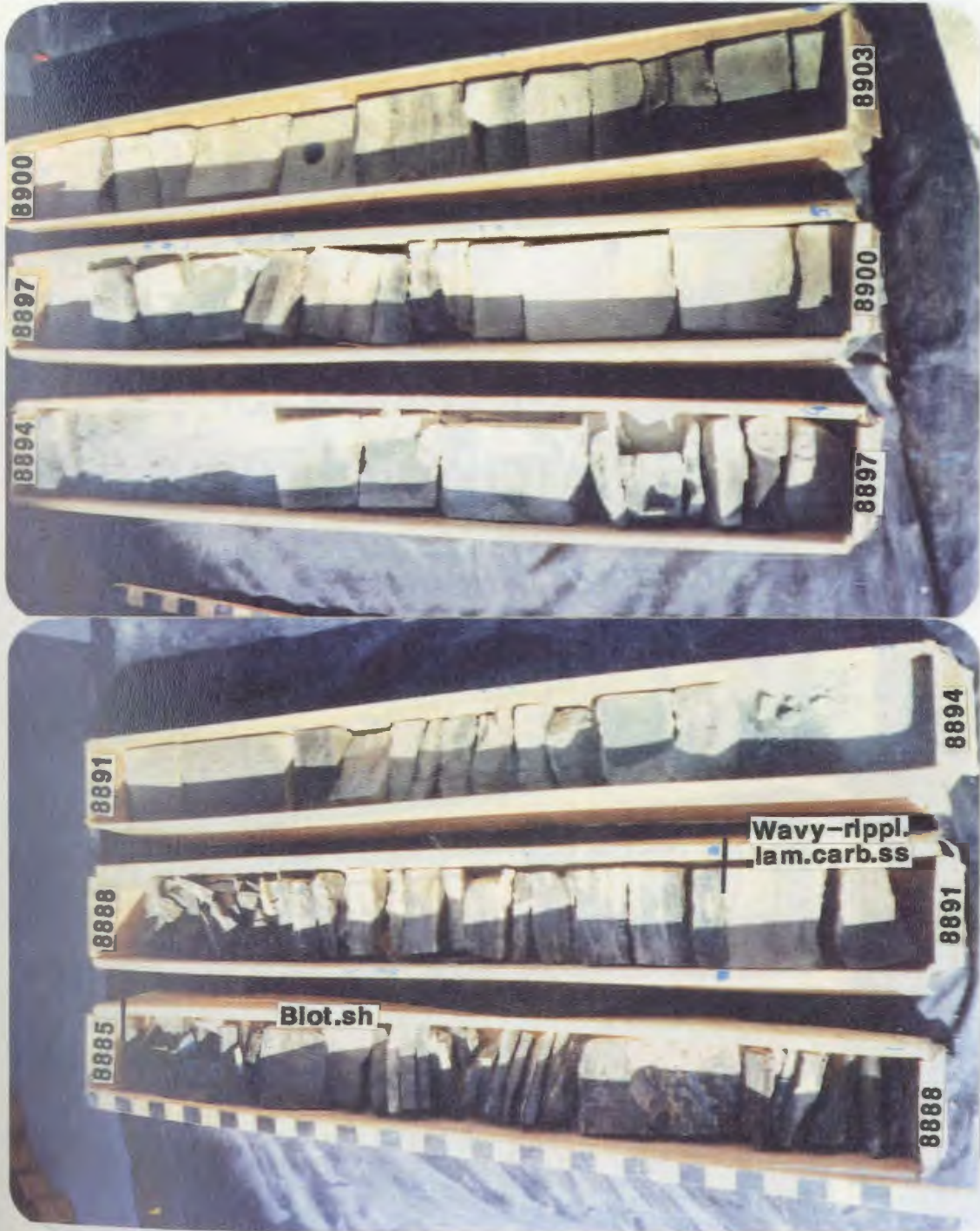
B3-61, C#2

APPENDIX I



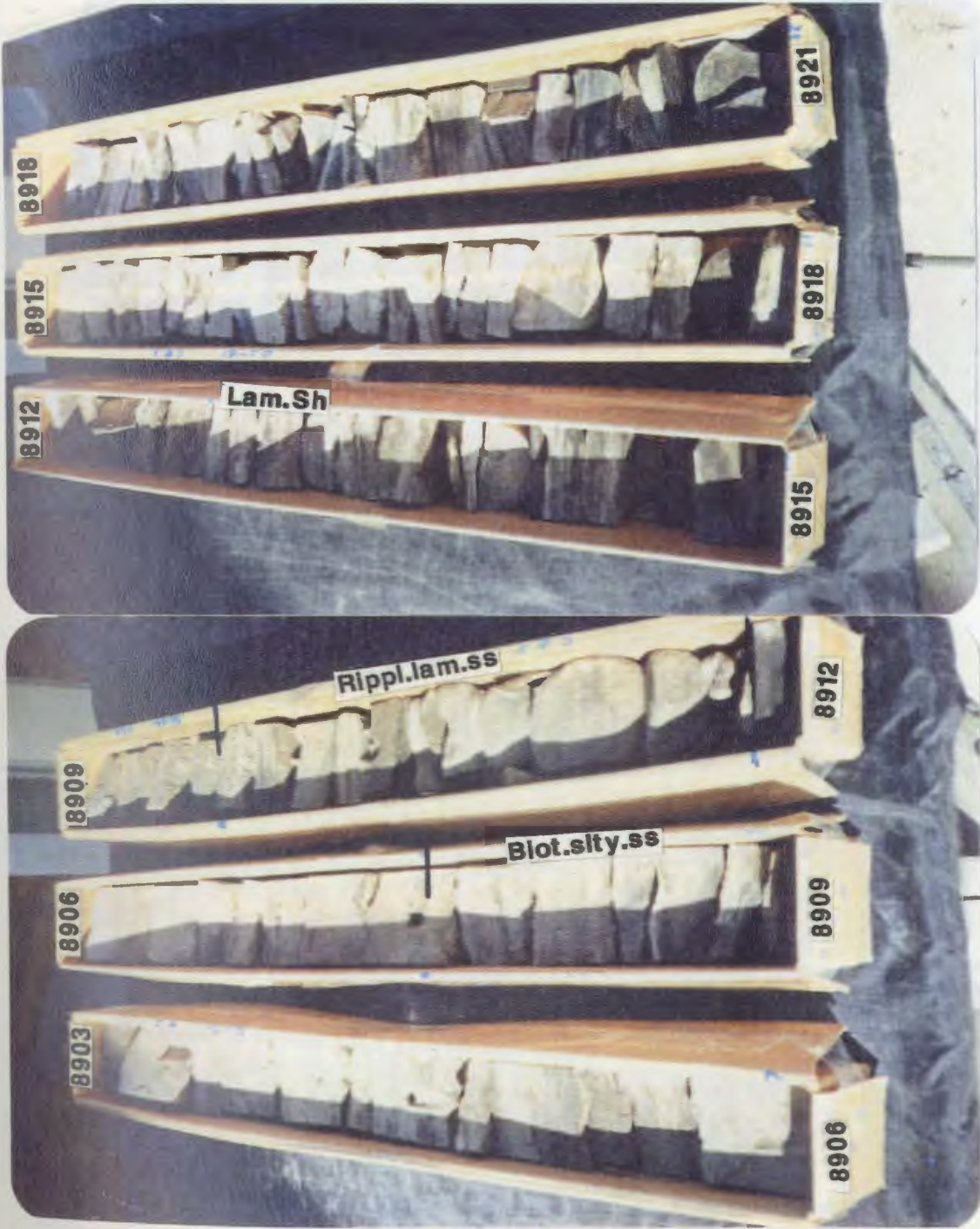
B3-61, C#2

APPENDIX I



B3-61, C#3

APPENDIX I



B3-61, C#3

APPENDIX I



B3-61,C#3

APPENDIX I



B3-61, C#3

APPENDIX I



B3-61, C#4

APPENDIX I



B3-61, C#4

APPENDIX I



B3-61, C#4

APPENDIX I



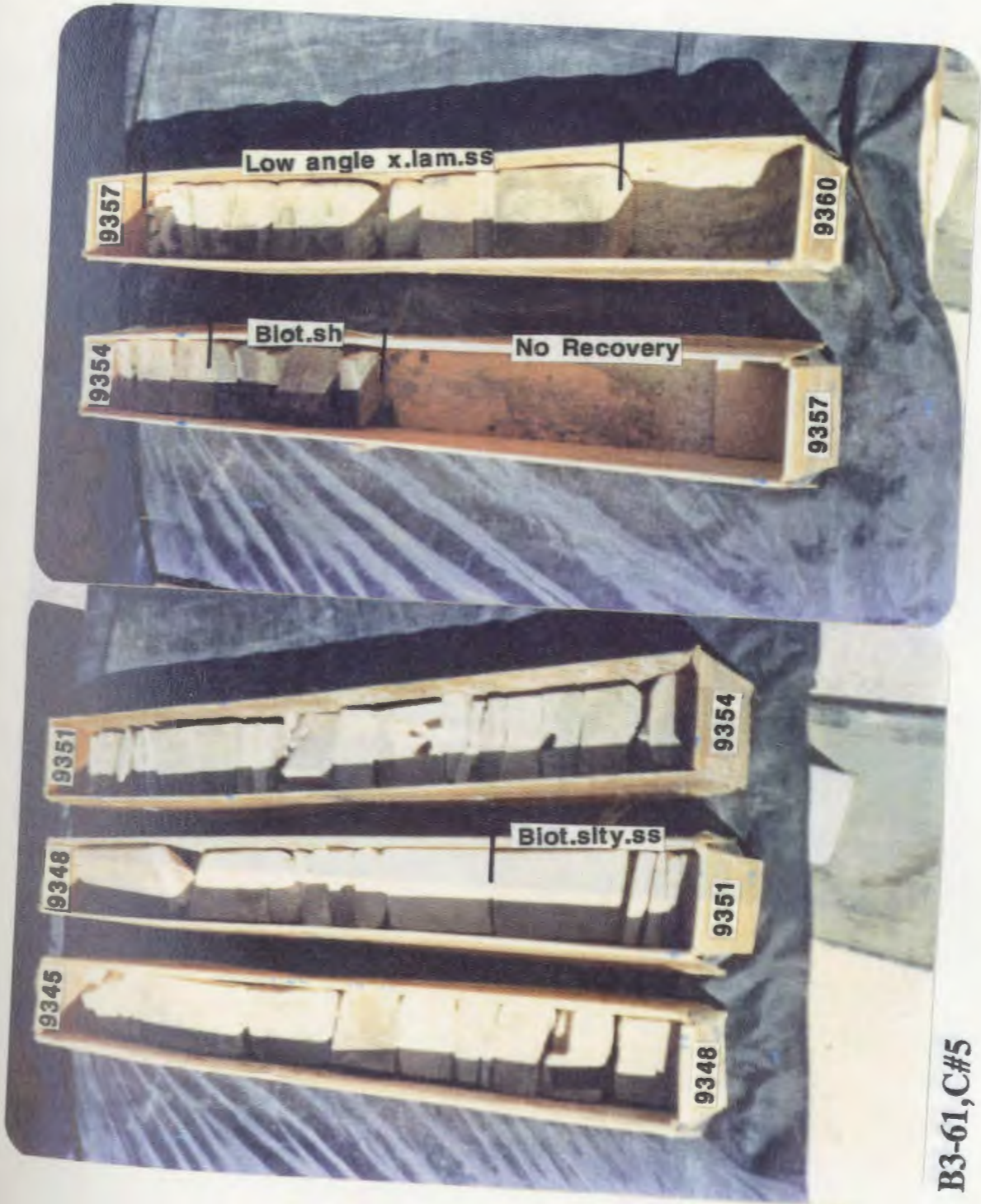
B3-61,C#5

APPENDIX I



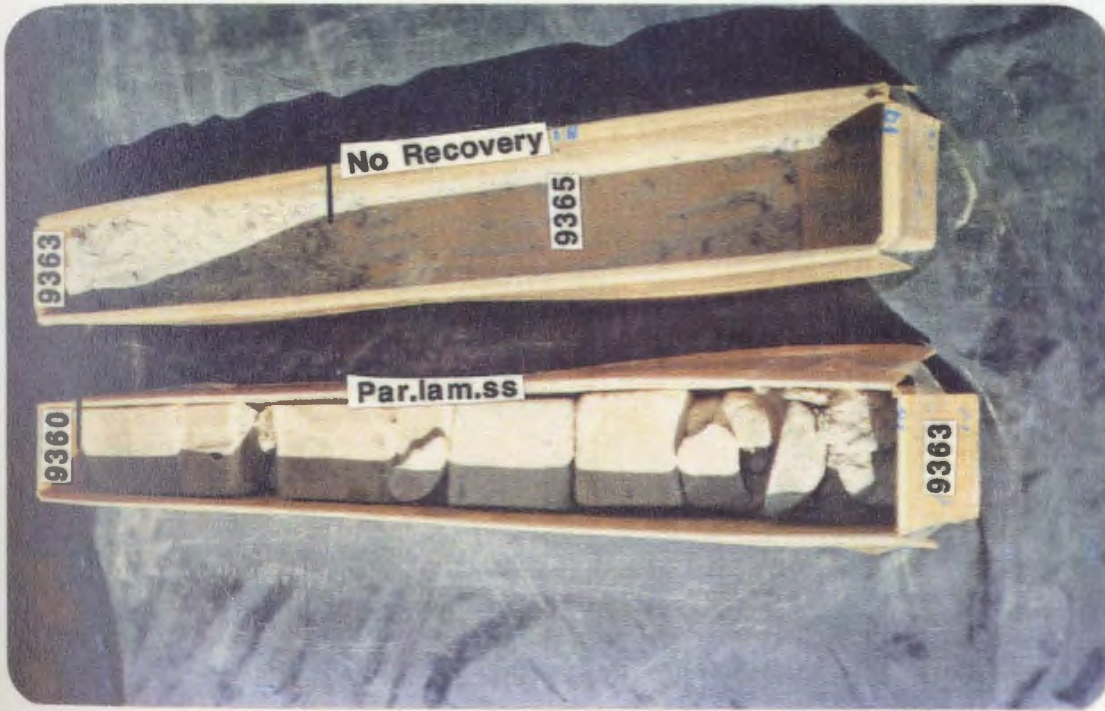
B3-61,C#5

APPENDIX I



B3-61, C#5

APPENDIX I



B3-61, C#5

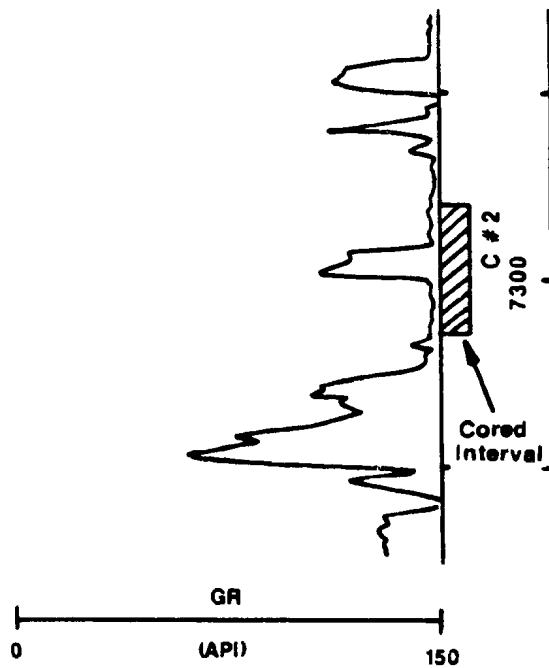
APPENDIX I

Figure App.I.20. Core Description (C#2) of Well C1-61,
Lower Acacus Formation, NC2 Concession,
Hamada Basin, NW Libya.

" Location of Well Shown in Figure.4 ".

C1-61

K.B. 2131 FT



Gamma-Ray Log (GR) Signatures and Cored Interval (7280-7315ft) for Well C1-61, Lower Acacus Formation, NC2 Concession, Hamada Basin, NW Libya.

" Depth divisions are 50 ft (15.24m) apart "

APPENDIX I

418

Well C1-61

Formation Lower Acacus

Concession NC2

Core No. 2

Interval 7280-7315ft

Hamada Basin, Libya

Depth (ft)	T.S.	Gross Lithology	Grain Size							Sed. Structures and Accessories	Rock Description	Lithofacies	Oil Stain			Porosity			DST Intv.	DST Result
			dy	sit	v/s	f/s	m/s	cs	vcs				h	m	L	gd	fr	pr		
7280		[Siltstone pattern]								=	SH, dk grn, occ. dk gy, fiss, mic. v. lam, non calc.	Finely lam. SH								
		[No Recovery pattern]								=			No Recovery							
7290		[Siltstone pattern]								=	SH, a/a (7280-7288ft), w/lent. silty sd lenses, biot. at 7315ft w/tr. glauc.	lam. SH								
		[Siltstone pattern]								◇ G										
7300		[Siltstone pattern]								=										
		[Siltstone pattern]								=										
7310		[Siltstone pattern]								◇										
		[Siltstone pattern]								ss										
7320		[Siltstone pattern]																		
7330		[Siltstone pattern]																		

Gross Lithology

- Siltstone
- Shale
- No Recovery

Sedimentary Structures

- Horizontal even parallel laminae
- Lenticular silty sand lenses
- Bioturbation

Accessories

- G** Glauconite

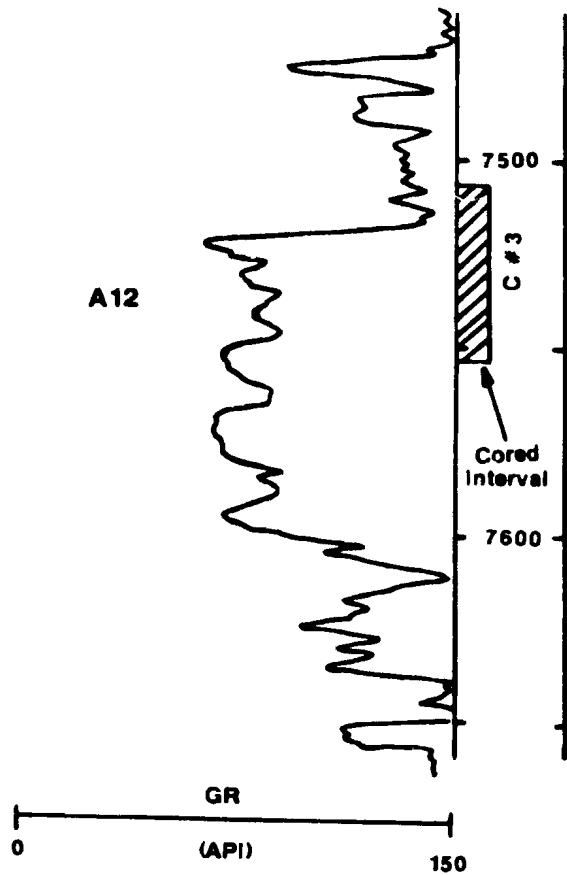
DST Result

APPENDIX I

Figure App.I.21. Core Description (C#3) of Well C1-61,
Lower Acacus Formation, NC2 Concession,
Hamada Basin, NW Libya.
Location of Well Shown in Figure.4 ".

C1-61

K.B. 2131 FT



Gamma-Ray Log (GR) Signatures and Cored Interval (7507-7555ft) for Well C1-61, Lower Acacus Formation, NC2 Concession, Hamada Basin, NW Libya.

" Depth divisions are 50 ft (15.24m) apart "

APPENDIX I

well C1-61

Formation Lower Acacus

Concession NC2
Hamada Basin, Libya

Core No. 3

Interval 7507-7555ft

Depth (ft)	T.S.	Gross Lithology	Grain Size						Sed. Structures and Accessories	Rock Description	Lithofacies	Oil Stain			Porosity			DST Intv.	DST Result
			dy	silt	vfs	fs	ms	cs				vcs	h	m	L	gd	fr		
7500																			
7510	•								SH, dk gy, occ. dk blk, fss, blk, mic, w/sily sd lenses at places.	Finely lam. SH									
7520	•																		
7530	•								SS, lt gy, crm, w/ish crm, vf-m grd, subang-subrd, m-w, sort, w/par lam., mud clasts, calc. in pts	par. lam. SS									
7540																			
7550									SLTY SS, dk gy, lt gy, v. sily, blot.	Biot. SLTY SS									
									SH, dk, gy, occ. dk blk, fss, mic, w/par.-subpar. micro lam.	Finely lam. SH									

Gross Lithology

-  Sandstone
-  Siltstone
-  Shale

Sedimentary Structures

-  Horizontal even parallel laminae
-  Lenticular silty sand insses
-  Bioturbation

Accessories

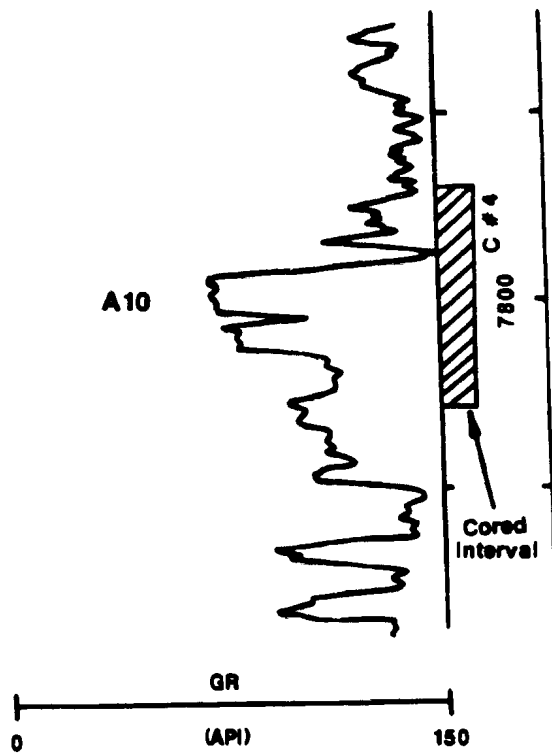
-  Mud clasts

DST Result

APPENDIX I

Figure. App.I.22. Core Description (C#4) of Well C1-61,
Lower Acacus Formation, NC2 Concession,
Hamada Basin, NW Libya.
" Location of Well Shown in Figure.4 "

C1-61
K.B. 2131 FT



Gamma-Ray Log (GR) Signatures and Cored Interval (7770-7828ft) for Well C1-61, Lower Acacus Formation, NC2 Concession, Hamada Basin, NW Libya.

" Depth divisions are 50 ft (15.24m) apart "

APPENDIX I

Well C1-61

Formation Lower Acacus

Concession NC2

Core No. 4

Interval 7770-7828ft

Hamada Basin, Libya

Depth (ft)	T.S.	Gross Lithology	Grain Size							Sed. Structures and Accessories	Rock Description	Lithofacies	Oil Stain			Porosity		DST Intv.	DST Result
			dy	slt	vfs	fs	ms	cs	vcs				h	m	L	gd	fr		
7770									ss	SH, dk gy, blot. No Recovery	Blot. SH								
									ss	SLTY SS, lt gy, dk gy, v. blot.	Blot. SLTY SS								
7780									ss	SH, a/a (7770-7771.5ft), occ. w/lent. slty sd lenses	Blot. SH								
									G	SS, lt gy, crm, vf. grd, subang-subrd, m. sort, w/tr. of glauc., calc.	Glauc. micro x-lam. SS								
7790									ss	SH, dk gy, dk grn, w/sltly sd lenses, blot. at the base	Blot. SH								
									F	SS, lt brn SS, lt brn, dk crm, f-m grd, subang-rd, w. sort, ferr. in pts, w/mud clasts, w/minor x-lam at the top, par. lam. at the base.	Ferr. par. lam. SS								
7800									ss	No Recovery SH, a/a (7800-7801ft), blot.	Blot. SH								
									ss	No Recovery SH, dk gy, dk grn, blot.	Blot. SH								
7810									G	SS, a/a (7782-7783.5ft), par. lam. No Recovery	Glauc. par. lam. SS								
										SH, gy, dk gy, dk grn, fls, flky, mic, v. lam.	Finely lam. SH								
7820										No Recovery									

Gross Lithology

- Sandstone
- Siltstone
- Shale
- No Recovery

Sedimentary Structures

- Low angle cross laminations
- Horizontal even parallel laminae
- Lenticular silty sand lenses
- Bioturbation

Accessories

- Mud clasts
- Glaucanite
- Iron oxide

DST Result

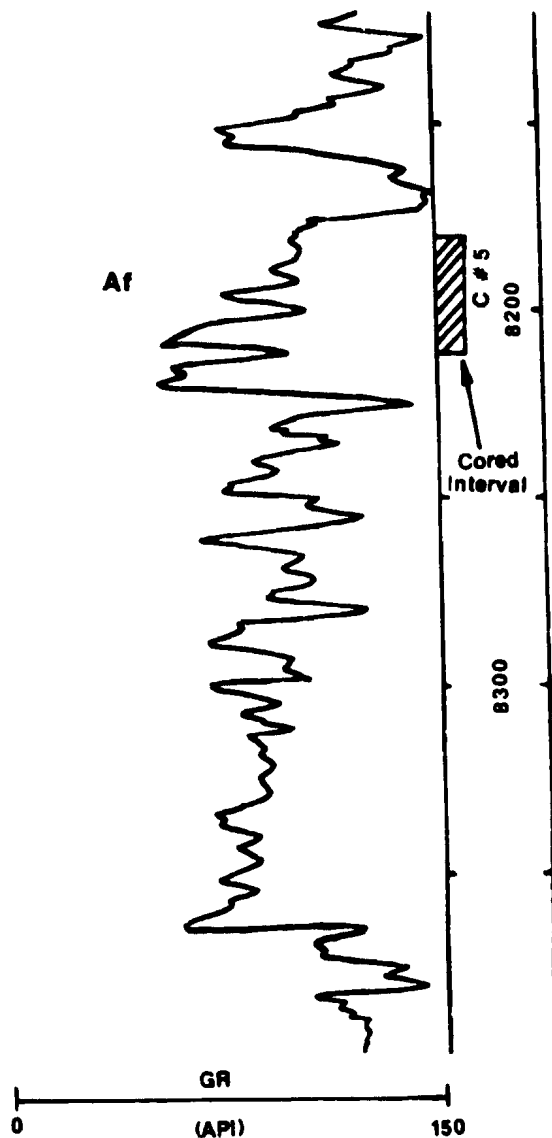
APPENDIX I

Figure App.I.23. Core Description (C#5) of Well C1-61,
Lower Acacus Formation, NC2 Concession,
Hamada Basin, NW Libya.
" Location of Well Shown in Figure.4 "

APPENDIX I

426

C1-61
K.B. 2131 FT



Gamma-Ray Log (GR) Signatures and Cored Interval (8180-8212ft) for Well C1-61, Lower Acacus Formation, NC2 Concession, Hamada Basin, NW Libya.

" Depth divisions are 50 ft (15.24m) apart "

APPENDIX I

Well C1-61

Formation Lower Acacus

Concession NC2
Hamada Basi, Libya

Core No. 5

Interval 8160-8212ft

Depth (ft)	T.S.	Gross Lithology	Grain Size						Sed. Structures and Accessories	Rock Description	Lithofacies	Oil Stain			Porosity			DST Intv.	DST Result
			dy	silt	vfs	fs	ms	cs				vcs	h	m	L	od	fr		
8180		[Sandstone pattern]							Horizontal even parallel laminae	SH, dk gy, occ. blk, fss, flky, mic, w/silty sd lenses at places, lam.	Lam. SH								
8190		[Sandstone pattern]							Bioturbation	SH, dk gy, subfss, biot.	Biot. SH								
8200	●	[Sandstone pattern]							Mud clasts	SS, lt gy f-vf, grd, ang-subang, pr. sort, w/mud clasts at places, Indist. Jam.	Indist. Jam f. grd SS								⊕
8210	●	[Sandstone pattern]							Mud clasts	SH, dk grn, occ. dk blk, v. biot. SS, lt gy, grnish gy, m. grd, frb, subang-rd, m-w sort, w/mud clasts, w/Indist. Jam.	Biot. SH Indist. Jam. m. grd SS								
8220		[No Recovery pattern]								No Recovery									
8230		[No Recovery pattern]																	

Gross Lithology

- [Sandstone pattern] Sandstone
- [Siltstone pattern] Siltstone
- [Shale pattern] Shale
- [No Recovery pattern] No Recovery

Sedimentary Structures

- [Horizontal lines] Horizontal even parallel laminae
- [Lenticular shape] Lenticular silty sand lenses
- [Wavy lines] Bioturbation

Accessories

- [Mud clast symbol] Mud clasts

DST Result

- [Water symbol] Water

APPENDIX I

Figure App.I.24. Core Photos (C#2-C#5) of Well C1-61,
Lower Acacus Formation, NC2 Concession,
Hamada Basin, NW Libya.

" Detailed Description of Lithofacies are
Included in Figures App.I.20-App.I.23 ".

APPENDIX I



C1-61,C#2

APPENDIX I



C1-61,C#2

APPENDIX I



C1-61,C#2

APPENDIX I



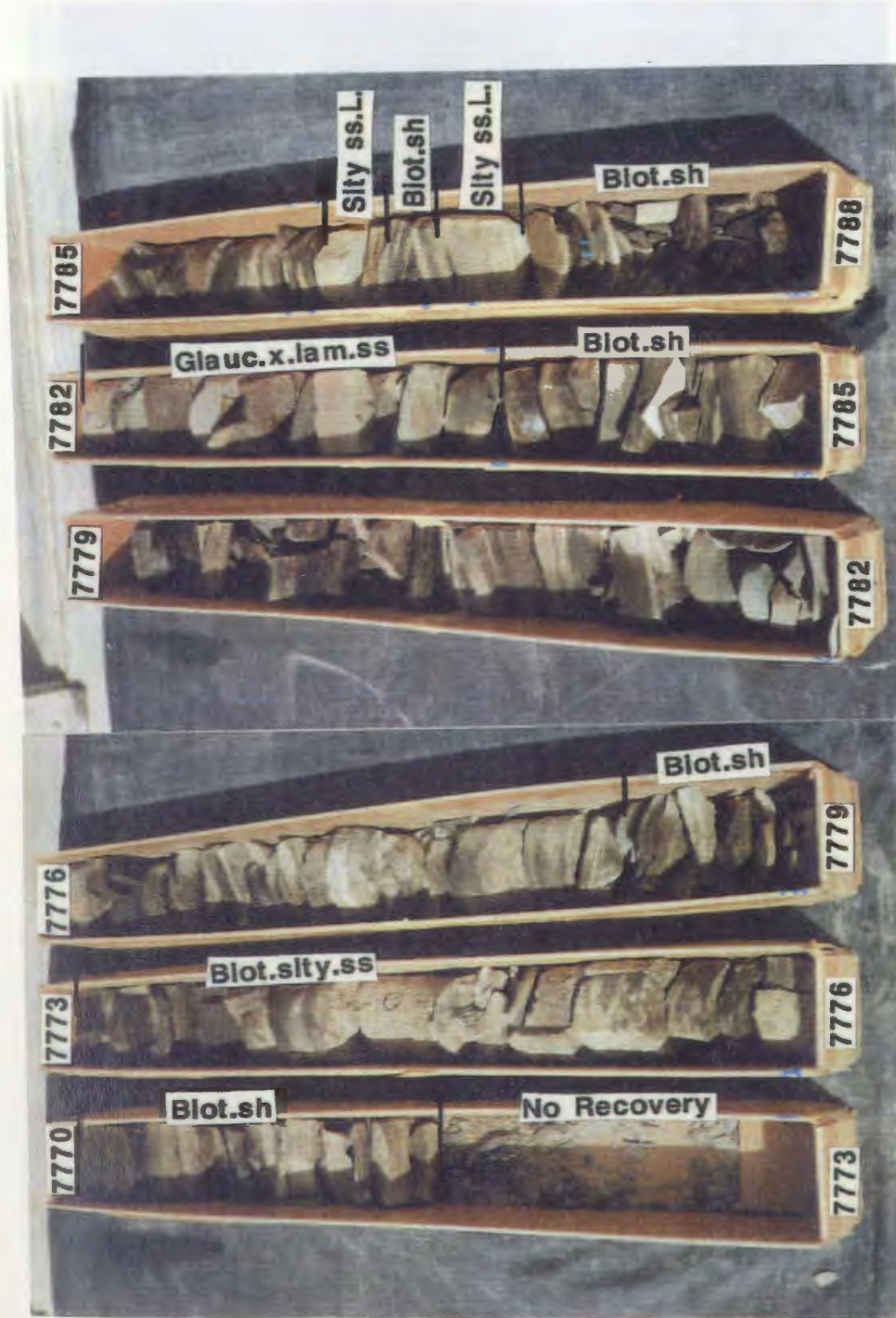
C1-61,C#3

APPENDIX I



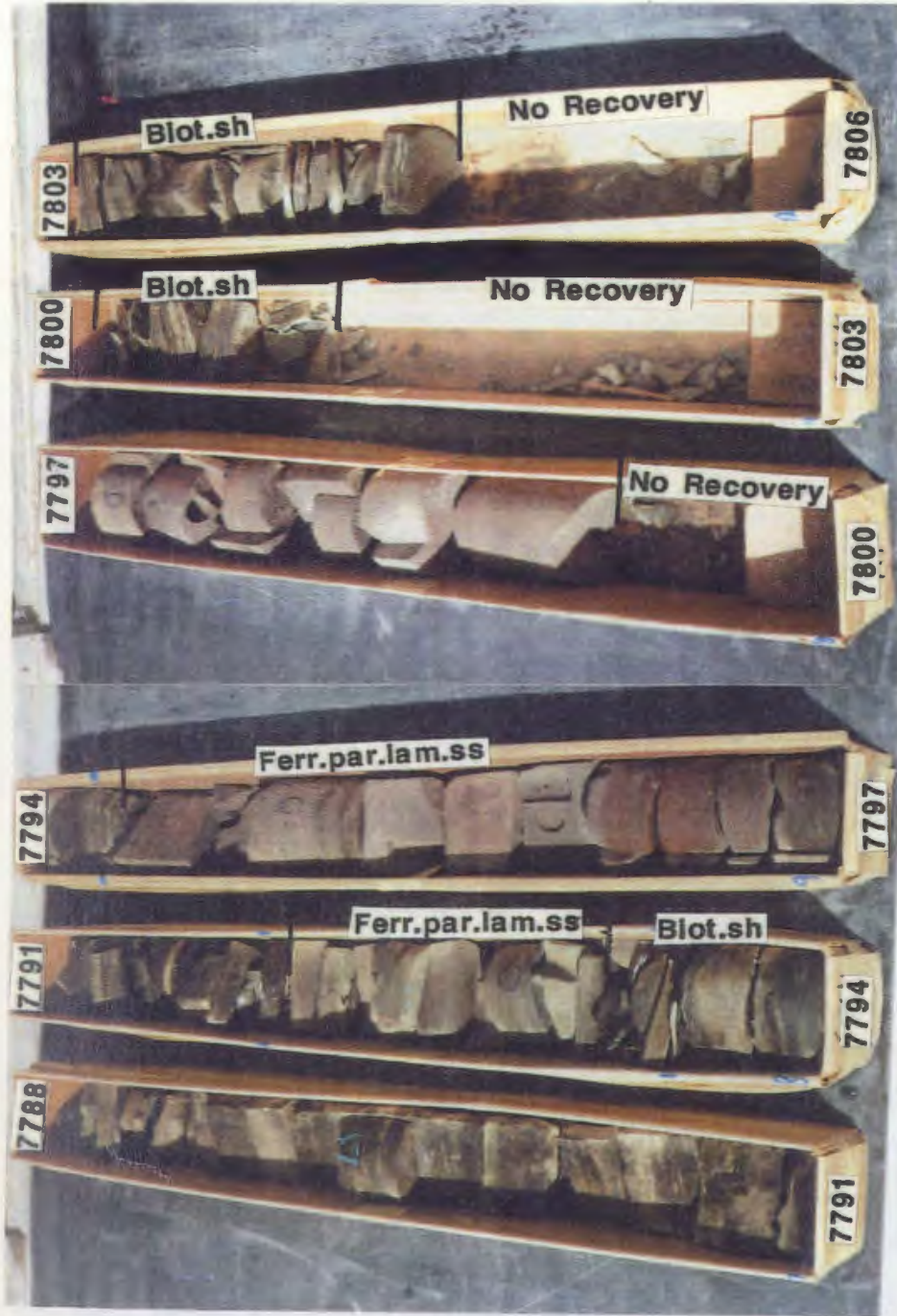
C1-61, C#3

APPENDIX I



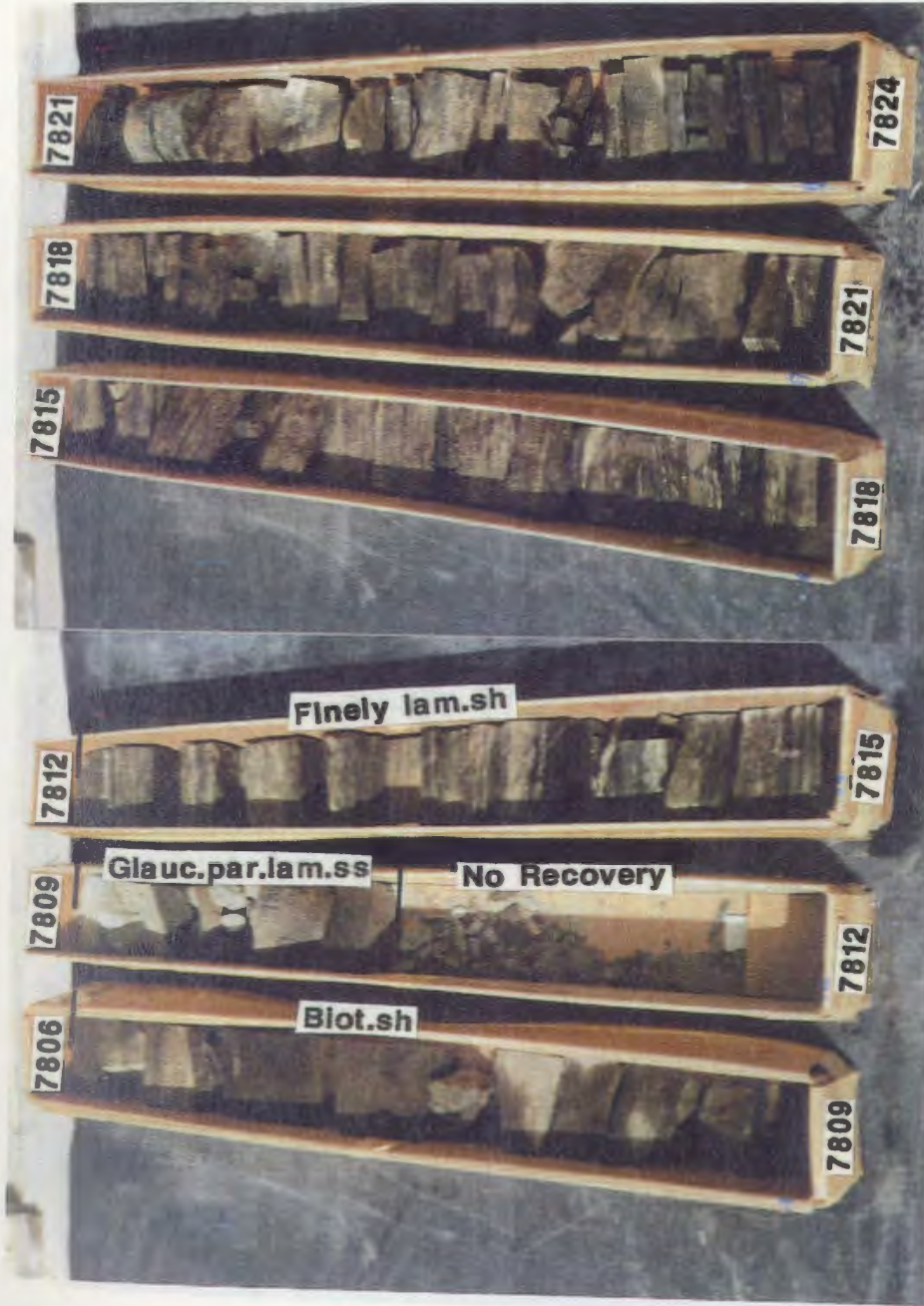
C1-61, C#4

APPENDIX I



C1-61, C#4

APPENDIX I



C1-61, C#4

APPENDIX I



C1-61,C#5

APPENDIX I



C1-61,C#5

APPENDIX I

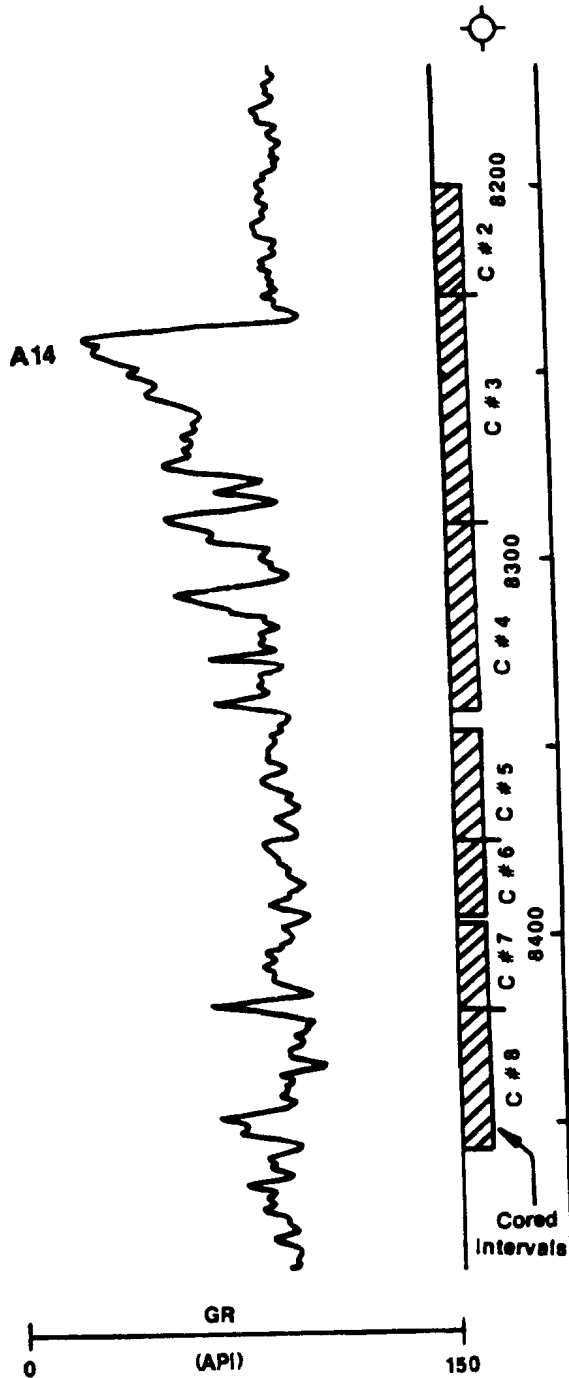
Figure App.I.25. Cores Description (C#2-C#8) of Well D1-61,
Lower Acacus Formation, NC2 Concession,
Hamada Basin, NW Libya.

" Location of Well Shown In Figure.4 ".

APPENDIX I

D1-61
K.B. 2078 FT

440



Gamma-Ray Log (GR) Signatures and Cored Intervals (8200-8230ft; 8230-8290ft; 8290-8340ft; 8345-8375ft; 8375-8395ft; 8397-8420ft; 8420-8456ft) for Well D1-61, Lower Acacus Formation, NC2 Concession, Hamada Basin, NW Libya.

" Depth divisions are 50 ft (15.24m) apart "

OBB-91

APPENDIX I

441

Well D1-61

Formation Lower Acacus

Concession NC2

Core No. 2

Interval 8200-8230ft

Hamada Basin, Libya

Depth (ft)	T.S.	Gross Lithology	Grain Size						Sed. Structures and Accessories	Rock Description	Lithofacies	Oil Stain			Porosity			DST Intv.	DST Result
			dy	sit	v/s	f/s	m/s	cs				vc/s	h	m	L	gd	fr		
8200		[Shale symbol]							=	SH,dk gy,dk grn,fiss,flky. v.lam.	Finely lam.SH								
8210		[Shale symbol]						=											
8220		[Shale symbol]						=											
8230		[Shale symbol]						=											
8240		[Shale symbol]																	
8250		[Shale symbol]																	

Gross Lithology

Sedimentary Structures

Accessories

DST Result

[Shale symbol] Shale

= Horizontal even parallel laminae

APPENDIX I

Well D1-61

Formation Lower Acacus

Concession NC2

Core No. 3

Interval 8230-8290ft

Hamada Basin, Libya

Depth (ft)	T.S.	Gross Lithology	Grain Size							Sed. Structures and Accessories	Rock Description	Lithofacies	Oil Stain			Porosity			DST Intv.	DST Result
			gy	silt	v/s	fs	ms	cs	vcs				h	m	L	gd	fr	pr		
8230									// ◆	SS, lt grn gy, f-m grd, frb, subang-rd, w. sort, w/micro x-lam. and mud clasts at the top, w/par.lam. at the base.	Low angle x-lam. SS								⊕	
8245									//	No Recovery SLTY SS, dk gy, silty, biot.	Biot SLTY SS									
8260									// S	No Recovery SLTY SS, a/a (9244-9252ft) w/cont.stru.	Biot. SLTY SS									
8275									// S	No Recovery SLTY SS, gy, dk gy, biot, w/cont.stru.	Biot. SLTY SS									
8290									//	No Recovery SH, dk gy, dk grn, fiss, w/some lam. at the top, v. Biot. at the base	Biot. SH									
8305																				

Gross Lithology

- Sandstone
- Siltstone
- Shale
- No Recovery

Sedimentary Structures

- Low angle cross laminations
- Horizontal even parallel laminae
- Contorted structure
- Bioturbation

Accessories

- Mud clasts

DST Result

- Water

APPENDIX I

443

Well D1-61

Formation Lower Acacus

Concession NC2

Core No. 4

Interval 8290-8340ft

Hamada Basin, Libya

Depth (ft)	T.S.	Gross Lithology	Grain Size							Sed. Structures and Accessories	Rock Description	Lithofacies	Oil Stain			Porosity			DST Intv.	DST Result
			dy	sit	vfs	fs	ms	cs	vcs				h	m	L	gd	fr	pr		
8290										==	SS, lt gy, vf. grd, frb, subang-rd, m. sort, lam., calc.	ParJam.SS								
										ss	SH, dk gy, grn, occ. blk, subflss, v. blot, mic. in pts.	Blot.SH								
8300										ss										
										ss										
8310										ss										
										ss	SLTY SS, tan, crm, lt gy, silty, blot, w/alternations of Sh. layers at (8316-8317) calc, w/wavy lam. at the base.	Blot SLTY SS								
8320										~										
										ss	SH, a/a (8292-8311ft) w/lent. silty sd lenses at (8330ft)	Blot.SH								
8330										◇										
										ss										
8340											No Recovery									

Gross Lithology

Sedimentary Structures

Accessories

DST Result

- Sandstone
- Siltstone
- Shale
- No Recovery

- Horizontal even parallel laminae
- Wavy laminations
- Lenticular silty sand lenses
- Bioturbation

APPENDIX I

Well D1-61

Formation Lower Acacus

Concession NC2
Hamada Basin, Libya

Core No. 5 & 6

Interval 8345-8375ft
8375-8395ft

Depth (ft)	T.S.	Gross Lithology	Grain Size							Sed. Structures and Accessories	Rock Description	Lithofacies	Oil Stain			Porosity			DST Intv.	DST Result
			cl	sl	vs	fs	ms	cs	vs				h	m	L	gd	lr	pr		
8340																				
8350									ss	SH, dk gy, dk grn, subfms, mic, blot, w/lent. slty sd lenses at places.	Biot. SH									
8360									◇	No Recovery										
8370									=	SH, dk gy, dk blk, fms, flky, occ. mic, w/lent. slty sd lenses, non calc, v. lam.	Finely lam. SH									
8380									◇	No Recovery										
8390									ss	SH, dk gy, dk grn, subfms, occ, mic, v. biot.	Biot. SH									
									ss	SLTY SS, lt gy, dk gy, slty, biot.	Biot SLTY SS									

Gross Lithology

- Siltstone
- Shale
- No Recovery

Sedimentary Structures

- Horizontal even parallel laminae
- Lenticular silty sand lenses
- Bioturbation

Accessories

DST Result

APPENDIX I

Well D1-61

Formation Lower Acacus

Concession NC2
Hamada Basin, Libya

Core No. 7

Interval 8397-8420ft

Depth (ft)	T.S.	Gross Lithology	Grain Size						Sed. Structures and Accessories	Rock Description	Lithofacies	Oil Stain			Porosity			DST Intv.	DST Result
			dy	ait	v/s	fs	ms	cs				vcs	h	m	L	gd	fr		
8390																			
8400		[Shale symbol]						=	SH, dk gy, dk grn, occ. blk, fiss, flky, mic, v. lam., non calc.	Finely lam. SH									
8410		[Shale symbol]						=											
8420		[No Recovery symbol]						ss	No Recovery SLTY SS, dk gy, slty, blot, occ. mic. No Recovery	Blot. SLTY SS				[Porosity symbol]					
8430																			
8440																			

Gross Lithology

- Siltstone
- Shale
- No Recovery

Sedimentary Structures

- Horizontal even parallel laminae
- Bioturbation

Accessories

DST Result

APPENDIX I

Well D1-61

Formation Lower Acacus

Concession NC2
Hamada Basin, Libya

Core No. 8

Interval 8420-8456ft

Depth (ft)	T.S.	Gross Lithology	Grain Size							Sed. Structures and Accessories	Rock Description	Lithofacies	Oil Stain			Porosity			DST Intv.	DST Result
			dy	sit	v/s	f/s	ms	cs	vcs				h	m	L	gd	fr	pr		
8420		[Lithology patterns: Sandstone, Siltstone, Shale, No Recovery]	[Grain Size columns]							~	SS, lt gy, crm, f-grd, subang-subrd, m. sort, w/ wavy lam., calc.	Wavy lam. SS								
	=									SH, dk gy, dk grn, flss, mic. in pts, v. lam.	Lam. SH									
	~ G									SS, lt gy, wtish gy, vf. grd, subang-subrd, pr-m sort, w/ wavy lam., tr. of glauc., calc.	Wavy lam. Glauc. SS									
8430										=	SH, a/a (8421-8424ft)	Lam. SH								
	ss									SH, dk gy, suf. flss, biot.	Biot SH									
8440										X	No Recovery									
		=	SH, dk gy, dk grn, flss, flky, mic. in pts, w/ lenty w/ lent. slty ad lenses, lam., w/ some cont. lam. at (8452ft).	Finely lam. SH																
8450		~	SLTY SS, dk gy, v. slty, biot.	Biot. SLTY SS																
		ss	SH, a/a (8435-8438ft).	Biot. SH																
8460																				
8470																				

Gross Lithology

- Sandstone
- Siltstone
- Shale
- No Recovery

Sedimentary Structures

- Horizontal even parallel laminae
- Wavy laminations
- Lenticular silty sand lenses
- Contorted structures
- Bioturbation

Accessories

- G Glaucanite

DST Result

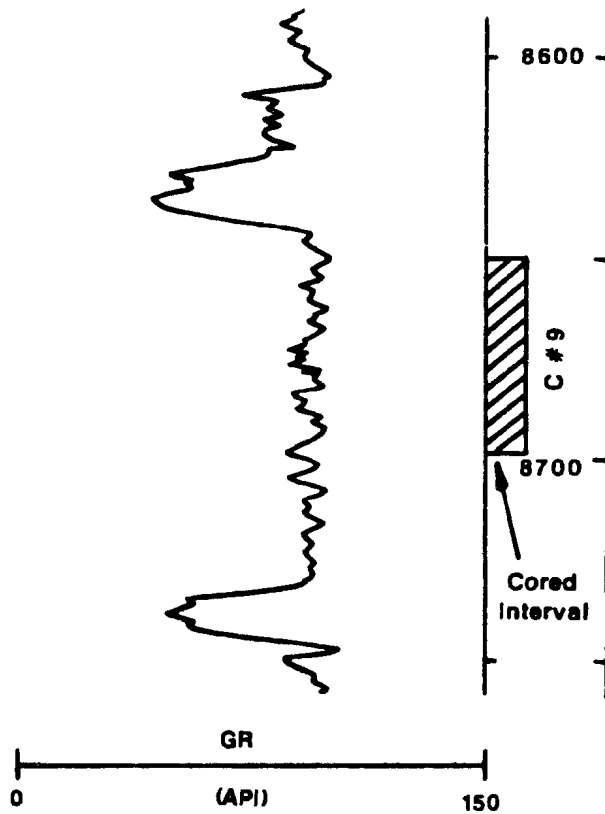
APPENDIX I

Figure App.I.26. Core Description (C#9) of Well D1-61,
Lower Acacus Formation, NC2 Concession,
Hamada Basin, NW Libya.

" Location of Well Shown in Figure.4 "

D1-61

K.B. 2078 FT



Gamma-Ray Log (GR) Signatures and Cored Interval (8650-8698ft) for Well D1-61, Lower Acacus Formation, NC2 Concession, Hamada Basin, NW Libya.

" Depth divisions are 50 ft (15.24m) apart "

APPENDIX I

449

Well D1-61

Formation Lower Acacus

Concession NC2

Core No. 9

Interval 8650-8698ft

Hamada Basin, Libya

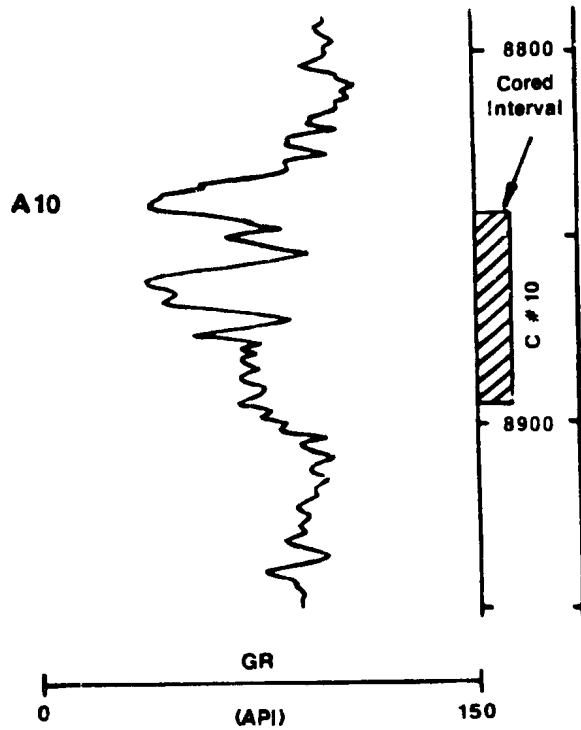
Depth (ft)	T.S.	Gross Lithology	Grain Size						Sed. Structures and Accessories	Rock Description	Lithofacies	Oil Stain			Porosity			DST Intv.	DST Result
			dy	sit	vis	fs	ms	cs				vcs	h	m	L	gd	fr		
8650									=	SH, dk gy, dk grn, occ. blk, flss, flky, comp., w/lent. silty sd lenses at places, occ. mic., v.lam, non calc.	Finely lam. SH								
8660									◊										▨
8670									=	SH, dk gy, occ. dk grn, subflss, v. blot, w/cont. a. tru. at (8692ft).	Blot. SH								
8680									∞										▨
8690									∞										
8700									∞										
									∞										
									∞										
									∞										
									∞										
									∞										
									∞										
									∞										
									∞										
									∞										
									∞										
									∞										
									∞										
									∞										
									∞										
									∞										
									∞										
									∞										
									∞										
									∞										
									∞										
									∞										
									∞										
									∞										
									∞										
									∞										
									∞										
									∞										
									∞										
									∞										
									∞										
									∞										
									∞										
									∞										
									∞										
									∞										
									∞										
									∞										
									∞										
									∞										
									∞										
									∞										
									∞										
									∞										
									∞										
									∞										
									∞										
									∞										
									∞										
									∞										
									∞										
									∞										
									∞										
									∞										
									∞										
									∞										
									∞										
									∞										
									∞										
									∞										
									∞										
									∞										
									∞										
									∞										
									∞										
									∞										
									∞										
									∞										
									∞										
									∞										
									∞										
									∞										
									∞										
									∞										
									∞										
									∞										
									∞										
									∞										
									∞										
									∞										
									∞										
									∞										
									∞										
									∞										
									∞										
									∞										
									∞										
									∞										
									∞										
									∞										
									∞										
									∞										
									∞										
									∞										
									∞										
									∞										
									∞										

APPENDIX I

Figure App.I.27. Core Description (C#10) of Well D1-61,
Lower Acacus Formation, NC2 Concession,
Hamada Basin, NW Libya.

" Location of Well Shown in Figure.4 ".

D1-61
K.B. 2078 FT



Gamma-Ray Log (GR) Signatures and Cored Interval (8845-8895ft) for Well D1-61, Lower Acacus Formation, NC2 Concession, Hamada Basin, NW Libya.

" Depth divisions are 50 ft (15.24m) apart "

APPENDIX I

Well D1-61

Formation Lower Acacus

Concession NC2

Core No. 10

Interval 8845-8895ft

Hamada Basin, Libya

Depth (ft)	T.S.	Gross Lithology	Grain Size						Sed. Structures and Accessories	Rock Description	Lithofacies	Oil Stain			Porosity			DST Intv.	DST Result
			dy	sl	vs	fs	ms	cs				vcs	h	m	L	gd	fr		
8840																			
8850									SS,lt gy,wtish gy,f-m.grd, subang-rd,occ.w.rd,m-w.sort,w/micro x-lam.at r at the top,w/parJam.at the base, occ.w/mud clasts,calc in pts.	Low angle x-lam.ss									
8860								No Recovery	No Recovery										
8870									SH,dk gy,occ.dk grn,subfiss, biot.	Biot.SH									
8880									SS,lt gy,wtish gy,f-m grd, subang-rd,w.sort,w/wavy lam,and mud dasts at the top, parJam.near the base, slty at the base.	Wavy lam. SS									
8890									SS,a/a (8866-8872ft),f-grd, parJam.	ParJam. SS									
									SH,dk gy,fiss,mic,vJam,occ. biot.at the base.	Lam.SH									
									SS,lt gy,wtish gy,vf.grd, subang-subrd,pr.sort,lam, calc.	ParJam. SS									
								No Recovery	No Recovery										

Gross Lithology

- Sandstone
- Siltstone
- Shale
- No Recovery

Sedimentary Structures

- Low angle cross laminations
- Horizontal even parallel laminae
- Wavy laminations
- Bioturbation

Accessories

- Mud clasts

DST Result

APPENDIX I

Figure App.I.28. Core Photos (C#2-C#10) of Well D1-61,
Lower Acacus Formation, NC2 Concession,
Hamada Basin, NW Libya.

" Detailed Descriptions of Lithifacies are
Included in Figures App.I.25-App.I.27 ".

APPENDIX I



D1-61,C#2

APPENDIX I



D1-61,C#2

APPENDIX I



D1-61,C#3

APPENDIX I



D1-61,C#3

APPENDIX I



D1-61,C#3

APPENDIX I



D1-61, C#4

APPENDIX I



D1-61,C#4

APPENDIX I



D1-61,C#4

APPENDIX I



D1-61,C#5

APPENDIX I



D1-61, C#5

APPENDIX I



D1-61,C#6

APPENDIX I



D1-61,C#7



D1-61,C#8

APPENDIX I



D1-61,C#8

APPENDIX I



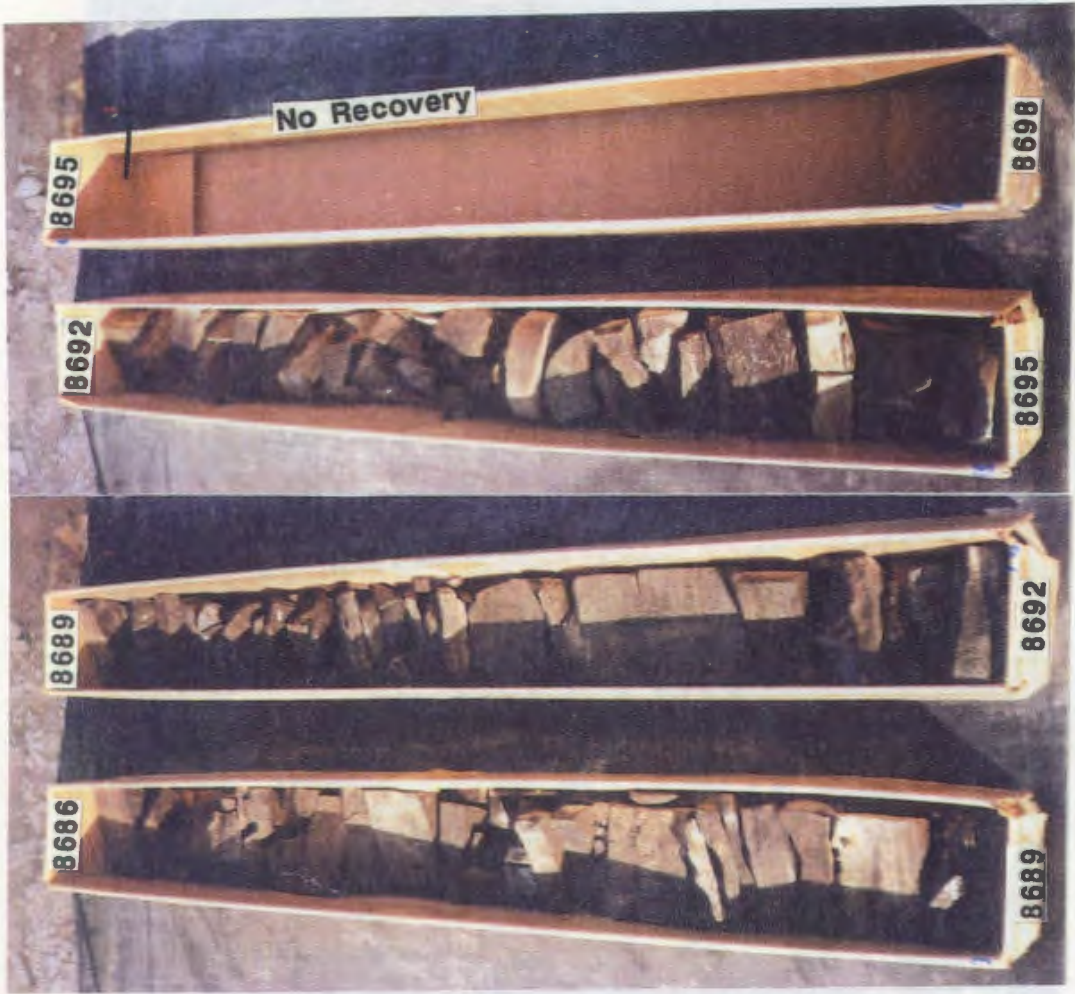
D1-61, C#9

APPENDIX I



D1-61, C#9

APPENDIX I



D1-61, C#9

APPENDIX I



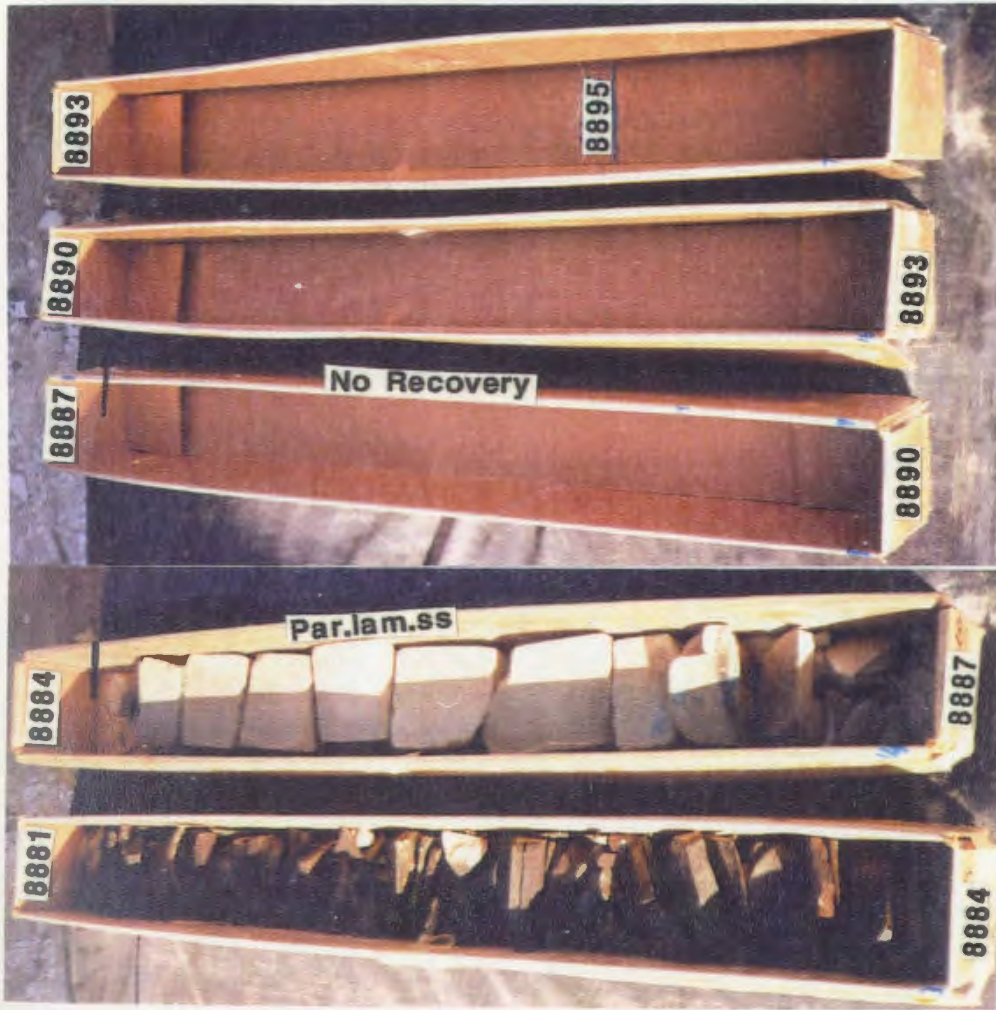
D1-61, C#10

APPENDIX I



D1-61, C#10

APPENDIX I



D1-61,C#10

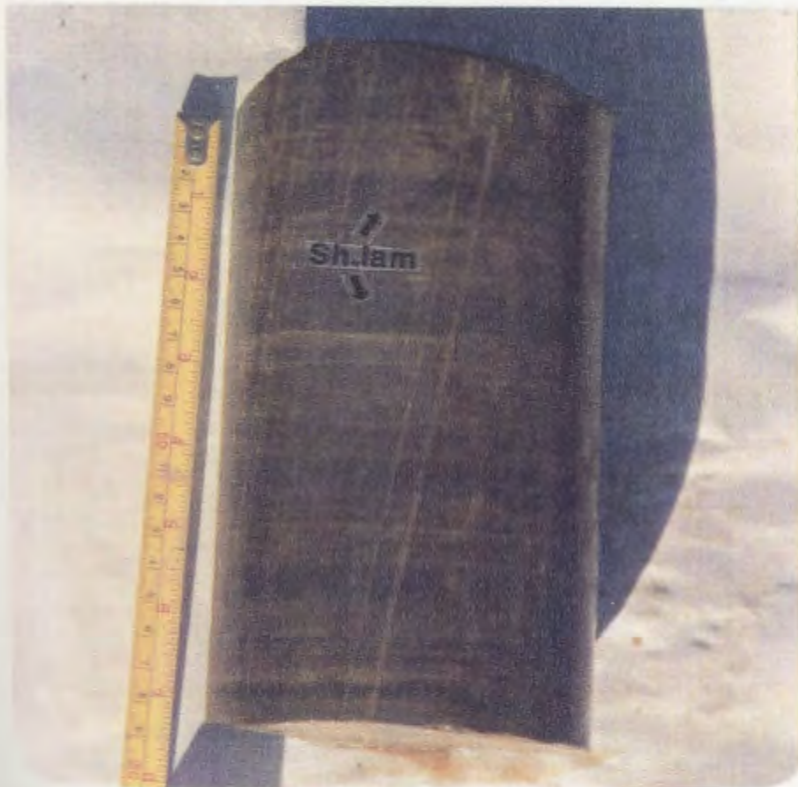
APPENDIX II

**Cores Illustrating Sedimentary Structures of
the Lower Acacus Formation, NC2 Concession,
Hamada Basin, NW Libya.**

- A-** Dark gray, greenish black shale (offshore-marine shale lithofacies), occasionally micaceous with rippled lenticular silty sand lenses (Silty.sd.L). Well A1-NC2 @ 7803ft (2379m).
- B-** Finely laminated dark shale, the laminae (Sh.lam) are centimeter thick. Well C1-NC2 @ 9679ft (2951m).



A



B

APPENDIX II

C-D. Soft sediment deformation (load features) (Lf) are locally preserved in the offshore-marine shale. Well A1-NC2 @ 7790ft (2375m), well C1-NC2 @ 9721ft (2964m) respectively.



C



D

APPENDIX II

- E-** Highly bioturbated (Biot) dark marine shale, indicating relatively slow depositional rate. Well A1-NC2 @ 7802ft (2379m).
- F-** Dark gray, greenish black shale, characterizes the offshore-marine lithofacies, with the lack of sedimentary structures. Well E1-NC2 @ 9141ft (2787m).



E



F

APPENDIX II

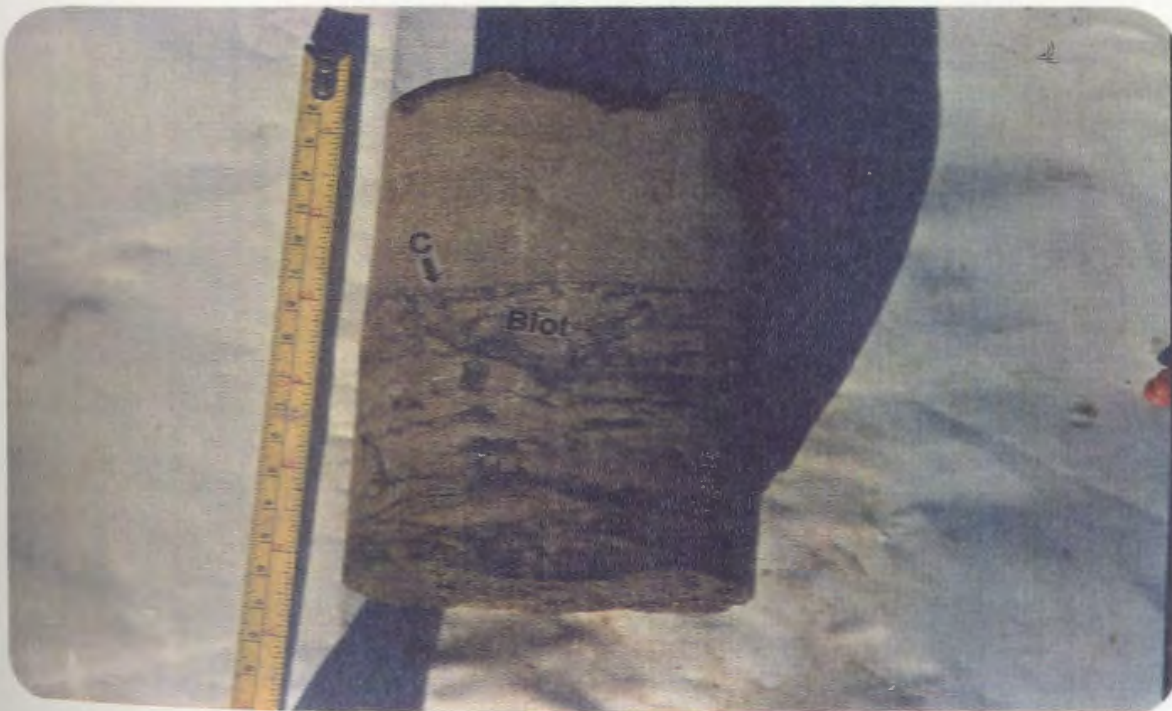
G- Bioturbated (Biot) and burrowed (Burr) silty sandstone (distal delta front lithofacies), with very distorted structures.

Well E1-NC2 @ 9515ft (2901m).

H- Bioturbated (Biot) silty sandstone with generally gradational contact (C) with the upper fine-medium grained sandstone (f-m. sst). Well C1-NC2 @ 9648ft (2941m).



G



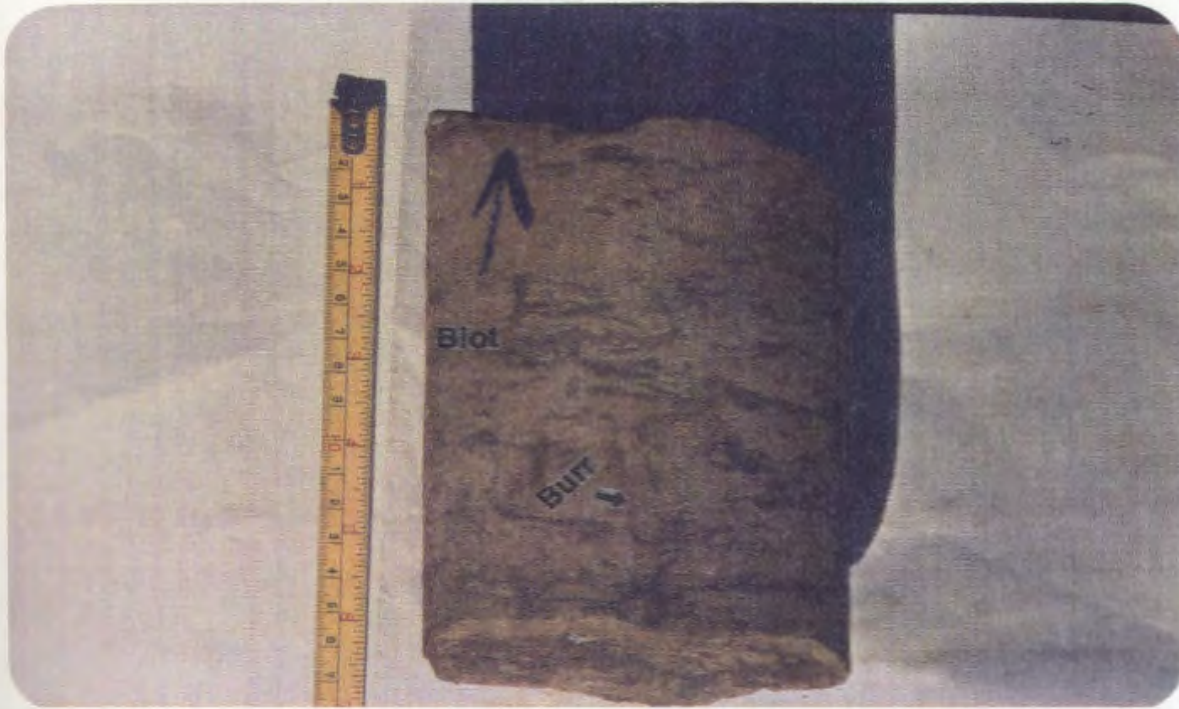
H

APPENDIX II

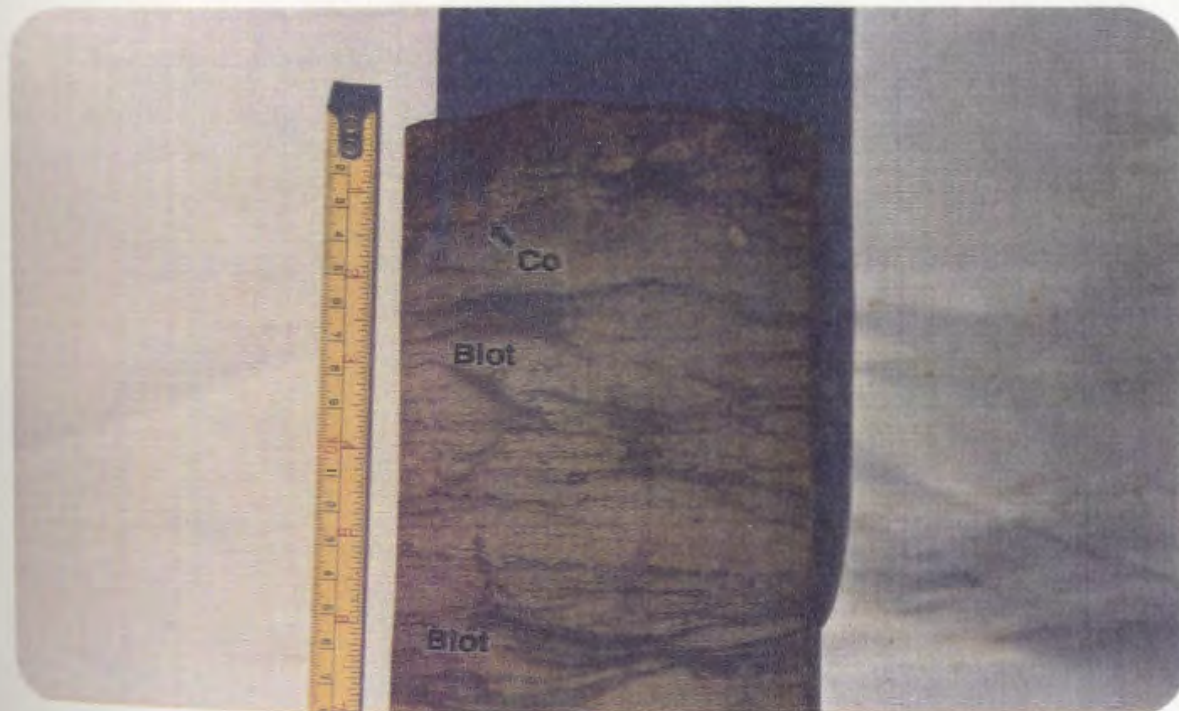
I- Very intensive bioturbated (Biot) and burrowed (Burr) silty sandstone (of marginal distal delta front lithofacies).

Well A1-NC2 @ 7826.5ft (2386m).

J- Slabbed bioturbated (Biot) silty sandstone, showing gradational contact(Co) with the upper hydrocarbon bearing, fine-medium grained sandstone (H,f-m sst). Note, the very distorted structures due to bioturbation. Well A1-NC2 @ 7823.5ft (2385m)



I



J

APPENDIX II

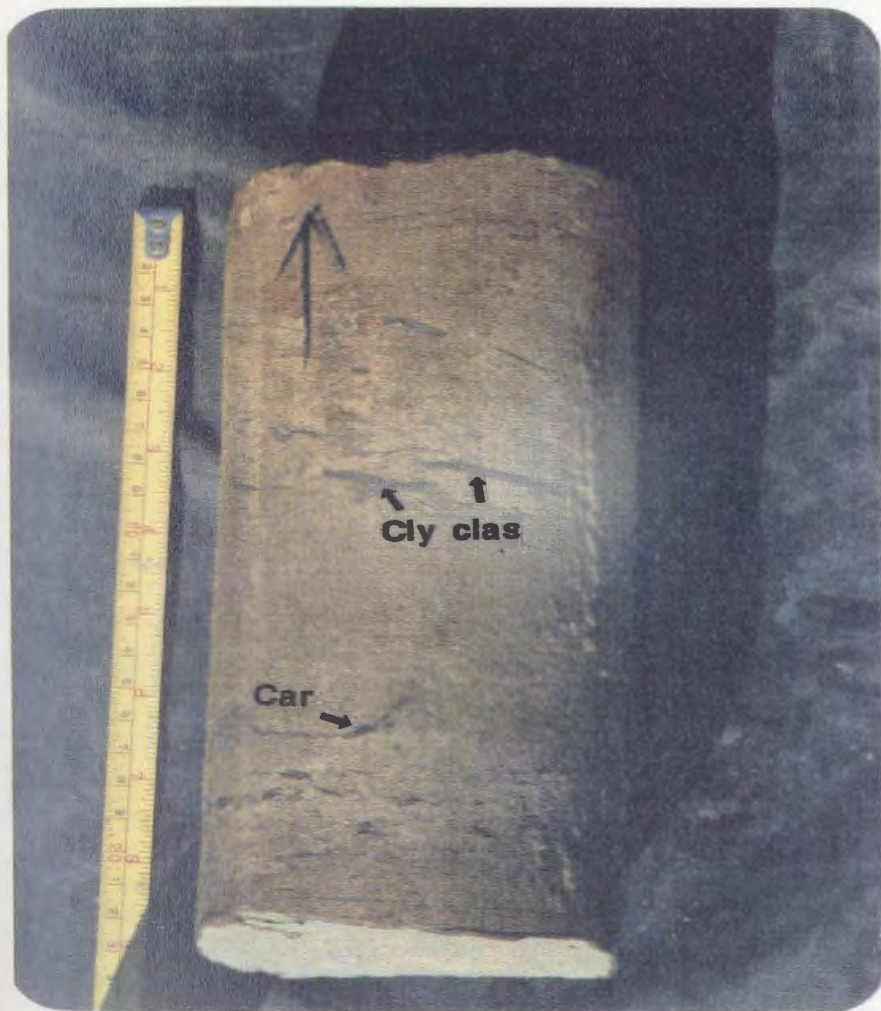
K- Fine-medium grained sandstone (proximal delta front lithofacies), with carbonaceous debris (Car), clay clasts (Cly clas).

Well C1-NC2 @ 9717ft (2962m).

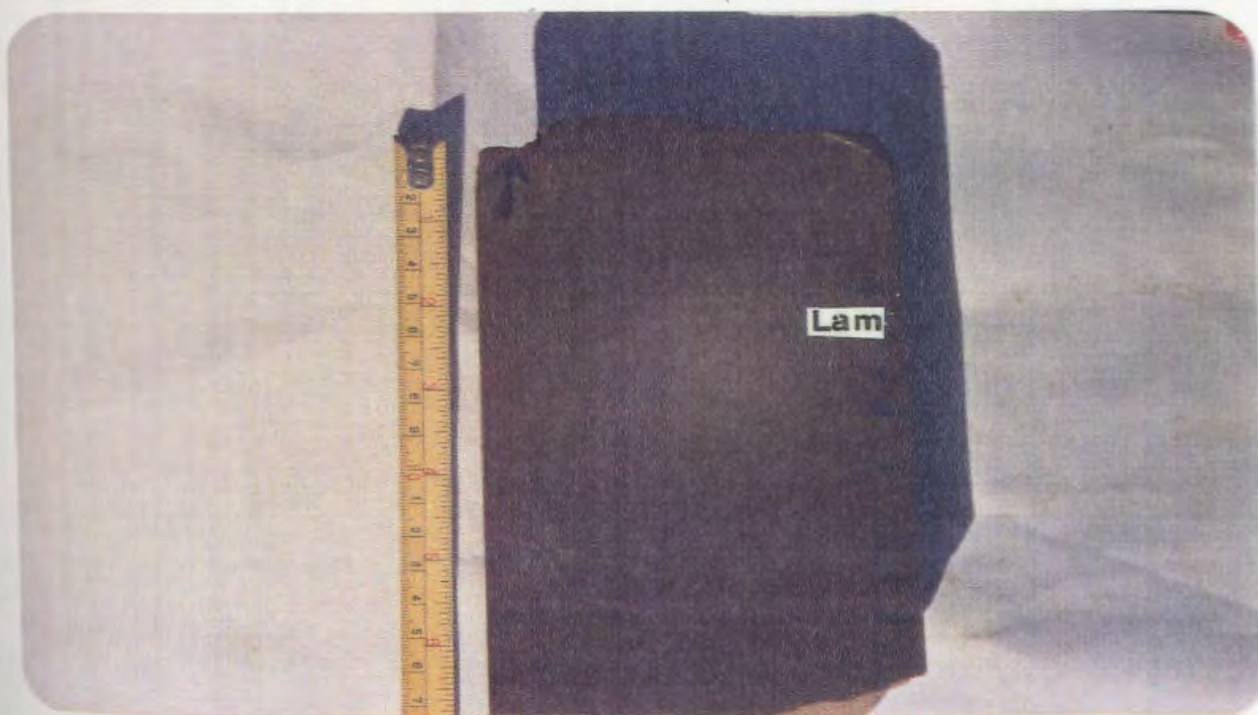
L- Slabbed core of fine-medium grained sandstone with horizontal to indistinctive lamination (Lam). Well E1-NC2 @ 9139ft (2786m).

Note: Oil stained sandstone.

K



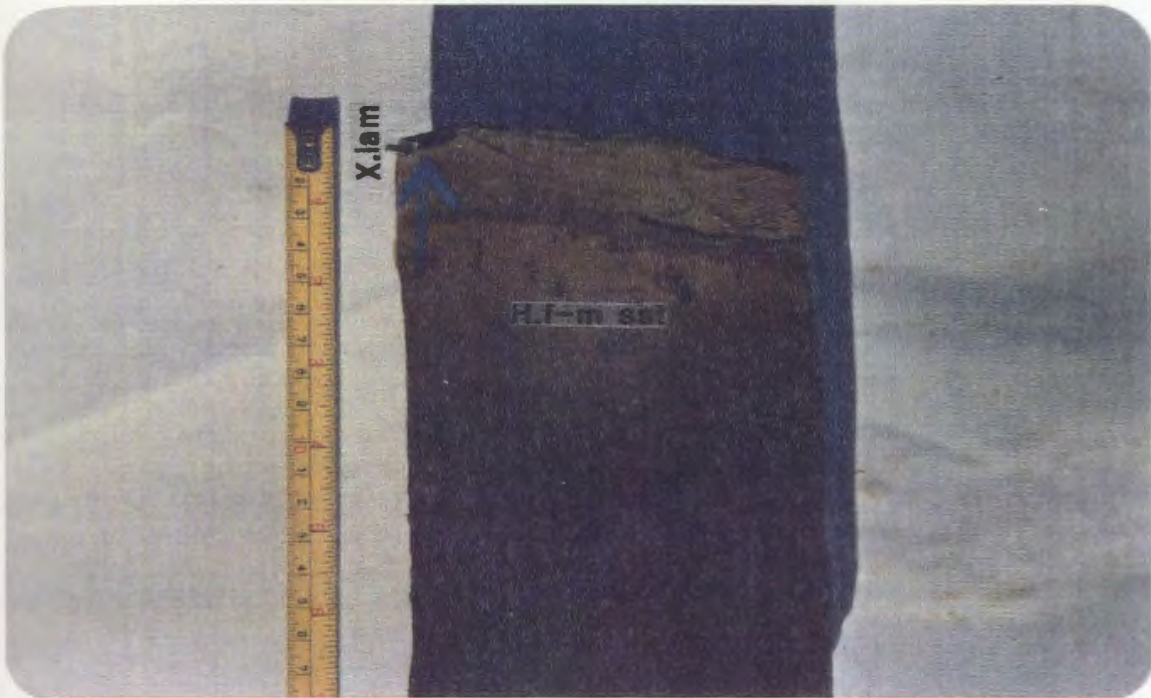
L



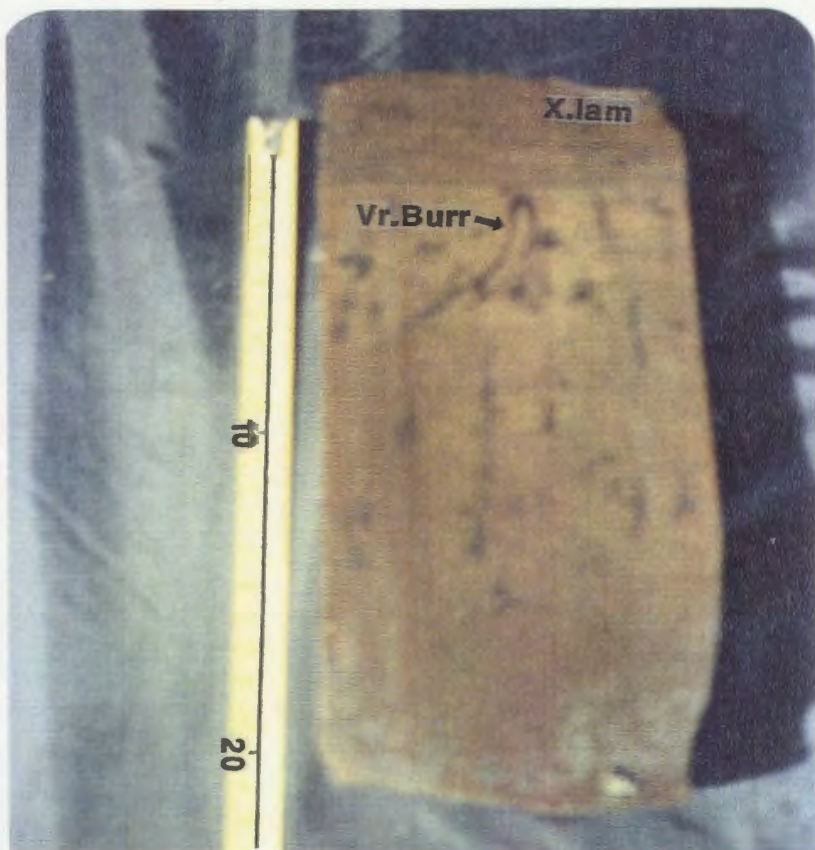
APPENDIX II

M- Slabbed hydrocarbon bearing, fine-medium grained sandstone (H,f-m sst), with low angle cross laminations (X.lam) at top of the unit, clay clasts (Cly clas), with some vertical burrows (Burr) may be seen in some places. Well E1-NC2 @ 9105ft (2776m). (sample from the oil column).

N- Slabbed core section in the fine-medium grained sandstone lithofacies (proximal delta front lithofacies), showing vertical burrows (Vr.Burr) (which may be skolithos trace fossils) indicating high energy environment. Note the cross lamination (X.lam) at top of the unit. Well E1-NC2 @ 9125ft (2725m).



M

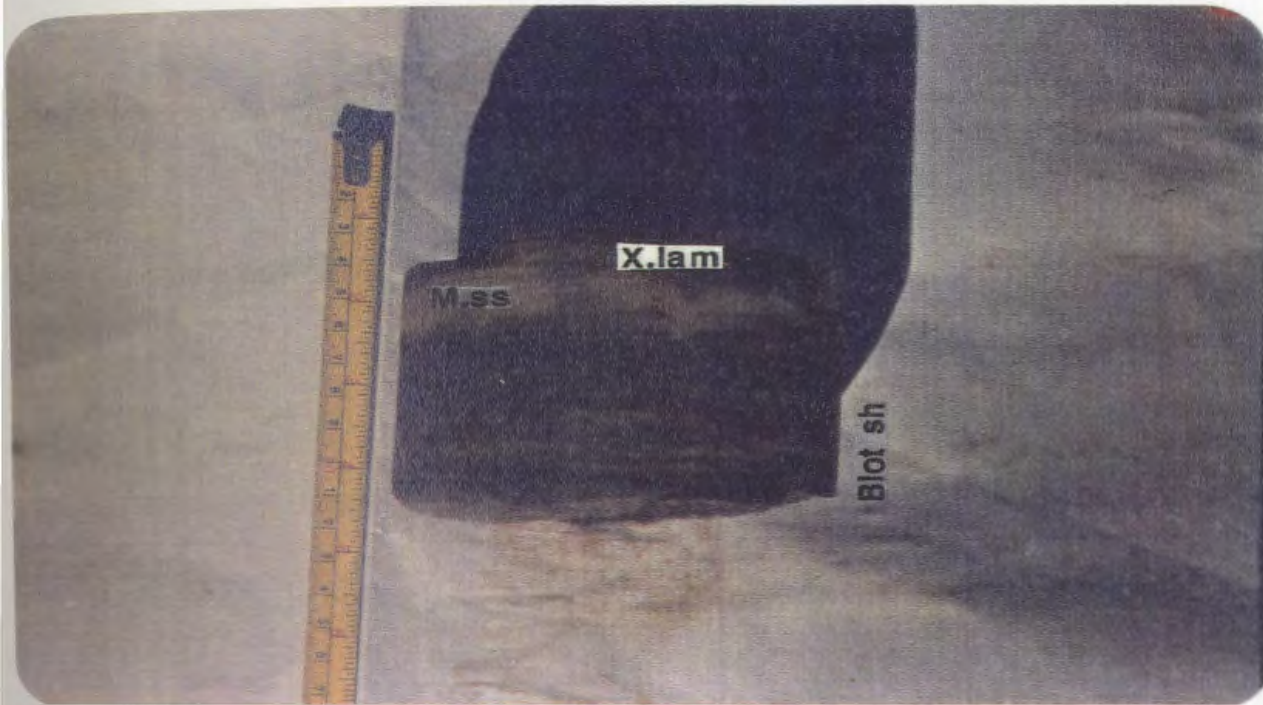


N

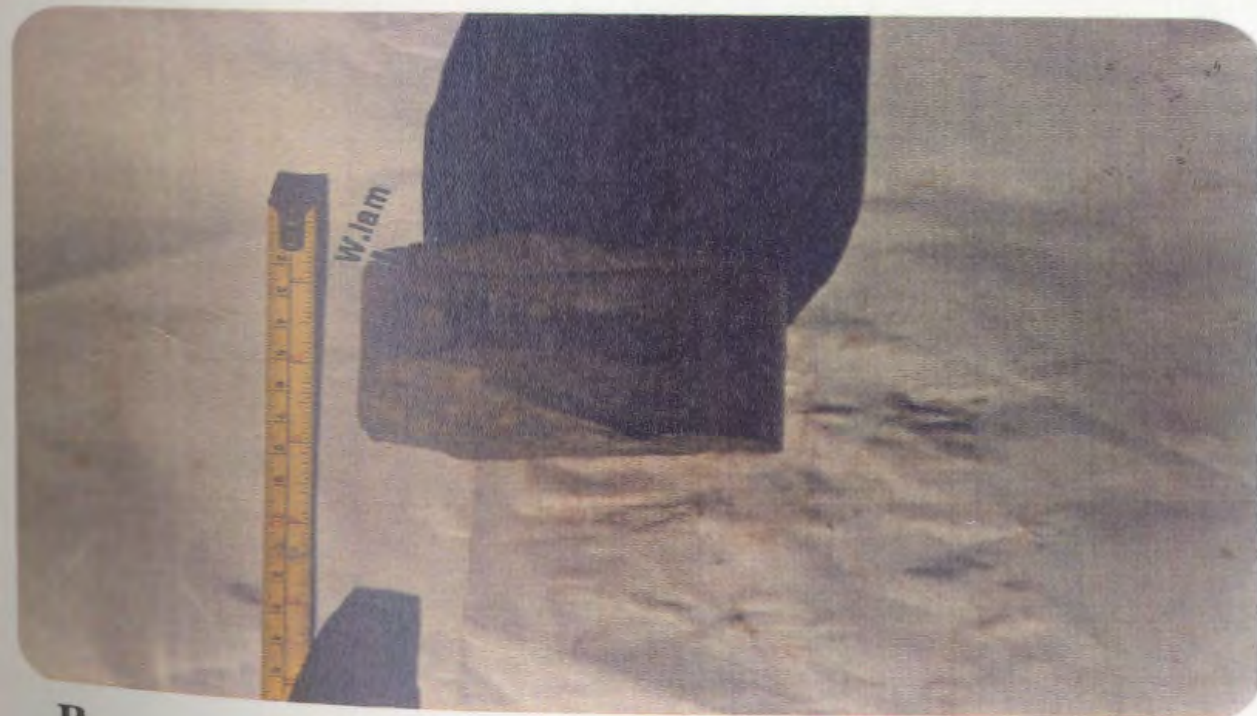
APPENDIX II

O- Marine sandstone lenses (M.ss) of destructional origin enclosed within the bioturbated marine shale (Biot.sh) (thin ranging from 1cm-1.5cm in this core). Well E1-NC2 @ 9132ft (2784m).

P- Marine sandstone with wavy laminations (W.lam), low angle cross lamnations (X.lam) may be seen, rarely with bioturbation. WellC1-NC2 @ 9670ft (2948m).



O

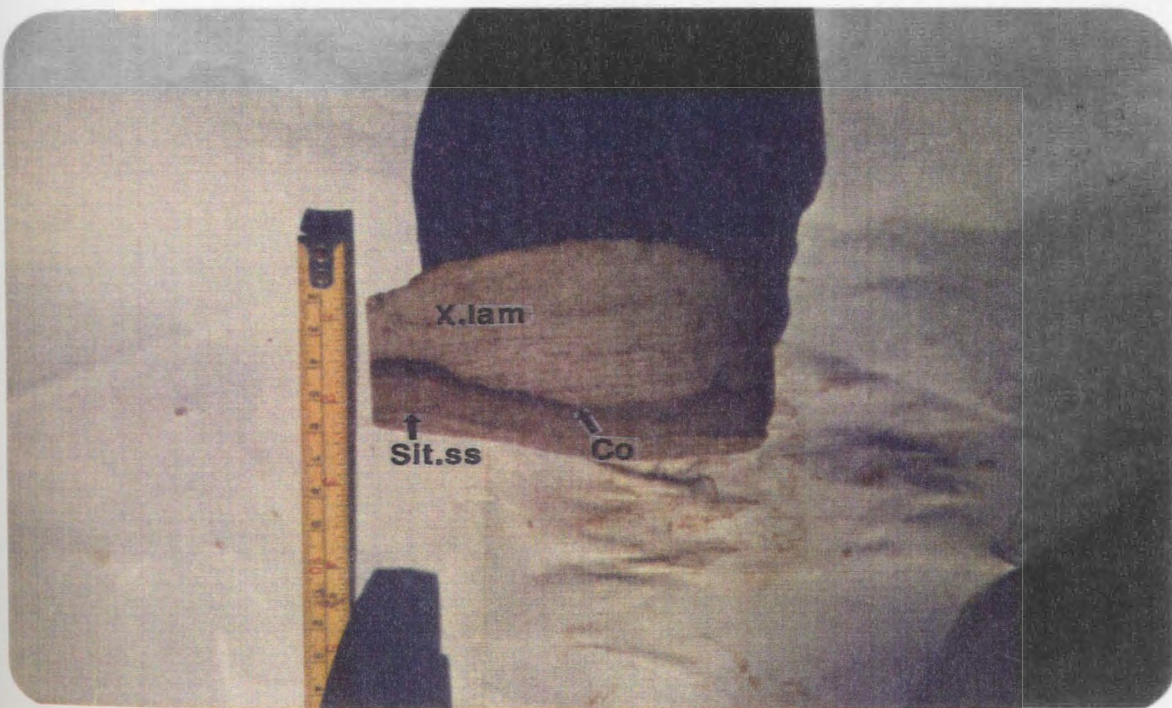


P

APPENDIX II

Q- Very fine-fine grained , glauconitic marine sandstone (M.sst), with some cross laminations (X.lam), and showing sharp contact (Co) with underlying very silty sandstone unit (Silty.ss).

Well Q1-23 @ 8464ft (2580m).



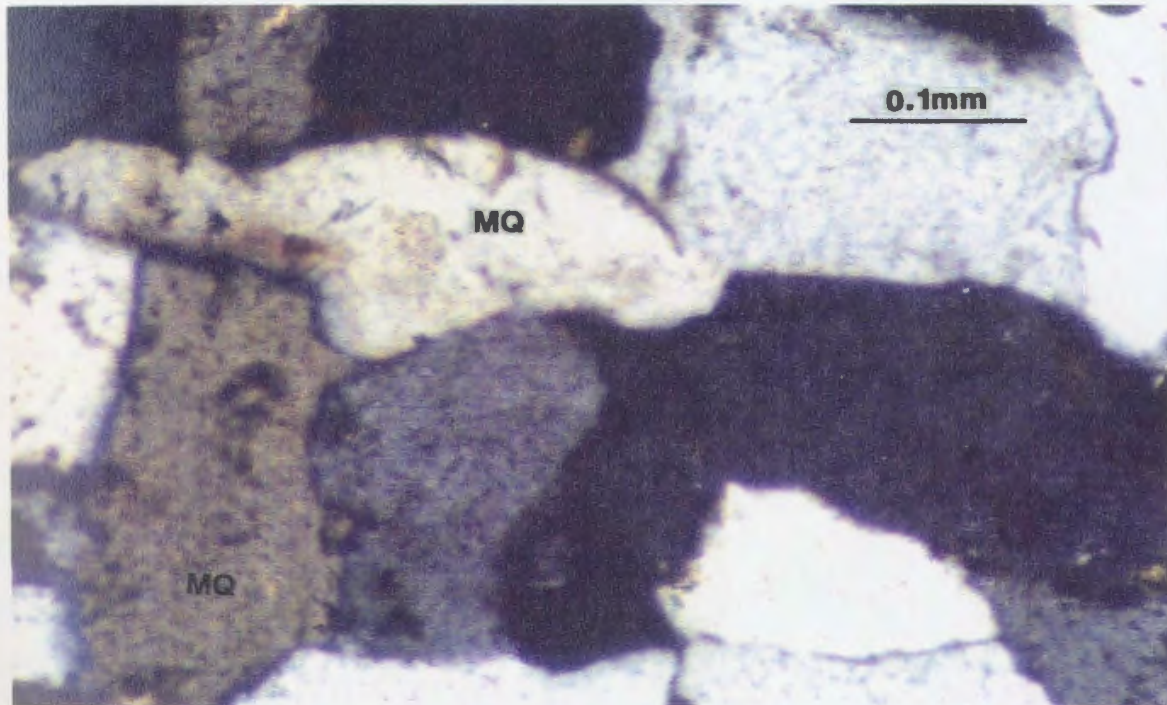
Q

APPENDIX III

**Thin-Section-Lithofacies
of the Lower Acacus Formation,
NC2 Concession, Hamada Basin, NW Libya.**

A- Fine-medium grained sandstone (proximal delta front Lithofacies), quartzarenite-sublitharenite sandstone, monocrystalline quartz (MQ) is the dominant mineral. Primarily silicate cemented (quartz supported).
Well T1-23 @ 8454ft (2577m).

X.N

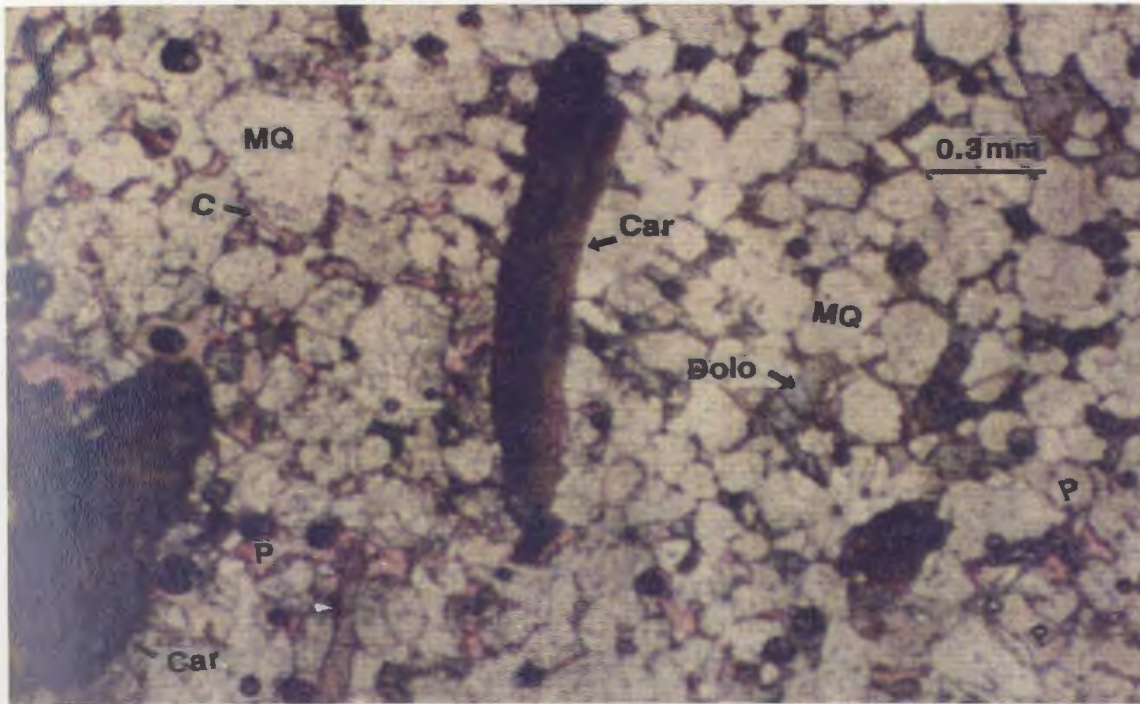


A

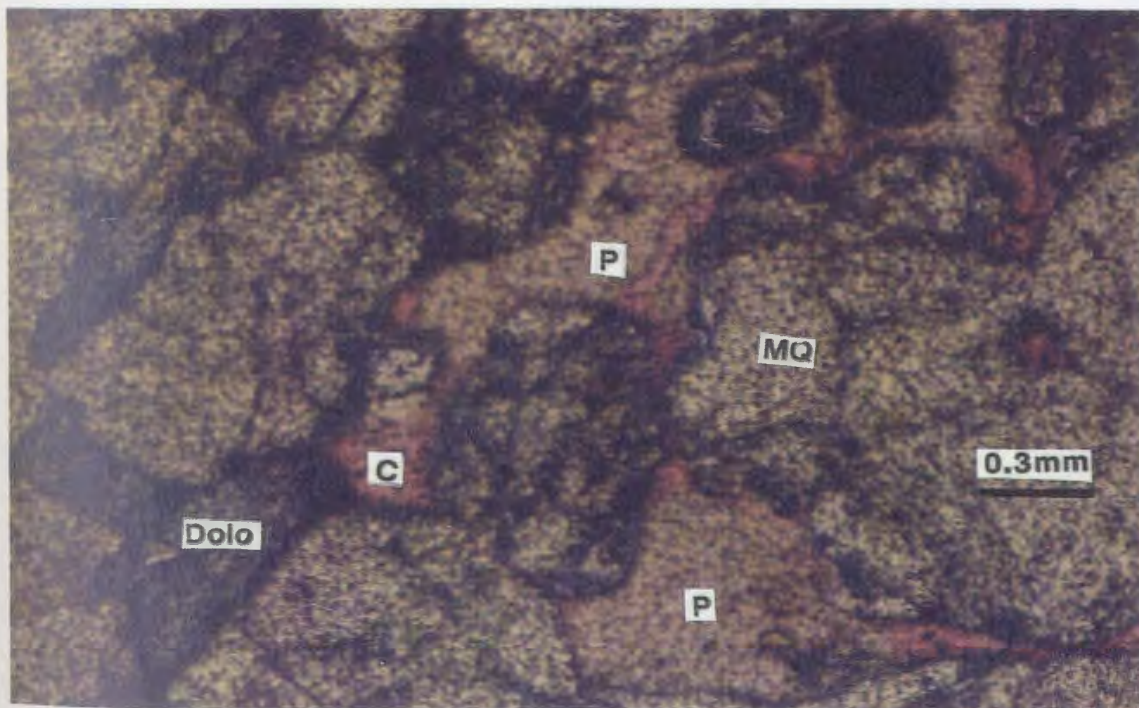
APPENDIX III

B- Fine-medium grained, carbonaceous (Carb), quartzarenite sandstone of the proximal delta front lithofacies, mainly composed of monocrystalline quartz (MQ), stringers of carbonaceous debris (Car) , showing partial dolomite (Dolo) and calcite (C) cements. This type of sandstone is relatively of high secondary porosity (P). Well C1-NC2 @ 9645ft (2940m).

C- Same sandstone type as the previous photo but in different view; fine-medium grained, quartzarenite sandstone, with partial calcite (C) and dolomite (Dolo) cements, relatively with high porosity. Note, the well developed large, oversized, intergranular secondary porosity (P). Well C1-NC2 @ 9645ft (2940m).



B

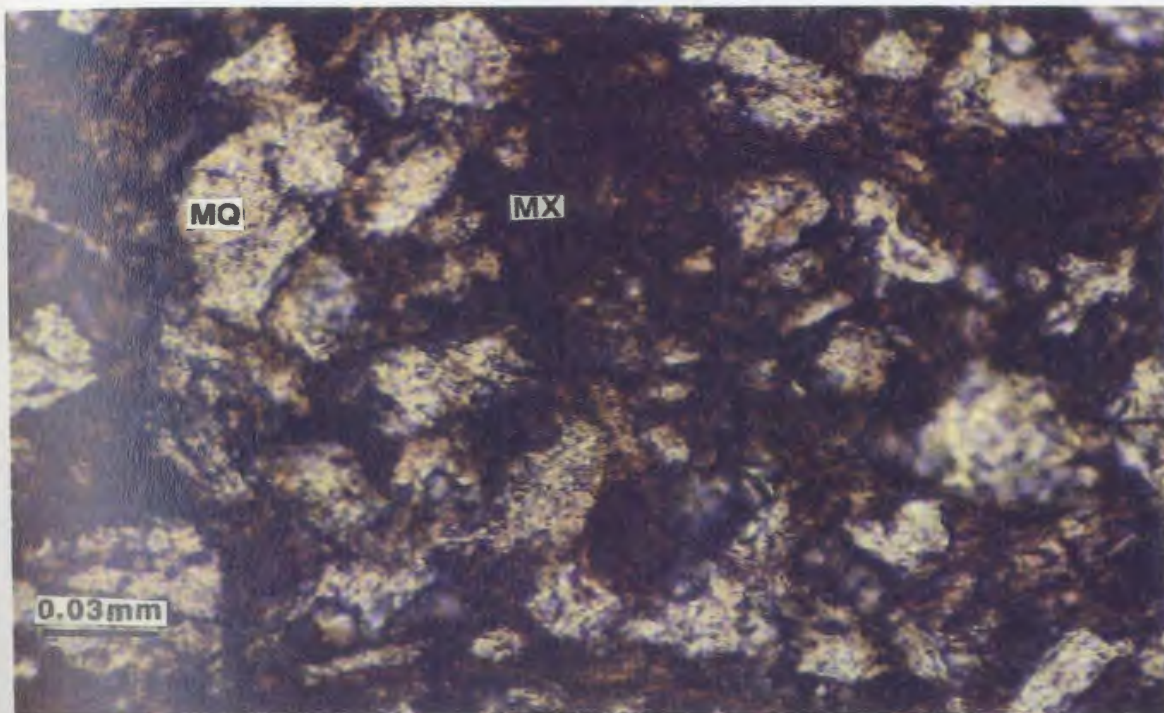


C

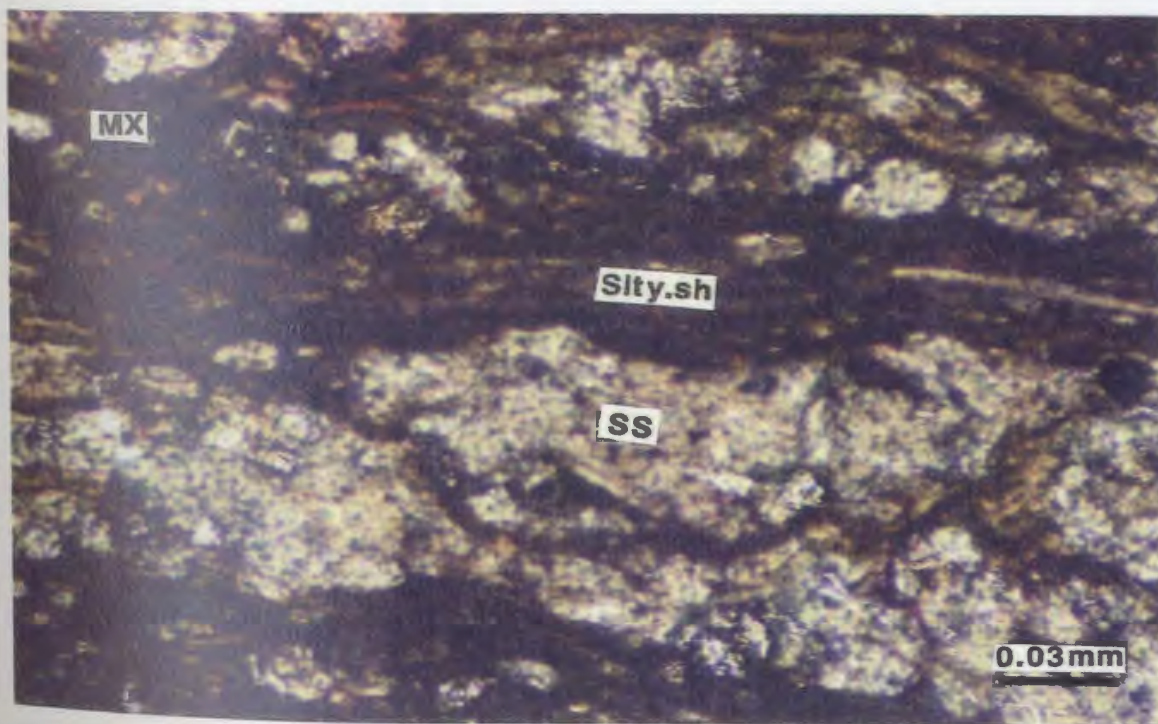
APPENDIX III

D- Clay-matrix (MX) rich bioturbated silty sandstone (distal delta front lithofacies), usually of low porosity. Well A1-NC2 @ 7817ft (2383m). MQ= monocrystalline Quartz.

E- Interbedded very fine grained sandstone (SS) and silty shale (Silty.sh) very common in the distal delta front lithofacies. Well E1-NC2 @ 9117ft (2779m). Note, the dispersed clay-matrix (MX) between the silty shale laminae.



D

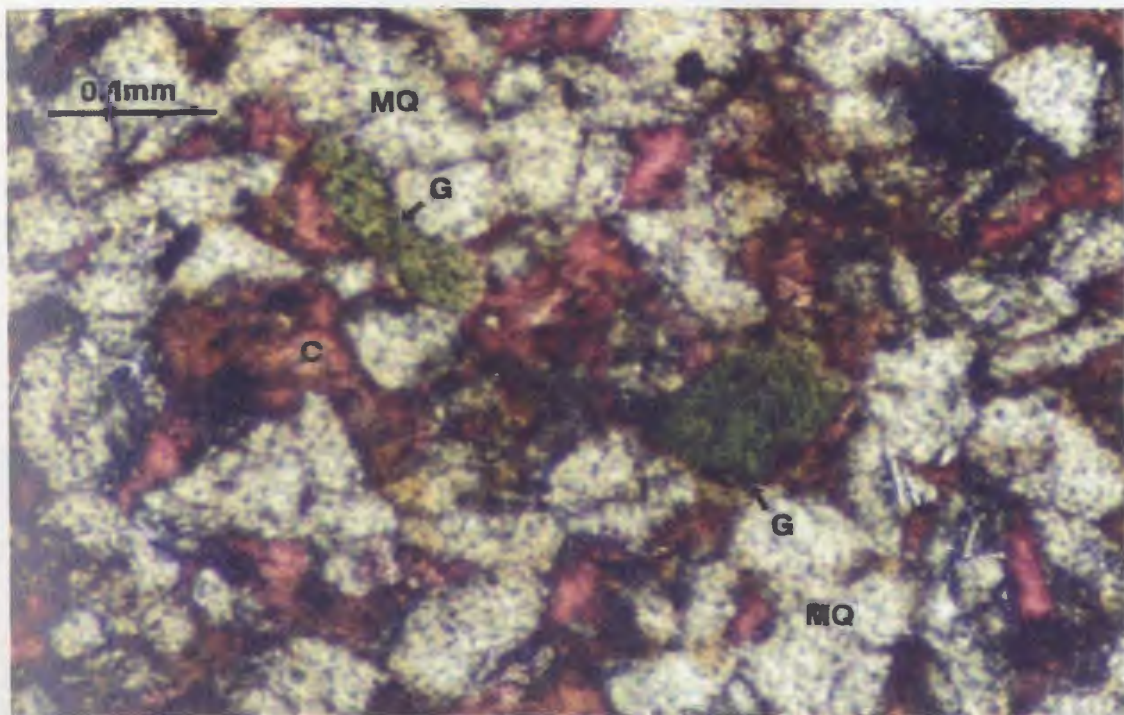


E

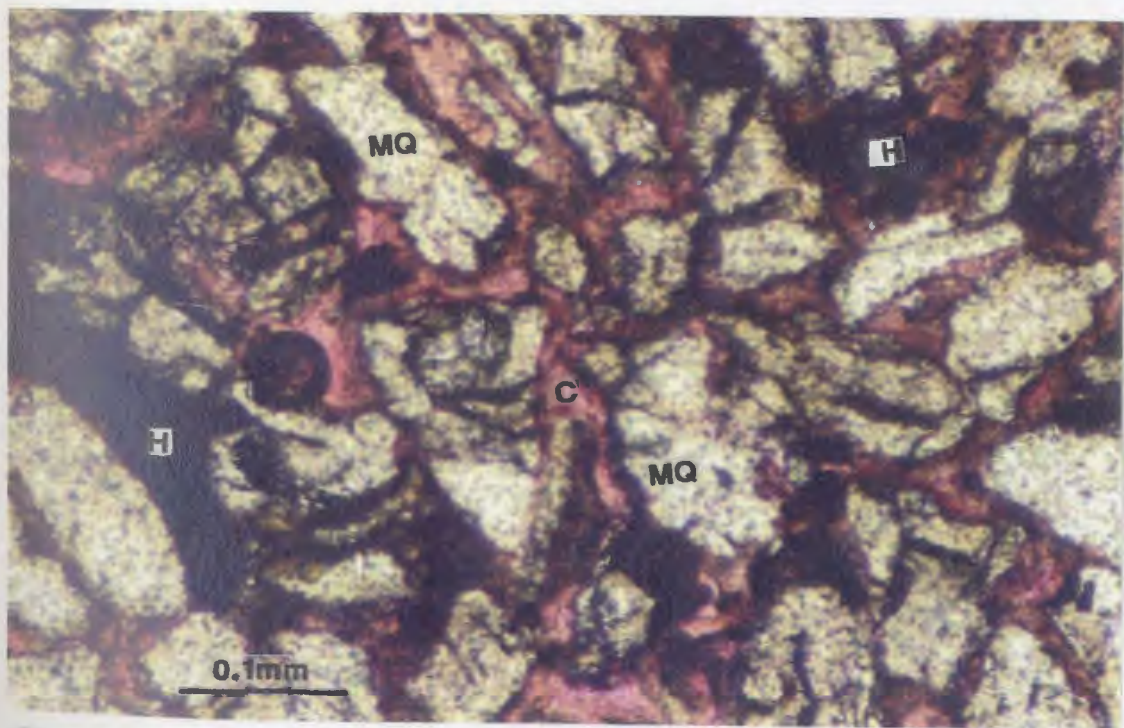
APPENDIX III

F- Very fine-fine grained carbonate sandstone (reworked marine sandstone lithofacies), sublitharenite, contains abundant monocrystalline quartz (MQ), abundant calcite cement (C) and occasionally with glauconite grains (G). Well Q1-23 @ 7461ft (2275m).

G- Carbonate cemented marine sandstone lithofacies, mainly composed of monocrystalline quartz (MQ) grains, calcite cement (C), characterized by floating grains and lack of silica cement. Note, some residual oil (H) filling secondary pores (where secondary porosity resulted mainly from calcite cement dissolution; very common in this type of sandstone).
Well Q1-23 @ 8180ft (2494m).



F



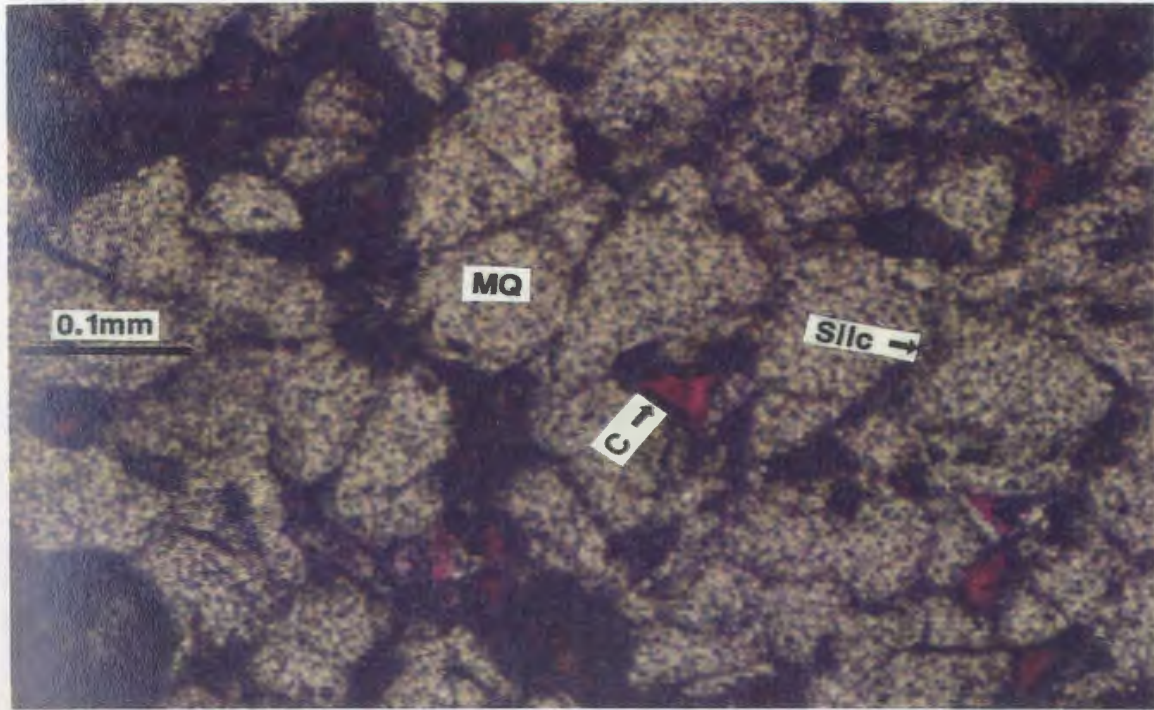
G

APPENDIX III

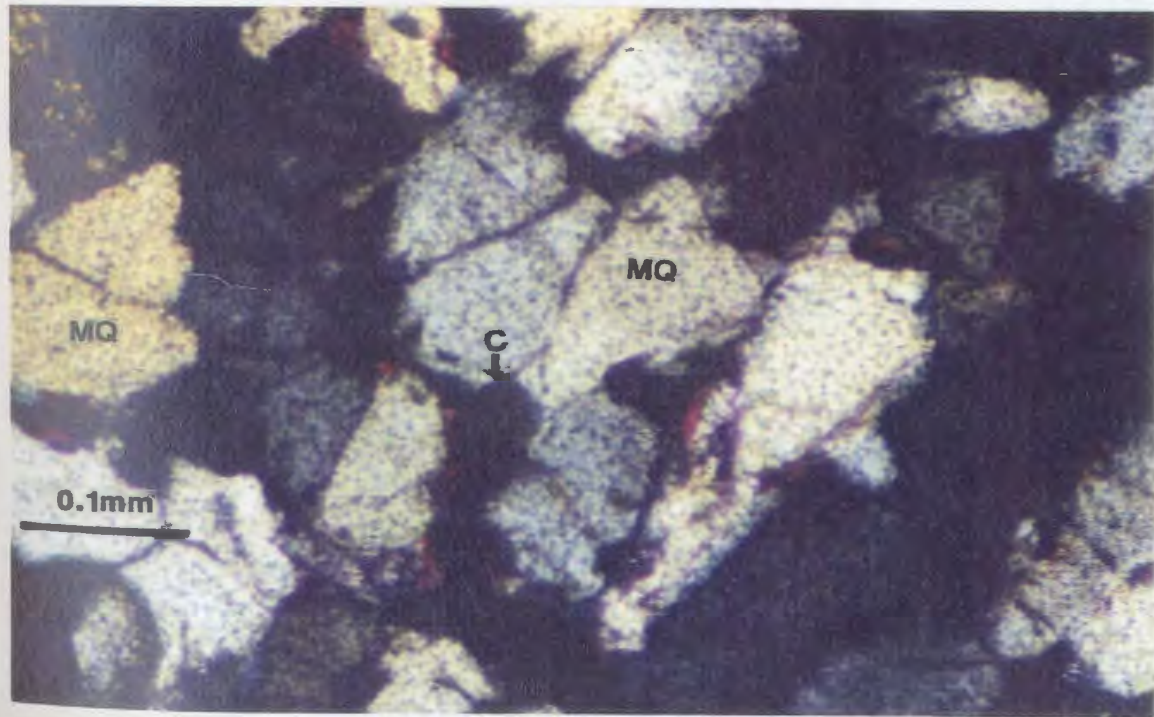
N-M Samples most representative of the upward decrease in grain size (upward increase in clay contents), and tend to confirm the fluvial origin (fluvial sandstone lithofacies) from 9353ft (2852m) to 9311ft (2839m) :

H- Sublitharenite, fine-medium grained sandstone, partially with silicate cement (Silc) through monocrystalline quartz (MQ) grains contacts, also carbonate cement (C) is present.
Well B3-61 @ 9353ft (2852m).

I- Same as previous photo but with crossed polarizers (X.N).



H

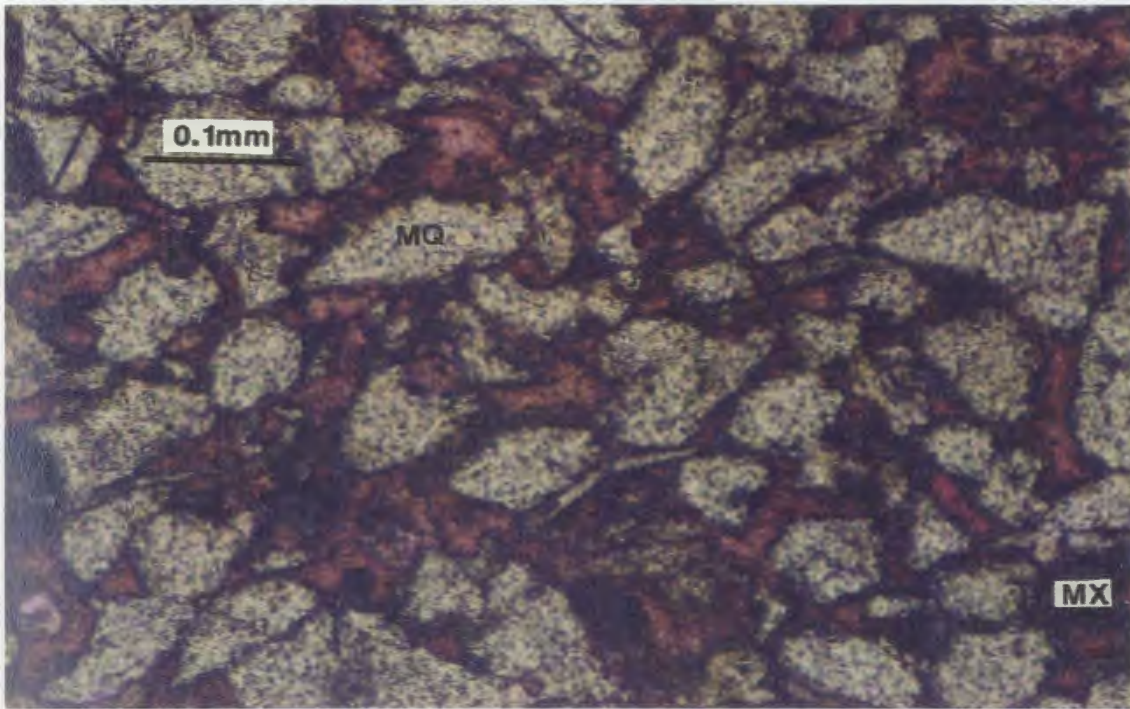


I

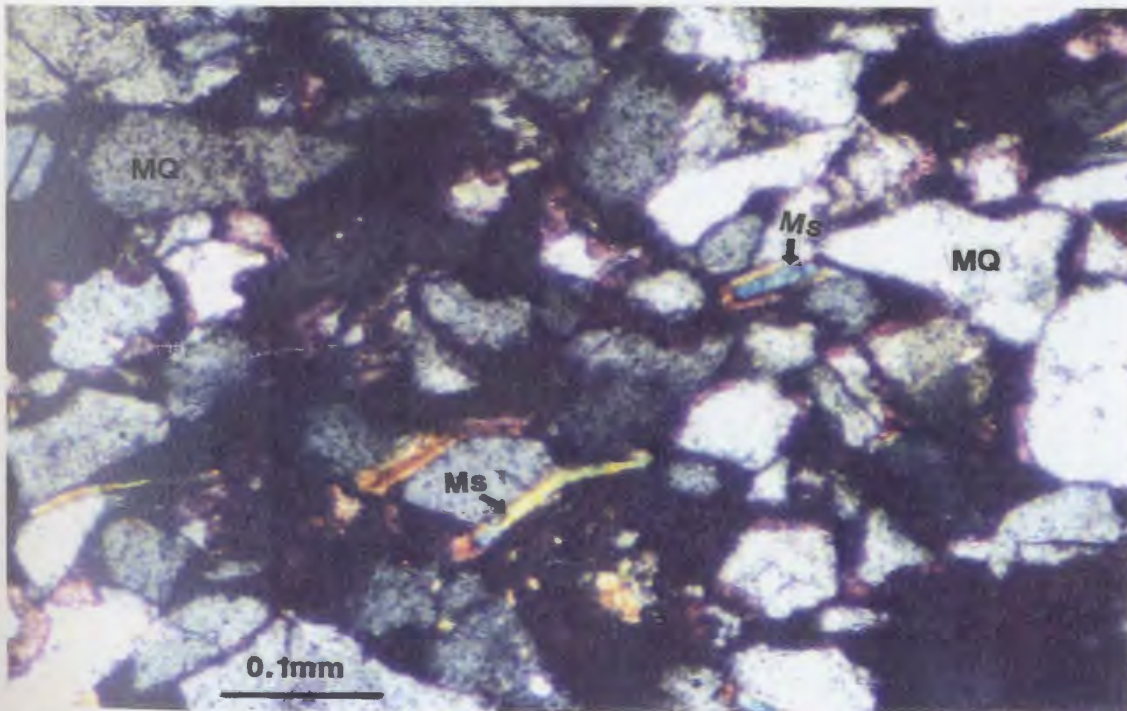
APPENDIX III

J- Sublitharenite-litharenite sandstone, with relative decrease in grain size of monocrystalline quartz (MQ), increase in clay contents (MX), and labile grains like muscovite (Ms), with abundant calcite cement (C). Well B3-61 @ 9328ft (2844m).

K- Same as previous photo but with crossed polarizers (X.N).



J

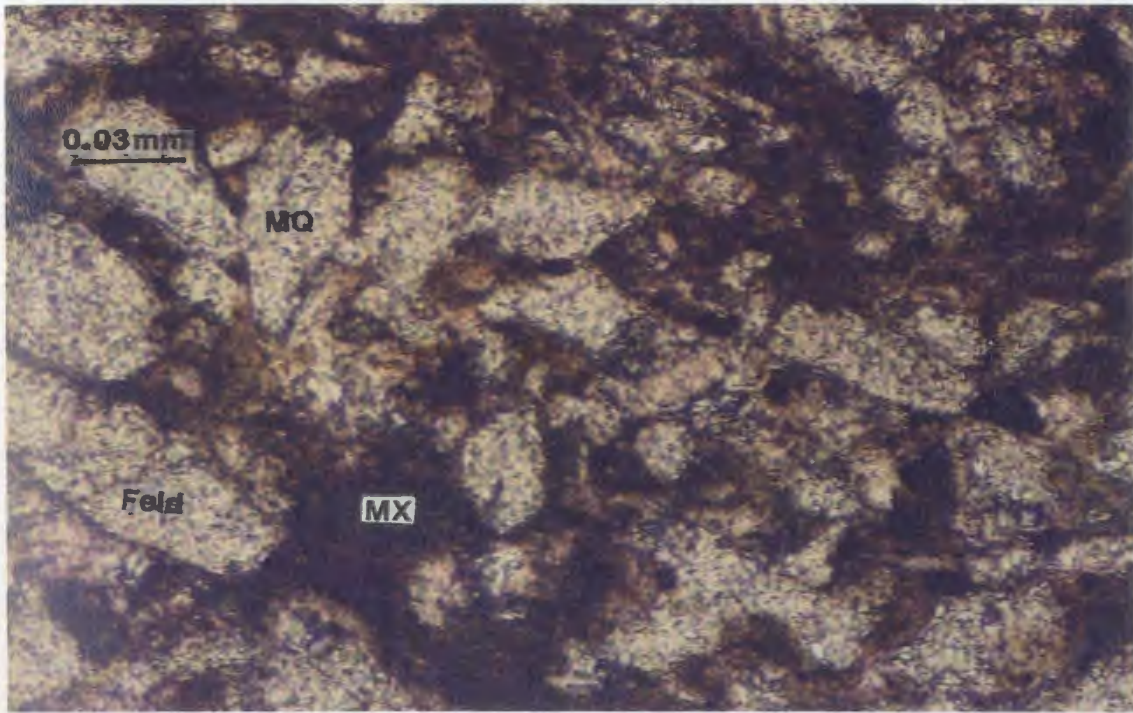


K

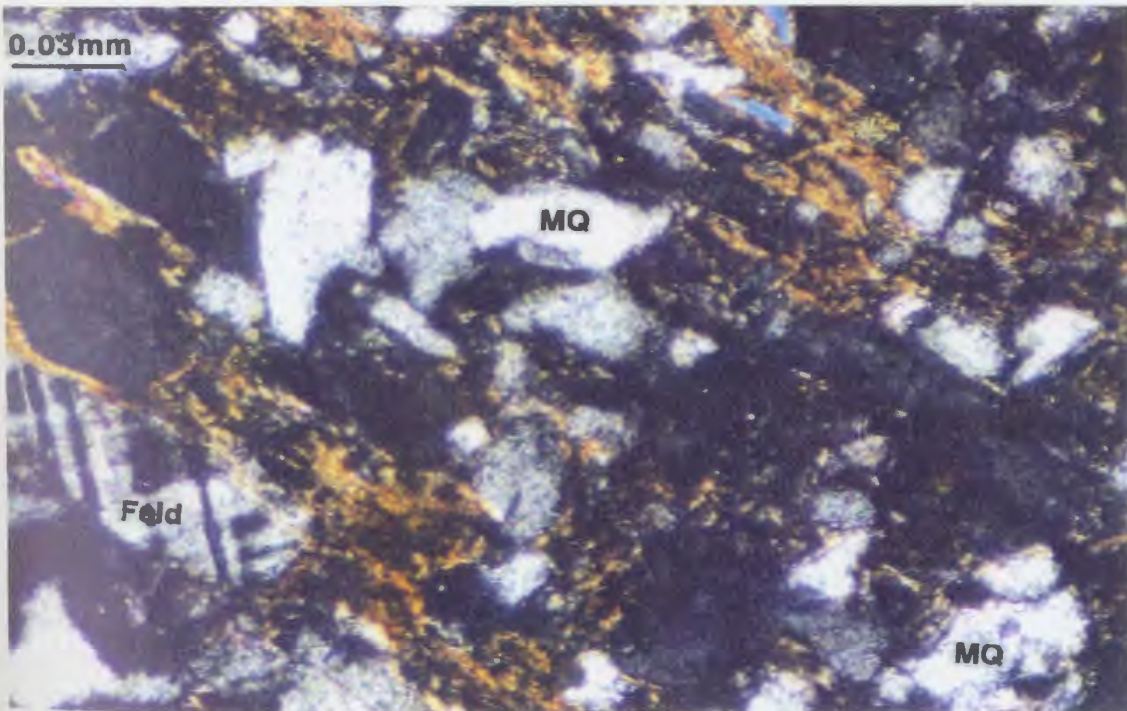
APPENDIX III

L- Clay-matrix rich (MX), litharenite sandstone (at top of fluvial sequence). Components are; monocrystalline quartz (MQ), feldspar (Feld), and clay matrix (MX). Well B3-61 @ 9311ft (2839m).

M- Same as previous photo but with crossed polarizers (X.N).



L



M

APPENDIX IV

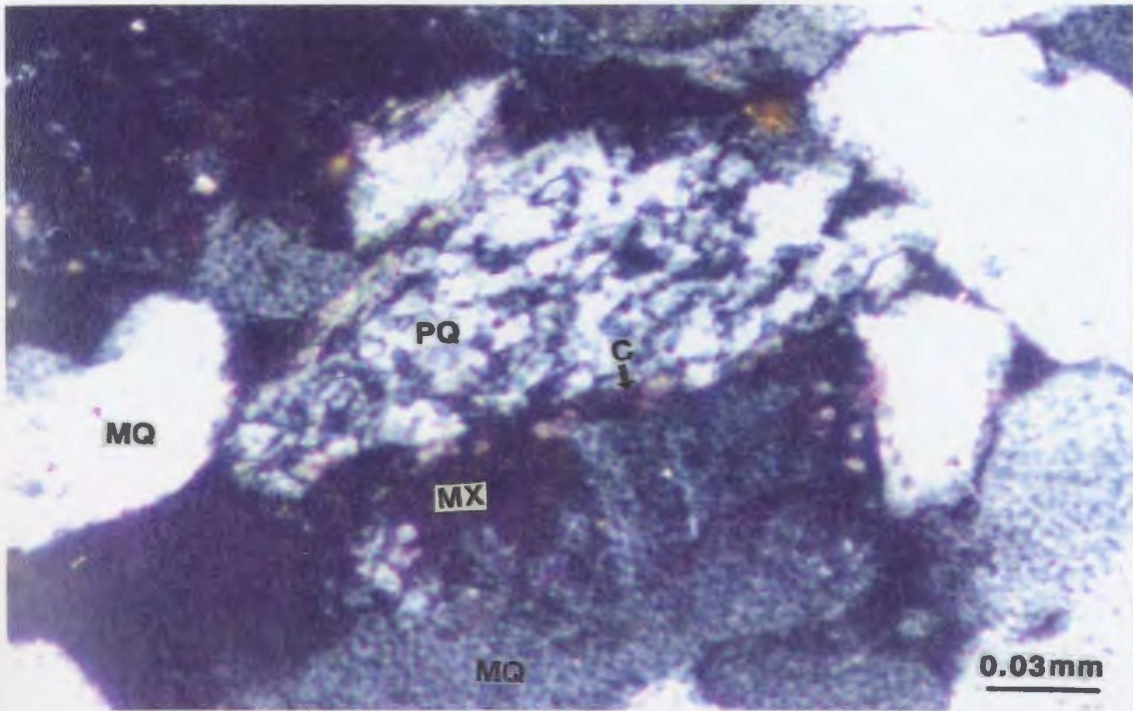
**Thin-Section-Petrographic Information
of the Lower Acacus Formation, NC2
Concession, Hamada Basin, NW Libya.**

A- Stretched quartz grains and foliated-like polycrystalline quartz (PQ) in the silty-fine grained sandstone of well D1-61 @ 8420ft (2567m). X.N

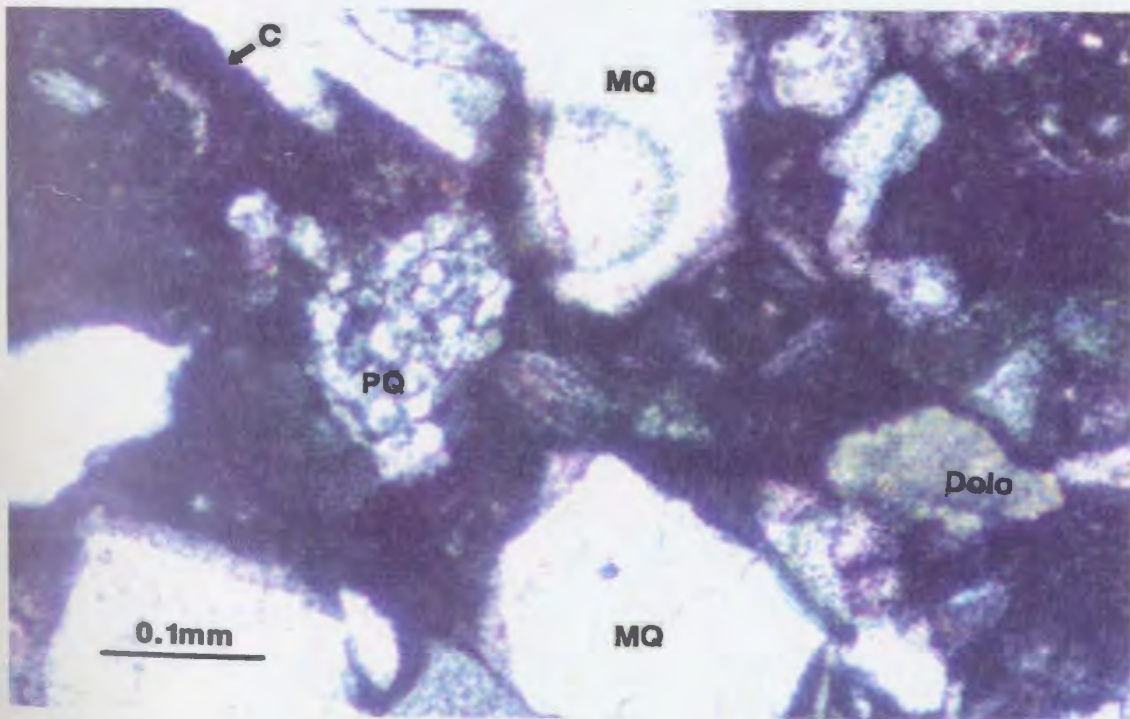
Components are: monocrystalline quartz (MQ), polycrystalline quartz (PQ), clay matrix (MX) and calcite cement (C).

B- Polycrystalline quartz (PQ) of metamorphic origin, in the sublitharenite, fine-medium grained sandstone of well D1-61 @ 8845ft (2697m). X.N

Components are: monocrystalline quartz (MQ), polycrystalline quartz (PQ), detrital dolomite (Dolo) and calcite cement (C).



A



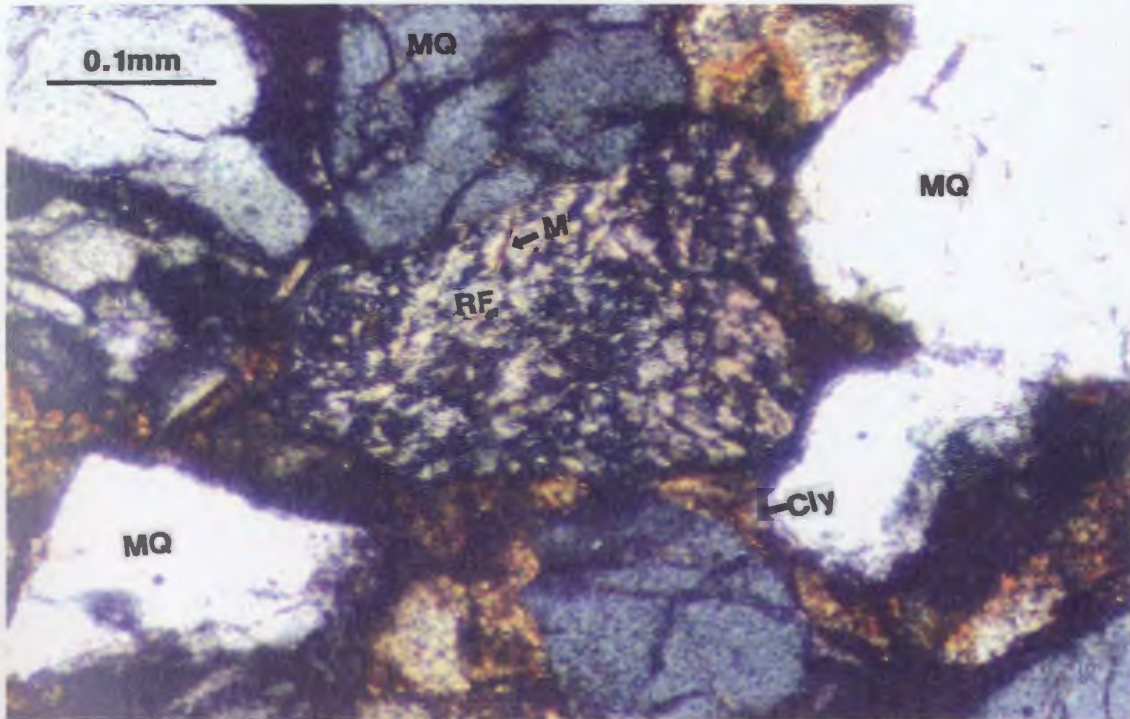
B

APPENDIX IV

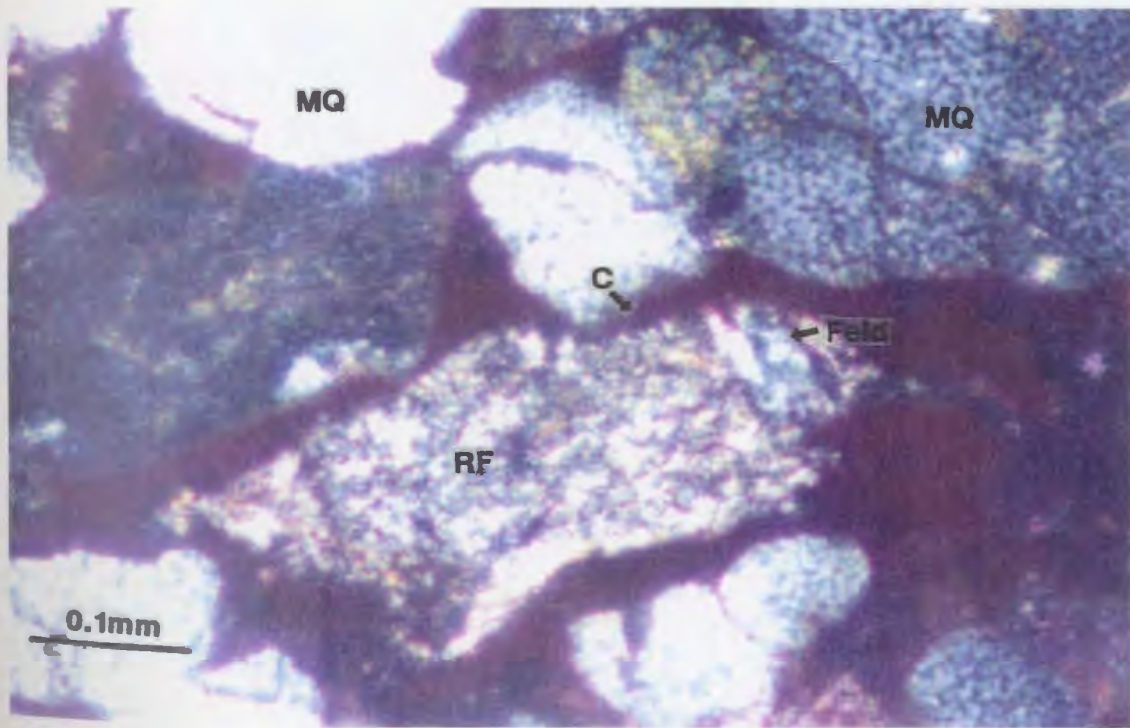
C- Possible altered rock fragment (RF); may be of volcanic or metamorphic origin, composed of very fine crystalline matrix occasionally with mica (M) and some unidentified crystals. Rock mainly composed of monocrystalline quartz (MQ), with some authigenic clay minerals (Cly). Sublitharenite, Fine-medium grained sandstone, well B3-61 @ 8969ft (2734m). X.N

D- Altered rock fragment (RF) with possible laths of feldspar crystals (Feld), in the sublitharenite, fine-medium grained sandstone, composed mainly of monocrystalline quartz (MQ) cemented by calcite (C). Well D1-61 @ 8236ft (2511m).

X.N



C



D

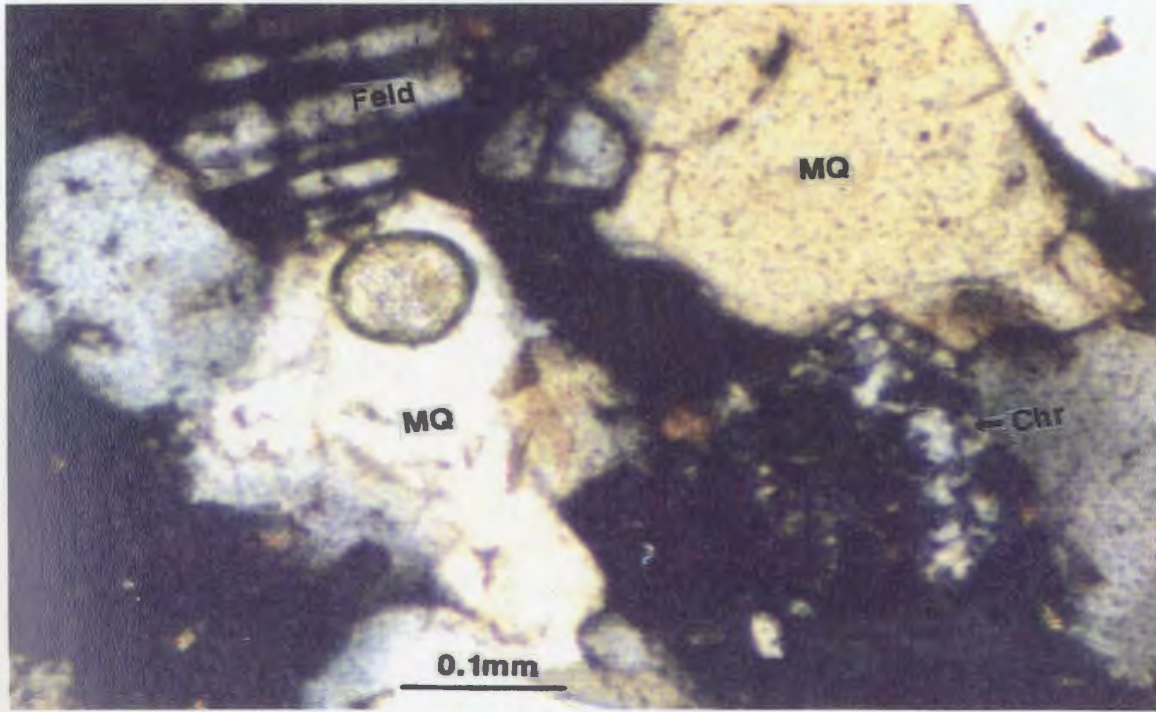
APPENDIX IV

E- Feldspar grain (Feld) exhibits albite twinning with the combination of detrital chert fragment (Chr), in the sublitharenite, monocrystalline quartz (MQ) supported, fine-medium grained sandstone of well T1-23 @ 8454ft (2577m).

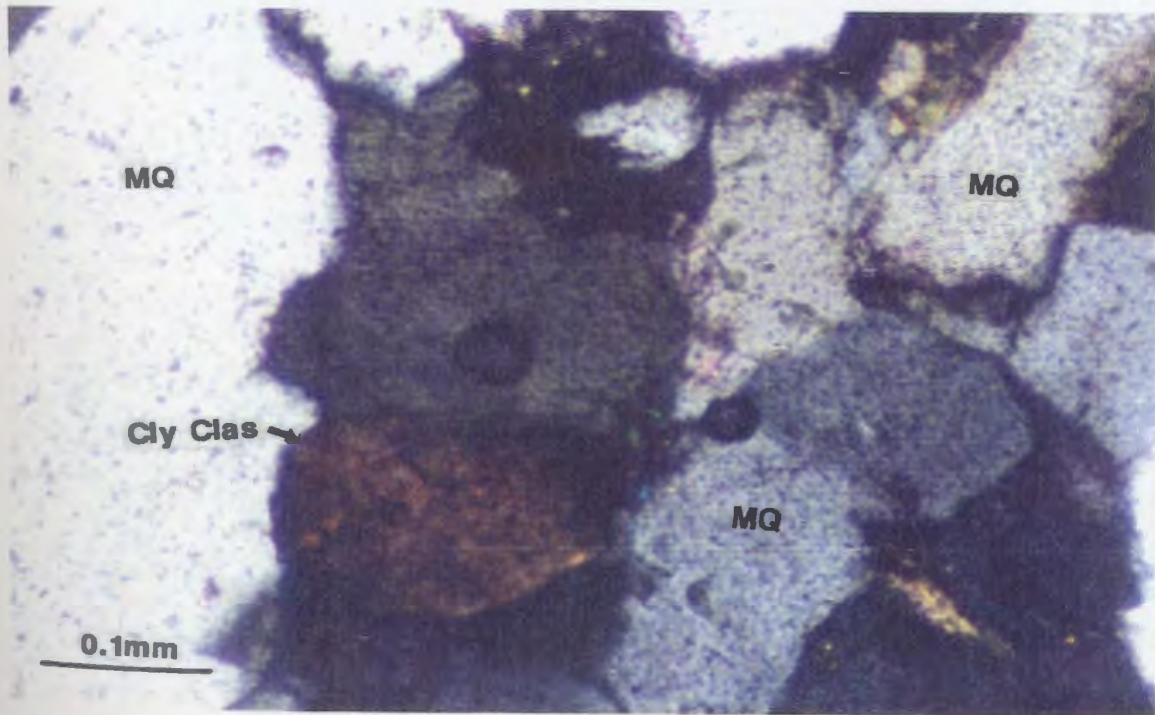
X.N

F- Individual clay clasts (Cly clas); with dark brown and extremely finely crystalline nature between monocrystalline quartz (MQ) grains. Sublitharenite, fine-medium grained, clean sandstone of well T1-23 @ 8454ft (2577m).

X.N



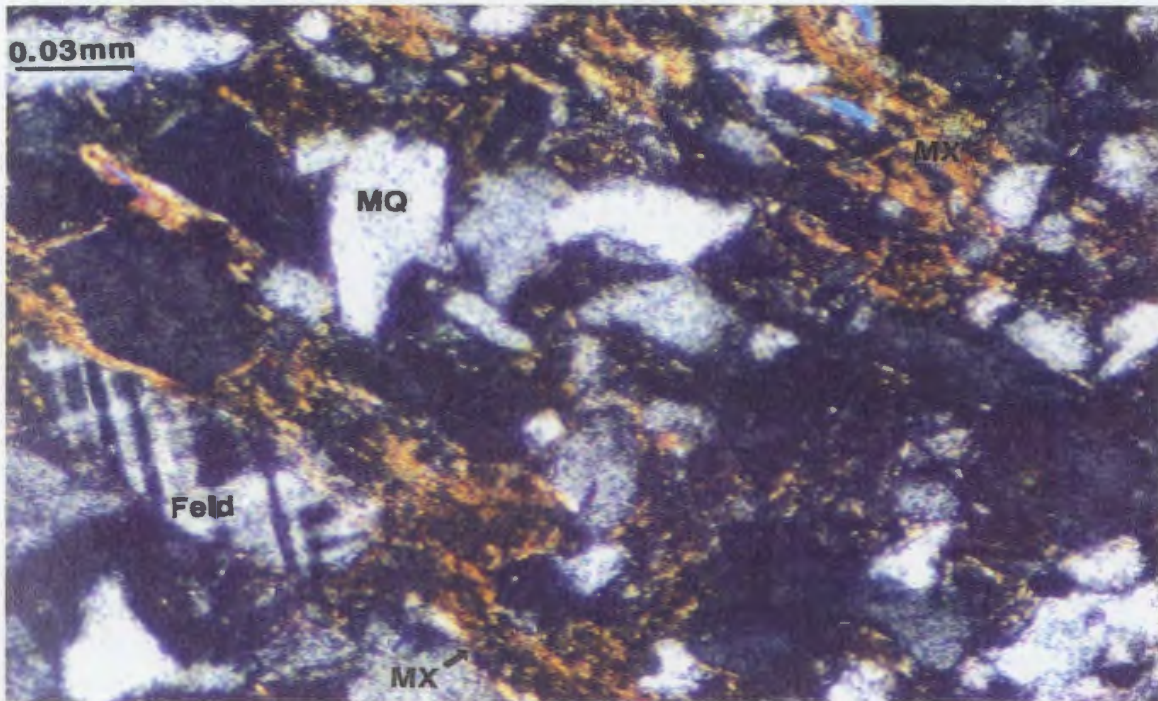
E



F

APPENDIX IV

G- Feldspar grain (Feld) with microcline (gridiron structure) twinning in the litharenite, fluvial clay rich , silty-v.fine grained sandstone of well B3-61 @ 9311ft (2839m). X.N
Components are: monocrystalline quartz (MQ), feldspar (Feld), mica muscovite (MS) and clay-matrix (MX).

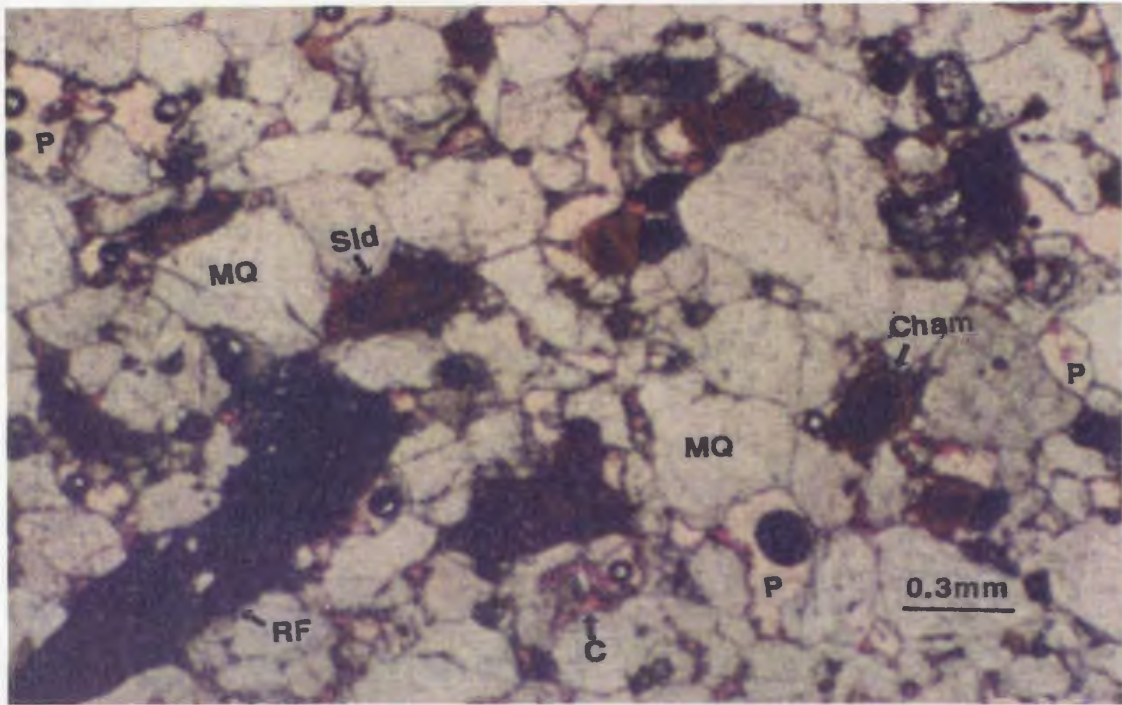


G

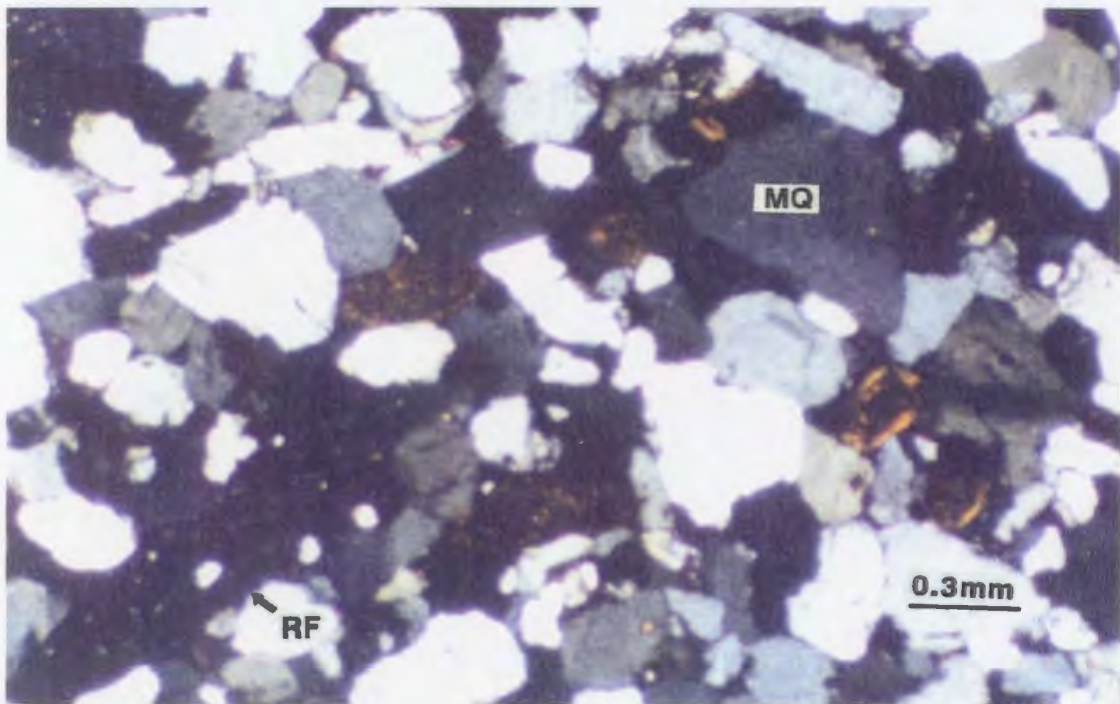
APPENDIX IV

H- Sublitharenite, fine-medium grained sandstone, showing rock fragment (RF); of dense isotropic to a crystalline texture, rock fragment such as this may be chert or volcanic in origin (VRF). Note, the oolitic texture of chamosite (Cham) and siderite-like eyes (Sid) between monocrystalline quartz (MQ) grains. Also note the secondary pore spaces (P) resulted mainly from dissolution of calcite (C) cement. Well B1-61 @ 8420ft (2567m).

I- Same as previous photo but with crossed polarizers (X.N).



H

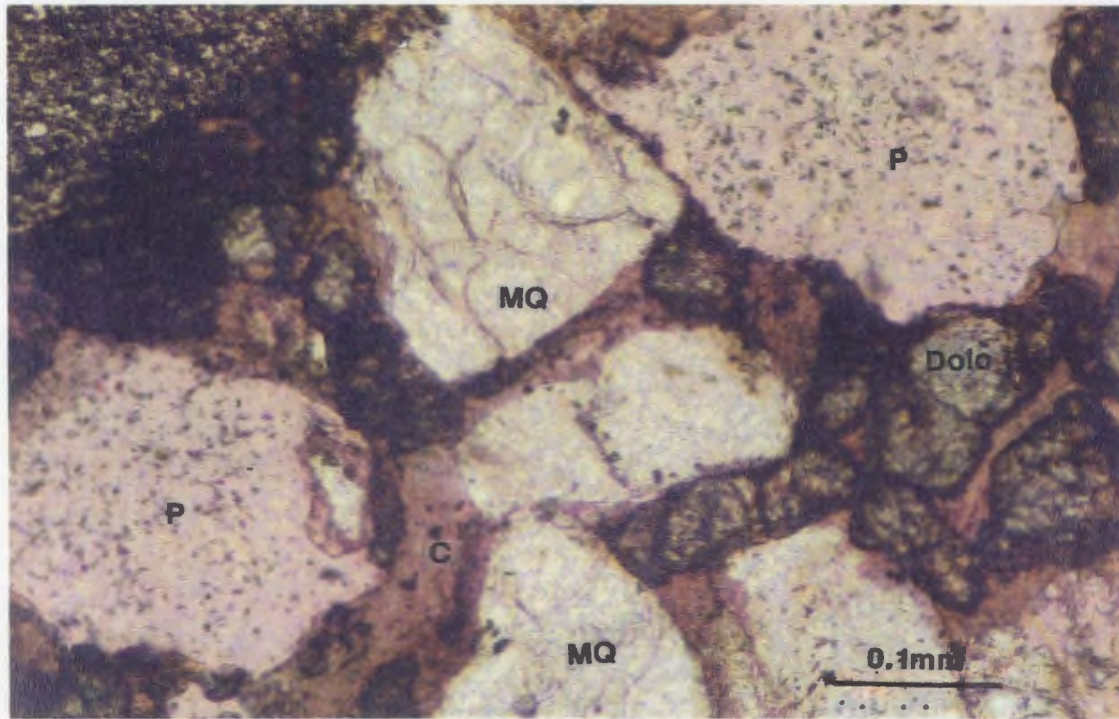


I

APPENDIX IV

J- Detrital dolomite grains (Dolo), identified by their rhombic shape of crystals, cloudy-brownish colour and their lack of response to stain. Sublitharenite, fine-medium grained sandstone, of well B3-61 @ 8893ft (2711m).

Components are: monocrystalline quartz (MQ), detrital dolomite (Dolo), secondary porosity (P) and calcite (C) cement.

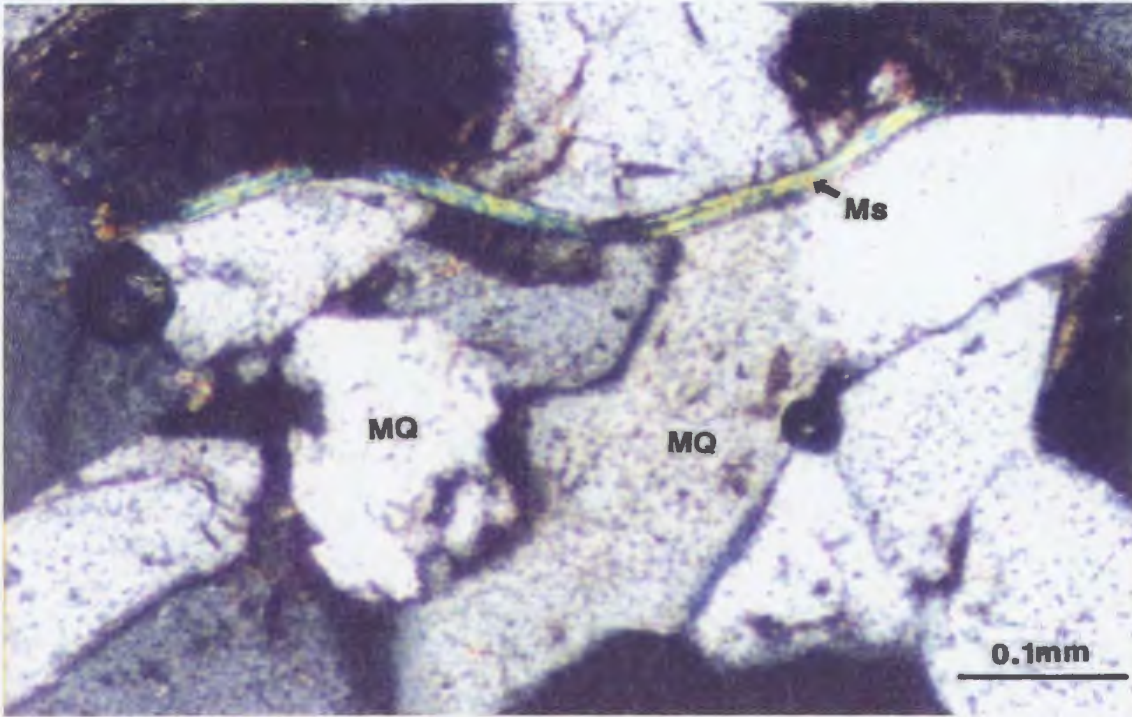


J

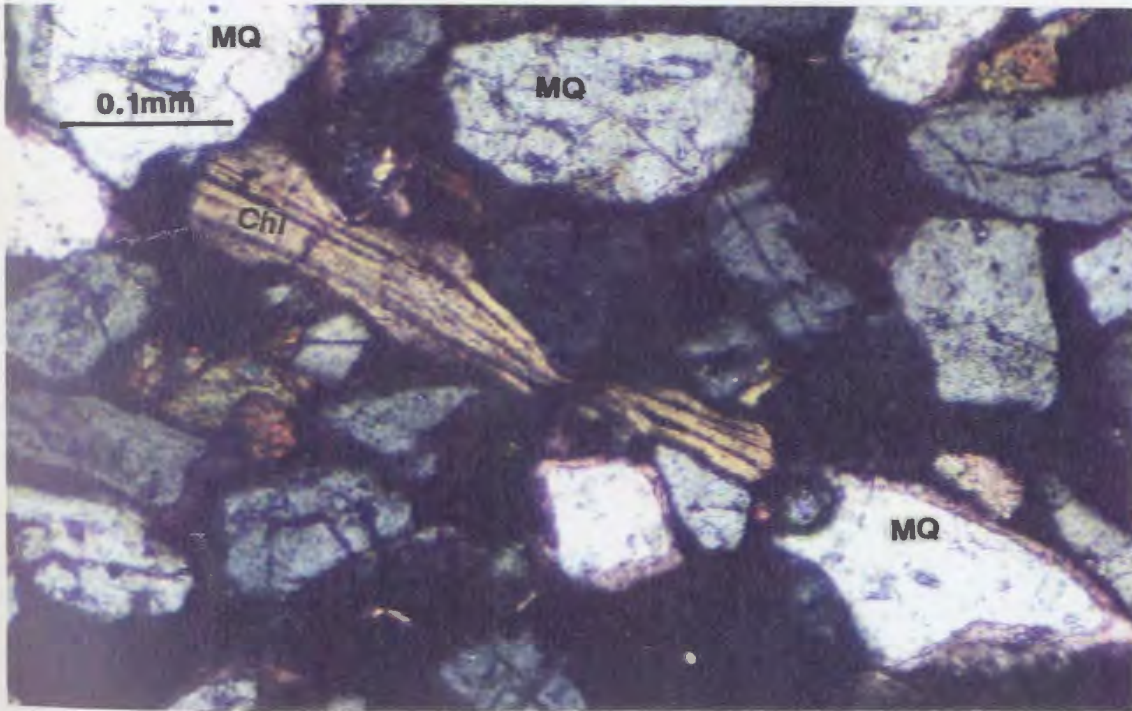
APPENDIX IV

K- Detrital mica muscovite (MS) with bright yellowish-blue birefringence, show some deformation between the rigid monocrystalline quartz (MQ) grains. Sublitharenite, fine-medium grained sandstone, of well T1-23 @ 8454ft (2577m). X.N

L- Detrital chlorite (Chl) grain shows some deformation between the rigid monocrystalline quartz (MQ) grains due to compaction. Sublitharenite, fine-medium grained sandstone, of well D1-61 @ 8845ft (2467m). Note, monocrystalline quartz (MQ) grains contain inclusions. X.N



K



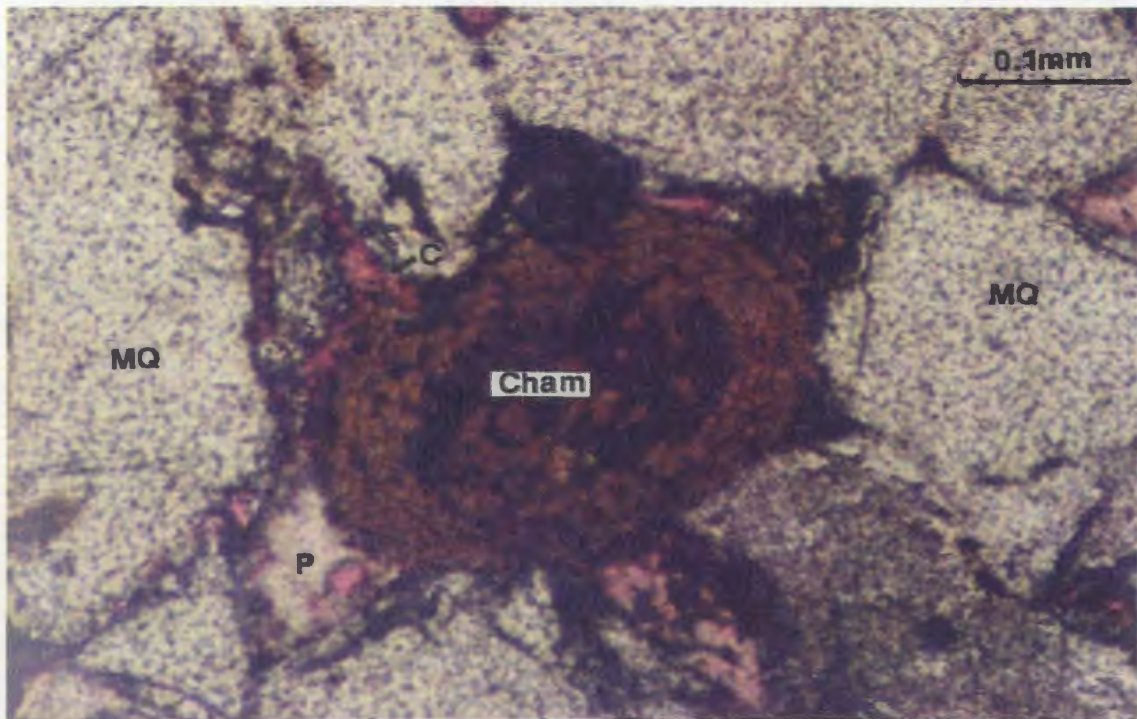
L

APPENDIX IV

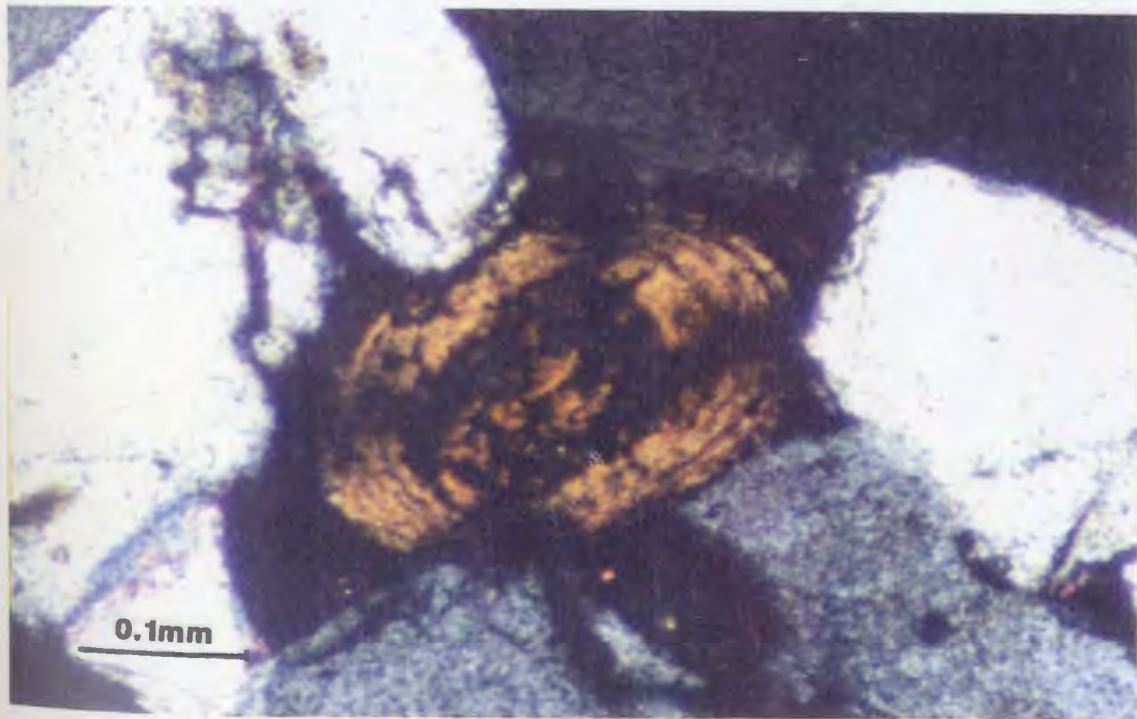
M- Chamosite (Cham) with oolitic texture between monocrystalline quartz (MQ) grains, is very common in the sublitharenite, fine-medium grained sandstone of well B1-61 @ 8420ft (2567m).

Note, dissolved calcite cement (C) yields secondary porosity (P).

N- Same as the previous photo but with crossed polarizers (X.N).



M



N

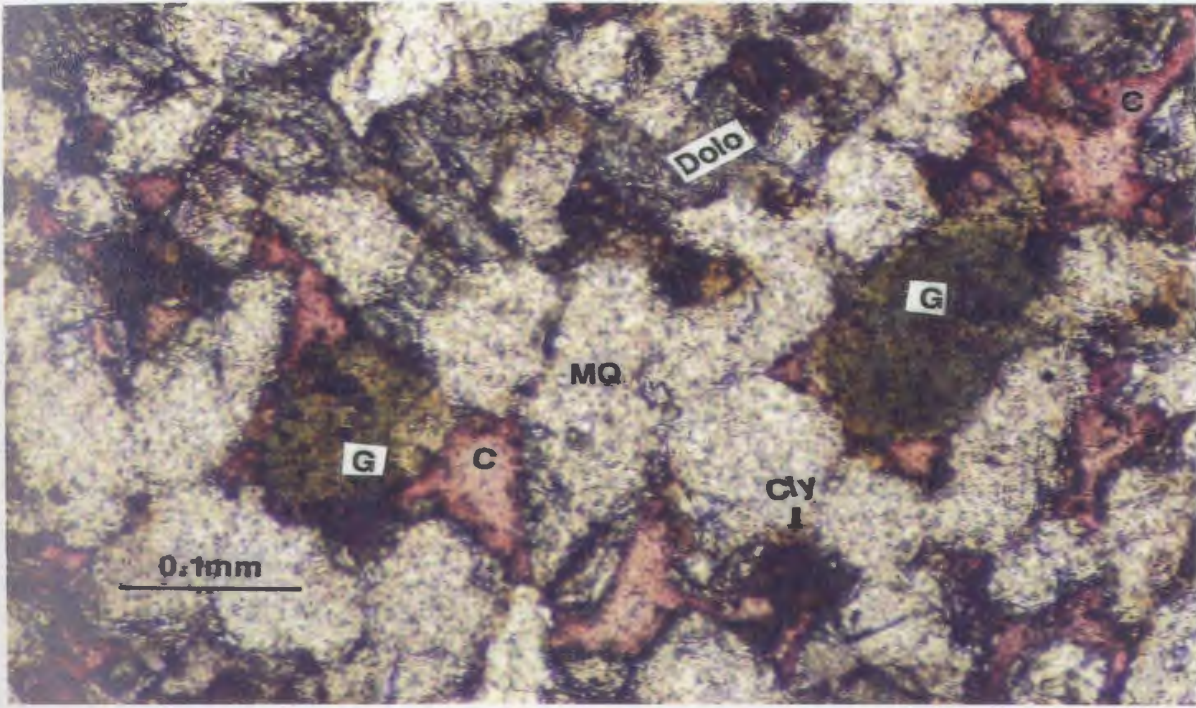
APPENDIX IV

O- Detrital glauconite (G) grains in the interpreted carbonate cemented marine sandstone lithofacies, with generally low porosity. Well Q1-23 @ 7471ft (2278m).

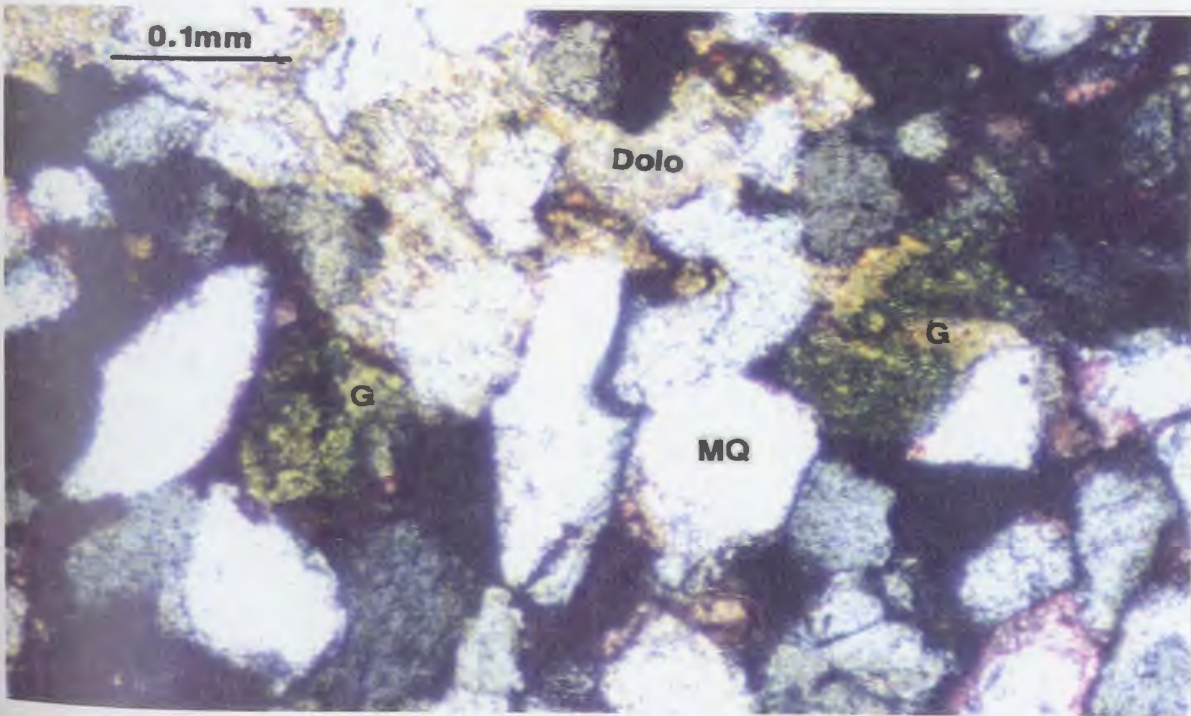
Components are: monocrystalline quartz (MQ), glauconite (G), partial calcite (C) cement, partial dolomite (Dolo) cement and authigenic clay minerals (Cly).

P- Same as previous photo but with crossed polarizers (X.N).

Note, glauconite grains are green in both ordinary (photo O) and polarized (photo P) lights.



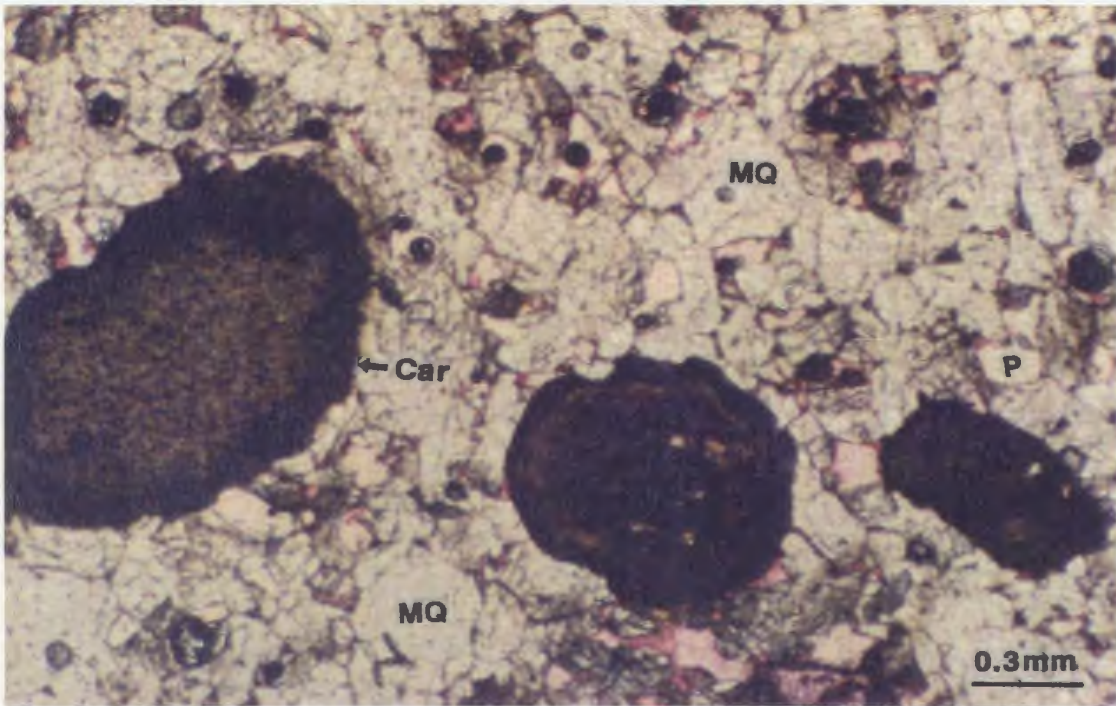
O



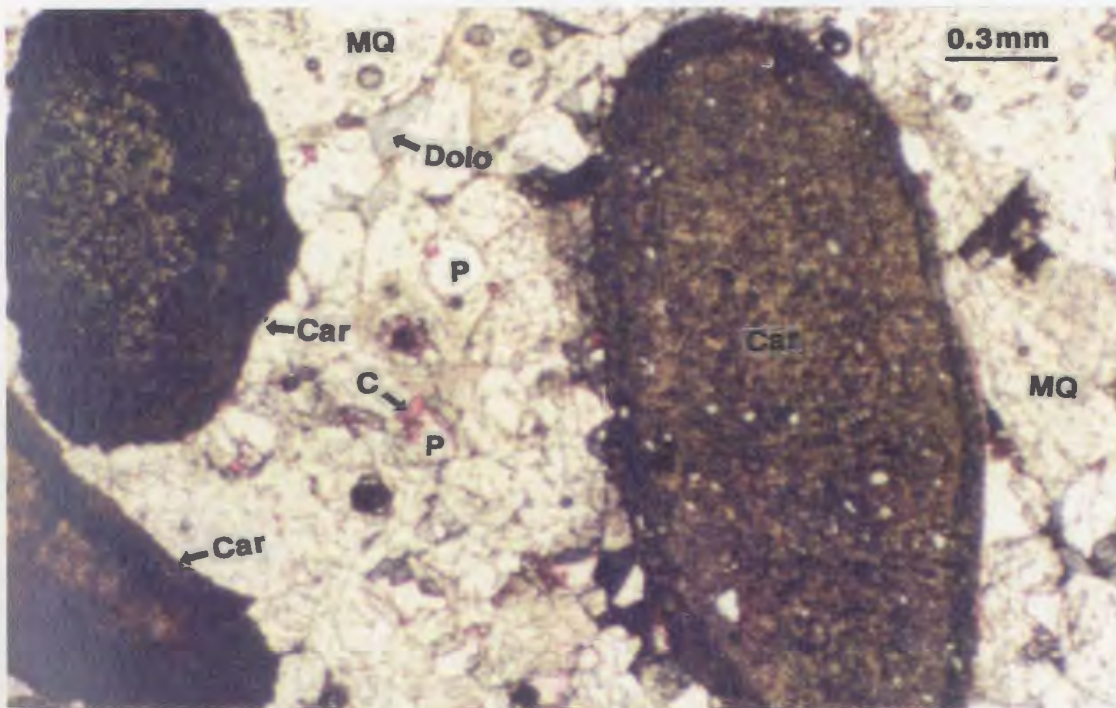
P

APPENDIX IV

Q-R Organic matter (carbonaceous debris) (Car) in well rounded shape very common in the sublitharenitic ,fine-medium grained sandstones (proximal delta front lithofacies) of well E1-NC2 @ 9105ft (2776m). Note, the patchy calcite (C) and dolomite (Dolo) cements between monocrystalline quartz (MQ) grains, partial cement dissolution may be seen through secondary pore spaces (P).



Q

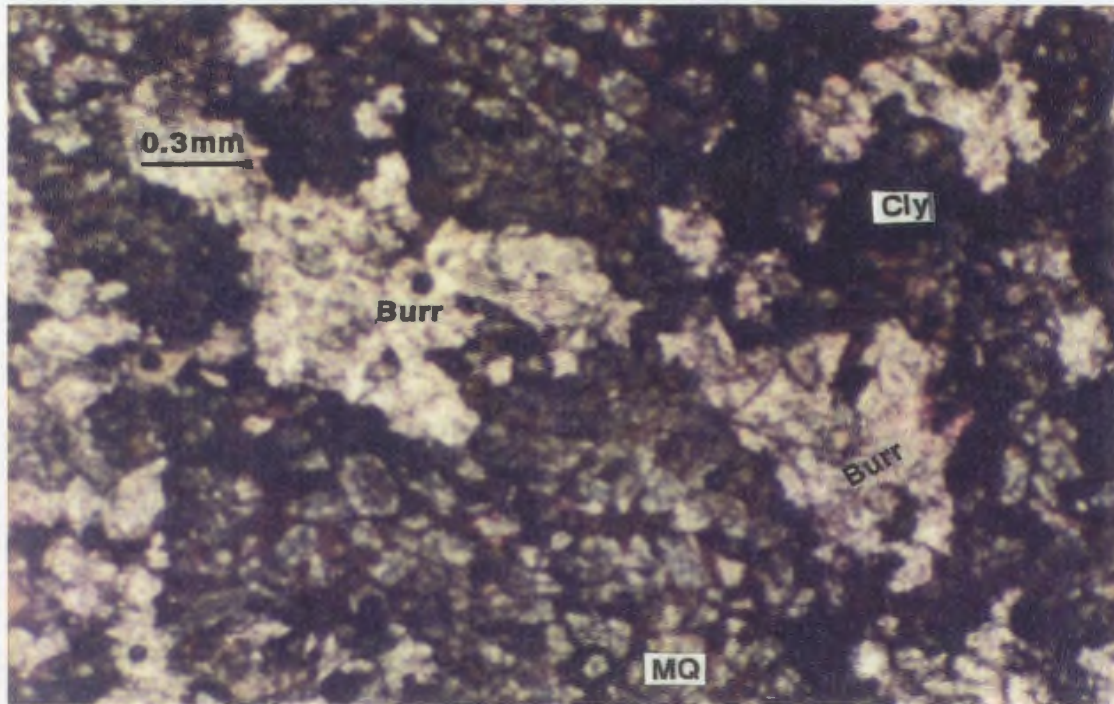


R

APPENDIX IV

8- Litharenite bioturbated silty sandstone in well A1-NC2 @ 7817 ft (2383m); showing burrows (Burr) have modified the original clay laminae. The clay (Cly) may line burrows.

Note, this is the typical distal delta front lithofacies in the study area in which the clay content (Cly) is high relative to the silty-v.fine monocystalline quartz (MQ).

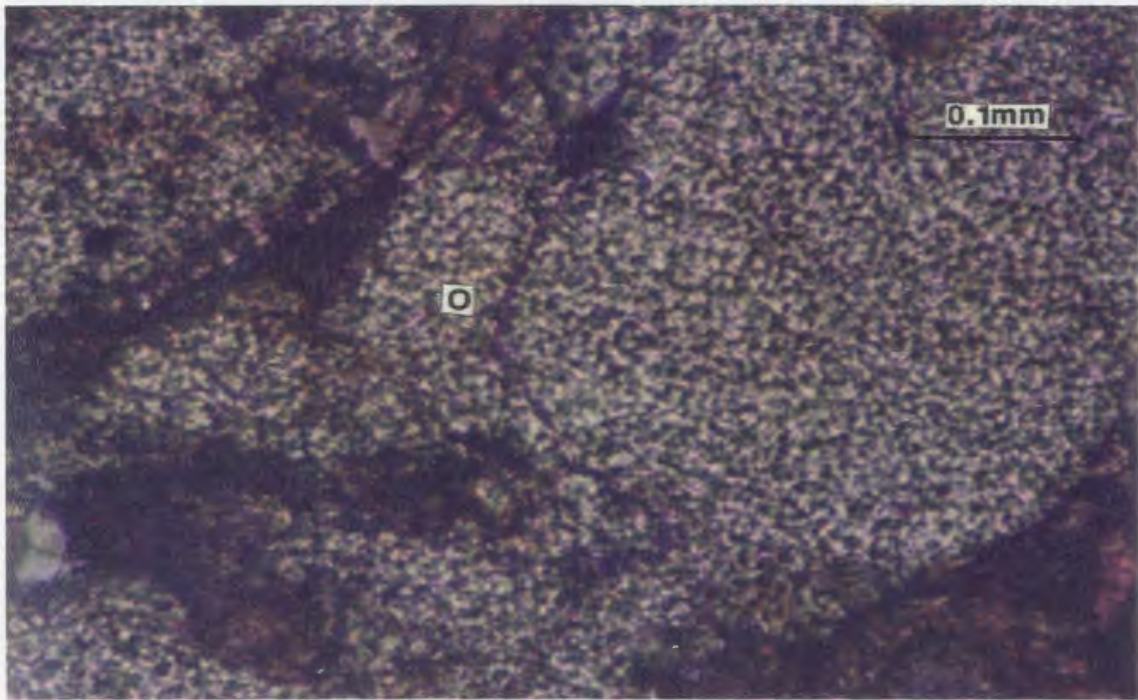


S

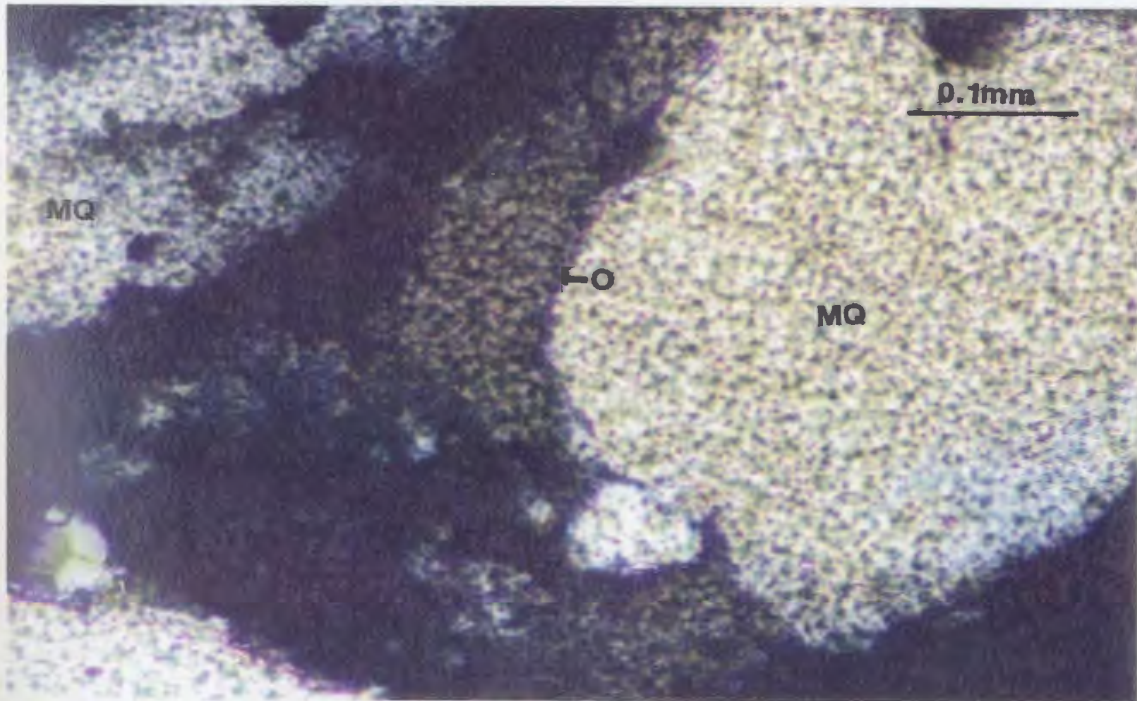
APPENDIX IV

T- Partial quartz cemented sandstone, quartz overgrowth (O) forms euhedral crystal termination with straight contact between adjacent monocrystalline quartz (MQ) grains. Quartz overgrowth (O) is much more abundant and pervasive in the well sorted, clean, cross-laminated, fine-medium grained sandstone of the proximal delta front lithofacies in well C1-NC2 @ 9622ft (2933m).

U- Same as the previous photo but with crossed polarizers (X.N).



T

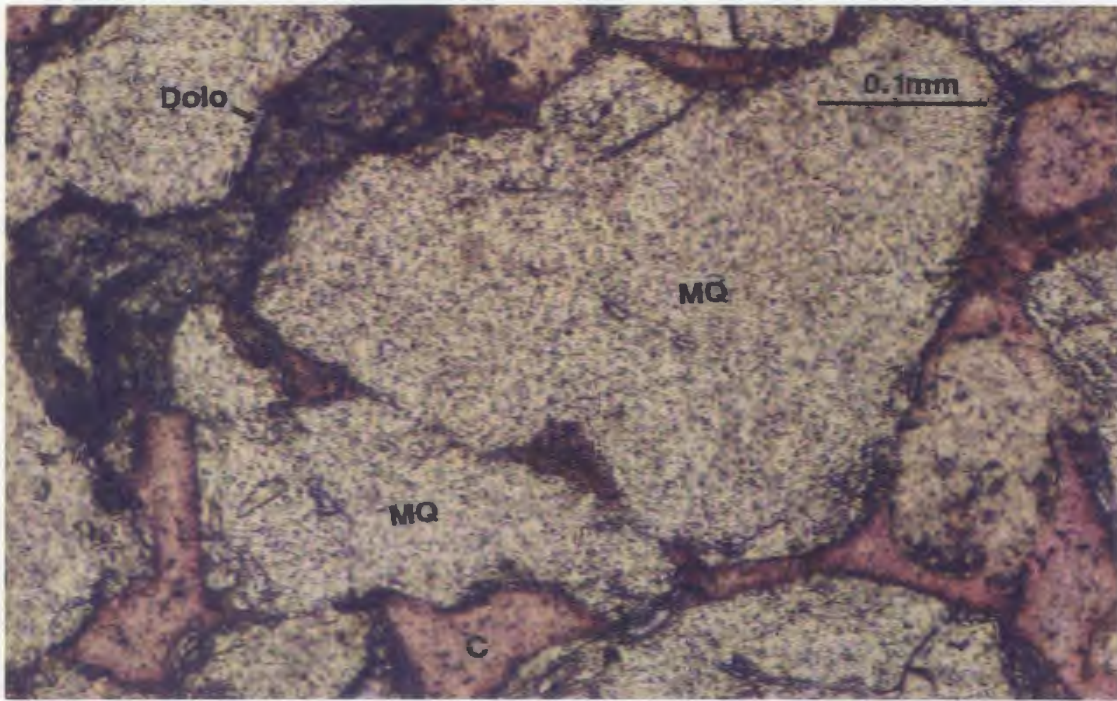


U

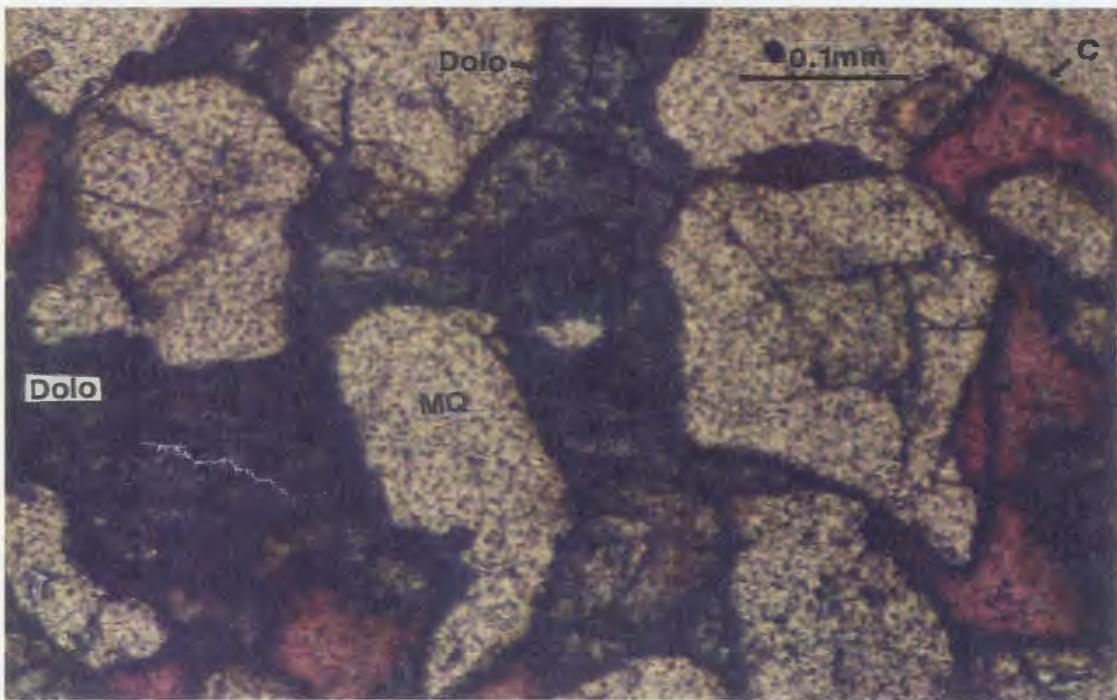
APPENDIX IV

V- Patchy calcite (C) and dolomite (Dolo) cemented sandstone (near shale-sand contact), the calcite (C) cement has been stained red, the dolomite (Dolo) cement show no response to staining; with moderate relief, rhombic outline and creamy-brownish gray colour. Sublitharenite-quartzarenite, with well sorted fine-medium grained monocrystalline quartz (MQ), well C1-NC2 @ 9703ft (2958m).

W- Patchy carbonate cemented sandstone, contains abundant calcite (C) and patchy dolomite (Dolo) cements. Quartzarenite, fine-medium grained monocrystalline quartz (MQ), well B3-61 @ 8756ft (2669m).



V

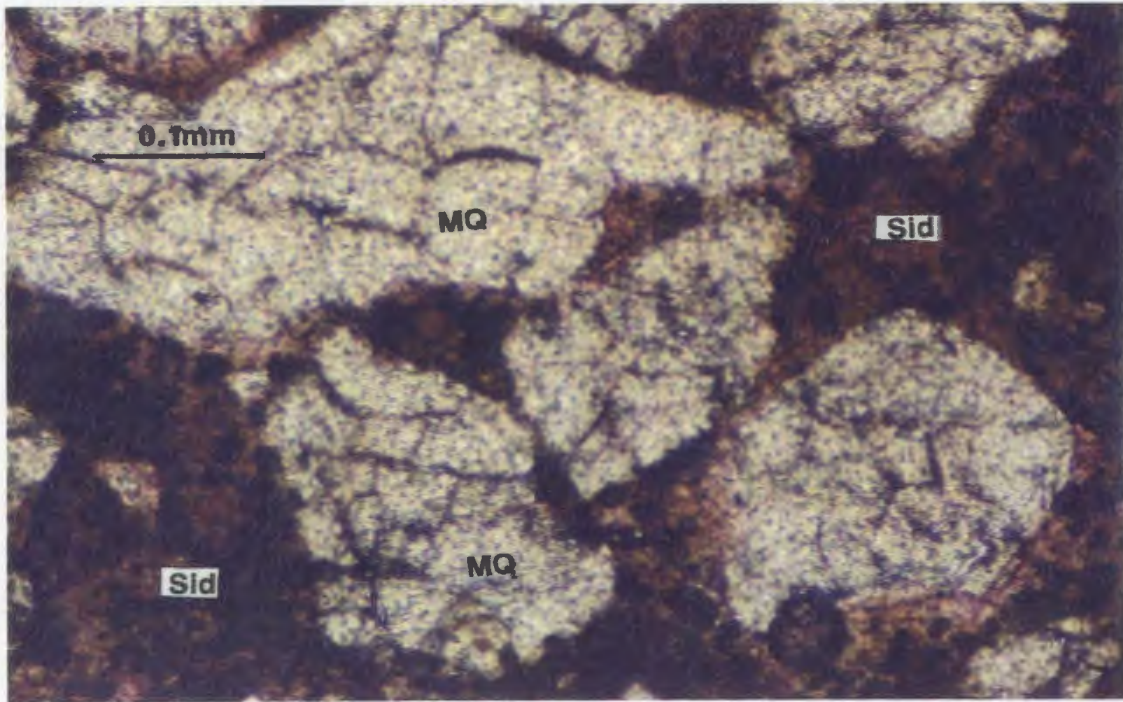


W

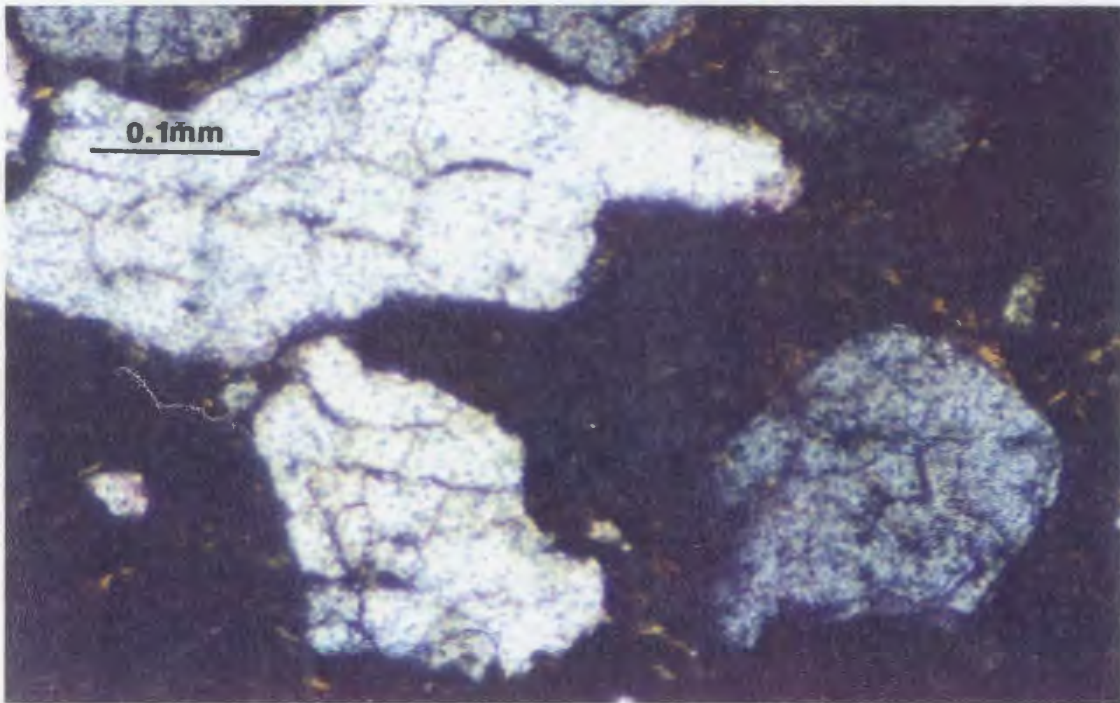
APPENDIX IV

X- Partial siderite (Sid) cement, showing some euhedral pore filling crystals with rhombic outline, and having typical brownish-yellow iron oxide coating (colour). In the sublitharenite, fine-medium grained monocrystalline quartz (MQ), of proximal delta front sandstone lithofacies in well B1-61 @ 8479ft (2585m).

Y- Same as previous photo but with crossed polarizers (X.N).



X



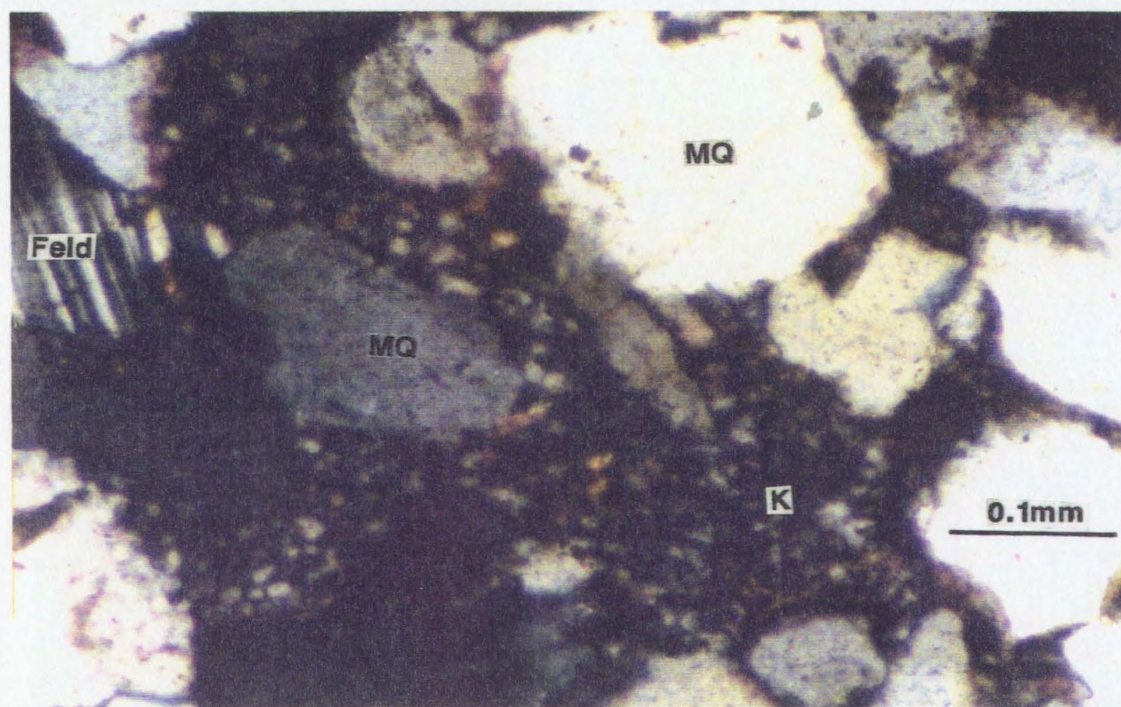
Y

APPENDIX IV

Z- Kaolinite cement (K) in the interpreted marine sandstone of well Q1-23 @ 8461ft (2579m) is identified by its fine crystal aggregates, vermicular texture, and low birefringence.

Kaolinite is very common in this type of sandstone and may contribute to reducing porosity. X.N

Components are: monocrystalline quartz (MQ), feldspar (Feld), and kaolinite cement (K).

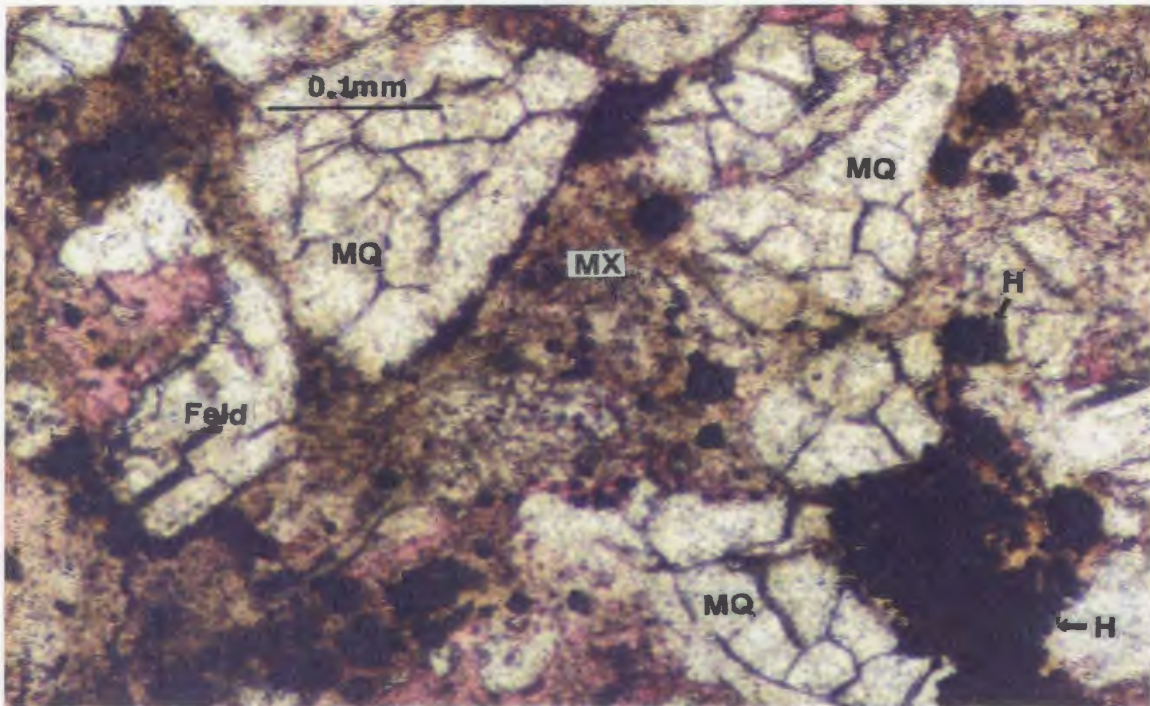


Z

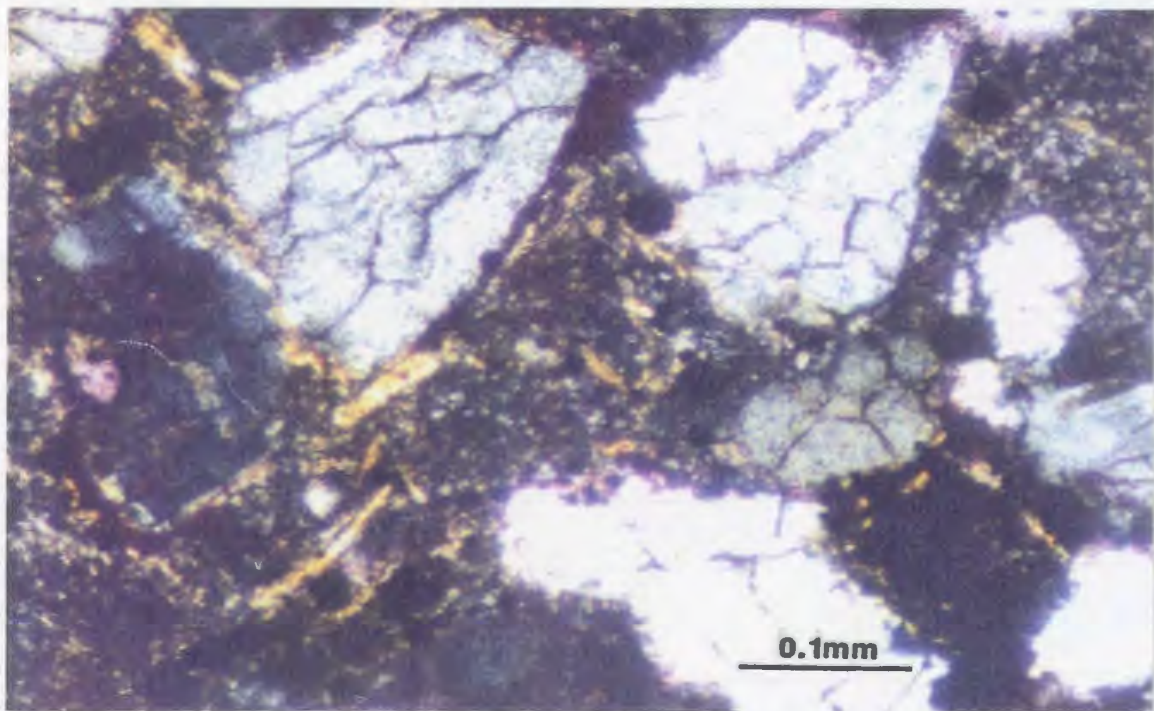
APPENDIX IV

ZZ- Hydrocarbon (H) droplets in clay-matrix (MX) probably kaolinite in the interpreted marine sandstone of well Q1-23 @ 8461ft (2579m). Note, the fractured monocrystalline quartz (MQ) grains, the partial dissolved feldspar grain (Feld) (left side of the photo) and the abundance of authigenic clays. All these may indicate this type of sandstone (lithofacies) underwent some diagenetic processes at some stages of its formation.

ZZZ- Same as previous photo but with crossed polarizers (X.N)



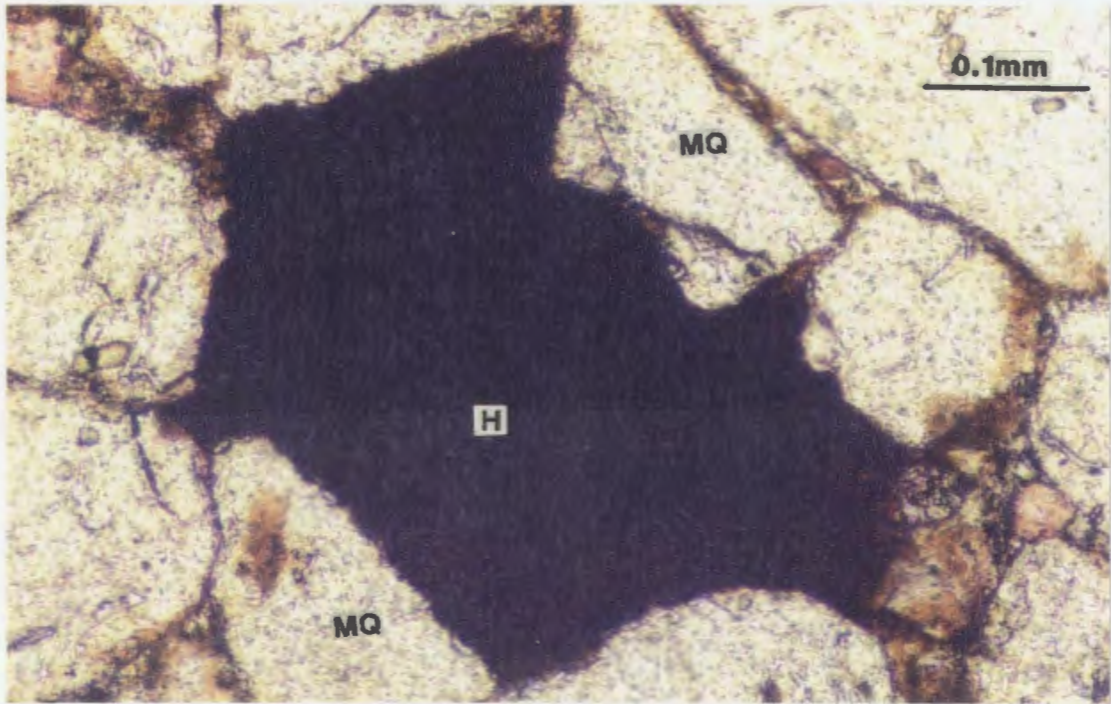
ZZ



ZZZ

APPENDIX IV

zzzz- Hydrocarbon (H) filling large pores between monocrystalline quartz (MQ) grains in reservoir sandstone (sample from the oil column) in well C1-NC2 @ 9703ft (2958m).

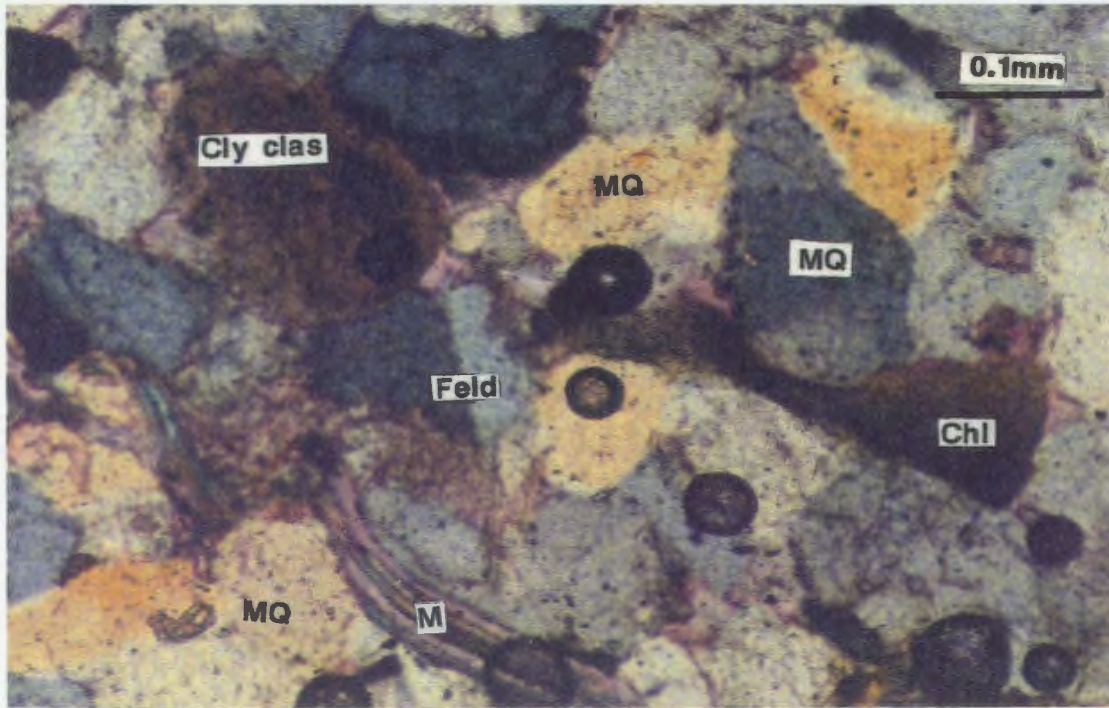


ZZZZ

APPENDIX IV

ZZZZZ- Deformation of some labile grains such as mica (M) sand chlorite (Chl) around the monocrystalline quartz (MQ) grains is very common in the silty sandstone (distal delta front) lithofacies, of well D1-61 @ 8420ft (2567m). Note, lack of intergranular pore-spaces associated with rock fragments. Detrital dark-brown clay clast (Cly clas) with very fine crystalline texture and partially dissolved feldspar (Feld) grains can also be seen.

X.N



ZZZZZ

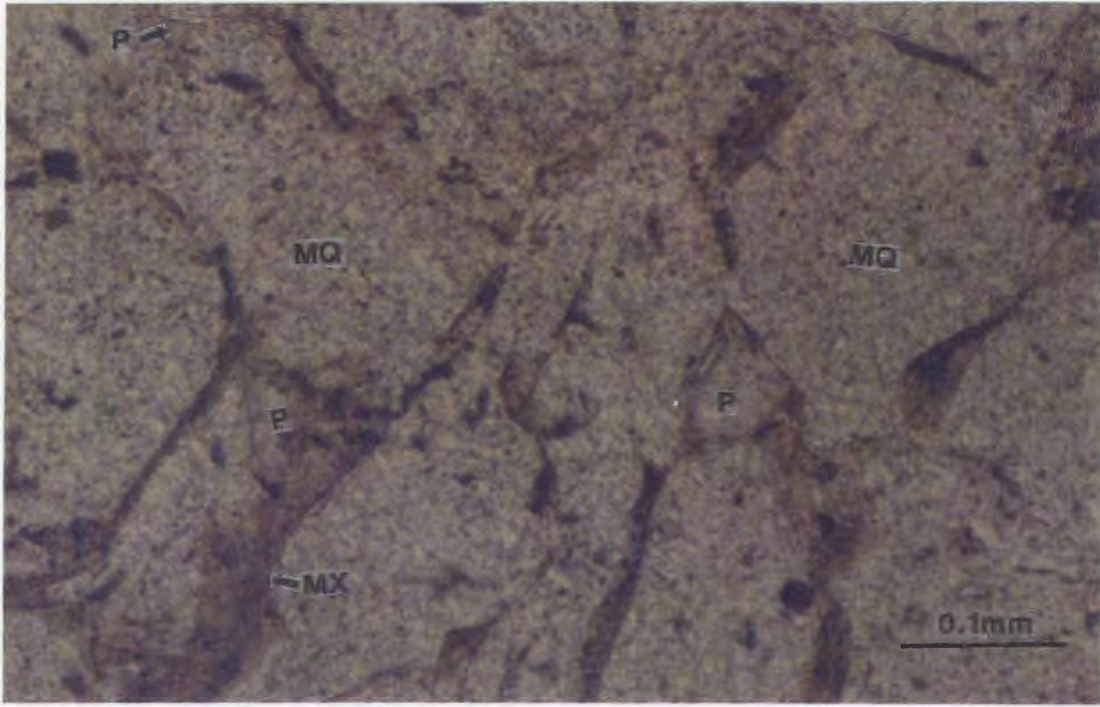
APPENDIX V

**Thin-Section-Porosity Type
of the Lower Acacus Formation,
NC2 Concession, Hamada Basin, NW Libya.**

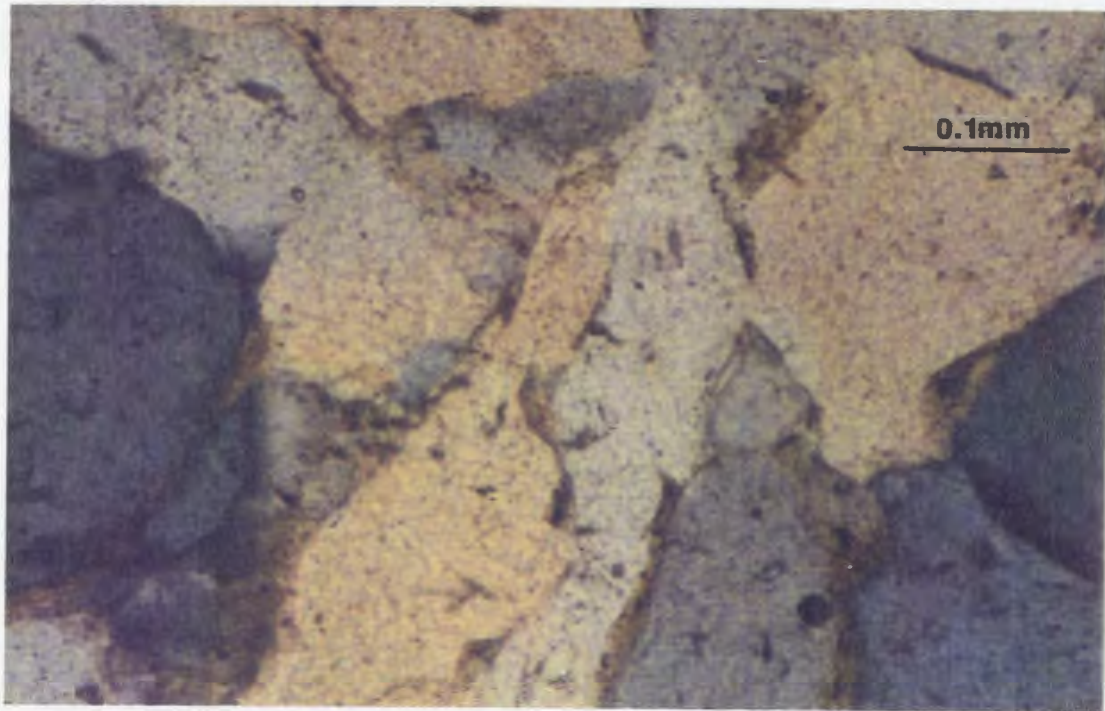
A-Thin-section photomicrographs showing residual primary porosity (P) in fine-medium grained, monocrystalline quartz (MQ) supported sandstone. Pores (P) are small, concavo-convex, triangular shape and of sharp, straight, uncorroded boundaries of the surrounding grains. Well T1-23 @ 8454ft (2577m).

Components are: monocrystalline quartz (MQ), clay-matrix (MX), primary porosity (P).

B- Same as previous photo but with partial crossed nicols (P.X.N).



A

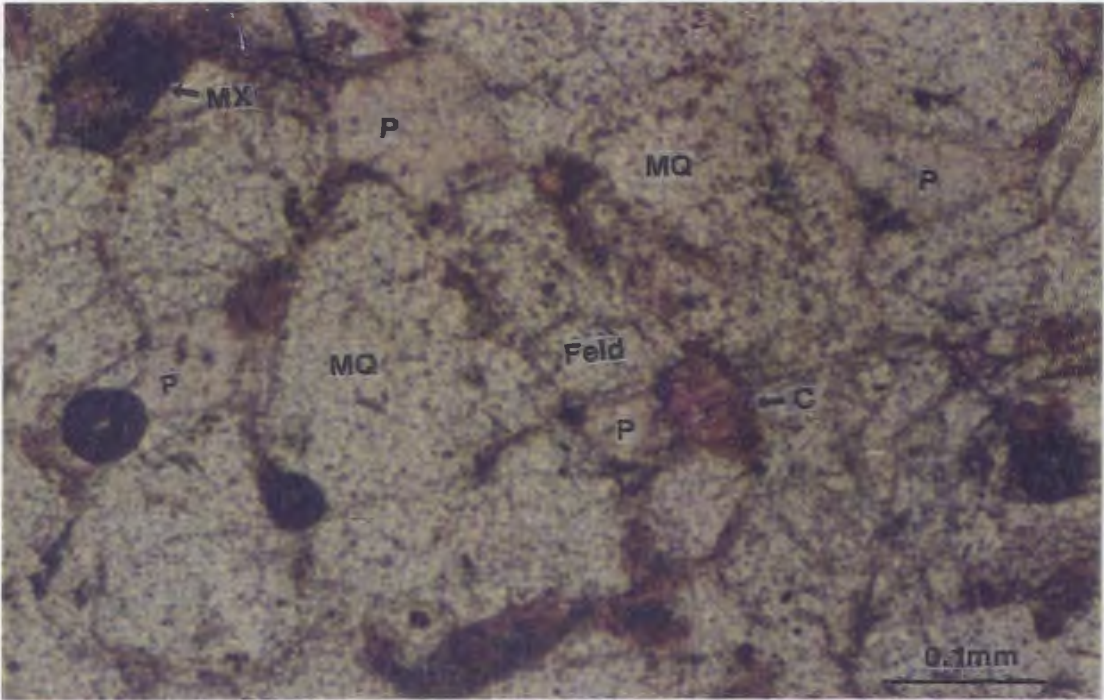


B

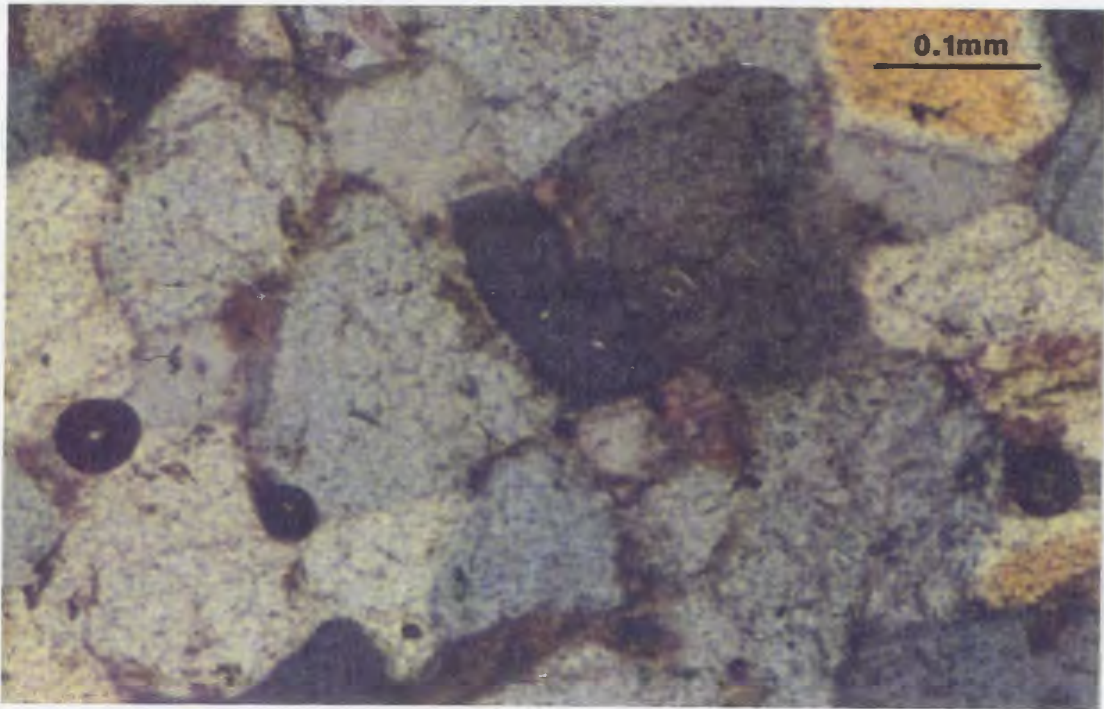
APPENDIX V

C- Thin-section photomicrographs showing secondary porosity (P) which is just replica of residual primary porosity in fine-medium grained, monocrystalline quartz (MQ) supported sandstone. Pores (P) are tiny with sharp uncorroded edges of adjacent quartz grains. Some pores show evidences of calcite (C) cement dissolution. Well B1-61 @ 8484ft (2587m). Components are: monocrystalline quartz (MQ), feldspar (Feld), calcite cement (C), clay-matrix (MX), secondary porosity (P).

D- Same as previous photo but with partial crossed nicols (P.X.N).



C



D

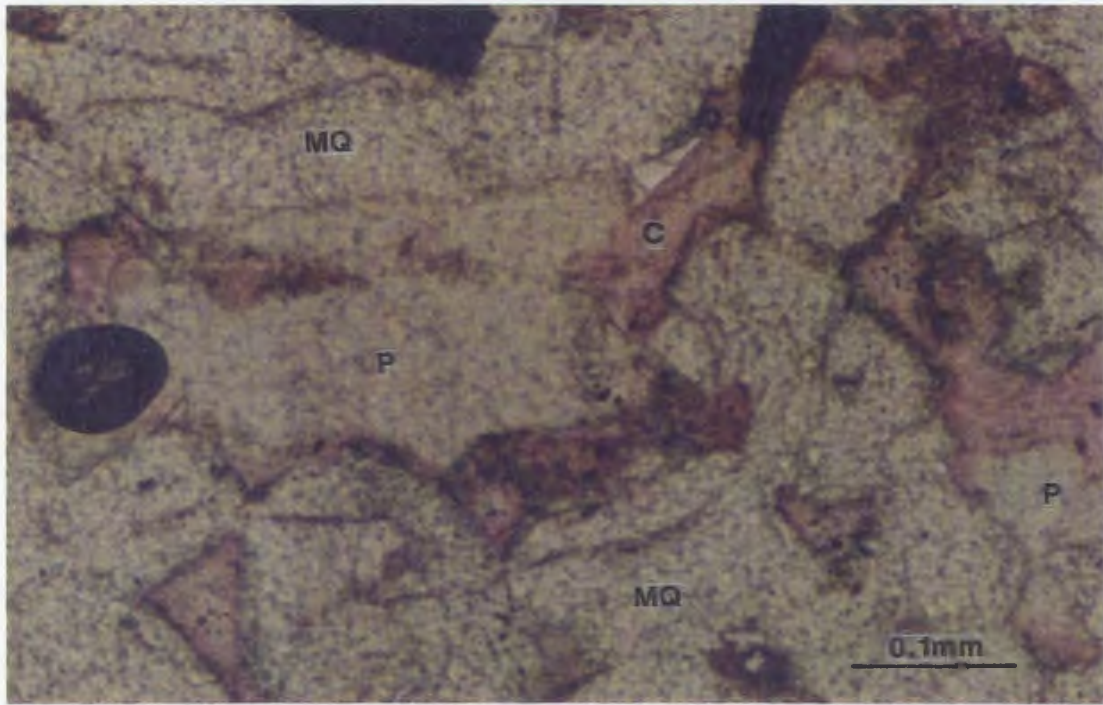
APPENDIX V

E- Thin-section photomicrographs showing secondary porosity (P) as a result of partial dissolution of calcite cement (C).

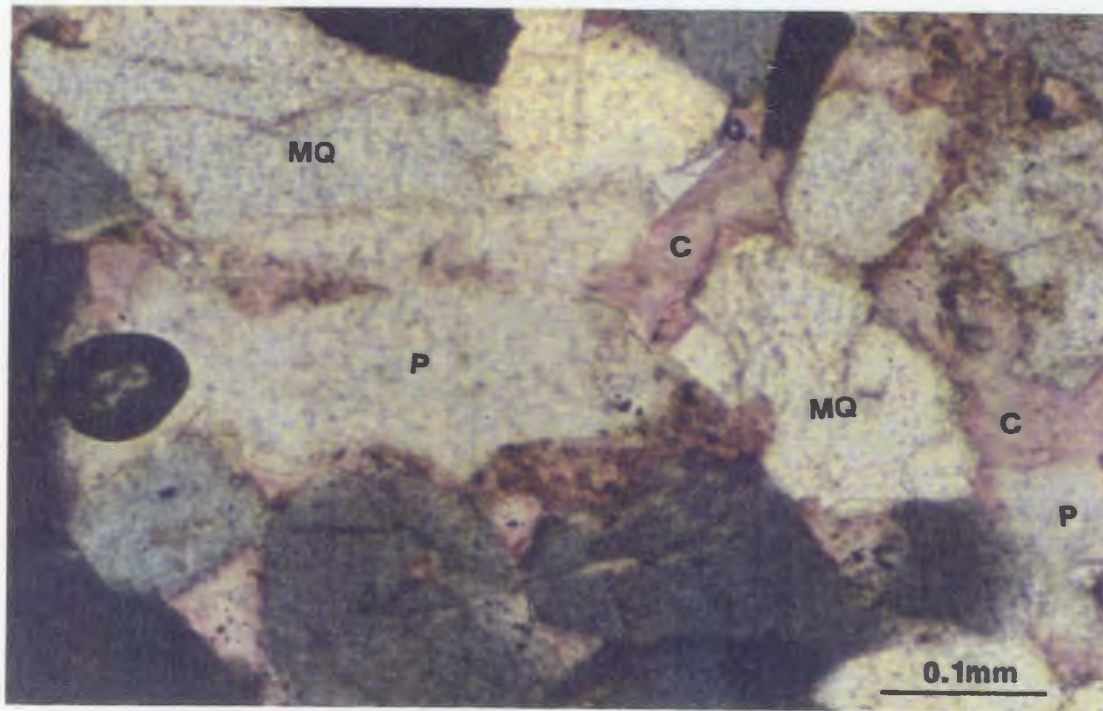
Note, remnant of non-dissolved calcite cement can be seen inside and at the edges of pores. Well C1-NC2 @ 9645ft (2940m).

Components are: monocrystalline quartz (MQ), calcite cement (C), secondary porosity (P).

F- Same as previous photo but with partial crossed nicols (P.X.N).



E



F

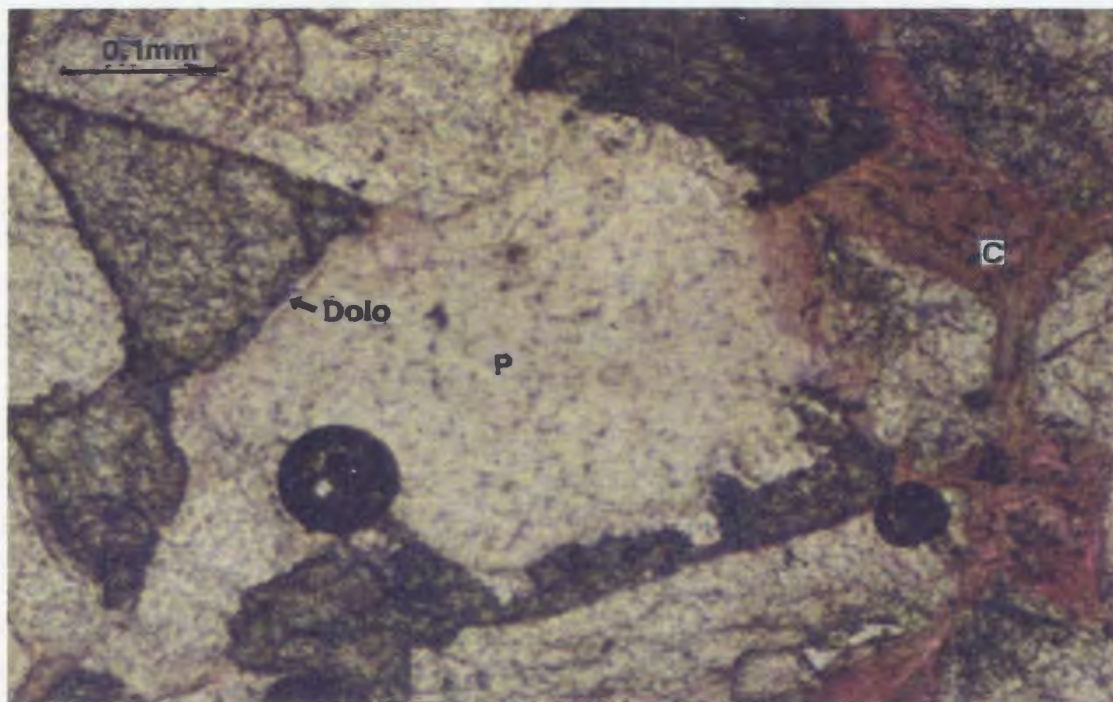
APPENDIX V

G- Thin-section photomicrographs showing secondary porosity (P) as a result of partial dissolution of dolomite cement (Dolo).

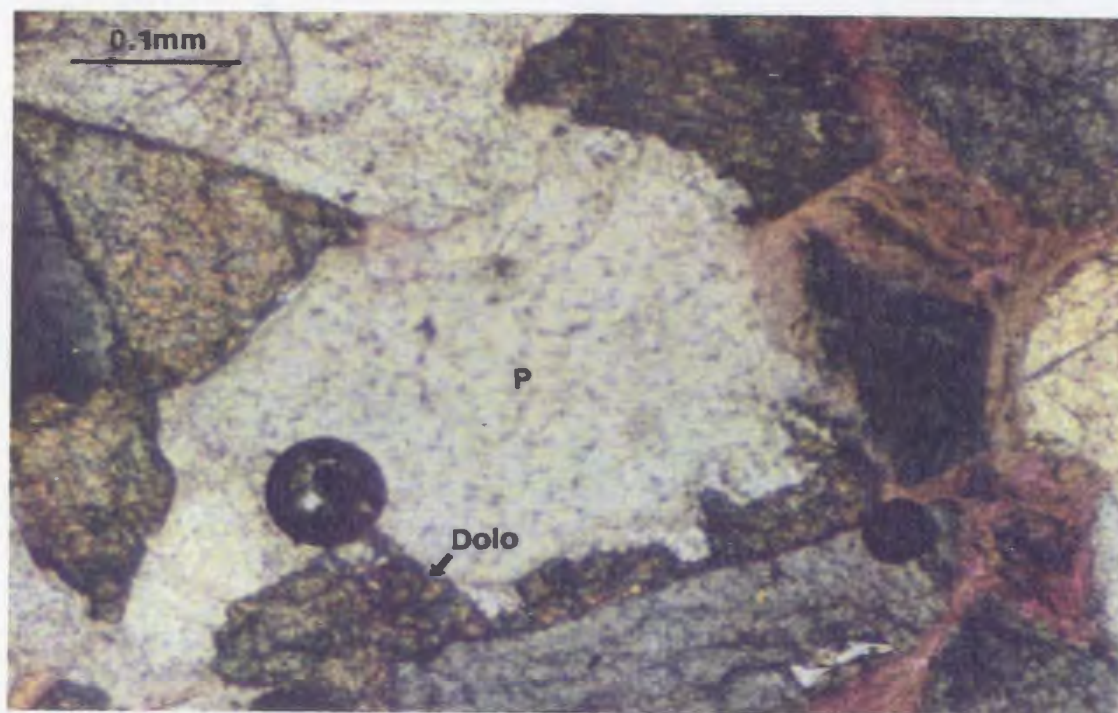
Note, remnant of non-dissolved dolomite cement can be seen at the edges of the pore (P). Well E1-NC2 @ 9131ft (2784m).

Components are : monocrystalline quartz (MQ), dolomite cement (Dolo), calcite cement (C), secondary porosity (P).

H- Same view as previous photo but with partial crossed nicols (P.X.N).



G



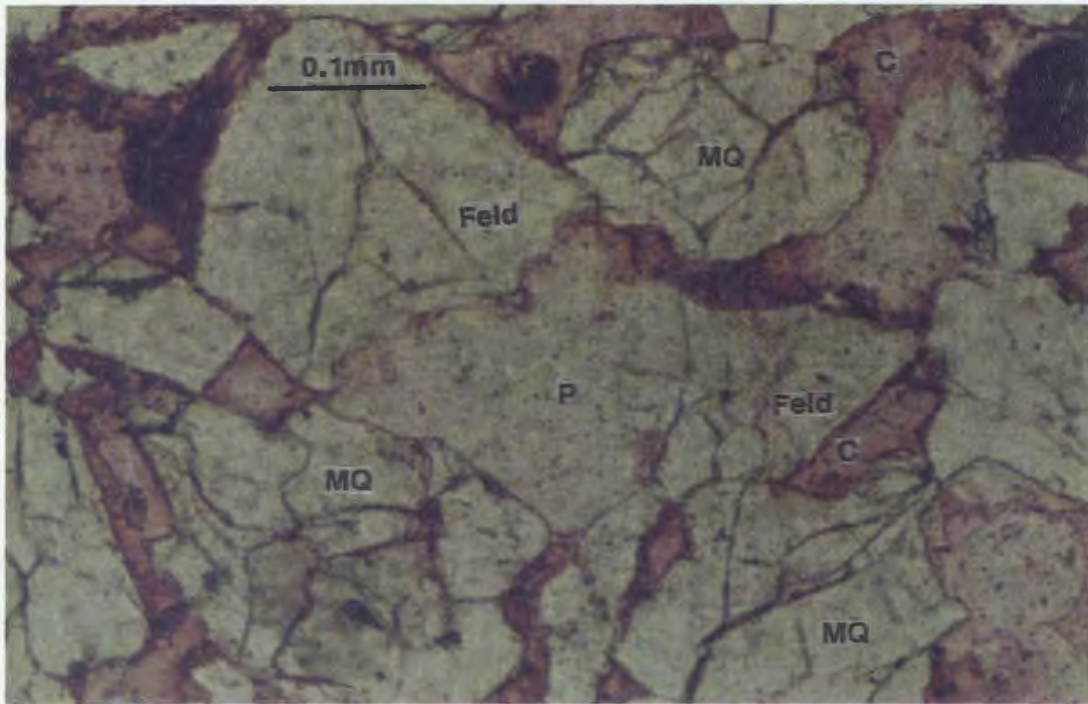
H

APPENDIX V

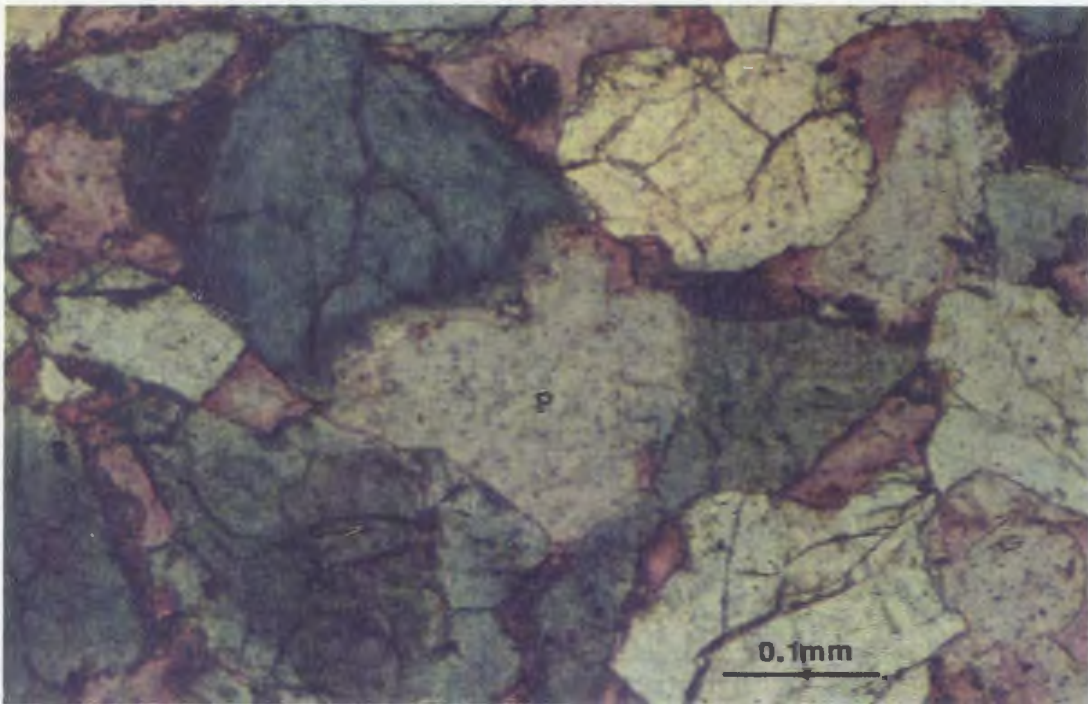
I- Thin-section photomicrographs showing secondary porosity (P) resulted from partial dissolution of unstable feldspar (Feld) grain (incomplete molds). Well C1-61 @ 7522ft (2293m).

Components are: monocrystalline quartz (MQ), feldspar (Feld), calcite cement (C), secondary porosity (P).

J- Same view as previous photo but with partial crossed nicols (P.X.N).



I



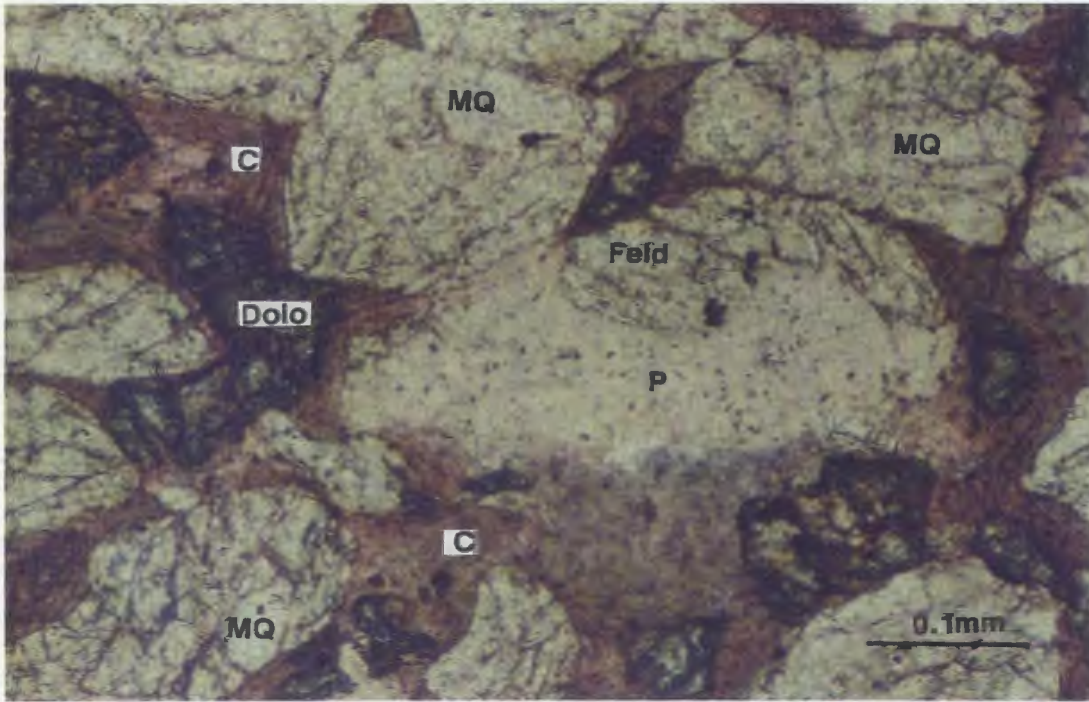
J

APPENDIX V

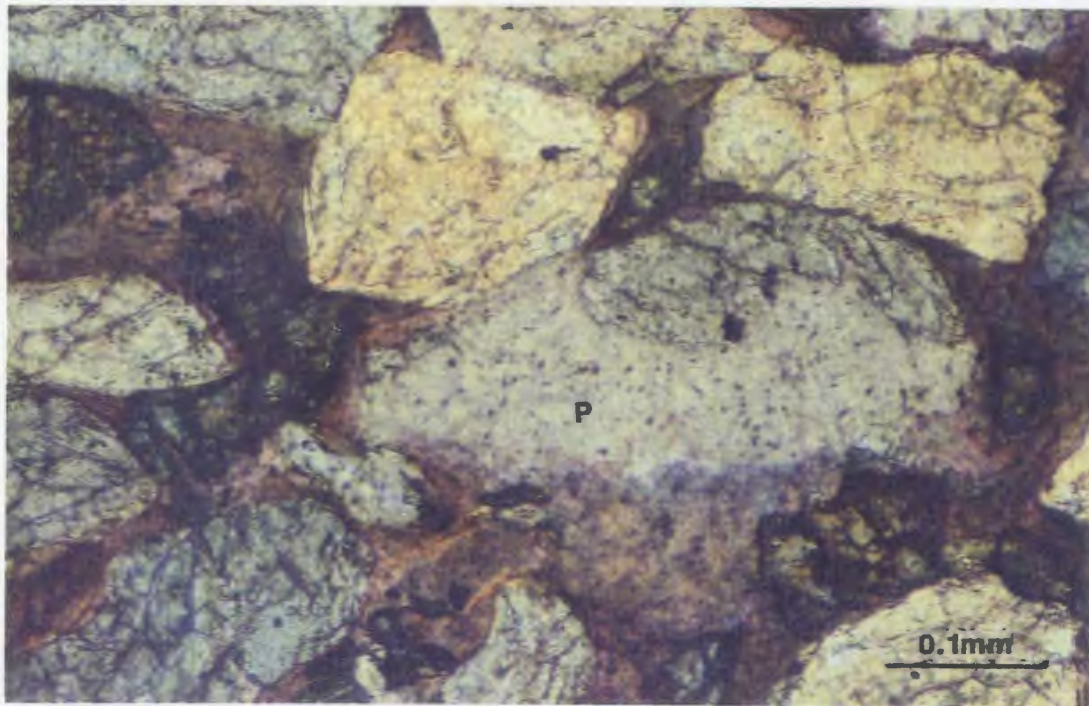
K- Thin-section photomicrographs showing secondary porosity (P) resulted from partial dissolution of unstable feldspar (Feld) grain (remnant of the non-dissolved feldspar grain can be seen in the pore). Well B3-61 @ 8893ft (2711m).

Components are: monocrystalline quartz (MQ), feldspar (Feld), detrital dolomite (Dolo), calcite cement (C), secondary porosity (P).

L- Same view as previous photo but with partial crossed nicols (P.X.N).



K



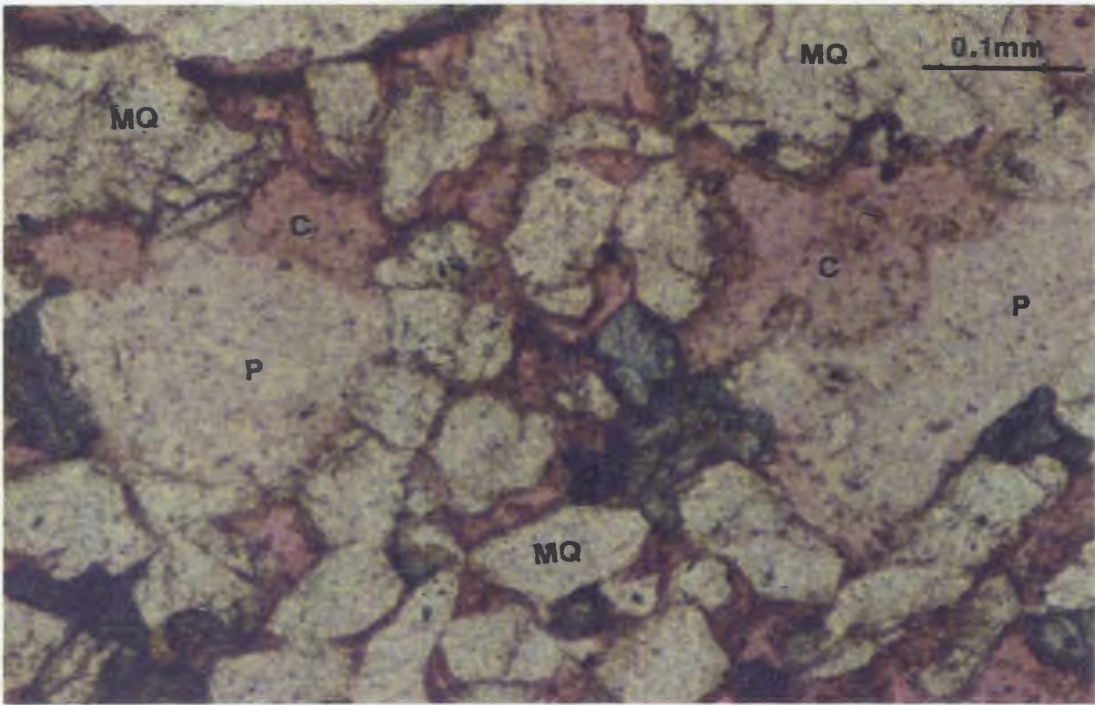
L

APPENDIX V

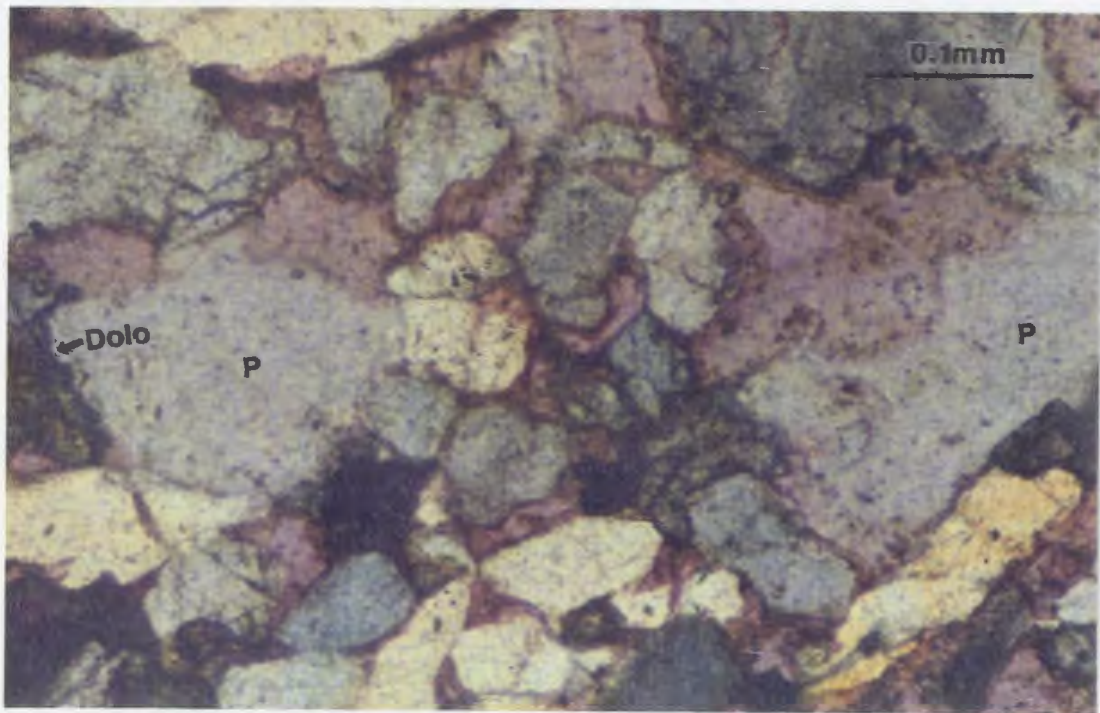
M- Thin-section photomicrographs showing pore-filling calcite cement (C) partially dissolved to produce secondary porosity (P). Well D1-61 @ 8236ft (2511m).

Components are: monocrystalline quartz (MQ), calcite cement (C), dolomite cement (Dolo), secondary porosity (P).

N- Same view as previous photo but with partial crossed nicols (P.X.N).



M

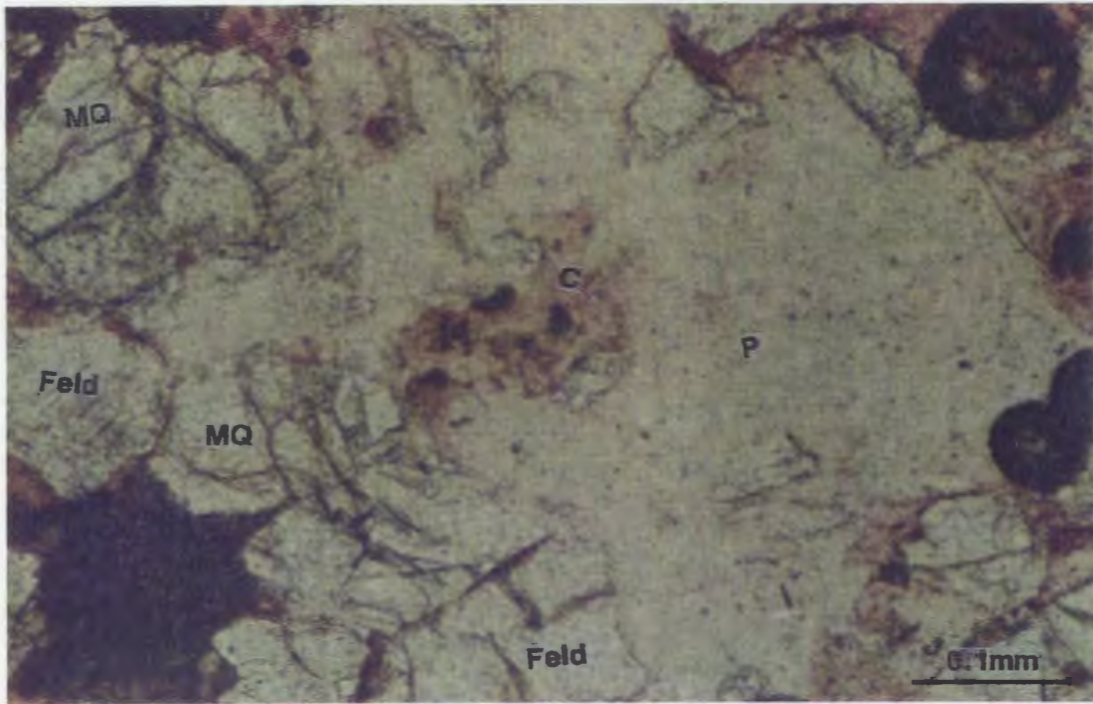


N

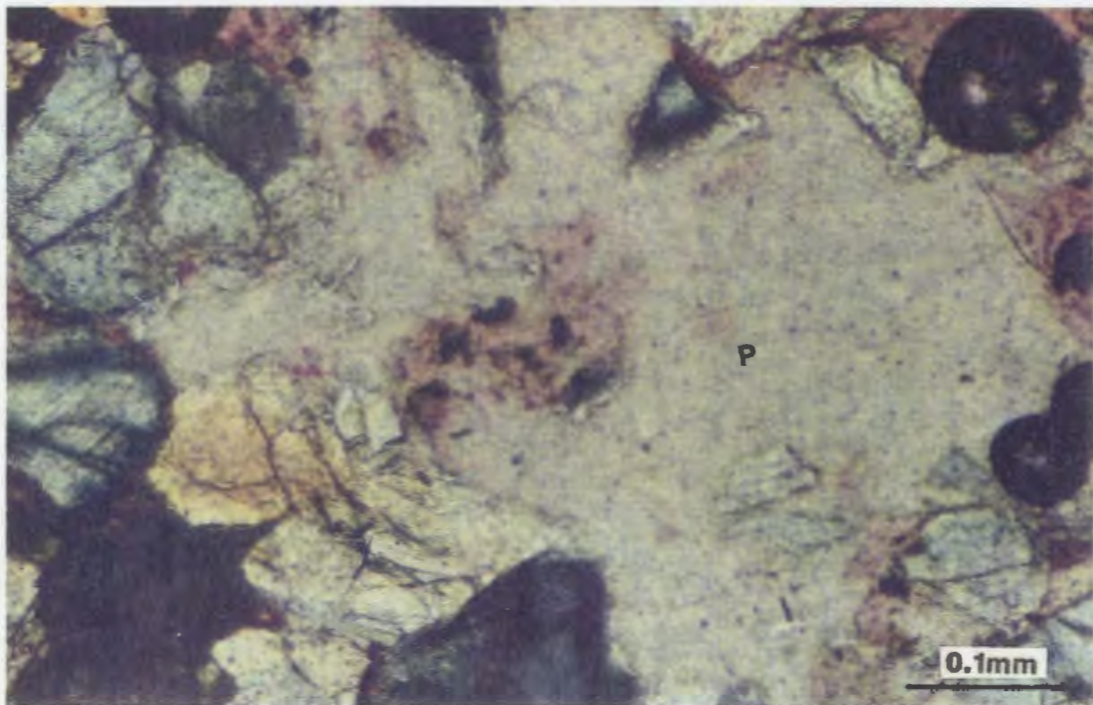
APPENDIX V

O- Thin-section photomicrographs showing oversized pores (P) resulted from near complete dissolution of calcite cement (C). Pores (P) with some floating grains and the surrounded quartz grains are heavily corroded. Well Q1-23 @ 8180ft (2494m). Components are: monocrystalline quartz (MQ), feldspar (Feld), calcite cement (C), secondary porosity (P).

P- Same view as previous photo but with partial crossed nicols (P.X.N).



O



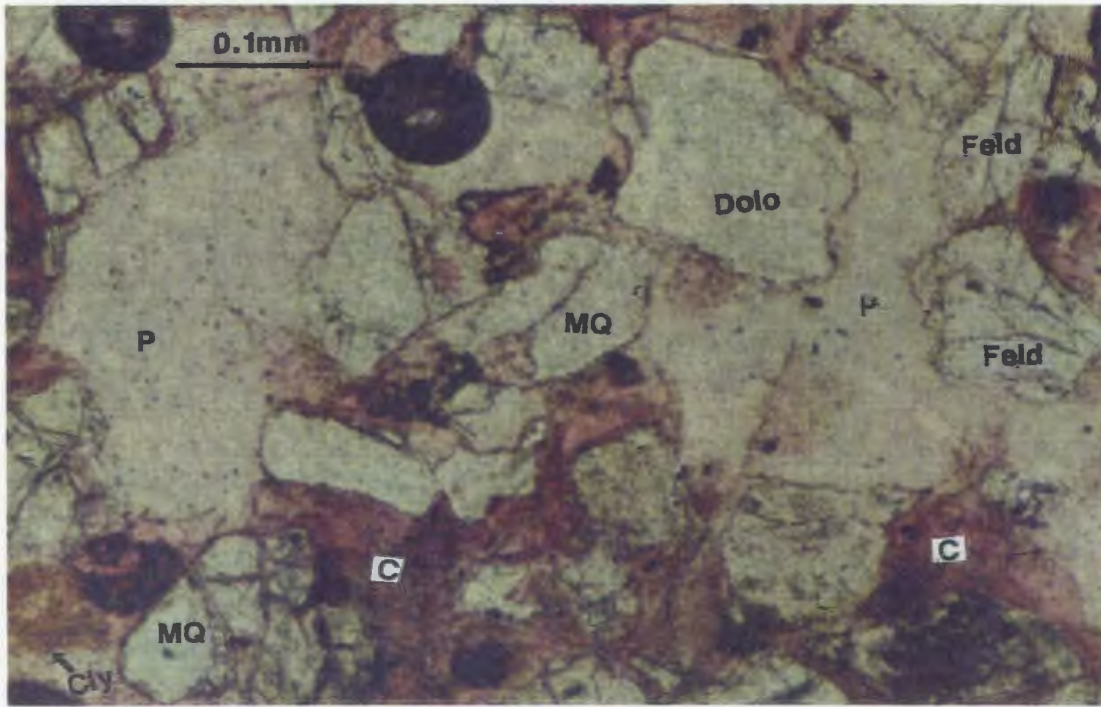
P

APPENDIX V

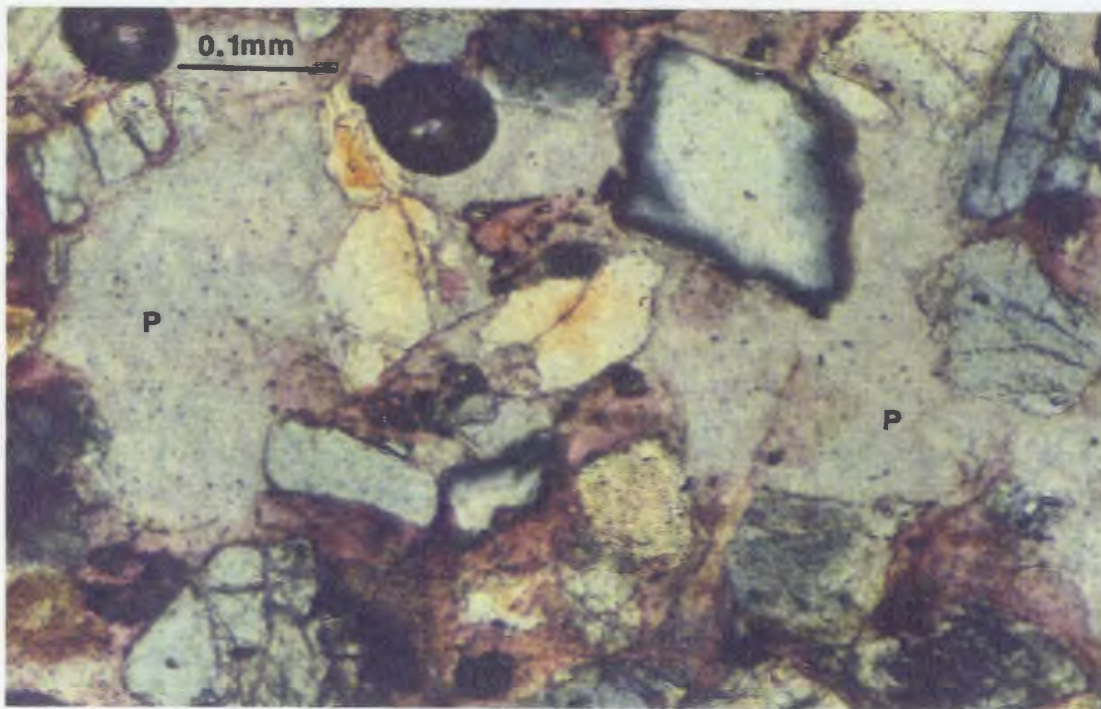
Q- Thin-section photomicrographs showing oversized pores (P) and inhomogeneous packing resulted from almost completely removed calcite cement (C). Note, the surrounded grains are heavily corroded by dissolved calcite cement. Well Q1-23 @ 8180ft (2494m).

Components are: monocrystalline quartz (MQ), feldspar (Feld), detrital dolomite (Dolo), clay minerals (Cly), calcite cement (C), secondary porosity (P).

R- Same view as previous photo but with partial crossed nicols (P.X.N).



Q

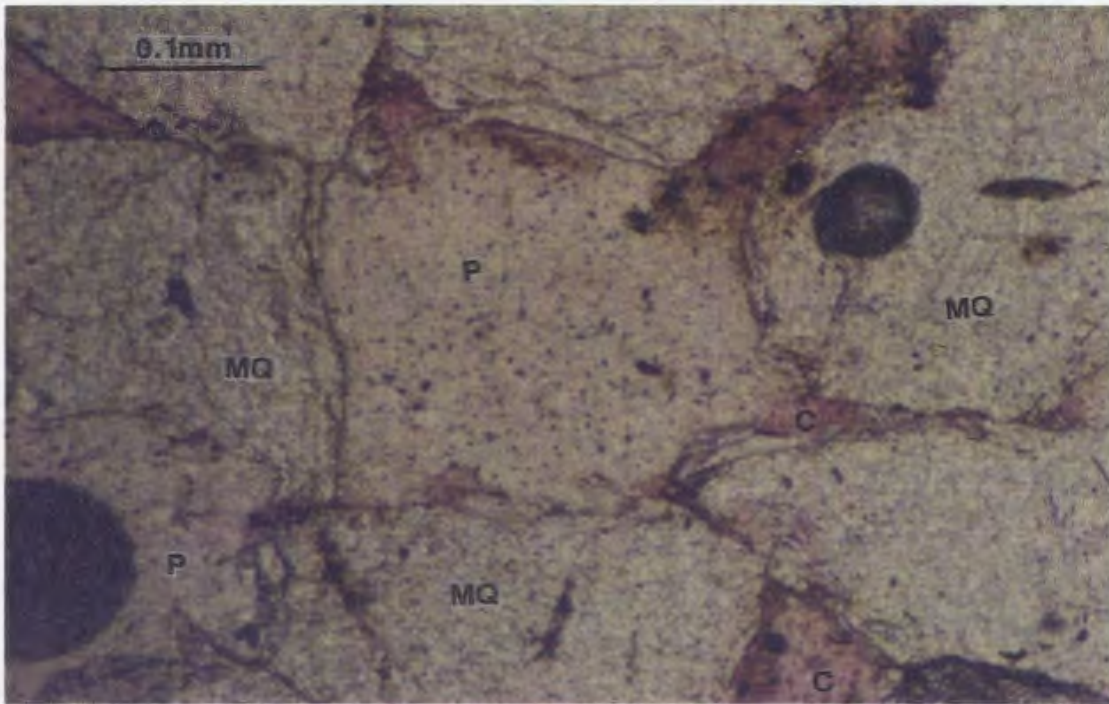


R

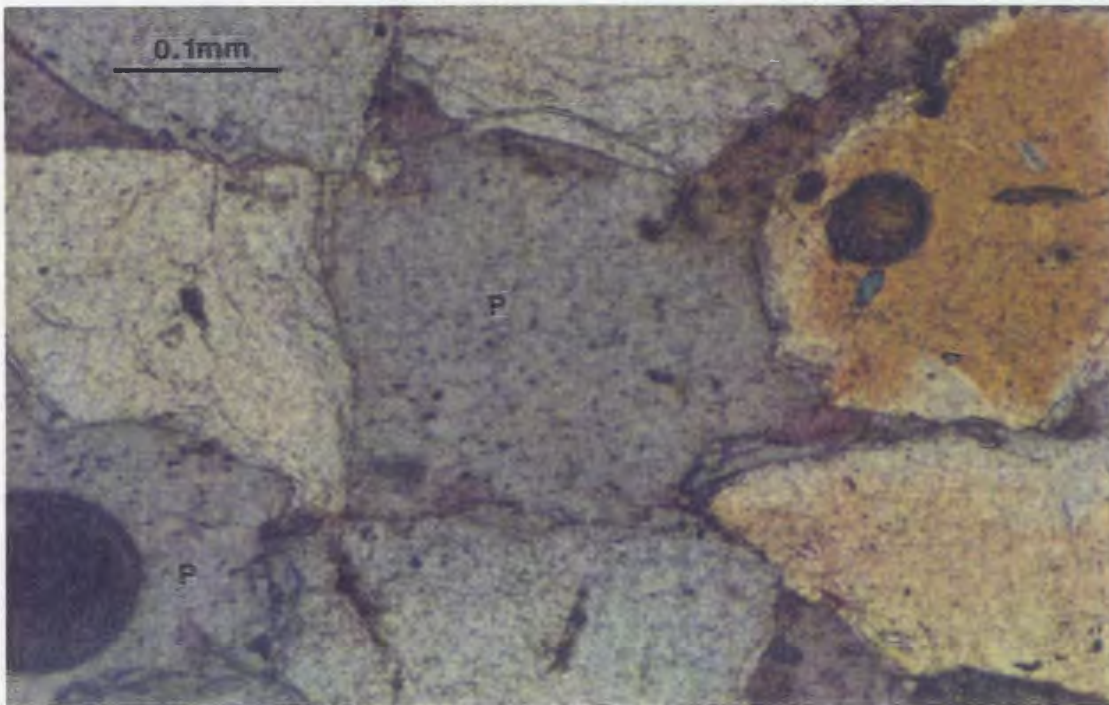
APPENDIX V

S- Thin-section photomicrographs showing secondary porosity (P) (recognizable molds) resulted from total dissolution of unstable grains where crystal outlines may be seen. Irregularity of pore edges occur with some corroded surrounded quartz grains. Well C1-NC2 @ 9703ft (2958m).
Components are: monocrystalline quartz (MQ), calcite cement (C), secondary porosity (P).

T- Same view as previous photo but with partial crossed nicols (P.X.N).



S



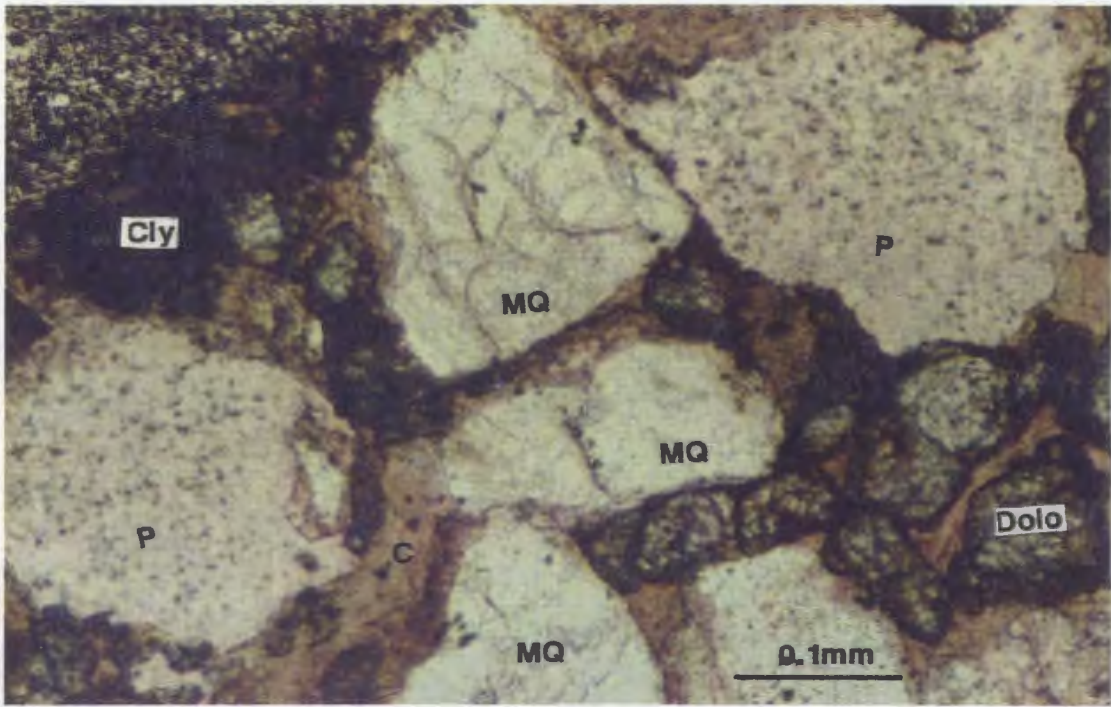
T

APPENDIX V

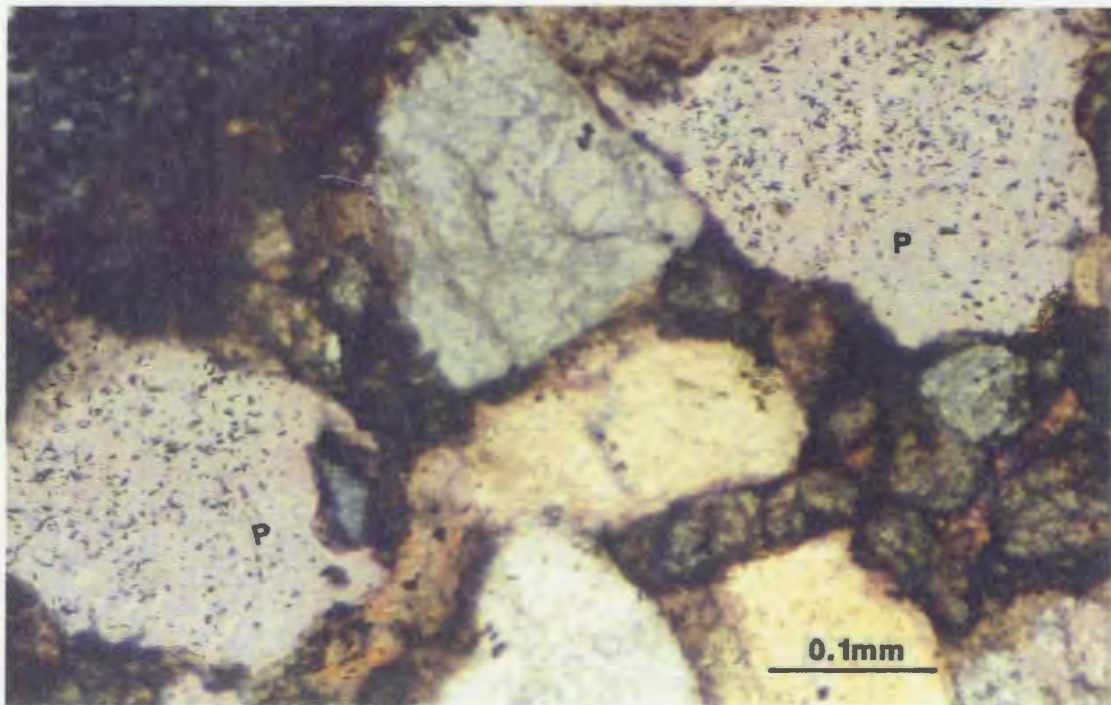
U- Thin-section photomicrographs showing recognizable molds of dissolved unstable grains; forming secondary porosity (P). Some remnant of the dissolved grain (probably feldspar (Feld) grain) may be seen inside the pore (at the left corner of the photo). Well B3-61 @ 8893ft (2711m).

Components are: monocrystalline quartz (MQ), feldspar (Feld), clay minerals (Cly), calcite cement (C), secondary porosity (P).

V- Same view as previous photo but with partial crossed nicols (P.X.N).



U



V

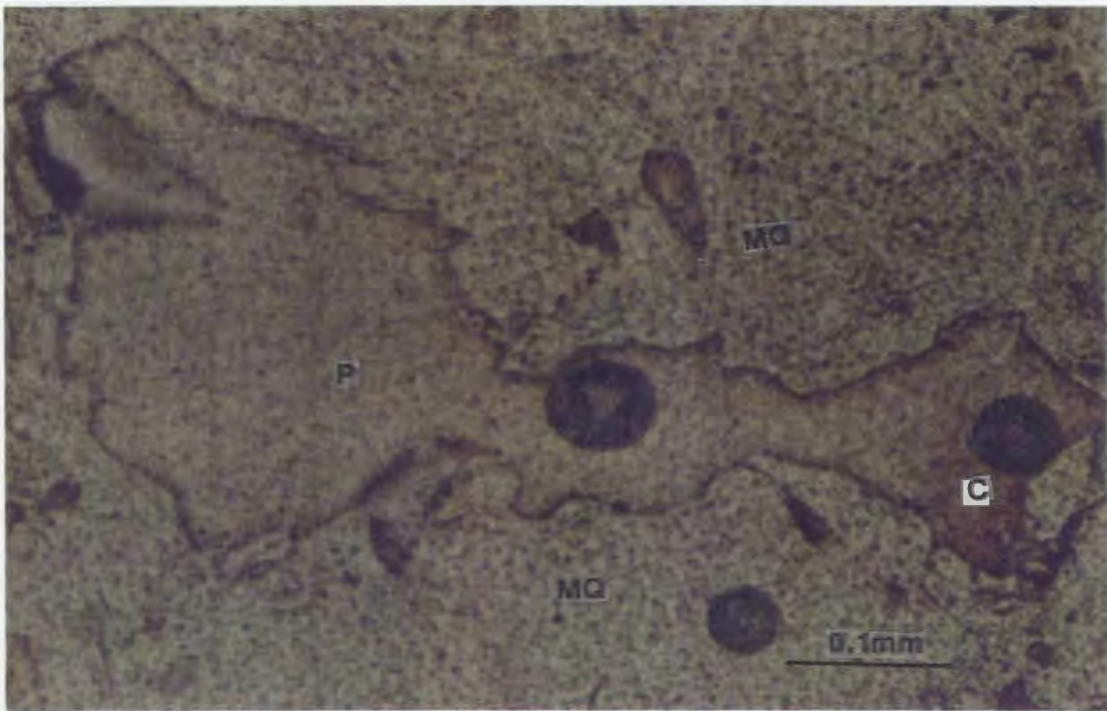
APPENDIX V

W- Thin-section photomicrography showing elongate pores (P) (<0.05mm) along the packed monocrystalline quartz grains (MQ); pores result from calcite cement (C) dissolution (calcite cement remnant is in the right side of the pore (P)). Heavily corroded surrounded quartz grains can be seen.

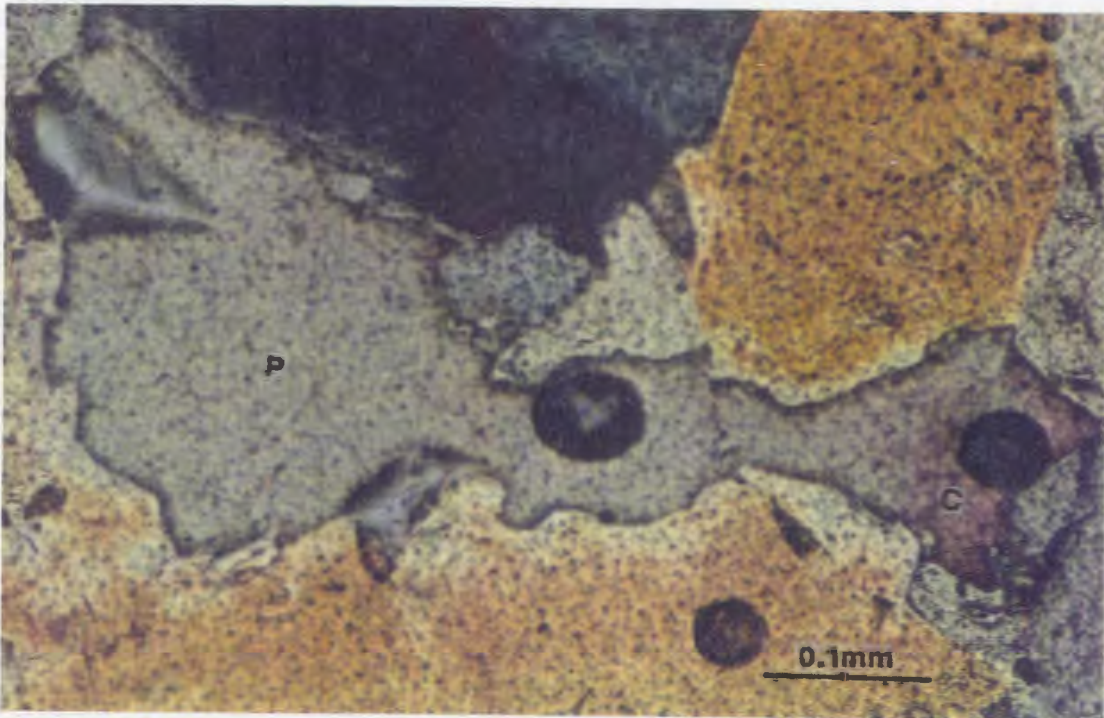
Well C1-NC2 @ 9725ft (2967m).

Components are: monocrystalline quartz (MQ), calcite cement (C), secondary porosity (P).

X- Same view as previous photo but with partial crossed nicols (P.X.N).



W



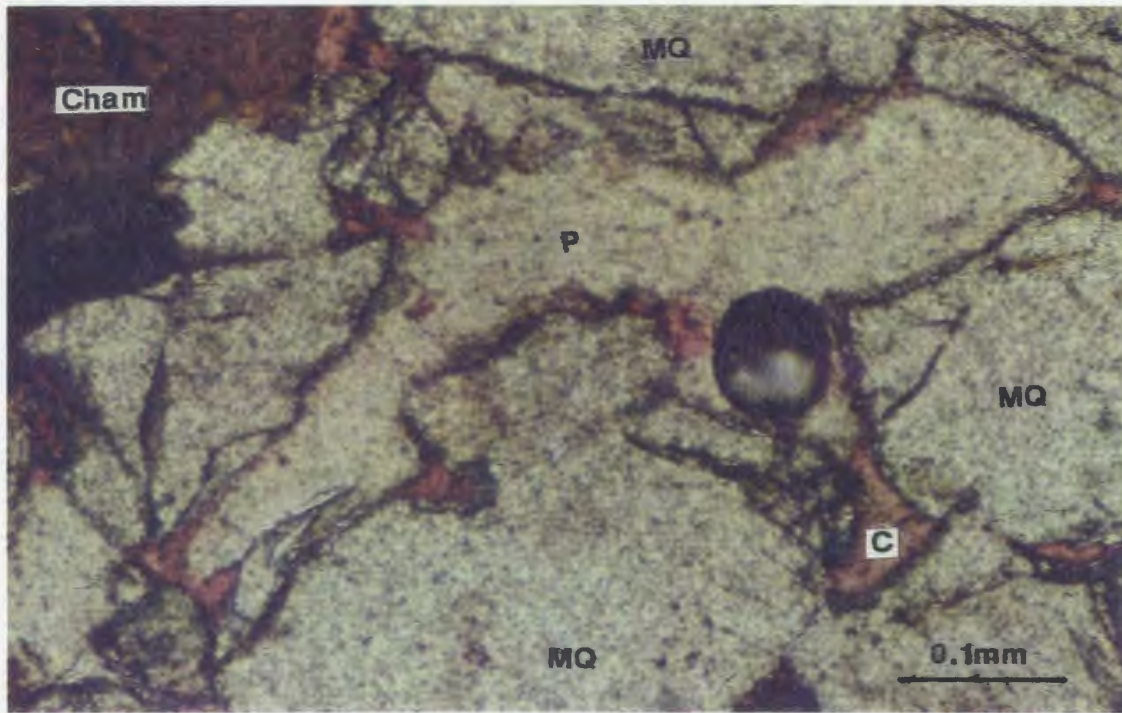
X

APPENDIX V

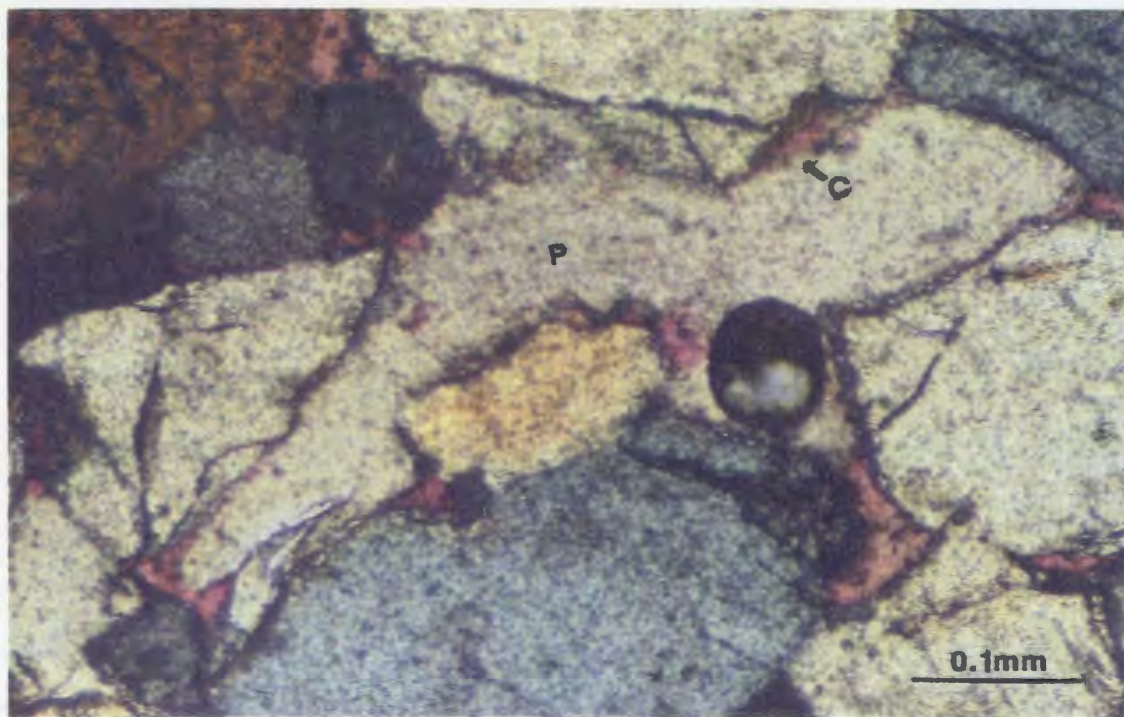
Y- Thin-section photomicrographs showing elongate pores (P) resulted from dissolution of calcite cement (C) along quartz grains (MQ) boundaries (remnant of calcite cement can be seen at some places inside the pore (P)). Well B1-61 @ 8420ft (2567m).

Components are: monocrystalline quartz (MQ), chamosite (Cham), calcite cement (C), secondary porosity (P).

Z- Same view as previous photo but with partial crossed nicols (P.X.N).



Y



Z

APPENDIX VI**Staining Method**

Prior to point counting, all thin sections examined in this study were stained for carbonates (calcite & dolomite) using Alizarin red S and Potassium Ferricyanide procedure recommended by Dickson (1965,1966). The method used for staining uncovered sandstone thin sections from the Lower Acacus Formation is here described in detail:

Dickson's method; Reagent:**Etching Solution:**

15ml of 36% Hcl dissolved in 500ml distilled water. Then topped up to 1000ml with distilled water.

Staining Solution:

- a- 0.2g. Alizarin red S dissolved in 100ml 1.5% Hcl solution.
- b- 2g. Potassium Ferricyanide crystals dissolved in 100ml 1.5% Hcl solution. (This solution must be freshly made for each staining session).
- c- Mix staining solutions a & b in the ratio 3 to 2.
(This combined solution lasts for one staining session).

Dickson's method; Procedure:

- 1- Immerse thin section in etching solution; for 10-15 seconds at 20°C.
- 2- Immerse the slide in dish of hot water before step (3) to avoid HCN fumes (gas).
- 3- Immerse specimen in the combined solution for 30-45 seconds.

(Best result will be obtained if the staining solution is warmed).

- 4- Wash the specimens gently using distilled water for a few seconds (hence, the stains are relatively soluble).
- 5- Dry the specimen surface quickly in a stream of warm air using hair drier or equivalent.

Note: Handle the specimen carefully; the stain is a thin surface film and is easily damaged.

This method produces the following colour differentiation between Calcite and Dolomite:

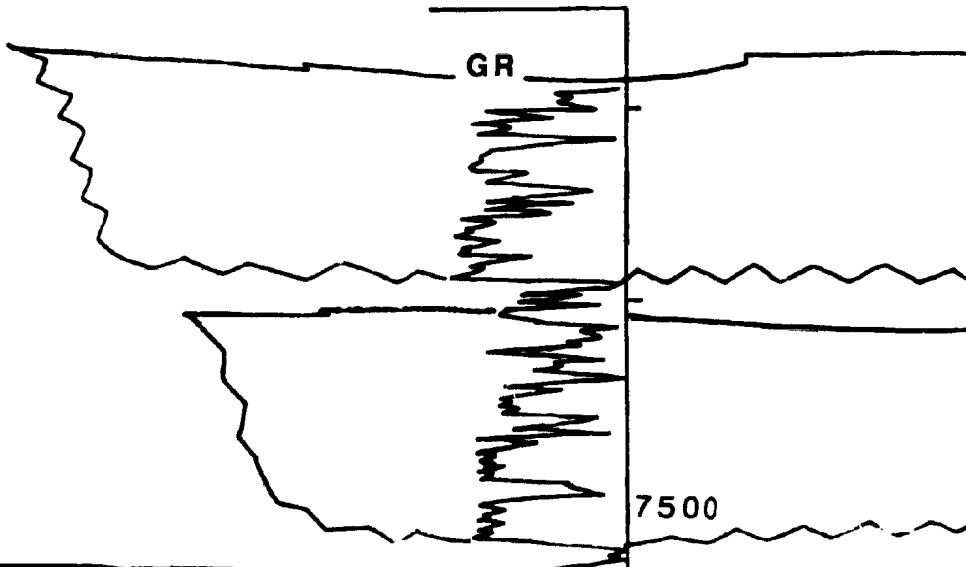
Calcite; varying from very pale pink to red.

Dolomite; no colour.

S

111-NC7

K.B.2076'



C7
76'

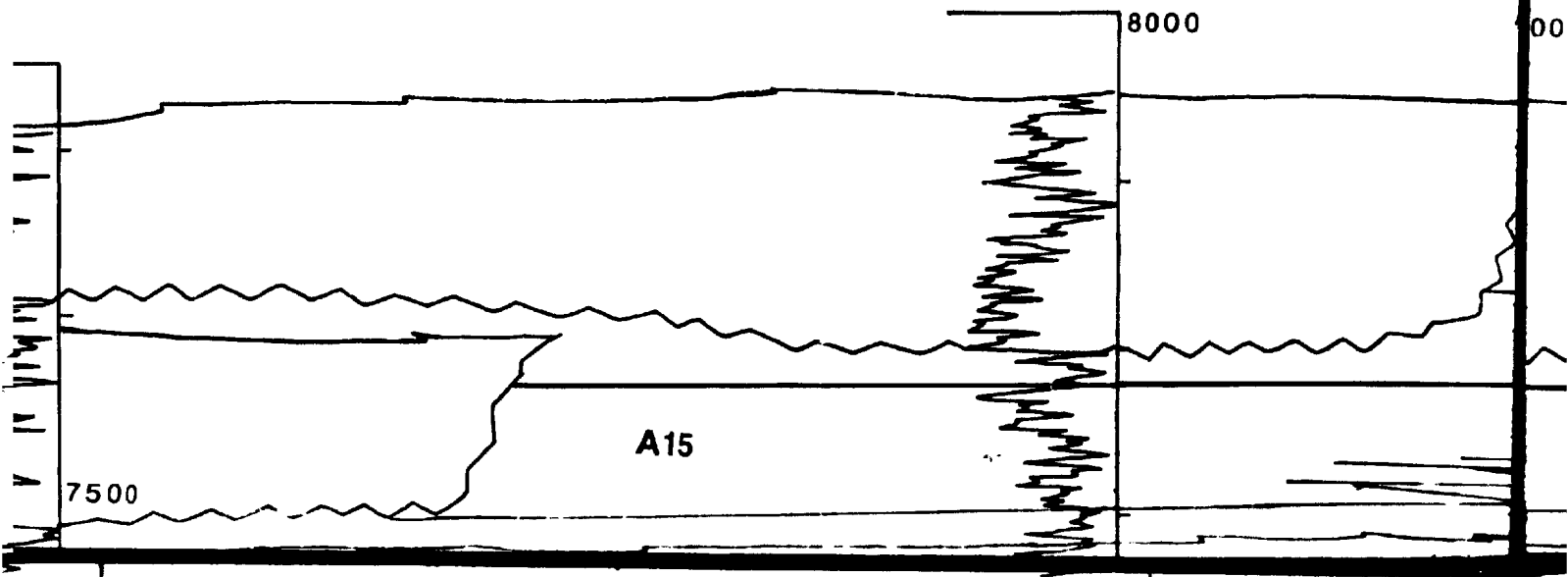
C1-NC7A
K.B.1990

A

40Km.



Hamada South

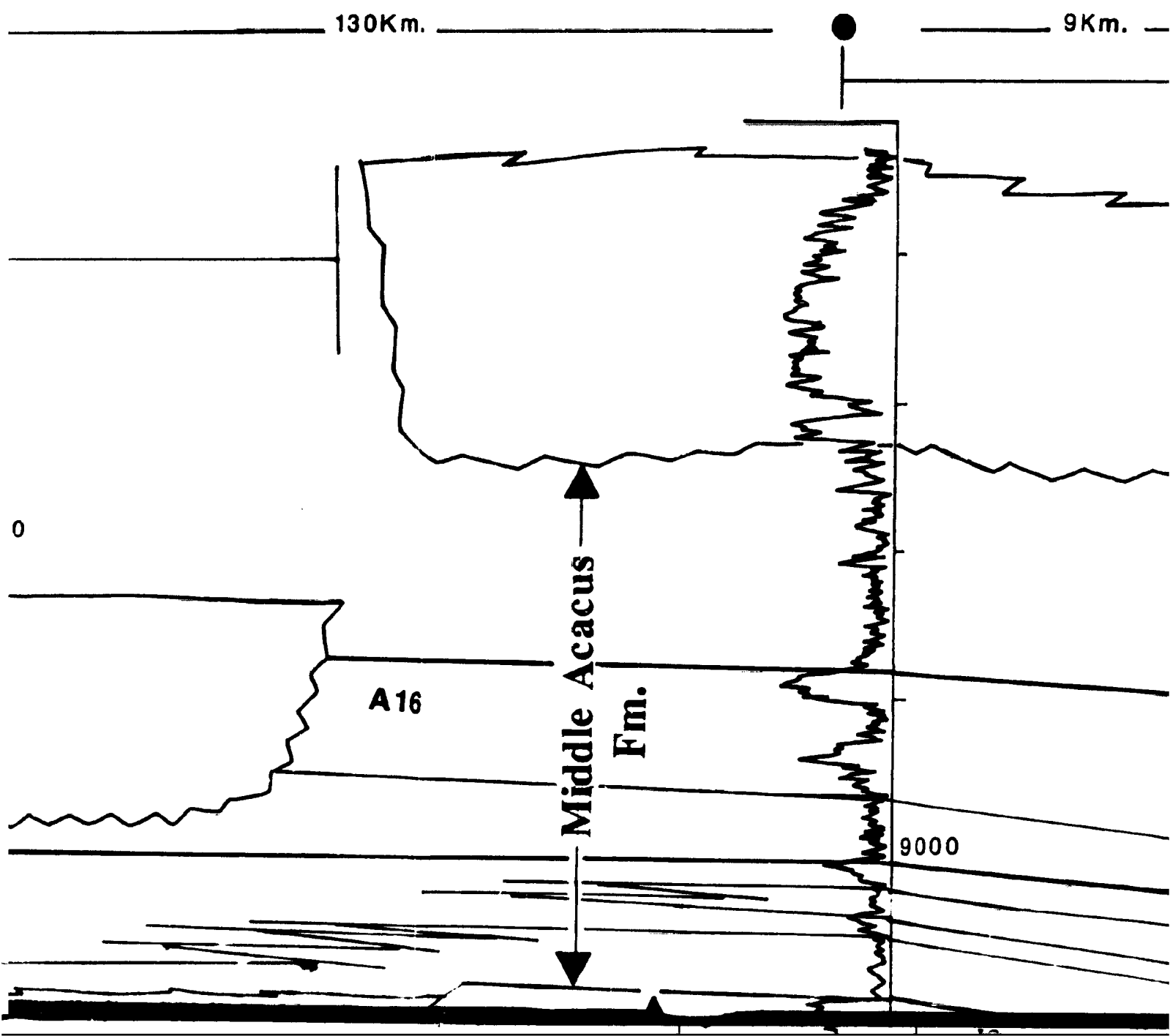


E1-NC2

K.B.1772

130Km.

9Km.



C1-NC2

K.B.1855

T1-23

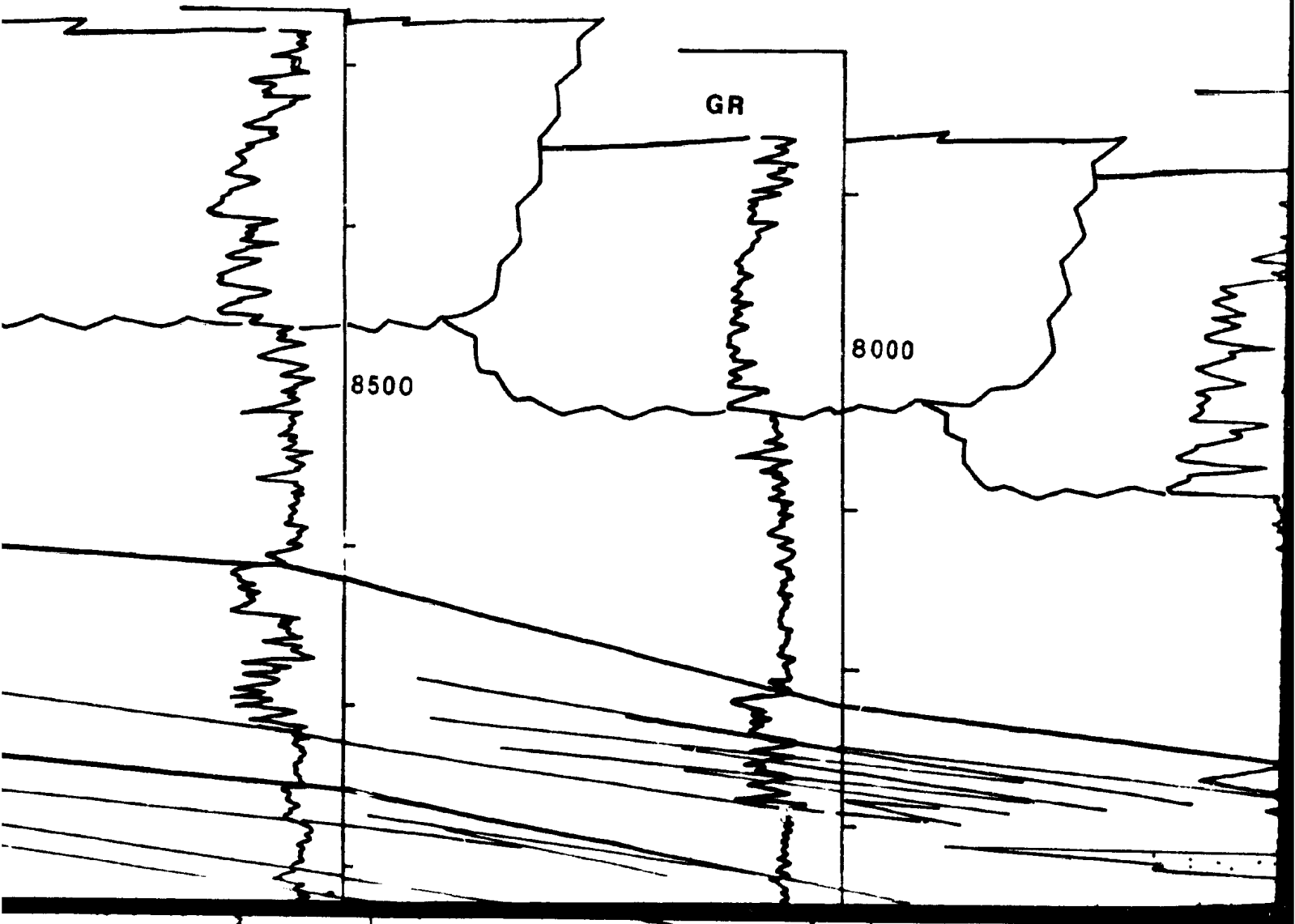
K.B.2056

E1-

K.B.2



NC2 Co



E1-23

K.B.2104

A1-NC2

K.B.2160

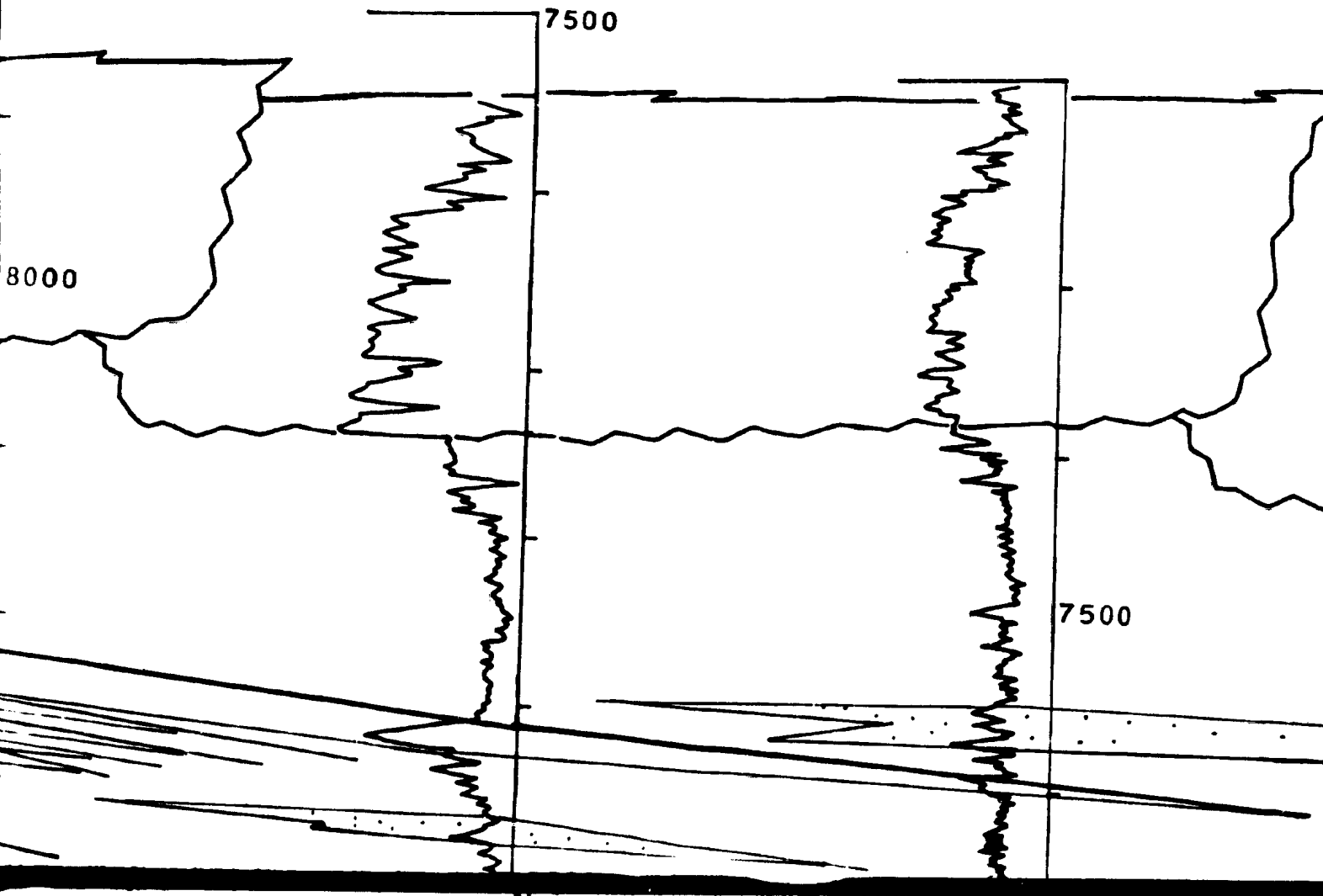
13Km.

15Km.

17Km.

Hamada North

NC2 Concession "Study Area"



2

Q1-23

K.B.2040

U1-23

K.B.2177

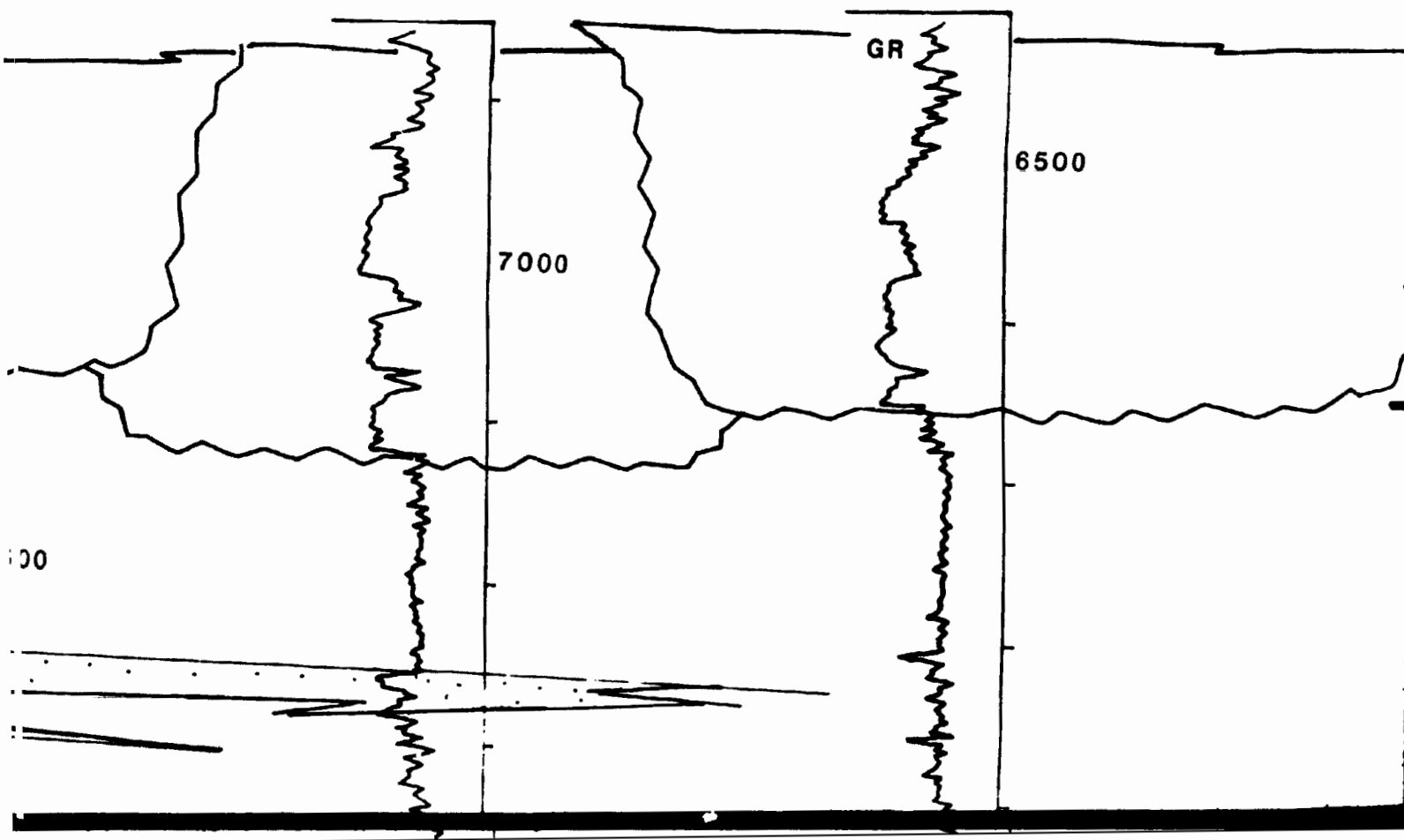
17Km.



19Km.



Outside Study Area



100

N

3

7



6500

Acacus Fm.
r Silurian

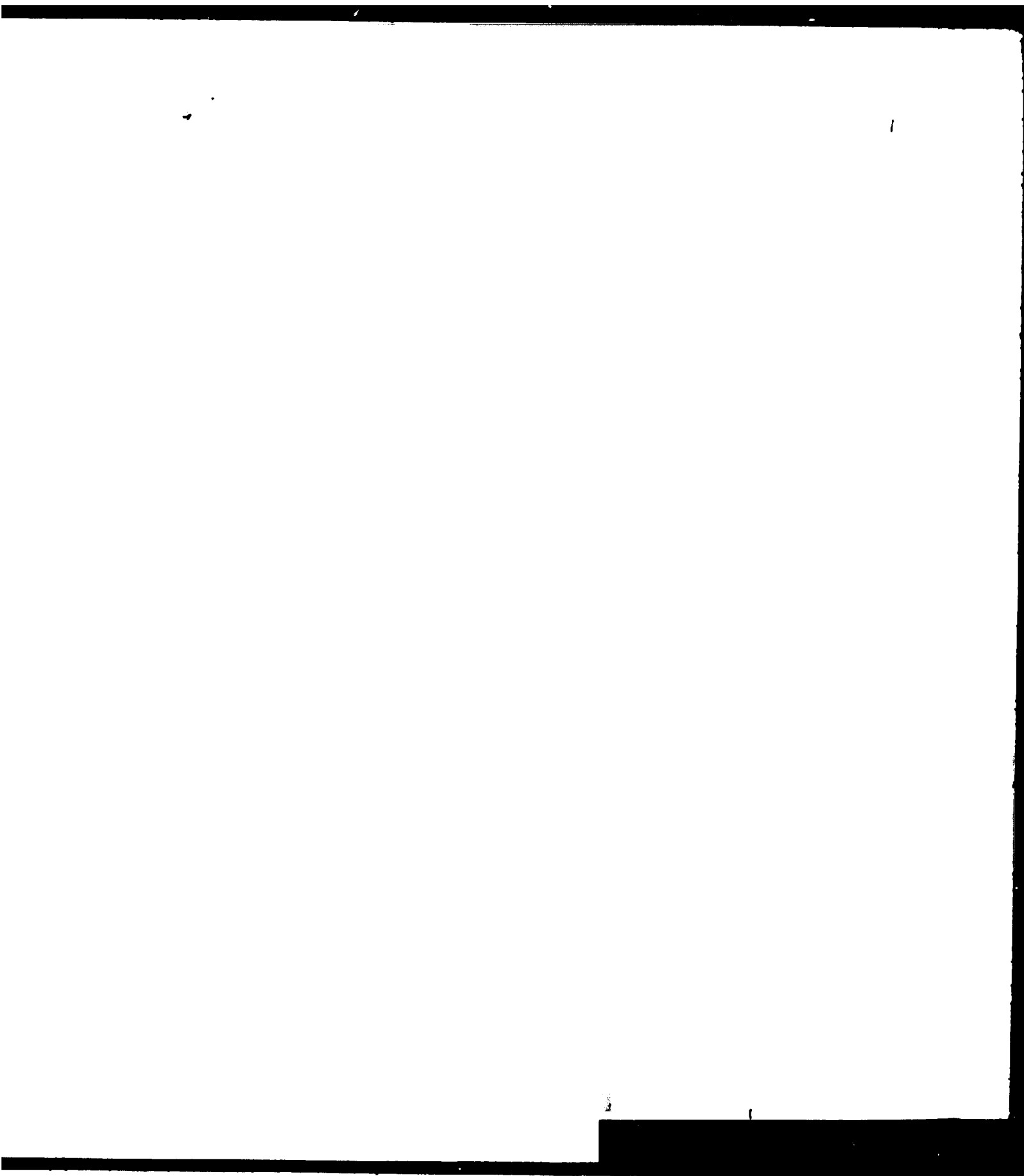


Upper Acacus Fm.

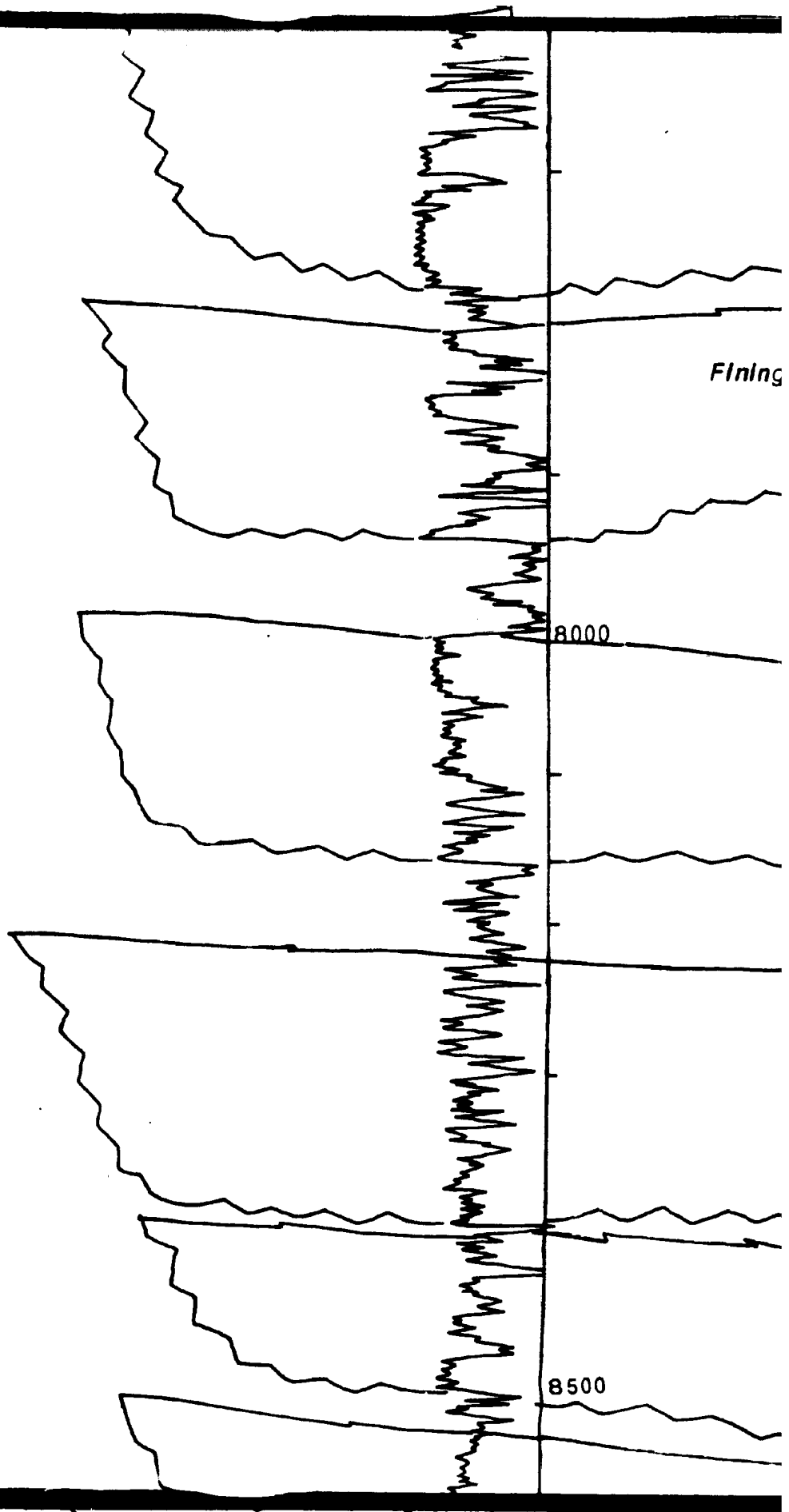


"Upper Silurian"





Acacus South Fm.



Flings

8000

8500

Fining-Upward Blocky Sand Log Facies

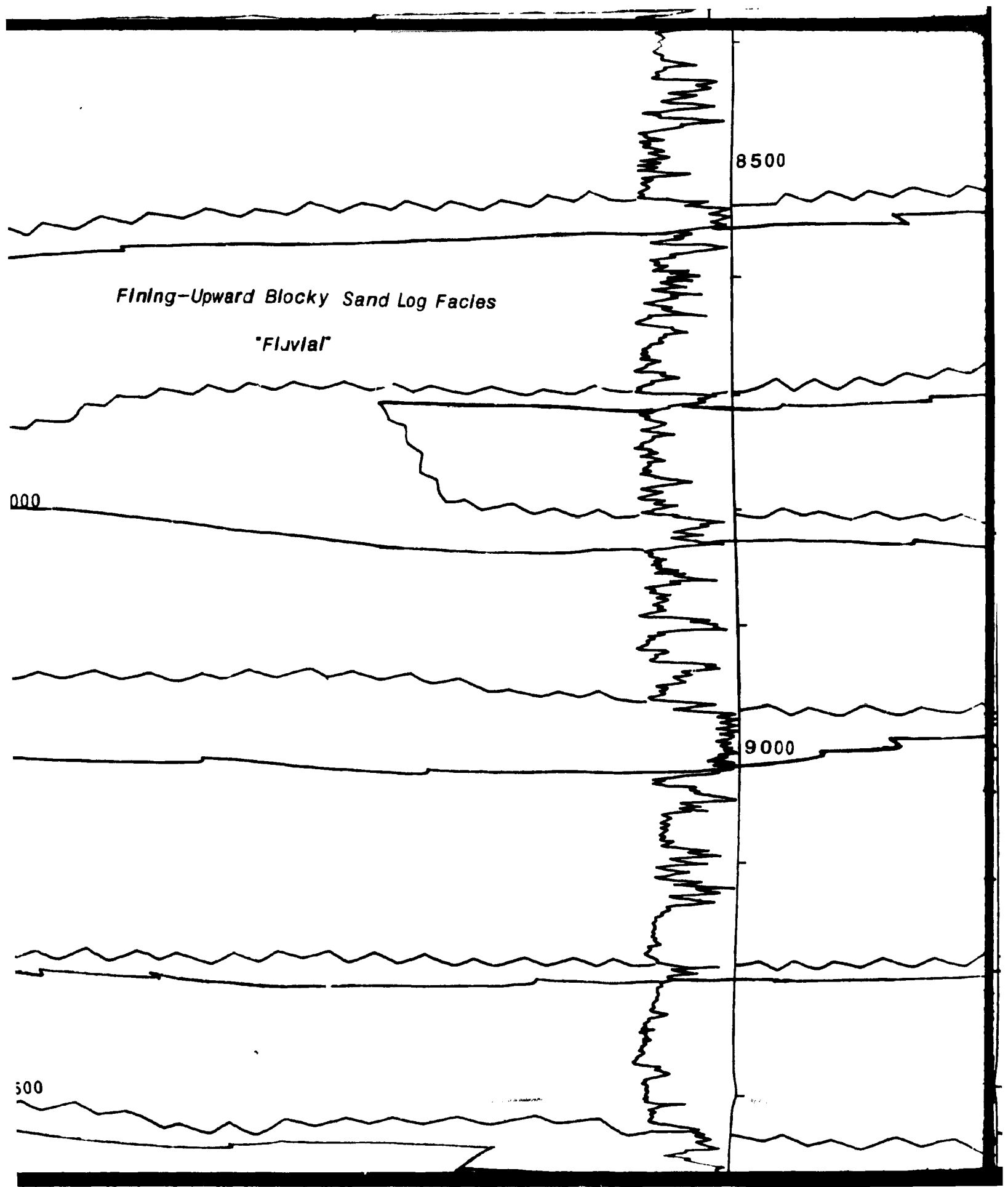
"Fluvial"

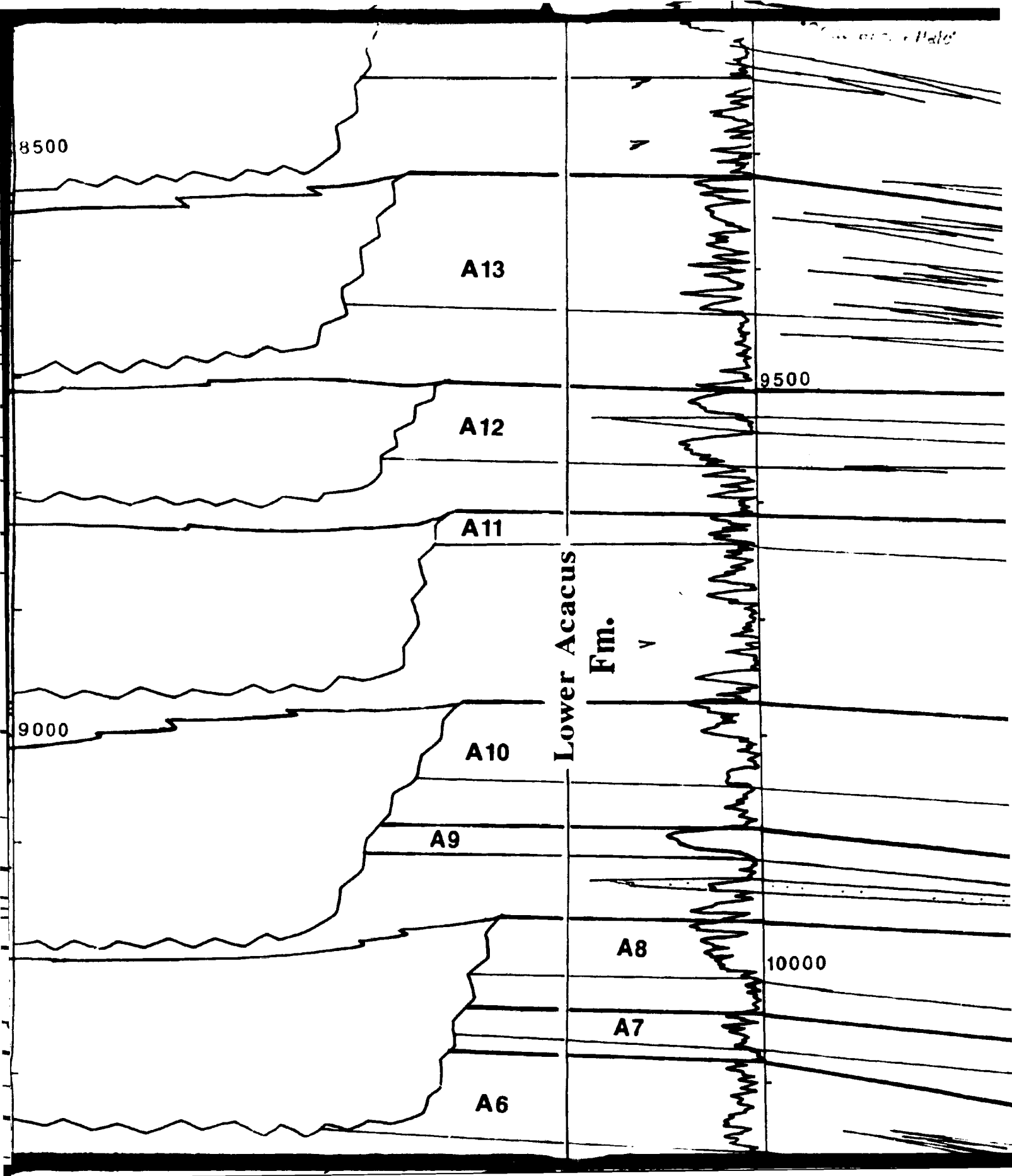
8500

000

9000

500





8500

A13

9500

A12

A11

Lower Acacus
Fm.

9000

A10

A9

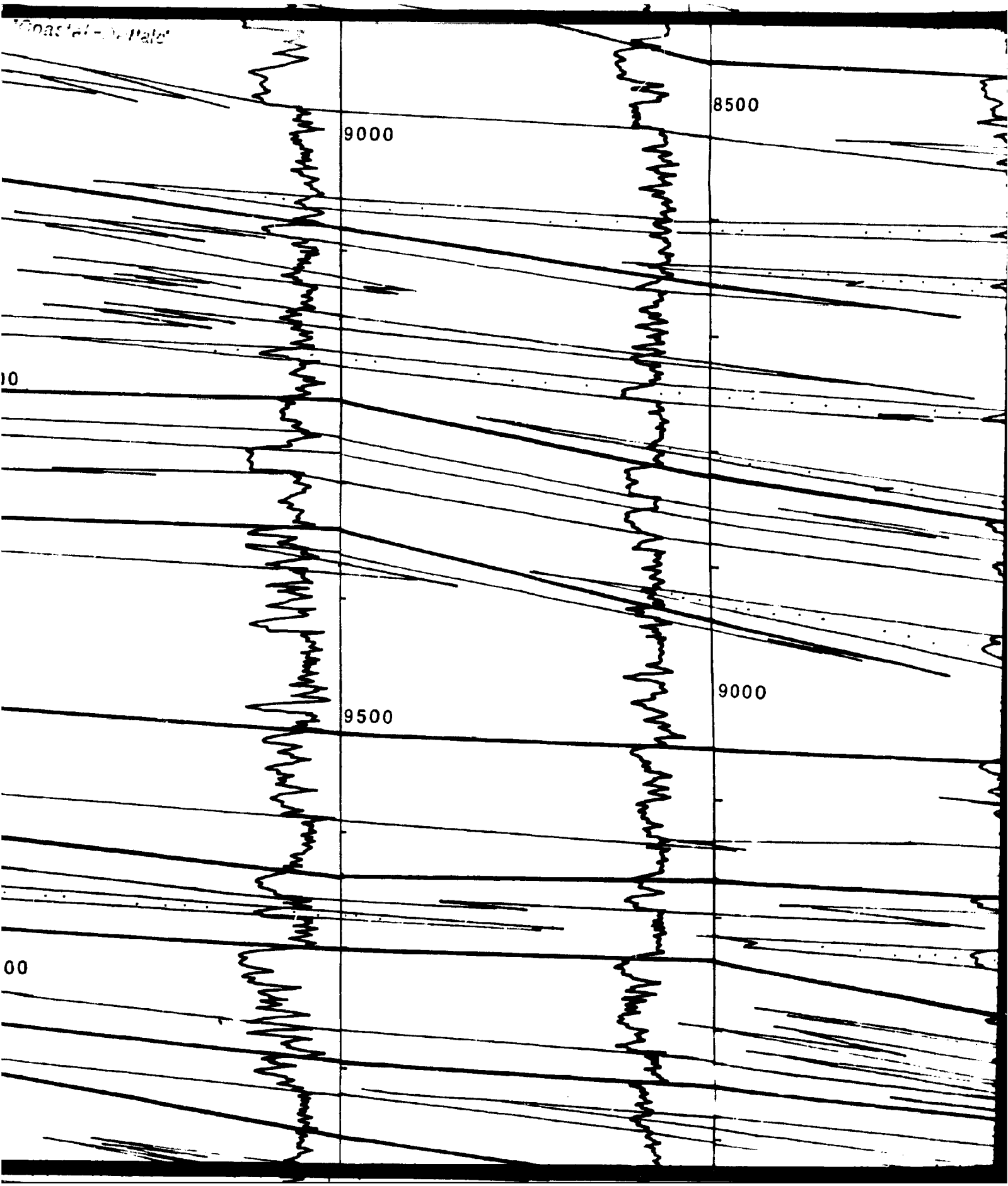
A8

10000

A7

A6

Coastal - Pale



8500

8000

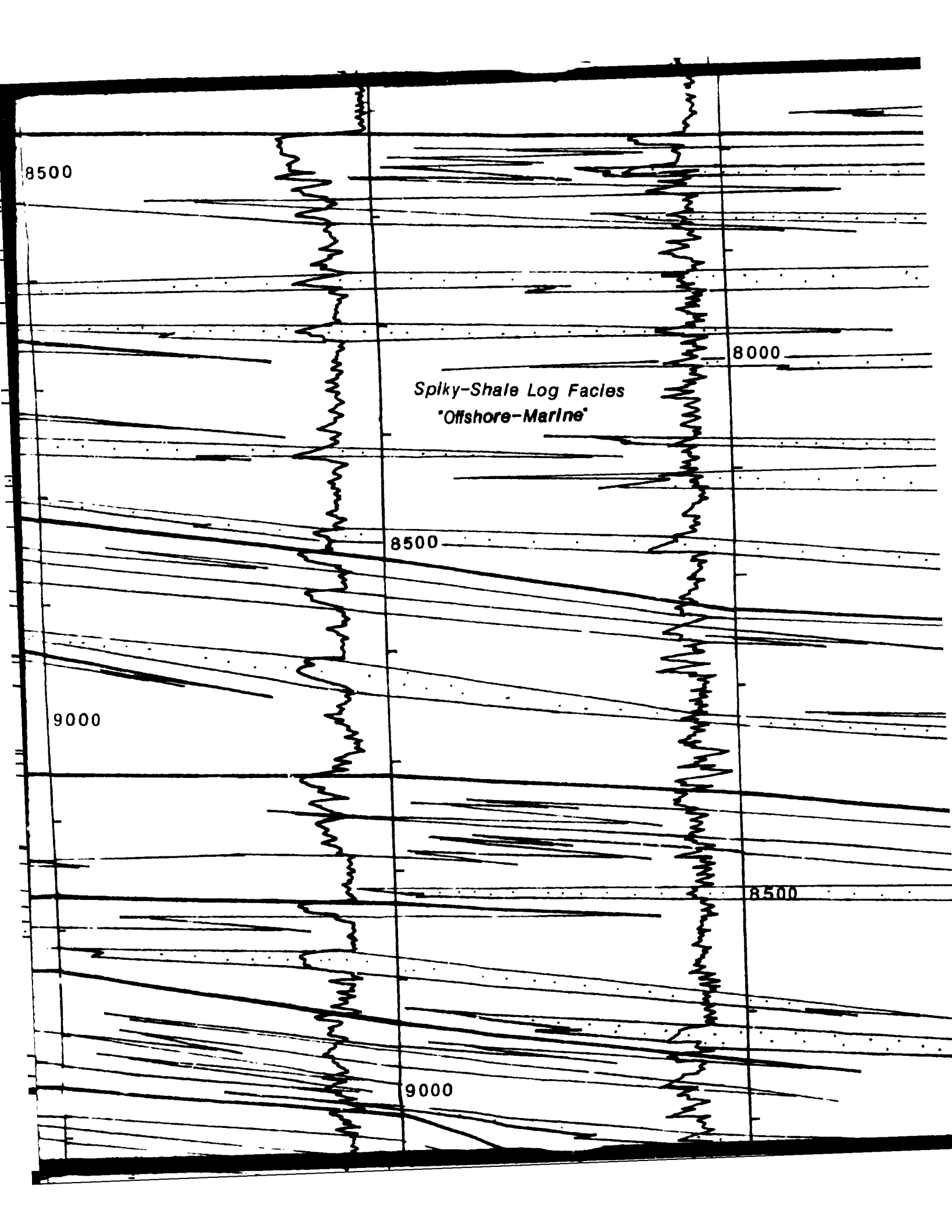
*Splky-Shale Log Facies
"Offshore-Marine"*

8500

9000

8500

9000



7000

7500

Marine Sand Log Facies
"Reworked-Marine"

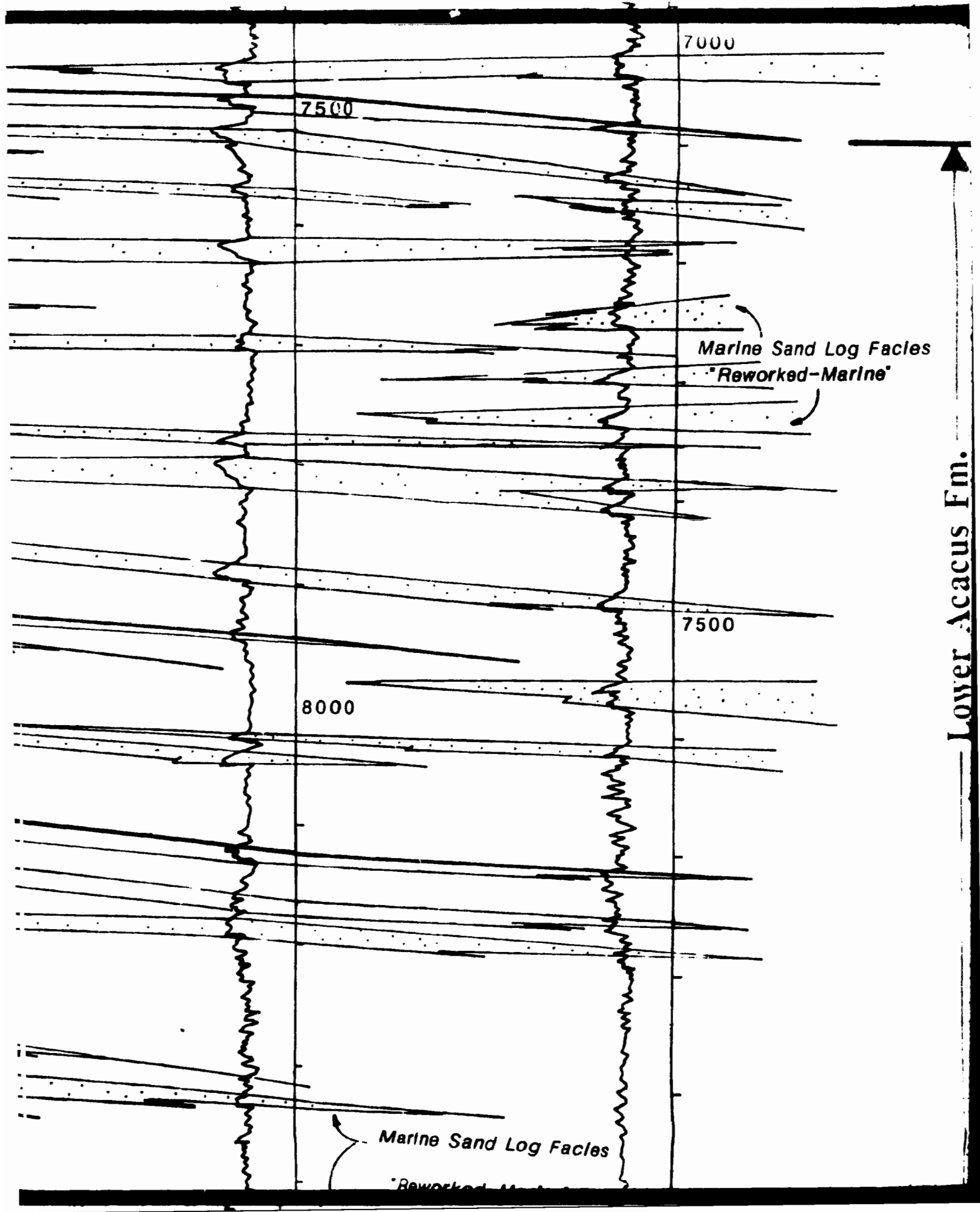
7500

8000

Marine Sand Log Facies

"Reworked-Marine"

Lower Acacus Fm.



100

Marine Sand Log Facies
"Reworked-Marine"

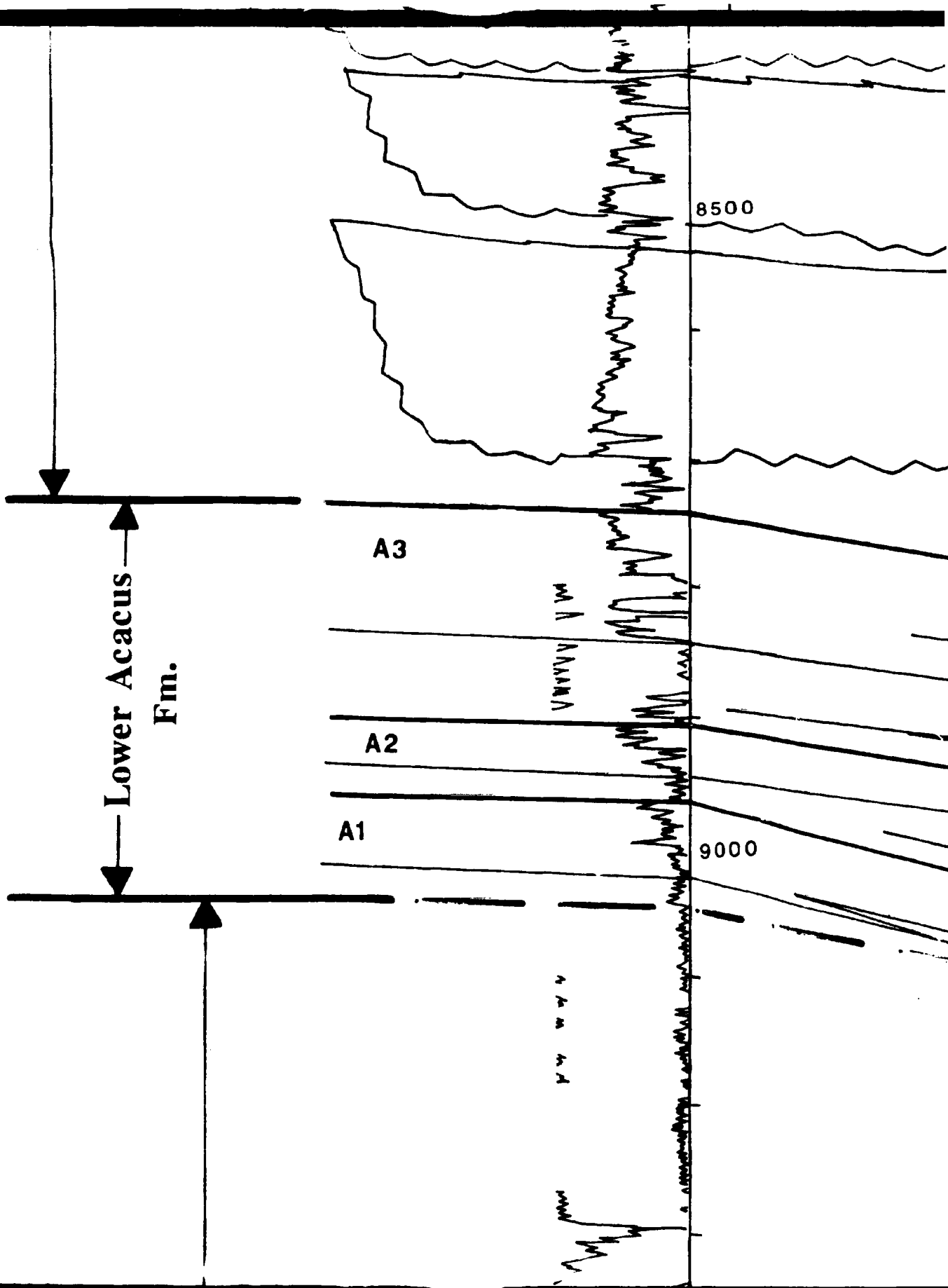
500

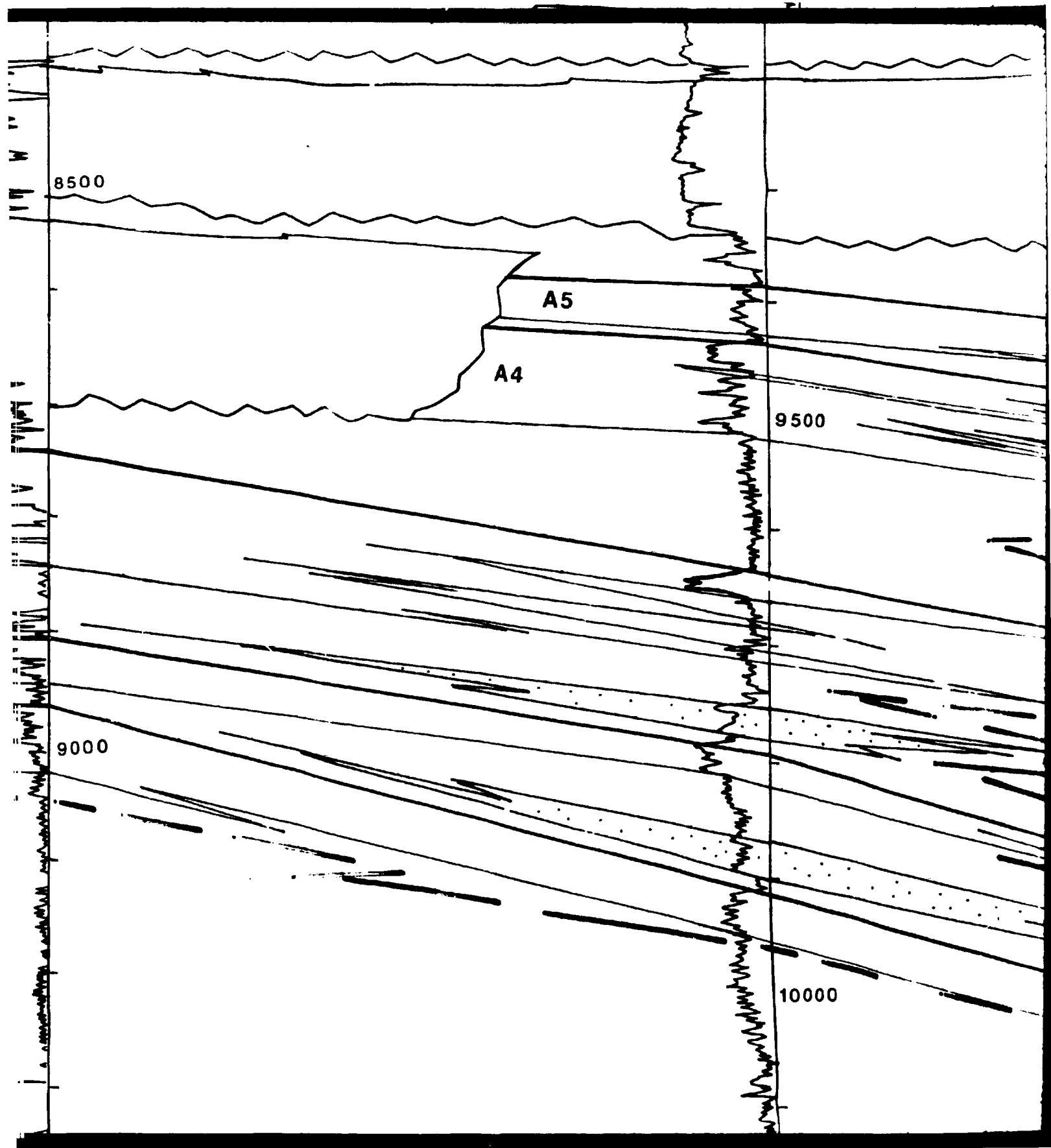
Lower Acacus Fm.

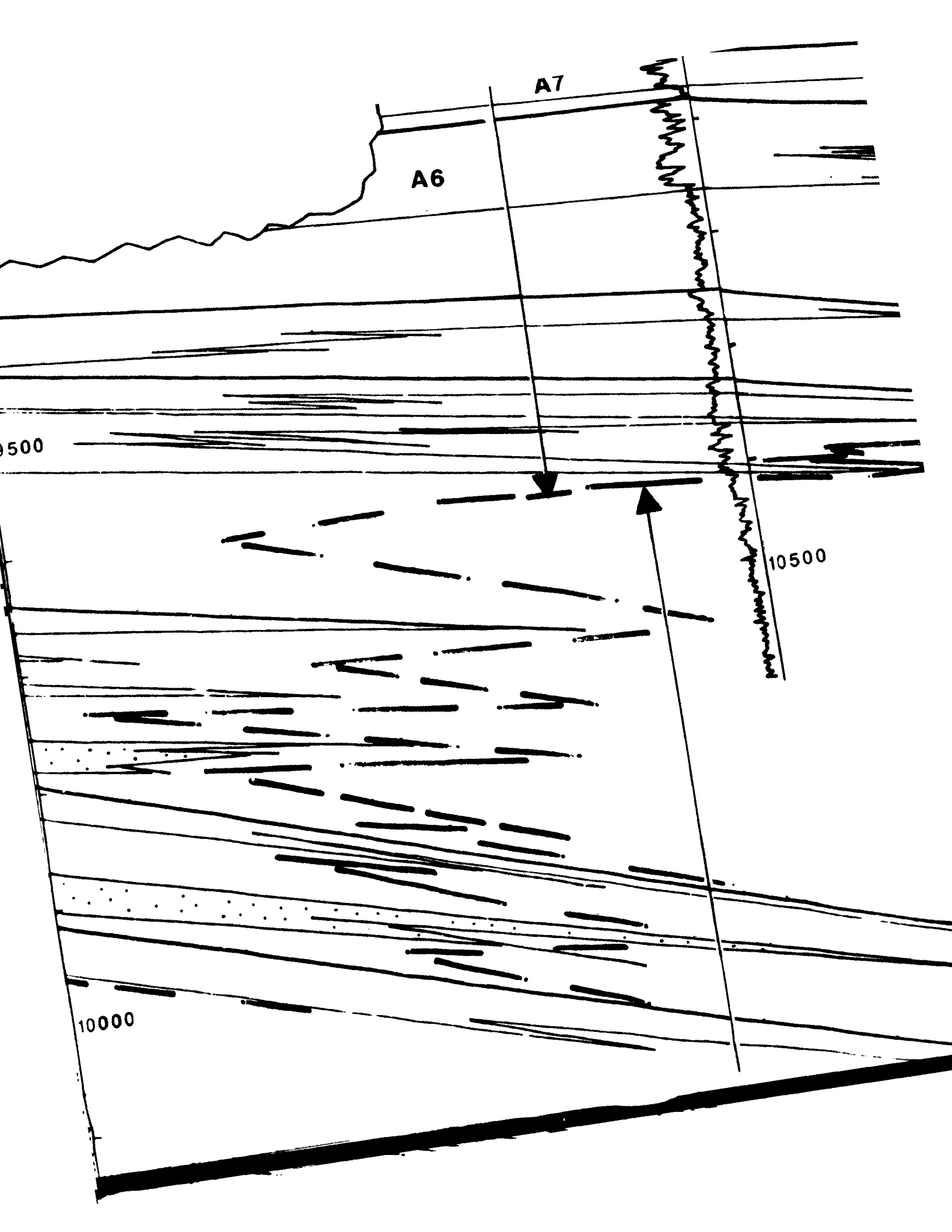
"Upper Silurian"

LEGI

LEGEND







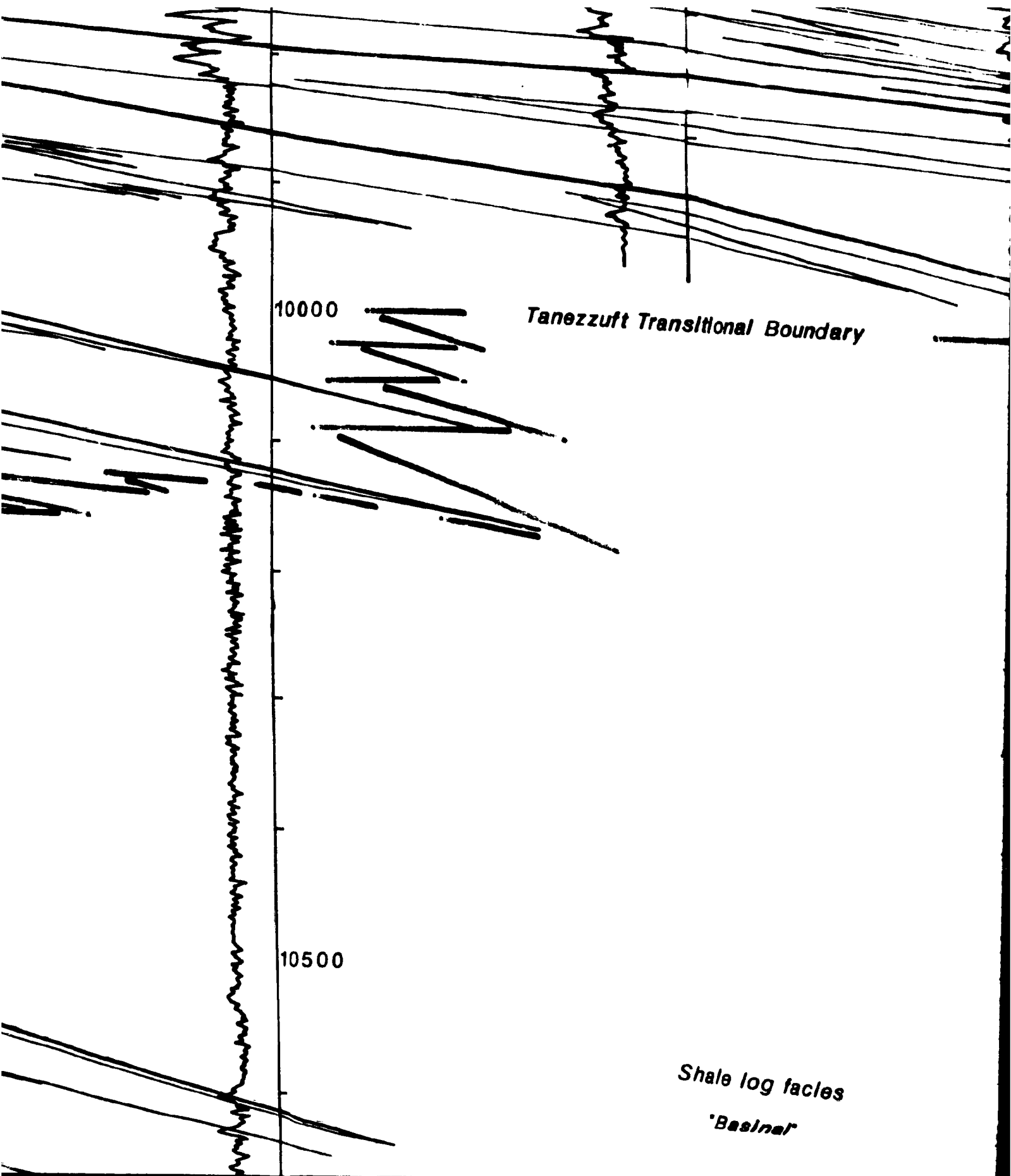
A7

A6

9500

10500

10000



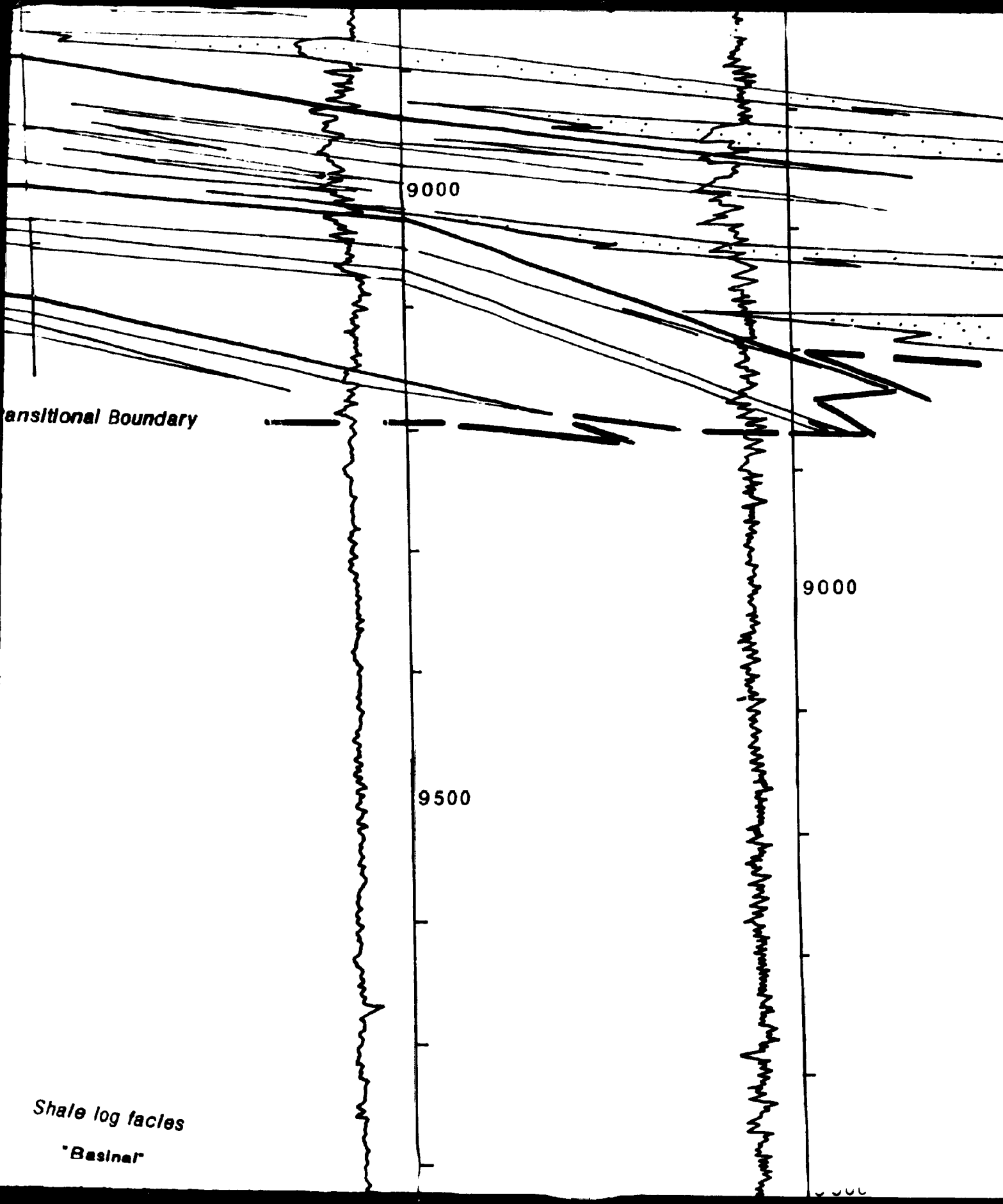
10000

Tanezzuft Transitional Boundary

10500

Shale log facies

'Basiner'



9000

Transitional Boundary

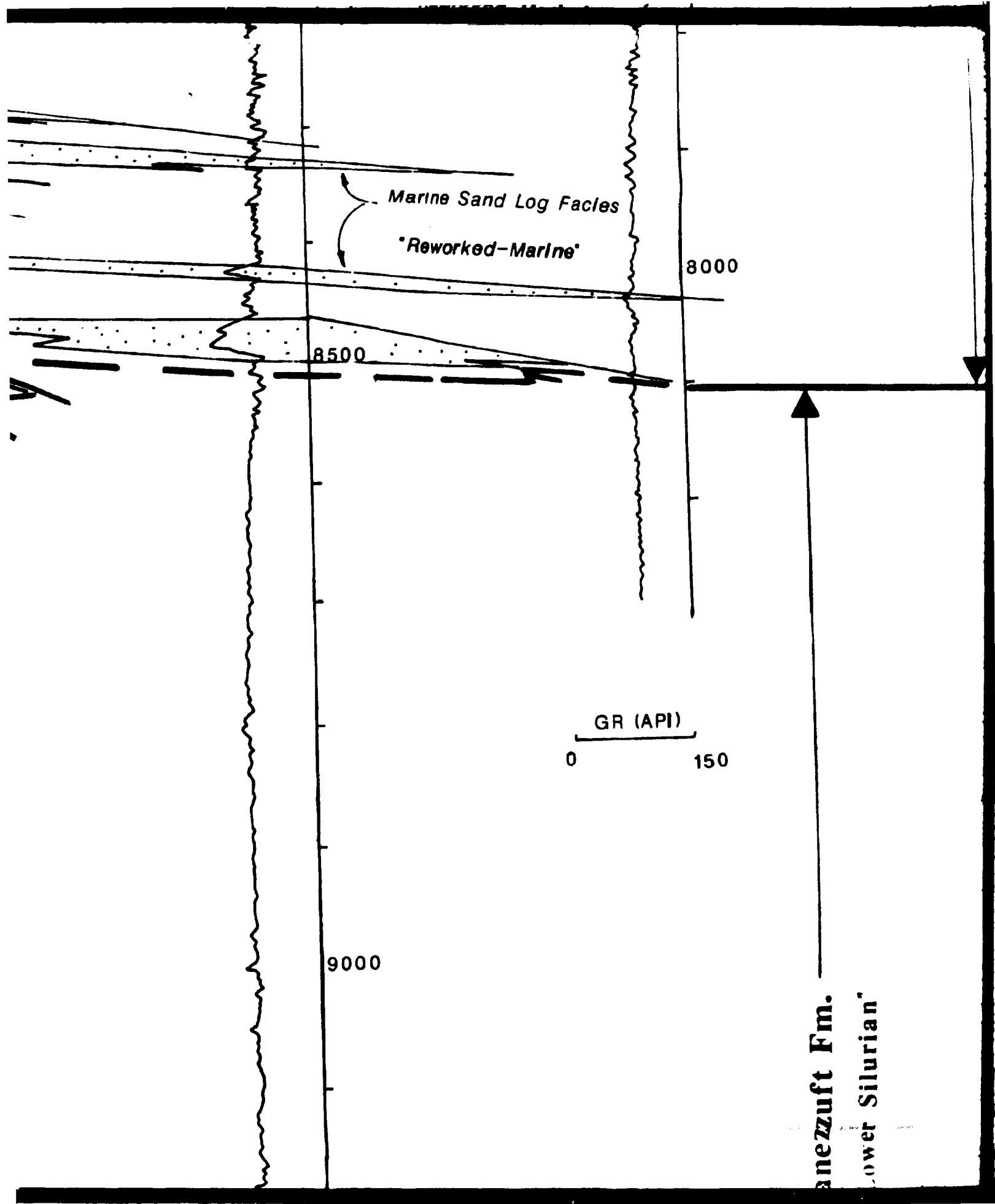
9000

9500

Shale log facies

"Basinal"

CCCC



Marine Sand Log Facies

"Reworked-Marine"

8000

8500

GR (API)

0

150

9000

anezuft Fm.
Lower Silurian

LEGEND



DRY HOLE



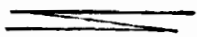
OIL WELL



OIL AND GAS WELL



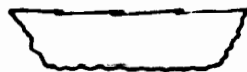
TOP GENETIC UNIT 'COARSENING-UPWARD SANDSTONE UNIT' LINE



FACIES LINE



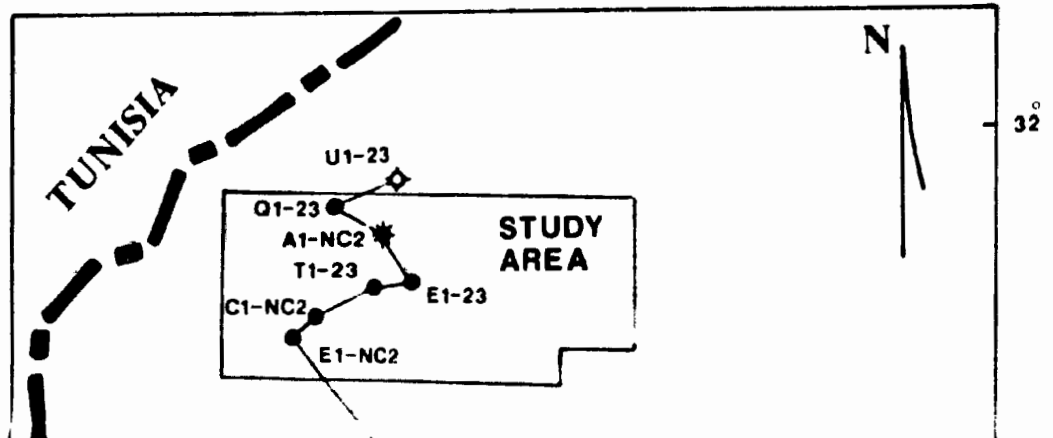
TANEZZUFT TRANSITIONAL BOUNDARY



FLUVIAL CHANNEL

A1-A14 LOWER ACACUS SANDSTONE UNITS

A15-A16 MIDDLE ACACUS SANDSTONE UNITS



WELL

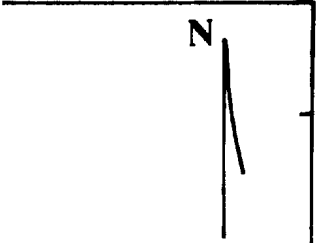
UNIT COARSENING-
TONE UNIT LINE

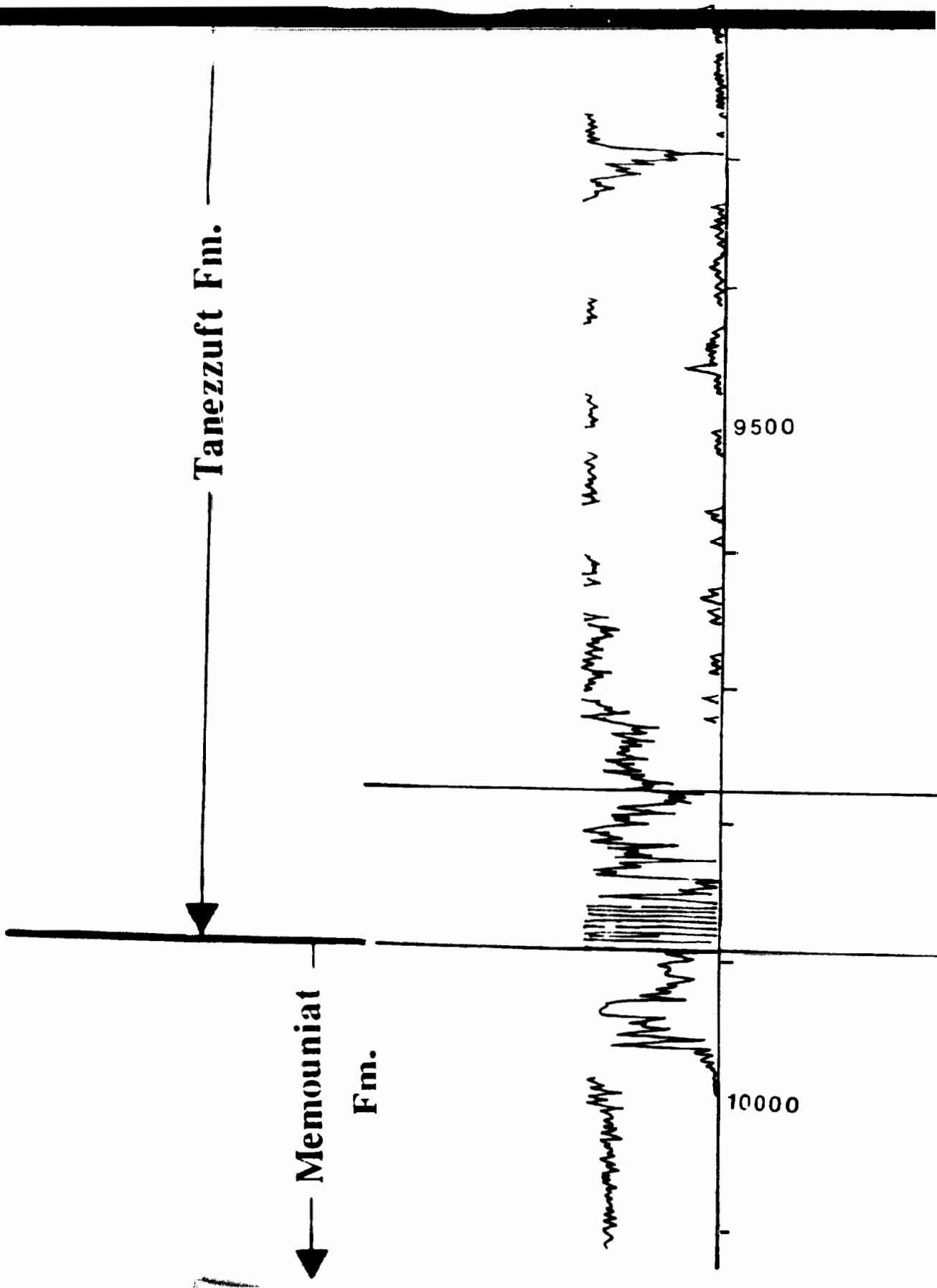
TRANSITIONAL
ARY

NEL

SANDSTONE UNITS

SANDSTONE UNITS





Tanezzuft Fm.

Memouniat Fm.

9500

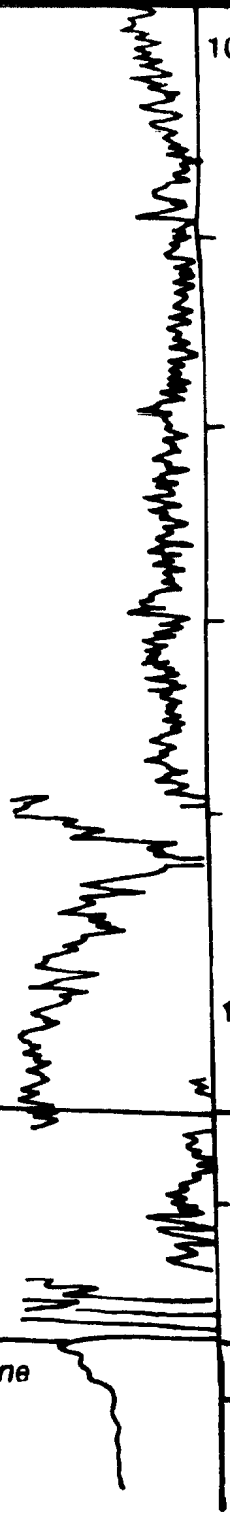
10000

Memouniat
a. ...

10000

10500

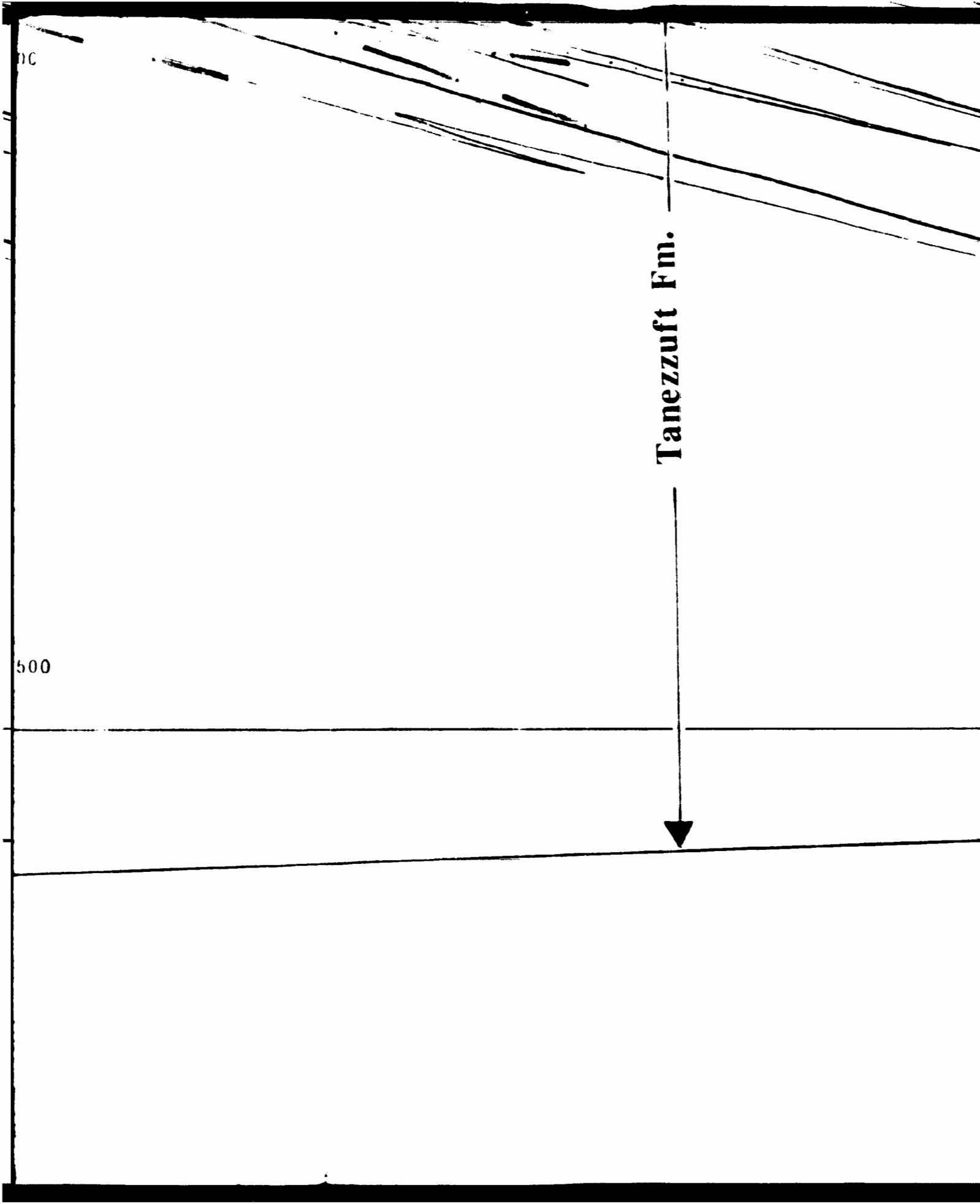
Terminal sandstone



00

Tanezzuft Fm.

500



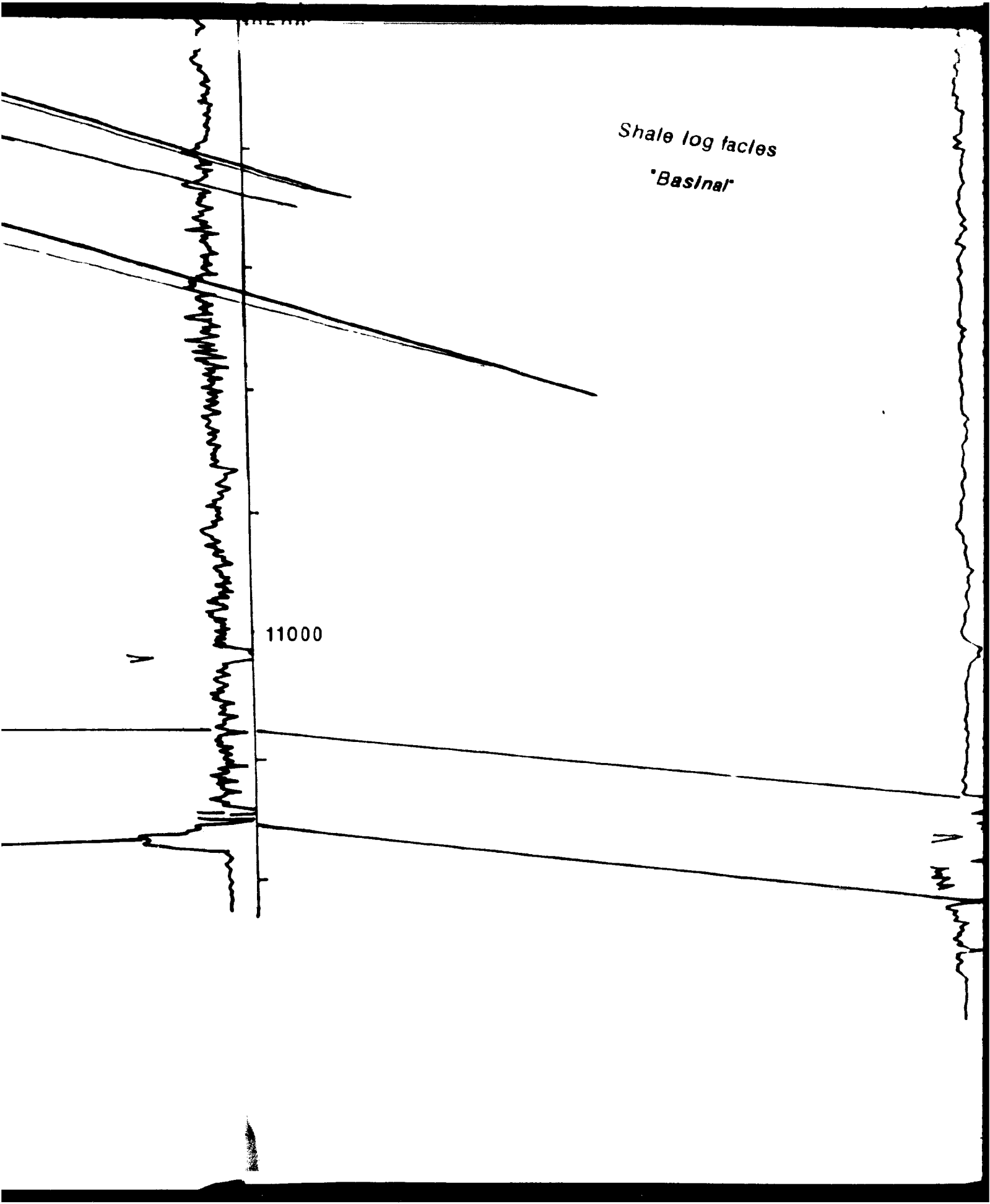
Shale log facies

'Basinal'

11000

V

V



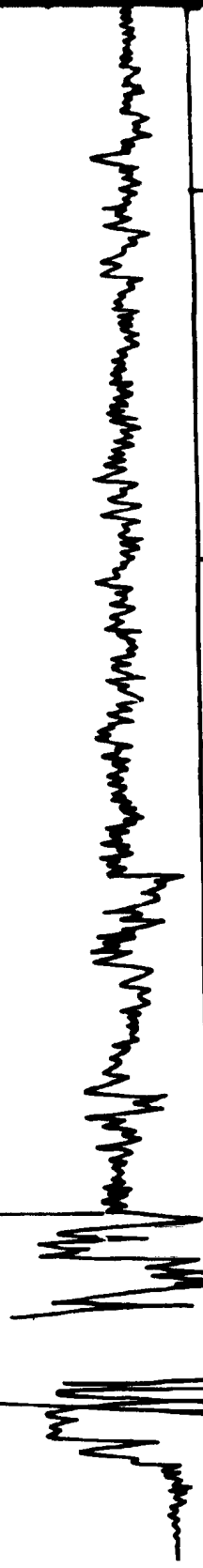
g facies

nal



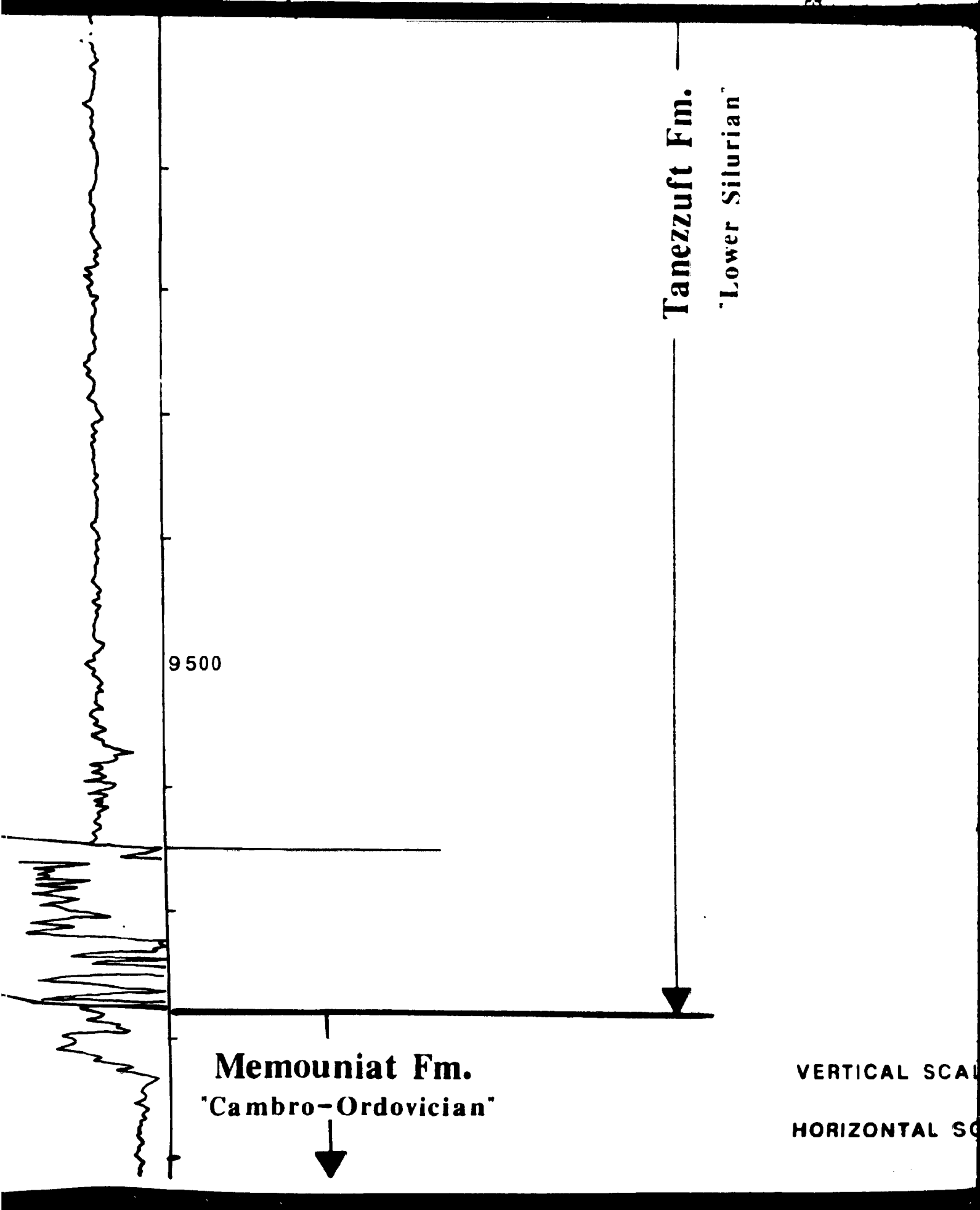
10000

Organic Shale



9500

10000



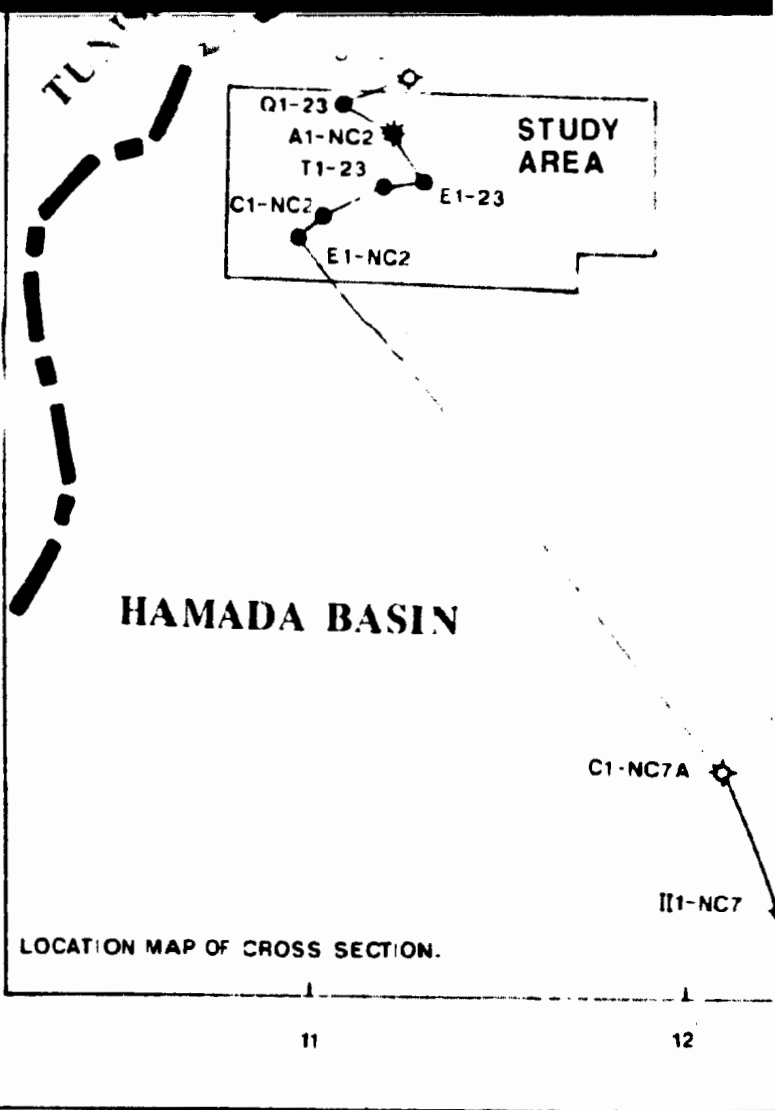
9500

Memouniat Fm.
"Cambro-Ordovician"

Tanezluft Fm.
"Lower Silurian"

VERTICAL SCALE
HORIZONTAL SCALE

Lower Silurian

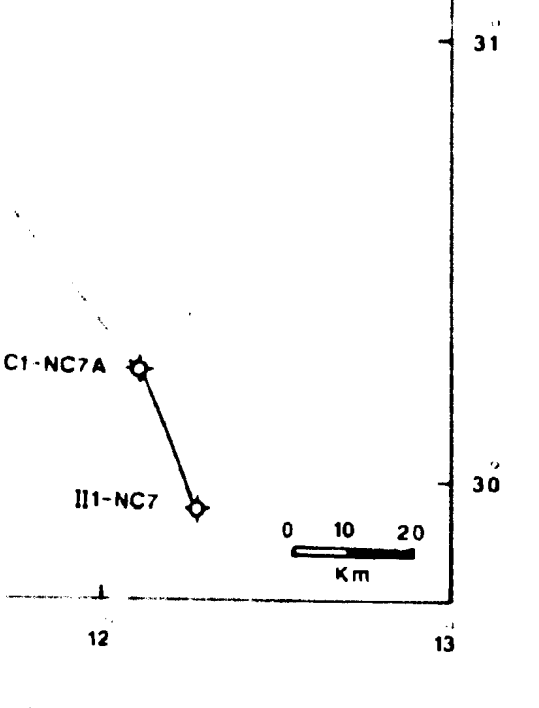


ENCLOSURE No. 1
N-S REGIONAL STRATIGRAPHIC CORRELATION
HAMADA BASIN, NW LIBYA

VERTICAL SCALE - 1 : 33.3 FT.

HORIZONTAL SCALE - AS INDICATED

DY
A



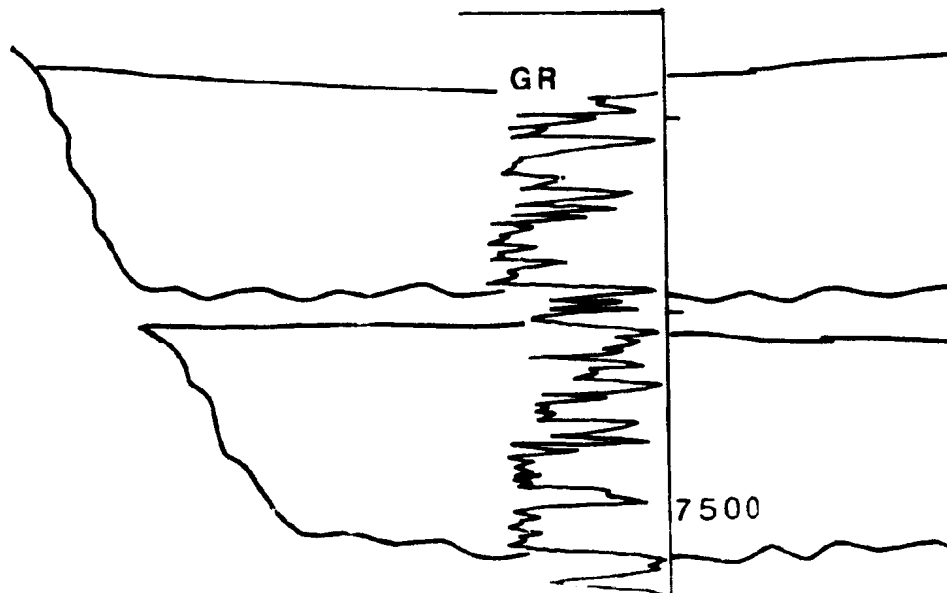
E No. 1
PHIC CROSS SECTION,
NW LIBYA.

OBE-91

S

111-NC7

K.B.2076



C1-NC7A

K.B.1990

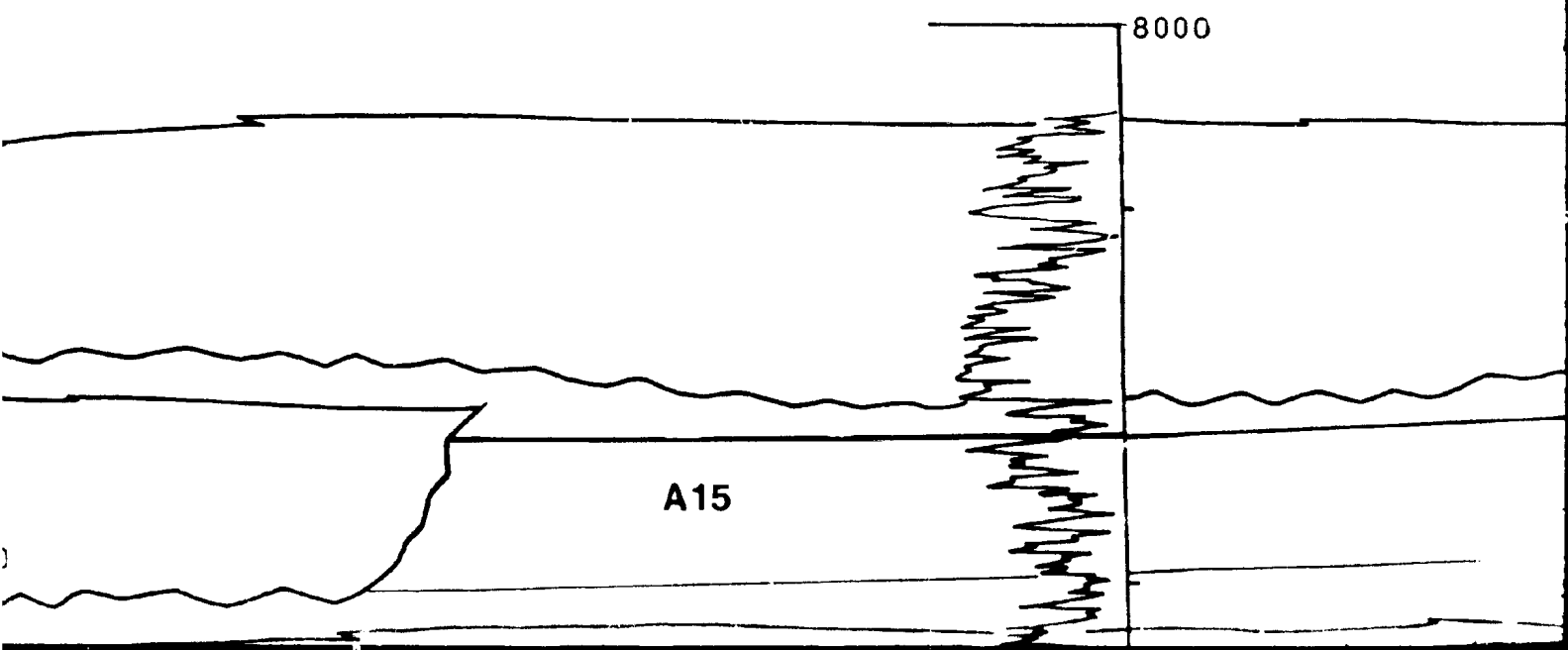
40Km.



Hamada South

8000

A15



C7A

90

B1-61

K.B.2037

95Km.

2K

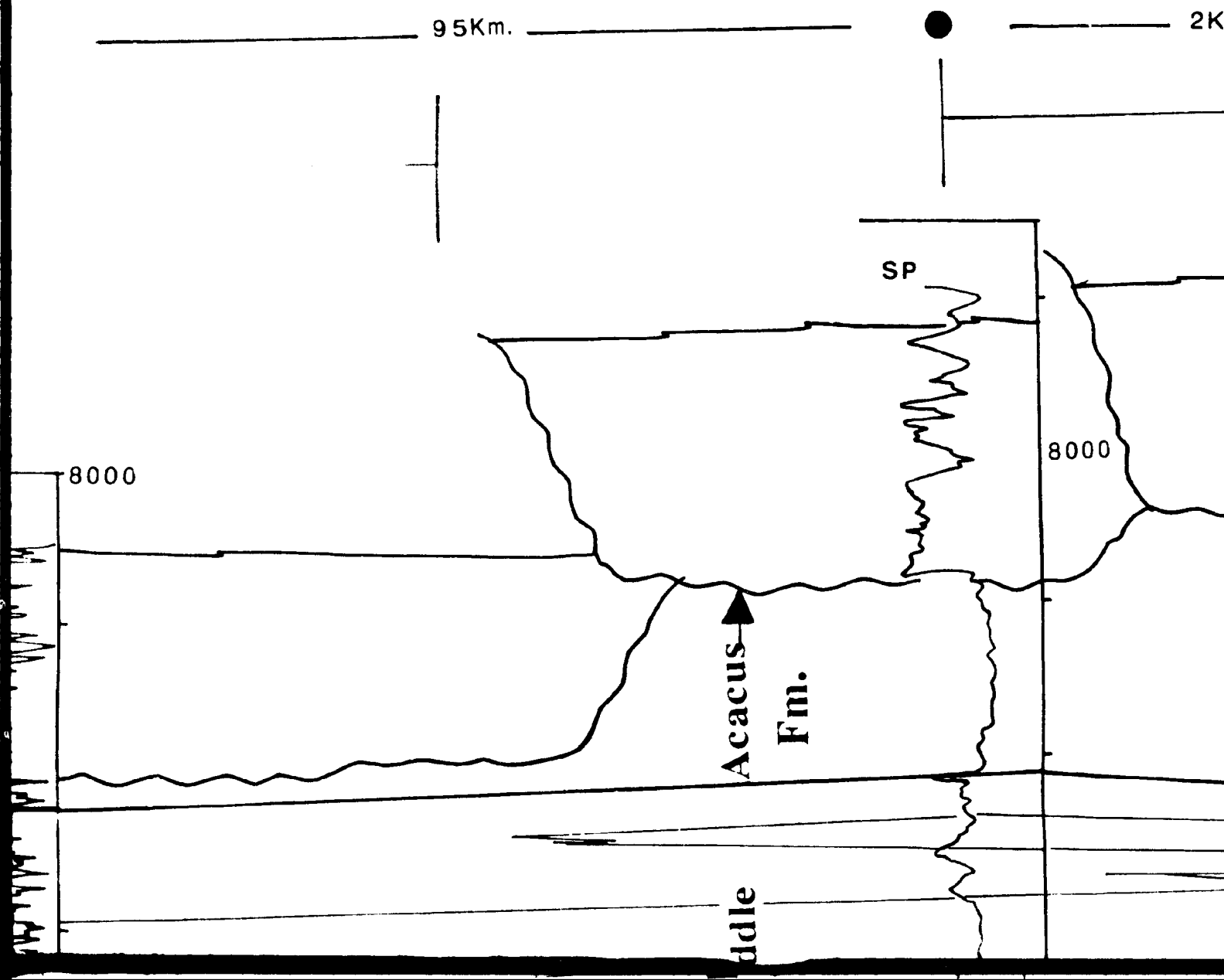
SP

8000

8000

Acacus
Fm.

iddle



B3-61

K.B.2050'

D1-61

K.B.2078'

2Km.



10Km.



3Km.

Hamada

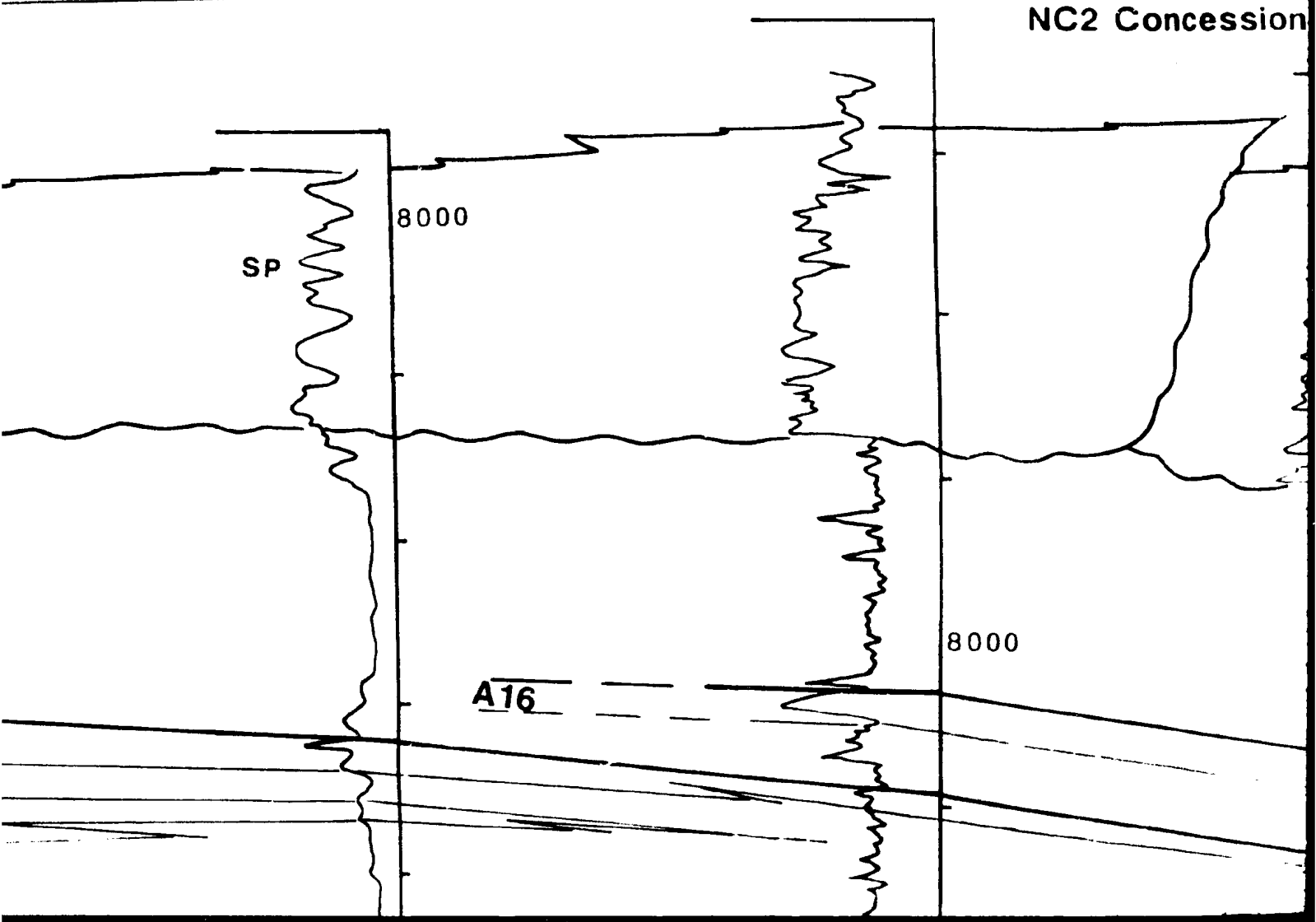
NC2 Concession

SP

8000

8000

A16



51
78

E1-23

K.B.2104

A1-NC2

K.B.2160

3Km.



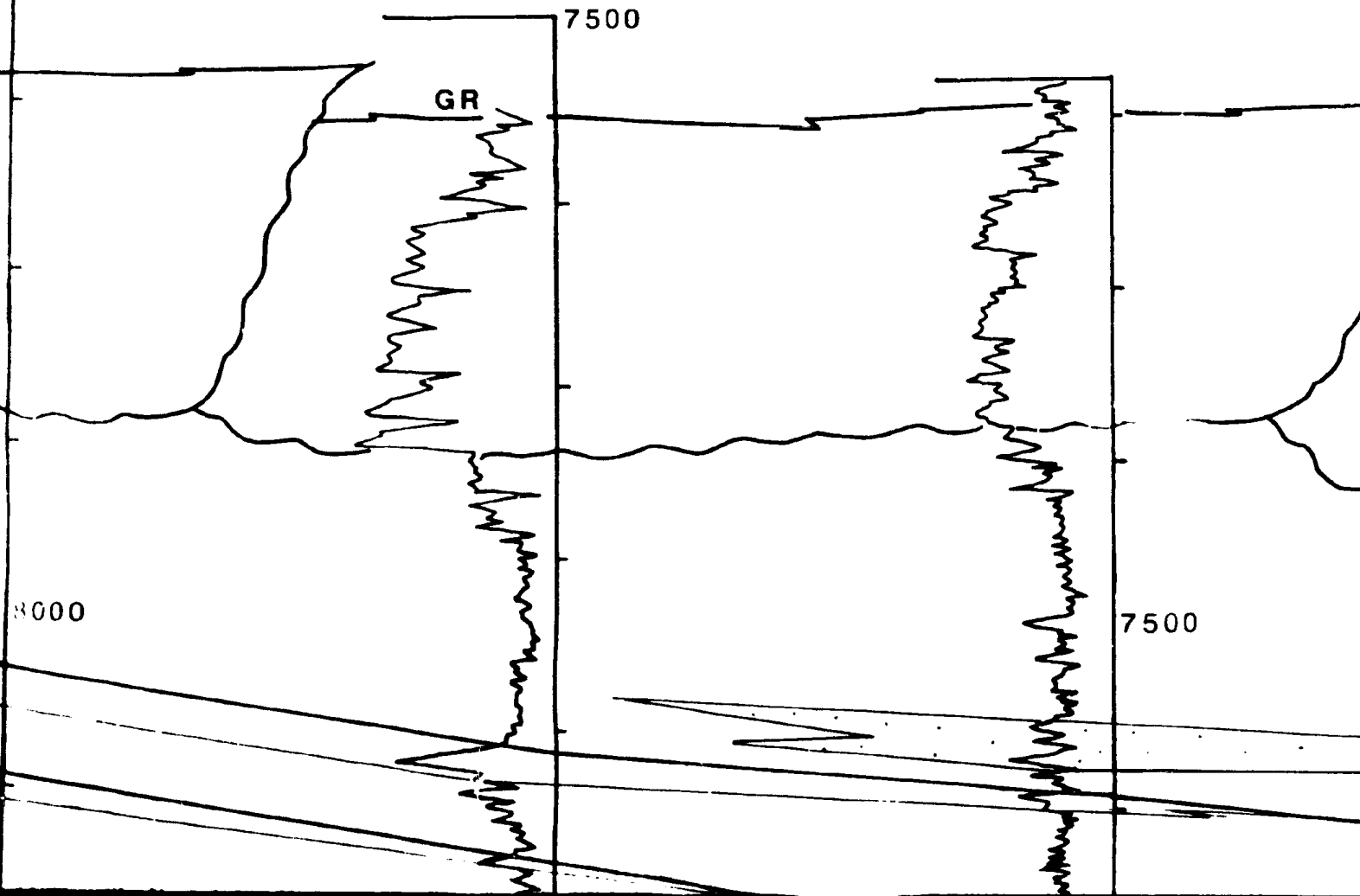
15Km.



17Km.

Hamada North

NC2 Concession "Study Area"

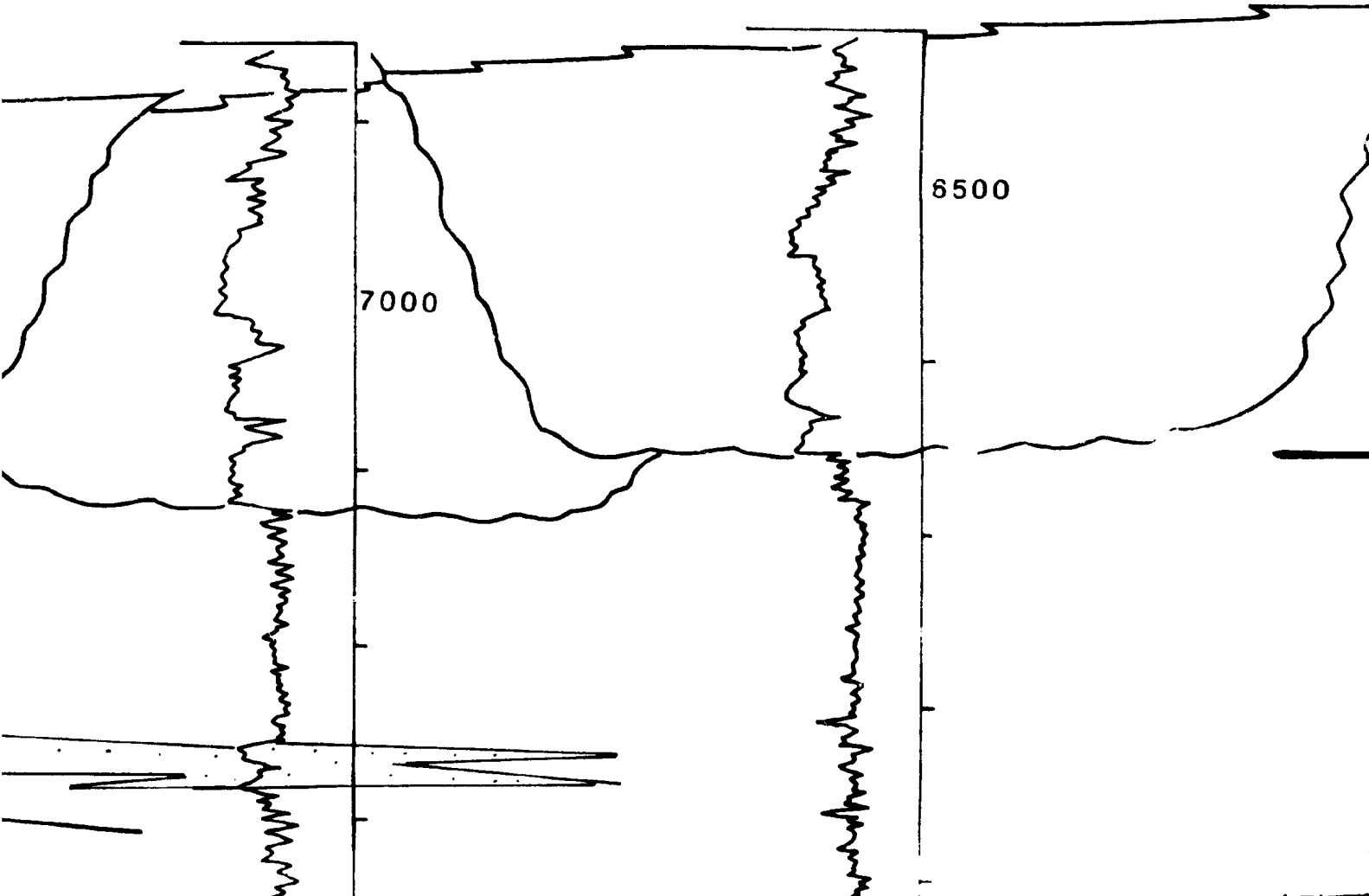
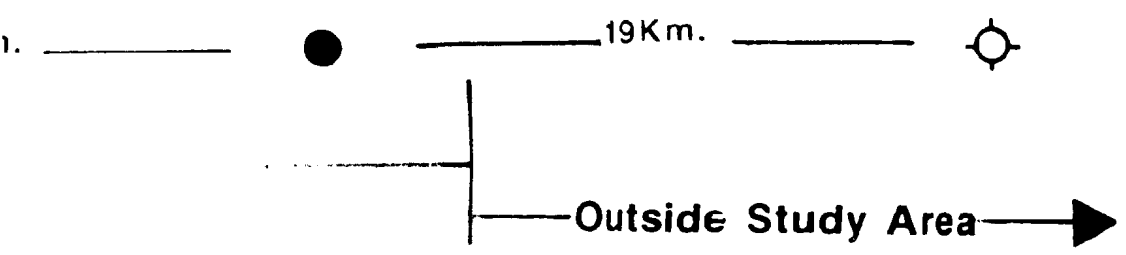


Q1-23

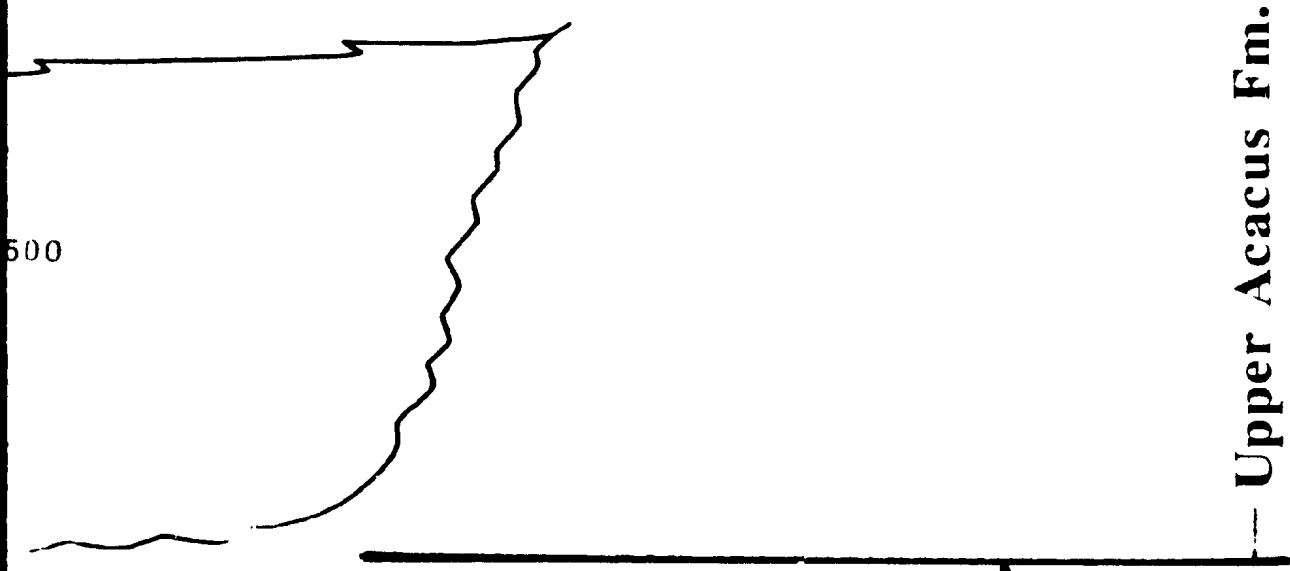
K.B.2040

U1-23

K.B.2177



N



500

Middle Acacus Fm.

Upper Silurian

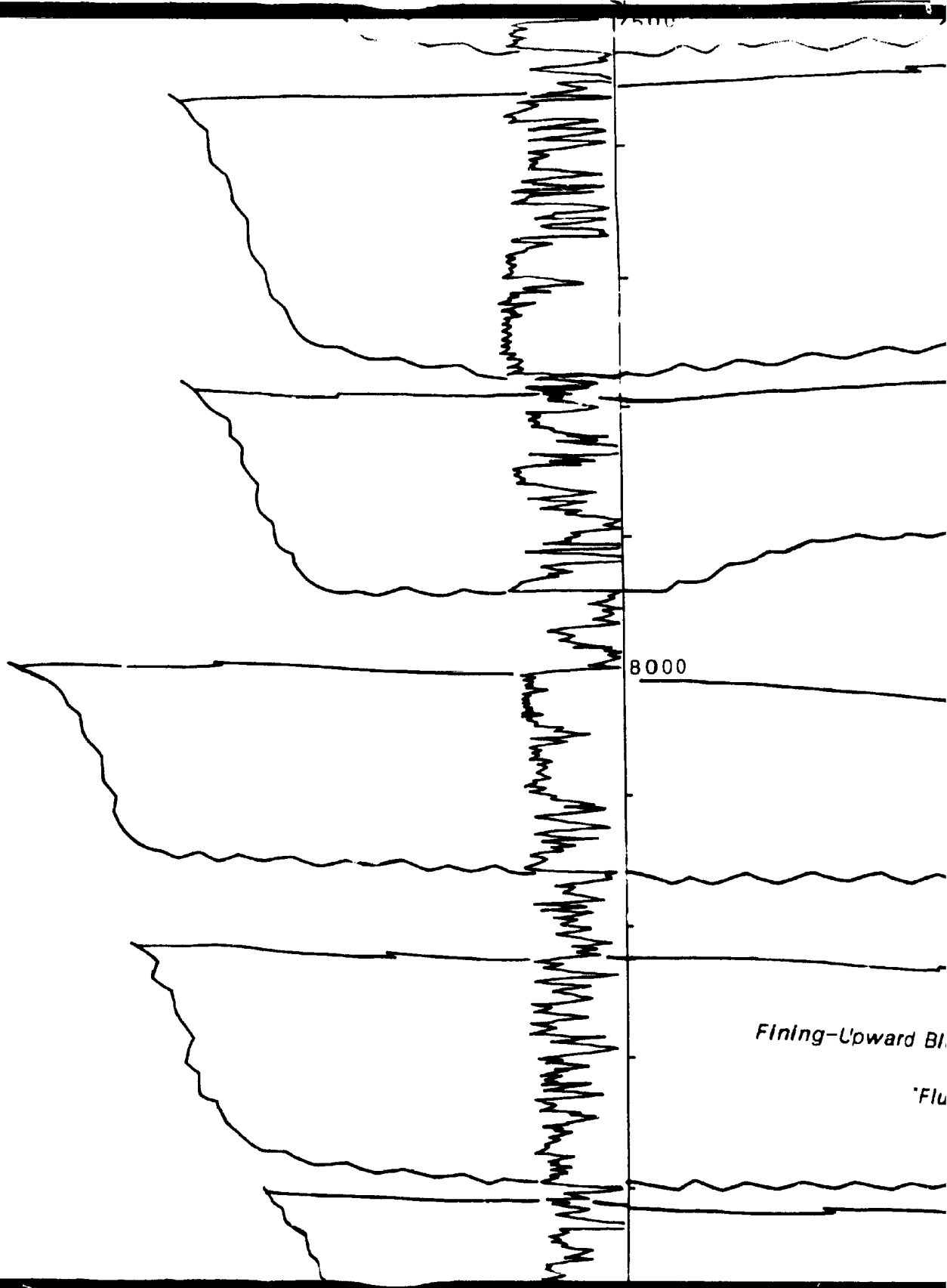
Upper Acacus Fm.

Upper Silurian

Marine Sand Log Facies

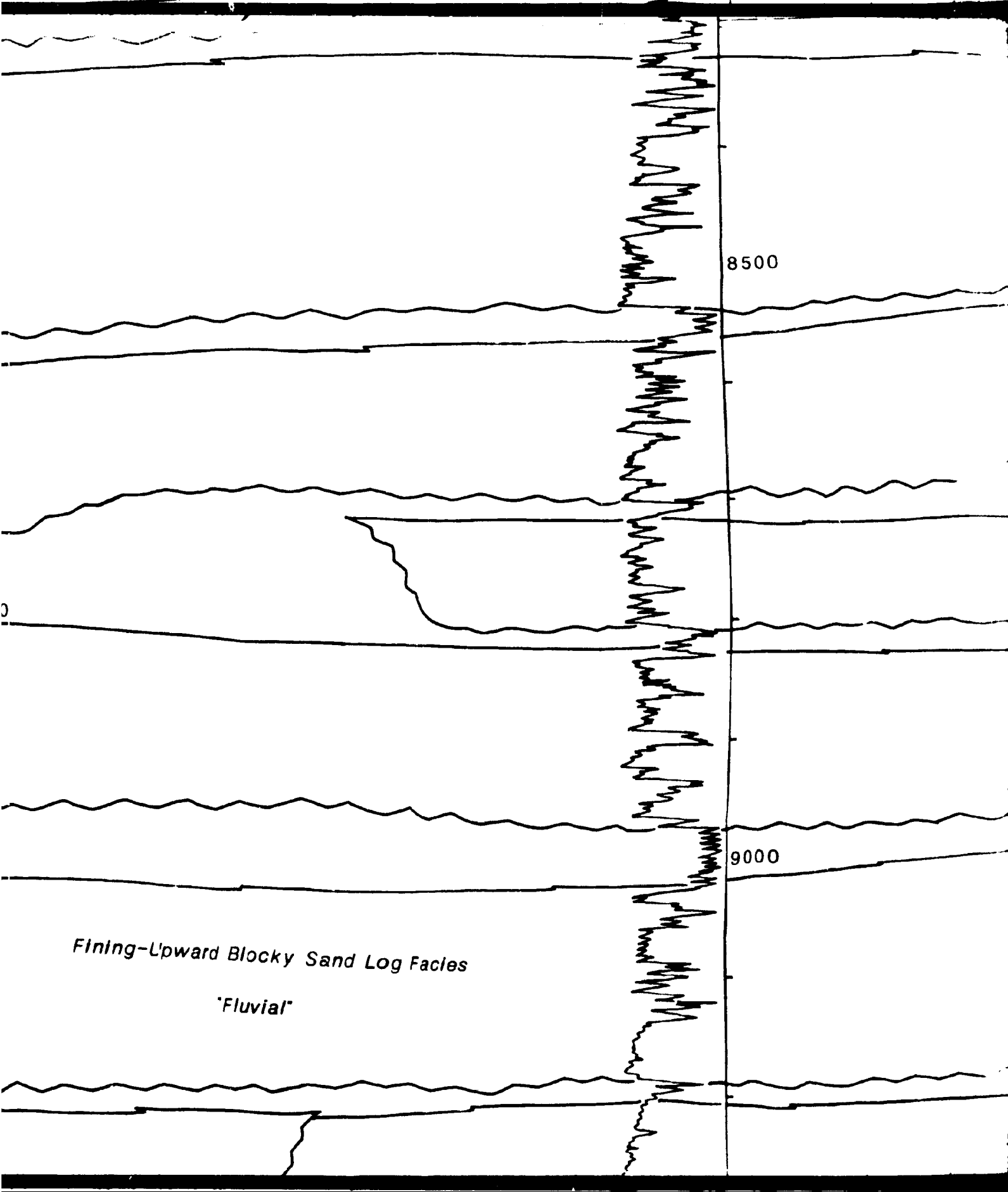
00

Acacus South Fm.



Fining-Upward Bl

Flu

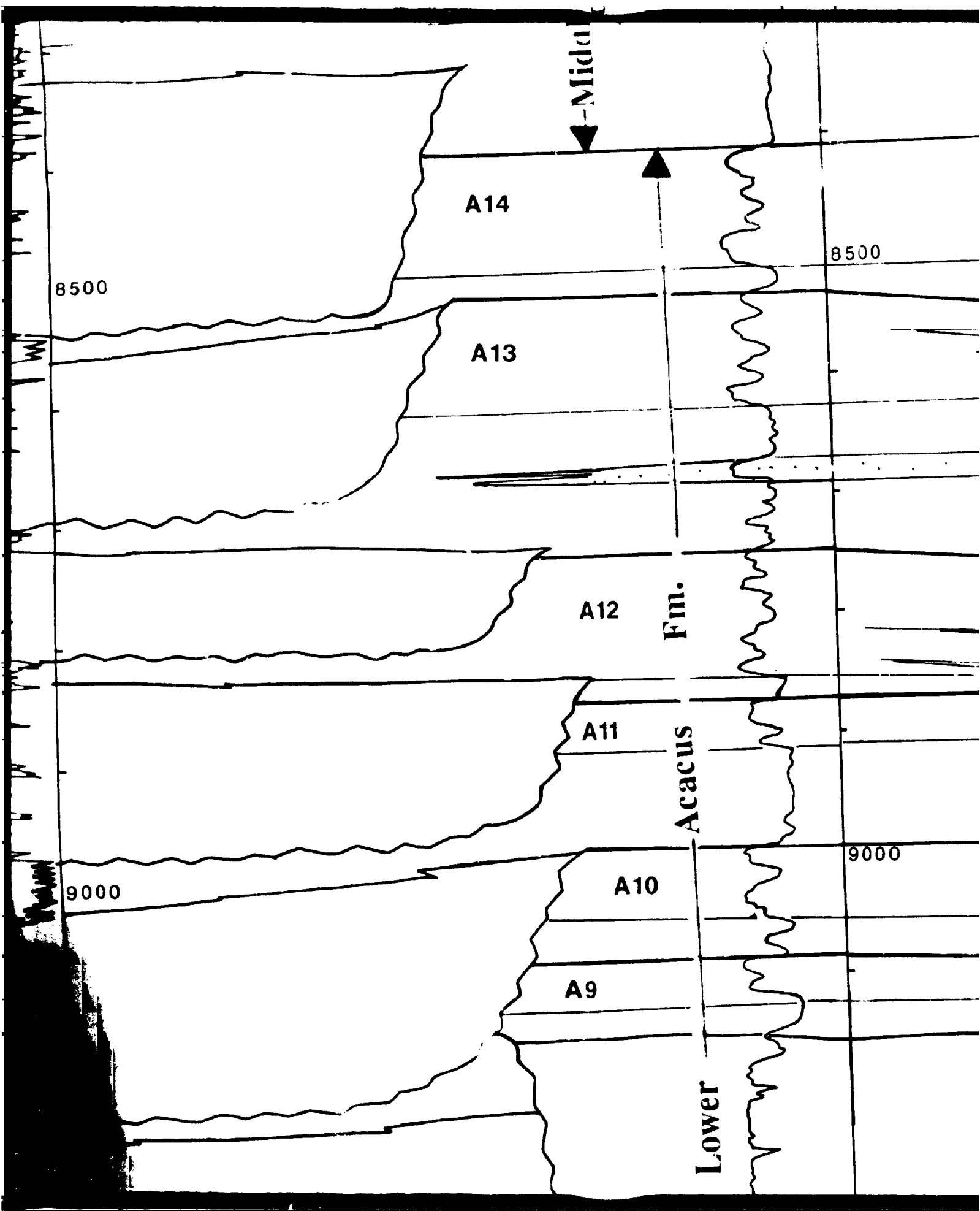


8500

9000

Fining-Upward Blocky Sand Log Facies

"Fluvial"



8500

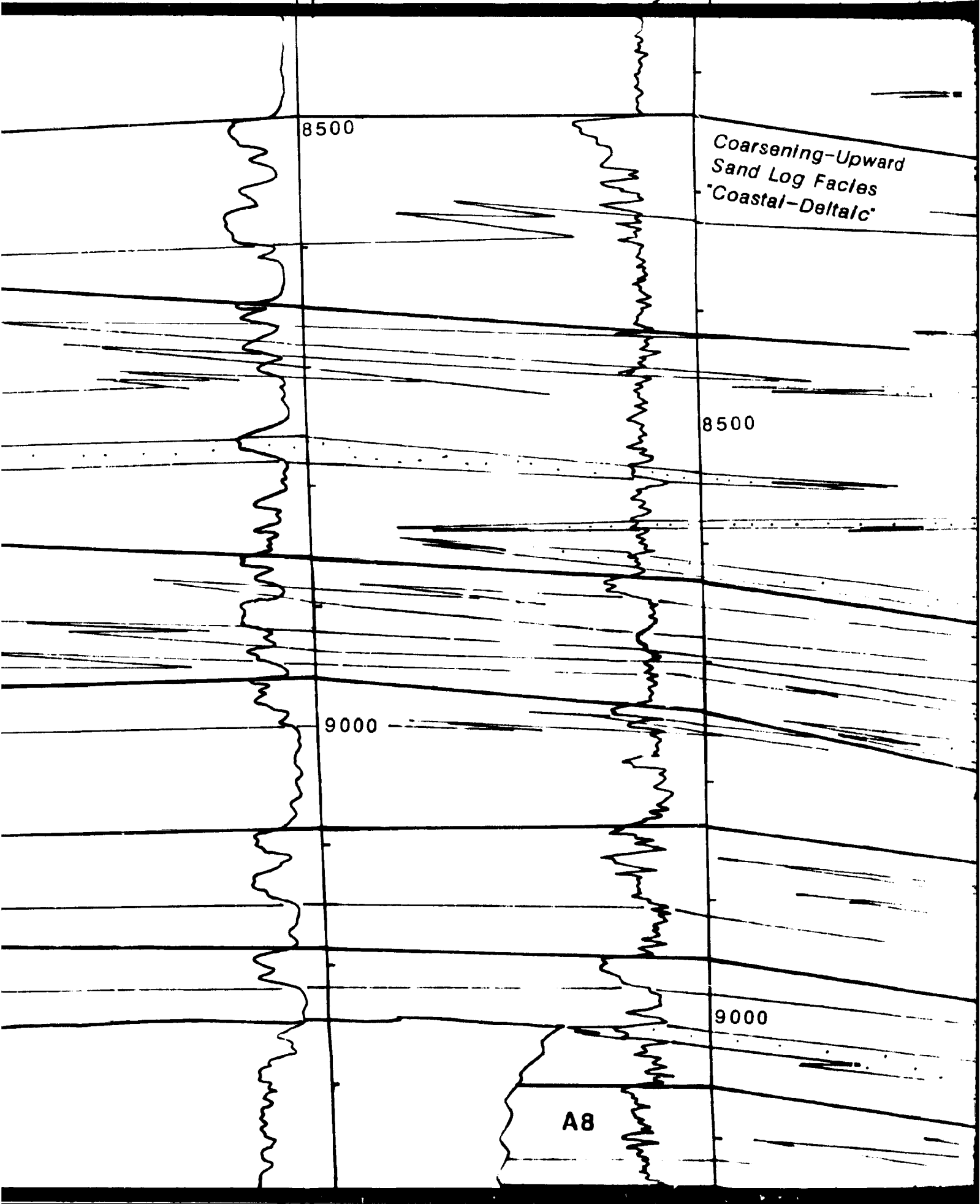
Coarsening-Upward
Sand Log Facies
'Coastal-Deltaic'

8500

9000

9000

A8



Coarsening-Upward
Sand Log Facies
'Coastal-Deltaic'

6000

8500

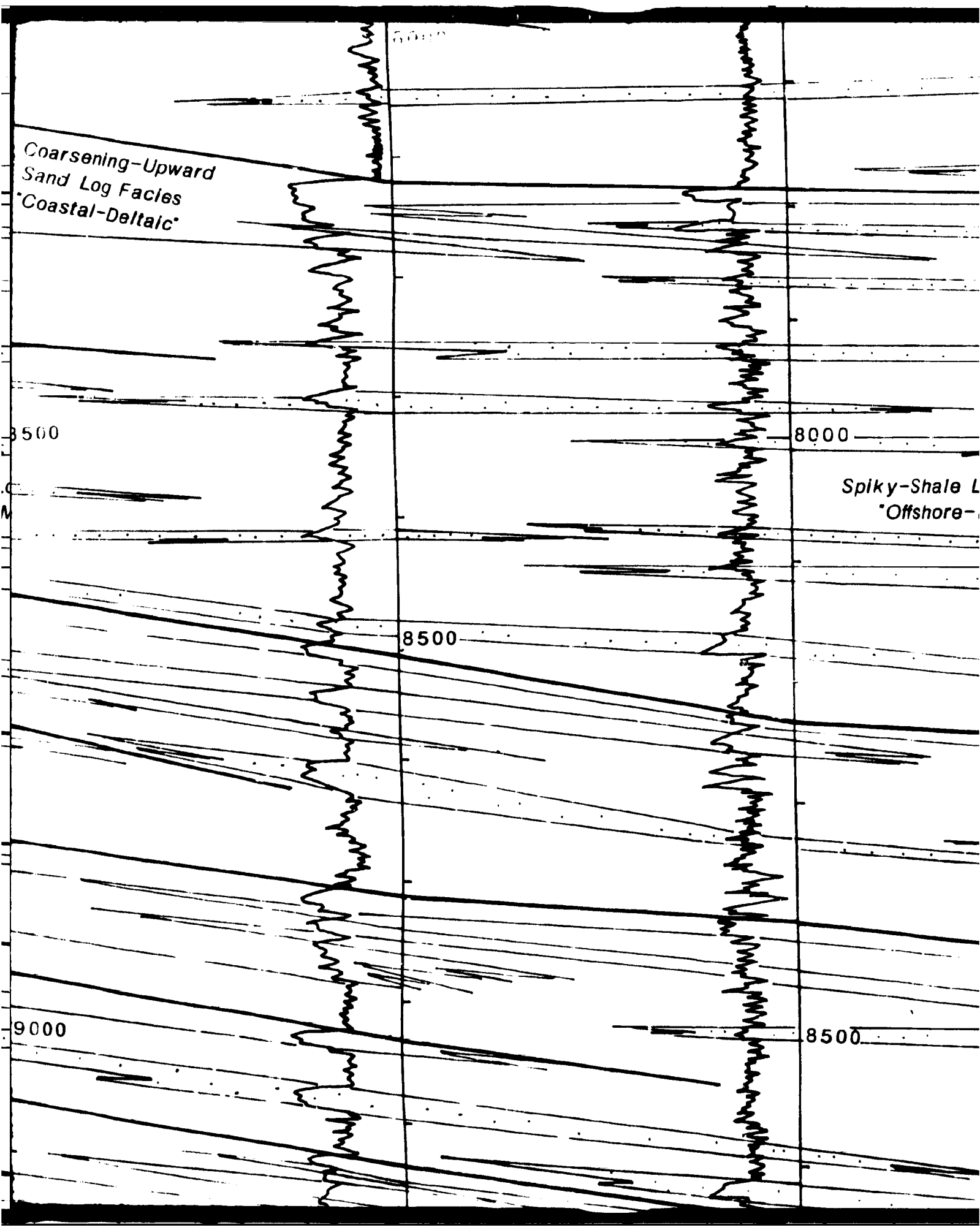
8000

Spiky-Shale L
'Offshore-

8500

9000

8500



Marine S

*Rewo

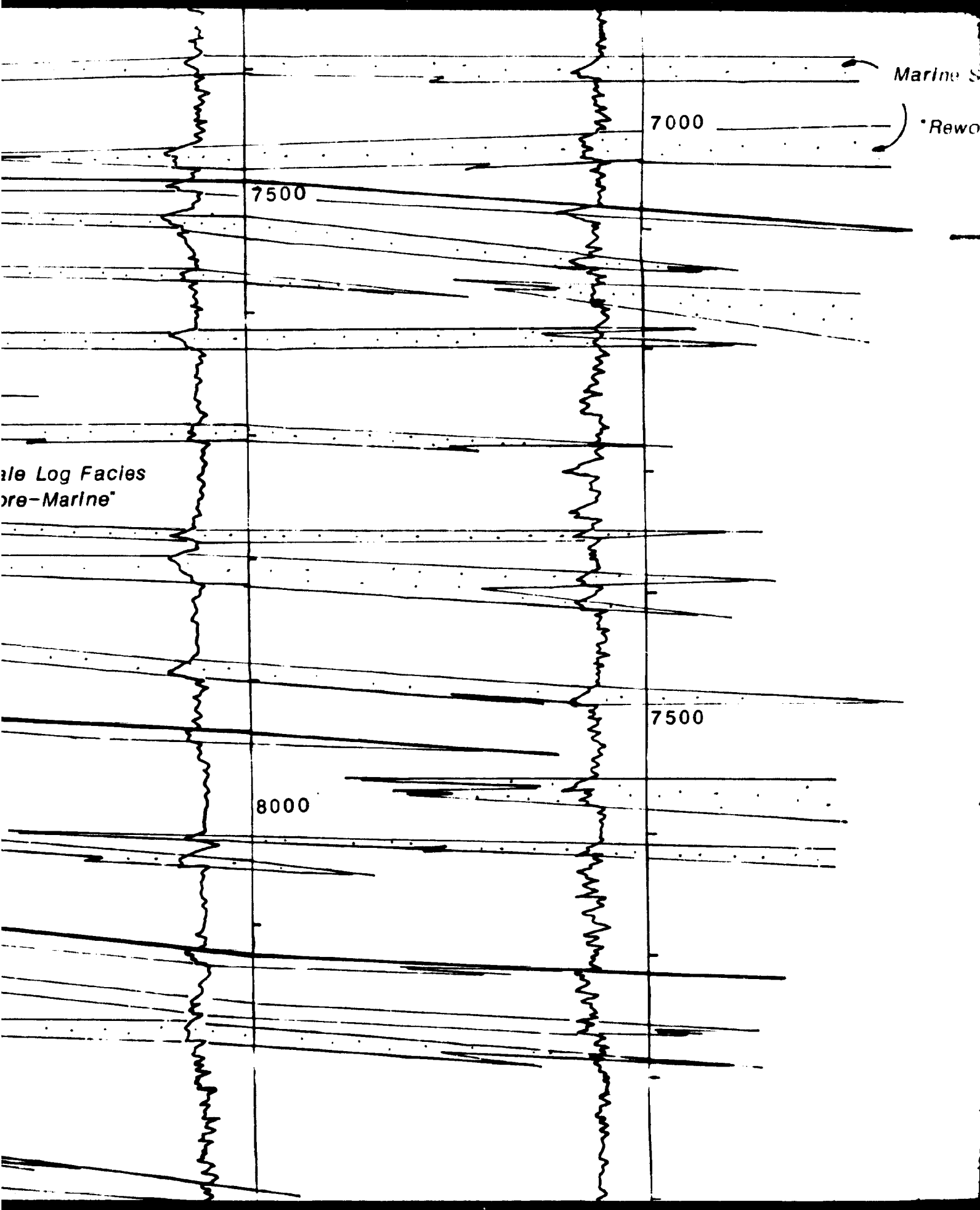
7000

7500

7500

8000

ale Log Facies
pre-Marine



Marine Sand Log Facies

7000

"Reworked-Marine"

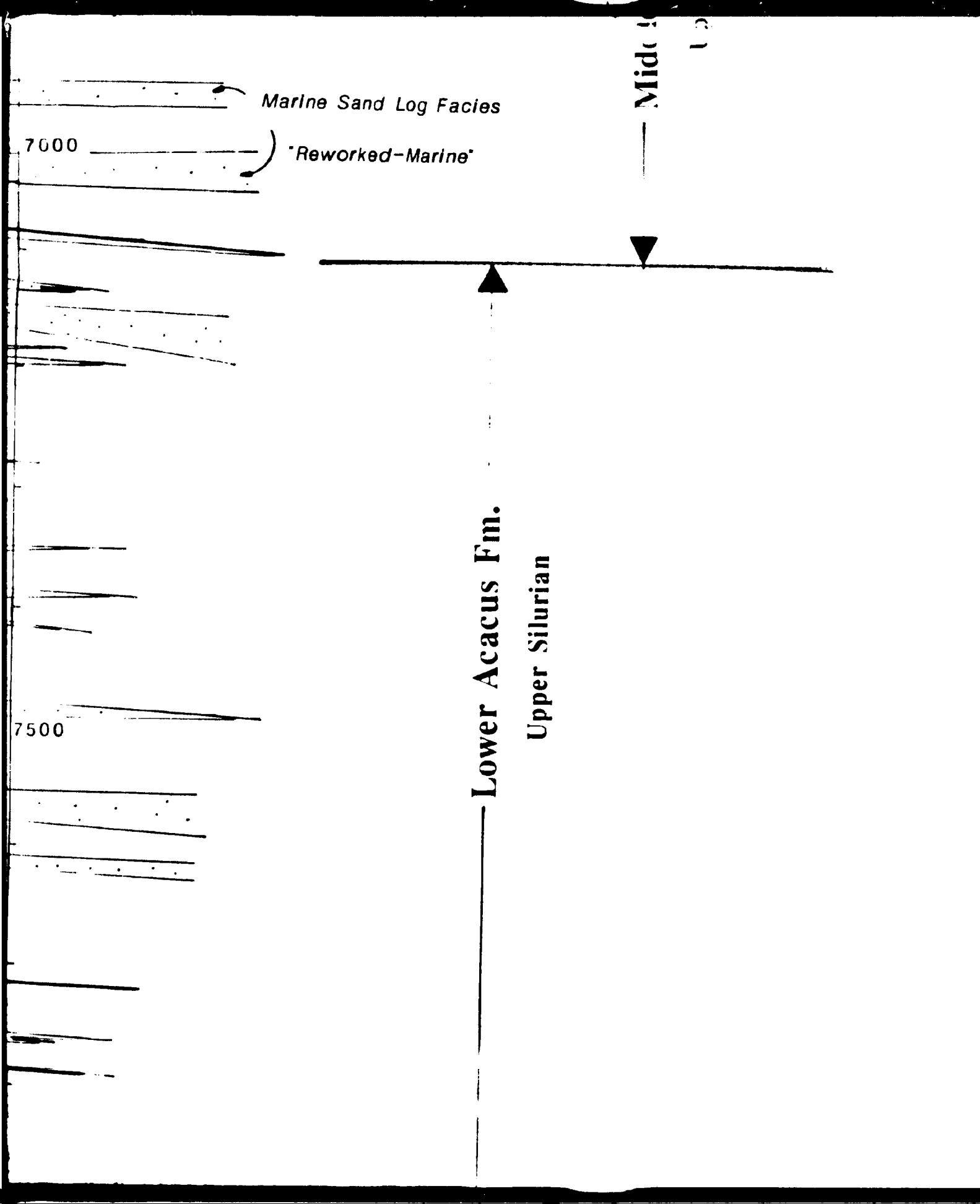
Mid

Up

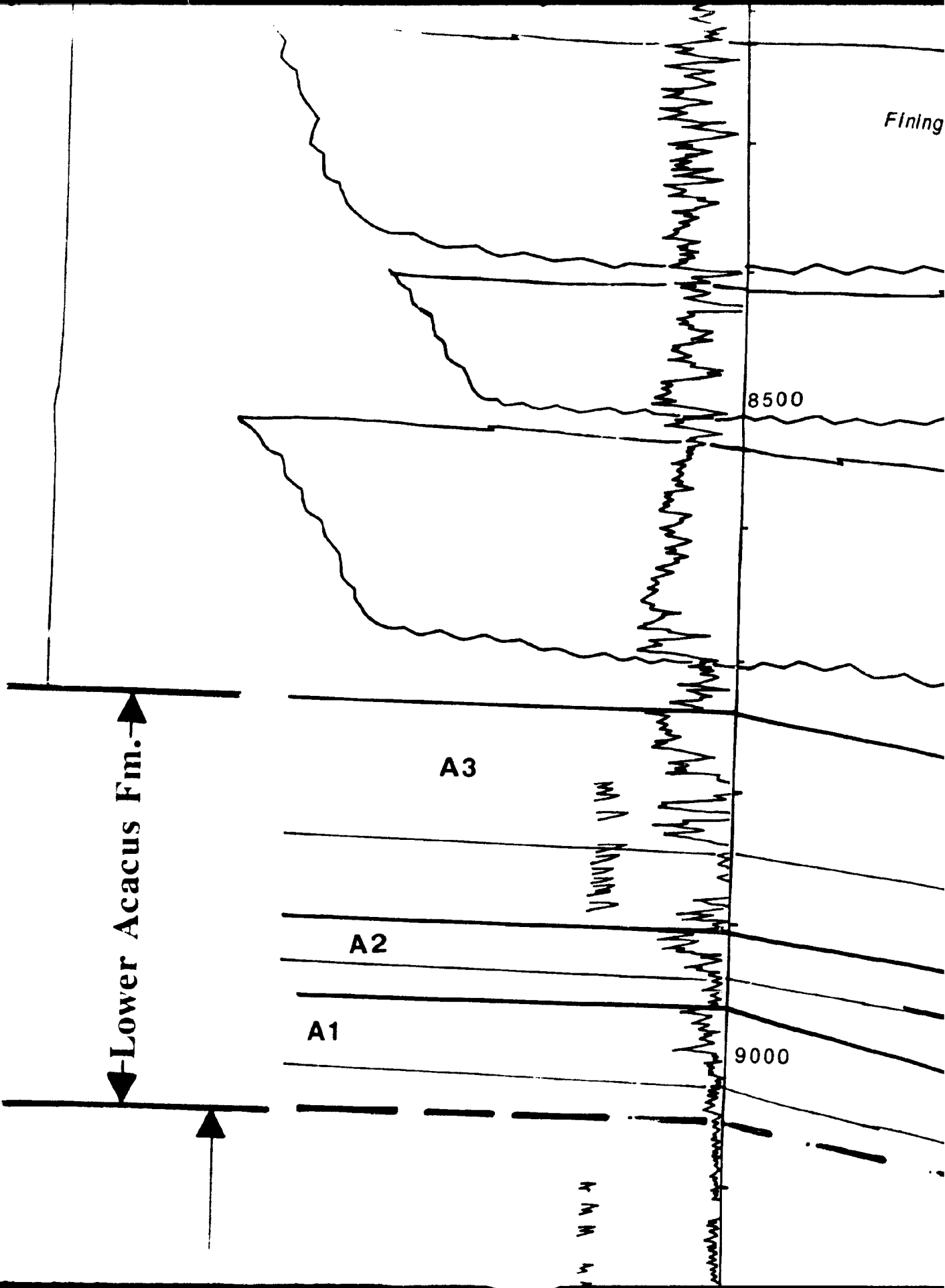
Lower Acacus Fm.

Upper Silurian

7500



1



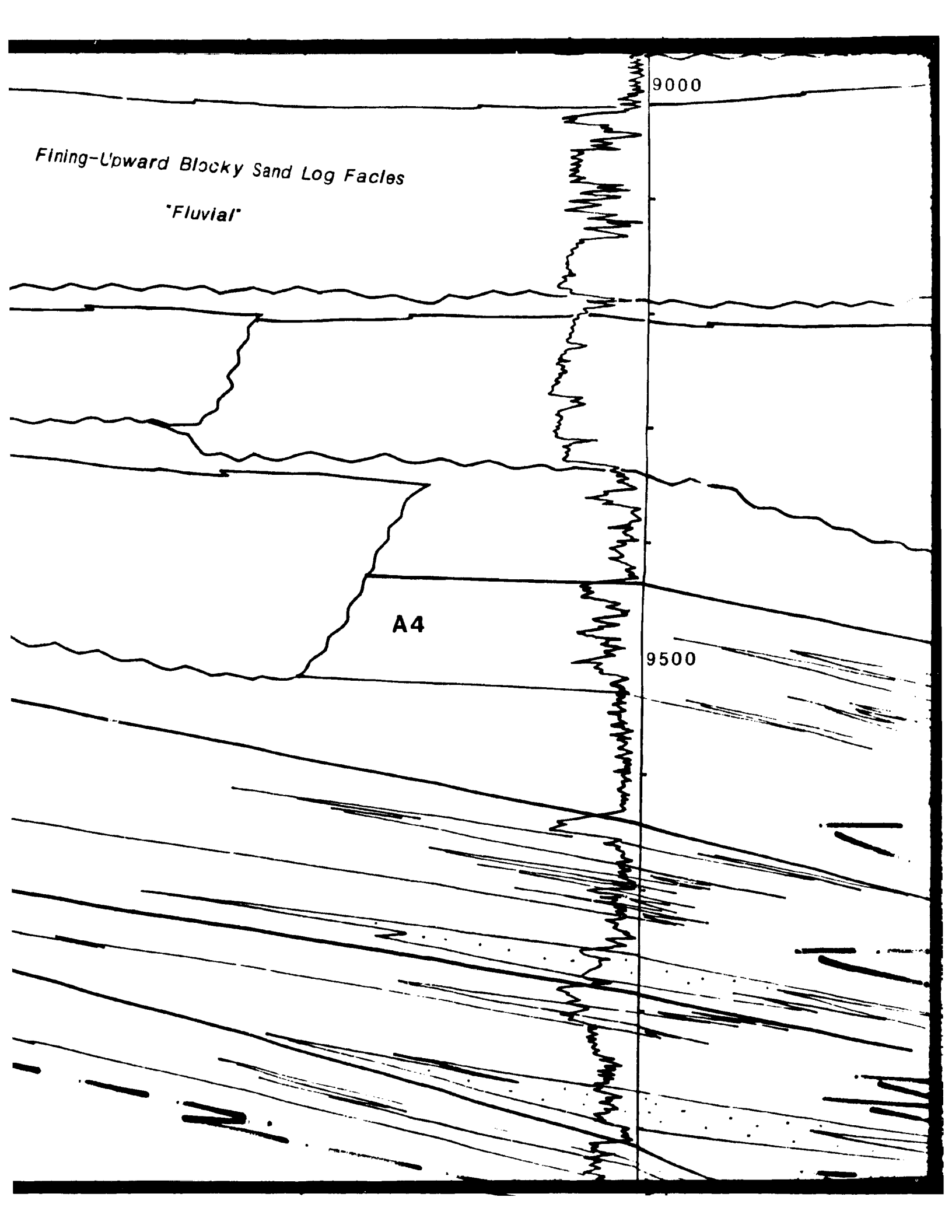
Fining-Upward Blocky Sand Log Facies

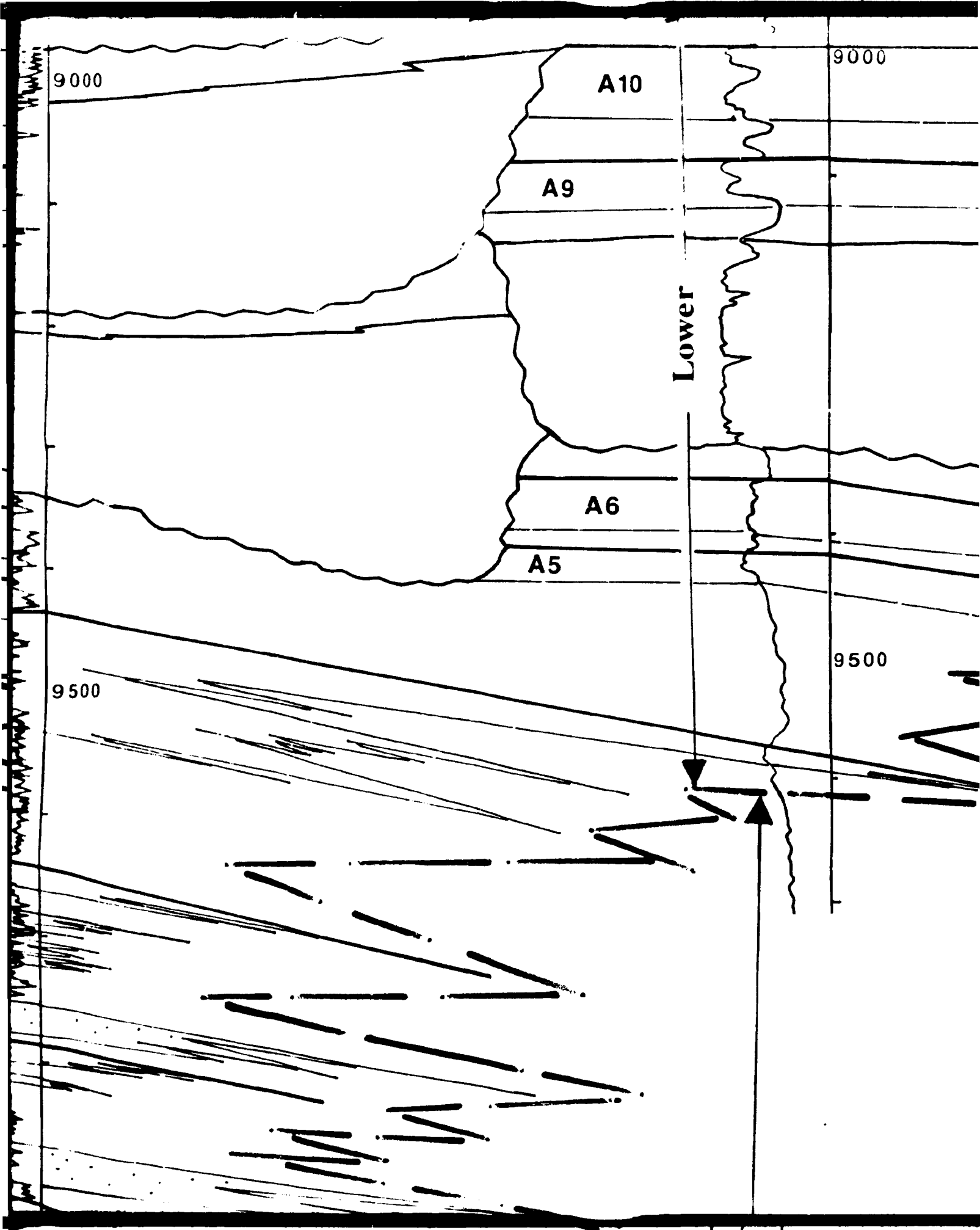
"Fluvial"

9000

A4

9500





9000

9000

A10

A9

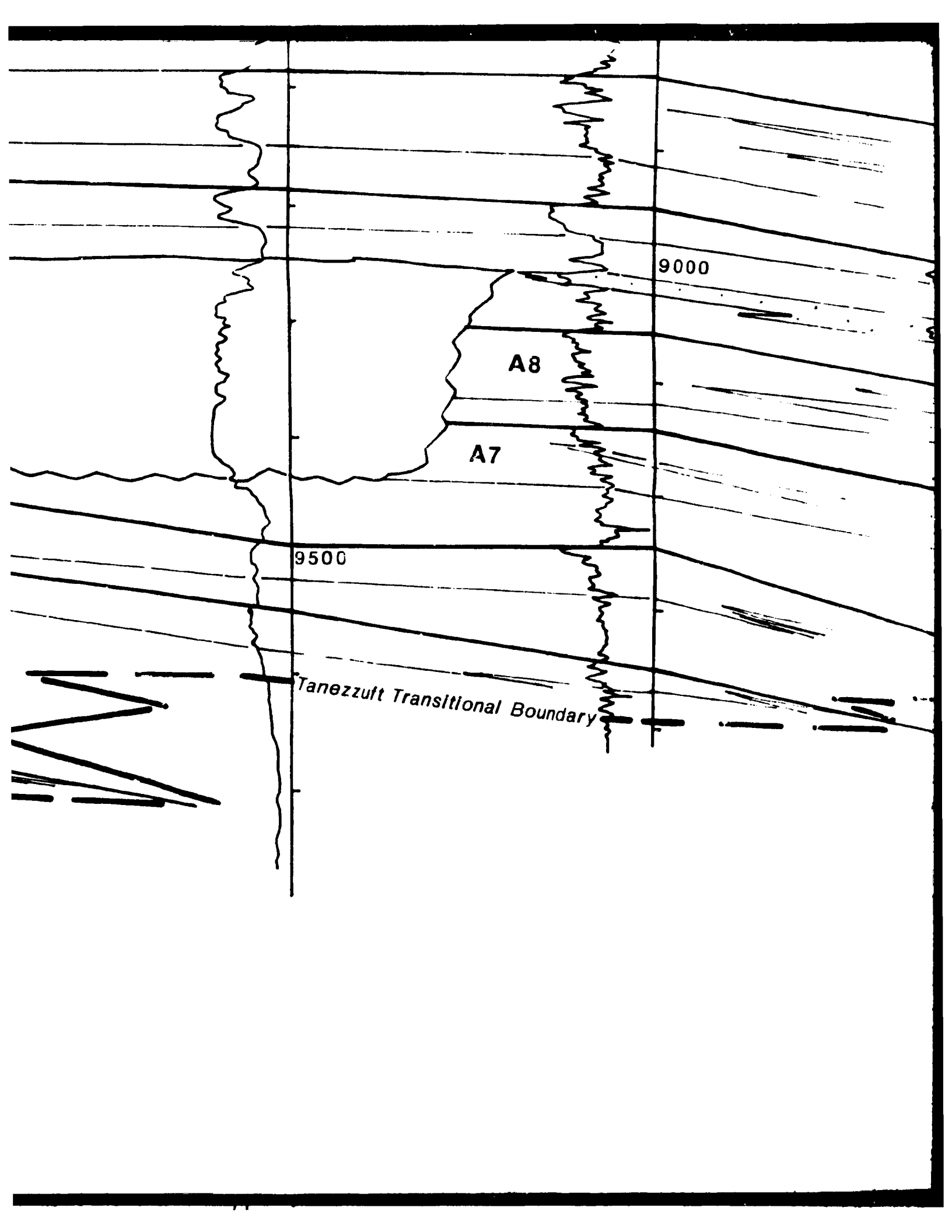
Lower

A6

A5

9500

9500



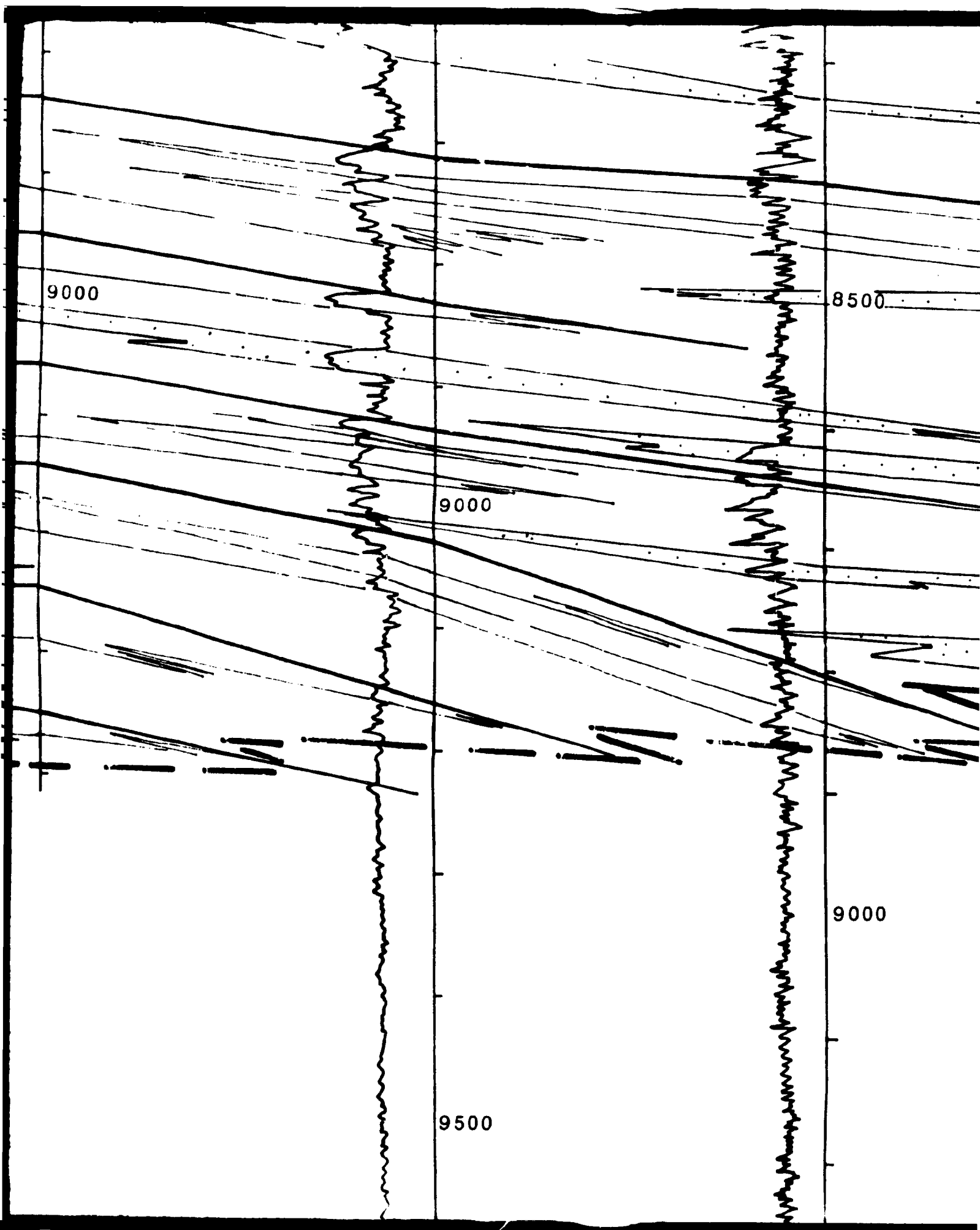
9000

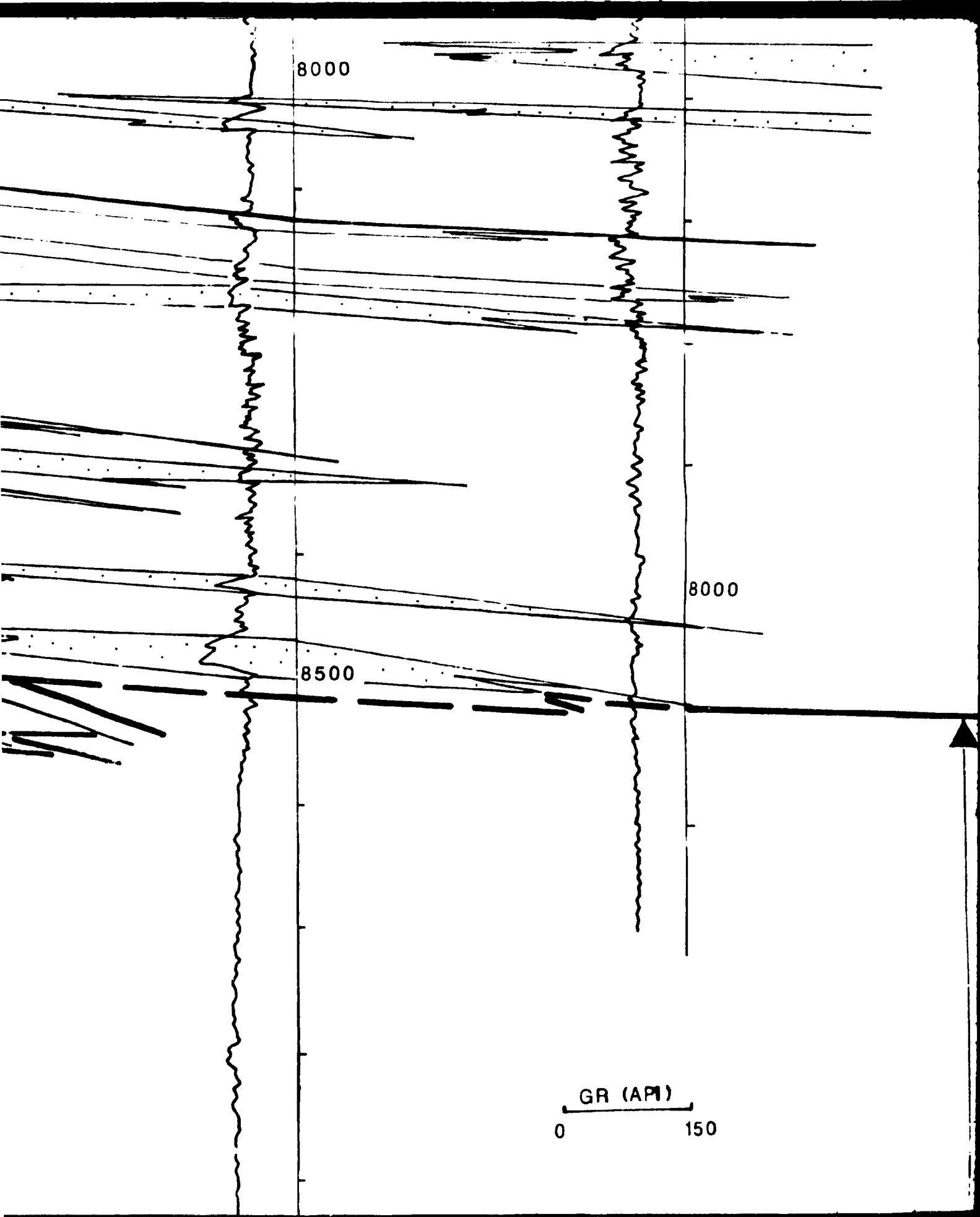
A8

A7

9500

Tanezzuft Transitional Boundary





8000

8000

8500

GR (API)
0 150

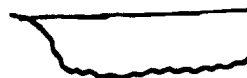
7500

Low

8000

21)

150



A1-A14

A15-A1

LEGEND

— DRY HOLE

— OIL WELL

— OIL AND GAS WELL

— TOP GENETIC UNIT "COARSENING-
UPWARD SANDSTONE UNIT" LINE

— FACIES LINE

— TANEZZUFT TRANSITIONAL
BOUNDARY

— FLUVIAL CHANNEL

-A14 LOWER ACACUS SANDSTONE UNITS

-A16 MIDDLE ACACUS SANDSTONE UNITS

Lower Acacus

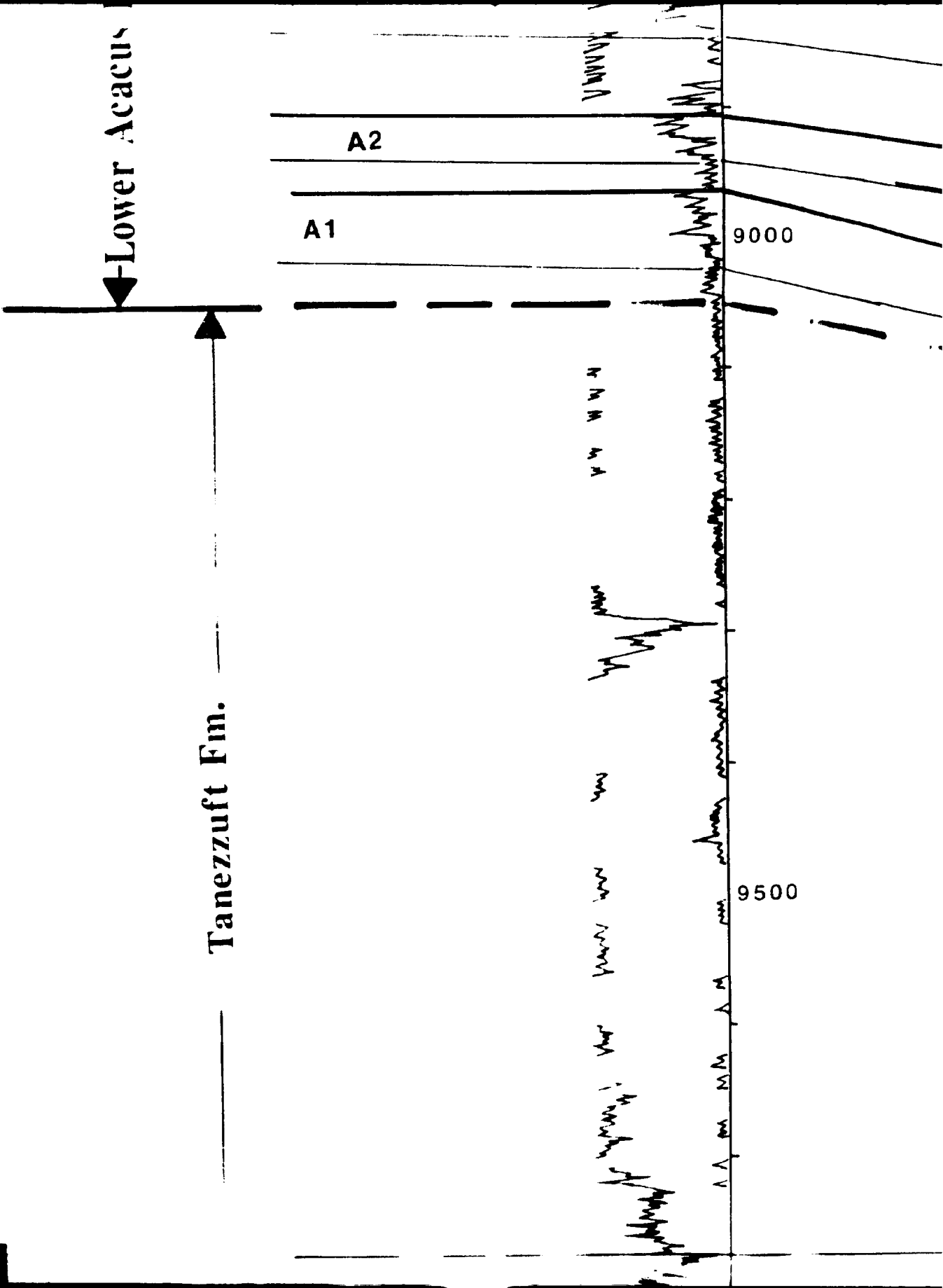
A2

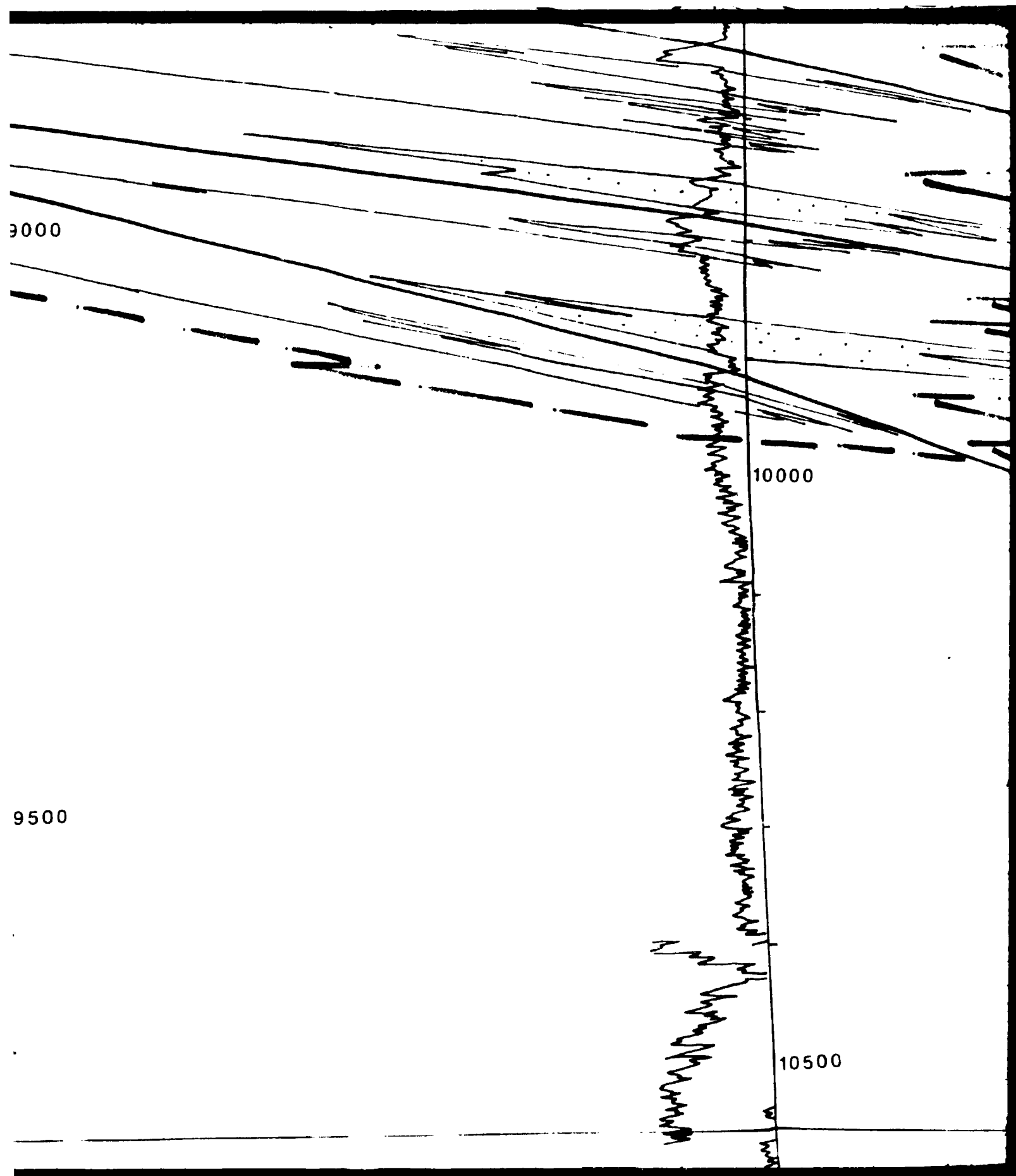
A1

9000

Tanezzuft Fm.

9500

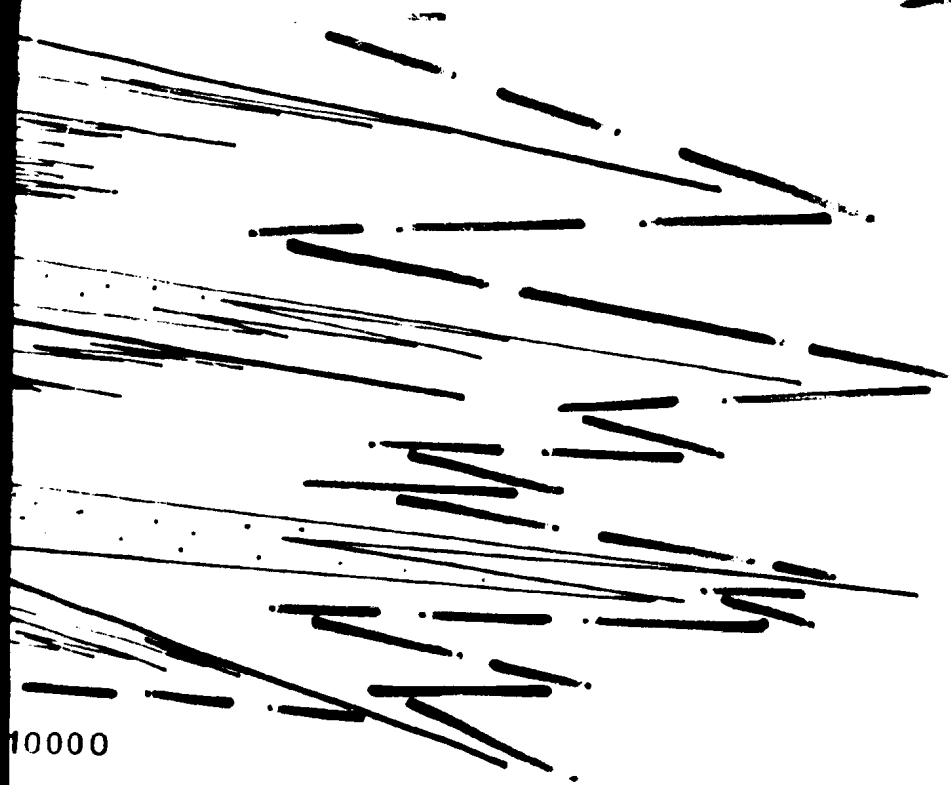




10000

10500

Tanezzufi Fm.



Shale Log Facies

"Basina"



9500

10000



9500

9500



9000

9500

GR (API)
0 150

Tanezzuft Fm.

(API)

150

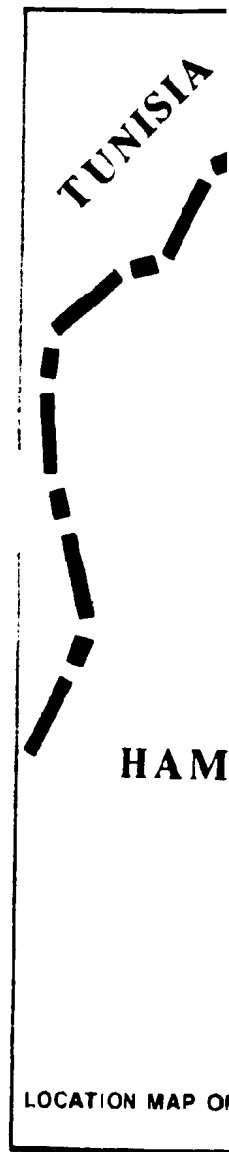
Tanezzuft Fm.

Lower Silurian



A1-A1

A15-A



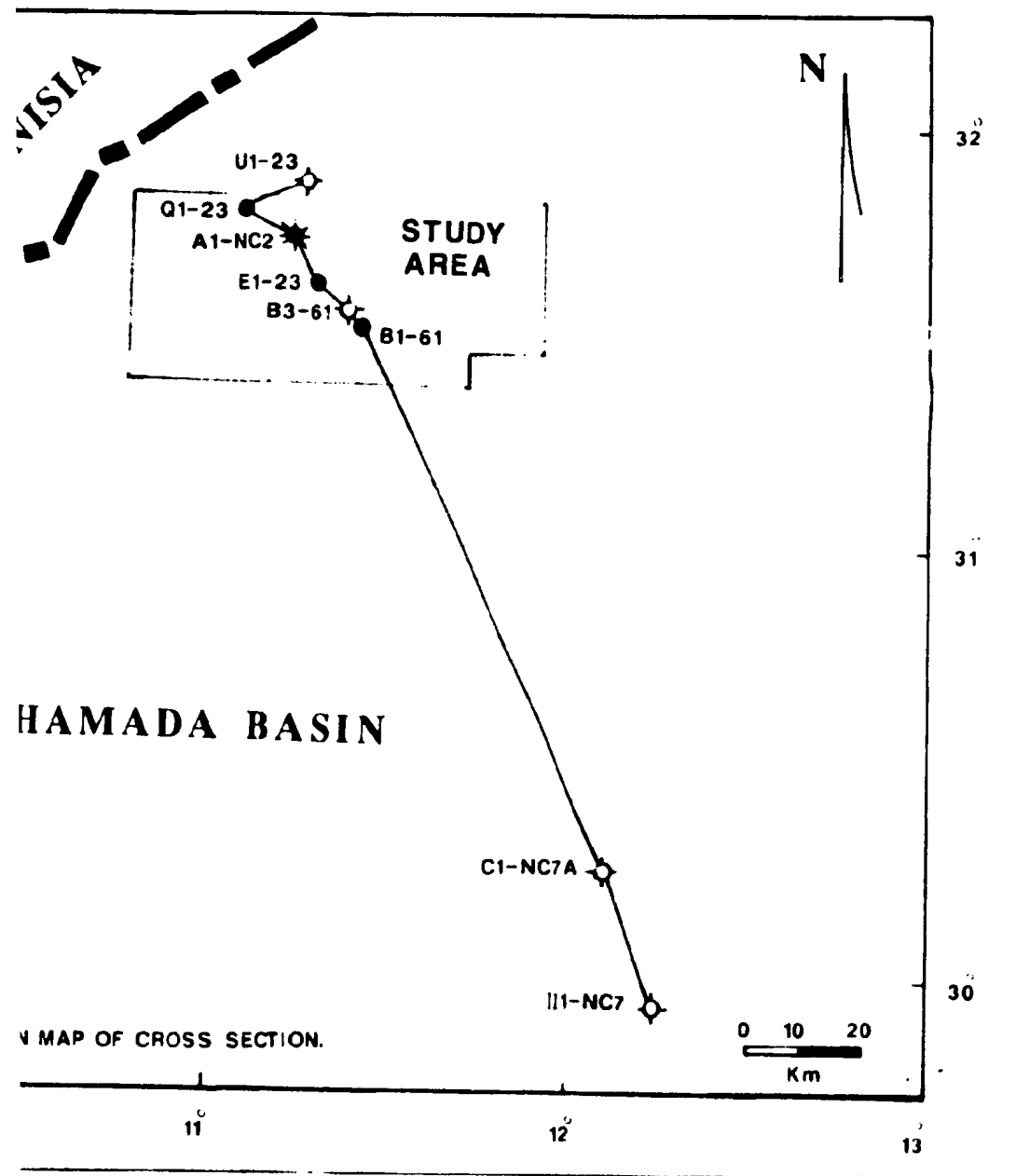
FACIES LINE

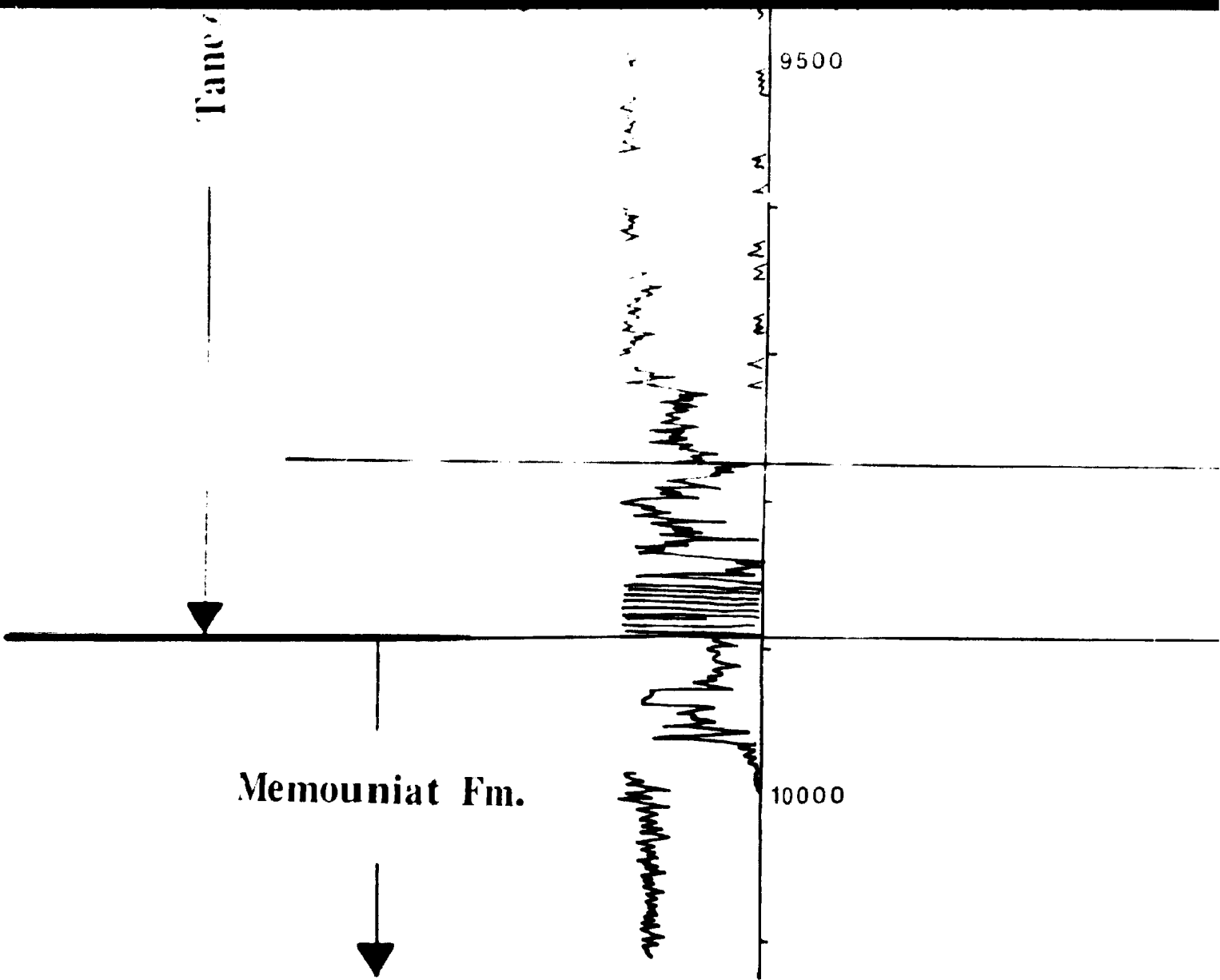
TANEZZUFT TRANSITIONAL
BOUNDARY

FLUVIAL CHANNEL

1-A14 LOWER ACACUS SANDSTONE UNITS

15-A16 MIDDLE ACACUS SANDSTONE UNITS





Tancos

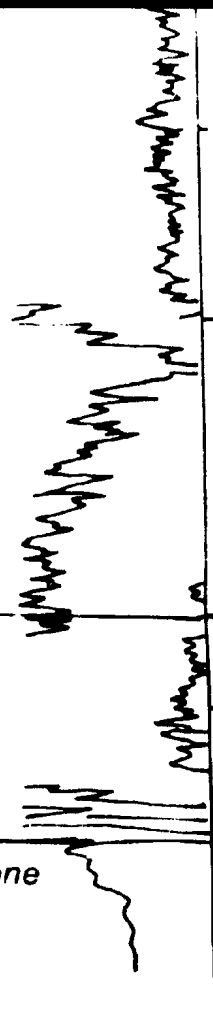
9500

Memouniat Fm.

10000

0

10

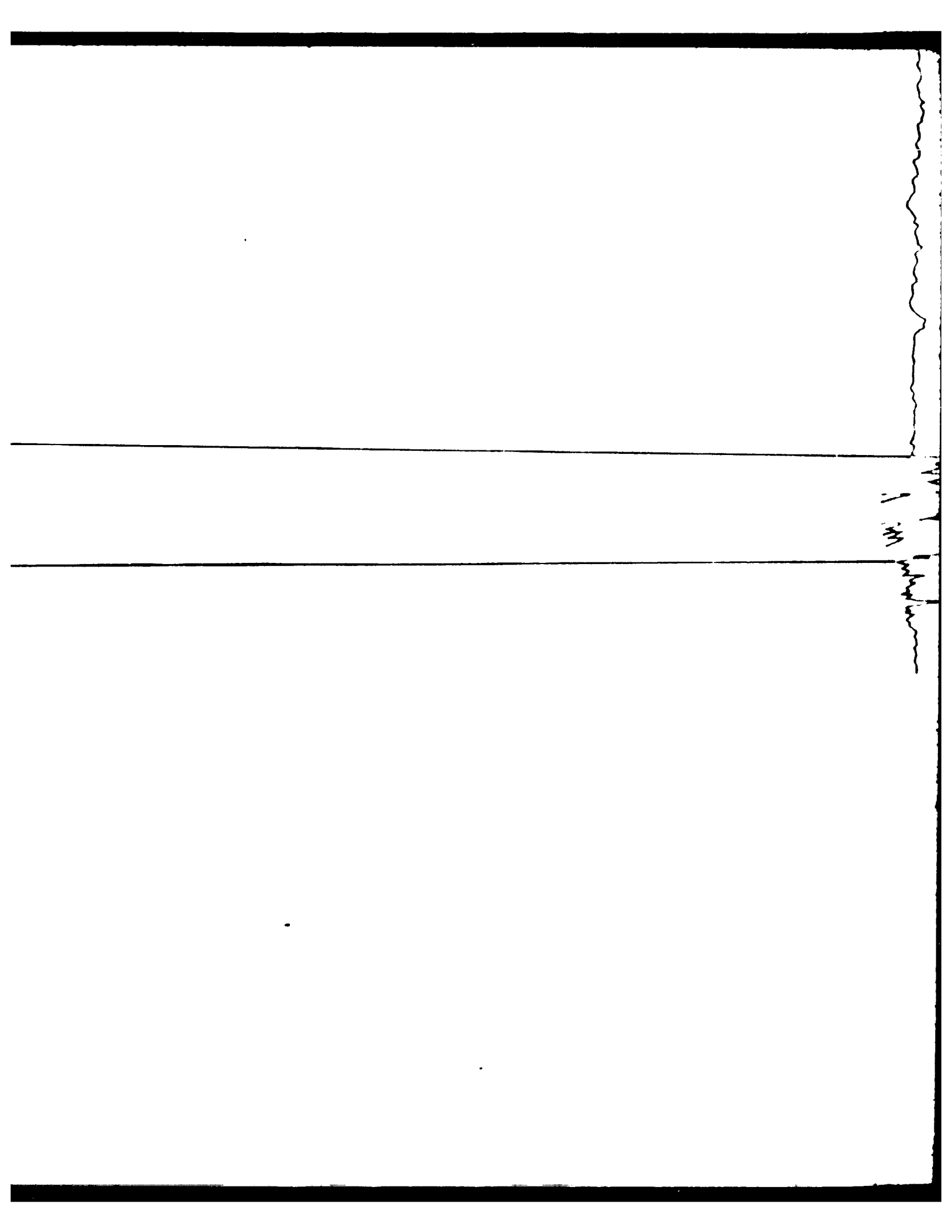


10500

Terminal sandstone

500

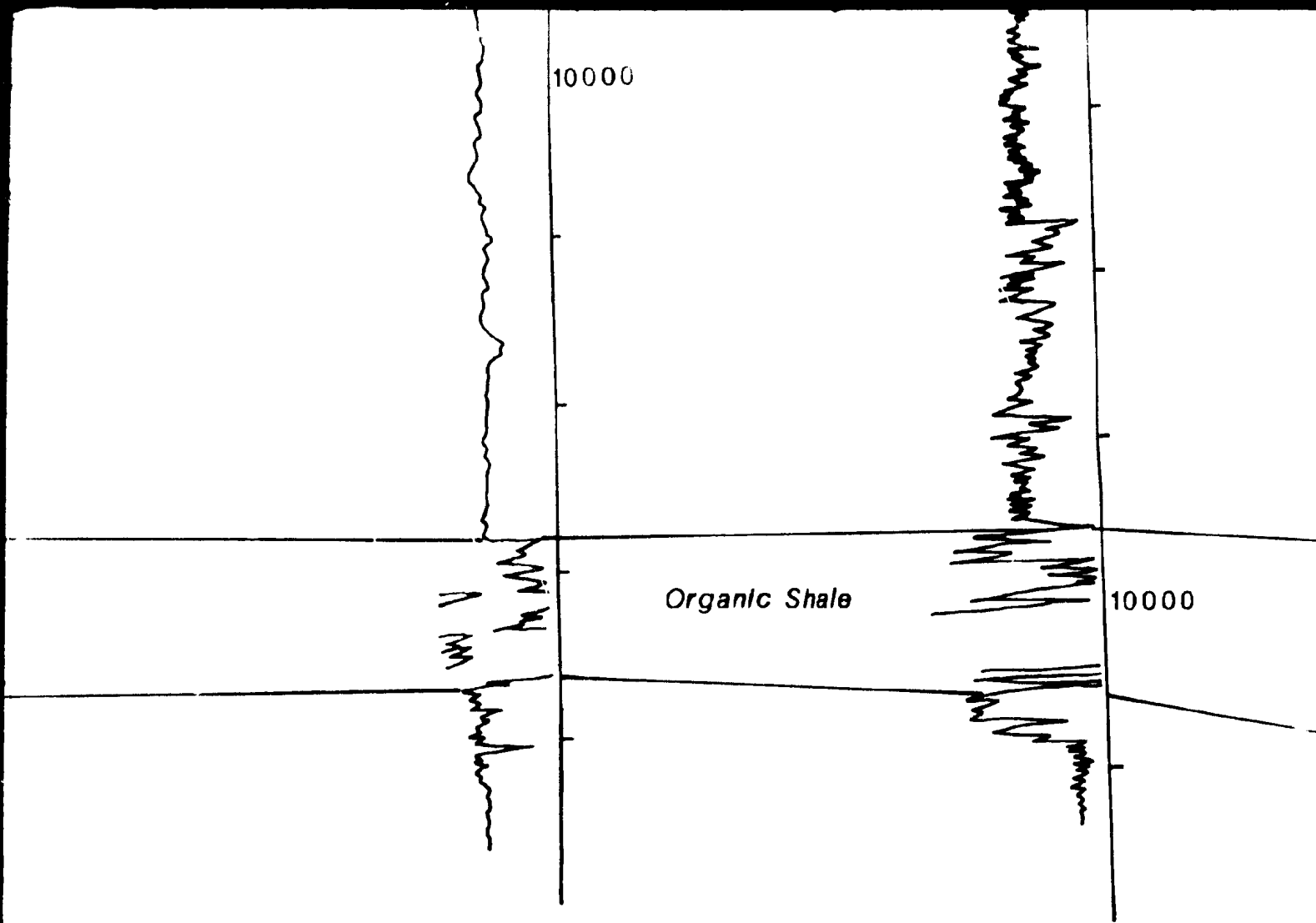




10000

Organic Shale

10000



9500

Memouniat Fm.
Cambro-Ordovician



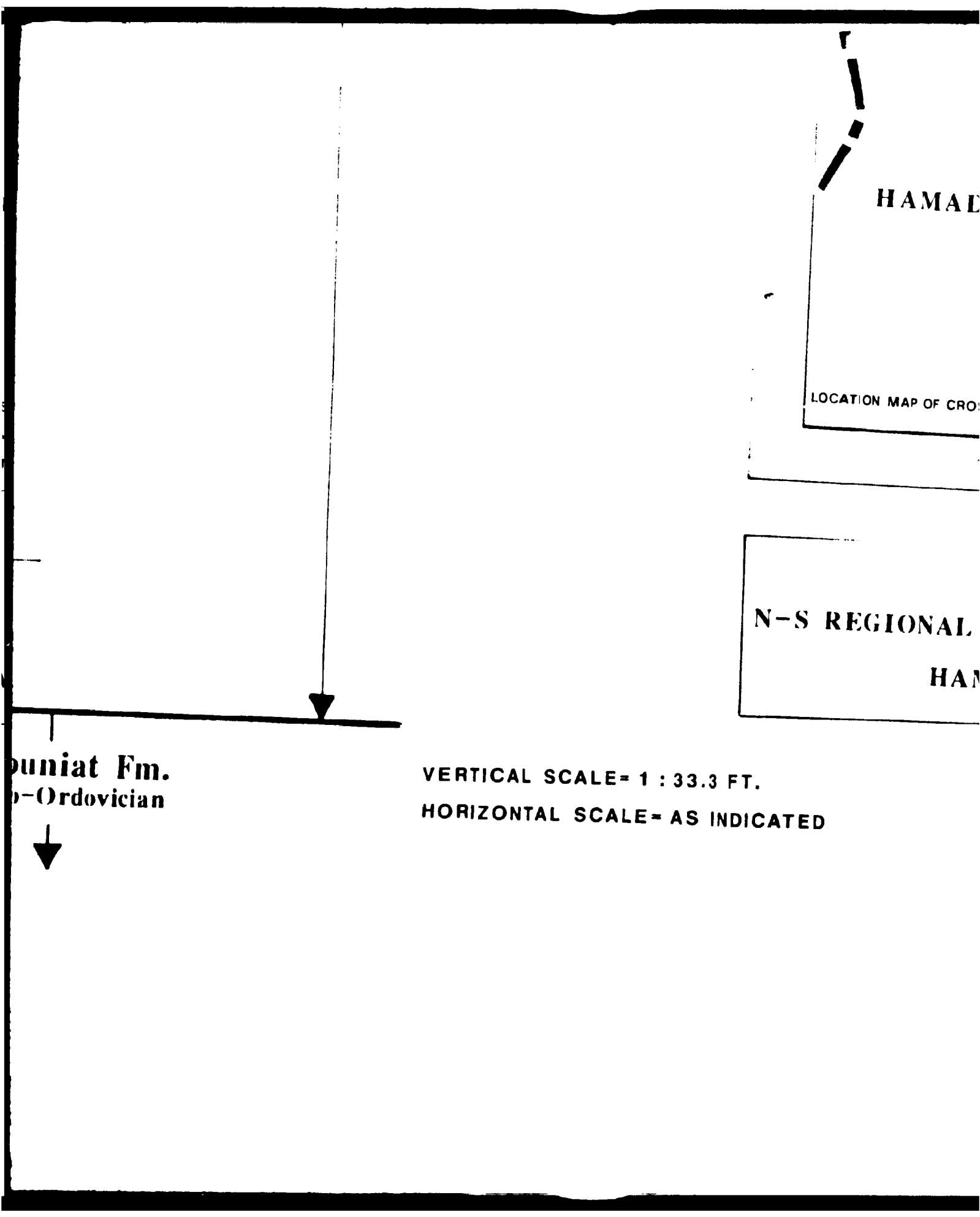
HAMAL

LOCATION MAP OF CRO

N-S REGIONAL
HAM

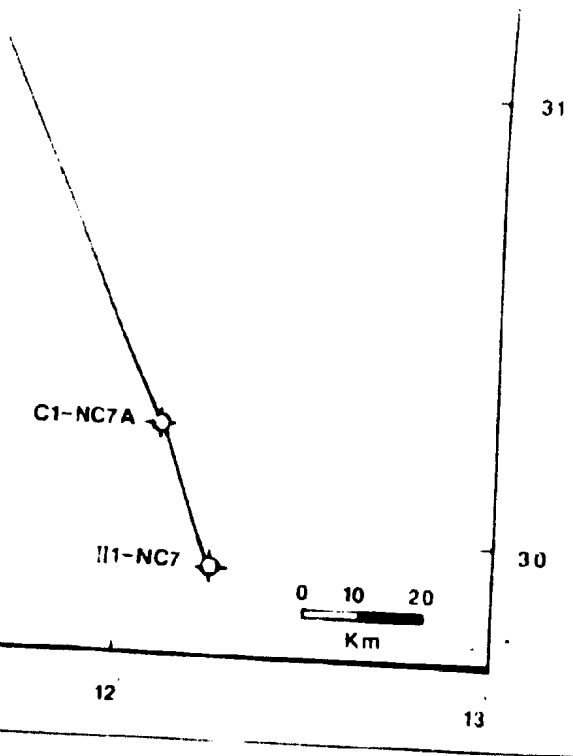
Duniat Fm.
p-Ordovician

VERTICAL SCALE = 1 : 33.3 FT.
HORIZONTAL SCALE = AS INDICATED



HAMADA BASIN

MAP OF CROSS SECTION.



ENCLOSURE No. 2

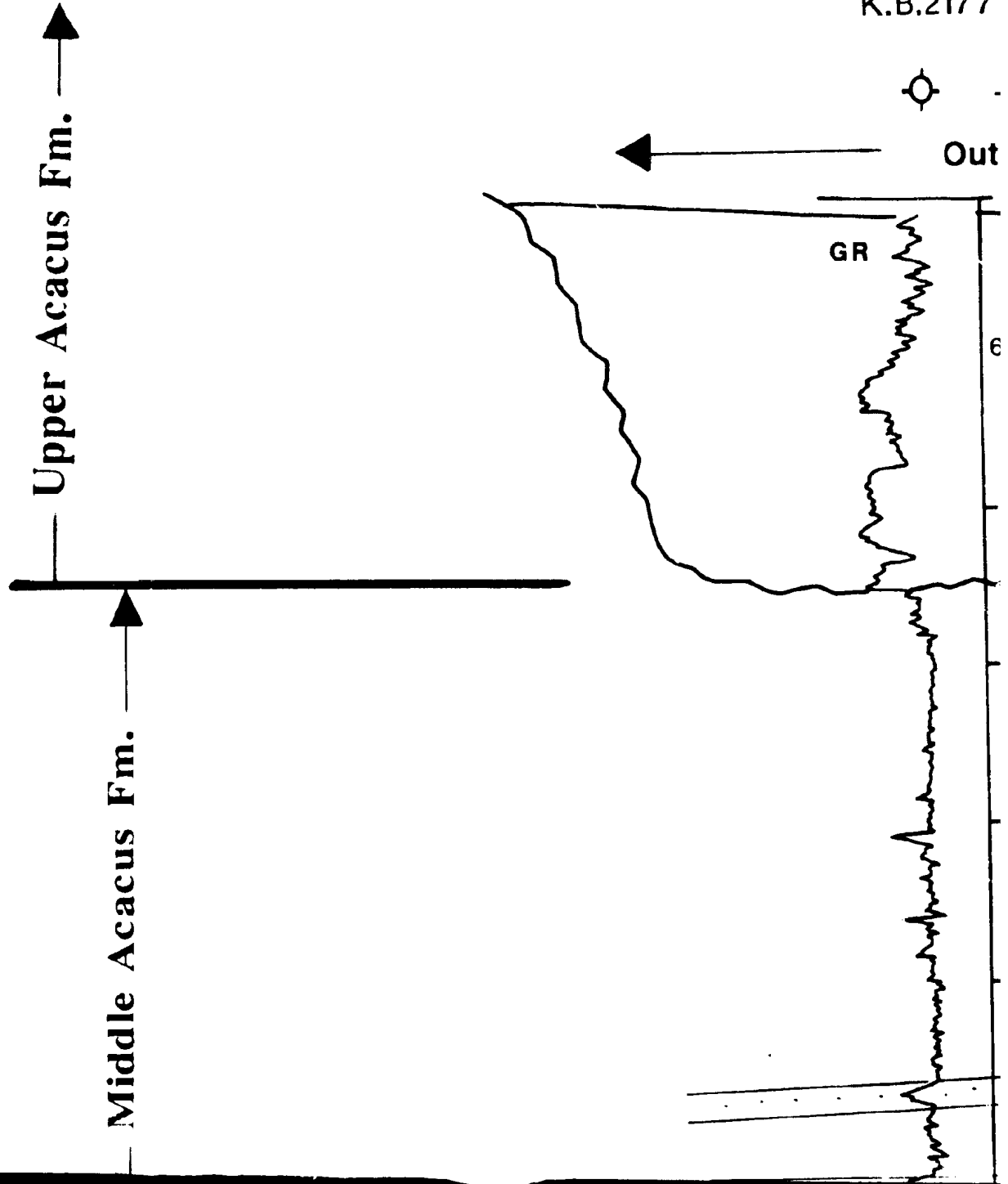
REGIONAL STRATIGRAPHIC CROSS SECTION,
HAMADA BASIN, NW LIBYA.

OBE-91

NWN

U1-23

K.B.2177



J1-23

K.B.2177

Q1-23

K.B.2040

A1-NC2

K.B.2160



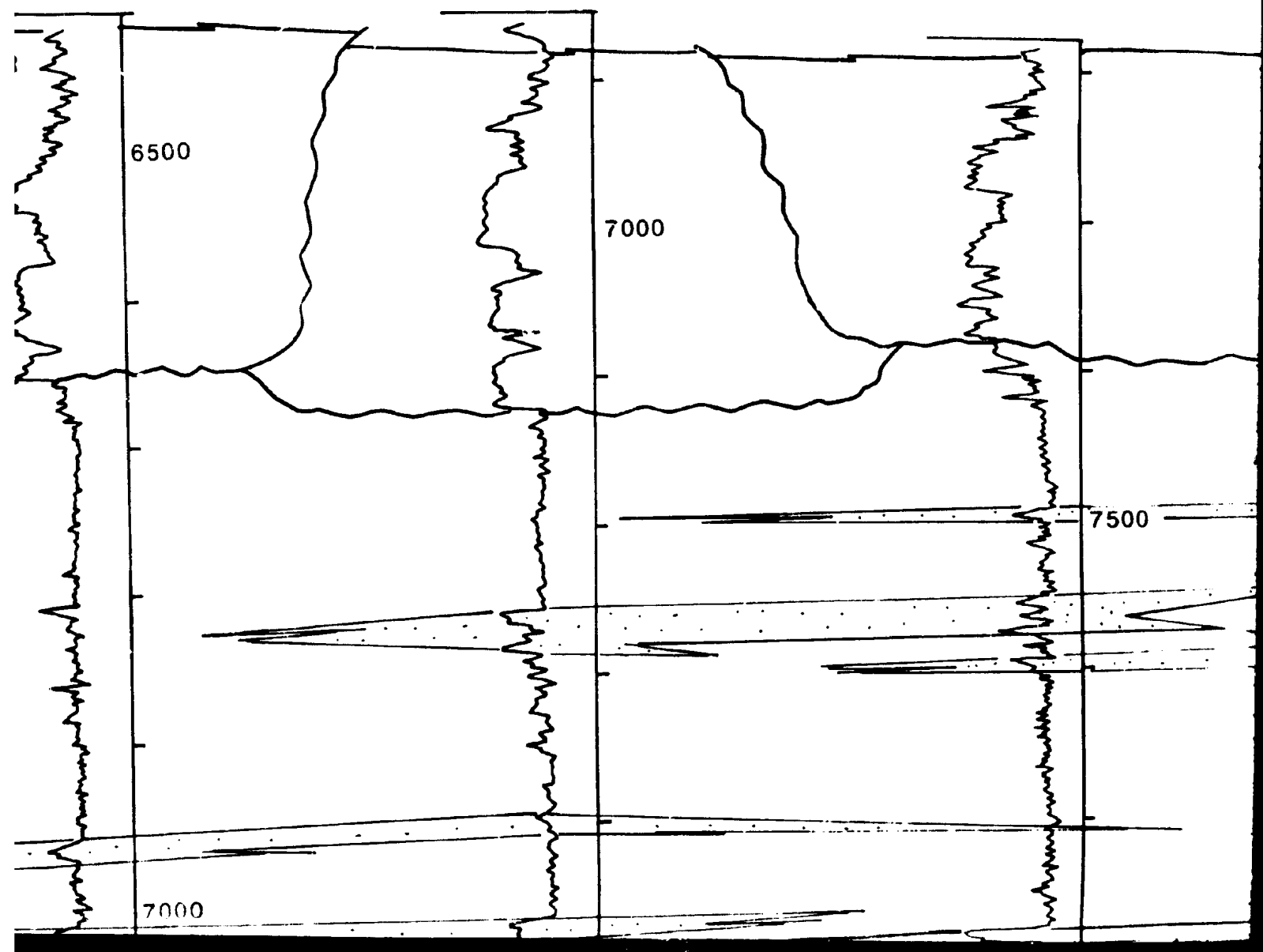
19Km.



17Km.



Outside Study Area



A1-NC2

K.B.2160

D1-M

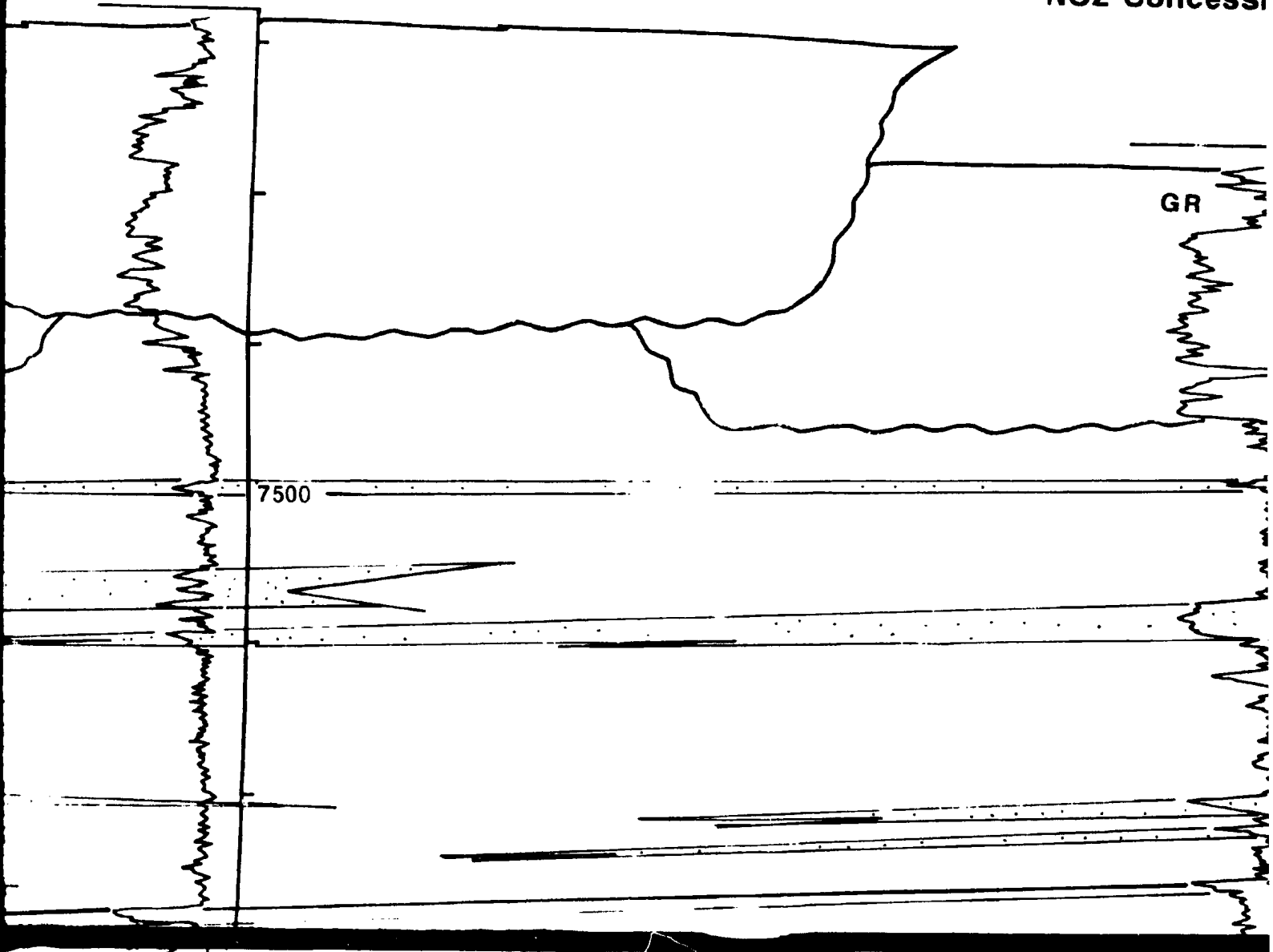
K.B.



47 Km.

Hama

NC2 Concessi



D1-NC2

K.B.1968

B2-NC2

K.B.1997

F1-NC2

K.B.1982



4Km.

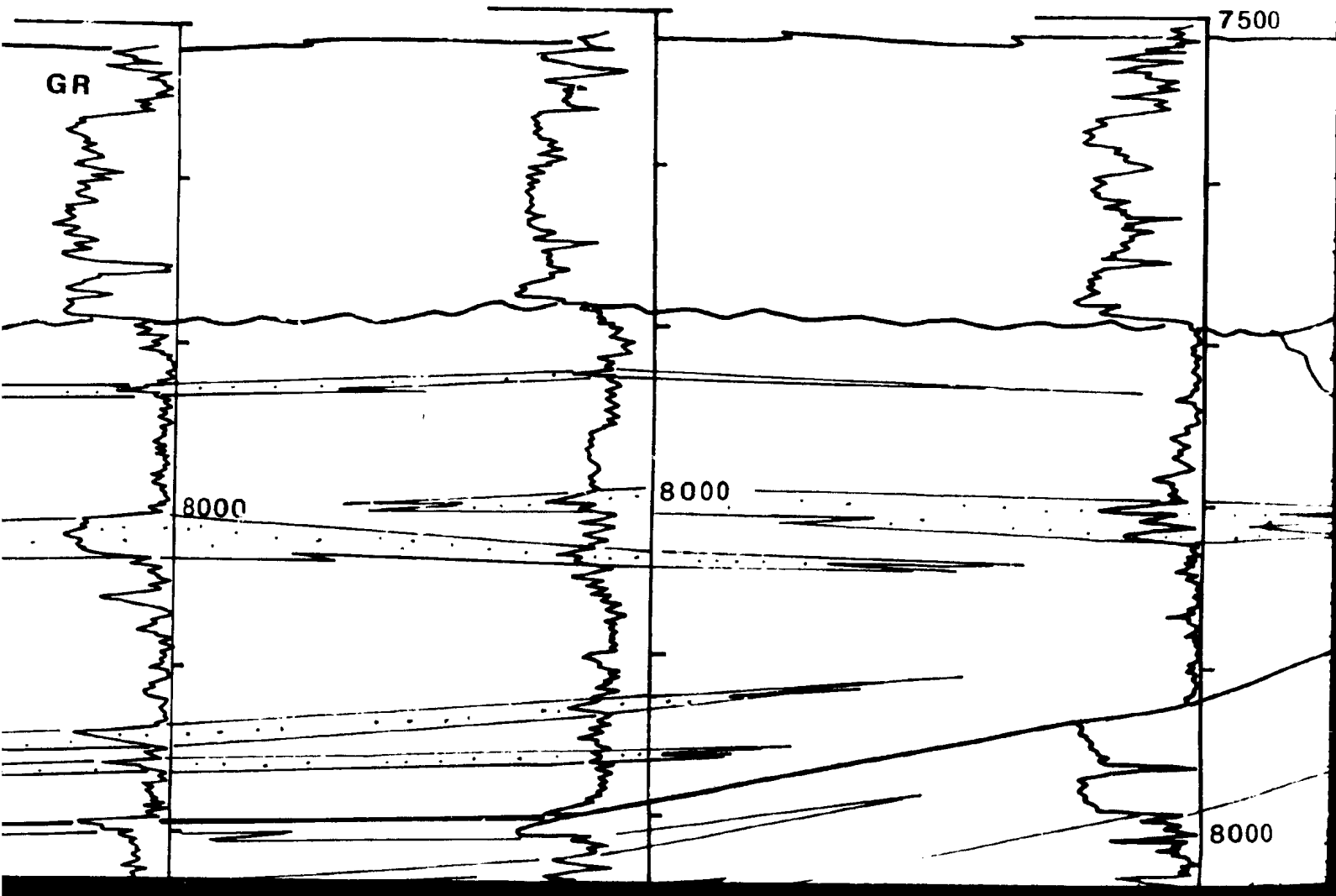


5Km.



Hamada North

Concession "Study Area"



F1-NC2

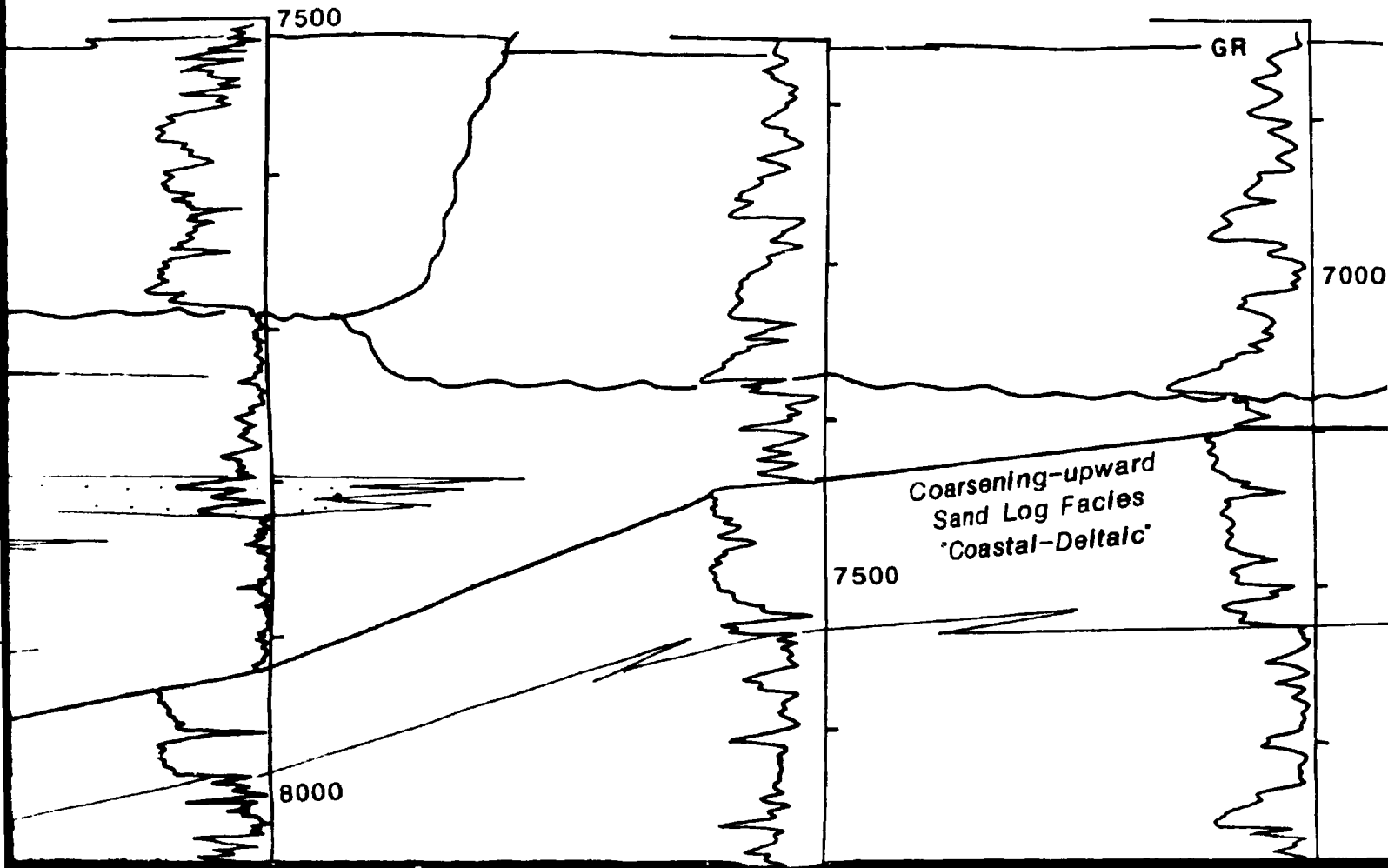
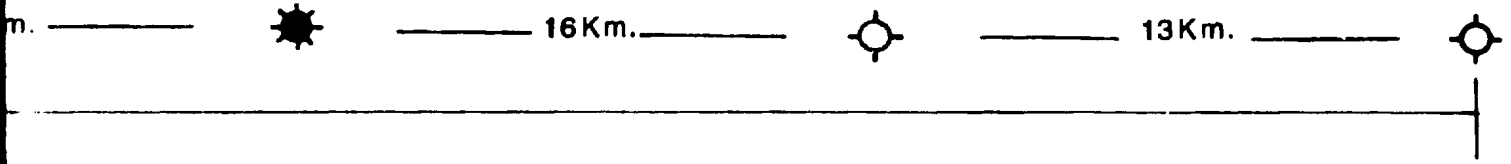
K.B.1982

A1-61

K.B.2141

C1-61

K.B.2131

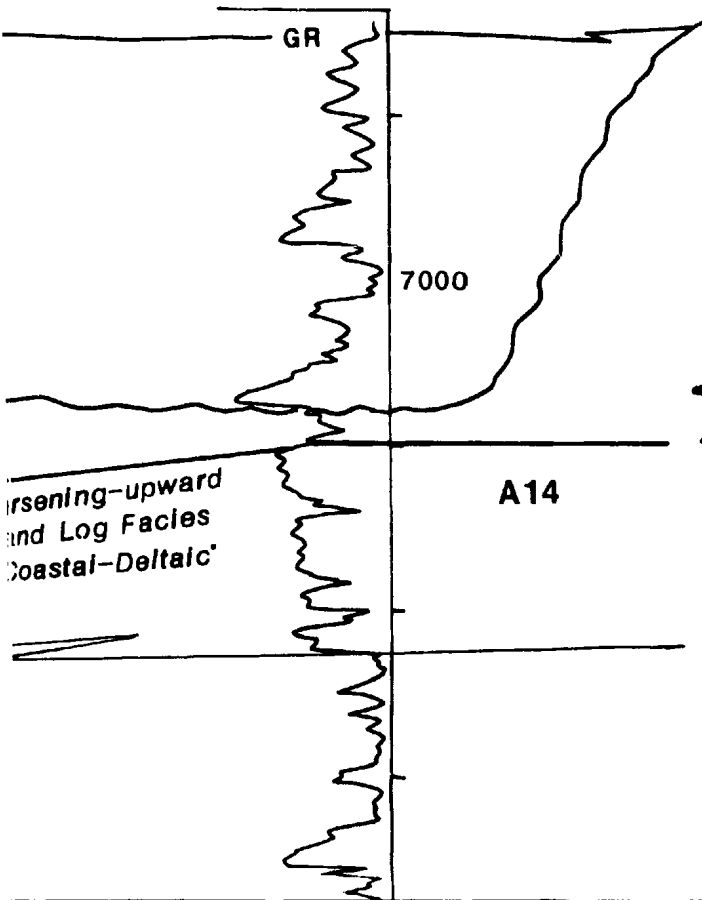
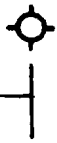


NE

C1-61

K.B.2131

13Km.



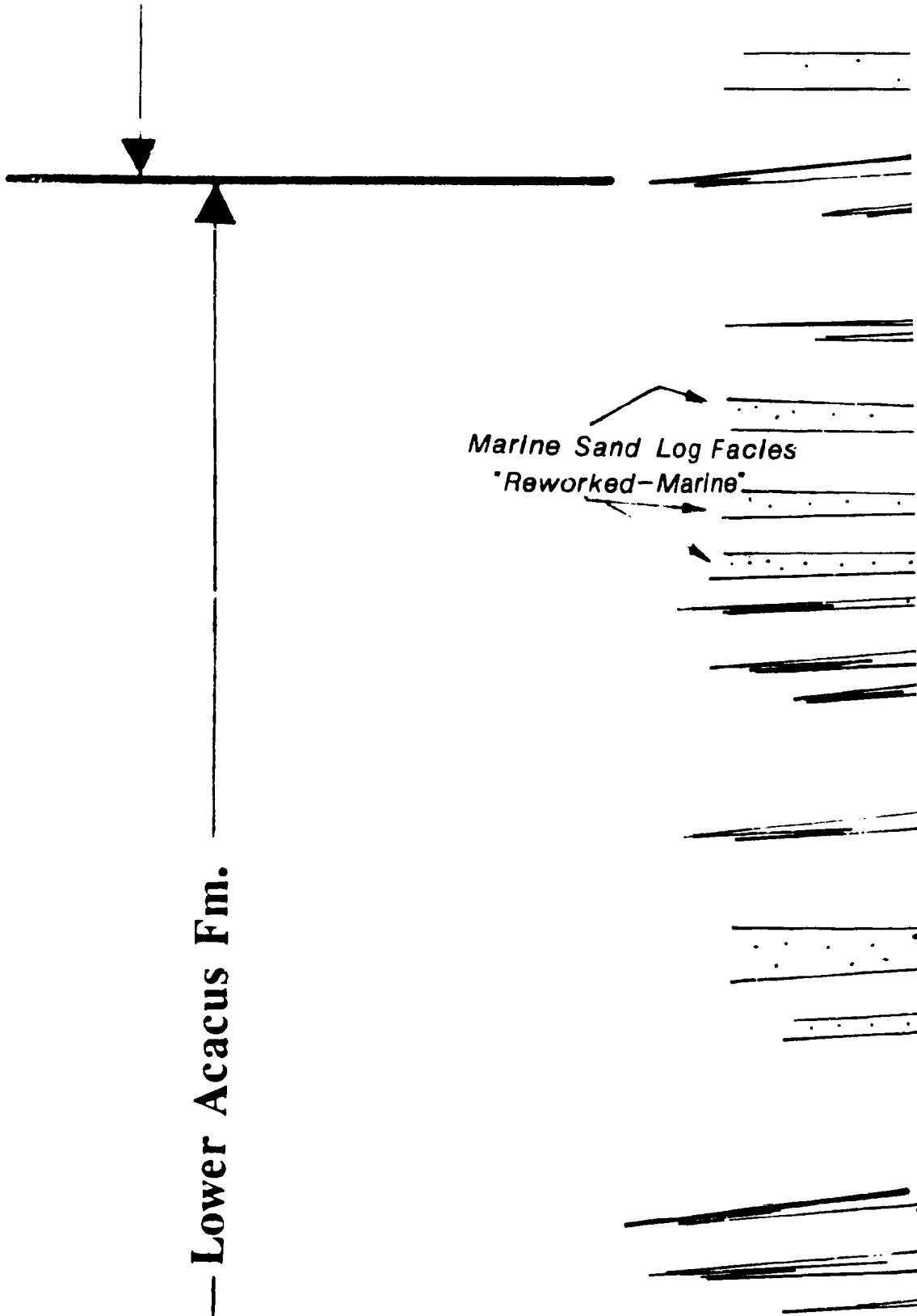
Middle Acacus Fm. "Upper Silurian"

Upper Acacus Fm.
Upper Silurian



Upper Acacus Fm. —↑
Upper Silurian"

m. "Upper Silurian"



Lower Acacus Fm.

Marine Sand Log Facies
"Reworked-Marine"

7000

7500

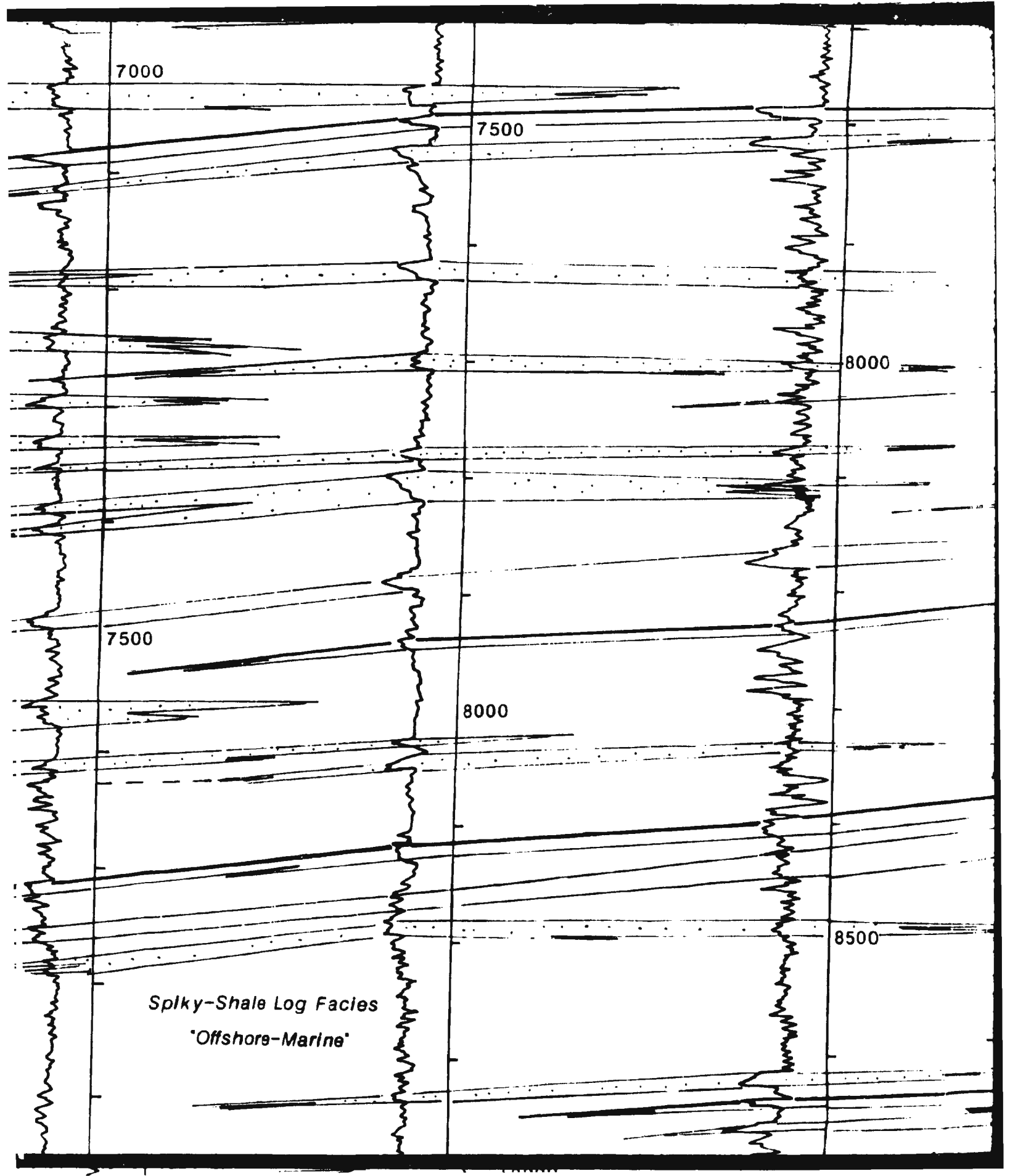
8000

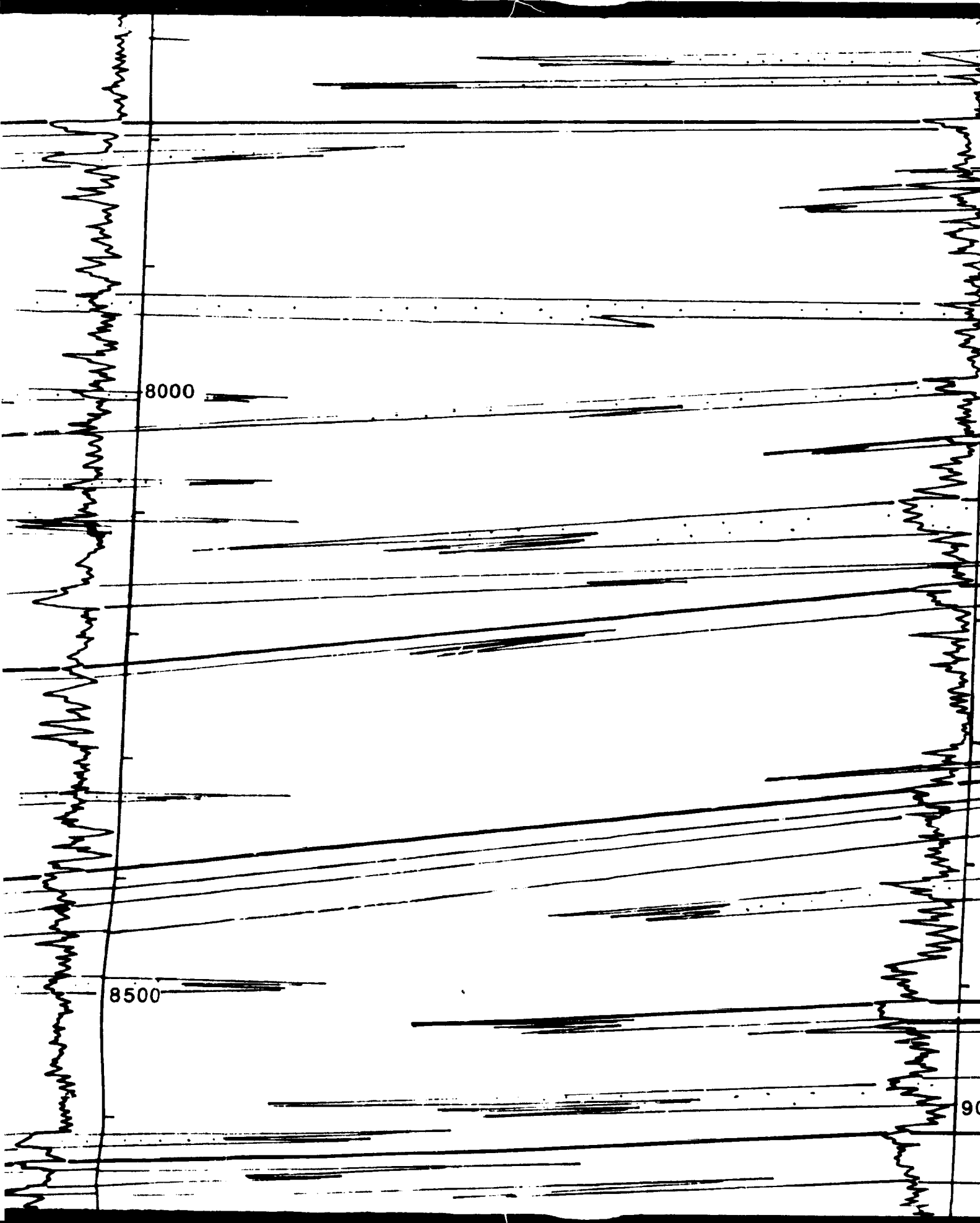
7500

8000

8500

Splky-Shale Log Facies
'Offshore-Marine'

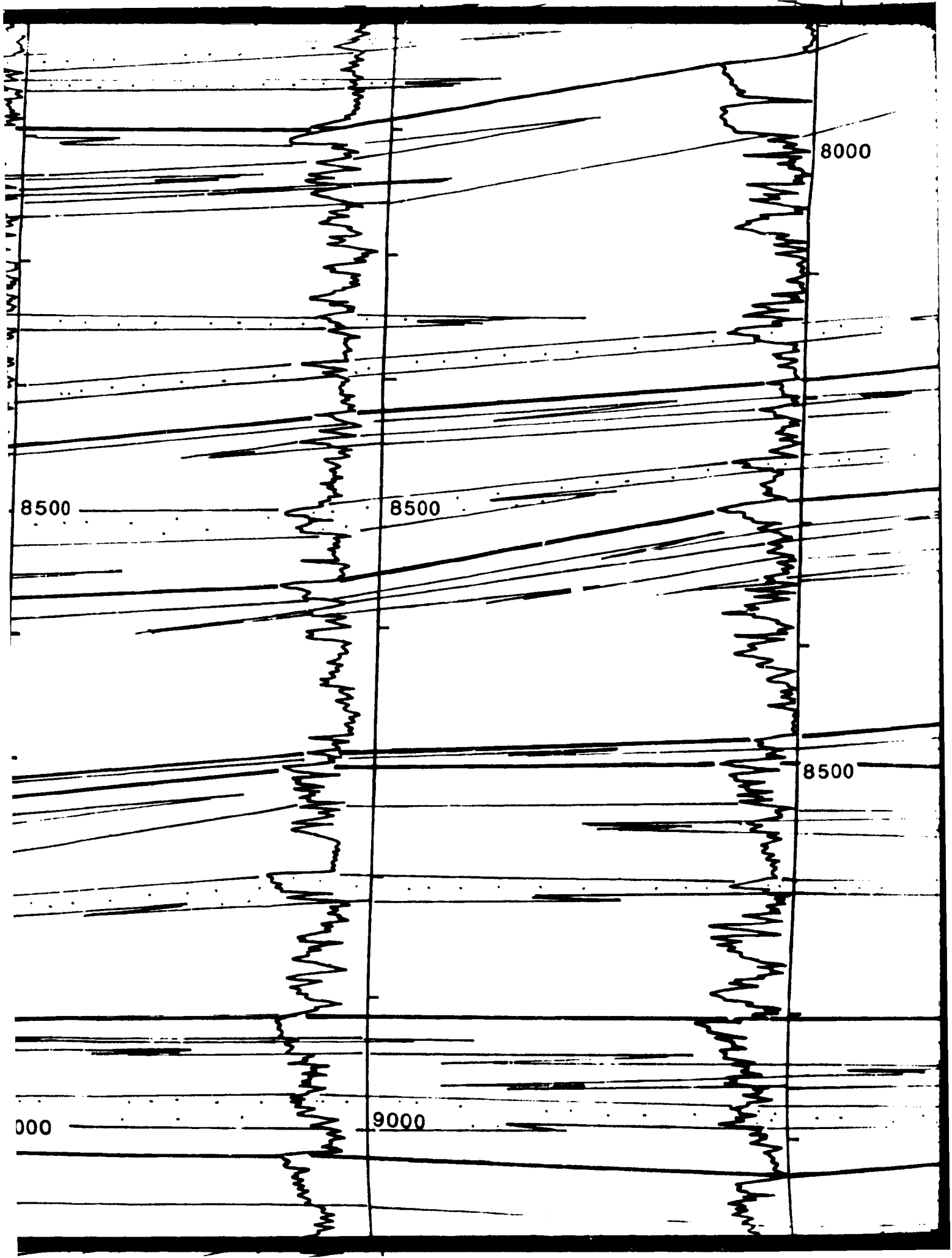




8000

8500

90



8000

8500

8500

8500

000

9000

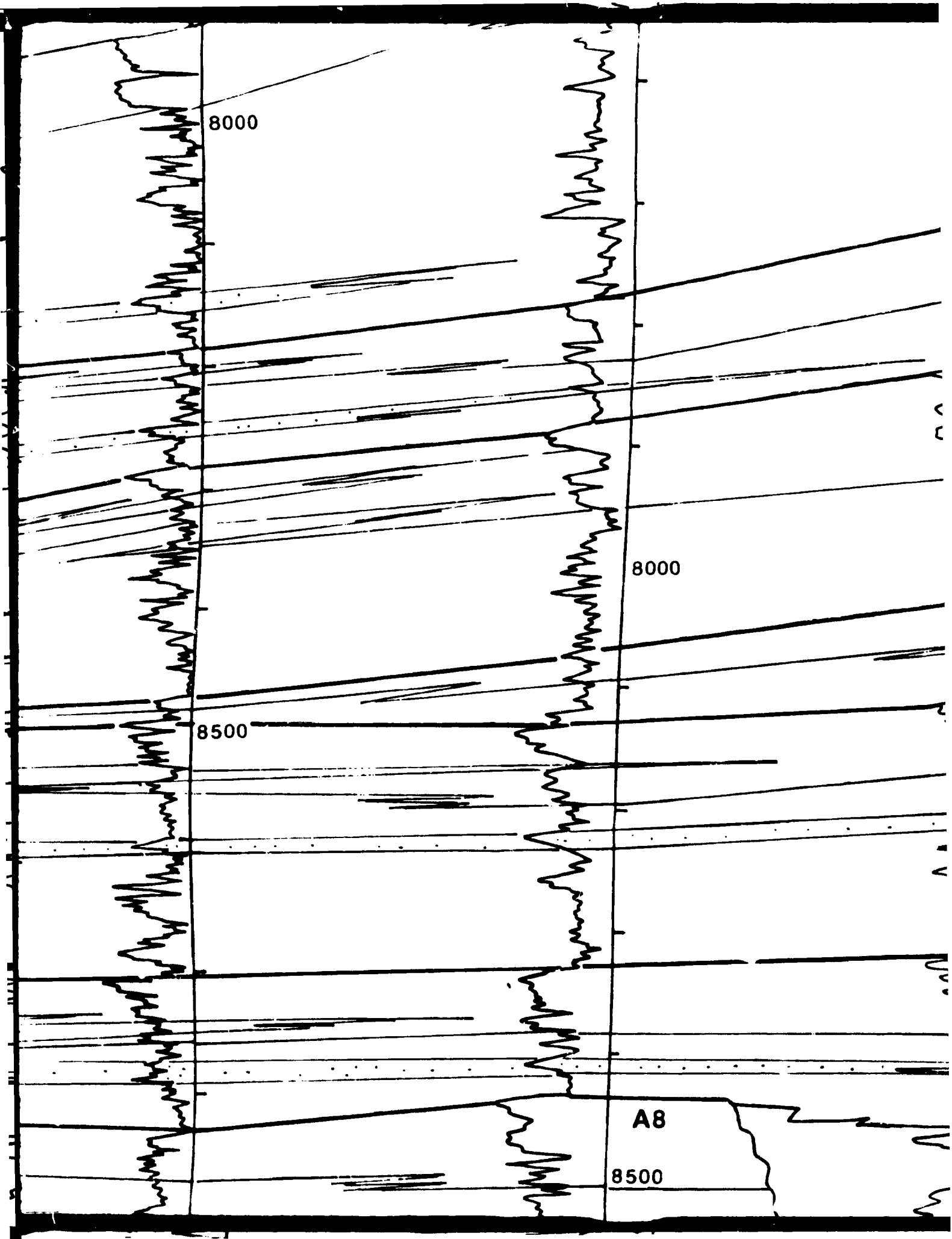
8000

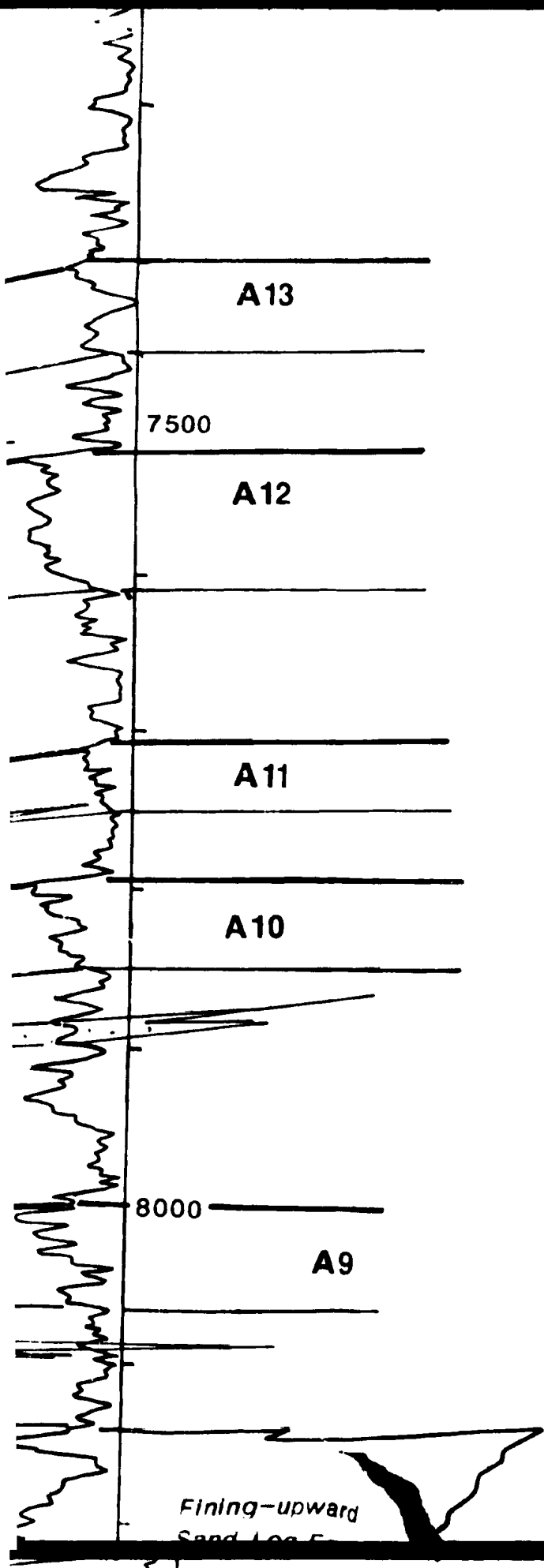
8000

8500

A8

8500





Lower Acacus Fm.

"Upper Silurian"

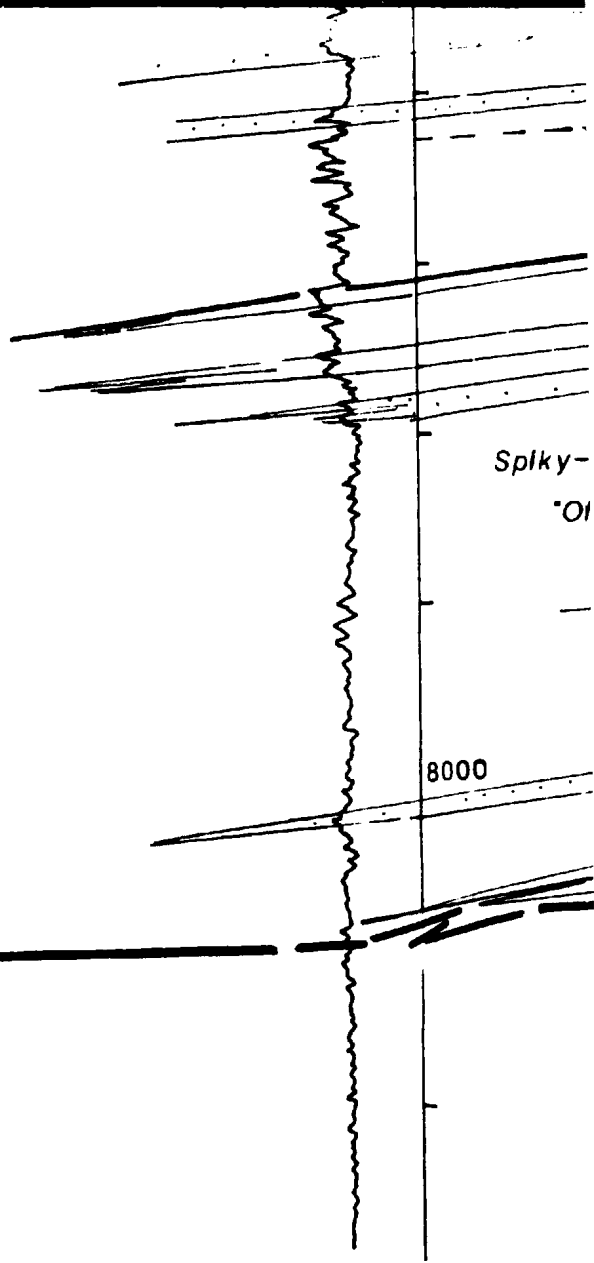
Upper Silurian



1



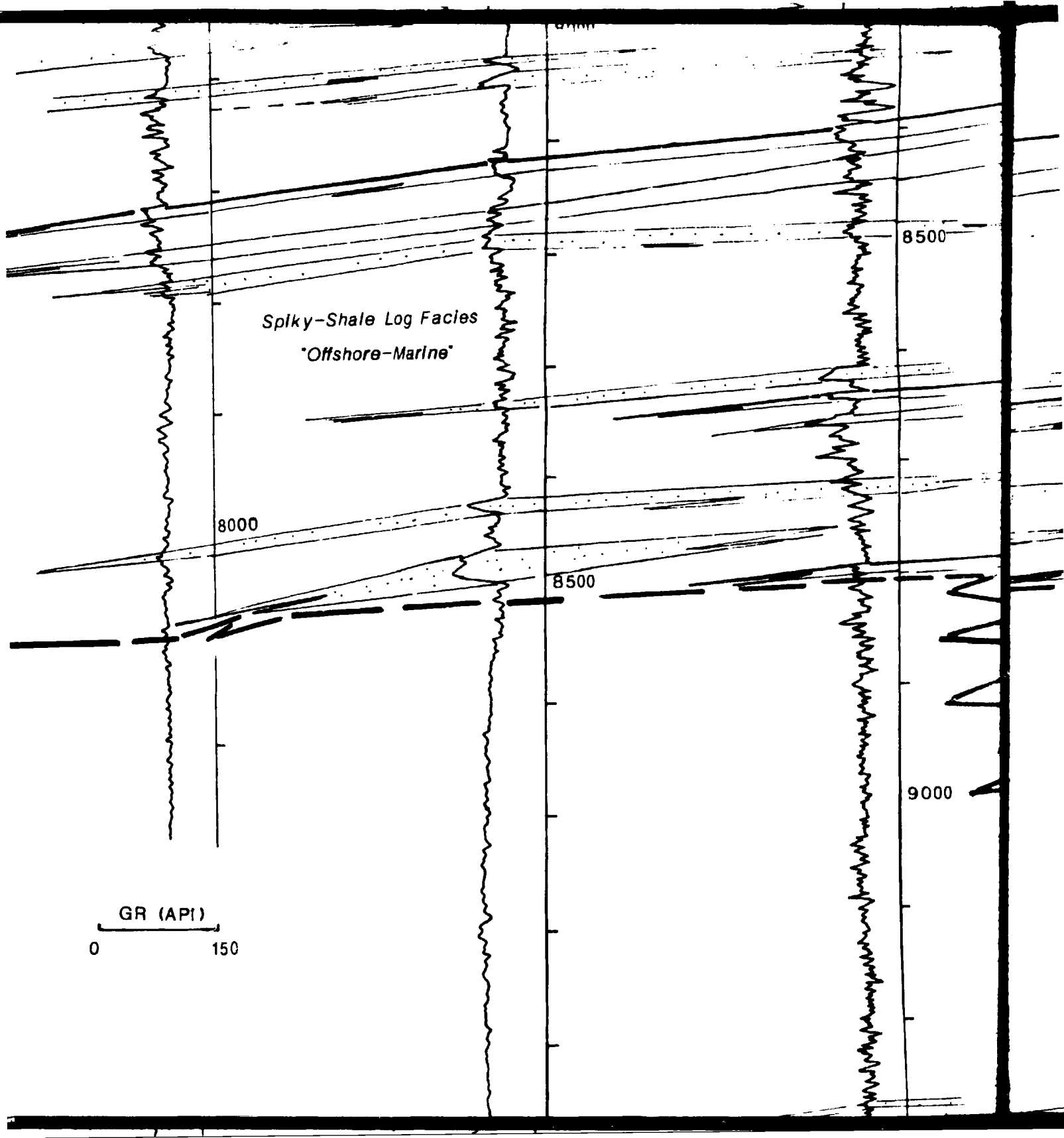
Lower Acacus F.



Splky-
"OI

8000

GR (API)
0 150



Splky-Shale Log Facies
'Offshore-Marine'

8000

8500

8500

9000

GR (API)
0 150

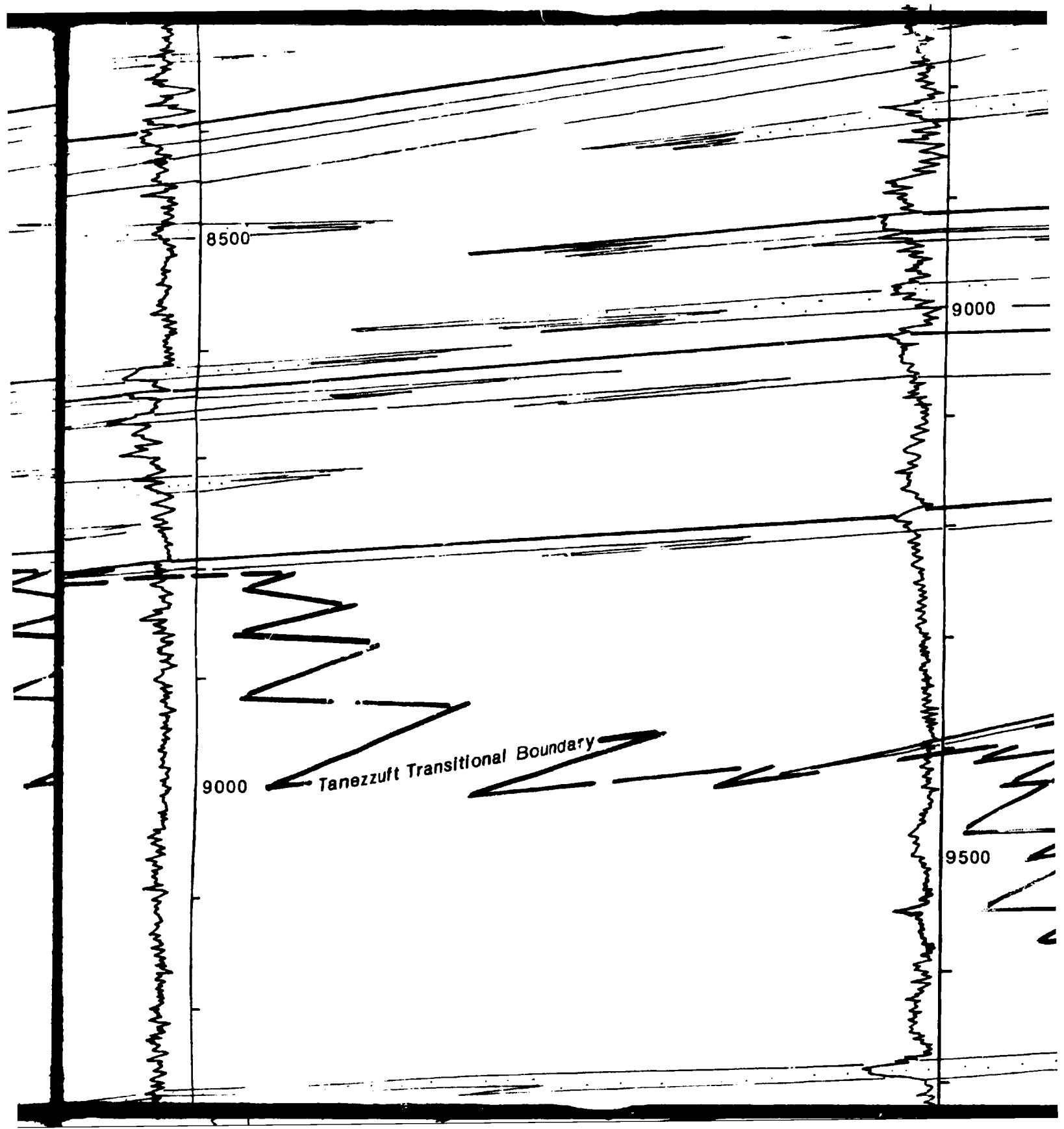
8500

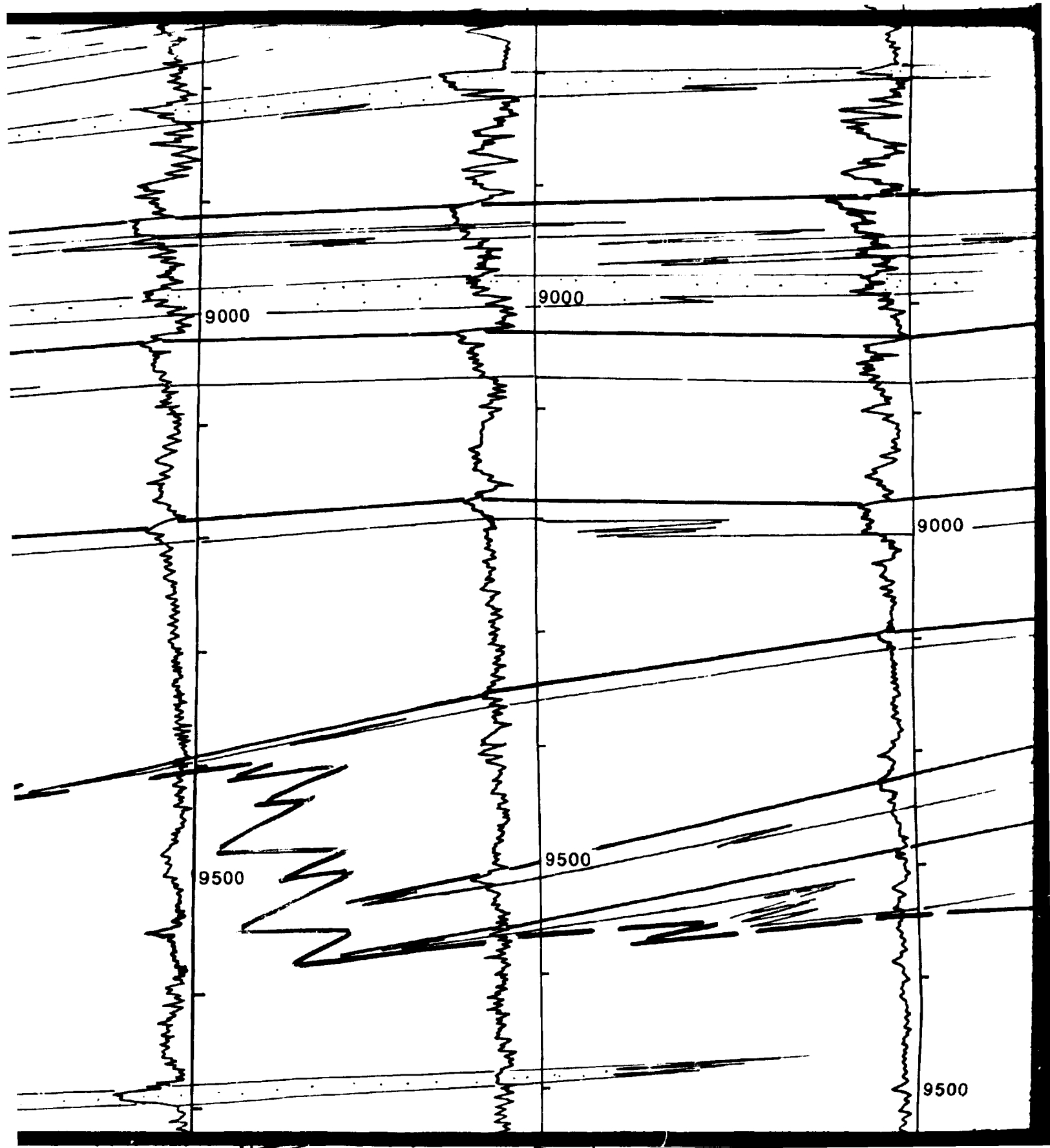
9000

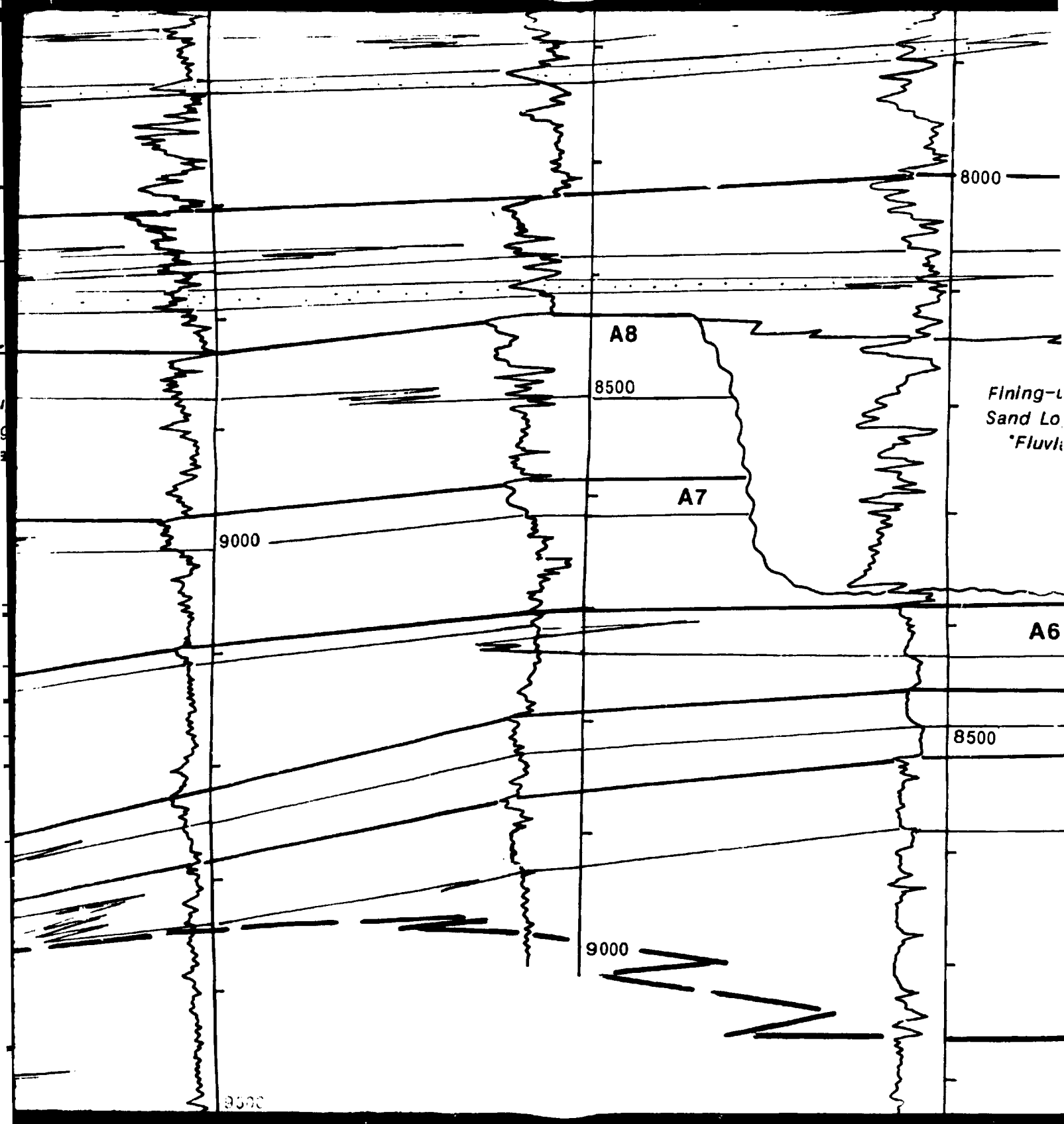
9000

Tanezzuft Transitional Boundary

9500







8000

A8

8500

A7

9000

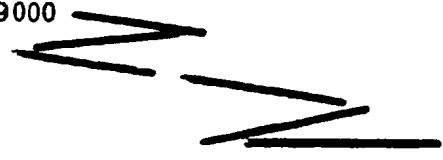
*Fining-
Sand Lo
Fluvial*

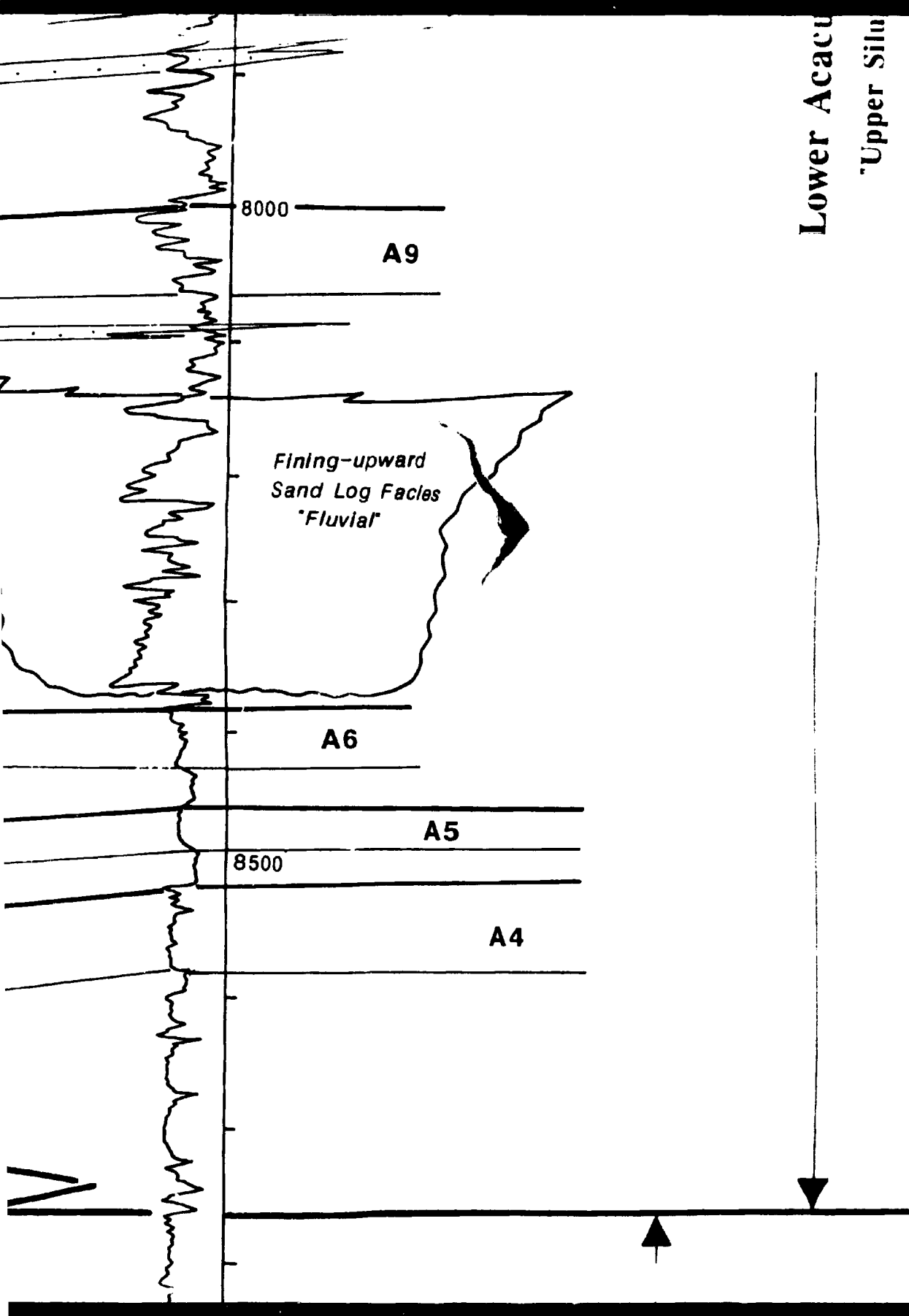
A6

8500

9000

9500





LOWER ACACUS

Upper Silurian

LEGEND



DRY HOLE



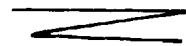
OIL WELL



OIL AND GAS WELL



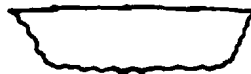
TOP GENETIC UNIT "COARSENESS
UPWARD SANDSTONE UNIT" LINE



FACIES LINE



TANEZZUFT TRANSITIONAL
BOUNDARY



FLUVIAL CHANNEL

A4-A14 LOWER ACACUS SANDSTONE UNIT



LEGEND

Y HOLE

WELL

AND GAS WELL

GENETIC UNIT 'COARSENING-
WARD SANDSTONE UNIT' LINE

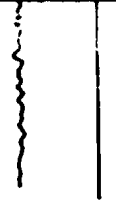
IES LINE

MEZZUFT TRANSITIONAL
BOUNDARY

VIAL CHANNEL

ER ACACUS SANDSTONE UNITS

1. 7.



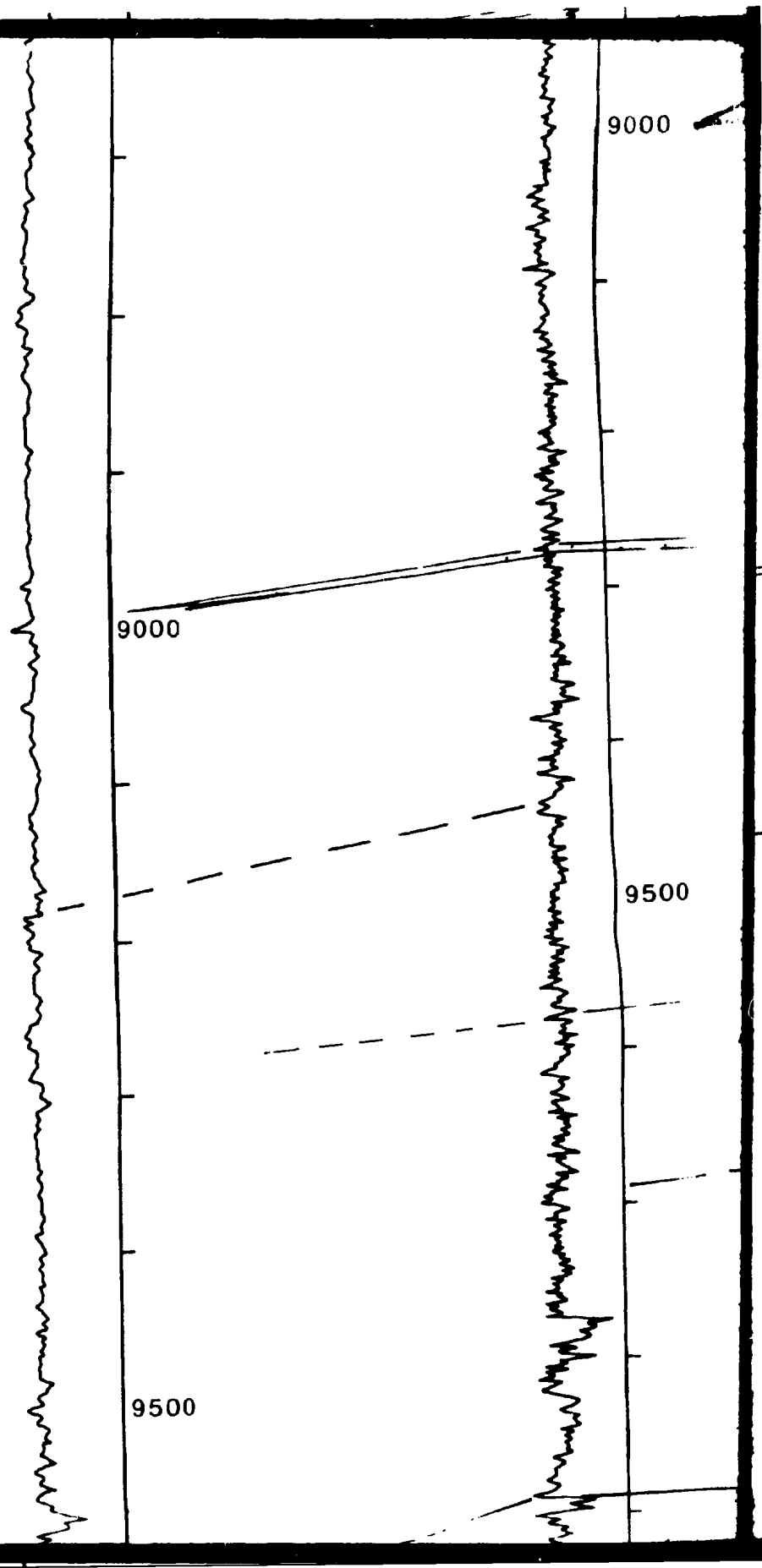
GR (AP?)
0 150

Tanezzuft Fm.

S

GR (API)
0 150

Shale Log Facies
"Basinal"



9000

9000

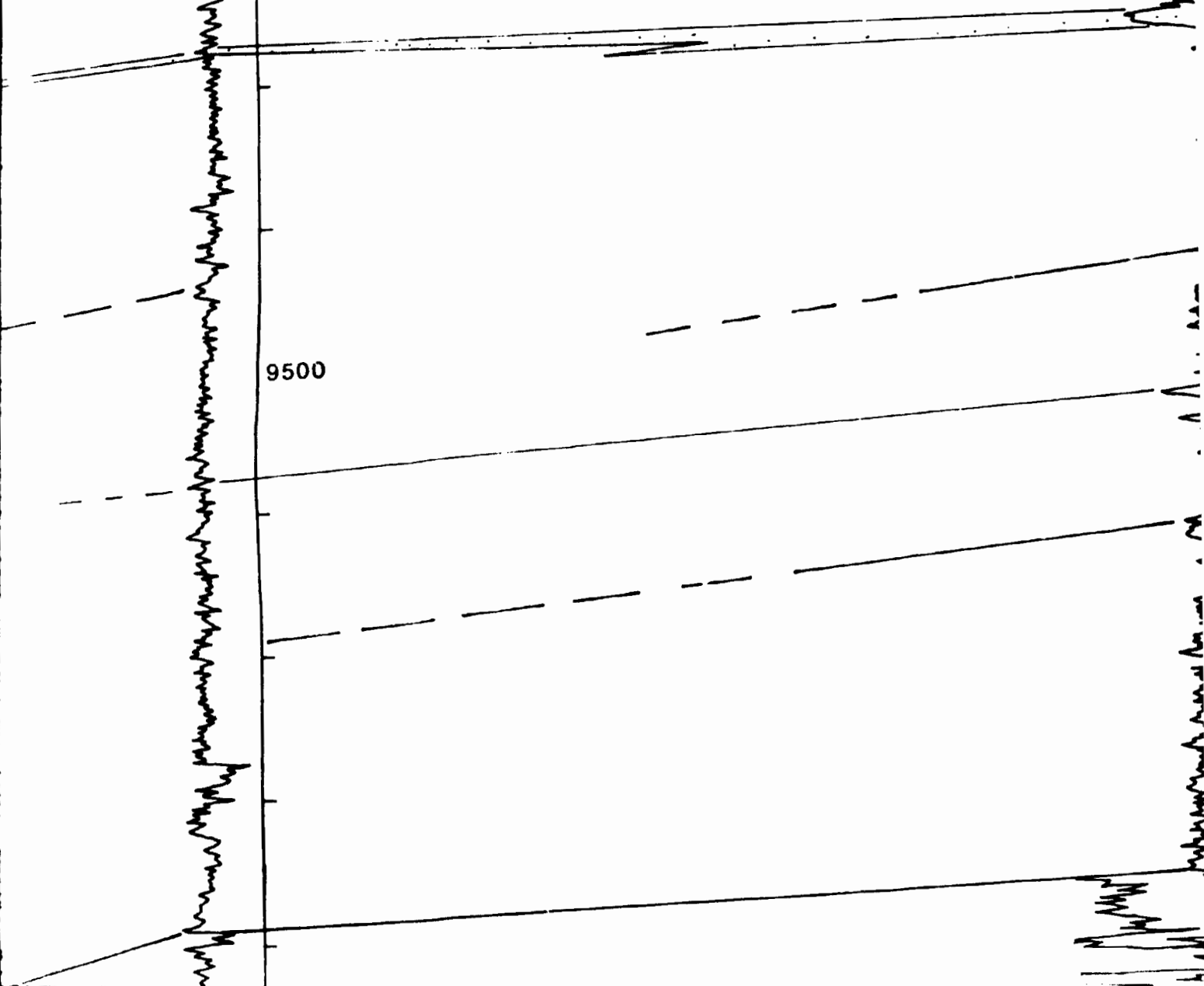
9500

9500

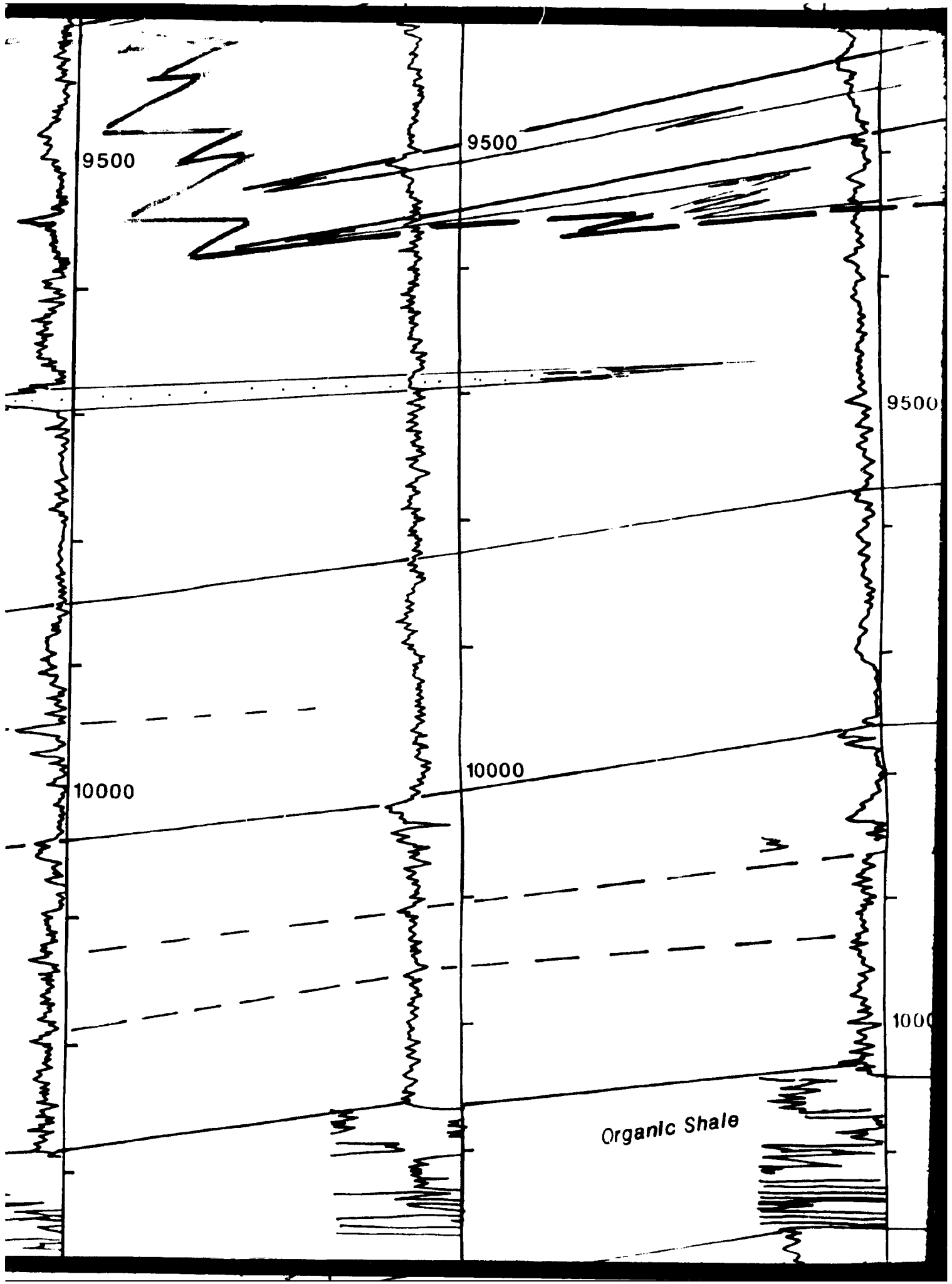
9000

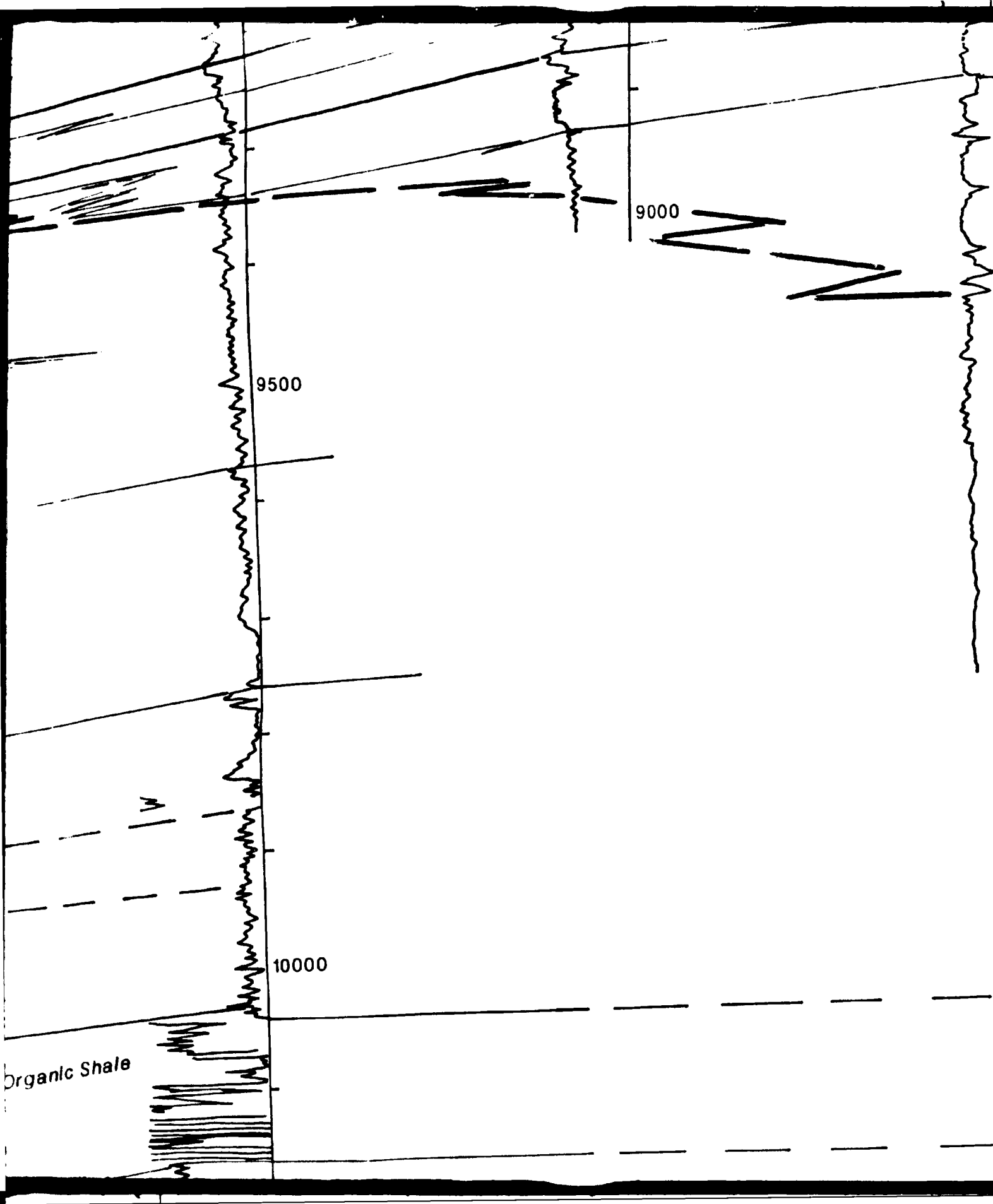
Tanezzuft Transitional

9500



Handwritten notes and symbols on the right margin, including a large 'A' and some illegible characters.



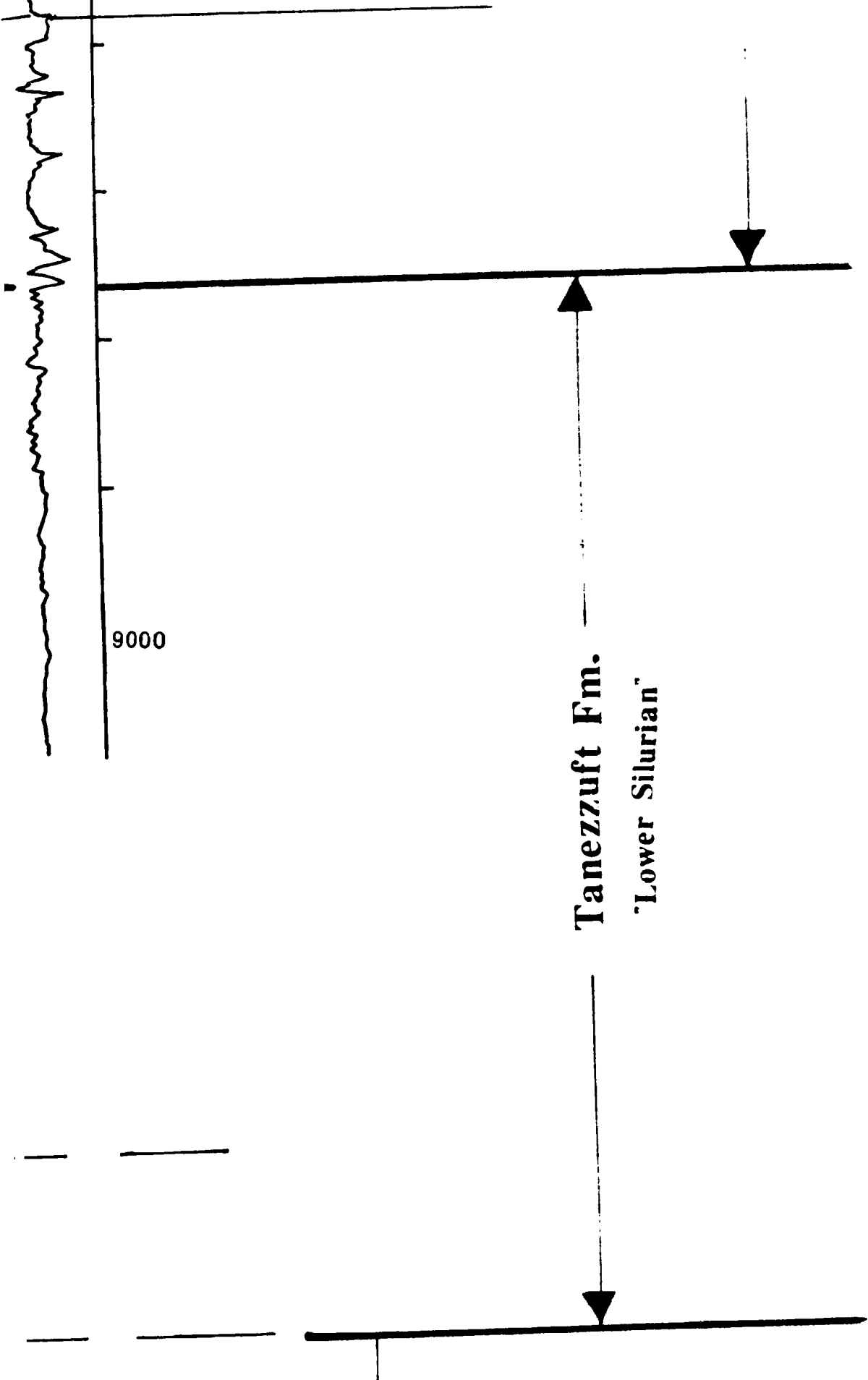


A4



9000

Tanezzuft Fm.
'Lower Silurian'

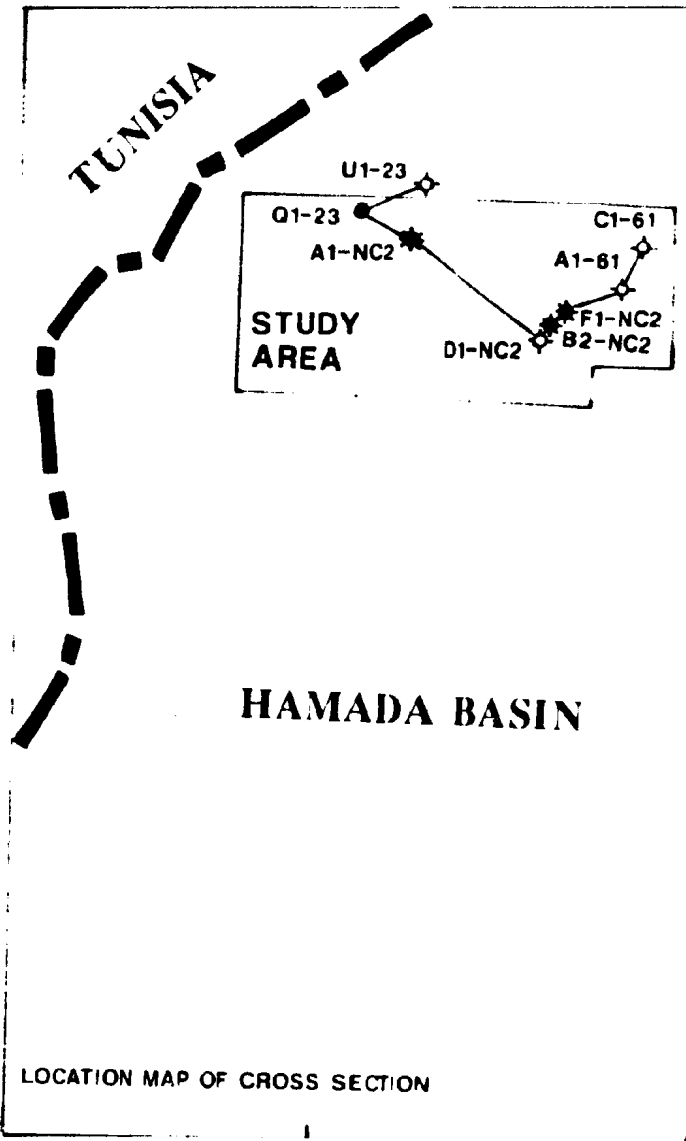


LYELLITE TRANS.
BOUNDARY



FLUVIAL CHANNEL

A4-A14 LOWER ACACUS SAND



LOCATION MAP OF CROSS SECTION

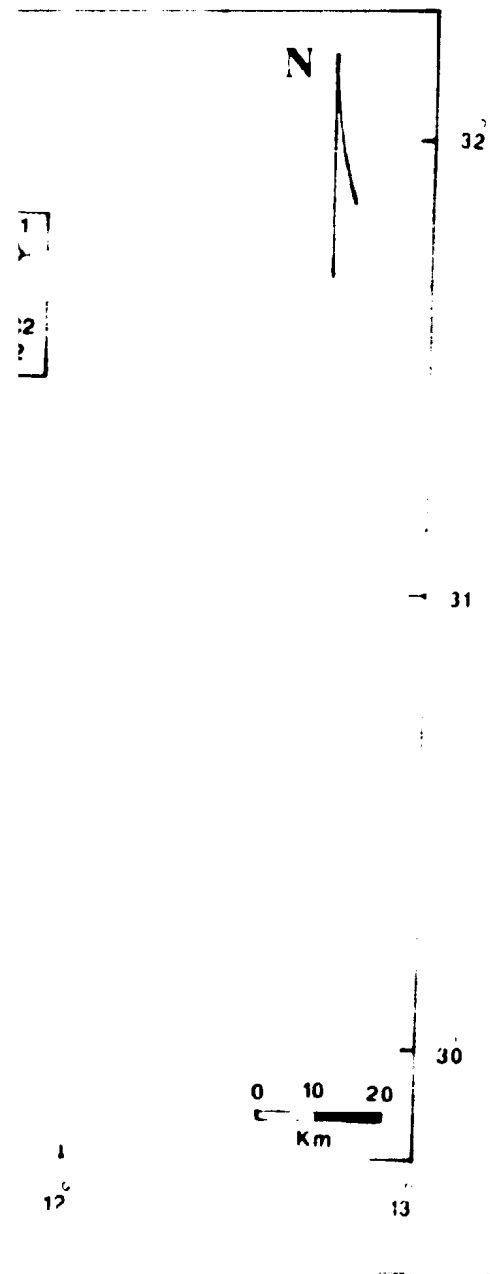
11°

12°

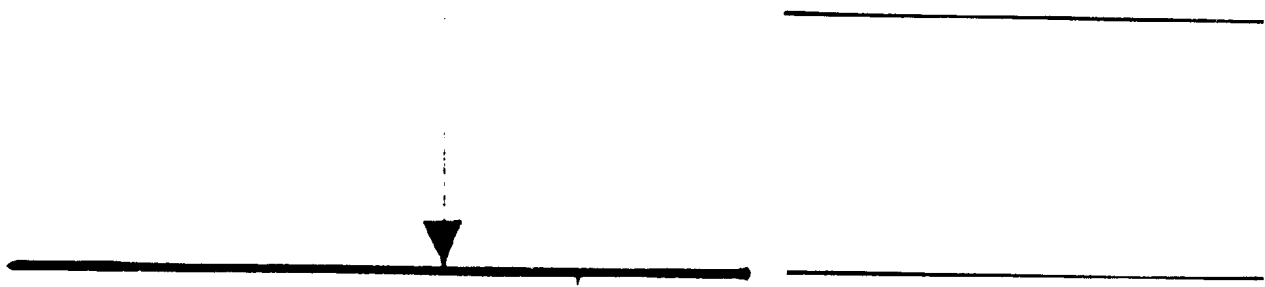
TRANSITIONAL
BARY

NNEL

SANDSTONE UNITS

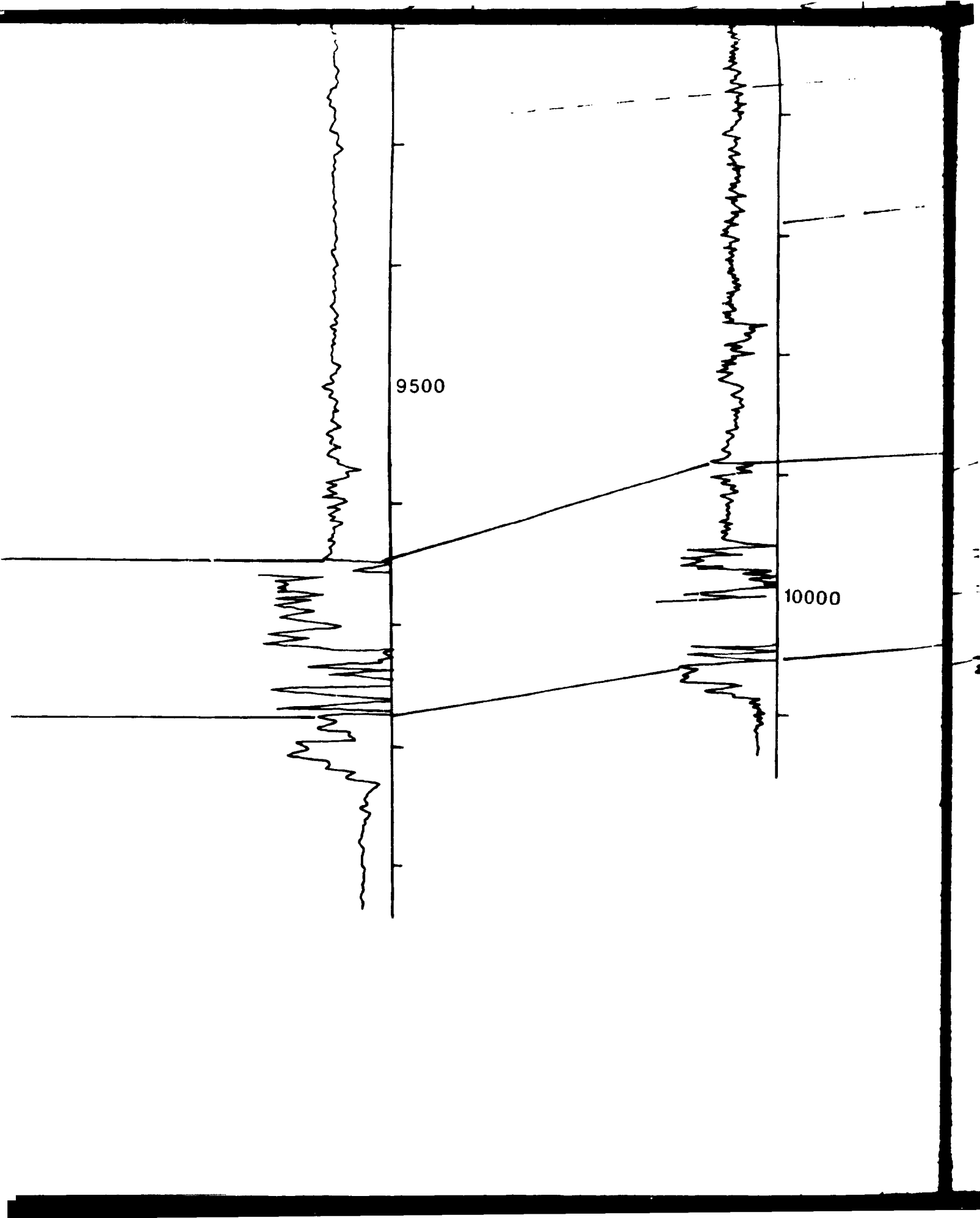


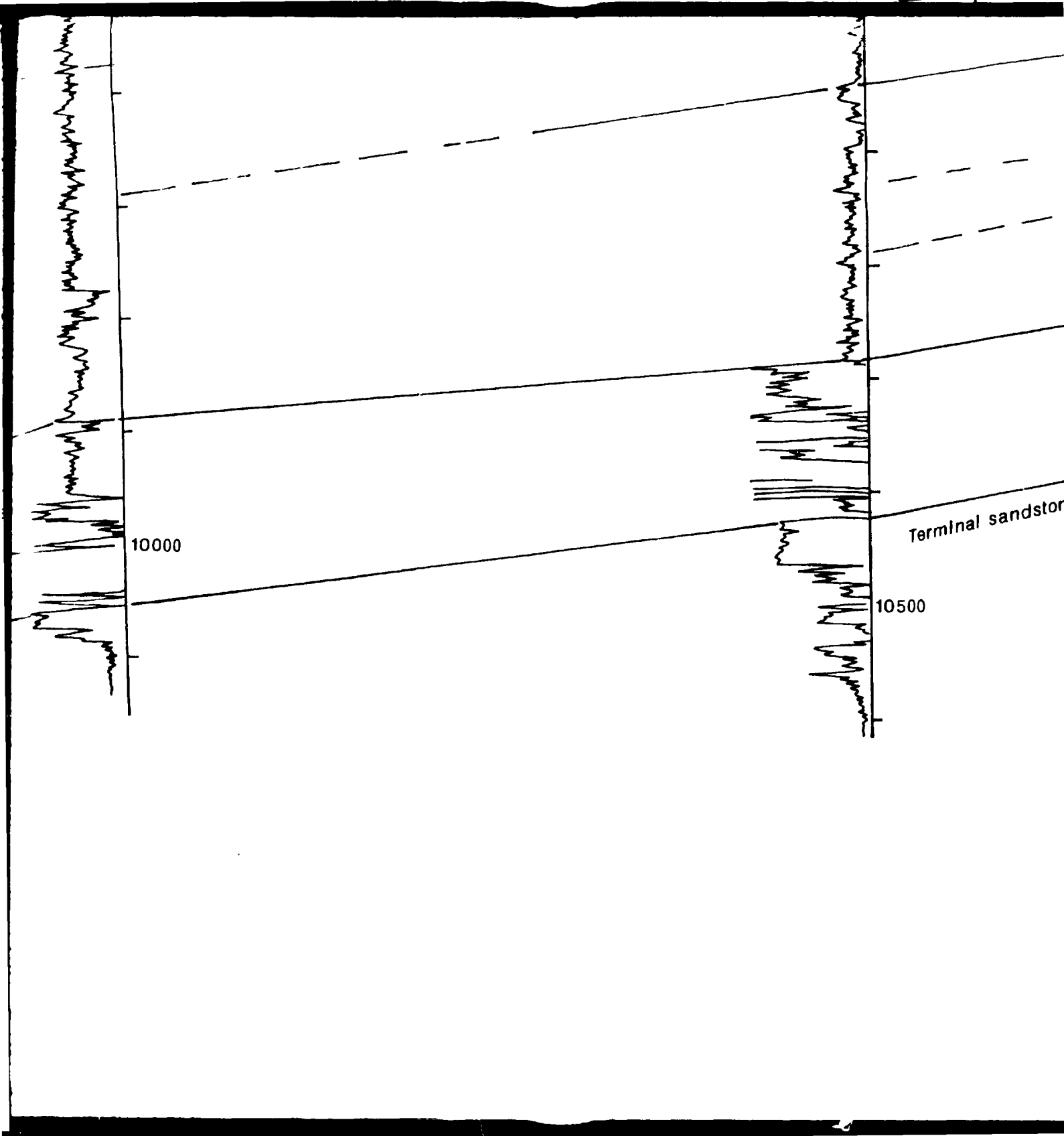
Tance



Memouniat Fm.



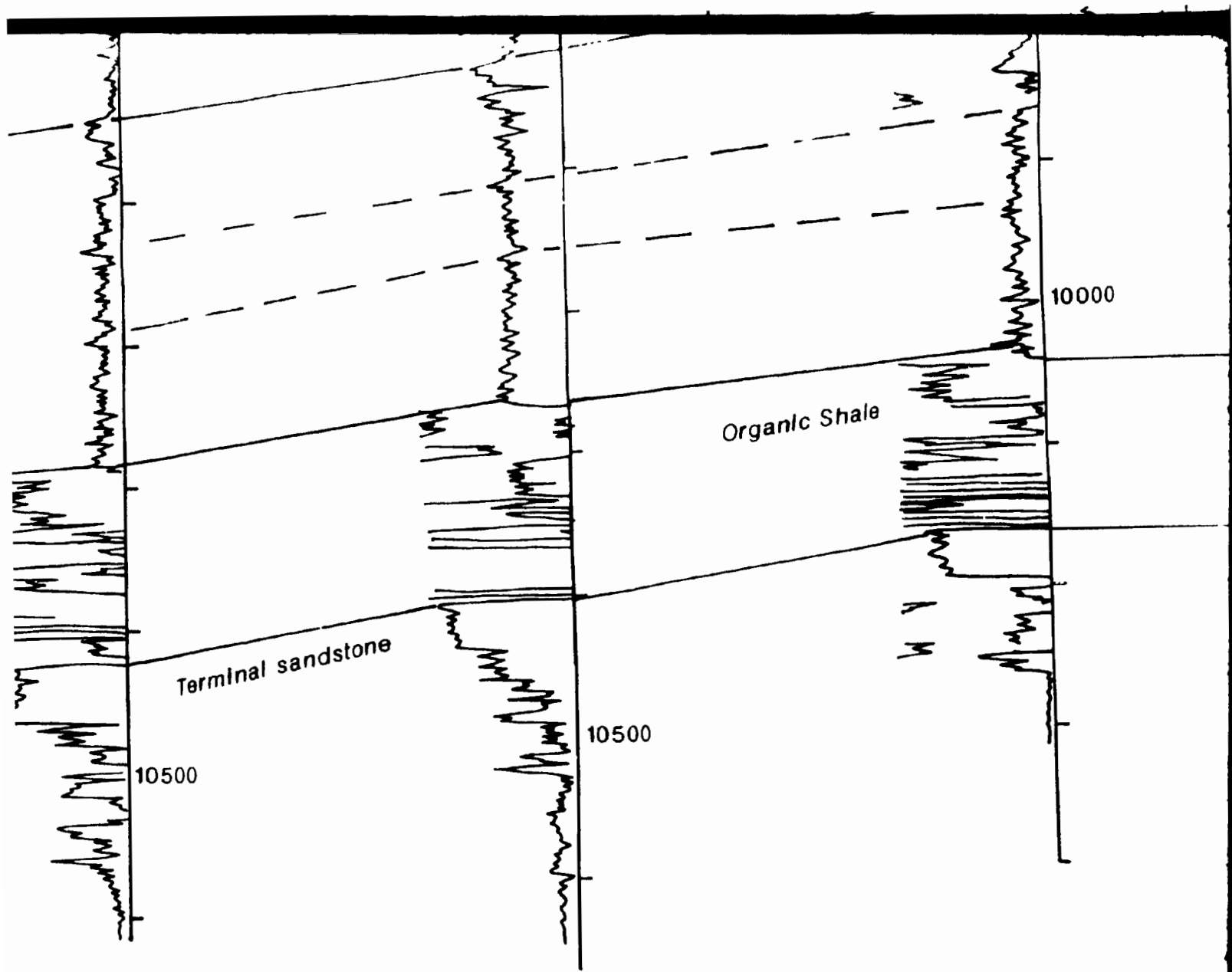




10000

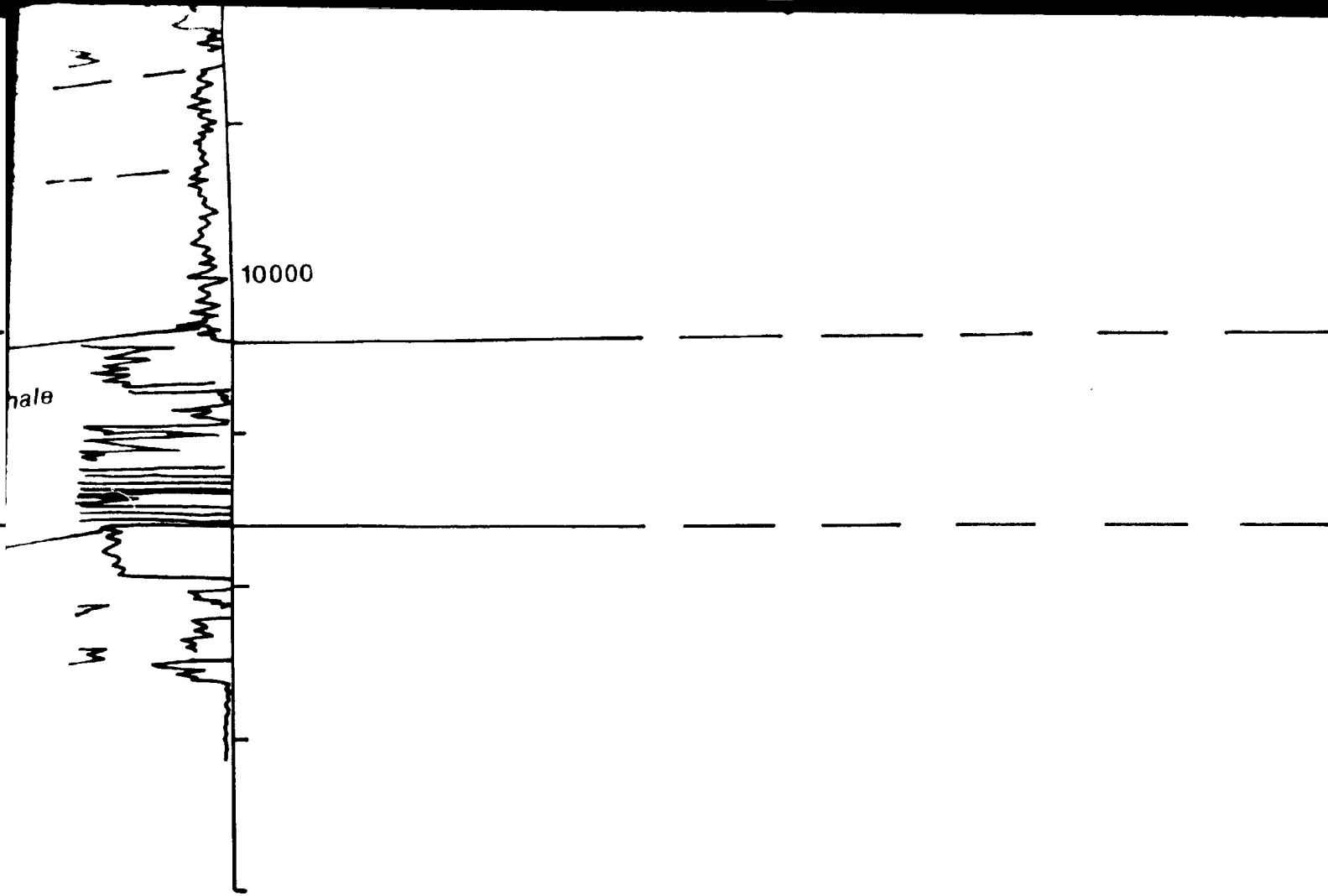
Terminal sandston

10500



10000

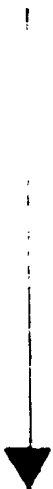
hale



Tane
Low



Memouniat Fm.
"Cambro-Ordovician"



VERTICAL SCALE

HORIZONTAL SCA

HAMADA BASIN

LOCATION MAP OF CROSS SECTION

0 10
Km

1 11
1 12

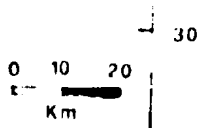
ENCLOSURE No.3

NE-NWN STRATIGRAPHIC CROSS SECTION

NC2 CONCESSION, HAMADA BASIN, NW LI

VERTICAL SCALE = 1 : 33.3 FT.

HORIZONTAL SCALE = AS INDICATED



30

13

RE No.3

CROSS SECTION,

BASIN, NW LIBYA.

OBE-91

ATED

N-S REGION

LOCATION



